Università Politecnica delle Marche

Scuola di Dottorato di Ricerca in Scienze dell'Ingegneria

Corso di Dottorato in Ingegneria Industriale

Enhancement of bio-based industrial by-products for innovative applications in engineering

Ph.D. Dissertation of:

Silvia Palmieri

Supervisor:

Prof. Francesca Tittarelli

Co-Supervisor:

Prof. Francesco Fatone

Co-Supervisor:

Prof. Maria Letizia Ruello

Ph.D. Course coordinator:

Prof. G. Di Nicola

XIX edition - new series

Università Politecnica delle Marche

Scuola di Dottorato di Ricerca in Scienze dell'Ingegneria

Corso di Dottorato in Ingegneria Industriale

Valorizzazione di sottoprodotti industriali a base biologica

per applicazioni innovative in ingegneria

Ph.D. Dissertation of:

Silvia Palmieri

Supervisor:

Prof. Francesca Tittarelli

Co-Supervisor:

Prof. Francesco Fatone

Co-Supervisor:

Prof. Maria Letizia Ruello

Ph.D. Course coordinator:

Prof. G. Di Nicola

XIX edition

Acknowledgements

I would like to dedicate this work to those who have always supported me and believed in me, even in my moments of doubts: my family and my friends.

But also to those who told me that I should give up because that was not for me and I would fail.

Abstract

L'estrazione e la produzione di risorse materiali hanno un impatto significativo sull'ambiente e sulla salute umana, oltre che sull'economia. Pertanto, ora, la salvaguardia e il risparmio delle risorse necessarie per il pianeta sta diventando sempre più importante nel campo dell'ingegneria e delle tecnologie.

L'ingegneria della materia, grazie allo sviluppo di materiali innovativi tramite il riutilizzo di vecchie risorse, offre diversi spunti per la realizzazione di materiali durevoli, multifunzionali e, soprattutto, attenti al consumo.

Difatti, il settore della ricerca sui materiali si sta focalizzando sempre più sulla valorizzazione di materie prime riciclate, ottenute da sottoprodotti industriali, per un'industria più sostenibile, a minore impatto ecologico, così da garantire un'economia circolare.

La presente ricerca si propone di supportare queste esigenze attraverso lo sviluppo e lo studio di materiali a base di sottoprodotti industriali a matrice biologica al fine di convertirli nuovamente in risorse per nuove applicazioni.

Lo studio si è focalizzato su vari materiali recuperabili da scarti industriali come derivati amidacei da industrie alimentari, fibre di cellulosa di carta igienica e poliidrossialcanoati (PHA) dal trattamento di acque reflue urbane, fibre di legno, di gusci di macadamia e da fondi di caffè e sulle loro possibili applicazioni.

In particolare, sono state realizzate e testate malte a base di calce idraulica rinforzate con fibre di cellulosa di scarto, in termini di proprietà meccaniche e di durabilità, per diminuire l'impatto ambientale dei materiali nel campo dell'ingegneria edile.

Sono state studiate le proprietà disinquinanti di alcuni derivati dell'amido (ciclodestrine) in termini di capacità di rimozione di COVs e del particolato per la creazione di filtri innovativi per il trattamento dell'aria.

Riguardo i PHA, sono state sperimentate diverse condizioni estrattive (convenzionali, in continuo e con Paar Reactor), includendo anche vari pretrattamenti (chimici e fisici) per valutarne le influenze sulle rese di estrazione. I polimeri estratti sono stati caratterizzati dal punto di vista meccanico, morfologico, chimico e termico.

Sono stati inoltre realizzati compositi a base di fibre di legno, di macadamia e di fondi di caffè, per produrre manufatti per il design tramite estrusione e stampaggio a compressione.

I risultati mostrano che la valorizzazione di queste materie secondarie è possibile, ottenendo risultati positivi in ogni campo proposto.

L'aggiunta di fibre di cellulosa recuperata nelle malte apporta benefici in termini di comportamento a flessione e capacità di tampone igrometrico.

L'aggiunta di ciclodestrine aumenta l'efficienza di rimozione di COVs e della frazione dimensionale PM1 dei filtri.

Si è dimostrato che i pretrattamenti sulla biomassa influenzano significativamente le proprietà dei polimeri estratti.

Infine, i compositi a base di PHA e fibre di legno si sono mostrati i più promettenti per lo stampaggio a compressione, presentando caratteristiche meccaniche e termiche comparabili a quelle di compositi contenenti PHA commerciale.

The extraction and production of material resources have a significant impact on the environment and human health, as well as on the economy. Even today, quality is synonymous with newness, for which a linear economic growth model is established, which has characterized history in the last century. Nowadays, safeguarding and saving the resources needed for the planet is becoming more and more important in the field of engineering and technologies.

Materials science and engineering, thanks to the development of innovative materials through the reuse of old resources, offers various ideas for the creation of durable, multifunctional and, above all, consumption-friendly materials.

In fact, the materials research sector is increasingly focusing on the enhancement of recycled raw materials, obtained from industrial by-products, for a more sustainable industry with a lower ecological impact, so as to ensure a circular economy.

The present research aims to support these needs through the development and study of materials based on biological matrix industrial by-products in order to convert them back into resources for new applications.

The study focused on various materials recoverable from industrial waste such as starch derivatives from food industries, cellulose fibers from toilet paper and polyhydroxyalkanoates (PHA) from the treatment of urban wastewater, wood fibers, macadamia shells and coffee grounds and their possible applications.

In particular, hydraulic lime-based mortars reinforced with recovered cellulose fibers were made and tested, in terms of mechanical properties and durability, to reduce the environmental impact of materials in the field of construction engineering.

The depolluting properties of some starch derivatives (cyclodextrins) were studied in terms of the ability to remove VOCs and particulate matter for the production of innovative filters for air treatment

Regarding the PHAs, various extraction conditions (conventional, continuous and with Paar Reactor) were tested, including various pre-treatments (chemical and physical) to evaluate their influences on extraction yields. The extracted polymers were characterized from a mechanical, morphological, chemical and thermal point of view.

Furthermore, composites based on wood fibers, macadamia and coffee grounds have been made to produce designer products by extrusion and compression moulding.

The results show that the exploitation of these secondary subjects is possible, obtaining positive results in each proposed field.

The addition of recovered cellulose fibers in mortars brings benefits in terms of flexural performance and hygrometric buffer capacity.

The addition of cyclodextrins increases the efficiency of removing VOCs and the PM1 dimensional fraction of the filters.

Biomass pre-treatments have significant influence on the properties of the extracted polymers.

Lastly, composites based on PHA and wood fibers have demonstrate to be the most promising composite for compression moulding, presenting mechanical and thermal characteristics comparable to those containing commercial PHA.

vii

"Populus me sibilat,
at mihi plaudo ipse domi,
simul ac nummos contemplor in arca."

Orazio, Satire
65 a.C.

Contents

Abbreviations

%w/V   Percentage weight on volume

%w/w   Percentage weight on weight

ΔP   Difference in pressure

μ   Water vapour resistance factor

3HO   3-hydroxyoctanoate

4HB   4-hydroxybutyrate

A   Area

a\b   aggregate\binder ratio

Ac   Acetone

Ac\MeOH   Mixture of Acetone and Methanol

ADF   Aerobic Dynamic Feeding

AN\AE   Anaerobic-aerobic process

ASTP   Activated Sludge Treatment Plant

ASTP   Activated Sludge Treatment Plant

ATR-FTIR   Attenuated Total Reflection Fourier Transform IR

BChl a   Bacteriochlorophyll a

BChl b   Bacteriochlorophyll b

BR   Butadiene Rubber

C%   Percentage consistency

C/C_0 Concentration at the final point on initial concentration

CA400   Calcareous sand

CEN   European Committee for Standardization

CENELEC   European Committee for Electrotechnical Standardization

CG   coffee ground

CGTase   Cycloglycosyltransferase

CP   Pure cellulose fibres

CP_30CG_Ex   Composite made with Commercial PHA and coffee grounds through extrusion

CP_30CG_Pm   Composite made with Commercial PHA and coffee grounds through compression moulding

CP_30MS_Ex   Composite made with Commercial PHA and macadamia shells through extrusion

CP_30MS_Pm   Composite made with Commercial PHA and macadamia shells through compression moulding

CP_30WF_Ex   Composite made with Commercial PHA and wood flour through extrusion

CP_30WF_Pm   Composite made with Commercial PHA and wood flour through compression moulding

CP_Ex   Commercial PHA composite made through extrusion

CP_Pm   Commercial PHA composite made through compression moulding

CREC   Recovered cellulose fibres

CRIC   Recycled cellulose fibres

CS   Chemical structure

CyDs   Cyclodextrins

d   density

d%   Ductility

DCM   Dichloromethane

d_f Paste diameter after 15 bumps;

d_i Initial diameter of the paste

DMF   N,N-Dimethylformamide

DPI   Degree of Polymerization

DSC   Differential scanning calorimetry

E   Young's Modulus

e%M   Deformation at the maximum load

EEA   European environment agency

EES   Engineering Equation Solver software

EP   epoxies

ESP   Electrostatic precipitations

EtOH   Ethanol

ETSI   European Telecommunications Standard Institute

Ex_Std   Standard Extraction

F   Force

GHG   Greenhouse gases

GPC   Gel permeation chromatography

GPW   Global Warming Potential

HB   3-Hydroxhybutirrate

HCl   Chloridic acid

HEPA   High efficiency particle arresting

Homo   Homogeization with pressure

HV   3-Hydroxyvalerate

IAQ   Indoor air quality

ITZ   Interfacial transition zone

KNO_3 Potassium nitrate

Ks   Stability constant

L   Distance

LCA   Life cycle assessments

LCI   Life Cycle Inventory

m   Mass

MBV   Moisture Buffering Value

Mc   Certain critical value for molecular weight

MCC   Multifunctional Cement-based composites

MeOH   Methanol

MFI   Melt Flow Index

$MgCl_2$ Magnesium Chloride

MIP   Mercury intrusion porosimetry

MMC   Mixed microbial culture

MMD   Molar mass distribution

Mn   Number average molecular weight

MS   Macadamia shell nuts fibres

Mw   Average molecular weight

MWD   Molecular weight distribution

MWh   Megawatt-hour

NaClO   Sodium hypochlorite

NF   Natural Fibre

NFRCs   Natural fibre–reinforced composites

NHL5   Natural hydraulic lime

NMR   Nuclear magnetic resonance

NRC   Natural Reinforced Composites

OPP   Oriented polypropylene

P(3HB)   Poly-3-Hydroxhybutirrate

P(3HB-3HV) Poly(3-hydroxybutyrate-co-3-hydroxyvalerate)

PAHs   Polycyclic aromatic hydrocarbons

PDI   Polydispersity index

PE   Polyethylene

PE   Population Equivalent

PHAs   Polyhydroxyalkanoates

PHB   Polyhydroxybutirrate

PHBV   Poly-3-hydroxybutirrate-co-3-valerate

PI   Polyimides

PLA   Polylactide Acid

PLA\CyDs   Polylactide acids fibres with cyclodextrins in powder

PLA+CyDs   Polylactide acids fibres with cyclodextrins in solution

PM   Particulate matter

PNSB   Purple non-sulfur bacteria

PP   Polypropylene

PPI   Pores per inches

PS   Polystyrene

PSB   Purple sulfur bacteria

PU   Polyurethane

PVC   Poly vinyl chloride

R   Resilience

RBDF   Rotating belt dynamic filter

RBF   Rotating Belt Filtration

R_c Compressive strength

REF   Reference

REI   Italian renewable energy incentives

R_f Flexural strength

RH   Relative Humidity

ROS   Reactive oxygen species

RP_30WF_Pm   Composite made with recovered PHA from PPB and wood flour through compression moulding

RP_Pm   Composite made with recovered PHA from PPB through compression moulding

rpm   Rotation per minute

S.C.E.N.A.   Short Cut Enhanced Nutrient Abatement

SBFR   Sequencing batch fermentation reactor

SBS   Sick building syndrome

SEM   Scanning Electron Microscope

Soxhlet   Extraction in continuous

Spheres   Glass Spheres

SSD   Saturated with dry surface

T   Toughness

Tc   Crystallization temperature

t_c Starting point of curing reaction

Td   Degradation temperature

Td 1\2   Temperature at half decomposition

Td max   Temperature at maximum rate decomposition

Td0   Initial Decomposition Temperature

t_f Fill time

Tg   Glass Transition Temperature

TGA   Thermo-gravimetric analysis

Tm   Melting temperature

T_w Uniform temperature or temperature of mould-wall

U   Velocity

Ultra   Homogenization with blades

U_{ssd} Percentage of maximum water absorption

VFAs   Volatile Fatty Acids

VOCs   Volatile Organic Compounds

v_{outlet} velocity of air flowing out

Vp   Total porosity volume

w\b   water\binder ratio

WF   Wood Flour

WHO   World Health Organization

WPCs   Wood Plastic Composites

WWTPs   Wastewater treatment plants

γ   shear rate

ΔHc   crystallization enthalpy

ΔHm   Melting enthalpies

ε   Strain

η   shear viscosity

ρa   Density of completely amorphous polymer

ρc   Density of completely crystalline polymer

ρs   Density

σ_M Maximum tensile strength

τ   shear stress

1. Chapter

Introduction

Description of the scientific and technological field:

Problems, Aims and Methods

1.1   **Preface**

"Waste is a waste only if you waste it. Otherwise it is a resource"

Ancona, T. Naik

Nowadays Europe relies heavily on material resources for almost all of the companies' activities. The extraction and production of material resources has a significant impact on the environment and human health, as well as on the economy. Even today, quality is synonymous of newness, for which a linear economic growth model is established, which has characterized the history in the last century. This model is founded on a market economy based on the extraction of raw materials, their production, consumption and on the disposal of waste, once the end-life has been reached. It is essential to reuse these resources in world economies, keeping their value high, offering value for longer periods and reducing the need to use virgin materials. While progress is being made in Europe by implementing an ambitious waste policy and the Circular Economy Framework, significant quantities of valuable resources are still being lost due to inefficient waste management practices.

A 'circular economy' approach would turn goods at the end of their service life into resources for others, closing loops in industrial ecosystems and minimizing waste. It would change economic logic because it replaces production with sufficiency: reuse what you can, recycle what cannot be reused, repair what is broken, remanufacture what cannot be repaired. Circular-economy business models fall in two groups: those that foster reuse and extend service life through repair, remanufacture, upgrades and retrofits; and those that turn old goods into as-new resources by recycling the materials[1].

In recent years, innovations in the field of materials science have transformed waste materials from the industrial sector into a complex tool for the reduction not only of the gas emissions due to the production of new goods, but also of the their disposal at their end of life, promoting their recovery and reuse for new applications.

This work has the propose of "closing the loop" for funding possible solutions for different kind of wastes coming from industrial sectors, recovering those materials and studying their characteristics and properties to enhance and valorise them in a new possible application.

Each chapter of my thesis is focused on a different wasted material: its source, its properties and a new possible application are investigated.

1.2   **Scientific field and problems**

Beyond climate change, the main challenges the world is facing today, as previously exposed, are the substantial increase in energy demand, food and material unsustainable consumption and production, and anthropogenic wastes generation. According to World Resources Institution, the planet is projected to hold 9.6 billion people by 2050, consuming the equivalent of 1.6 planet's resources, with a consequent high amount of wastes generated[2]. Consequences of the unsustainable consumption and production patterns are resource depletion, climate change, air and water pollution, loss of biodiversity and of fertile soil, amongst other environmental, social, and economic challenges[3,4,5]. Almost 30% of the food produced globally is lost or wasted at some point along the food supply chain[4,6] causing all these serious issues[7,8].

Referring to the circular economy, the fields of application are varied and vast, so to define an application target[9] is necessary. In literature, in fact, the circular economy issue is tackled from different points of view: from the economic one[10] to the implementation method[3]. Therefore, to define the action target is essential: Figure 1.2.1 summarizes the main known targets[9].
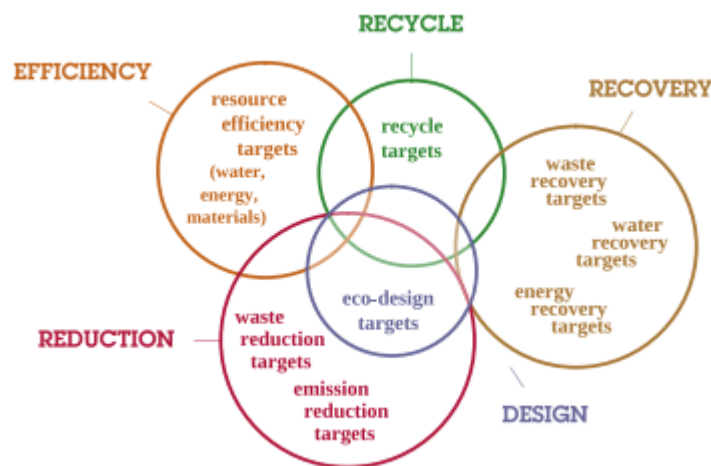
Figure 1.2.1 Main existing Circular Economy targets by areas of application [9]

This study is focused on the section of recovery of waste materials in order to enhance by-products promoting the reduction of human footprint and the reuse, recycling and recovery of various wastes.

1.2.1   Decreasing the human footprint on the environment by enhancing secondary products

The development of new approaches in supply chain management research are addressed at the promotion of efficient resource use and the reduction of environmental impacts, all while considering the profitability and productivity of all stages of the supply chain. This perspective, aims at reducing the ecological impacts of anthropic activities without sacrificing quality, cost, reliability and performance, balancing the relationships between supply chain management and the natural environment.

Reducing environmental impacts and getting economic benefits by recovering by-products, and by reducing both water consumption and organic load, is the aim of the implementation of an eco-efficiency process.

In this context, it is important not only the recovery of the material itself, but also the demand for it in the market: from the beginning of its process as raw material up to its disposal. On the one hand, there is a need to reduce the consumption of raw materials, raising awareness among the population and a more conscious use of the resource, promoting recycling, reuse and avoiding the purchase of disposable materials; on the other side there is the market that offers non-reusable products even if eco-sustainable.

Nowadays the consumer pays much more attention to the eco-sustainability of the product than in previous years, looking for biodegradable plastics or taking advantage of the purchase of products from intensive farming. Nevertheless, terms such as biodegradability are still confused or wrongly understood: in fact, the population often misunderstands the fact that a product is biodegradable or eco-sustainable with the possibility of being released into the environment rather than properly disposed of. This attitude, wrong for any kind of economy (both linear and circular), leads to an accumulation of waste that has a huge environmental footprint. It is important that the consumer clearly understands the durability of the various products, so that they can be disposed of in the most suitable way reducing the environmental impact.

The market should cooperate by moving towards this perspective, enhancing recycled and recovered products, facilitating companies in production and encouraging consumption to purchase.

1.2.2   Recycling of bio-based industrial by products

The disposal of wastes is one of the main costs for a company. The addition of value in a recycled or recovered material can be increased creating a communication between companies. In fact, some company have the possibility to use the waste of another industry to produce their own goods: many textile companies utilize recycled PET for

making fleece clothing. For example, the US-based company Patagonia began making recycled polyester from PET bottle waste in 1993.

Another interesting example is the Colombia-based Diseclar, which developed a manufacturing process that turns recycled plastic and agro-industrial waste into durable furniture suitable for indoor and outdoor use. By combining non-degradable plastic waste and agro-industrial waste, such as sugarcane pulp, coffee residues, and rice chaff, the company creates furniture with the look and feel of solid wood. In their first year of production, Diseclar aimed to recycle 300,000 kg of plastic and 192,000 kg of agro-industrial waste.

The use of plastics in association with other materials permit to create new composites and to reduce the amount different wastes. Association of two (or more) different materials permits to create a composite: an innovative material, with the combination of the chemical and physical properties of the single components. Recently, the use of plastics in association with wood-based materials to make Wood Plastic Composites (WPCs) represents one option for recycling, which is explored in the present work. WPCs have gained a substantial market in the last decade, due to transformative technological advancements in compounding and processing. The WPC global market was as high as 3.0 million tonnes/year in 2014, and is forecast to double by 2020[11,12].

In the present work, wood flour, macadamia shell flour and coffee grounds coming from industrial wastes were used as reinforcing materials to make composites in association with polyhydroxyalkanoates, to be used in design manufacture (as furniture and auto interior parts). These three materials came from three different industries of the Australian market and represents a large piece of the global market concerning since 2012 (Figure 1.2.2).
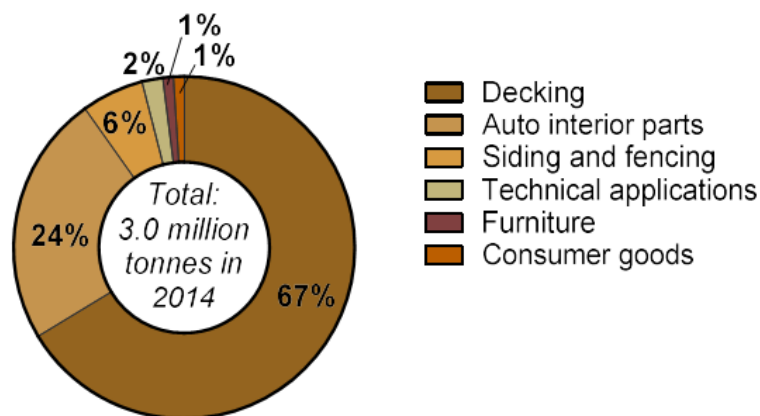
Figure 1.2.2 Market segment of Wood Plastic Composites (WPC) in Europe (2012)[11]

The recovery of particular waste materials, mainly from urban wastewater treatment plants and industrial wastes is the core of this dissertation, which is the result of a collaboration with SMART-Plant Innovation Action (www.smart-plant.eu). SMART-Plant includes the whole train of wastewater and sewage sludge treatment within any type of wastewater treatment plant. These have emerged through the implementation of the EU funded Horizon 2020 Innovation Project of SMART-Plant. The full-title of SMART-Plant project is "Scale-up of low-carbon footprint material recovery techniques in existing wastewater treatment plants".

1.2.3 Wastewater Treatment Plants

During the last years, wastewater treatment plants (WWTPs) have moved from the concept of 'waste treatment', aimed at discharging treated wastewaters, to a much broader concept: wastewater contains important resources that should be recovered in wastewater treatment plants to generate value-added products such as renewable energy, biofertilizers and water for different purposes. The recycling of resources through innovative recovery processes is only a recent objective in wastewater treatment systems: it makes the processes of the plants more efficient, it reduces the amount of waste and it provides environmental and economic benefits[13].

The ultimate aim for the plant would be to become energy self-sufficient with zero external energy supply. Sustainability in wastewater management needs to consider not only treatment of sewage, but also the potential for resource recovery from the treatment[14].

For these reasons, WWTPs moved into a new concept of 'water resource recovery facility': this transformation from pollutants removal to valuable resources frames wastewater management in the broader context of the circular economy[13,14].

In this new concept of plants, the energy recovery is interpreted in a wider sense. To achieve the aim of Zero Energy WWTPs, the objective is not only the already known water reuse, which can be one of the methods of recycling treated wastewater for beneficial purposes (such as agricultural or industrial processes), but also to invest on the other sub-products present in the plants[13–15].

Biogas production (the main resource of anaerobic treatment systems) is widely diffused as an alternative source of energy, for the recovery of thermal, electrical and mechanical energy, to be consumed either inside (also achieving energy self-sufficiency) or outside the plant.

Also recovered nutrients from the wastewater are particularly interesting: in fact, they can be utilized as soil amendments or fertilizers for beneficial uses in agriculture. In particular, substances as Ammonium (NH_4^+) and Phosphorous (P) are advantageous

because NH_4^+ predominates in anaerobic reactor effluents and can be useful for fertigation purposes; whereas P (recovered as struvite or salts) becomes essential for preventing eutrophication in the aquatic environment[14,16].

Furthermore, this new generations plants permits to recover also other precious materials that can be originated from cellulosic primary sludge and biopolymers rich sludge.

The cellulosic sludge can be separated by upstream dynamic sieving[15]. The Cellulosic Primary Sludge can be anaerobically digested to produce biogas, or, under optimal acidogenic fermenting conditions it produces Volatile Fatty Acids (VFAs)[16].

For what concerns biopolymers recovery (polyhydroxyalkanoates), primary and secondary sewage sludges are potential feedstock[17]. Polyhydroxyalkanoates have comparable properties to petrochemical plastics and can also serve as biofuel or building blocks for the synthesis of various chemicals[18].

While some of the above-mentioned reuse and recovery approaches towards wastewater are already efficiently implemented, some of them still lack the convenient technology together with social-technological planning and design methodology to identify their potential end-use and market requirements. This study treats the last two materials, cellulose fibres and polyhydroxyalkanoates, recovered from the WWTP of Carbonera, Treviso Province, Italy. These recovered materials and this work are part of SMART-Plant European project, and they directly come from one of the partners of the project.

1.2.3.1   *Cellulose fibres from Cellulose Primary Sludge*

Cellulosic material in the toilet paper, which is the major organic component in the urban influent that enters the municipal treatment plants [15], holds a great potential as one of the most recoverable products from wastewater flows. The potential recovery of cellulose strictly depends to the daily use of toilet paper: this means that the consumption is extremely variable, heterogeneous and closely related to the degrees of urbanization, sanitation, sewage infrastructures and waste transport. The potential recovery has to be referred to specific territorial scale: variable ranges of data are reported in the scientific literature basing on the country, equal to 49 ± 23 g toilet paper $p^{-1}d^{-1}$ in America, to 31 ± 21 g toilet paper $p^{-1}d^{-1}$ in Europe, to 5 g toilet paper $p^{-1}d^{-1}$ in Asia and to 1 toilet paper g $p^{-1}d^{-1}$ in Africa[19–21].

Assuming that toilet paper contains approximately 85% of cellulosic compounds[22], the maximum potential recovery of cellulose varies in a range between 42 g toilet paper $p^{-1}d^{-1}$ in the most industrialized countries and 1 g toilet paper $p^{-1}d^{-1}$ in developing countries.

Several research activities and European projects have focused on the recovery of resources from wastewaters (Pioneer_STP, SMART-Plant and INCOVER are only some

examples). Specifically, projects such as SMART-Plant, have implemented the recovery of cellulosic fraction in wastewater treatment plants (WWTPs) through the integration of the dynamic separation technology into conventional treatment flow schemes. This unit easily allows to separate a greater fraction of solids and to retain the cellulose fibers more efficiently while replacing the traditional primary sedimentation[15]. The separated material; on the other hand, needs to be industrially washed and dried to extract the recovered cellulose fibers (Figure 1.2.2).

Figure 1.2.3 Recovered Cellulose Fibres

CirTec (a SMART-Plant partner) has developed a flow scheme with filter for primary treatment (Salsnes Filter[TM]) and separation of cellulosic fibres to produce a highly concentrated sludge. The produced fine sieved fraction has a very heterogeneous composition containing mainly cellulosic fibres originating from toilet paper. The result is a market-ready cellulose that has been cleaned, dried and disinfected. Some of the cellulose fibres used in this study have been gently provided by CirTec.

1.2.3.2   *Polyhydroxyalkanoates*

Rapid depletion of petroleum reserves and persistence of conventional synthetic plastics in the environment are considered important ecological problems. Thus, alternatives to petroleum-based plastics are needed. Biopolymers are a group of polymers with similar properties to petroleum-based plastics, produced from renewable sources also by different types of bacteria using carbon as substrate[23].

Polyhydroxyalkanoates (PHAs) are an example of biopolymer. They are commonly known as bioplastic and have the advantage to be biodegradable and biocompatible.

It has been estimated that globally, production capacities of bioplastics till 2025 is going to increase from around 2.11 million tonnes in 2020 to approximately 2.87 million tonnes [17,24,25]. However, the main obstacle to the growth of bioplastic market is its high production cost, poor recycling facilities and inefficient waste handling technology[17,26].

The production of PHA from pure bacterial cultures is extremely studied, but until few years ago it was very limited because of the high costs. In fact, for pure cultures the major portion of the production cost is spent on media sterilization and maintenance of reactor[27]. Hence, to search for worthwhile and cost-effective feedstock alternatives for PHA production has become imperative.

Wastewater treatment sludge containing mixed microbial cultures is a potential feedstock for PHA production. In fact, the use of wastewater treatment sludge for producing PHA will also reduce the environmental burden of sludge disposal permitting an advantage not only for the environment, but also for the valorisation of a sub-product[14,17,28,29]. Rapidly increasing population, urbanization and industrialization leads to production of excess amount of sludge, making it readily available. PHA-storing bacteria, that store these polymers as carbon source and energy reserve[30], are well-known to grow in activated sludge processes of WWTPs. The series of operations needed for microbial production of PHAs are well known in the literature[27,31–36].

On-going pilot-scale and new technologies developed in recent years offer fundamental experience to produce PHA from waste materials in enough quantities to inspire value chains and investment within first bio-based value chains[17,29,45,46,37–44]. The disadvantages on these plastics recycling and recovery concerns the limits in applications: products coming from wastewater resources have strict standards to guarantee the safety of those materials for some applications. Those standards are determined by the European Committee for Standardization (CEN), the European Committee for Electrotechnical Standardization (CENELEC) and the European Telecommunications Standards Institute (ETSI). For these reasons, applications in hygienic fields or in foods fields (such as food packaging or biomedical engineering) can not be considered in this work.

Basing on the feedstock and on the growing conditions of the cultures, the chemical structure of the polymer might change[29,40,47,48], therefore to control them constantly is determinant. The most common structures of PHAs are homopolymers of 3-polyhydroxybutyrate (PHB) and copolymers with 3-hydroxyvalerate (HV). Other PHA monomers comprise, 3-hydroxybutyrate, 3-hydroxy-2-methylbutyrate, 3-hydroxyvalerate, and 3-hydroxy-2-methylvalerate, and 3-hydroxyhexanoate. PHA, as insoluble corpuscles in the cytoplasm, are a widespread microbial mechanism in nature to store carbon and energy within the cells under unfavourable growth and nutrient conditions. The metabolism of PHA synthesis is encoded by *phaC* gene, characteristic of microbes with PHA-storing capacity.

In the wastewater treatment plant of Carbonera, a town in the Province of Treviso (Italy), there is a pilot plant (Figure 1.2.3) working on the biological nitrogen removal and P-bioaccumulation via-nitrite during the treatment of anaerobic supernatant.

The full-scale plant has a treatment capacity of 40,000 PE and it treats around 15,000 m^3/day of municipal wastewater without any industrial contribution. The water line is composed by preliminary treatments, primary sedimentation, biological reactor (Schreiber process), secondary sedimentation, disinfection and final filtration[49].

The sludge line is composed by a static pre-thickener followed by dynamic thickening (installed during the experimental period) of mixed primary and secondary sludge, equalization tank for thickened sludge, anaerobic digester and the Short-Cut Enhanced Nutrients Abatement (S.C.E.N.A.) system for the treatment of sludge reject water.

It accounts of the following subprocesses: (i) cellulosic primary sludge fermentation to enhance the production of Volatile Fatty Acids and release nitrogen and phosphorus (i.e. ammonia and phosphate); (ii) solid and liquid separation of the fermentation products and recovery of struvite form the sewage sludge fermentation liquid by the addition of Mg(OH)$_2$ to facilitate the precipitation; (iii) ammonium conversion to nitrite accomplished in a sequencing batch reactor; (iv) selection of PHA storing biomass in a sequencing batch reactor by the alternation of aerobic feast conditions and followed by anoxic famine conditions for denitritation driven by internally stored PHA as carbon source; (v) PHA accumulation using a fed-batch reactor to maximize the cellular PHA content of the biomass harvested from the selection stage[49].
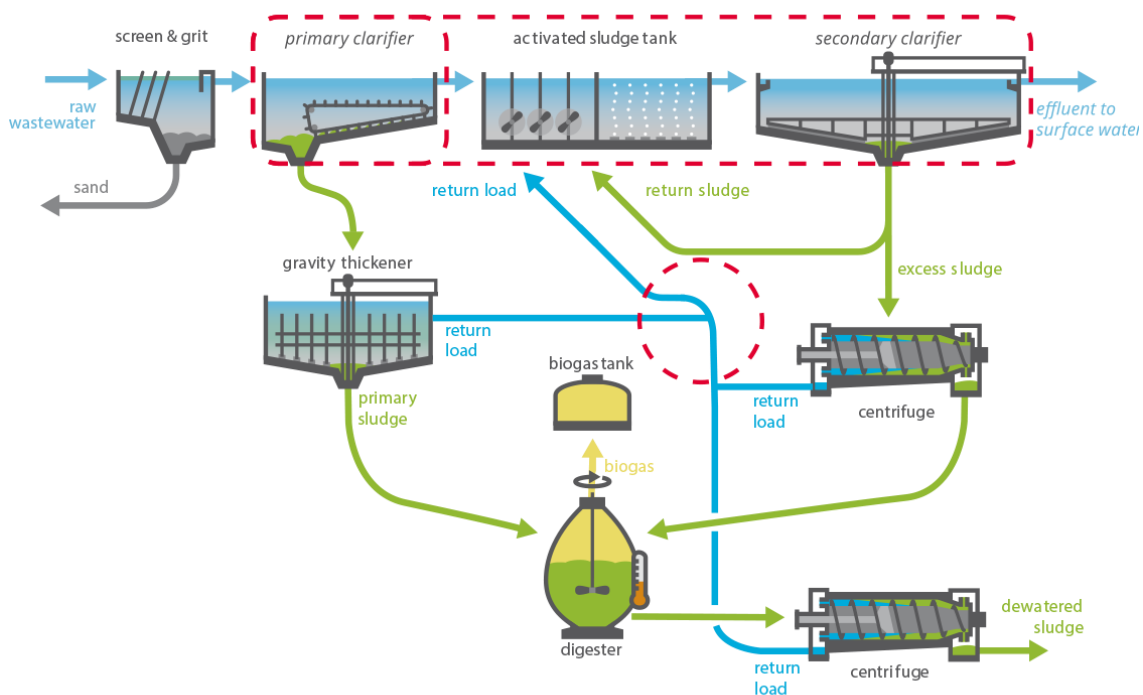
Figure 1.2.4 Schematic representation of Carbonera pilot plant (www.smart-plant.eu).

1.2.4   **Foods waste**

Food waste has been recognized as a global issue due to its environmental, economic, and social impacts with global consequences, requiring a change in political actions[50,51,3].

Food waste and losses mobilize a remarkable amount of natural resources. It consumes around 25% of all water used by agriculture each year, 23% of all cropland, equivalent to all cropland in Africa, while it generates around 8% of annual global greenhouse gases emissions [3,7,8].

In previous studies reported in literature[3,4,52,53], the amount of food wasted per capita by consumers in Europe and North America is 95-115 kg\year, while in Africa and Asia is only 6-11 kg\year. Indeed, Food Loss is equally serious in industrialized countries as in the developing one. The two terms "Food Waste" and "Food Loss" are usually used with the same intention, but the meanings are different. "Food Loss" refers to food lost in earlier stages of production (for instance during storage or transportations); "Food Waste" refers to items thrown away (usually by supermarkets or consumers).in the step of consumption.

The European Commission acknowledged the importance of foods loss and waste prevention and included it as a part of Circular Economy Package[8]. Foods loss and waste management within the Circular Economy framework represents a new stream of research oriented towards understanding food loss in the initial stages of supply chains[3,6]. To our best knowledge, to date, few studies focused on foods loss and waste according to the Circular Economy perspective. In recent years, various studies are focused on transforming food waste into energy and on implementing food sharing models to reduce the waste without defining an explicit Circular Economy framework.

In a recent study[6], the Italian company Barilla, one of the world's main pasta producer, provided its data to analyze pasta losses, waste and its causes along the entire life cycle, from field to table (Figure 1.2.4), showing that most of the waste and loss that occur in this supply chain could be reused or recycled under the Circular Economy perspective.

Total Food loss and waste per stage
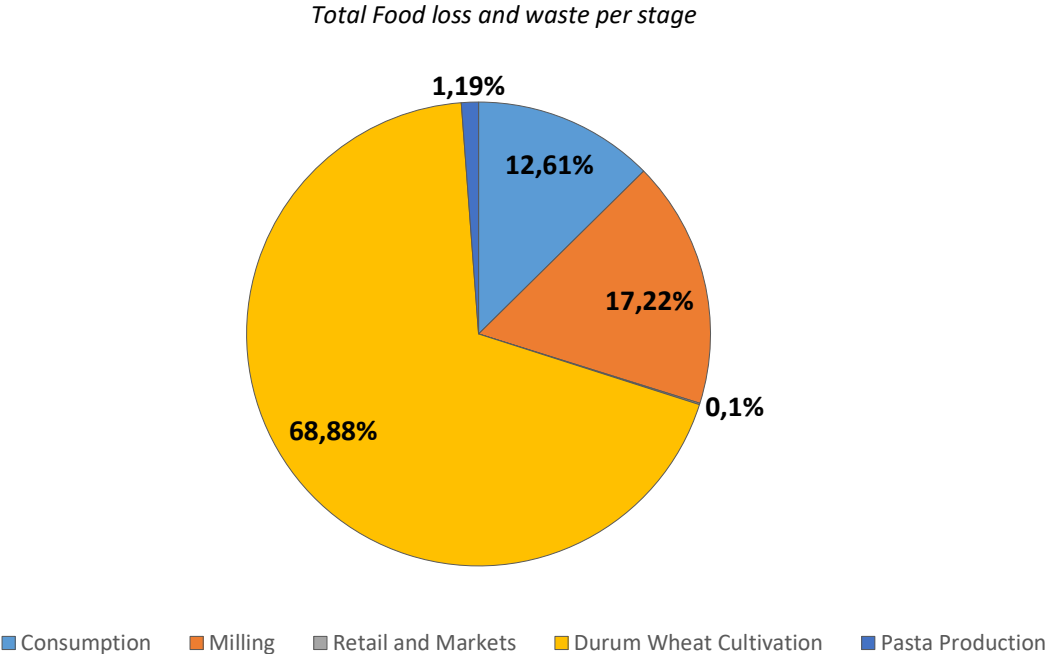
Figure 1.2.5 Total Food loss and waste per stage [6]

In this study, according to the Circular Economy perspective, waste management should not focus only on waste prevention but, since Food Loss and Waste are inevitable, also on the energy recovery, recycling and reusing in other materials.

The European Commission encourage all countries to a change their approach in production, consumption, processing, storage, recycling, and disposal of biological resources. In this light, developments in bio-economy research and innovation will improve the management of the biological resources.

Regarding the potentially marketable components present in foods wastes and co-products, the aim is to exploit high value components present in foods such as proteins, polysaccharides, fibers, flavor compounds, and phytochemicals as nutritionally and pharmacologically functional ingredients. This valorization can be achieved through the extraction of high-value components which can be recycled as nutritionally and pharmacologically functional ingredients, as fillers for composites, or can be chemically transformed to improve their qualities. The Waste Framework Directive (2008/98/EC) defines recycling and recovery: *"Recycling"* means any recovery operation by which waste "materials are reprocessed into products, materials or substances" whether for the original or other purposes. It includes the reprocessing of organic material but does not include energy recovery and the reprocessing into materials that are to be used as fuels or for backfilling operations. *"Recovery"* means any operation "the principal result of which

is waste" serving a useful purpose by replacing other materials which would otherwise have been used to fulfil a particular function, or waste being prepared to fulfil that function, in the plant or in the wider economy. The European Commission is also promoting the term *"Reuse"* which refers to using products more than once, for the same purpose. Reusing products is a good way to reduce the amount of waste generated, and ultimately landfilled.

The next chapters propose explorative applications for wastes derived from WWTPs and foods found in literature for industrial sectors such as air filtration systems for indoor environments, building construction and bioplastic processing.

1.2.4.1   *Starch*

Starch (Figure 1.2.6) is the most significant form of carbon reserve in plants in terms of amount, universality of its distribution among different plant species, and its commercial importance. Corn, tapioca, wheat, rice, and potato are some of the most consumed foods and just the most common sources of starch. According to an investigation of the Global Industry Analysis Inc[54], the global starch consumption reached 133.5 million metric tons in 2018, driven primarily by the diversity and sheer number of end-use applications in both food and non-food industries. The application of non-conventional raw materials as complementary sources provides a possible solution for the cost reduction of raw material in industries, besides offering new products with differentiated characteristics.

Starch extraction from roots and tubers uses grating with water and sieves to separate the starch slurry from residual mass. The starch is recovered by decantation or centrifugation; usually this type of extraction has a yield of around 60-70% in weight[55].
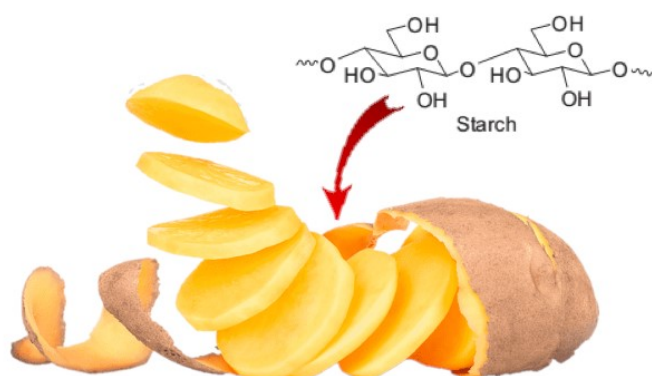
Figure 1.2.6 Starch source and chemical structure structure

The agro-food industry provides interesting opportunities for the application of this concept, due to the water consumption levels and wastes involved. Crispy chips are a

practical example: the general flow process includes potato discharge, washing, peeling, slicing, blanching, frying, quality control and packaging. For all these processes, food industries (as pasta or crispy chips producer) needs high water consumption, for washing, peeling, slicing, blanching or in mixing operations generated wastewaters and other wastes with high content in starch[56].

Many industries in the food production sectors are already recovering starch and other nutrients from their plants, permitting the valorisation of these secondary products in different fields[57–60].

1.3   **Objectives**

1.3.1   **New materials for old sectors**

In this thesis, different materials are presented, applicable in various sectors of industrial engineering. Cellulose, starch and polyhydroxyalkanoates have been studied and, if necessary, modified to be inserted within a specific industrial sector in order to transform waste into a resource and, when possible, suggest a possible change to reduce the environmental impact of some materials.

The industrial sectors suggested for the application of these new materials are some of the most common and impactful in the world of engineering: the building materials, the air treatment systems and lastly, the bioplastic extraction and processing sector.

1.3.1.1   *Building Materials*

Concrete is the fundamental materials for contemporary construction techniques. Since its invention (thousands of years ago) this material has undergone many technological developments, but it is still mainly used for its effective structural properties and for its ease of processing.

The *construction industry* represents the productive sector with the greatest number of human and technological resources employed and in which the highest number of raw materials are used[61]. Concrete, the most used material in construction, is the most employed human-made product in the world[62,63]

However, concrete and other cement-based composites are porous materials[64], and therefore they are subject to wear due to the infiltration of pathogens from the external environment. This requires constant and demanding maintenance work, aimed at preserving the functionality of the structure. For this reason, civil and infrastructural engineering are increasingly focusing on innovative control systems for reinforced concrete structures, that guarantee safety in their use and efficient operation[65]

In addition to improving durability, another goal that encourages the technological evolution of cement-based materials is the introduction of multiple functions in the same constructive element, in addition to the simple structural use. The needs of modern society have become more complex compared to the past, and a wide range of studies aims to improve the quality of life in buildings through the pollutant's removal and the enhancement of structural safety.

An interesting solution to these different problems is the production of innovative and multifunctional cement-based materials and mortars, characterized by different performance, thanks to the insertion of specific admixtures into the composites.

The present dissertation is integrated into this field of study, through the development of non-structural composites realized with the addition of cellulose fibers from different origins (pure cellulose, recycled cellulose and recovered cellulose fibers), in order to decrease the amount of binder in the mixture, but increasing the other performances (as insulation or indoor comfort). A significant increase in sustainability of mortars/concretes production can be achieved by replacing virgin raw materials with renewable and/or so-called ''waste ones''[66–68]. Although recovered cellulose fibers from other industrial activities are often used in the building engineering applications[69], the cellulose recovered from municipal wastewater have never been considered until now. The use of this recovered resource will be a relevant change not only from the economic but also environmental since cellulose coming from WWTPs can substitute virgin cellulose.

The effect of the addition of recovered cellulosic fibers at different percentages on the properties of hydraulic lime-based mortars is tested for non-structural applications. The properties of mortars that are manufactured with the same dosages of pure cellulose fibers and of recycled cellulose from newspapers are further compared. Finally, technical feasibility and economic considerations are discussed to promote the valorization of recovered cellulose and its economic assessment in the building sector.

1.3.1.2   *Air filtration sector*

Each year, more than 4 million people die early because of outdoor air pollution, according to the World Health Organization (WHO). The main culprits are fine particles with diameters of 2.5 micrometers or less (PM2.5) which can penetrate deep into the lungs, heart and bloodstream, causing diseases and cancer[60].

The mix and toxicity vary from place to place and over time: for example, in Asia, soot from residential heating and cooking is the biggest source of PM2.5 and VOCs. In European countries, Russia, Turkey, South Korea, Japan and the eastern United States, agricultural emissions such as ammonia are the leading source. Desert dust boosts air

pollution in northern Africa, the Middle East and central Asia. It is not clear which source is the most dangerous[61].

The association between various air pollutants (from SO_2 and PM 2.5-10 to NO_2) seems to support a negative effect not only on cardiovascular and respiratory health systems, but also as a mental wellbeing. In fact, the subjective perception of air pollution - that is the assessment of levels of air pollution made by individuals in their near environment - is also found to be associated with wellbeing. From smog hanging over cities to smoke inside the home, air pollution poses a major threat to health and climate. The combined effects of ambient (outdoor) and household air pollution cause about seven million premature deaths every year (Figure 1.3.2), as a result of increased mortality from stroke, heart disease, chronic obstructive pulmonary disease, lung cancer and acute respiratory infections[70,71,72].
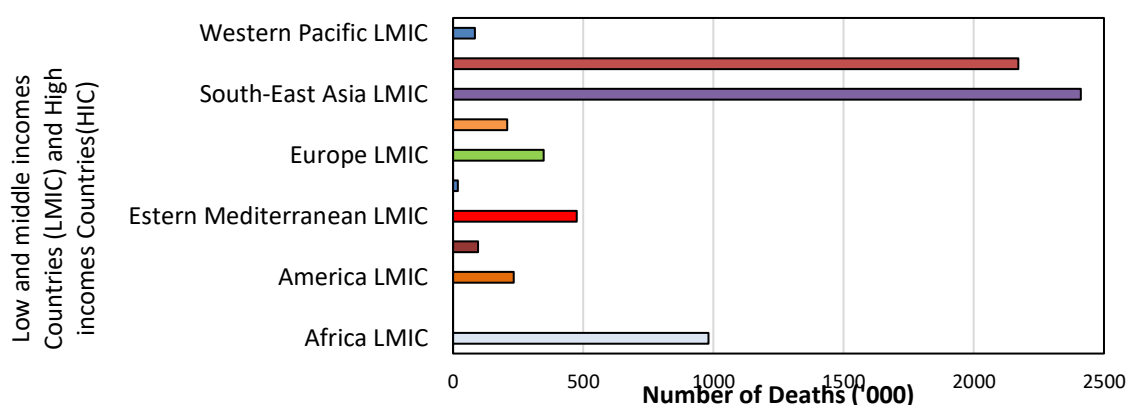
Figure 1.3.1 Total deaths attributable to the joint effects of household and ambient air pollution in 2016 by region and incomes countries (low and middle (LMIC) and high (HIC) [60]

More than 80% of people living in urban areas that monitor air pollution are exposed to air quality levels that exceed WHO guideline limits, with low- and middle-income countries suffering from the highest exposures, both indoors and outdoors[71,72].

Air filtration industry has evolved tremendously since the introduction of the first air filters in the 1930s. Now, with a variety of filtration technologies and styles to choose and industry standard criteria to judge filtration performance, filter media designed to maintain system cleanliness, improve indoor air quality, and reduce energy consumption simultaneously can be adopted. Attention to the entire lifecycle cost of filters, and not just their initial purchase price, is crucial.

In this dissertation a preliminary study of a new type of filter based on modified starch and polylactic acid polymer produced and characterized for the filtration of particulate matter (PM) and enhanced adsorption of Volatile Organic Compounds (VOCs) is reported. The study is based on the possibility of transforming starch in cyclodextrins[73–

[76] and on the application of cyclodextrins coming from wasted sources in air filtration system. The study is inspired by the possibility of transforming starch in cyclodextrins and on the application of cyclodextrins coming from wasted sources of starch in air filtration system. However, this study has been limited to the use of pure cyclodextrins for two reasons: the first one is to have a blank line and to understand if the project could it be applicable, avoiding uncertainties coming from secondary cyclodextrines; the second one is to optimize the project road map reserving the time required to prepare cyclodextrins coming from wasted starch sources only to further studies explicitly focused on the impact and efficiency of not pure cyclodextrins.

1.3.1.3   *Bioplastic extraction and processing*

At the moment the chemical industry is divided between continuing the production of traditional plastics, and developing a broad range of biodegradable and compostable plastics[77].

Today bioplastics have been considered as a better solution to the increasing demands for truly sustainable growth. In developing the new generation of plastic products made from renewable feedstock, the ability of biodegradability, compost-ability should be taken into account to evaluate the contributions to the environmental impacts of bioplastics[78,79] by Life Cycle Analysis (LCA).

Biopolymers are classified according to their source:

1. **Natural biopolymers**: These biopolymers are extracted from natural raw materials. The first type of biopolymer includes polysaccharide (starch, cellulose, alginate, carrageenan, and chitosan), protein (wheat gluten, soy protein, collagen, and gelatin), and lipids (waxes, glycerides)[78].

2. **Synthetic biodegradable polymer**: Polymers produced by chemical synthesis from biomass monomers, such as PLA. Others can be derived from petroleum resources; examples of petroleum-based biodegradable polymers include PCL and PVA[78].

3. **Produced by microorganisms**: Produced directly by natural or genetically modified microorganisms, such as polyhydroxyalkanoates (PHA), including poly-3-hydroxybutyrate (PHB) and poly-3-hydroxybutyrate-co-3-hydroxyvalerate (PHBV)[78].

Thanks to its characteristics (biodegradability, biocompatibility, chemical-diversity), PHA has attracted much commercial and research interests, especially for its manufacture from renewable carbon resources[41,42].

At present, PHA is not cost competitive compared to fossil-derived products. For this reason, in recent years, researchers are trying to reduce the cost of this biopolymer working on its production and extraction. For what concerns PHA production, as previously exposed in section 1.2.1.2, it is possible to produce it using microorganism present in WWTPs, which make the entire process extremely relevant. Nevertheless, regarding the extraction process, the cost is still too high because of the difficulties on the recovery and on the purification process.

This dissertation proposes different pre-treatment (physical and chemical) and different extraction techniques (conventional, in continuous and in more extreme conditions) to estimate their influence in the recovery. This aspect is studied not only in the perspective of yield, but also analyzing the performances of the extracted product. Moreover, PHA coming from two types of biomasses: one comes from wastewater sludge (mixed culture) and another from a selected culture composed by purple phototrophic bacteria (PPB) is also presented.

Lastly, being the WPCs' market in growing, the realization of composites made with the addition of wood flour, macadamia shell and coffee grounds (coming from common wastes of Australian industries) to PHA have been realized and presented. These composites are manufactured with two of the commonest techniques in polymer processing: extrusion and compression moulding.

1.4   Research methods

Given the vastness of the studied materials and the different fields of application, to base the research method directly on the single studied material is necessary. This choice allows not only to model the research method on the chosen material, but also to identify the field of the possible applicability based on the characteristics of the material, thus facilitating the process of "transformation" of the secondary product from waste to resource.

The research method has been modelled in two parts: the initial phase involves the preliminary study of the material and its origin, researching in literature how this is usually present and where it is normally expected. The chemical-physical characteristics have been analysed and the standards regulating the various applications proposed are therefore sought. Furthermore, an important part of the research is dedicated to the study of the fundamental properties of polymers, in order to evaluate their potential use and behaviors in multifunctional materials.

In each chapter of this dissertation, a secondary product will be presented with:

- an introduction with the state of the art of the single material and the possible applications,
- the methods used for its characterization
- the discussion of test results
- the conclusions of the work, resuming the key points and the limits of the study.

2.Chapter

Fundamentals of Polymer Science and Processing

Fundamentals of polymers chemistry and polymer processing to understand and correlate their structure with their chemical-physical properties and applications.

2.1   **Introduction**

The continuous development of the modern process industries gives great importance to the properties of materials, including many new chemical substances whose physical properties have never been measured experimentally. This is especially true for polymeric substances. The design of manufacturing and processing equipment requires considerable knowledge of the processed materials and related compounds. Also for the application and final use of these materials this knowledge is essential.

The major aim of the present chapter is twofold:

1. To correlate the properties of known polymers with their chemical structure, establishing structure–properties relationships.

2. Introduce two of the main techniques for the processing of polymers in industries, presenting the different variables that may influence the final product[80–83].

Macromolecules are giant molecules in which more atoms are linked together by covalent bonds. They may be linear, as branched chains or as three-dimensional networks.

There are thousands of chemical compounds of interest in science and practice; however, the number of structural and functional groups, which constitute all these compounds, is much smaller.

Physical property of a compound is determined by a sum of contributions made by the structural and functional groups in the molecule. These group contributions are often called *increments*. Such a group contribution is necessarily an approximation, because it is not necessarily the same in another environment. The fundamental assumption of the group-contribution technique is *additivity*. This assumption is valid only when the influence of any one group in a molecule or in a structural unit of a polymer is not affected by the nature of the other groups.

In this chapter, basic concepts of polymer chemistry will be introduced, presenting the typologies of polymers and their characteristics. Successively, the attention will be focused on the thermophysical and thermochemical properties[80]. In the last part of the chapter the polymer processing parameters will be analyzed, and the two processing methods used in this dissertation (extrusion and compression moulding) will be presented in order to describe all the variables considered during the studies presented in Chapters 6 and 7.

2.2   **Basic concepts of polymer chemistry**

Macromolecules ad *polymers* may be linear, slightly branched, or highly interconnected. In the latter case the structure develops into a large three-dimensional network.

The small molecules used as the basic building blocks for these large molecules are known as *monomers.*

The size of a polymer molecule may be defined either by its *mass* or by the number of repeat units in the molecule. This latter indicator of size is called the ***degree of polymerization*** (DP or DPI). The relative molar mass of a polymer is thus the product of the relative molar mass of the repeat unit and the DP.

Usually, molecules of relative molar mass of at least 1000 or a DP of at least 100 are considered to fall into the domain of polymer chemistry. The vast majority of polymers in commercial use are organic in nature, that is they are based on covalent compounds of carbon. The other elements involved include hydrogen, oxygen, chlorine, fluorine, phosphorus, and sulfur.

Polymer molecules are also subjected to various secondary intermolecular forces such as *dipole forces* between oppositely charged ends of polar bonds and *dispersion forces,* which arise due to perturbations of the electron clouds about individual atoms within the polymer molecule. *Hydrogen bonding*, which arises from the particularly intense dipoles associated with hydrogen atoms attached to electronegative elements such as oxygen or nitrogen, is important in certain polymers, notably proteins. Hydrogen bonds have the effect of fixing the molecule in a particular orientation[83].

In polymer science is essential to understand the chemical structure of a compound to predict its behavior in certain conditions. For this propose, the study of the polymer starts from the monomers that form the molecule.

The first step in this analysis is the check of the basic units: if the they are identical, it is *homo-polymer*; if there are more kinds of basic units (e.g. two or three) it is a *copolymer*. In that case the composition of the macro- molecule may vary from ordered repetition to random distribution.

In essence, there are only two really fundamental characteristics of polymers: their chemical structure and their molar mass distribution pattern.

The chemical structure (CS) of a polymer comprises:

1. The nature of the repeating units

2. The nature of the end groups

3. The composition of possible branches and cross links

4. The nature of defects in the structural sequence

The molecular weight distribution (MWD) or molar mass distribution (MMD) informs us about the average molecular size and describes how regular (or irregular) the molecular size is.

CS and MMD are two fundamental characteristics that determine all the properties of the polymer. In a direct way they determine the cohesive forces, the packing density (and potential crystallinity) and the molecular mobility (with phase transitions). In a more indirect way, they control the morphology and the relaxation phenomena, i.e. the total behavior of the polymer[80].

In all the molecules atoms arranges in different way, so in polymer chemistry geometrical arrangements of chains can be discerned in two categories[83]:

a. Arrangements fixed by the chemical bonding, known as *configuration*s. The configuration of a chain cannot be altered unless chemical bonds are broken or reformed (cis- and trans-isomers for example).

b. Arrangements arising from rotation about single bonds, known as *conformations*.

These concepts are fundamental in the physical state of a material: in fact, in dilute solutions the molecules are in continuous motion and assume different conformations in rapid succession; in the solid state, many polymers have typical conformations, such as folded chains and helical structures.

The precise arrangement of these asymmetric carbons gives rise to three different possible stereochemical arrangements. Firstly, when all asymmetric carbon atoms adopt identical configurations, the resulting polymer is *isotactic*. Secondly, if the arrangement of asymmetric carbon atoms is regularly alternated, the polymer is *syndiotactic*. Lastly, where a no regular structure is known as *atactic*.

All these configurations are represented in Figure 2.2.1[80].
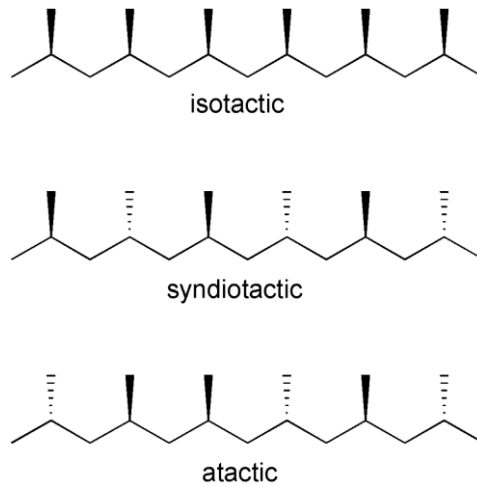
Figure 2.2.1 Representation of isotactic, syndiotactic and atactic configurations[83]

2.2.1   **Polymer Structure**

The polymer molecule consists of a "skeleton", which may be a linear or branched chain or a network structure, and peripheral atoms or atom groups. Polymers of a finite size contain *end groups*, which do not form part of the repeating structure.

Usually they do not affect the physical properties, but they can be determinant for the chemical ones.

2.2.1.1   *Structural Groups*

Every polymer structure can be considered as a summation of structural groups. A long chain may consist mainly of bivalent groups, but any bivalent group may also be replaced by a trivalent or tetravalent group and so on[80–83]. Some of the main structural groups are reported in Figure 2.2.2.
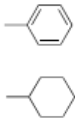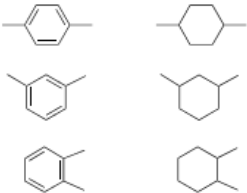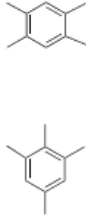
Groups	Monovalent	Bivalent		Trivalent	Tetravalent
1. Hydrocarbon groups	$-CH_3$	$-CH_2-$		$>C-$	$>C<$
	$-CH=CH_2$	$-CH=CH-$		$>CH=C-$	$>C=C<$
2. Non-hydrocarbon groups	$-OH$	$-O-$			
	$-SH$	$-S-$			
	$-NH_2$	$-NH-$			
	$-F$	$\overset{O}{\underset{\parallel}{-C-}}$		$-N<$	$>Si<$
	$-Cl$				
	$-Br$	$-\overset{O}{\underset{O}{\overset{\parallel}{\underset{\parallel}{S}}}}-$			
	$-I$				
	$-C\equiv N$				

Figure 2.2.2 Main structural groups[83]

2.2.1.2   *Chains*

Linear chain polymers can be distinguished into two main classes:

1. *Homochain polymers*, containing only carbon atoms in the main chain. These polymers are normally prepared by addition or chain-reaction polymerization.

2. *Heterochain polymers*, which may have other atoms (originating in the monomer functional groups) as part of the chain.

Stereoregularity plays a very important role in the structure of polymers, especially on proteins, nucleic acids and other substances of biological importance. Stereoregularity is the essential requirement for crystallinity in polymers and it is strictly related to structure composition: for example, in general atactic polymers cannot crystallize, but if the pending group is only small, like OH in polyvinyl alcohol, crystallization is possible.

Crystalline regions are formed from the stereoregular components of the macromolecules, which, given the nature of the polymerization processes from which the macromolecules are built up, represent only a proportion of the overall material. It is often possible that an essentially isotactic polymer will contain a syndiotactic segment and vice versa. Chain branching may also occur, thereby reducing local regularity in structure and inhibiting

crystallization. Occasionally co-polymerization is the reason for the co-existence of the amorphous regions with the crystalline phases.

So, the organization and the composition of chains are determinant for the polymer structure and properties because they influence the behavior of the polymer[80–83].

2.2.1.3   *Co-polymers*

As previously exposed, the presence of two or three different monomers is named *copolymer*. Copolymers can be distinguished into alternating-, random-, graft-, and block copolymers (Figure 2.2.3).

Shortly*, alternating copolymers* may be considered as homo-polymers with a structural unit composed of two different monomers; r*andom copolymers* are obtained from two or more monomers, which are present simultaneously in one polymerization reactor. In *graft polymerization* a homopolymer is prepared first and in a second step one or two monomers are grafted onto this polymer; the final product consists of a polymeric backbone with side branches. In *block copolymerization* one monomer is polymerized, after which another monomer is polymerized on to the living ends of the polymeric chains; the final block copolymer is a linear chain with a sequence of different segments.

Alternating Copolymers   *Graft Copolymers*

                                          A
                                          |
-A-B-A-B-A-B-A-   -B-B-B-B-B-B-B-B
                                          |
                                          A
                                          |
                                          A

Random Copolymers   *Block Copolymers*

-A-A-A-B-A-B-B-   -A-A-A-A-B-B-B-B
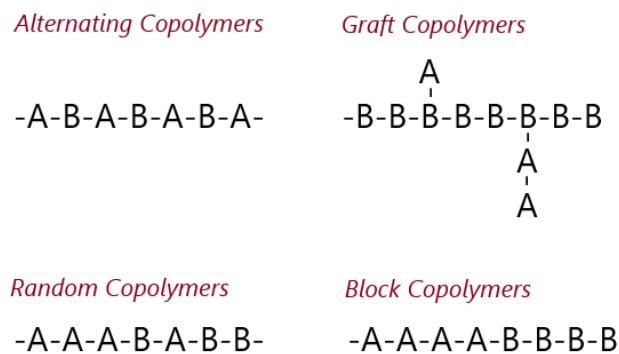
Figure 2.2.3 General copolymer structures

Polymers obtained by condensation polymerisation of purely bifunctional monomers, must be linear. The chains produced in addition polymerisations may have a number of short or long branches randomly attached along their axes: branching affects the properties of a polymer in the molten state and in solution[83].

2.2.2   **Polymer Crystallinity**

The polymeric chains are found in two forms: *Lamellar* crystalline form in which the chains fold and make lamellar structure arranged in the regular manner and *amorphous*

form in which the chains are in the irregular manner. The lamellae are embedded in the amorphous part and can communicate with other lamellae via tie molecules. Polymer may be amorphous or semi-crystalline in nature.

The percentage of crystallinity is given by Equation 1:

$$\% \ Cristallinity = \frac{\rho c(\rho s - \rho a)}{\rho s(\rho c - \rho a)} \cdot 100 \ ...... \qquad ....(\text{Equation 1})$$

Where **ρc** is the density of the completely crystalline polymer, **ρa** is the density of the completely amorphous polymer and **ρs** is the density of the sample[80].

Figure 2.2.4 reports the three possible structures in polymers, whom identify different grades of crystallinity.

Amorphous   Semi-cystalline   Crystalline
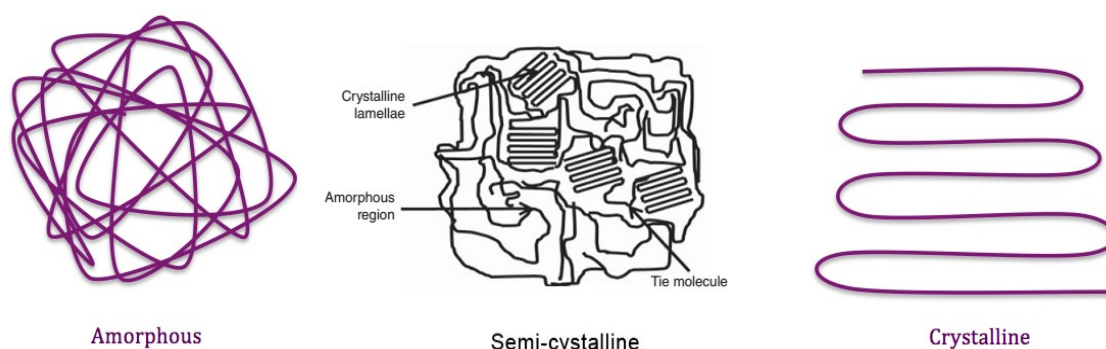
Figure 2.2.4 Schematic representation of amorphous, semi-crystalline and crystalline structures

A typical range of crystallinity can be defined as amorphous (0%) to highly crystalline (>90%). The polymers having simple structural chains as linear chains and slow cooling rate will result in good crystallinity.

In slow cooling, sufficient time is available for crystallization to take place. Polymers with high degree of crystallinity are rigid with high melting point, but their impact resistance is low. Amorphous polymers are soft with lower melting points. A solvent can penetrate the amorphous part more easily than the crystalline part.

When the molten polymer is cooled down, the crystalline lamellae grow in radial direction from a nucleus along the three dimensions leading to a spherical structure called spherulite (Figure 2.2.5). Spherulites diameter depends on various parameters such as

the number of nucleation sites, polymer molecule structure and rate of cooling. Due to highly ordered lamellae, the spherulite shows higher density, hardness, tensile strength, and Young's modulus. The elasticity and impact resistance are shown, because the lamellae are connected to amorphous regions[77,84,85].
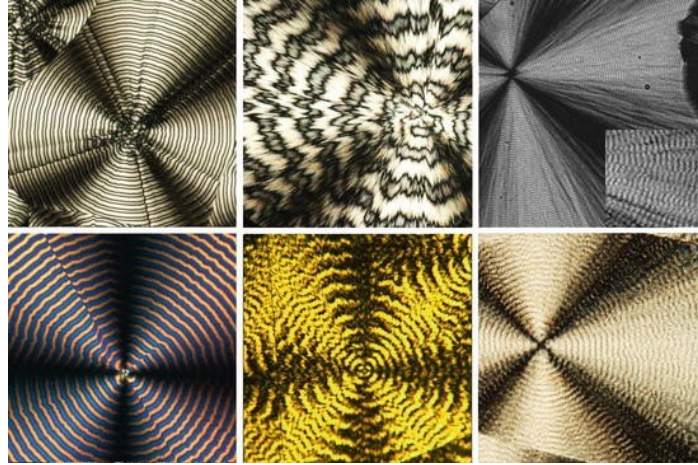
Figure 2.2.5 Spherulites analysed with SEM [84,85]

It is now generally accepted that the morphology of a polymer depends on the contributions of three different macro-conformations: (a) the random coil or irregularly folded molecule as found in the glassy state, (b) the folded chain, as found in lamellar structures and (c) the extended chain.

A semi-crystalline polymer exhibits a different structure: crystalline regions disturb the amorphous phase and reduce its segmental mobility. This reduction is at its maximum in the immediate vicinity of the crystallites; at large distances from the crystallites the properties of the amorphous phase become equal to those of the bulk amorphous material. The main consequence of this reduced mobility is an extension of the glass transition region towards the high temperature side. In terms of properties, semi-crystalline thermoplastics have good strength, and good chemical resistance, but they typically lack in impact resistance[80,81,83,86,87].

2.2.3   Polymer Classification

The most usual method for polymers classification considers their response to a thermal treatment dividing them into thermoplastics, thermosets and elastomers.

Thermoplastics are polymers which melt when heated and re-solidify when cooled; *Thermosets* are polymers which do not melt when heated but, at sufficiently high temperatures, decompose irreversibly.

Elastomers are polymeric materials whose dimensions can vary enormously under stress conditions and then return to their original values (or almost) when the stress is interrupted. Elastomers are usually thermosets (requiring vulcanization) but may also be thermoplastic (such as polyolefins or co-polymers of styrene and butadiene).

There is a useful chemical distinction between the two groups (thermoplastics and thermosets), with the elastomers that have properties of both two main groups[80,81,83,86,87].

2.2.3.1   *Thermoplastic polymers*

Most thermoplastic polymers are used in high-volume, widely recognized applications, and are often called commodity plastics.

The most common commodity thermoplastics are polyethylene (PE), polypropylene (PP), polyvinyl chloride (PVC) and polystyrene (PS). These thermoplastics have in common the general repeat unit $-(CHX-CH_2)-$, where $-X$ is $-H$ for PE, $-CH_3$ for PP, $-Cl$ for PVC, and a benzene ring for PS. In their simplest forms, the thermoplastics are linear, carbon chain polymers. There are methods for creating branches, especially in polyethylene, while still maintaining thermo-plasticity. Increased branching tends to decrease the density, melting point, and certain mechanical properties of the polymer, but increases transparency and impact toughness[83].

2.2.3.2   *Thermoset polymers*

There are many important examples of thermoset polymers, sometimes referred to as resins. The thermoplastic PE can be treated by electron radiation or chemical means to form chemical bonds between adjacent chains called crosslinks. In this process, some of the carbon–hydrogen or carbon–carbon bonds in the linear chain are broken, forming bridges between the chains. The result is that unlike linear PE, crosslinked PE has no distinct melting point due to limited chain mobility and degrade upon heating. This is a common characteristic of thermoset polymers. Due to their three-dimensional structure, they cannot be reshaped upon heating. Instead, they tend to remain rigid, or soften only slightly, until the backbone begins to break, leading to polymer degradation. Generally, thermosets are stiffer than thermoplastics. In fact, the crosslinks tend to increase the long-term thermal and dimensional stability of the polymer, such that thermosets find wide use in very large and complex parts where thermal stability is important. The chemical structures of thermosets are generally much more diverse than the commodity thermoplastics [83]. The most common types of thermosets are the epoxies (EP), polyurethanes (PU), and polyimides (PI).

2.2.3.3   *Elastomers*

A related, yet distinctly different, class of crosslinked polymers are the *Elastomers.*

Though they are structurally different than the thermosets, they are usually included in thermosets because they tend to decompose when heated, rather than flow. The presence of crosslinks in some polymers allows them to be stretched, or elongated, by large amounts[83]. Polymers that have more than 200% elastic elongation (three times the original length) and can be returned to their original form are termed elastomers. They are like thermoplastics in that they readily elongate, but the presence of crosslinks limits the elongation prior to breakage and allows the polymer to return to its original shape. Natural rubber is an important elastomer. Crosslinks are added to an emulsion of rubber, called latex, through the addition of heat and sulphur. The sulphur creates chemical bonds between the rubber chains in a process known as vulcanization. Other common elastomers are polyisoprene, butadiene rubber and silicones[80].

2.2.4   **Mechanical Properties**

It is of great importance to be familiar with some basic mechanical properties of the material before its application in any field, such as how much it can be stretched, how much it can be bent, how hard or soft it is, how it behaves on the application of repeated load and so on.

2.2.4.1   *Strength*

In simple words, the strength is the stress required to break the sample. There are several types of strength, namely tensile (stretching of the polymer), compressive (compressing the polymer), flexural (bending of the polymer), torsional (twisting of the polymer), impact (hammering) and so on. The polymers follow the following order of increasing strength*: linear < branched < cross-linked < network[86].*

Factors Affecting the Strength of Polymers

1.   Molecular Weight (Mw): The tensile strength of the polymer rises with the increase in molecular weight and reaches the saturation level at some value of the molecular weight. At lower molecular weight, the polymer chains are loosely bonded by weak van der Waals forces and the chains can move easily, responsible for low strength, although crystallinity is present. In case of large molecular weight polymer, the chains become large and hence are entangled, giving strength to the polymer.
2.   Cross-linking: The cross-linking restricts the motion of the chains and increases the strength of the polymer.

3.   Crystallinity: The crystallinity of the polymer increases strength, because in the crystalline phase, the intermolecular bonding is more significant. Hence, the polymer deformation can result in the higher strength leading to oriented chains[86],[80].

2.2.4.2   *Percent Elongation to Break*

It measures the percentage change in the length of the material before fracture (Figure 2.2.6). It is a measure of ductility. Thermoplastic have a very high value of elongation to break (>100%), whereas thermosets have a very low one (<5%)[86,80,83].

Figure 2.2.6 Elongation to break the polymer[86].

2.2.4.3   *Young's Modulus*

Young's Modulus or Tensile Modulus is the ratio of stress to the strain in the linear elastic region (Figure 2.2.7). It is a measure of the stiffness of the material[86].

$$E = \frac{\sigma}{\varepsilon}$$
(Equation 2)

Where σ is the tensile stress and ε is the tensile strain.
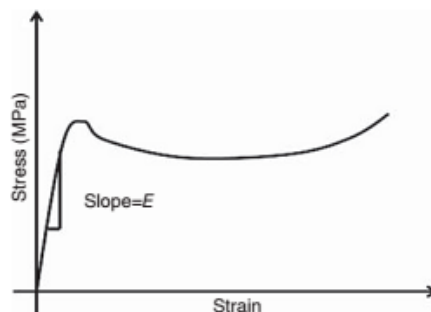
Figure 2.2.7 Young's Modulus of a polymer[86]

2.2.4.4   *Toughness*

The toughness of a material is given by the area under a stress–strain curve and it indicates the energy absorbed by the material before it breaks. A typical stress–strain curve is shown in Figure 2.2.8, which compares the stress–strain behaviour of different types of materials[86,80,83].

Rigid polymers possess high Young's modulus (such as brittle polymers), ductile polymers can possess similar elastic modulus, but with higher fracture toughness. Elastomers have low values of Young's modulus and are rubbery in nature. The yield strength of the plastic polymer is the stress where the elastic region (linear portion of the curve) ends (Figure 2.2.8). The tensile strength is the stress corresponding to the fracture of the polymer. The tensile strength may be higher or lower than the yield strength (Figure 2.2.8a). The mechanical properties of the polymer are strongly affected by the temperature. A typical plot of stress versus strain is shown in Figure 2.2.8b. From the plot, it is clear that with the increase in temperature, the elastic modulus and tensile strength are decreased, but the ductility is enhanced[86].

(a)   *(b)*
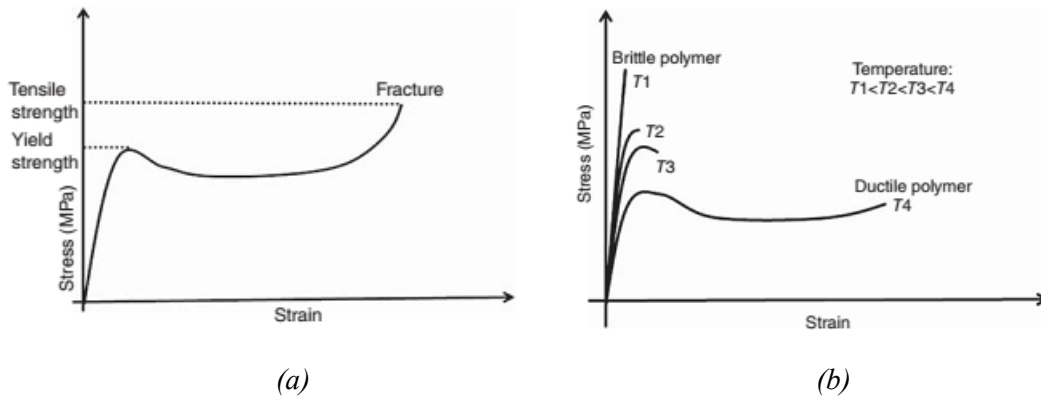
Figure 2.2.8 a) Yield strength and Tensile strength of polymers; b) Effect of temperature on the mechanical performances of polymers[86].

2.2.4.5   *Viscoelasticity*

There are two types of deformations: elastic and viscous. In the elastic deformation, the strain is generated when the constant load (or stress) is applied, and this strain is maintained until the stress is not released. On removal of the stress, the material recovers its original dimensions completely, that is the deformation is reversible[86].

In viscous deformation, the strain generated is not instantaneous but time dependent. The strain keeps on increasing with time when a constant load is applied; when the load is

removed, the material does not return to its original dimensions completely, causing an irreversible deformation.

2.2.5   **Thermal Behaviour**

The study of a polymer can not be complete without a deep analysis of its behaviour under the temperature change. The effect of temperature on a polymer can have a determinant impact on its structure, and this kind of analysis permits to extrapolate many information about the structure (and the nature) of the polymer.

Three factors affect the essential nature of a polymeric material and determine whether it is glassy, rubbery, or fibre-forming under a given set of conditions: the flexibility of the macromolecule, the magnitude of the forces between the molecules, and the stereoregularity of the macromolecules. It is possible to shortly describe the *glassy state* as a sort of "frozen state" where the molecules can vibrate slightly but are not able to move significantly in the amorphous region of the polymer at lower temperature. In this state, the polymer is brittle, hard and rigid analogous to glass[86,80,83].

When the polymer is heated, the polymer chains are able to wiggle around each other, and the polymer becomes soft and flexible similar to rubber. This state is called the *rubbery state*.

The temperature at which the glassy state makes a transition to rubbery state is called the *glass transition temperature* (Tg). Note that the glass transition occurs only in the amorphous region, and the crystalline region remains unaffected in the semi-crystalline polymer. While Tg is the property of the amorphous region of the polymer, the crystalline region is characterized by the melting point[86] (Tm).

The three main temperatures to consider in the study of thermal properties of polymers are the *glass transition temperature* (**Tg**), the *melting temperature* (**Tm**), also known as transition temperatures; and the *degradation temperature* (**Td**), which indicates a range of temperature where the molecule starts to degrade. Before to describe all these temperatures and their variation basing on the polymer structure, it is essential to introduce the particular case of semi-crystalline polymers.

As previously reported, semi-crystalline polymers have both amorphous and crystalline regions: this means that the study of thermal properties can be more problematic, because these polymers will show the transition corresponding to both of the regions. Thus, the semi-crystalline polymers have true melting temperatures (Tm) at which the ordered phase turns to disordered phase, whereas the amorphous regions soften over a temperature range known as the glass transition (Tg)[80,83].

Factors affecting transition temperatures

The Tg is the property of the amorphous region of the polymer, whereas the crystalline region is characterized by Tm. In thermodynamics, the transitions are described as first and second order transitions. The value of Tg is not unique because the glassy state is not in equilibrium. Tg is a second order transition, whereas Tm is a first order transition.

Transition temperatures are extremely structure-sensitive, partly due to steric effects, partly due to intra- and inter-molecular interactions.

The value of Tg depends on several factors such as molecular weight, measurement method, and the rate of heating or cooling[80,83]. The Tg depends on the mobility and flexibility of the polymeric chains. If the polymeric chains can move easily, then the glassy state can be converted to the rubbery state at lower temperature, that is, Tg is lower. If somehow the mobility of the chains is restricted, then the glassy state is more stable, and it is difficult to break the restriction causing the immobility of the polymer chains at the lower temperature, because more energy is required to make the chains free.

The usual factors that influence Tg are summarized in:

1.   **Intermolecular Forces**. Strong intermolecular forces cause higher Tg.

2.   **Chain Stiffness.** The presence of the stiffening groups (such as amide, sulfone, carbonyl, p-phenylene etc.) in the polymer chain reduces the flexibility of the chain, leading to higher Tg.

3.   **Cross-Linking.** The cross-links between chains restrict rotational motion and raise Tg. Hence, higher cross-linked molecule will show higher Tg than that with lower cross-linked molecule.

4.   **Pendant groups.** The presence of pendent group can change Tg. Bulky pendant groups as a benzene ring, can restrict rotational freedom, leading to higher Tg. Flexible pendant groups as aliphatic chains, limits the packing of the chains and hence increases the rotational motion, tending to less Tg value.

5.   **Plasticizers.** Plasticizers increase chain flexibility and reduce the intermolecular cohesive forces between the polymer chains, which in turn decrease Tg.

6.   **Molecular Weight.** Tg is increased with the molecular weight. The molecular weight is related to Tg by the Fox–Flory Equation (Equation 3):

$$Tg = T_{g, \infty} - \frac{K}{Mn} \qquad\qquad \text{(Equation 3)}$$

where Tg, is the glass transition temperature at the molecular weight of infinity, and K is the empirical parameter called Fox–Flory parameter related to the free volume inside the polymer. It is observed that Tg is increased up to the molecular weight of approximately 20 000, but after this limit, Tg is not affected appreciably[80,83].

Also Tm is strictly related to the chemical structure of the material. In fact, non-structural-groups present on the chains of the polymer are determinant for the change in Tm.

Tm is increased if double bonds, aromatic groups, bulky or large side groups are present in the polymer chain, because they restrict the flexibility of the chain. The branching of chains causes the reduction of Tm, as defects are produced because of the branching.

2.2.5.1 *Decomposition Temperature*

Polymer degradation is a change in the properties – tensile strength, colour, shape, etc. – of a polymer under the influence of one or more environmental factors such as heat, light or chemicals. The way in which a polymer degrades under the influence of thermal energy in a certain atmosphere is determined by the chemical structure of the polymer itself and by the presence of traces of unstable structures (impurities or additions)[80,83].

Thermal degradation does not occur until the temperature is so high that primary chemical bonds are separated. It begins typically at temperatures around 150–200 °C and the rate of degradation increases as the temperature increases.

For many polymers thermal degradation is characterised by the breaking of the weakest bond and is consequently determined by a bond dissociation energy[80].

The process of thermal decomposition is characterised by a number of experimental indicators[80]:

a. **The temperature of initial decomposition (Td_0).** Temperature at which the loss of weight during heating is just measurable (inclination point of the loss of weight/ temperature curve).

b. **The temperature of half decomposition ($Td_{1/2}$).** Temperature at which the loss of weight (at a constant rate of temperature rise) reaches 50% of its final value.

c. **The temperature of the maximum rate of decomposition (Td_{max})**, it corresponds to the inflection point (at a standardised rate of temperature rise) of the weight loss curve .

d.   The amount of residue char in the case of pyrolysis (normally around 900°C).

The types of polymer degradation can be divided into three general categories: *chain depolymerisation, random scission* and *substituent reactions.*

Chain depolymerisation is the successive release of monomer units from a chain end or at a weak link, which is essentially the reverse of chain polymerisation This depolymerisation begins at the ceiling temperature. A "weak link" may be a chain defect, such as an initiator fragment, a peroxide or an ether linkage arising as impurities.

This depolymerisation is characterised by a) the major product is monomer, b) the decrease of degree of polymerisation is initially negligible, and accordingly the mechanical properties do not deteriorate fast and c) the rate of depolymerisation gradually decreases[80].

Random degradation occurs by chain rupture at random points along the chain, giving a disperse mixture of fragments which are usually large compared with the monomer unit. Random scission is characterised by a) the major products are typically fragments with molecular weights up to several hundreds (monomers, dimers, trimers, etc.), b) the decrease of molecular weight is initially appreciable, and accordingly the mechanical properties deteriorate rather fast and c) the rate of degradation is initially rapid and approaches a maximum[80].

Degradation by substituent reactions occurs by modification or elimination of substituents attached to the polymer backbone. This type of polymer undergoes degradation reactions in oxygen free circumstances, e.g. during extrusion, at processing temperatures of 200 °C[80].

Tg, Tm and Td are fundamental not only for the study of materials performances, but also to determine the range of processability of those materials. From the thermal study, in fact, the manufactory process and conditions[80] are decided.

2.3   Polymer Processing

Polymer processing is commonly defined as the activity performed on polymeric materials to increase their usefulness. It involves not only the shaping but also the synthesis, transformation, compounding, functionalization, and stabilization of materials.

This part of the chapter introduces the relevant characteristics about morphology of polymer structures and its influence on their physical behaviour; analysing the relationship between processing routes and the rheology of polymers, also with some aspects of heat transfer. The aim of this part is to relate the behaviour of these materials to their process in a simple manner. Successively, the processing methods (extrusion and compression moulding) examined in this study will be described after an overall presentation of the physical basis of polymer processing.

2.3.1   The physical basis of polymer processing

As already described in Section 2.2.3, thermoplastics and thermosets have very different behaviour under thermal conditions which influence their physical properties. In fact, the thermosetting processes is characterized by irreversible chemical change, after shaping, in the solidification stage. In practice, the whole process, for resins or rubber products for example, is carried out in a mould, to give a shaped and solidified product at the end. Usually, the chemical hardening is caused by the formation of chemical cross-links between the polymer chains and it depends on additives to promote the development of these cross-links[85,88,89,86].

The liquid stage is a polymer melt and this implies a high temperature process. The solidification stage is simply to cool/freeze the shaped melt. These are the thermoplastic processes, which are characterized by reversibility of the solid-liquid transition. There are also some important consequences of this reversibility: there is a ceiling temperature for the product in service, which is that at which the materials begin to soften again[88].

Table 2.3-1 compares thermoplastic and thermosets materials basing on materials properties and their rheology.

Table 2.3-1 Comparison of thermoplastics and thermosets[88]

Thermoplastic	Thermosets
Use melt in liquid shaping stage	Use lower Mw liquid or rubbery polymers at shaping stage
Harden by freezing the melt	Harden by chemical reaction, often cross-linking of chains
Liquid-solid reversible	Liquid goes irreversibly to solid
Scrap recovery possible	Scrap cannot be recovered

Ceiling service temperature	Often can withstand high temperature
Processing of melt usually orientates polymer chains	Can be processed with low orientation

2.3.1.1   *Viscosity*

The viscosity of a fluid is a measure of its resistance to deformation at a given rate. For liquids, it corresponds to the informal concept of "thickness": viscosity is the material property which relates the viscous stresses in a material to the rate of change of a deformation (the shear rate). Although it applies to general flows, it is easy to visualize and define in a simple shearing flow, such as a planar Couette flow (Figure 2.3.1).

Consider two plates separated by a distance h and the space between them is occupied by a fluid. One plate moves to the other with a velocity (U). The movement is resisted by a viscous reaction of the fluid. Since the movement is in shear the reaction is the shear viscosity. The shear stress can be defined by the force (F) acting on the moving plate (its area A) and the shear rate is found from the velocity (U) relative to distance (L).
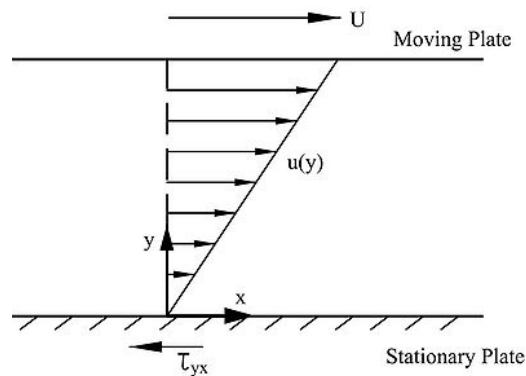
Figure 2.3.1 Couette flow representation

Shear stress $\qquad\qquad \tau = \dfrac{F}{A}$ $\qquad\qquad$ (Equation 4)

Shear rate $\qquad\qquad \gamma = \dfrac{U}{L}$ $\qquad\qquad$ (Equation 5)

The shear rate is a derivative, it is the rate of change velocity of the shearing fluid through the thickness. The velocity is maximum immediately adjacent to the moving plate and zero adjacent to the stationary plate.

From these equations is possible to obtain η, the coefficient of shear viscosity, which is proportionally constant between the shear stress and the shear rate.

$$\tau = \eta\gamma \qquad\qquad \text{(Equation 6)}$$

In polymer processing, viscosity is a parameter that must be considered because the value of the shear stress clearly depends on the rate of shear and the viscosity of the fluid. If the fluid is of low viscosity the shear stress needed to distort it will be small.

Most of the polymeric materials of practical use exhibit "viscoelastic" behaviour during flow, meaning that they exhibit not only viscous behaviour but also elastic (rubberlike) behaviour in the liquid state.

The viscosity of a polymer is proportional to its molecular weight (Mw) when it is lower than a certain critical value (Mc): the polymer having Mw ≤ Mc is referred to as "unentangled" polymer, and the polymer having Mw ≥ Mc is referred to as "entangled" polymer[88,82,87,90,91].

Before proceeding with the description of manufacturing processes it is important to remember that high rates of shear are not necessarily involved in high processing speeds. The shear rate γ is concerned with the rate of distortion of the fluid elements. The shear rate depends principally on the nature of shaping, fluid-distorting process, rather than the speed at which the process is run. Much less variation in γ will result from running the machinery slowly or fast. In Table 2.3-2 there are few examples of shear rates of processes [88,89].

Table 2.3-2 Shear rates of processes[85]

Process	Shear rate (s⁻¹)
Compression moulding	1-10
Calendering	10-100
Extrusion	100-1000
Injection moulding	$1000-10^5$
Reverse roll coting	3×10^3

Viscosity depends strongly on temperature. In liquids it usually decreases with increasing temperature, whereas in gases viscosity increases with increasing temperature.

According to the kinetic theory of gases, viscosity should be proportional to the square root of the absolute temperature, in practice, it increases more rapidly (Figure 2.3.2).

In a liquid molecular interchange are similar to those developed in a gas, but there are additional substantial attractive, cohesive forces between the molecules of a liquid (which are much closer together than those of a gas). Both cohesion and molecular interchange contribute to liquid viscosity. The impact of increasing the temperature of a liquid is to

reduce the cohesive forces while simultaneously increasing the rate of molecular interchange [84,87,88].

The former effect causes a decrease in the shear stress while the latter causes it to increase. The result is that liquids show a reduction in viscosity with increasing temperature. With high temperatures, viscosity increases in gases and decreases in liquids, the drag force will do the same.

The knowledge of solution or melt rheology of polymers is keystone information for the polymer processing industry. Understanding the solution rheology of polymers is a key factor in developing suitable models for the solution polymerization process[88].
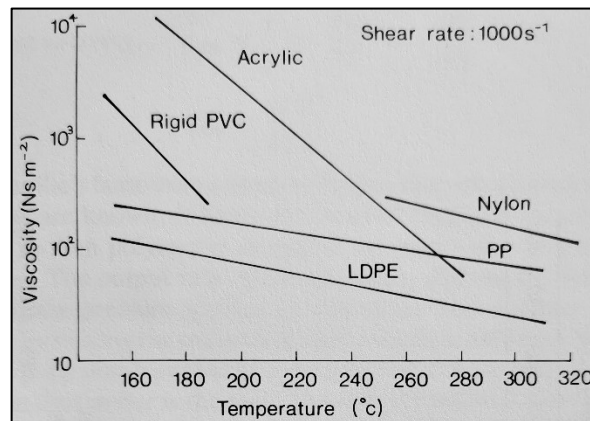
Figure 2.3.2 Effect of temperature on different polymer viscosity[88]

The significance of this appears in high shear rate process, such as injection moulding and extrusion, which are carried out at high temperatures.

Different polymers require different conditions for processing, and standard methods specify a driving weight and temperature for each polymer type. This classification is based on the melt flow index (MFI), the melting behaviour of the polymer class, the thermal capacities and solidification process.

The *MFI* is usually used to compare grades within a polymer type. The *melt flow rate* is an indirect measure of molecular weight, with high melt flow rate corresponding to low molecular weight. At the same time, melt flow rate is a measure of the ability of the material's melt to flow under pressure. It is inversely proportional to viscosity of the melt at the conditions of the test, though it should be borne in mind that the viscosity for any such material depends on the applied force.

The MFI must be treated with caution because it cannot be used to compare polymer types, thus MFI values for polyethylene cannot be compared for with those of polypropylene or polystyrene[88].

The originally solid polymer must be heated to above its melting or softening point: the heat for this propose comes from two sources. The first is the external heat supplied, for instance, by electrical resistance heater bands on the barrels of extruders and injection moulding machines or steam jacketing on internal mixers. The second source is heat generated by viscous dissipation in a highly viscous fluid being sheared at high shear rates. Many internal mixing processes use steam heating only for the first two or three batches and when the equipment is fully heated, require only the heat generated by working the polymer (as happens for the rubber mixing). The total energy to heat a polymer from a temperature to another can be found from its specific heat, latent heat of fusion and the weight produced. The energy derived from viscous dissipation can be found from the power consumption of the machine when loaded compared with its power consumption empty. The difference is due to the heater bands[88].

These differences in polymers are important in designing processes: the partially crystalline polymers have appreciable latent heats of fusion, which must be supplied during melting in addition to the heat needed simply to heat the mass of the polymer. The crystalline ones have values for latent heat with the result that these materials require greater heating than do the amorphous to raise their temperature from ambient to the appropriate processing temperature. Table 2.3-3 reports some examples of thermal properties of different polymers[88].

Table 2.3-3 Thermal properties of different polymers

Polymer	Specific heat ($kJkg^{-1}°C^{-1}$)	Melting latent heat ($kJkg^{-1}$)	Process temperature (°C)	Total heat to process ($kJkg^{-1}$)
Nylon 6.6	1.67	130	280	570
Polycarbonate	1.26	-	300	350
Polyethylene, HD	2.30	209	240	720
Polypropylene	1.93	100	250	550
Polystyrene	1.34	-	200	240

The next consideration is the various means of solidifying into the final form. Once again, there are two broad division; liquid systems, which solidify by chemical change, and thermoplastics, which solidify by freezing.

In *liquid systems* a wide variety of chemical reactions is employed. Often these reactions require elevated temperatures to proceed at a reasonable speed and heated plant is thus frequently to be found, as static or continuous processing ovens or hot press etc.

For example, liquid resins have chemical cross-linking, so the introduction of additives before shaping promotes or accelerates the reaction; the vulcanization process of rubbers is usually conducted at elevated temperatures, under pressure to contain volatile reaction products[88]. Normally, in this technique, sulphur is employed as a cross-linking agent in addition to other substances to promote the speed and smoothness of the reaction.

Instead, in the *freezing of melts* the two main differences from the melting process are:

1) There is no contribution from work (W), so all heat must be removed by conduction[88](heat transmission that occurs from the higher temperature zone to those with lower temperature);

2) Usually to return to ambient temperature by the end of the process is not needed. Thus, although the moulding or extrudate must be cooled, the target temperature may be higher than ambient. This temperature is the eat distortion temperature and it is the maximum temperature at which the moulding may be removed from a mould without danger of its distortion, either during removal or when completing its cooling ambient by natural cooling[88].

2.3.2 Mixing

The mixing process can alter the physical form of the polymer to be readily handled at the final conversion stage of its processing. However, before polymer can be used to make products, it is generally added with ingredients to alter the properties of the material (making it harder or more flexible) and to prevent the degradation of the polymer in service or during processing[87,88,90].

Additives in mixing can be used as *reinforcing fillers* to toughen polymers, where the reinforcement effect depends on the fine particle size of the added filler; as *non-reinforcing filler*, added to cheapen the mix or to stiffen it or reduce its tack (such as calcium carbonate or limestone); and as *protective additives*, as antioxidants, heat stabilizer, antiozonants, antistatic agents or processing lubricants (internal or external)[88].

The type of plant required for the mix depends on the physical form of the polymer and additives. Raw materials are supplied in a large variety of forms which include granules and powders of various particle size, liquid medium molecular weight resins or latex. Clearly, the machinery required specifics to mix ingredients, reinforcing fillers, stabilizers etc without overheating the components. Two basic mixing functions can be

identify: *blending* (or extensive mixing or distributive mixing) and *compounding* (or intensive mixing or dispersive mixing)[88].

The first one consists in stirring together the ingredients: the result is a mixture of powders where the individual powder remains and can be separated (although in practice is very difficult). Usually blending is necessary when the fabricating process offers some compounding actions (as happens for powder prior to extrusion); or when thermosetting powders are blends of powders resin and fillers which disperse upon fusion of the resin during moulding.

The *compounding* involves a more intimate dispersion of the additives into the polymeric matrix, requiring generally a physical change in the components, a high shear forces and the polymer has to be in the molten state during the mixing procedure. It is used when an accurate distribution and dispersion of interactive ingredients is needed or when a large amount of modifying ingredients are used.

Figure 2.3.3 reports as examples a high speed mixer (usually known as Henschel mixer) for blending and the internal mixer for compounding, in which a ram operates to keep the material between the rotors and the resultant thin layers are alleged to allow better cooling thanks to a larger cooling surface[88].

(a)   (b)
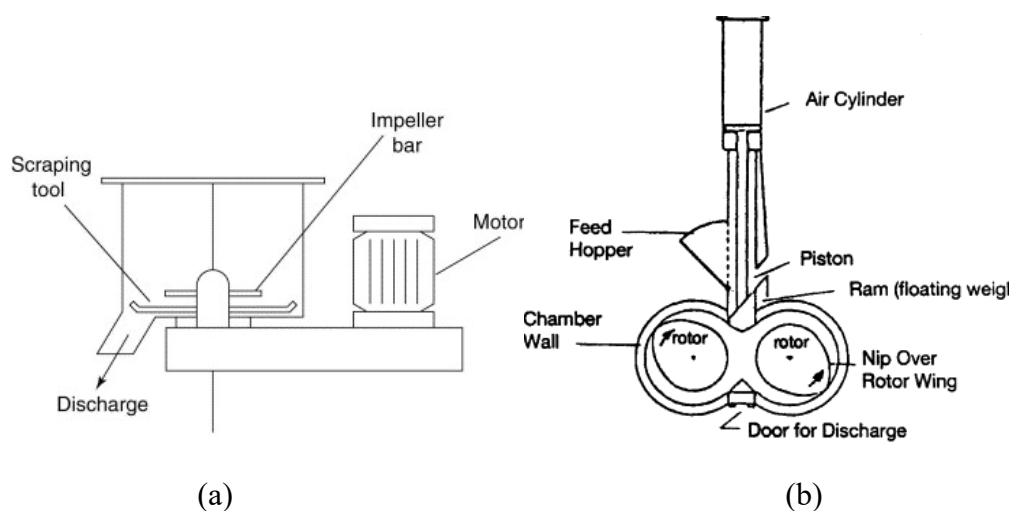
Figure 2.3.3 a)High-Speed mixer for blending; b)Intermix mixer for compounding[88]

2.3.3   Extrusion

The extrusion process comprises the forcing of a plastic or molten material through a shaped die by means of pressure. In modern process, screws are used to progress the polymer in the molten or rubbery state along the barrel of the machine. The most widely

used type is the single screw machine (Figure 2.3.4). Twin screw extruders are also used when superior mixing or conveying is important[87,90,92].

Basing on the class of polymers (thermoplastic, thermosets and elastomers) some considerations are necessary. Thermoplastic materials soften when heated and solidify when cooled. If the extrudate does not meet the specifications, the material can generally be reground and recycled. Thus, the basic chemical nature of a thermoplastic usually does not change significantly as a result of the extrusion process. Thermosets undergo a crosslinking reaction when the temperature is raised above a certain temperature. This crosslinking bond the polymer molecules together to form a three-dimensional network. This network remains intact when the temperature is reduced again. Crosslinking causes an irreversible change in the material. Therefore, thermosetting materials cannot be recycled as thermoplastic materials[88,92]..

2.3.3.1   *Basic extrusion process*

Materials can be extruded in the molten state or in the solid state: generally, polymers are extruded in the molten state. If the polymer is fed to the extruder in the solid state and the material is melted as it is conveyed by the extruder screw from the feed port to the die, the process is called plasticating extrusion. In this case, the extruder performs an additional function, namely melting, besides the regular extrusion function.

In melt fed extrusion, the extruder acts purely as a pump, developing the pressure necessary to force the polymer melt through the die[88,92].

Screw extruders are divided into single screw and multi screw extruders: the single screw extruder is the most important extruder used in the polymer industry. Its key advantages are relatively low cost, straightforward design, ruggedness and reliability, and a favourable performance/cost ratio[92].

The machine (Figure 2.3.4) consists essentially of an Archimedean screw fitting closely in a cylindrical barrel, with just sufficient clearance to allow its rotation. Solid polymer is fed in at one end and the profiled molten extrudate emerges from the other. Inside the polymer melts and homogenizes.

Generally, the feed material flows by gravity from the feed hopper down into the extruder barrel. Some materials do not flow easily in dry form and special measures have to be taken to prevent hang-up (bridging) of the material in the feed hopper. As material falls down into the extruder barrel, it goes in the annular space between the extruder screw and barrel, and is further bounded by the passive and active flanks of the screw flight: the screw channel. The barrel is stationary, and the screw is rotating. As a result, frictional forces will act on the material, both on the barrel as well as on the screw surface. These

frictional forces are responsible for the forward transport of the material, at least as long as the material is in the solid state[88,92,93].

As the material moves forward, it will heat up as a result of frictional heat generation and because of heat conducted from the barrel heaters. When the material temperature exceeds the melting point, a melt film will form at the barrel surface, where the solids conveying zone ends and the plasticating zone starts[92].
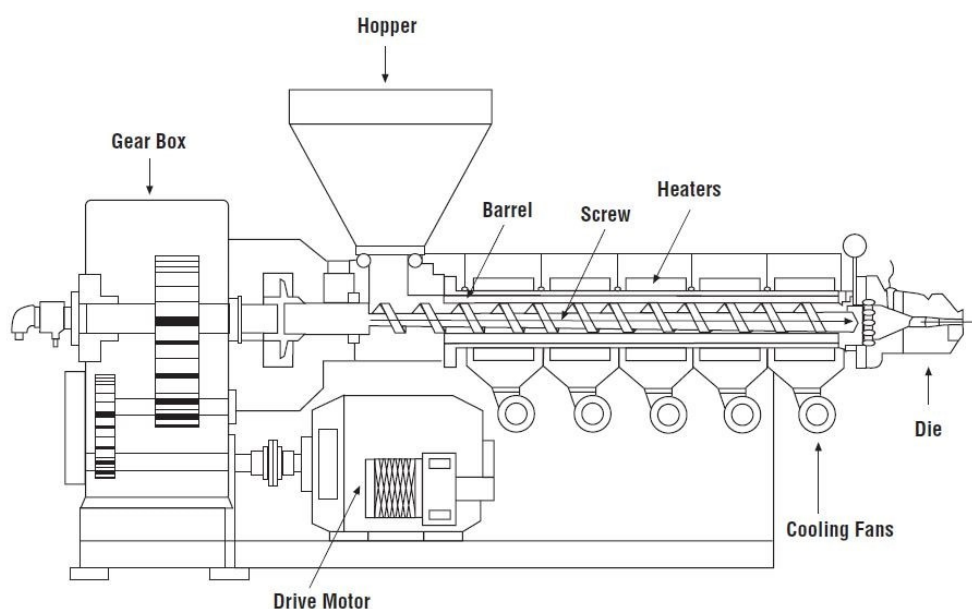
Figure 2.3.4 Main features of a single screw extruder[92]

The boundaries of the functional zones will depend on polymer properties, machine geometry, and operating conditions. Thus, they can change as operating conditions change. However, the geometrical sections of the screw are determined by the design and will not change with operating conditions. As the material moves forward, the amount of solid material at each location will reduce as a result of melting. When all solid polymer disappears, the end of the plasticating zone is reached and the melt conveying zone starts. In the melt-conveying zone, the polymer melt is simply pumped to the die. As the polymer flows through the die, it adopts the shape of the flow channel of the die. Thus, as the polymer leaves the die, its shape more or less corresponds to the cross-sectional shape of the final portion of the die flow channel. Since the die exerts a resistance to flow, a pressure is required to force the material through the die (*diehead pressure*)[88,92].

The diehead pressure is determined by the shape of the die (particularly the flow channel), the temperature of the polymer melt, the flow rate through the die, and the rheological

properties of the polymer melt. It is important to underline that the diehead pressure is caused by the die, and not by the extruder.

The extruder simply has to generate sufficient pressure to force the material through the die[88].

The screw of an extruder has one or two flights spiralling along its length. The diameter to the outside of the flight is constant along the length to allow the close fit in the barrel. The core is of varying diameter and so the spiralling channel varies in depth. In general, the channel depth decreases from feed end to die end although variants can be for special purposes. A consequence of this decreasing channel is the increasing pressure along the extruder that derives the melt through the die[88,92].

The length of the channel can be divided in four zones: feed zone, compression zone, metering zone and die zone, which will be examined separately.

a. **Feed zone.** The function is to pre-heat the polymer and convey it to the subsequent zones. The screw depth is constant and the length of this zone is such as to ensure a correct rate of feed[88].

b. **Compression zone.** This zone has decreasing channel depth and several functions: firstly, it expels air trapped between the granules; secondly, heat transfer from the heated barrel walls is improved as the material thickness decrease; thirdly, the density change during melting is accommodated. Basing on polymer the screw design is varied to facilitate these operations: if the polymer melts relatively sharper, as happens for nylon, a very short compression zone is needed, so design of the screw changes (Figure 2.3.5)[88,92].
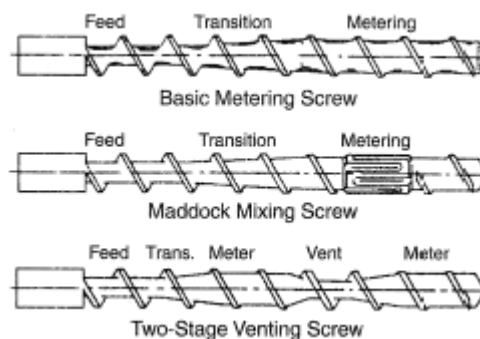
Figure 2.3.5 Variations in screw design[92]

c. **Metering zone.** The screw depth is constant because the function is to homogenize the melt and hence to supply a homogeneous material at constant temperature and pressure[88] to the die region.

d. The die zone. This is the final zone of an extruder, which terminates in the die itself. Usually it comprises a perforated steel plate (breaker plate) and a sieve pack of two or three layers of wire gauze on its screw side. The breaker plate needs to sieve out extraneous materials (like ungelled polymer or dirt), to allow head pressure and to remove the turning memory from the melt. These last two functions are important because the head pressure provides the driving force for the die, and in many cases the polymer "remembers" its history of turning along the spiral screw, even after it has been through the die and this can result in a twisting distortion in the product. When the melt receives a long mechanical treatment as happens with the screw, the chain alignment modifies manifesting a tendency towards elastic recovery of this alignment as preferred energetic configuration[88].

2.3.3.2 *Extruder components*

2.3.3.2.1 Barrel and Feed Throat

The extruder barrel is the cylinder that surrounds the extruder screw and the feed throat is the section of the extruder where material is introduced into the screw channel: it fits around the first few flights of the extruder screw[92].

The geometry of the feed port should be such that the material can flow into the extruder with minimum restriction. Cross-sections of various feed port designs are shown in Figure 2.3.6.
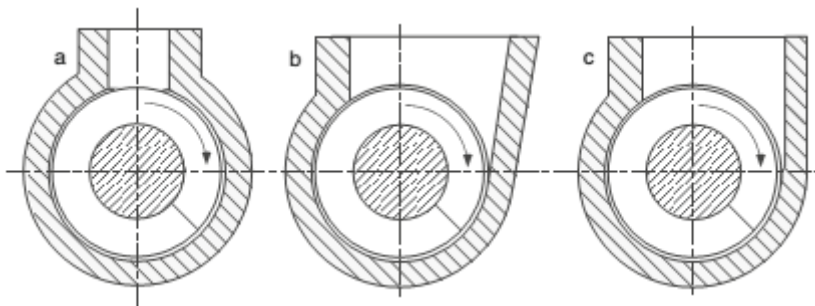
Figure 2.3.6 Cross-sections of various feed port designs[92]

Figure 2.3.6a shows the usual feed port design, Figure 2.3.6b shows an undercut feed port often used on melt fed extruders. The danger with this design is the wedging section between screw and feed opening. If the melt is relatively stiff and / or highly elastic, significant lateral forces will act on the screw. These forces can be high enough to deflect the screw and force it against the barrel surface. This problem is more severe when this geometry is used for feeding solid polymer powder or pellets. This geometry, therefore, should only be used for feeding molten polymers. A better geometry would be the one shown in Figure 2.3.6c with an undercut to improve the intake capability, but the

pronounced wedge is eliminated by a flat section oriented more or less in the radial direction[92].

The shape of the inlet opening is usually circular or square. The smoothest transition from feed hopper to feed throat will occur if the cross-sectional shape of the hopper is the same as the shape of the feed opening.

The extruder barrel is simply a flanged cylinder. It must withstand relatively high pressures, as high as 70 MPa (10,000 psi), and should possess good structural rigidity to minimize sagging or deflection. Many extruder barrels are made with a wear - resistant inner surface to increase the service life. The two most common techniques are nitriding and bimetallic alloying[92].

Some extruders have additional functionalities along the barrel as the *vented extruders*. A vented extruder (Figure 2.3.7) is equipped with one or more openings (vent ports) in the extruder barrel, through which volatiles can escape. Instead of the extraction of volatiles, the vent port can be used to add certain components to the polymer, such as additives, fillers, reactive components, etc. This adds versatility of vented extruders, with the benefit that the extruder can be operated as a conventional non-vented extruder by simply plugging the vent port and, possibly, changing the screw geometry[92].
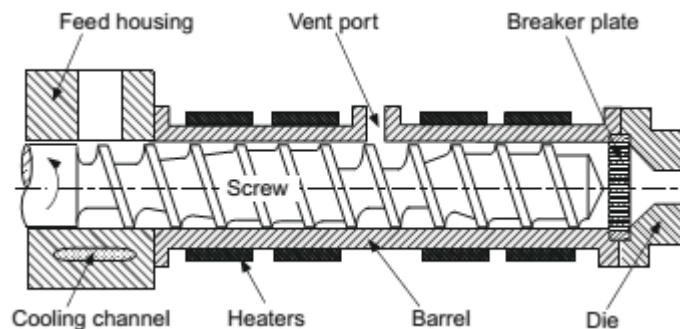
Figure 2.3.7 Vented extruder[92]

The feed hopper feeds the granular material to the extruder. In most cases, the material will flow by gravity, unaided, from the feed hopper into the extruder. Unfortunately, this is not possible with all materials. Some bulk materials have very poor flow characteristics and additional devices may be required to ensure steady flow into the extruder. Sometimes this can be a vibrating pad attached to the hopper to dislodge any bridges as soon as they form. In some cases, stirrers are used in the feed hopper to mix the material (and prevent segregation) and /or to wipe material from the hopper wall, if the bulk material tends to stick to the wall[92].

Square feed hoppers with rapid compression usually work well with bulk materials with uniform pellet size. *Crammer feeders* are used for bulk materials difficult to handle. Other materials, particularly those with low bulk density, tend to entrap air. If the air cannot escape through the feed hopper, it will be carried with the polymer and eventually appear at the die exit. In most cases, this will cause surface imperfections as small explosions when the air escapes from the die.

2.3.3.2.2   Screw

The extruder screw is the heart of the machine. The rotation of the screw causes forward transport, contributes to a large extent to the heating of the polymer, and causes homogenization of the material. In simple terms, the screw is a cylindrical rod of varying diameter with a helical flight(s) wrapped around it. The outside diameter of the screw, from flight tip to flight tip, is constant on most extruders. The clearance between screw and barrel is usually small. Generally, the ratio of radial clearance to screw diameter is around 0.001, with a range of about 0.0005 to 0.0020[92].

The proper design of the geometry of the extruder screw is of crucial importance to the proper functioning of the extruder. If material transport instabilities occur as a result of improper screw geometry, even the most sophisticated computerized control system cannot solve the problem.

Regardless of the details of the screw geometry, it is important that the screw has sufficient mechanical strength to withstand the stresses imposed by the conveying process in the extruder.

An important requirement for the extruder screw is the ability to transmit the torque required to turn the screw. The most critical area of the screw in this respect is the feed section. In fact, in the feed section the cross-sectional area of the root of the screw is generally the smallest and the torsional strength the lowest. Furthermore, the entire torque has to be transmitted, while further downstream only a fraction of the total torque has to be transmitted[92].

Generally, the objective of a screw design is to deliver the largest amount of output at acceptable melt quality, considering also all the other parameters that act on the screw (as pressure, erosion, flight width, etc.)[87,88,90,92,93]. The more common types of screw are reported and classified.

a.   The Standard Extruder Screw (Figure 2.3.8)

Total length: 20–30 D

Length of feed section: 4–8 D

Length of metering section: 6–10 D

Number of parallel flights: 1

Flight pitch: 1 D (helix angle 17.66°)

Flight width: 0.1 D

Channel depth in feed section: 0.15–0.20 D

Channel depth ratio: 2–4
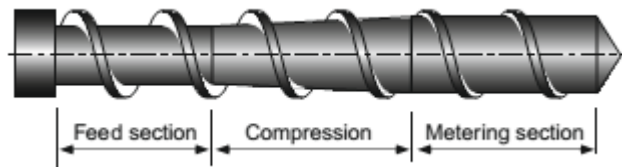
Figure 2.3.8 Standard extruder screw [92]

The standard extruder screw is still the most used, but significant improvements have been made on the screw design basing on the designed performances.

There are a large number of modifications of the standard extruder screw in use today basing on the model proposed in Figure 2.3.8.

An example is the standard screw with additional flight in the feed section (Figure 2.3.9)

Figure 2.3.9 Standard screw with additional flight in the feed section[92]

The additional flight is intended to smooth out the pressure fluctuation caused by the flight interrupting the in-flow of material from the feed hopper every revolution of the screw. An additional benefit of the double-flighted geometry is that the forces acting on the screw are balanced; thus, screw deflection is less likely to occur. On the negative side, the additional flight reduces the open cross-sectional channel area and increases the contact area between solid bed and screw[92].

b.   *Devolatilizing extruder screws*

Devolatilizing extruder screws (Figure 2.3.10) are used to extract volatiles from the polymer in a continuous fashion. Such extruders have one or more vent ports along the length of the extruder through which volatiles escape. Some of the applications of vented extruders are: removal of monomers and oligomers in the production of polymers; removal of reaction products of condensation polymerization (e. g., water, methanol) and oligomers from nylon and polyesters; removal of air with filled polymers, particularly with glass fibre reinforced polymers; and the removal of water from hygroscopic polymers or other solvents.

The screw consists of at least five distinct geometrical sections. The first three sections, feed, compression, and metering are the same as on a conventional screw. After the metering section there is a rapid decompression followed by the extraction section, which, in turn, is followed by a rapid compression and a pump section. Two important functional requirements for good devolatilization are zero pressure in the polymer under the vent port and completely molten polymer under the vent port[92].
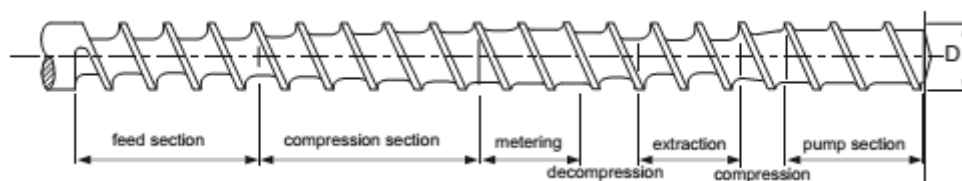
Figure 2.3.10 Two-stage devolatizing extruder screw[92]

c.   *Vented extruder screw*

The conventional vented extruder screw is shown in Figure 2.3.11. In many cases, mixing sections are incorporated into the metering section of the screw to improve the homogeneity of the melt entering the extraction section. The volatiles travel with the polymer up to the vent port. This type of venting is referred to as forward devolatilization. The length of the extraction zone is usually 2 to 5 D. The channel depth in the extraction section is large, particularly if the polymer foams in the extraction section. In this case, the helix angle is often increased from the conventional 17.66° to 40°[92].
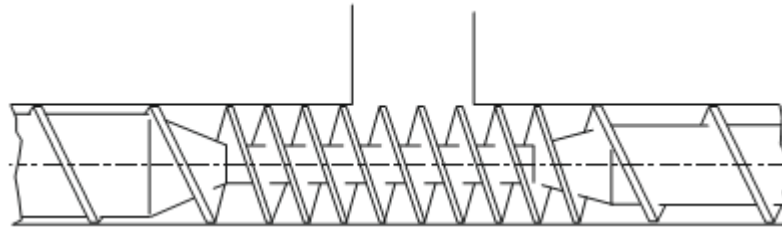
Figure 2.3.11 Extraction section with multiple flight[92]

2.3.3.2.3   Dies

The objective of an extrusion die is to distribute the polymer melt in the flow channel such that the material exits from the die with a uniform velocity. The actual distribution will be determined by the flow properties of the polymer, the flow channel geometry, the flow rate through the die, and the temperature field in the die[85,87,89.]

If the flow channel geometry is optimized for one polymer under one set of conditions, a simple change in flow rate or in temperature can make the geometry non-optimum. Except for circular dies, to obtain a usable flow channel geometry for a wide range of polymers and for a wide range of operating conditions is essentially impossible. For this reason, adjustment capabilities into the die are often incorporates in order to change the distribution externally while the extruder is running. The flow distribution is generally changed in two ways: by changing the flow channel geometry (by means of choker bars, restrictor bars, valves, etc.) and by changing the local die temperature. Mechanical adjustment capabilities complicate the design of the die but enhance its flexibility and controllability.

The die, where the forming of the polymer takes place, is one of the most critical parts of the extruder. The rest of the extruder basically has only one task: to deliver the polymer melt to the die at the required pressure and consistency. Thus, the die forming function is a very important part of the entire extrusion process. Some of the more common types of dies are reported and classified[85,89].

a.   *Film and Sheet Dies*

Dies for flat film are essentially the same as dies for sheet extrusion. The difference between sheet and film is primarily the thickness. Webs with a thickness of less than 0.5 mm are generally referred to as film, while webs with a thickness of more than 0.5 mm are generally referred to as sheet.

Some example of dies for films and sheets are reported in Figure 2.3.12. The flow can be adjusted adding the flex lip adjustment, that allows fine adjustments of the extrudate thickness; and the choker bar, which can be locally deformed by a number of bolts located along the width of the die. The deformation of the choker bar causes a change in the height of the flow channel and, thus, allows an adjustment of the flow distribution in the die. A third adjustment possibility is the die temperature. Local heating or cooling of certain die sections enhance or restrict flow: temperature adjustment will be more effective with polymers whose viscosity is quite sensitive to temperature as most amorphous polymers[89].
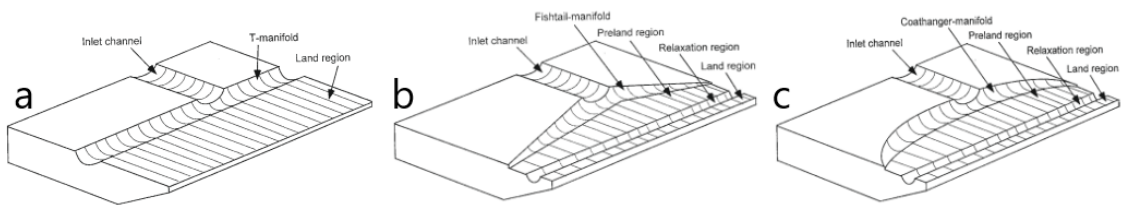
Figure 2.3.12 a) T-die; b) Fishtail die; c) Coat hanger die

b. *Pipe and Tubing Dies*

The difference between pipe and tubing is mainly determined by size. Small diameter products (less than 10 mm) are generally referred to as tubing, while large products are generally referred to as pipe. Annular products can be extruded on in- line dies and crosshead dies. In the crosshead die the polymer melt makes a turn as it flows through the die (Figure 2.3.13). The direction of the inlet flow is perpendicular to the outlet flow. The polymer melt makes a 90° turn and splits at the same time over the core tube. The polymer melt recombines below the core tube; this is where a weld line forms. After the 90° turn, the polymer melt flows through the annular flow channel where it adopts more or less the shape of the final land region[89].
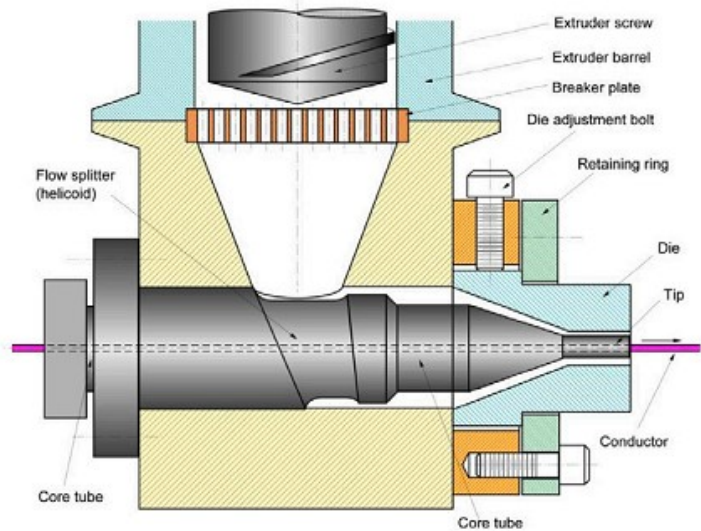
Figure 2.3.13 Crosshead die[89]

In most crosshead dies, the location of the die relative to the tip can be adjusted by means of centring bolts. This allows adjustment of the wall thickness distribution and concentricity[89].

2.3.3.3 *General flow mechanism*

The flow can be divided in three phases that start with the *melting*. As the polymer is conveyed along the screw a thin film melts at the barrel wall. The screw scrapes off the melted film during the rotation and the molten polymer move down to the core and sweep up again to establish a rotary motion in front of the leading edge of the flight. The entire process is progressive until all the polymer is melted. The *conveying* is the second phase where with a friction with both screw and barrel, leading to the principal transport mechanism (drag flow). This is literally dragging along by the screw of the melt as the result of frictional forces and it is the equivalent to the viscous drag between stationary and moving plates separated by a viscous medium. Pressure is high at the output end, low at the feed end and a pressure gradient opposes the drag flow. So, the pressure acts only as an opposition. The final component of the conveying is a leak flow that opposes to the drag flow because there is a finite space between screw and barrel through the material can leak backwards[85].

Therefore the total conveying flow can be sum in:

TOTAL CONVEYING FLOW= DRAG FLOW − PRESSURE FLOW − LEAK FLOW

The final part of the flow mechanism is the *heating and cooling* phase. The whole system is thermostatically controlled to give precise control of the melt temperature. The length of the machine is divided into sections to allow variation of temperature for optimum processing. The running condition may be regarded as lying between the extremes of adiabatic running (with heat coming only from viscous dissipation) and isothermal running (when the temperature is constant in all the sections and heat is supplied by heaters or removed by coolers to compensate changes in melt temperature)[85].

To fully understand the entire process, one also has to know and appreciate the properties of the material being extruded. The characteristics of the polymer determine, to a large extent, the proper design of the machine and the behaviour of the process.

2.3.3.4   *Influence of polymer properties*

Some of the most important properties of the bulk material are the bulk density, the coefficient of friction, and particle size and shape. From these properties, the transport behaviour of the bulk material can be described with reasonable accuracy.

2.3.3.4.1   Bulk density

The bulk density is the density of the polymeric particles, including the voids between the particles.

Low bulk density materials ($\rho < 0.2$ g /cc) tend to cause solids conveying problems, either in the feed hopper or in the feed section of the extruder. Materials with irregularly shaped particles tend to have a low bulk density; examples are fibre scrap or film scrap (flakes). When the bulk density is low, the mass flow rate will be low as well. Thus, the solids conveying rate may be insufficient to supply the downstream zones with enough material. Special devices and special extruders have been designed to deal with these low bulk density materials. A crammer feeder (Figure 2.3.14) is a device used to improve the solids transport from the feed hopper into the extruder barrel[88,93].
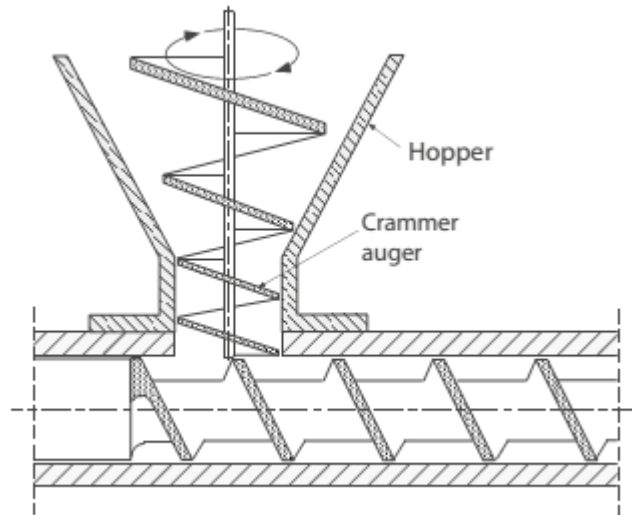
Figure 2.3.14 Crammer feeder[89]

2.3.3.4.2   Coefficient of friction

The coefficient of friction of the bulk material is another very important property. Internal and external coefficient of friction can be distinguished. The internal coefficient of friction is a measure of the resistance present when one layer of particles slides over another layer of particles of the same material. The external coefficient of friction is a measure of the resistance present at an interface between the polymeric particles and a wall of a different material of construction. The coefficient of friction is simply the ratio of the shear stress at the interface to the normal stress at the interface. Friction itself is the tangential resistance offered to the sliding of one solid over another.

Some of the variables that affect the coefficient of friction are temperature, sliding speed, contact pressure, metal surface conditions, particle size of polymer, degree of compaction, time, relative humidity, polymer hardness, etc. The coefficient of friction is very sensitive to the condition of the metal surface. The coefficient of friction of a polymer against an entirely clean metal surface is very low initially, as low as 0.05 or less. However, after the polymer has been sliding on the surface for some time, the coefficient of friction will increase substantially and may stabilize at a value about an order of magnitude higher than the initial value[85].

a.   *Particle size and shape*

The range of polymeric particles used in extrusion is quite wide, from about 1 micron to about 10 mm. Particle size can be determined by a variety of techniques, microscopic measurement being one of the most common techniques.

The transport characteristics of particulate solids are quite sensitive to the particle shape. Both the internal and external coefficient of friction can change substantially with variations in particle shape even if the major particle dimensions remain unchanged. Small differences in the pelletizing process can cause major problems in a downstream extrusion process. Variations in the ratio of regrind to virgin polymer can cause variations in the extrusion process.

The ease of solids transport is often determined by the particle size. Pellets are generally free-flowing and do not have a strong tendency to entrap air. From a solid conveying point of view, pelletized materials are the easiest to work with. Granules are often free-flowing, sometimes semi-free-flowing; they are more likely to entrap air. Semi-free-flowing granules may require special feeding devices (such as a vibrating pad on the hopper) to ensure steady flow. Powders tend to be cohesive and also tend to entrap air. Therefore, in most cases, special precautions have to be taken to successfully extrude powder material[85,89,90,93].

b.   *Newtonian Fluid*

A fluid whose viscosity is independent from the shear rate. Most low viscosity liquids and gases behave as a Newtonian fluid. In a plot of shear stress versus shear rate, a Newtonian fluid will exhibit a linear relationship; therefore, Newtonian fluids are also referred to as linear fluids[85,90,93].

c.   *Non-Newtonian Fluid*

A fluid whose viscosity is dependent on the shear rate. High viscosity polymer melts behave as non-Newtonian fluids, with the viscosity reducing with increase shear rate. Another type of non-Newtonian fluid is a dilatant fluid. The viscosity of a dilatant fluid increases with the shear rate increase (pseudo-plastic behaviour). The shear stress-shear rate relationship of non- Newtonian fluids is non-linear. The concepts of shear rate, shear stress, and viscosity are extremely important in developing a thorough understanding of the extrusion process (and other polymer processing operations)[85,89,90,93].

2.3.4   **Compression Moulding**

Compression moulding is the oldest mass production process for polymer products.

Compression moulding encompasses different techniques in processing plastics such as the basic arc compression moulding process (Figure 2.3.15), the transfer moulding process, resin transfer moulding process, compression-transfer moulding process, and other moulding processes. These compression moulding methods provide different capabilities to fabricate products meeting performance requirements using different materials.
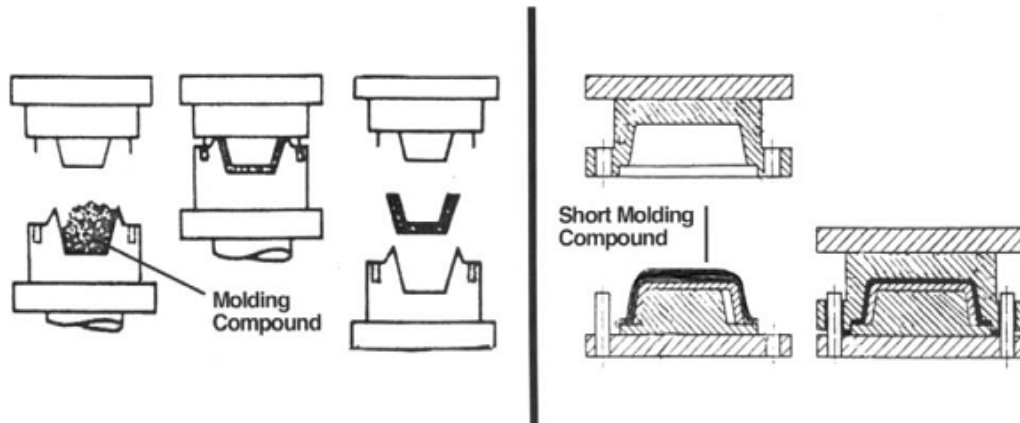
Figure 2.3.15 Schematics of compression moulding plastic materials

In this processing method of moulding, the moulding material, generally preheated, is first placed in an open, heated mould cavity. The mould is closed with a top force or plug member, pressure is applied to force the material into contact with all mould areas, while heat and pressure are maintained until the moulding material has cured. The process employs thermosetting resins in a partially cured stage, either in the form of granules, putty-like masses, or preforms[85].

Compression moulding is a high-volume, high-pressure method suitable for moulding complex, high-strength fiberglass reinforcements. Advanced composite thermoplastics can also be compression moulded with unidirectional tapes, woven fabrics, randomly oriented fibre mat or chopped strand.

The advantage of compression moulding is its ability to mould large, fairly intricate parts. Furthermore, it is one of the lowest cost moulding methods compared with other methods such as transfer moulding and injection moulding; moreover it wastes relatively little material, giving it an advantage when working with expensive compounds[85,89].

2.3.4.1   *General process*

In the compression moulding process, a thermoplastic or partially polymerized thermosetting polymer is placed in a heated cavity (Figure 2.3.16), usually in a preheated and preformed shape vaguely corresponding to that of the cavity; the mould begins to

close and pressure is applied to the preform, forcing it to further heat up close to the mould temperature, and flow to fill the mould cavity.

After charging the mould, the press is closed bringing the two parts of the mould together. This allows the moulding material to melt and flow through filling the cavity between the two parts of the mould, and at the same time pushing out any entrapped air ahead of the melt so as to fill the mould cavity completely. After holding the plastic in the mould for the time specified for a proper cure under the required temperature and pressure, the pressure is released, the mould opened, and the solid moulded plastic part discharged. In a modern high-speed automatic compression press all the operations are performed automatically[94].

The necessary preheating and mould heating temperatures and mould pressure may vary considerably depending upon the thermal and theological (refers to the deformation and flow properties of the plastic) properties of the plastic.

In the process, the polymer undergoes complete polymerization (cross linking). Then the mould is opened, the part is ejected, and the cycle starts again. This process wastes very little material (no runners and sprue) and can produce large parts. However, it is difficult to produce parts with very close tolerances because the final size of the compression melded article depends on the exact amount of the preform. Furthermore, the process does not easily lend itself to moulding of intricate parts with deep undercuts[85,89].

(a)   (b)
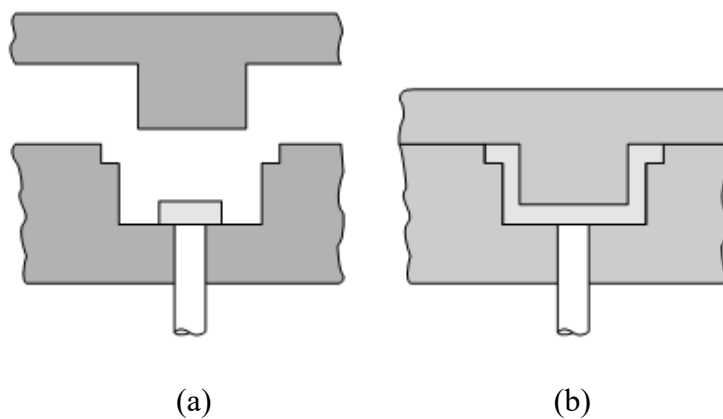
Figure 2.3.16 Schematic illustration of compression moulding process with mould open (female cavity on the bottom)(a) and mould closed (b)[89].

For a typical compression moulding of thermoset material a slight excess of material is usually placed in the mould to insure it being completely filled and this excess is squeezed out between the mating surfaces of the mould in a thin, easily removed film known as flash. As shown in Figure 2.3.17 flash can form in different positions based on how it is to be removed. Different methods are used to remove flash such filing, sanding, and/or

tumbling. In the case of a thermoplastic, the moulding temperature cycle is from heating to plasticizing the plastic, to cooling in the mould under pressure, the pressure released, and the moulded article removed. When thermosets are used the mould need not be cooled at the end of the moulding operation or cycle, as the plastic will have hardened and can no longer flow or distort.
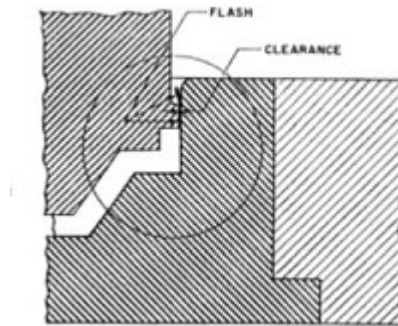
Figure 2.3.17 Example of vertical flash in a mould

The advantages of compression moulding over other moulding operations are the simplicity of the moulds, which makes them less expensive to manufacture and maintain, and the relatively small amount of waste produced. Disadvantages include relatively slow cycle times and geometrical limitations to the mouldable parts. Moreover, during the preform-heating part of the cycle, the main problems to be considered are heat transfer and flow (or elastic deformation) of the compressed particulate matter.

Both compression moulding and injection moulding are used to produce discrete parts of widely differing geometries, but the difference in resin type commonly used between the two processes dictates very different mould conditions. In compression moulding, the mould is heated so that the polymer will cure. In injection moulding, the mould is cold so that the molten polymer will freeze.

Another consequence of making thermoset polymer parts by compression moulding is that reject parts cannot be reprocessed. To overcome some of these limitations, transfer moulding was developed. Transfer moulding is a hybrid between compression moulding and injection moulding, in which the charge is melted in a separate pot, which is part of the heated mould, and then transferred under pressure by a ram, through runners and gates, into the mould cavity. Transfer moulding cycles tend to be shorter than compression moulding cycles[85,93,89].

Figure 2.3.18 represents the various stages of the compression moulding cycle from the point of view of the plunger force needed to close the mould at a constant rate.
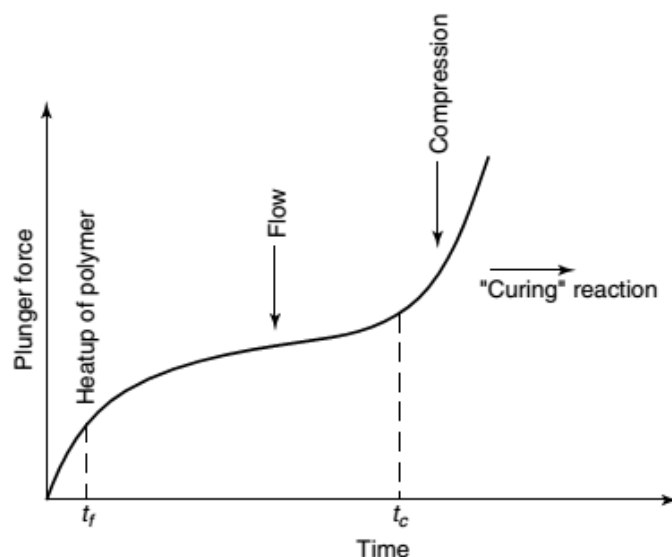
Figure 2.3.18 Schematic representation of the plunger force applied during compression moulding[89].

In the first region, the force increases rapidly up to the fill time (t_f) as the preform is squeezed and heated. At t_f, the polymer is in the molten state and is forced to flow and fill the cavity. Filling terminates at t_c, when compression of the polymer melt begins, to compensate for the volume contraction that occurs during polymerization. The bulk of the curing process takes place after t_c. In order to derive relationships for the flow and pressure characteristics, the time period $t_f < t < t_c$, is simply needed to be considered since prior to t the polymer is melt and after t_c it is cured.

During the considered time interval, the polymer is assumed to be heated to a uniform temperature, T_w, that is equivalent to the mould wall temperature.

A knowledge of the temperature, conversion, thermal properties of the polymer and molecular weight distribution as a function of thickness and reaction time is essential in determining the required compression mould cycle or the time and temperature in the post-curing step[93,89].

There is also the possibility to use a mould held between the heated platens of a hydraulic press: in this case the prepared quantity of moulding compound is placed in the mould (usually by hand) and the mould placed in the press (Figure 2.3.19). Usually this is a laboratory scale solution.

In this kind of moulding the cycle starts when the mould reaches the set temperature under the decided pressure conditions.
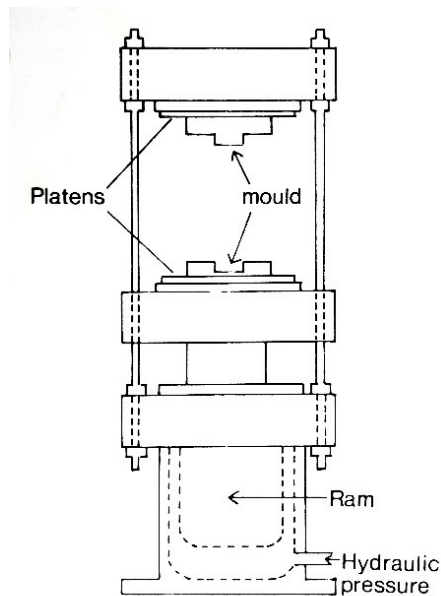
Figure 2.3.19 Original compression moulding press[89]

2.3.4.2   *Moulds*

The moulds used in Compression Moulding can be classified in three general types:

2.3.4.2.1   Flash Moulds

This type of mould is widely used because simple to construct and holds the part thickness and density within close limits. As the mould closes, the excess material escapes over the land where it forms a very thin fin.

This fin hardens first, preventing the escapement of the mould charge. Flash type moulds (Figure 2.3.20) can be loaded by volume since excess material is permitted to escape. Material lost through flashing is higher than for other types of compression moulds, but the original mould cost is relatively low[94].
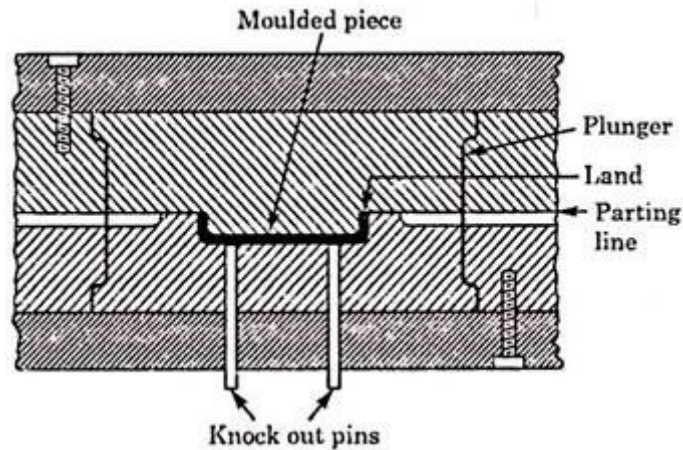
Figure 2.3.20 Flash moulds scheme[89]

2.3.4.2.2   Positive Moulds

The characteristics of positive type mould (Figure 2.3.21). are deep cavity and a plunger that compresses the compound at the bottom of the mould. As there is very little escapement of material, it is necessary to weight the charge accurately if the size of the part is to be controlled. Such moulds are used for high impact materials and parts requiring deep draw[94].
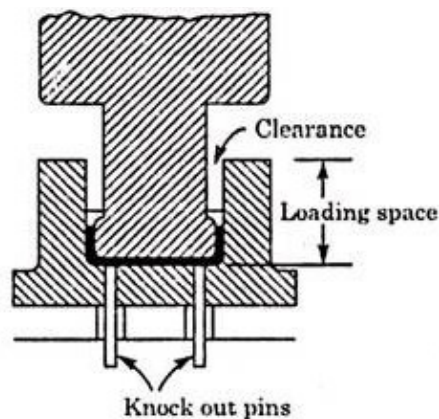
Figure 2.3.21 Positive Moulds scheme[89]

2.3.4.2.3   The semipositive mould

The semipositive mould (Figure 2.3.22) is by far the most popular. It combines the best features of the positive and the flash moulds. Since its design includes a plastic material well of larger diameter, with a tight-fitting force above the cavity, the material is trapped fairly positively and the plastic is forced to flow into all corners of the cavity. As the

material picks up more heat and becomes fluid, it escapes between the force and cavity sidewalls as flash, allowing the force to scat on the land area[94].
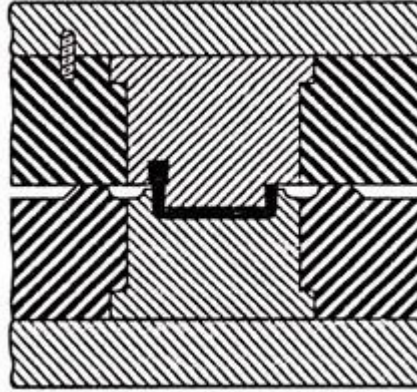
Figure 2.3.22 The semi-positive mould scheme[89]

2.3.4.3   *Process defects and remedies*

The defects in compression moulded parts can be classified into two categories: surface defects that affect the visual appearance and internal defects that influence the mechanical properties. Surface defects can be masked by post-processing such as painting by spray coating after moulding. Many defects can be avoided or reduced by optimizing the moulding material, process conditions and part design[95].

2.3.4.3.1   Voids

Voids or porosities are generated if air is entrapped inside the moulded part. These voids significantly deteriorate mechanical properties such as interlaminar shear strength and flexural strength. Most of the air bubbles are generated during the mixing and compounding stages[95].

2.3.4.3.2   Blisters

As the internal pressure of volatiles or entrapped air is released at the moment of mould opening, interlayer cracks may be created near the part surface. These cracks are called blisters. They often appear to be dome-shaped bulges. They also can be created at elevated temperatures by the expansion of entrapped air. The formation of blisters can be decreased either by the vacuum application in the mould to minimize the entrapment of air or volatiles or by the use of coupling agents and contaminant reduction in the resin formulation to increase the interlaminar shear strength[95].

2.3.4.3.3   Delamination

Delamination can result from either poor fibre wetting with resin or residual stress that is caused by a non-uniform temperature distribution and/or incomplete curing. Hence, delamination is usually observed near the centreline of thick sections. To lessen this problem, to use a relatively slow catalyst in order to obtain uniform curing reaction is most effective. This remedy, however, can increase the process cycle time[95].

2.3.4.3.4   Knit line and Sink marks

A knit line is generated when two or multiple flow fronts join or merge to form a single flow front (Figure 2.3.23). Along the knit line, the fibre is aligned parallel to the knit line. As a result, the strength in the direction normal to the knit line is significantly lower than in the parallel direction. If the load is applied in the transverse direction relative to the knit line, matrix cracking is easily initiated, and the part can fail. The most common location of knit line formation is behind moulded-in holes that are made by core pins in the mould[93].

Sink marks are small depressions appearing on the surface usually located opposite to the ribs or bosses (Figure 2.3.23). Even though they do not deteriorate the mechanical properties, they affect the visual appearance of the final product leading to varying gloss on the flat surface. To avoid this problem, a low-profile additive can be added to the resin formulation. However, it is more effective to optimize the part design. It is recommended to avoid thick sections directly near the rib or boss. If possible, to use a protruding corner instead of a square or rounded corner at the rib juncture[95] is preferable .

(a)   (b)
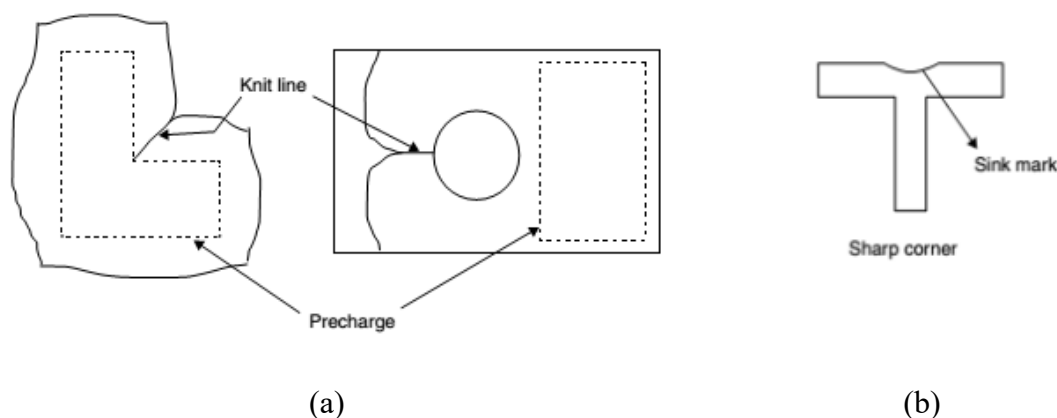
Figure 2.3.23 a) Formation of knit line in two different shaped moulds; b) Illustration of sink mark[95]

2.3.4.3.5   Fibre separation

Fibre separation or fibre segregation takes place when the fibre does not migrate with the resin flow in the mould. As a consequence, the fibre content becomes non-uniform leading to a higher than nominal fibre content in the upstream and a lower than nominal fibre content in the downstream. The fibre separation is more significant as the fibre content and fibre length are increased. Moreover, the fibre oriented parallel to the flow direction are more susceptible to fibre separation than those oriented normally to the flow direction[95] (Figure 2.3.24).

| (a) | (b) |
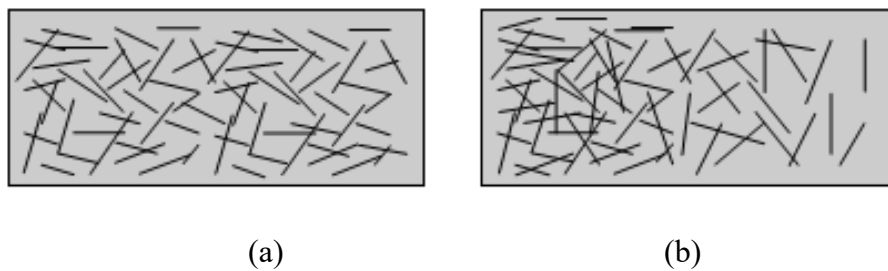
Figure 2.3.24 (a)Homogeneous suspension; b) Fibres separation in a heterogeneous suspension[95]

3. Chapter

Cellulose-based

Mortars

State of the art, methods and application of cellulose fibers coming from wastewater sludge

3.1   **Introduction**

Concretes, mortars and other cement-based composites are the most common structural materials in the construction industry.

The hydraulic binders-made composites were discovered and used thousands of years ago, and, thanks to their immediate effectiveness, their modern production techniques have remained very similar to antiquity. However, the great technological development of materials science and nanotechnology in recent decades, has allowed new opportunities for the development of cementitious mixtures, through the introduction of new techniques and innovative materials. This permit creating composites with many additional characteristics (besides structural properties) aimed at improving safety and life quality inside buildings. About 40% of the global energy is mainly used for the production of mortars and concretes[66]: therefore, a significant increase in sustainability of mortars/concretes production can be achieved by replacing virgin raw materials with renewable and/or so called ''waste ones''[67,68] . Since recovered cellulose fibres from other industrial activities are often used in building applications[67], also the cellulose recovered from municipal wastewater becomes an attractive possibility to consider in this application field.

This chapter analyses the evolution of hydraulic binders-based materials, with a presentation of all the materials considered in this study and their sustainability. Successively, composites added with natural fibres are introduced, analysing the effect of the type of the fibre on the composite properties. Lastly, the description of the methods used for the application of cellulose fibres in mortars and the obtained results are discussed. In the last part of this chapter, technical feasibility and economic considerations to promote the valorisation of recovered cellulose and its economic assessment in the building sector are considered.

Since the aim of this study is to investigate the possibility of cellulose recovery from municipal wastewater and its valorisation in the building sector, the effect of the addition of recovered cellulosic fibres at different percentages (0%, 5%, 10%, 15% and 20% added by volume) on the properties of hydraulic lime-based mortars was tested for non-structural applications. Also the properties of mortars manufactured with the same dosages of pure cellulose fibers and cellulose fibers recycled from newspapers were further compared. This study gives a perspective about the substitution of virgin cellulose with recovered one from WWTPs, in order to obtain mortars with better, or at least comparable, properties by avoiding the use of virgin resources when it is not necessary.

3.2   Cement-based materials: history and evolution

The most used composite material in construction, in which Portland cement is a key component, is concrete. Although modern concrete production techniques have developed just in the last two centuries, artificial conglomerates have a very ancient origin, given that civilizations such as Assyrians[97], Egyptians and, later, Greeks[98] used similar artificial materials.

However, it was the Romans who optimized this constructive technique, with the use of the *Opus caementicium*, producing very advanced works and infrastructures for the time (Figure 3.2.1)[99].

Figure 3.2.1 Example of ancient artefacts: Roman Pantheon, Rome 218AD

After the fall of the Roman Empire, in the 5th century, these constructive techniques were set aside and forgotten, until the humanistic reawakening, after the 14th century, when the texts of *Pliny the Elder* and *Vitruvius* were rediscovered. In the following centuries, the continuous approach to the rediscovery of concrete led to the discovery of *hydraulic lime*, which marks the technological transition from Roman's Opus caementicium to modern concrete[100]. In these years, the development of the chemistry knowledge and of cooking techniques, ed to the manufacture of Portland cement at the beginning of the 19th century[101].

The name "Portland" derived from the similarities found between the "artificial stone", obtained by mixing cement with water and aggregates (today called "concrete" or "mortar"), and the limestone from the British isle of Portland, extensively used as a building stone throughout the British Isles at that time[102].

During the industrial revolution and until the present day, the techniques of production and processing of cement have continuously evolved, and innumerable patents have been registered[63].

Today, cement is used as a binder in a wide range of construction products, with particular emphasis on concretes and mortars. Both are based in similar compositions, which essentially include Portland cement, aggregates and water, being mainly differentiated by the size of the aggregates (coarser in concrete). Cement-based products are generally considered *two-phase* materials, constituted by a cementitious matrix and aggregates. The matrix consists of a cement paste, resulting from the cement hydration, with the function to bind the aggregates together, and create a material similar to an artificial stone (Figure 3.2.2).

Several additives can be used to improve or correct workability, setting time, mechanical strength or durability of these mixtures.
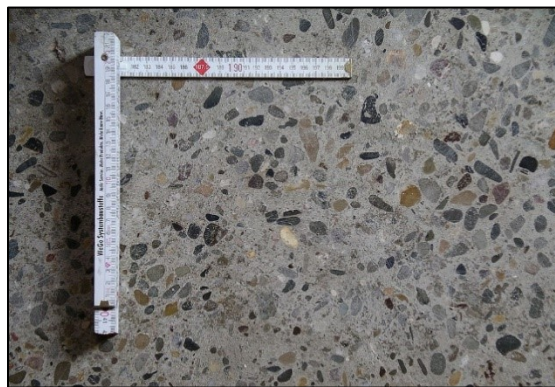
Figure 3.2.2 Traditional concrete surface. Aggregates are distinguishable from the cement matrix

3.3   **Overview of multifunctional binder-based materials**

The technology linked to cementitious materials has certainly reached important milestones, but, in recent decades, the needs of the building industry have become numerous and increasingly complex. Buildings are no longer required to have a simple structural function, but to contribute to the daily well-being of its inhabitants[103].

For this reason, the European Union is very active in the production of laws and standards for the regulation of the wholesomeness of living environments and structural safety [104].

This needs to implement construction materials with new functions, in order to introduce new technological systems to improve the use of living space. In the last decades, many researchers have been focused on the development of cement-based products capable of performing autonomous tasks without the need of external devices, the so-called *Multifunctional cement-based composites* (MCC)[105].

As already mentioned, cementitious materials such as mortar and concrete can be considered "two-phase" materials: the cement matrix consists of the *reagent* part of the mixture, i.e. the hydraulic binder; the *inert* part is instead represented by the aggregates, held together by the cement paste which compose the "backbone" of the material. The coarse and fine aggregates traditionally used are gravel and sand, but these can be replaced by other materials, depending on the properties sought in the composite.

Such functionalities are obtained by adding specific admixtures in the compositions, resulting into functional cement matrixes. For example, mortars and plasters can be realized with artificial or natural lightweight aggregates, in order to increase the porosity of the material, obtaining thermal insulation [106], and a similar approach can be used to realize sound-absorbing or sound-insulating plasters (Figure 3.3.1)[107].

Figure 3.3.1 Hydraulic lime-based plaster realized with natural organic aggregates (cork) for thermal insulation and acoustic absorption

Adsorbent materials (as cork or cellulose), capable of eliminating pollutants[108], or photocatalyst materials (as TiO_2) which decompose harmful products (such as VOCs) can be inserted into the mixtures[109].

The mechanical properties of the cement paste can be also improved considerably by inserting different types of fibres[110–112], with a natural or industrial origin, which can improve the mechanical behaviour of the composite, in particular the tensile one through the "bridging effect"[113].

Vegetable or cellulose fibres exhibit a set of important advantages, such as wide availability at relatively low cost, bio- renewability, ability to be recycled, biodegradability, non-hazardous nature, zero carbon footprint, and interesting physical and mechanical properties (low density and well-balanced stiffness, toughness and strength)[114,115]. Natural fibres (NF) can be found in a wide variety of morphologies – diameter, aspect ratio, length, and surface roughness – and form – mainly strands, pulp or staple. Moreover, their surface can be easily modified in order to have a more hydrophilic or hydrophobic character or to attach functional groups. Although brittle building materials have been reinforced with vegetable fibres since ancient times, the

concept of NF reinforcement in cement-based materials was developed in 1940s, when these fibres were evaluated as potential substitutes for asbestos fibres[114,115].

3.4 Materials for mortars manufacturing

The study of materials used in mortars production is essential to choose the best composition parameters for the mix design, in order to obtain certain mechanical properties. For these reasons, it is necessary to describe all the components that take part in the mix to evaluate their function and their composition.

3.4.1 Hydraulic Binders

The monolithic properties of mortars and concretes derive from the action of a binder with "hydraulic behavior".

3.4.1.1 *Natural Hydraulic Lime*

Hydraulic lime is a hydraulic binder primarily composed of calcium hydroxide ($Ca(OH)_2$). The hydraulic lime production differs from Portland cement in the cooking time and in the quality of the clay[116]. Composites made with hydraulic lime show lower mechanical strength and a lower elastic modulus than cement-based materials, due to the lower reactivity of lime powder. However, the hydraulic lime-based materials are more breathable, thanks to their greater porosity.

In this work, Natural Hydraulic Lime NHL5 provided by Fornace Brigliadori, Sant'Arcangelo di Romagna (RN), Italy (Figure 3.4.1), has been used for the realization of pastes.according to UNI EN 459-1:2010.

Figure 3.4.1 Natural Hydraulic Lime NHL5

3.4.2   **Aggregates**

The *aggregate* can be defined as "inert", because it does not contribute to the chemical reactions of the hardening process (such as hydraulic binders), but it forms the main framework of the material, held together by the binder paste.

The aggregate used in this research for the realization of mortars, is a *Calcareous sand*, CA 400 (Figure 3.4.2) with a grain size less than 3mm kindly provided by Gola della Rossa Mineraria Spa, Serra San Quirico (AN), Italy.
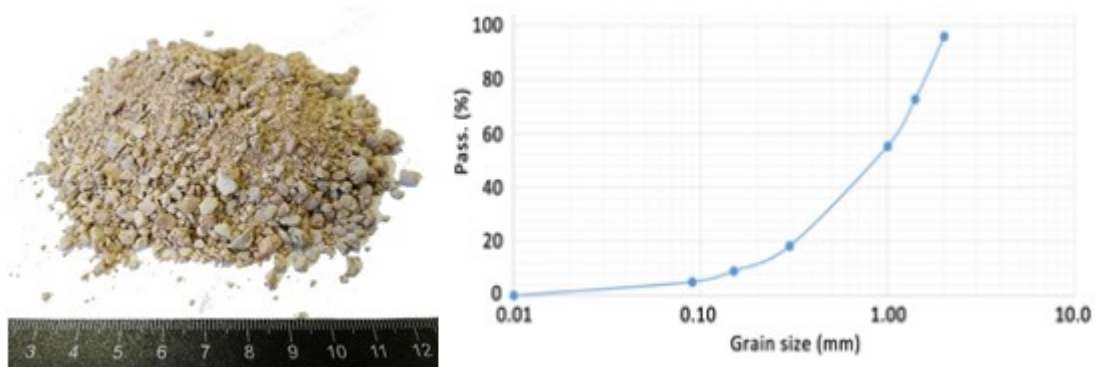
Figure 3.4.2 CA 400 calcareous sand and its grain size distribution

The humidity of the aggregate is an important factor for the realization of cement composites, because it can modify the composition ratios of the mixture[108]. For this reason, it is advisable to consider an aggregate in a *Saturated* Surface *Dry Surface* (SSD condition)[117,118].

3.4.3   **Fibers**

In this dissertation cellulose fibers of different origins are discussed, in order to evaluate their influence in the mixture. The different tested cellulose fibers have been chosen with dimensions comparable to the fibers recovered from WWTPs.

Some properties of fibers are essential for the calculation of the mix design as their apparent density and the water absorption.

3.4.3.1   *Pure cellulose fibers (CP)*

Arbocell B400 (Figure 3.4.3) are highly cellulose fibers provided by J. RETTENMAIER & SOHNE (JRS). These fibers have an average length of 900 µm and an average thickness of 20 µm.
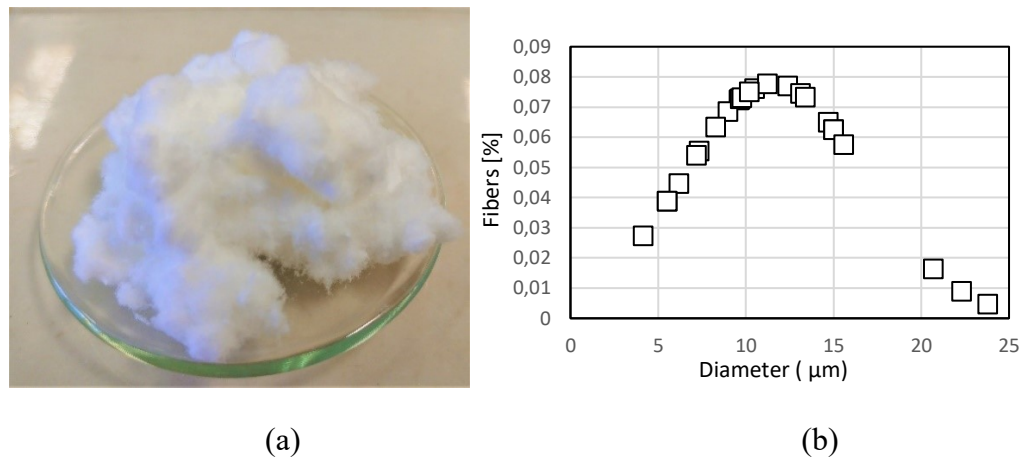
Figure 3.4.3 a) Pure Cellulose fibres; b) Fibres distribution

The results obtained by the Scanning Electron Microscope (SEM) (Figure 3.4.4) microstructural analyzes and the EDAX analysis (Table 3.4-1) (performed with a ZEISS 1530-Carl Zeiss, Oberkochen, Germany equipped with a Schottky emitter) permit to evaluate the average diameter, the aspect of the fiber and the elementary composition.. In particular, the aim of EDAX analysis is to investigate on the presence of different element from carbon (C), hydrogen (H) and oxygen (O) that compose the chemical backbone. The aspect of this type of fibers appears smooth and uniform: the average diameter is 11.6 µm with a high presence of calcium (Ca) and sulphur (S). The amount of water absorbed by cellulose fibers to reach the Saturated Surface Dry (SSD) is 63% and the calculated apparent density is 0.47 g cm^{-3}.
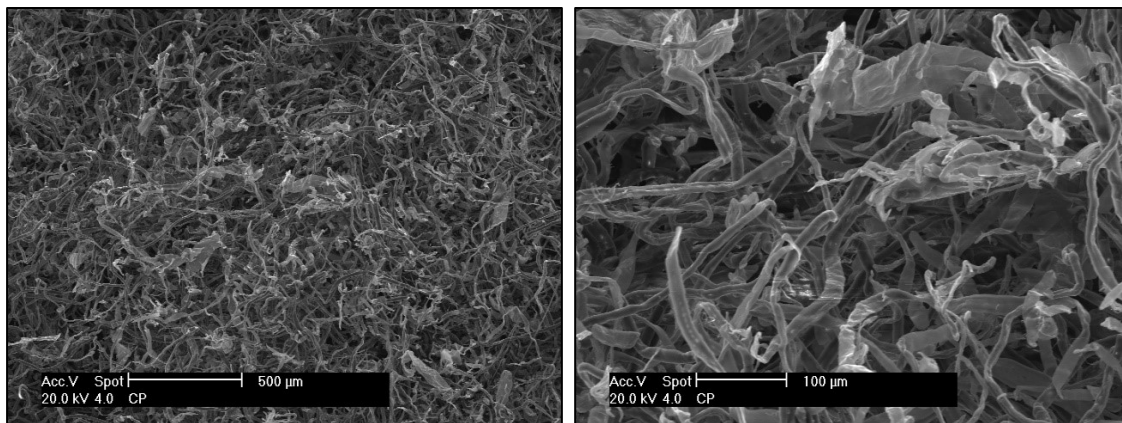
Figure 3.4.4 SEM analysis of Pure Cellulose fibres

Table 3.4-1 EDAX analysis of Pure Cellulose fibres

Element	Weight [%]
Al	17.74
Si	-
S	10.94
K	-
Ca	71.32
Fe	-
Total	100

3.4.3.2   *Recycled cellulose fibers (CRIC)*

Arbocell ZZC 900 *(*Figure 3.4.5) are technical raw cellulose fibers coming from the recycling process of papers provided by J. RETTENMAIER & SOHNE (JRS). These fibers have an average length of 1000 µm and an average thickness of 45 µm.

(a)   (b)
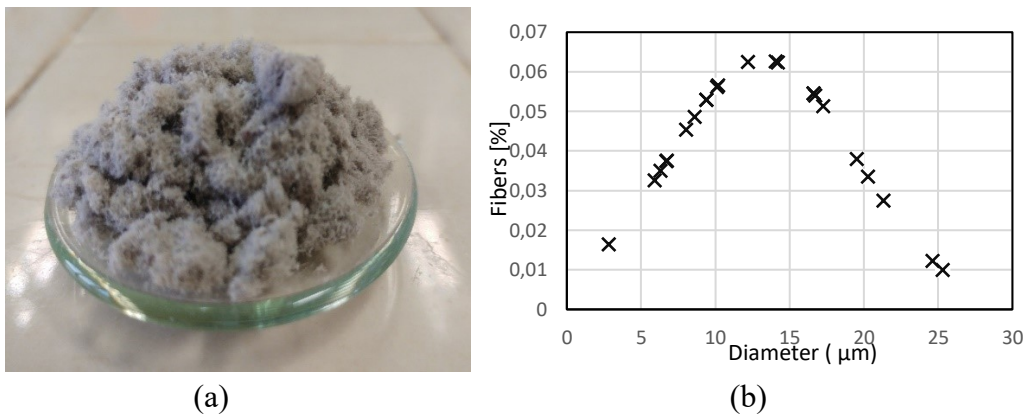
Figure 3.4.5 a) Recycled Cellulose fibres; b) Fibres distribution

The aspect of recycled fibers appears rough and inhomogeneous (Figure 3.4.6)*,* with the presence of white ribbons on the structure. This is the usual structure of fibers after chemical and physical process, typical of recycling treatments, that cause hornification of the fibers structure[119–123]. The average diameter is 13 µm and, from the EDAX analysis (Table 3.4-2), with a very high presence of calcium (Ca) and silicon (Si) probably due to the recycling process. The amount of water absorbed by cellulose fibers to reach the Saturated Surface Dry (SSD) is 78% and the calculated apparent density is 0.39 g cm^{-3}.
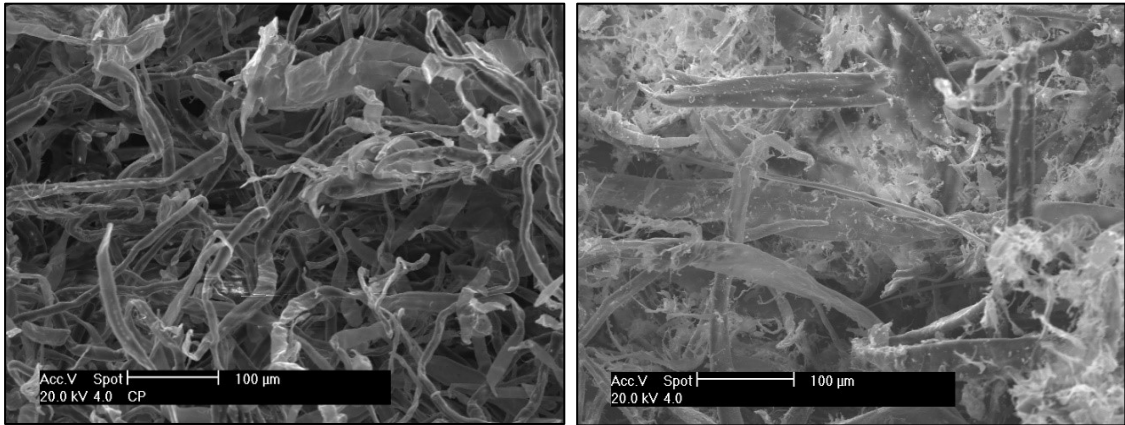
Figure 3.4.6 SEM analysis of Recycled Cellulose fibres

Table 3.4-2 EDAX analysis of Recycled Cellulose fibres

Element	Weight [%]
Al	7.4
Si	43.98
S	-
K	-
Ca	48.61
Fe	-
Total	100

3.4.3.3   *Recovered cellulose fibers (CREC)*

These recovered cellulose fibers (Figure 3.4.7) are provided by CirTec BV. CirTec BV is a partner of SMART-Plant Project (smart-plant.eu) and its core business is the recovery of cellulosic fibers from WWTPs using Rotating Belt Filtration (RBF) units in industrial scale with the same configuration of the demonstrative plants of Falconara and Carbonera. The length of CREC is 1000 μm, measured according to literature[15].

(a)   (b)
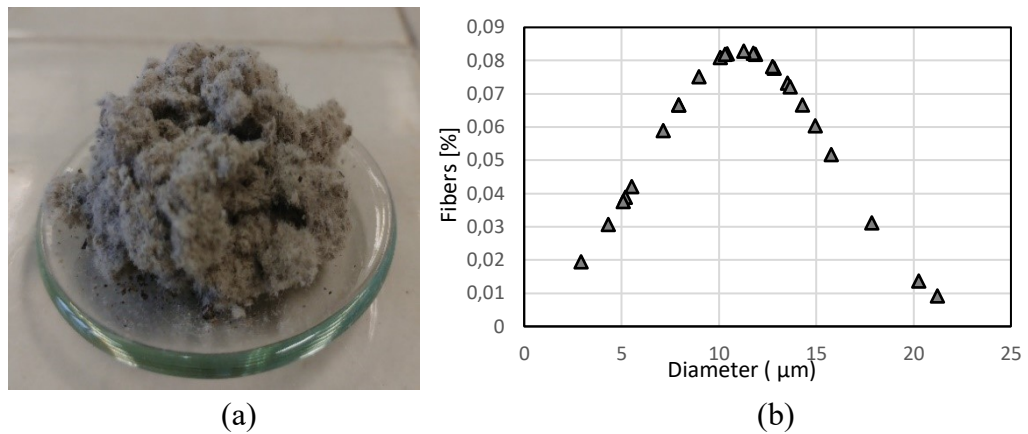
Figure 3.4.7 a) Recovered Cellulose fibres (CREC); b) Fibres distribution

The aspect of recovered fibers is homogeneous, but with the presence of small impurities due to the origin and the recovery process in the WWTP (Figure 3.4.8). In this case, there are no white ribbons on the structure, meaning that the recovery process does not change the chemical composition in lignin, hemicellulose and cellulose of the fiber, respect to the recycled filler[119–123]. The average diameter is 11.1 µm and, from the EDAX analysis (Table 3.4-3), various element because of the recover process are present. Calcium (Ca), iron (Fe), potassium (K), sulphur (S) and silicon (Si) are usually present in the effluent in form of salts, ions or other inorganic compounds. The amount of water absorbed by these cellulose fibers to reach the Saturated Surface Dry (SSD) is 119% and the calculated apparent density is 0.46 g cm^{-3}.
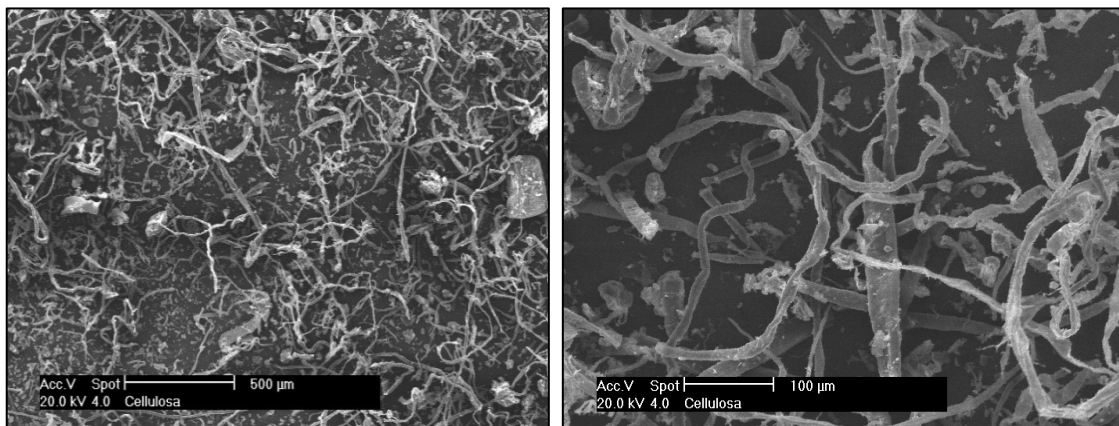
Figure 3.4.8 SEM analysis of Recovered Cellulose fibres from WWTPs

Table 3.4-3 EDAX analysis of Recovered Cellulose fibres from WWTPs.

Element	Weight [%]
Al	0.88
Si	2.03

S	0.16
K	1.01
Ca	94.11
Fe	1.81
Total	100

3.4.4   **Mortars**

Pastes have been manufactured with a water/cement = 0.63 and an aggregate/cement = 3 by weight in order to reach a stiff consistency (UNI EN 1015:3-2010) for all the mixes. Different mortar mix designs have been compared both by adding increasing dosages of CREC fibers and by using pure fibers (CP) and by recycled ones (CRIC) from newspapers in the same proportions.As reference (REF), a paste without filler (0%) addition is prepared. Fibers have been added in the mortar mix at 5%, 10%, 15% and 20% by mortar volume[124,125]. Mix proportion and workability of pastes are reported in Table 3.5-1. To better disperse each fiber addition, fillers are added gradually and in SSD condition to the mix.

Table 3.4-4 Mix Design (g/L) and Workability results

Specimen	Units	Water	NHL5	CA400	CP	CRIC	CREC	Slump(cm)
Reference	*g*	295	467	1402	0	0	0	118
CP 5%	*g*	281	445	1335	22	0	0	118
CRIC 5%	*g*	281	445	1335	0	19	0	117
CREC 5%	*g*	281	445	1335	0	0	22	117
CP 10%	*g*	268	425	1274	43	0	0	108
CRIC 10%	*g*	268	425	1274	0	35	0	115
CREC 10%	*g*	268	425	1274	0	0	42	115
CP 15%	*g*	256	406	1219	61	0	0	108
CRIC 15%	*g*	256	406	1219	0	51	0	107
CREC 15%	*g*	256	406	1219	0	0	60	111

CP 20%	*g*	246	389	1168	78	0	0	107
CRIC 20%	*g*	246	389	1168	0	65	0	111
CREC 20%	*g*	246	389	1168	0	0	77	109

NHL5 has been initially mixed with sand and cellulose to obtain a homogeneous matrix, water has been subsequently added and the blend mixed for 3 minutes. In all mixes, aggregate and fibers have been added in SSD condition. The addition of fibers may cause the formation of agglomerates in the paste, for this reason it is extremely important to add the fibers gradually, taking care to mix the paste properly, allowing the homogeneous dispersion of the fibers in the mix.

Mortar specimens have been cured at T = 20 ± 2 °C and RH = 95 ± 3% for 7 days and then at T = 20 ± 2 °C and RH = 50 ± 3% for the following 21 days before testing, according to UNI EN 1015-11:2007.

All the mortars have been characterized in fresh and hardened conditions in order to investigate on the effect of filler additions.

3.5   Methods

3.5.1   Fresh mortars characterization

3.5.1.1   *Workability*

The workability of the pastes has been evaluated by means of slump test to the *flow table*, according to UNI EN 1015-3:2007 standard.
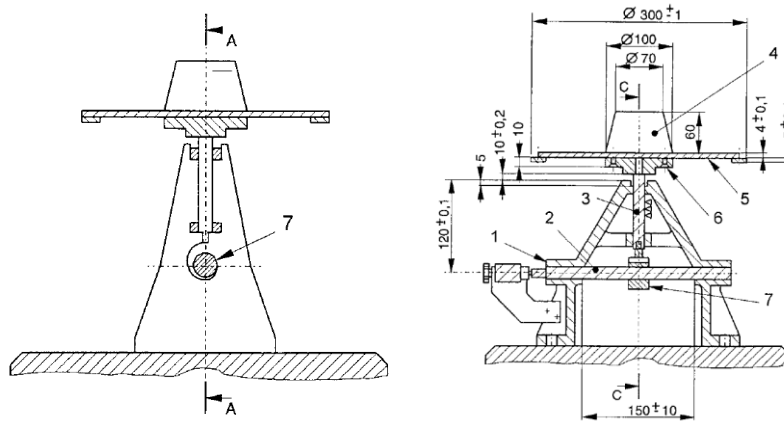
Figure 3.5.1 Schematic structure of the flow table apparatus, UNI EN 1015-3:2007

The test evaluates the *percentage consistency* (C%) of the fresh mixture by measuring the expanded diameter of the sample after 15 bumps at the flow table, through Equation 7:

$$C(\%) = \frac{d_f - d_i}{d_i} \cdot 100 \qquad \text{(Equation 7)}$$

Where d_f = sample diameter after 15 bumps; d_i = initial diameter of the sample (100 mm).

The results (Table 3.5-2) show that all pastes reach a stiff consistency according to UNI EN 1015-3:2010.

Table 3.5-1 Flow values and C% of pastes (UNI EN 1015-3:2007)

Mixtures	Flow value (mm)	C (%)
Reference	118	18
CP 5%	118	18
CRIC 5%	117	17
CREC 5%	117	17
CP 10%	108	8
CRIC 10%	115	15
CREC 10%	115	15

CP 15%	108	8
CRIC 15%	107	7
CREC 15%	111	11
CP 20%	107	7
CRIC 20%	111	11
CREC 20%	109	9

3.5.2   Hardened mortars characterization

3.5.2.1   *Microstructural characterization*

In order to correlate the obtained results with microstructure, *mercury intrusion porosimetry* (MIP) has been performed using a *Thermo Fisher 240 Pascal* porosimeter to analyse the pore distribution and the total porosity volume (V_p) of pastes (Figure3.5.3a). Three small fragments for each composition have been tested after 28 days of curing and the average results are reported. Moreover, Scanning Electron Microscopy (SEM) observations have been performed using a SEM PHILIPS XL20 equipment (Figure 3.5.3*b*) on small pieces of graphite coated paste specimens after 28 days of curing.
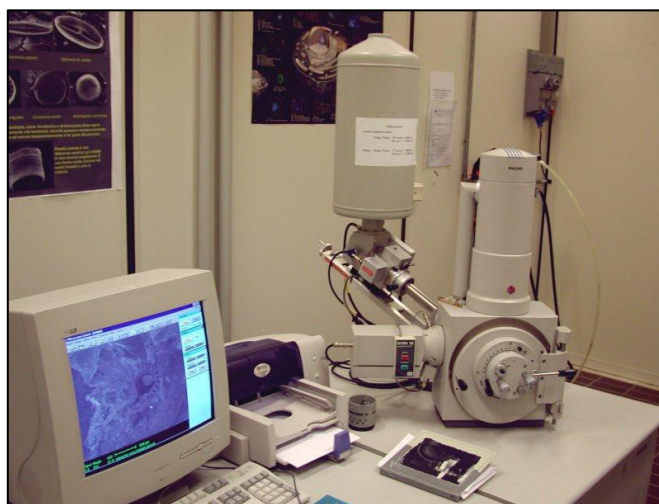
(a)   (b)

Figure 3.5.2 Instrumentation for microstructural characterization: a) Mercury intrusion porosimeter, b) Scanning electron microscope (SEM)

3.5.2.2   *Mechanical properties*

After 28 days of curing, the density (ρ, in g dm^{-3}) of hardened mortars has been calculated according to UNI EN1015-11:2007.

Compressive and flexural strength (R_c and R_f) tests have been carried out on at least three prisms (40 mm x 40 mm x160 mm) according to the Italian standard UNI EN1015-11:2007 using a 'Galdabini' hydraulic press (Figure 3.5.4) with a precision of 1% and equipped with load cells. The average results of three specimens for each mix has been reported.

Figure 3.5.3" Gabaldini" Hydraulic press for mechanical tests

3.5.2.3   *Hygrometric behavior*

In literature[126,127] other cellulose-based fibers, as hemp, have improved the water vapour transfer and humidity storage capacities[128] of mortars. Therefore, these mortars, if applied as renders in indoor applications, have the potential to improve also the indoor microclimate, the comfort and health of occupants and allow to reduce the energy demand of building[129,130,131].

The mortars manufactured in this study could therefore influence the Indoor Air Quality (IAQ) positively in terms of water vapour permeability[132] and moisture buffering capacity (MBC)[110,133].

The interactions of the mortars with the environmental RH have been studied both in static (Water Vapour Permeability) and dynamic (Moisture Buffering Capacity) conditions.

3.5.2.3.1   Water vapour permeability

Water vapour permeability measurements have been carried out according to the UNI EN 1015-19:2007 to assess the water vapour transfer and humidity storage capacities of mortars as reported previously[126–128,134].

Cylindrical mortar specimens (d = 12.5 cm; h = 3.0 cm) have been placed on the top of a sample-holder with a saturated solution of potassium nitrate (KNO_3) inside (RH = 93 ± 3% at T = 20 ± 2 °C).

The containers have been placed in a climatic chamber at T = 20 ± 2 °C and RH = 50 ± 5% and the test started. On the side surface, the specimens have been sealed with a non-breathable film in order to guarantee the unidirectional flow of the water vapour from inside to outside, due to the difference of RHs.

The mass of the specimens has been monitored day by day until stationary conditions were achieved. The average results of the test are reported in terms of the water vapour diffusion resistance factor, **μ** (defined as the ratio between the vapour permeability of stagnant air δa (kg $(Pams)^{-1}$) and the vapour permeability of the material δp (kg $(Pams)^{-1}$) at the same temperature and pressure[68,135]).

Furthermore, if applied as renders in indoor applications, these mortars also have the potential to improve indoor microclimate and consequently the comfort and health of occupants[129–131].

3.5.2.3.2   Moisture Buffering Capacity

The moisture buffering value (MBV) quantifies the capacity of a material to absorb and release moisture from/to the environment where it is placed.

In this dissertation, the influence of cellulose fibers on MBV of mortars has been assessed by a simplified version of the NORDTEST method[136] where specimens have been cyclically exposed to different relative humidity (RHs) for fixed periods.

The exposure to different RHs has been carried out by placing the specimens inside two boxes containing a saturated solution of magnesium chloride ($MgCl_2$, RH = 33%) and sodium chloride (NaCl, RH = 75%), respectively. The boxes have been kept inside a climatic chamber to maintain the temperature constant at 20 ± 2 °C.

 Four cycles have been carried out. The amount of water vapour absorbed or released by the specimens during each step has been determined by measuring the weight of the specimens before changing boxes. The practical MBV (g $(m^2\% RH)^{-1}$) was calculated as the amount of moisture changed by the material per surface unit and RH gradient[68].

3.6   **Results and Discussion**

3.6.1   **Correlation between microstructural analysis and mechanical performances**

The use of fibers coming different types of woods and\or origin in composites, is already well investigated in literature, and from these previous studies is evident that the fiber composition in terms of presence of cellulose, hemicellulose and lignin is determinant for the performances of the composite.

During processes as purification or paper recycling, the wetting ability of fibers decreases, resulting in a decrease in fiber plasticity, paper tensile, burst index and an increase in brittleness[96,120,122] . This deterioration of the properties is mainly due to the irreversible structural changes in the fiber wall caused by the pulping method, drying condition and the amount of non-cellulosic concomitants (hemicellulose, lignin and extractives)[122].

For this reason, it is fundamental to consider the microstructural aspect of the fiber, in order to understand how its structure may interact with the other components of the composite.

In this case, there are gradual differences between the three different fiber: in fact, observing the fibers in Figure 3.6.1, Figure 3.6.2 and Figure 3.6.3, it is evident that CRIC is highly different from CREC because of the presence of white ribbons (a specific formation that highlights the hornification of the fiber[106,107,108]), but the structure of CP is in an intermediary state between the other two. In fact, CP presents the main fiber structure as CREC, but there is also the sporadic presence of white ribbons, probably due to the purification process.

The addition of fibers generally decreases the workability of mortars[137] as in this case. However, despite the differences in fibers microstructure (Figure 3.6.1, Figure 3.6.2 and Figure 3.6.3), all mortars belong to the same workability class equal to stiff (according to UNI EN 1015-6:2007) .
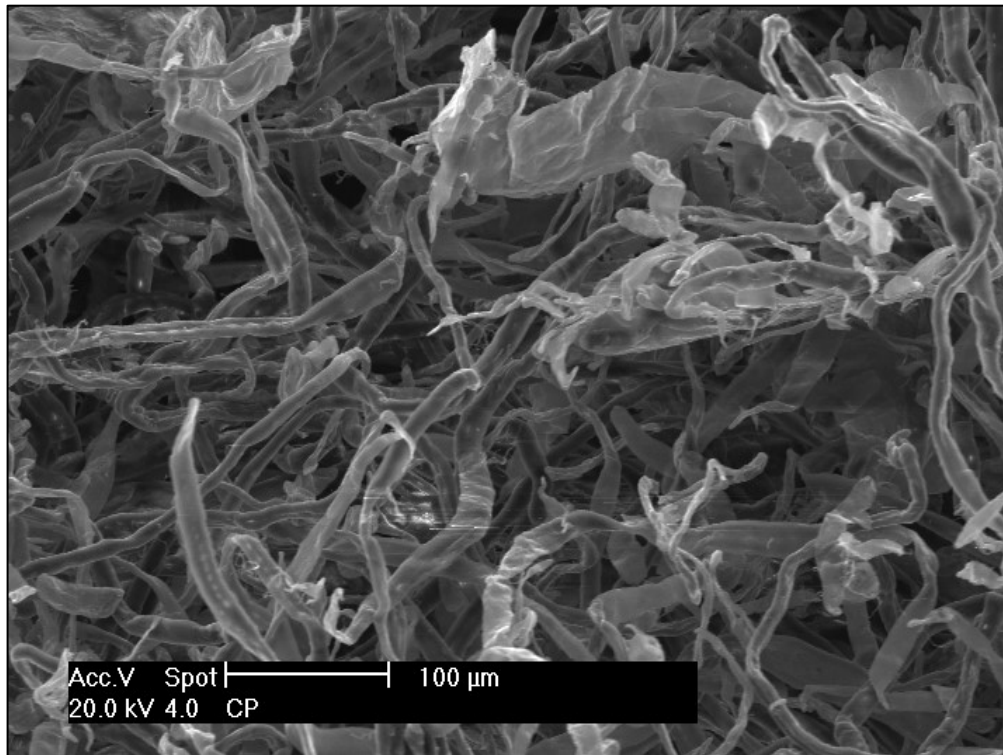
Figure 3.6.1 Pure Cellulose
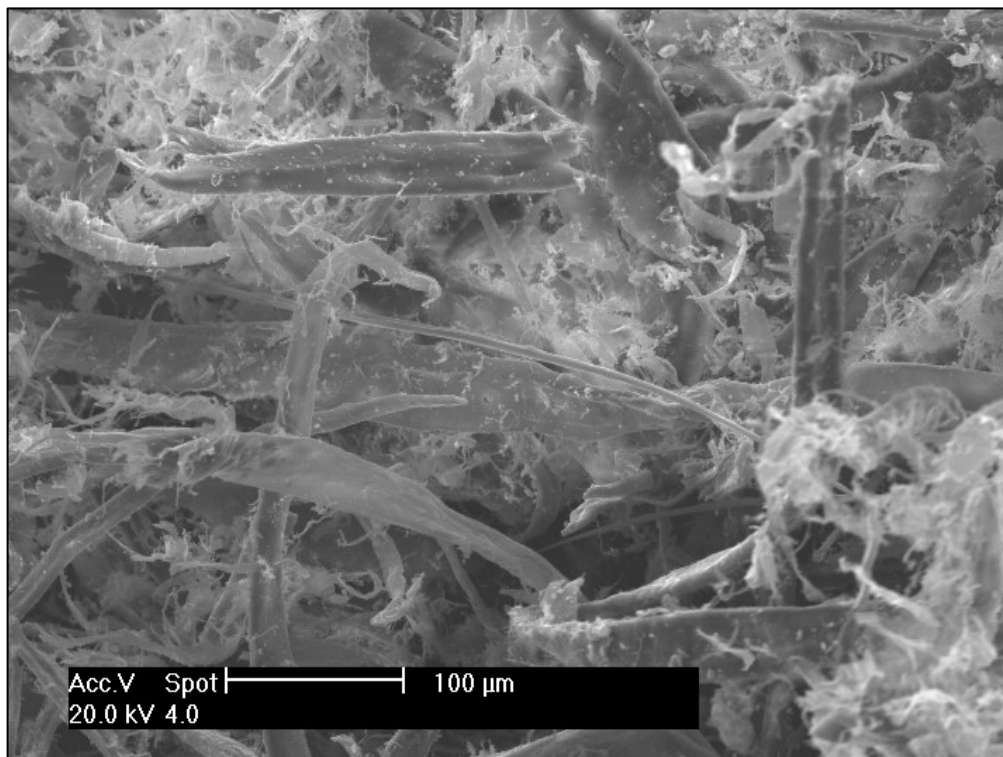
Figure 3.6.2 Recycled Cellulose
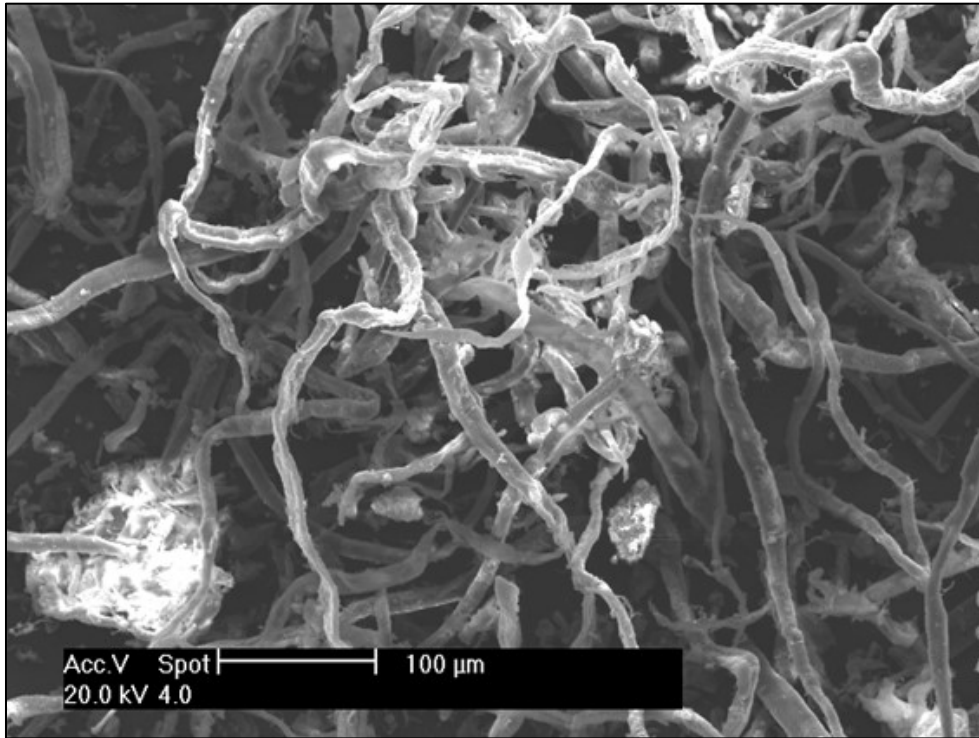
Figure 3.6.3 Recovered Cellulose

In mortars, agglomerates of fibers may form during the mixing process; however, SEM observations of mortars show a good dispersion of cellulose fibers, regardless their origin (Figure 3.6.1, Figure 3.6.2 and Figure 3.6.3).

Moreover, more particles of binder paste are present on the surface of CREC fibers, than in CP and CRIC fibers. More adhered paste particles suggest a better adherence between fibers and matrix. This gives a better Interfacial Transition Zone (ITZ) as shown in Figure 3.6.4, Figure 3.6.5 and Figure 3.6.6, where the limit between fibers and paste is less evident than in other mortars.

The best adherence of CREC fibers to the binder paste could be due to their rougher surface as observed in Figure 3.6.3. It is well known that a rougher surface gives a better adherence of fibers to the binder paste[66,115,138–143]. Moreover, in CRIC fibers the pulping method induces irreversible structural changes in the fibers by reducing the hemicellulose and lignin content[119,123]. Hemicellulose consists of highly hydrophilic polysaccharide chains, which are the main contributor to water absorption[143]. It has been reported[120] that, as a consequence, also the wetting ability, plasticity, ductility, stiffness and tensile strength of fibers decrease and they tend to collapse into ribbons and flocks.
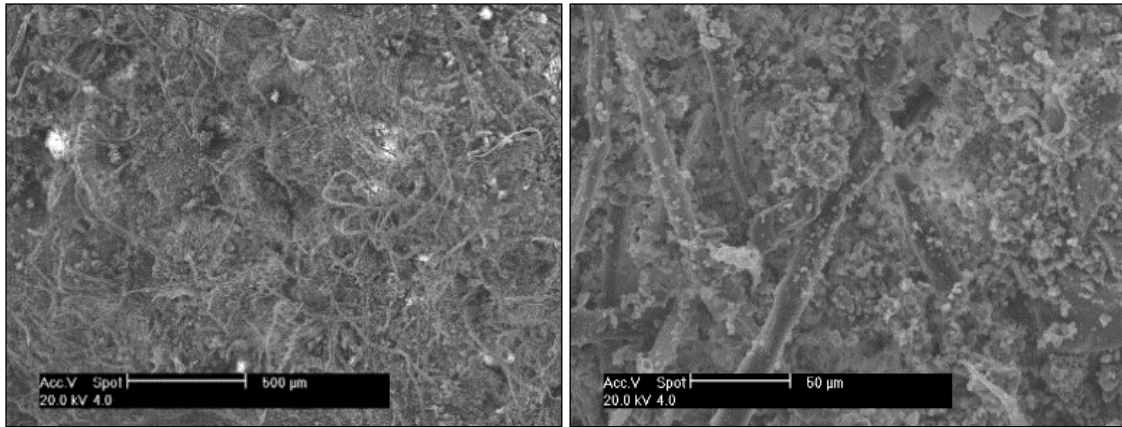
Figure 3.6.4 SEM observation of mortars with 20% of CP fibers additions
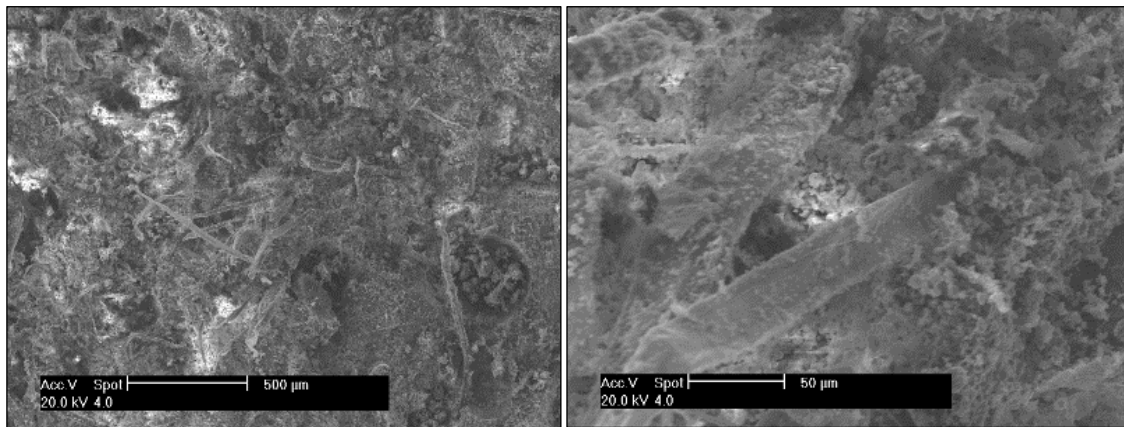
Figure 3.6.5 SEM observation of mortars with 20% of CRIC fibers additions
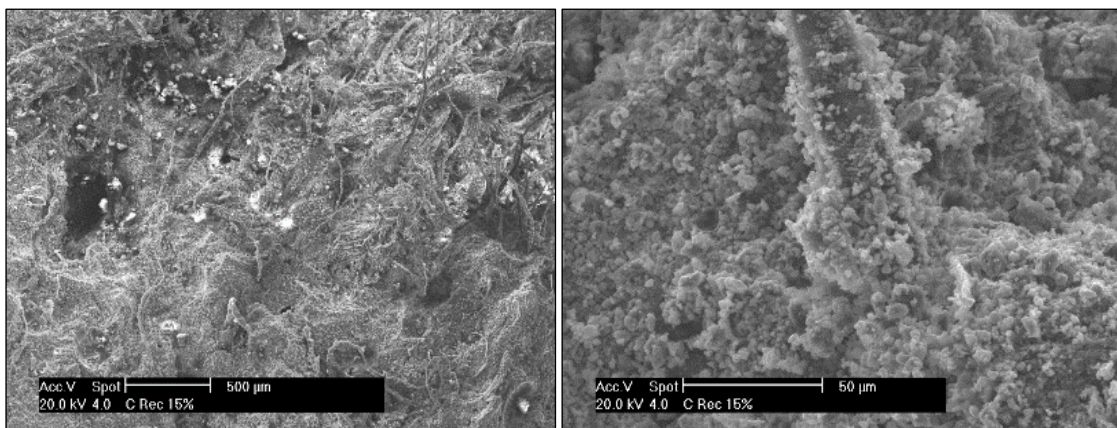
Figure 3.6.6 SEM observation of mortars with 20% of CREC fibers additions

Higher amount of cellulose fibers causes higher presence of pores and an increase in their diameters in mortars. Specifically, the total accessible porosity increases from 31% (REF) to 34% (CREC 20%), 36% (CP 20%) and 37% (CRIC 20%). Whereas the REF mortar

shows a unimodal pore size distribution, mortars with fibers have a bi-modal pore size distribution with the second peak moving to bigger pores, especially for CRIC, as reported in Figure 3.6.7. This is due to the porous structure of added cellulosic fibers and the additional ITZ between fibers and binder paste[143,144].
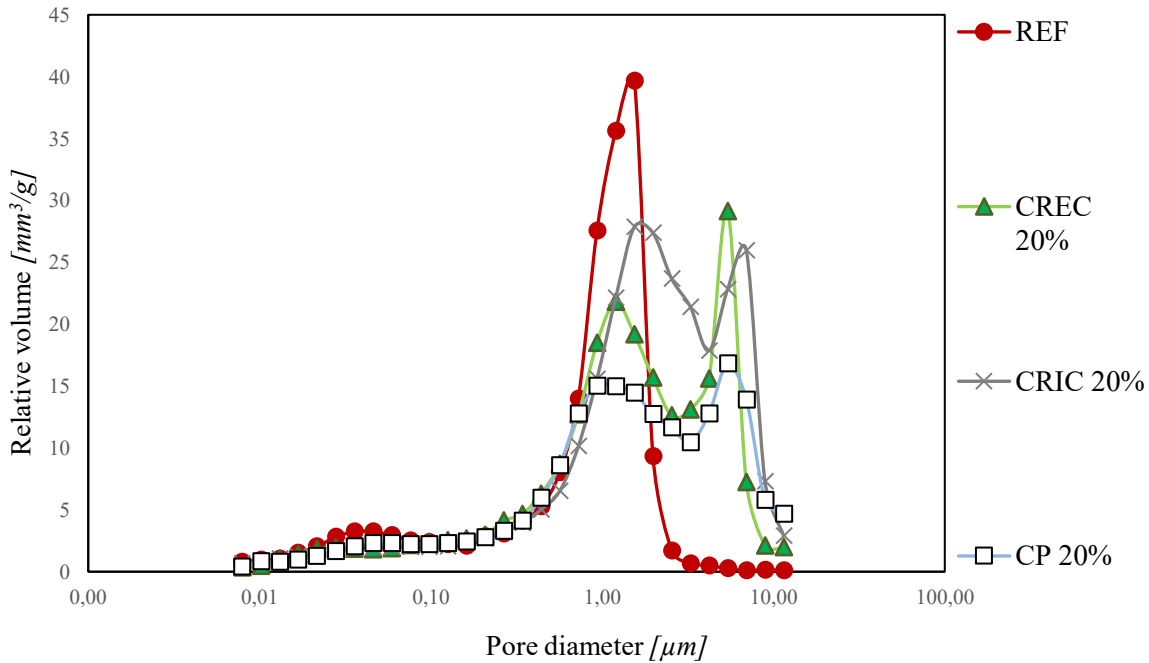
Figure 3.6.7 Pore size distribution of mortars with 0% and 20% of cellulose fibers addition

As expected, an increased addition of fibers, the lightest ingredient of the mortars, by increasing porosity and reducing the binder paste content, gives a reduction in density as reported in Figure 3.6.8.
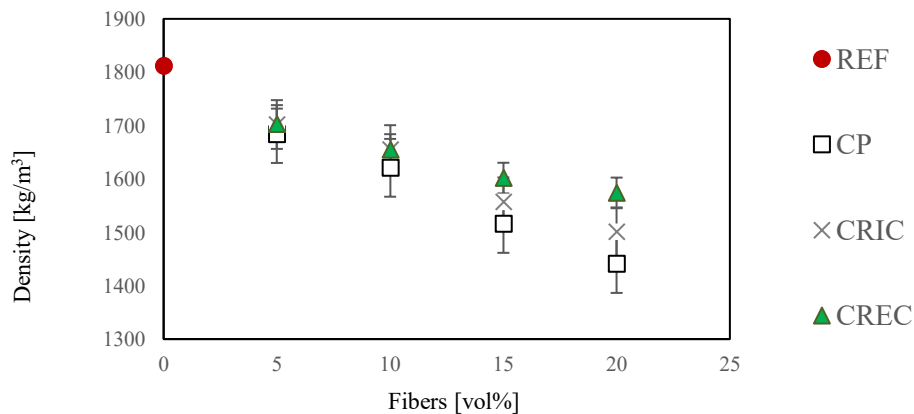
Figure 3.6.8 Density of different mortars

Consequently, an increased addition of fibers gives a reduction of the compressive strength of the composites.

For 20% added cellulose, the compressive strength of mortars reaches the 26% (CP), 32% (CRIC) and 46% (CREC) of the value of the reference mortar (REF) (Figure 3.6.9). The addition of fibers, by inducing more voids, lighten and weaken the material[145].

Anyway, at the 20% fibers addition the residual R_c is most elevated in CREC mortar probably due to the best adhesion of the binder paste on CREC fibers as highlighted in the SEM observations (Figure 3.6.4, Figure 3.6.5 and Figure 3.6.6).
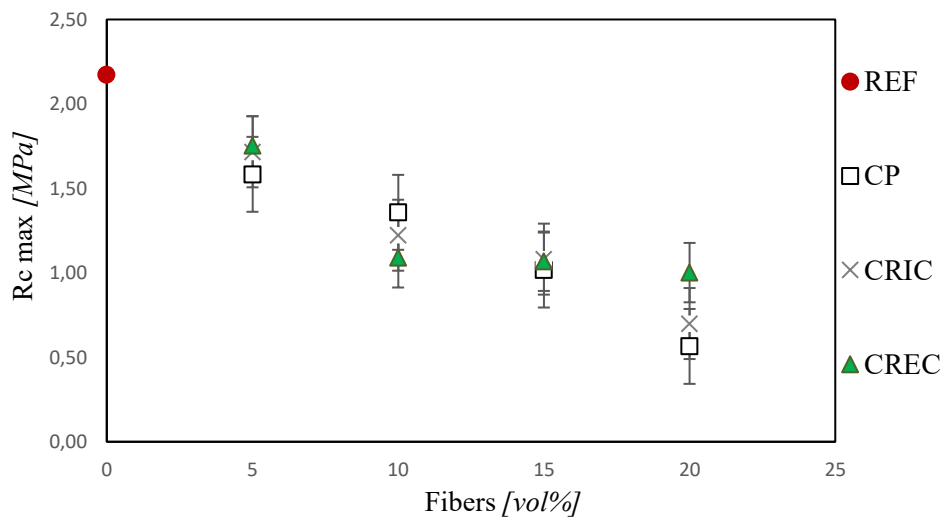
Figure 3.6.9 Compressive strength (R_c) of different mortars
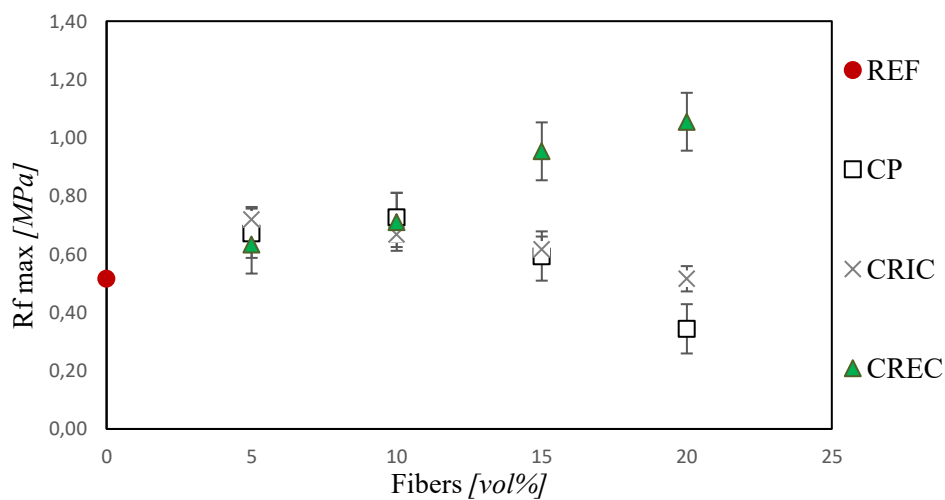
Figure 3.6.10 Flexural strength (R_f) of different mortars

Usually fibers improve the flexural behavior of mortars thanks to the bridging effect that increases the resistance to crack propagation of brittle matrices [134,146]. However, in this case, the addition of cellulose fibers by reducing the binder content also lighten and increase porosity and therefore weak the composite. For these reasons, despite of the type of the fiber, beneficial effect in terms of R_f was found until 10% of fibers addition (Figure 3.6.10) when the bridging effect overcomes the weakening effect. At higher dosages of CP and CRIC, R_f starts to decrease and at 20% of cellulosic addition become comparable (CRIC) or even lower (CP) compared to REF.

Differently, despite the reduction in density and in R_c values, for CREC mortars the flexural strength (Figure 3.6.10) always increases with fiber additions, up to 200% at 20% of cellulose addition. This is due to their higher aspect ratio and better adherence between the binder paste and CREC fibers compared to CRIC and CP fibers, as already observed and discussed, respectively. It is well known that both a higher aspect ratio and higher adherence of fibers enhance their bridging effect against cracks propagation in mortars.

3.6.2   **Hygrometric behavior: Water Vapour Permeability and Moisture Buffering Capacity**

Reduced water vapor permeability is a negative factor in mortars since it does not allow proper drying of penetrating water and impairs the elimination of water vapor that occurs within buildings. In Table 3.6-1 water vapor resistance factor (μ) of all the mixes has been reported: REF has the highest value of μ and the addition of cellulose fibers always decreases, even if slightly, the μ of mortars. A low value of μ indicate higher values of permeability. The cellulose fibers addition in mortar implies an increase in critical pore size and total open porosity. According to Poiseuille's law, permeability depends on open porosity and connected pores size[147]. For these reasons, the most permeable mix is CRIC 20%, that has the highest open porosity and shifted to highest diameters.

Table 3.6-1 Comparison of $\bar{\mu}$ and MBV results of different mortars

Specimen	μ	MBV [g/m²·%UR]
REF	11.2	0.07
CP 5%	11.0	0.11
CP10%	10.9	0.13
CP 15%	10.0	0.13
CP20%	9.5	0.15

CRIC 5%	10.7	0.10
CRIC 10%	10.0	0.11
CRIC 15%	9.9	0.11
CRIC 20%	8.9	0.11
CREC 5%	10.2	0.12
CREC 10%	10.1	0.13
CREC 15%	10.0	0.15
CREC 20%	9.7	0.17

The higher transpiration of mortar gives a higher moisture penetration depth[148] that implies a higher MBV[149,150] ; which improves the human health in indoor applications. MBV increases also with hygroscopic materials as those cellulose based[136,148] thanks to their structure composition. Regardless the type of cellulose fibers considered in this study, MBV of mortars slightly increase with their addition. This is true especially for CREC mortars perhaps due to their higher affinity to water compared to CP and CRIC fibers where the submitted previous treatments have decreased their wetting ability as already discussed in Section 3.6.1.

3.7   **Sustainability and assessment of cellulose recovery**

In the last years, the recovery and reuse of cellulosic material interest new and emerging economic sectors. In general, nine categories of cellulose-based products could be identified as textile, non-woven, wood and timber, pulp/paper and board, cellulose dissolving pulp, cellulosic films, building materials, cellulosic fiber composites and green chemicals. Considering the characteristics of the cellulose in the wastewater and the market possibilities, fine sieved fraction separated by dynamic filter represents an innovative opportunity [14]. Several international projects were developed in this direction highlighting that the fine-screening of influent would provide specific operative cost of 53W/m^3 with significant positive contribution to WWTPs processes further along the treatment chain by making wastewater treatment more efficient and result in a product (mainly cellulose) that could be recovered and valorized (i.e. EU Screencap (screencap.eu), H2020 SMART-Plant (smart-plant.eu)). The recovered cellulose can be used as raw material for new paper products, adhesion binders for asphalts or as fibrous reinforcement material in bricks after properly separation and refining[16,113,151]. The use of

natural fibers as the adsorbent is another emerging trend in environmental engineering[152,153]. However, the choice of the specific applications and the recovery market sectors request inlet materials with diverse standards based on the available amounts and the final productive application. Therefore, the sustainability of the recovery needs to be supported both by global mass balance of the recovered potentiality and by functional tests for the final reuse. Given the promising results obtained from the experimentation and, given the eco-sustainable structure of this work, it is decided to consider also the impact that these pre-mixed mortars could have on the market. This point of view is necessary to understand the feasibility of a possible start-up of this product, for this reason, the preliminary study is carried out referring to plants and companies in the Italian territory and, more specifically, from the Marche region.

The experimental results show that CP fibers can be replaced by CREC fibers in mortars to improve their lightweight, flexural behavior, hygrometric properties and to reduce their capillary water absorption. The use of recovered cellulose in mortars not only permits the waste-resource valorization, but also limits the environmental impact derived using pure cellulose. The CREC fibers production is experimentally determined and fitted in a previous experimental study based on the WWTPs of Falconara and Carbonera (province of Ancona and Treviso , Italy)[154]. Consequently, considering the data reported by this study on real scale, based on the same technology used by CirTec B.V., the potential recovering of cellulose fibers coming from this plant could be predicted equal to 9.2 grams of cellulosic material for m^3 of influent wastewater. Indeed, in a territorial application with medium size wastewater treatment plant (50.000 PE) and large size wastewater treatment plant (150.000 PE), the recoverable theoretical material is estimated respectively in the range from 110 kg per day to 331 kg per day. To obtain 1 ton of mortar with 5% of cellulose fibers by volume, 7.80 kg of CP, 6.18 kg of RIC and 5.82 kg of REC are needed. From this point of view, a hypothetical medium size WWTP (50.000 PE) plant could supply a daily production from 102 to 356 sacks per day of pre-mixed mortar with respectively 20% and 5% of REC fibers by volume; whereas a large size WWTP (150.000 PE) plant from 305 to 1069 sacks per day, respectively. Referring to a small-medium company producing cementitious products, such as Diasen srl (Sassoferrato, Province of Ancona, Italy), 800 sacks per day of 25 kg pre-mixed mortar are produced, so it is possible to satisfy this type of need.

This preliminary investigation on the production of pre-mixed mortars shows very promising results and it seems to be practicable not only for the recovering of cellulose from WWTPs, but also for the production of the pre-mix in a middle size company for both of the considered mixes. The use of this pre-mixed mortars would permit a more ecological and sustainable choice for the environment transforming a waste in a resource and the production of a renewed product on the market, giving benefits to WWTPs and building construction companies.

Moreover, in indoor applications the improved lightweight, flexural behavior and hygrometric properties of CREC mortars enhance the IAQ with increased comfort and healthy for occupants: this permits to limit the use of conventional active systems as dehumidifiers or air-conditioning system which consume energy.

3.8   **Conclusion**

To investigate the possibility of valorising CREC coming from RBF of municipal wastewater in the building sector, CREC fibres have been characterized and added in hydraulic lime-based mortars at the amount of 0%, 5%, 10%, 15%, 20% by volume.

 Meanwhile, the properties of mortars manufactured with the same dosages of CP and CRIC fibers have been compared. The results showed that the use of CREC fibres in mortars not only allows to valorise a waste but even limits the environmental impact of adding CP fibre.

The obtained results further indicated that CREC fibers, as CP and CRIC fibers, slightly increased the water vapor permeability and the moisture buffering capacity of mortars. This implies an improvement in the human comfort and health if these mortars are applied as renders in indoor applications and a reduction in the use of conventional active systems, as dehumidifiers or air- conditioning systems, which consume energy.

As expected, all cellulose fibers, regardless their origin, lightened the mortars and reduced their compressive strength. However, thanks to their higher aspect ratio and better adherence to the binder paste, the residual compressive strength is most elevated in mortars with CREC fibers. Moreover, for the same reasons, the flexural strength increases with the addition of fibers only in mortars with CREC fibers.

Finally, a preliminary balance showed that a large size WWTP (150.000 PE) plant can supply a daily production from 305 to 1069 sacks per day of pre-mixed mortar with 20% and 5% of REC fibers by volume, respectively, that is the average production of a small-medium company producing cementitious products

4. Chapter

PLA-Cyclodextrins composites for air filtration systems

Preparation and characterization of an electrospun PLA-cyclodextrins filter for simultaneous high-efficiency PM and VOCs removal

.

4.1   **Introduction**

In section 1.2.2.1 starch is introduced as one of the main components pin the waste water of many agri-foods-industries, and company as Barilla or others corporations are investing on the recovery of this secondary material to reduce the food losses and wastes.

This chapter considers the possibility to use a well-known starch derivate called *Cyclodextrin (CyD)* as a component for air filtration systems with the purpose of blocking particulate matters and also molecules as volatile organic compounds (VOCs). This chapter is a preliminary step on the use of new materials as air filtrating systems.

In literature, previous researches have already worked on the synthesis of cyclodextrin and starch based polymers for sorption of azo dyes and other pollutants from aqueous solutions[71-74, 159–165.]. The results have demonstrated that they can be used for the removal of those pollutants, thanks to their particular structure which permits to block very small molecules[155,161]. Until now, cyclodextrins have been used as pharmaceutical carriers or for the removal of pollutants in wastewater[161,162], but never in indoor air treatments. For this reason, the attention has been focused on the possible applicability of CyDs in indoor air treatments and pure CyDs have been used in this preliminary step also to avoid the addition of other variables as the presence of impurities.

In particular, the attention is focused on the production of a filter made with electrospun fibres of polylactic acid (PLA) functionalized with cyclodextrins (CyD) in order to realize a new type of filter for the air pollution reduction in indoor environments. This type of filter has been designed to join the filtration of particulate matter (PM) with the adsorption of VOCs to increase the IAQ. Thanks to the electrospinning technique, the diameters of the produced fibres can be controlled, increasing the filtration area of the filter. The designing process of this innovative filtration system considers not only the needs in terms of low-cost materials for the replacement of the filter, but also the design requirements creating a hexagonal filter that can be modulable on panels for applications of different scales.

However, in this preliminary work for indoor air treatments, commercial cyclodextrins have been used. The obtained results, if promising, could be useful for further studies focusing on the actual use of cyclodextrins coming from wasted starch sources and on the evaluation of their purity level.

In the following sections, the fundamental concepts about the indoor air quality and the air filtration theory are presented, with a short description about why and how pollutants are dangerous for human health. Moreover, also the different categories of pollutants are introduced shortly.

4.2   The Indoor Air Quality

The Global Burden of Disease project puts air pollution as the fourth greatest risk after high blood pressure, dietary risks and smoking.

The risk is more linked to the concentration of pollutants integrated over time more than to the concentration of pollutants that can be detected. Since nowadays, most of the time is spent indoors, the presence of contaminants in indoor environments have an important impact on human health as in the "sick building syndrome" (SBS).

However, it might not be easy to achieve high level indoor air quality. The pollutants that spread into indoor environments come from a series of possible sources that are not easily recognizable, such as furniture, interior surfaces, paints, detergents, air fresheners, appliances, combustion, in addition to cigarette smoke, which is the source of a great variety of pollutants such as organic substances, formaldehyde and particulate matter of all sizes.

Furthermore, special emphasis placed on building "airtightness" by the building construction industry in order to improve the energy efficiency of buildings has made more difficult to obtain better indoor air quality through natural ventilation.

The air quality of the indoor environment is capable of affecting human comfort in a multitude of ways, depending on the contaminant. Airborne contaminants range from toxic substances such as carbon monoxide to nuisance matter such as large dust particles. The body is a complex interaction of numerous functions such as inhalation, digestion of food, and excretion of wastes. While all these functions are being performed, the human body fights off armies of pollutants through built-in defence mechanisms. Throughout this daily body functioning, the human body remains in a state of balance, known as homeostasis. Disease or illness occurs when the body's homeostasis is disrupted. Becoming ill is dependent on the interrelation of a variety of factors, such as the body's genetic makeup, the environment to which the body is exposed, and the degree of stress exerted on the body.

The most significant paths for air contaminants to enter the body are through:

• Inhalation;

• Skin absorption;

• Ingestion.

Most air contaminants enter the human body through the process of inhalation. The main function of inhalation is to provide oxygen to the body's cells and to remove excess carbon dioxide. It is easily understandable that, if the air reaches the alveoli (where the exchange between oxygen and carbon dioxide occurs) also some of the contaminants present in the air can reach them.

In 2009 the European Environment Agency reported a study about the expected changes on the health because of the impact of air pollution caused by particulate matter in terms of loss in statistical life expectancy (months), that can be attributed to anthropogenic contributions to PM2.5 for the year 2000 and for 2020[163].

This survey, reported in Figure 4.2.1, showed **a reduction in months life losses** from 2000 for all the European states, where almost all the countries with a reduction from 2 to 9 months changed to 2-4 months in 2020 with the maximum loss up to 6-9 months of loss[163]

Estimated losses in life expectancy attributable to exposure to fine particulate matter (PM2.5) from anthropogenic emissions for 2000 (left) and 2020 (right)
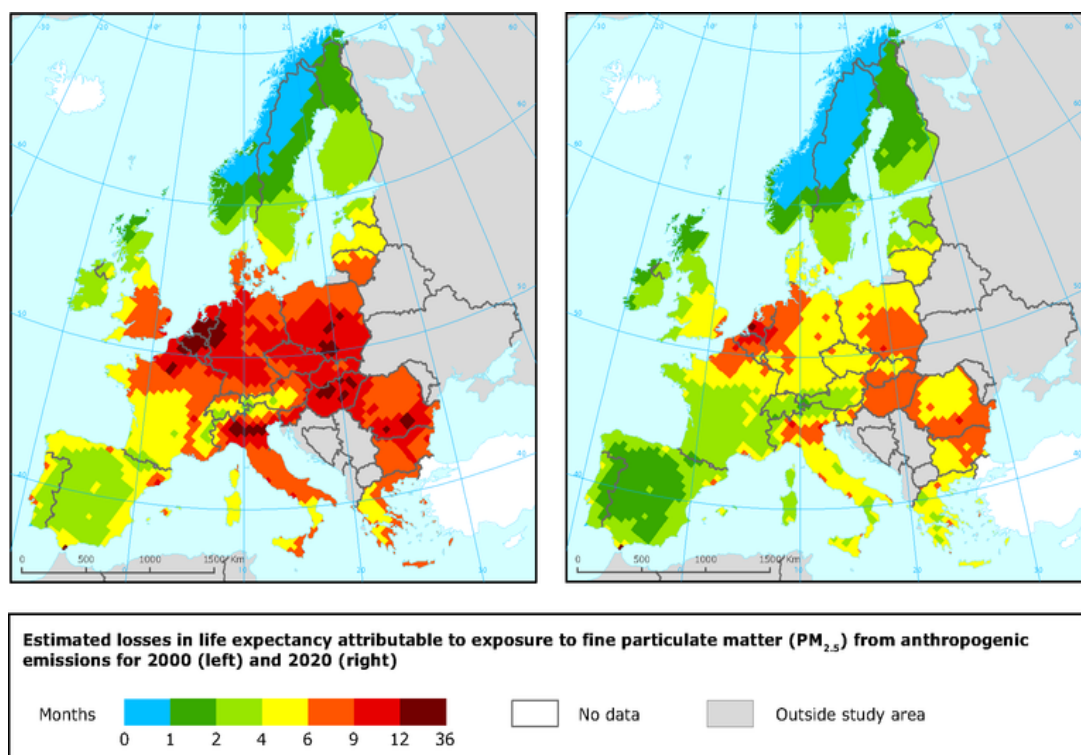
Figure 4.2.1 Estimated losses in life expectancy caused by the exposure of PM2.5 emissions for 2000 (left) and 2020 (right)

Fibres and particles greater than 5 μm (microns) in aerodynamic diameter which enter the respiratory system are generally intercepted by mucous, nose hair and cilia in the trachea.

Once trapped by these mechanisms, the particles are expelled from the body by coughing and sneezing.

Fibres and particles smaller than 5 μm in aerodynamic diameter are too small to be filtered by the respiratory defence systems. Particulate matter falling into this category are of concern due to their ability to by-pass the human defences and enter the lungs. The smaller the particle, the easier the passage into the human respiratory system and the greater possibility to cause harm[164].

4.3   Pollutant categories

The main change in the atmospheric composition is primarily due to the combustion of fossil fuels, used for the generation of energy and transportation. Air pollutants differ for their chemical composition, reaction properties, emission, persistence in the environment, ability to be transported in long or short distances and their eventual impacts on human and/or animal health[60,164].

4.3.1   Gaseous pollutants

Sulphur dioxide (SO_2), nitric oxide (NO_x), carbon monoxide (CO), ozone and Volatile Organic Compounds (VOCs) are some of the main pollutants present in the atmosphere.

Nitrogen oxides are emitted as NO, which rapidly reacts with ozone or radicals in the atmosphere forming NO_2. The main anthropogenic sources are mobile and stationary combustion sources. Moreover, ozone in the lower atmospheric layers is formed by a series of reactions involving NO_2 and VOCs, a process initiated by sun light. CO, on the other hand, is a product of incomplete combustion, majorly caused by road transport. While the anthropogenic SO_2 results from the combustion of sulphur-containing fossil fuels (principally coal and heavy oils) and the smelting of sulphur containing ores, volcanoes and oceans are its major natural sources[165].

Lastly, a major class are the *Volatile Organic Compounds (VOCs)* as Polycyclic Aromatic Hydrocarbons (PAHs). This class of molecules have multiple cycles, precluding benzene from being considered a PAH[165]. Benzene is a widely present volatile organic compound, the main source of which in the outside air is constituted by automotive gasoline. In indoor environments, benzene can be emitted by cigarette smoke and various possibly contaminated products, such as glues, adhesives, solvents, varnishes and paints. Benzene is one of those pollutants for which the policies adopted over the years have been successful, greatly reducing emissions and levels in the air. The fundamental actions carried out for the reduction of benzene are in the road transport sector, namely the introduction of the catalytic converter of the car fleet and the reduction of the benzene

content in fuels. Also in other sectors the reductions are evident, even if their relative weight on the total is in any case not very significant.

Figure 4.3.1 shows the trend of industrial emissions from 2007 to 2016 for the 33 member countries (including the EU-28 Member States, Iceland, Liechtenstein, Norway and Switzerland) reported by the European Environment Agency (EEA). In 10 years, the emissions from the industries have been considerably reduced, but the levels are still high due to the wide presence of these pollutants in every single sector.
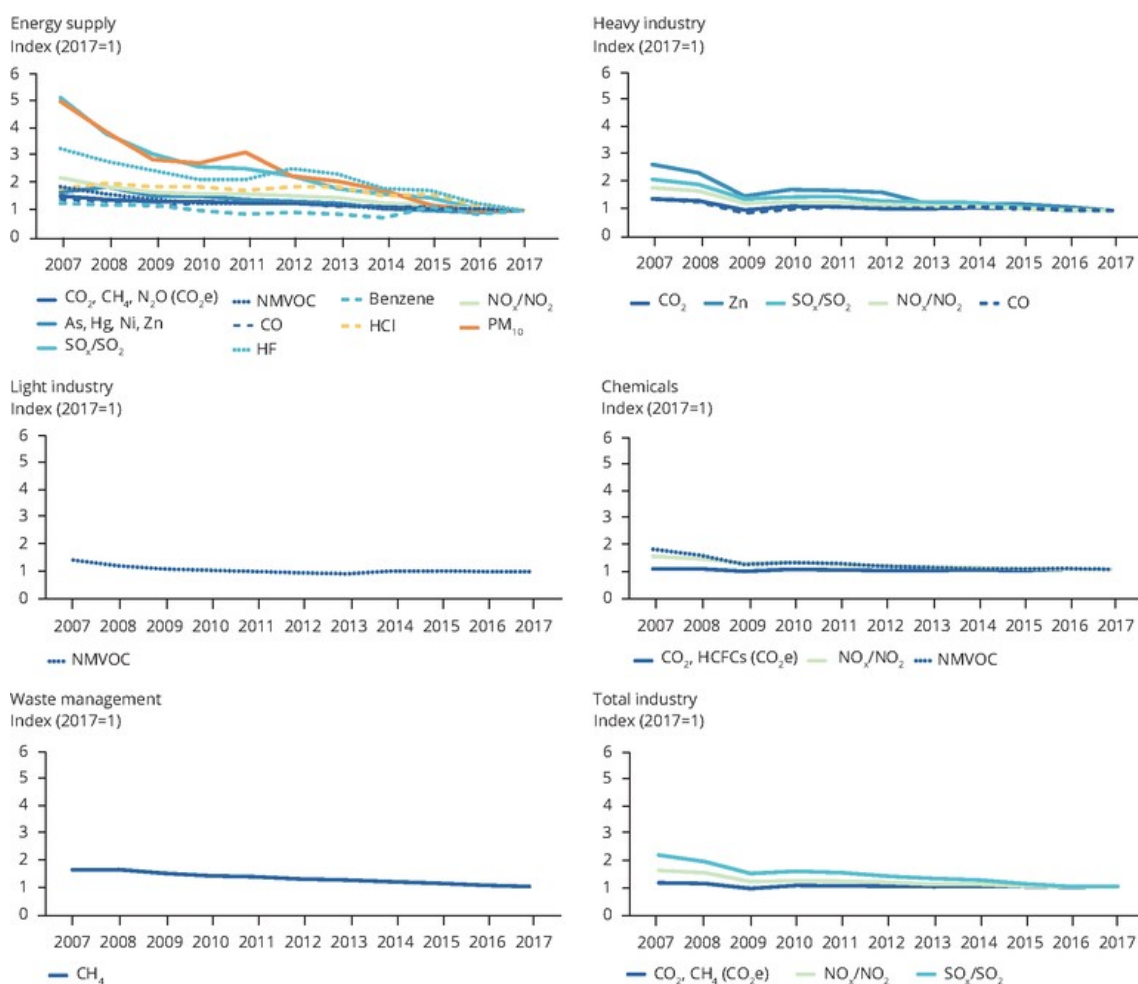
Figure 4.3.1 European industrial air pollutant and emissions in 2007 to 2016 by industry sector[166].

The World Health Organization (WHO), through the IARC (International Agency for Research on Cancer), classifies the exposing agents, assessing their degree of risk, according to general criteria shared by the international scientific community[167].

UNI EN ISO 16000-5 and UNI EN ISO 16017 are the norms regulating the VOCs concentrations. The WHO set the limits for the human exposure to benzene, its derivates (toluene, ethylbenzene and xylene) and other pollutants in order to prevent the health risk. These limits are reported in Table 4.3-1 referring to the WHO guidelines for indoor air quality[167].

Table 4.3-1 WHO limits[71,167]

Contaminant	WHO limit
Benzene	1.7 µg/m³
Formaldehyde	0.1 mg/m³ for 30 min exposure
CO	7 mg/m³ for 24 hours exposure
NO$_2$	200 µg/m³ for 1 hour indoor
PAHs (benzo(a)pyrene)	8.7×10^{-5} per ng/m³ indoor

4.3.2   Persistent organic pollutants

This term is used to classify a toxic group of chemicals that can persist in the environment for long periods of time, with effects that can affect the food chain. This includes pesticides, dioxins, furans and polychlorinated biphenyls (PCBs). Dioxins are formed during incomplete combustion and whenever materials containing chlorine (e.g. plastics) are burned. Emitted in the atmosphere, dioxins tend to deposit on soil and water but, being water insoluble, they do not contaminate ground water sources. Most dioxins in plants come from air and dust or pesticides and enter the food chain where they bio-accumulate due to their ability to be stably bound to lipids[165].

4.3.3   Heavy metals

Heavy metals include basic metal elements such as lead, mercury, cadmium silver nickel, vanadium, chromium and manganese. They are natural components of the earth's crust; they cannot be degraded or destroyed, and can be transported by air, and enter water and human food supply.

The risk of this contaminant is strictly dependant on their concentration: in fact, the presence of this metals in low concentration is essential to maintain the normal metabolic reaction in the human body but, in high, they can cause the bio-accumulation process in the human body[165]. Bioaccumulation means an increase in the concentration of a chemical in a biological organism over time, compared to the chemical's concentration in the

environment. It occurs when an organism absorbs a substance at a rate faster than that at which the substance is lost or eliminated by catabolism and excretion.

4.3.4   **Particulate Matter**

Major sources of particulate pollution are factories, power plants, re-fuse incinerators, motor vehicles, construction activity, fires, and natural windblown dust. This is the generic term used for a type of air pollutants, consisting of complex and varying mixtures of particles suspended in the breathing air, with various size (Figure 4.3.4) and compositions.

Among the parameters that play an important role for eliciting health effects are the size and surface of particles, their number and their composition. The composition of PM varies, as they can absorb and transfer a multitude of pollutants: their major components are metals, organic compounds, material of biologic origin, ions, reactive gases, and the particle carbon core.

The size of the particles varies and different categories have been defined: *Ultra-fine particles*, smaller than 0.1 mm in aerodynamic diameter, *Fine particles*, smaller than 1 mm, and *Coarse particles*, larger than 1 mm. The size of the particles determines the site in the respiratory tract that they will deposit (Figure 4.3.3): PM10 particles deposit mainly in the upper respiratory tract while fine and ultra-fine particles are able to reach lung alveoli. PM10 is the fraction of particles collected with a selection system having an efficiency established by the standard (UNI EN12341 / 2001) and equal to 50% for the aerodynamic diameter of 10 μm. Similar considerations apply to PM2.5 (UNI EN14907 / 2005).
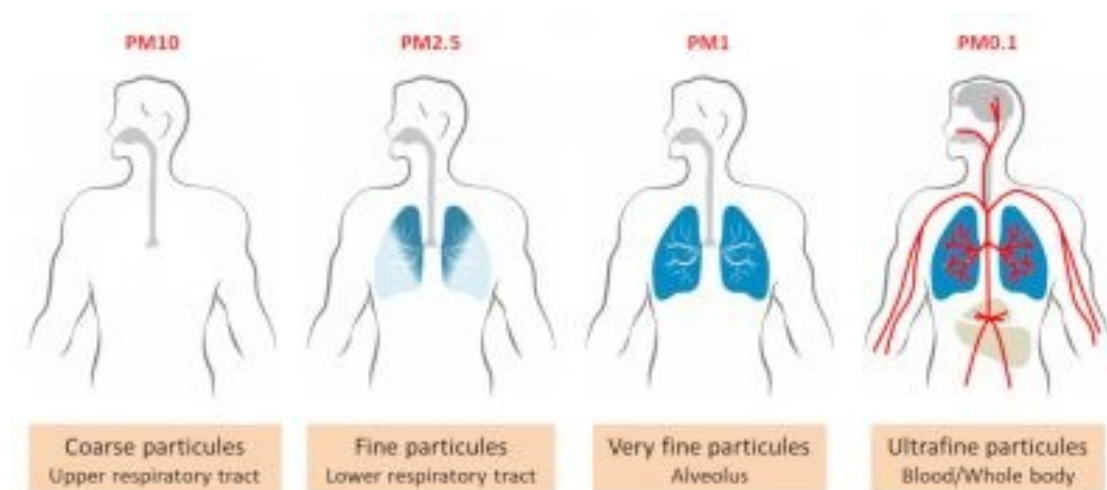
Figure 4.3.2 Affection of PM size on the respiratory tract.

4.3.5   **Biological contaminants**

Biological contaminants include bacteria, viruses, animal dander and cat saliva, house dust, mites, cockroaches, and pollen. There are many sources of these pollutants. By controlling the relative humidity level in a home, the growth of some sources of biologicals can be minimized. A relative humidity of 30-50 percent is generally recommended for homes. Standing water, water-damaged materials or wet surfaces also serve as a breeding ground for molds, mildews, bacteria and insects. House dust mites, the source of one of the most powerful biological allergens, grow in damp, warm environments. Some biological contaminants trigger allergic reactions, including hypersensitivity pneumonitis, allergic rhinitis, asthma. Some diseases, like humidifier fever, are associated with exposure to toxins from microorganisms that can grow in large building ventilation systems.

However, these diseases can also be traced to microorganisms that grow in home heating and cooling systems and humidifiers. Mold, dust mites, pet dander and pest droppings or body parts can trigger asthma. Biological contaminants, including molds and pollens can cause allergic reactions for a significant portion of the population.
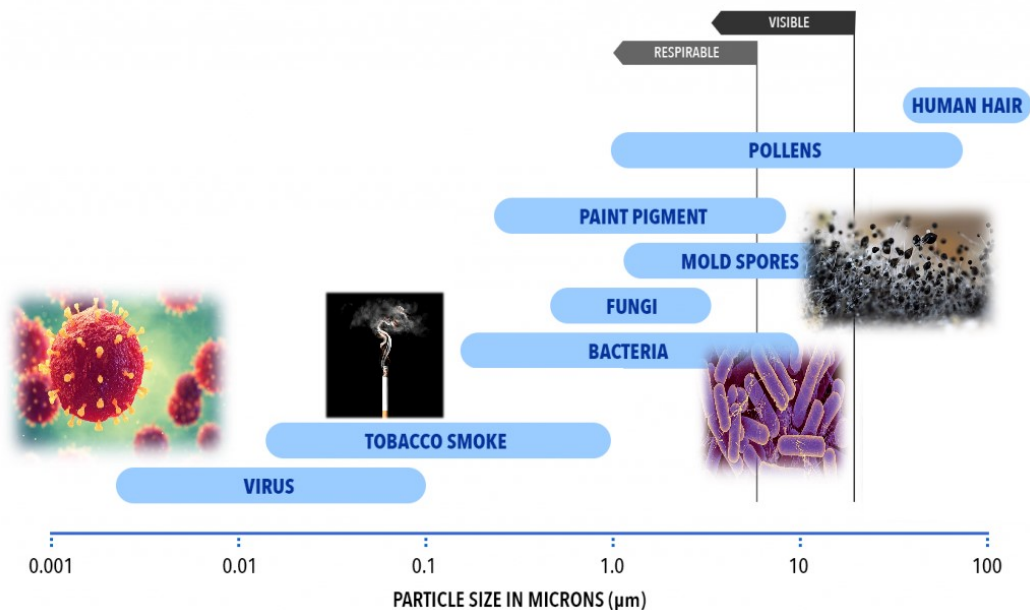
Figure 4.3.3 Representation of the dimensions of various contaminants

4.3.6   The importance of Air Filtration

Air filtration is the most effective and widespread method to remove particulate matters (PM) and other pollutants from the air stream and now the engineering sector is investing their resource on the study of technologies and parameters to control the indoor environment to follow the WHO guidelines for IAQ.

Nowadays, with a variety of filtration technologies and styles to choose and industry-standard criteria by which to judge filtration performance, it's possible and practical to specify air filters with filter media designed to maintain Heating, Ventilation and Air Conditioning (HVAC) system cleanliness, improve indoor air quality, and reduce energy consumption simultaneously. Attention to the entire lifecycle cost of filters[168] and on the selection of materials, and not just their initial purchase price, is crucial.

However, ventilation systems can also be major sources of airborne pollutants as a result of inadequate system design, distribution, cross-contamination, etc.

4.4   Overview on collection air filters

Ensuring clean indoor air quality requires the assistance of effective air filtration systems. Understanding how the different filtration systems perform is critical when designing for a certain degree of air cleanliness, because different variables have to be considered in order to facilitate the air flow and to achieve the expected removal efficiency.

4.4.1   High Efficiency Particle Arresting

HEPA (High Efficiency Particle Arresting) filters are known to be amongst the most efficient filters available for trapping particles of different diameter. They are designed to be over 99.99% efficient, and are routinely used for air filtering in locations such as hospital operating theatres, respirators, vehicles etc.

Their mechanism of air filtration essentially consists of a pleated sheet of fibre with high surface area. Particles being forced through this sheet are trapped through three major mechanisms called diffusion, interception and impaction, each of which becomes more remarkable depending on the particle sizes (Figure 4.4.1).
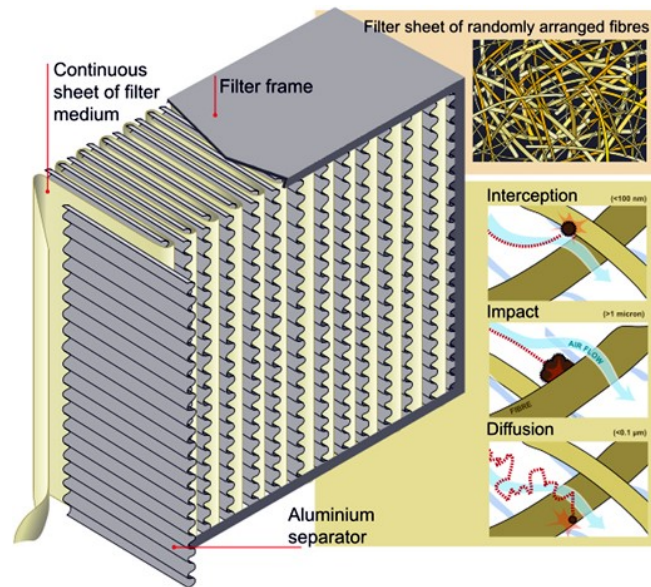
Figure 4.4.1 HEPA filter representation

4.4.2   Polyurethane Foams

Polyurethane is a synthetic polymer which forms from the re-action of a polyol (a long-chained alcohol) with a diisocyanate. Depending on the type of polyol used, different types of poly- urethane can be formed. The reticulated type polyurethane foam is a porous, low-density type of foam characterised by a three-dimensional skeletal structure lacking membrane between the strands. The porosity of the foam is typically 95% but it can be as high as 98%. Each foam has a nominal number of Pores Per Inch (PPI), which determines how dense the foam is. Increasing the PPI of the foam will make it denser. Currently reticulated foam is used in water filters and air filters in air-conditioning units.

As HEPA filters, they are physical filters since they trap particles on the surface of their fibres. As particles travel through the foam, with a very elevated internal surface area, they alikely adhere to it. The random arrangement of the ribs and nodes in open-cell foams makes the flow of air or water inside it necessarily non-laminar, increasing the probability that particles in the flow come into contact with it.

Polyurethane foams filters (Figure 4.4.2) are not nearly as efficient as HEPA filters. Nevertheless, they have the advantage of being adaptable to specific needs. The PPI and thickness of the polyurethane foam filter can be fine-tuned to find the optimal compromise between efficiency and pressure drop. Increasing the PPI makes the foam more efficient as a filter. Similarly, increasing the thickness of the foam filter will also increase the efficiency. At the same time however, increasing the PPI or the thickness the pressure drop will also increase. Because of this, the efficiency and pressure drop of foam filters can be tuned to some optimal value.

Figure 4.4.2 Polyurethane Foam filters

4.4.3   **Nano-fibres filters**

Non-woven nano-fibre mats are an emerging technology. The most common process for nanofiber production involves electrospinning[169], an innovative technology where polymers are extruded through a very thin nozzle and sprayed onto a collector[170]. The plastic fibers thus produced are normally between 1 mm and 50 nm thick. The large number of fibers produced using this method form a mat, which can be used as a filter. The efficiency of these filters is extremely high being comparable to HEPA filters or even superior at smaller particle sizes.

An enormous advantage, widely studied in literature, for nanofiber mats can be the functionalization with a wide variety of components both during and after production to increase the filtration efficiency of the filter[171–175]. For example, nanofibers have been functionalized with fungicidal or bactericidal materials[176].Very low concentrations of functionalization are required to obtain fungicidal and bactericidal activity.

As for HEPA filters, the mats need to be replaced on a yearly basis. The very high efficiency of these mats at very small particle size might be a disadvantage since it implies that the filter would become fully loaded more quickly, so the low cost of the filter is essential.

4.4.4   **Electrostatic precipitation**

Its air filtration mechanism consists of a number of wide parallel plates charged to very high voltages. A particle charger, which is often a thin series of wires charged with an opposite polarity with respect to the plates, is often placed up- stream of the plates[177]. When the air is forced to flow through the charged plates, corona discharges occur which charge the particles, cause them to become attracted to the plates and deposit on them as dust. Small amounts of ozone are generated as a by-product[178] by the high voltage plates.

The voltage on the Electrostatic Precipitators (ESPs) plates can be positive or negative, or alternating.

This technology is used regularly in smoke stacks and other scenarios where fine particles present in the air need to be deposited to clean the air. ESPs are not used in hospitals since the technology works best at particle sizes above 0.03 mm or 0.1 mm, so they are useless for virus[174] or other pollutants smaller than 0.03 mm. Nevertheless, the overall efficiency is much lower than that of HEPA filters and fibre mats[178].
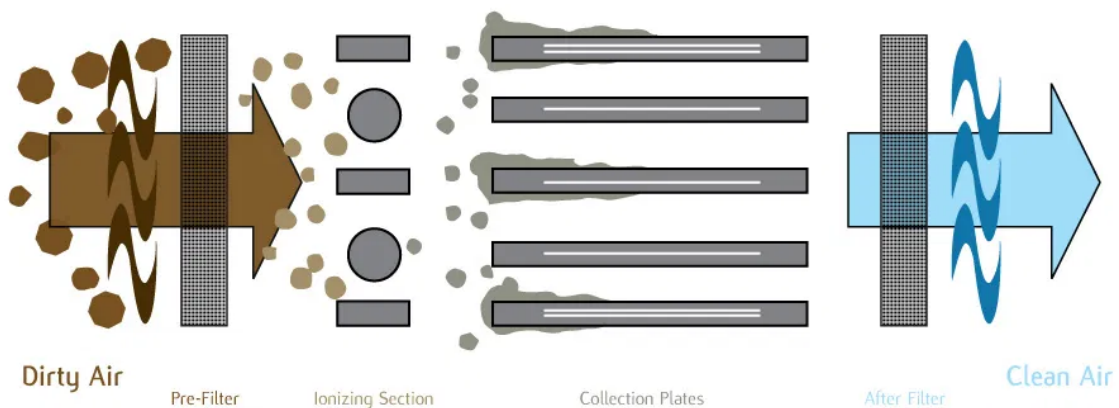
Figure 4.4.3 Schematic representation of ESPs composition.

4.4.5   **Wet scrubbing**

Wet scrubbers (Figure 4.4.4) are not normally used as standalone filters, but in conjunction with other technologies[178,179] .They operate by making small particles heavier by the addition of water, making it easier for the secondary filter to collect the liquid droplets, much easier to collect than the original particles. The gas being filtered is first made to come into contact with a very fine mist of liquid droplets which have either been formed previously (using, for example, a very fine nozzle and high water pressure) or which are formed by impaction of the gas being filtered itself, travelling at high speeds. The fine mist of water traps the offending particles, increasing their weight substantially. The mist can then be removed from the air by passing it through a fine cloth, through a cyclonic separator[184].

Figure 4.4.4 Wet Scrubber

All these filters are designed for different engineering applications: a study on the air composition and the application field for the filter's design permits to improve not only the filtration efficiency, but also to prevent an excessive energy consumption becoming even a more sustainable solution.

A recent study[180] on the influence of the filter morphology for the removal of pollutants highlights that to reduce exposure to indoor PM2.5, high efficiency particulate air (HEPA) filters are commonly installed in air-handling units. In traditional HEPA filters, the fibres diameters are normally micrometric, and the filters usually consist of many layers. Although high particle removal efficiency can be achieved with such filters, the large air resistance can significantly increase energy consumption in heating, ventilation, and air-conditioning systems. Figure 4.4.5 represents the difference between a traditional filter composed by micrometre scale-fibres and an innovative filter with fibers at nanometric scale.
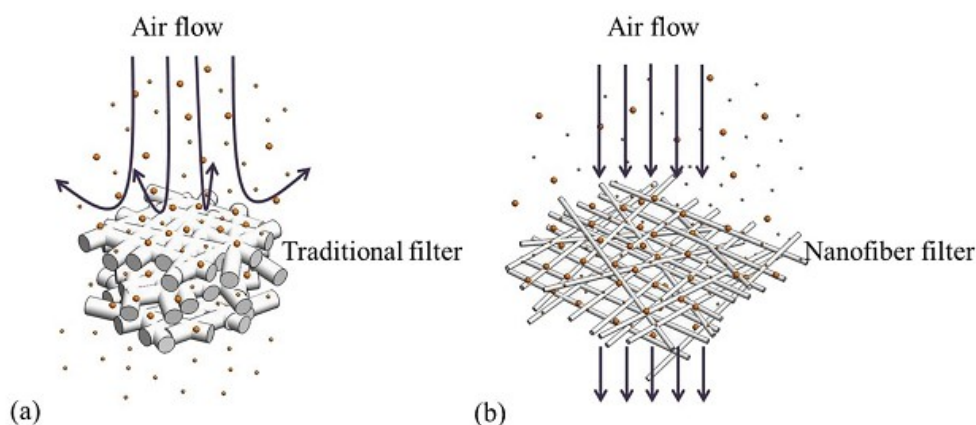
Figure 4.4.5 Schematic of (a) Traditional HEPA filter for capturing particles with large air resistance, and (b) a nanofiber air filter for capturing particles with low air resistance[180]

Due to the gas slip effect, the pressure drop across nanofiber filters tends to be lower than that across the traditional filters[180,181]. Therefore, nanofiber air filters can potentially be applied in indoor environments to lessen exposure to PM2.5 of both indoor and outdoor origin with reduced energy consumption.

4.5   Overview on the Collection Mechanism

4.5.1   Impaction, Interception and Diffusion

Consider a particle in a gas stream moving toward or being carried toward a target. If the particle touches the target, it will likely stick to the target due to inter-surface forces. The target may be a liquid droplet, as in the case of wet scrubbers, or a fibre, as in a fabric filter baghouse.

The three mechanisms by which the particle touches the target are illustrated in Figure 4.5.1. In each mechanisms, a large number of targets will increase the probability that a particle will touch a target[182].
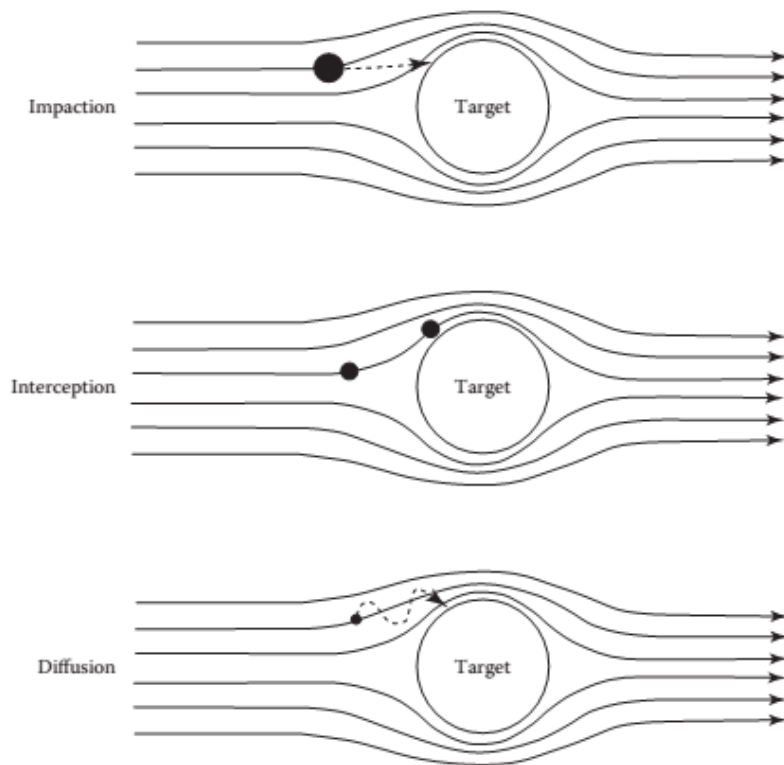
Figure 4.5.1 Representation of the impaction, interception and diffusion[182] collection mechanism

4.5.1.1   *Impaction*

Large particles moving toward the target have mass, and therefore momentum, which causes each particle to travel in a straight line toward the target. The particle leaves the streamline as the streamline bends to move around the target. The greater the mass of the particle, the more likely that it will travel in a straight line. Also, as the velocity difference between the particle and the target increases, the particle will have increased momentum and will be more likely to be carried into the target. The smaller the radius of curvature, the less likely that a particle will follow the streamline. Therefore, small targets are more likely to be impacted than large targets[182].

4.5.1.2   *Interception*

Particles of roughly 0.1–1 μm diameter are carried by the gas streamline sufficiently close to the surface of the target in order to touch it. These particles have insufficient inertia to leave the gas streamline and are carried with the streamline[182]. Interception is a relatively weak mechanism for particle collection compared to impaction. The impact between the path of the streamline and the particle happens randomly, and this is why particles in this size range are difficult to collect compared to larger and smaller particles[188].

4.5.1.3   *Diffusion*

Diffusion of extremely small, submicron particles is a result of Brownian motion. The mass of the particles is very small and the number of collisions with air molecules is low. Therefore, random collisions with air molecules cause the particle to bounce around[182].

4.5.2   **Electrostatic Attraction**

If particles acquire a charge and are placed in an electric field, the electrostatic force will move the particles across gas flow streamlines. Electrostatic forces on small particles can be quite large, making this a very effective mechanism for particle collection. This mechanism is utilized in electrostatic precipitators[177,178,182].

4.5.3   **Gravity**

The force of gravity is sufficient to pull very large particles out of a gas stream. Some mechanical separators are designed to slow a gas stream to allow particles to settle, but this type of collection mechanism is very weak, especially for light particles.

4.6   Fundamentals of Electrospinning Process

Electrospinning is currently the only technique that allows the fabrication of continuous fibers with diameters down to few nanometres. The method can be applied to synthetic and natural polymers, polymer alloys, and polymers loaded with chromophores, nanoparticles, or active agents, as well as to metals and ceramics. Fibers with complex architectures, such as core–shell fibers or hollow fibers, can be produced by special electrospinning methods. It is also possible to produce structures ranging from single fibers to ordered arrangements of fibers. Electrospinning is not only employed in university laboratories, but also in industry[183, 192].

Electrospinning of functional polymeric nanofibers has attracted considerable attention in the past decade due to the simplicity of the process and the enhanced properties associated with the size of the fibers[184–186].

One potential application for electrospun nanofibers is in the field of filtration where the nanowebs can provide separation of tiny particles due to the different interception mechanism.

4.6.1   Theory of Electrospinning

The most common electrospinning process is the needle- based technique; improved variations of this process will be depicted later (Figure 4.6.1). This simple system consists of a metal-tip extrusion system, a high-voltage supply and a grounded collector. When a liquid is slowly pushed through a needle, a droplet of liquid is formed, exhibiting a hemispherical surface. Then the droplet can be subjected to different forces: if the pressure applied on the liquid in the syringe is continuous, a liquid jet is ejected from the needle[169,183,187,188].
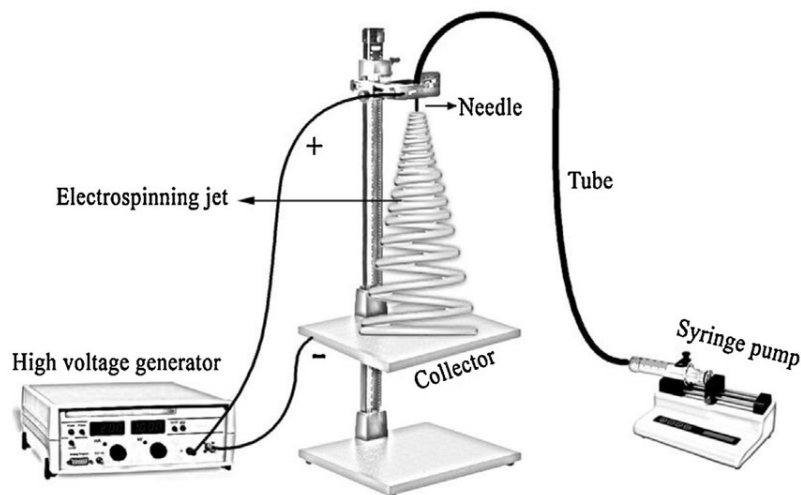
Figure 4.6.1 Electrospinning process representation.

If the filament formation is only governed by capillary through the needle/spinneret, even if a mechanical stretching is subsequently applied to the extruded filament, naturally by gravity or with the assistance of a mechanical setup, the resulting fibre diameter is usually in the range of mm or μm, not below[187].

The breakthrough, which enables to come down to the nanoscale, is the contribution of electrostatics. Due to the effect of the high electric field and surface tension, the hemispherical surface of the extruded droplet is extended to create a conical shape, known as the Taylor cone[188,187]. When this value is reached, the rounded tip inverts and emits a liquid jet. This fluid electrodynamics phenomenon is the first step of the electrospinning and electro- spraying processes.

During the flight from the needle to the collector, solvent evaporation occurs, which permits to collect solid fibers. The longitudinal forces induced by the external electric field are responsible for a straight path during the first part of the flight. Then, when the solvent evaporates, the fibre diameter is slowly reduced thus generating lateral repulsive forces[187].

4.6.2   Morphology of electrospun fibres

The morphology of the electrospun fibers is strongly affected by solution and electrospinning parameters such as polymer concentration, solvent, capillary size, flow rate, working distance, and applied potential[169,183,187–190]. Among these parameters, solution concentration and viscosity have been found to be the most important factors affecting fibre diameter[189].

Studies with various polymer systems demonstrate that the fibre diameter increases significantly as the solution concentration increases and this increase follows a power law relationship[171,174,184,188,189,191,192]. The solution viscosity is related to the extent of polymer chain entanglement and thus plays a critical role not only in the fibre size but also in its homogeneity. Below a certain critical value, the electrospinning jet breaks up and electro-spraying occurs, where beads or droplets are formed[187], as shown in Figure 4.6.2.
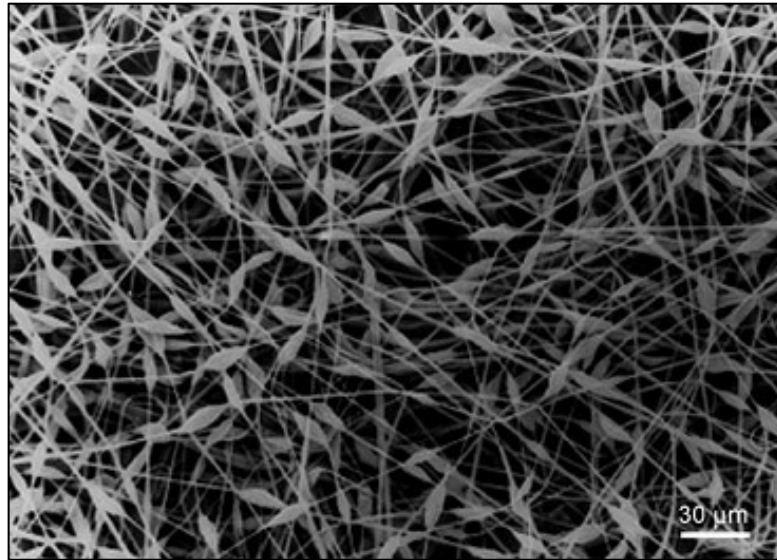
Figure 4.6.2 Example of beads structure in electrospun fibres

Other parameters such as the dielectric constant and boiling point of the used solvent may also play a significant role in the homogeneity of electrospun fibres; however, to isolate these parameters and study their effect on fibre morphology[187] is more difficult. Figure 4.6.3 represents some of the parameters affecting the morphology.
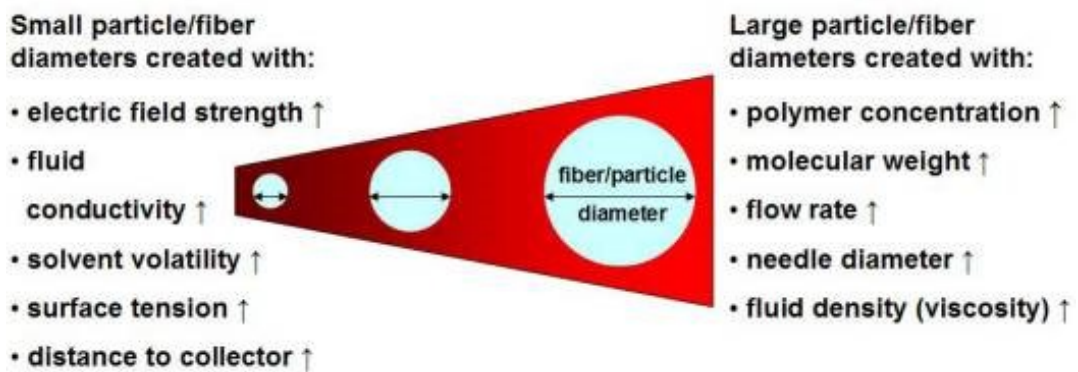
Figure 4.6.3 Schematic representation of relationship between electrospinning parameters and morphology of the fibres.

4.7   **Materials**

4.7.1   **Polylactide Acid (PLA)**

Polylactide (Figure 4.7.1) or polylactic acid (PLA) is a synthetic, aliphatic polyester from lactic acid (LA). For industrial applications, such as fibers, films, and bottles, the chain length n should be between 700 and 1400.

PLA is made from Lactide Acid, found in plants and animals as a by-product or intermediate product of metabolism. Therefore, LA and the hydrolytic degradation products of PLA are non-toxic by its nature. After hydrolysis, PLA is biologically degradable by common microorganisms. Only in an industrial composting facility the high temperature (60 °C) and humidity required for the hydrolysis is achieved. At temperatures below its glass transition point (e.g., 55 °C, depending on co-monomer content), PLA is as stable as Polyethylene terephthalate (PET) or Polybutylene terephthalate (PBT).

Figure 4.7.1 PLA granules

4.7.1.1   *Chemical Structure*

Lactide is a chiral molecule that exists in two optical forms: L-lactide and D-lactide (Figure 4.7.2). There are many different ways to synthesize PLA, but ring-opening polymerization of lactide is the most common[193].
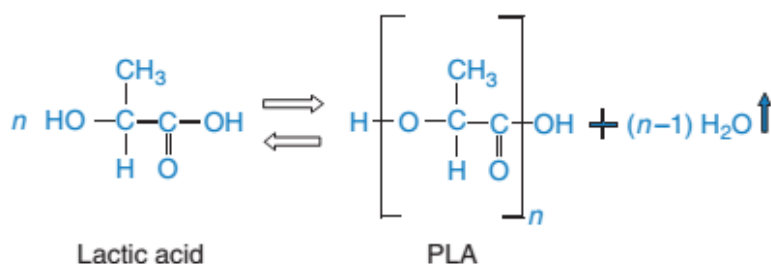
Figure 4.7.2 From Lactide acid to Polylactide[194]

 The polymerization of lactide leads to the formation of semi-crystalline PLA polymers. PLA has three different structures: poly(L-lactide) (PLLA), poly(D-lactide) (PDLA), and poly(D,L-lactide).

In packaging applications, poly(D,L-lactide) with 90% L-lactide has been widely used. Increasing the D-lactide concentration produces PLA polymers with a more crystalline structure and PLA films with better thermal stability, mechanical strength, and barrier properties[195].

4.7.1.2   *Physical Properties*

Polylactic acid can be processed by injection moulding, film extrusion, blow moulding, thermoforming, fibre spinning, and film forming[196–201]. It has better thermal processability compared to other bioplastics, such as PHA, polyethylene glycol (PEG), or poly(ε-caprolactone) (PCL).

Figure 4.7.3 compares the glass transition temperature (Tg) and melting temperature (Tm) of PLA with those of other polymers.
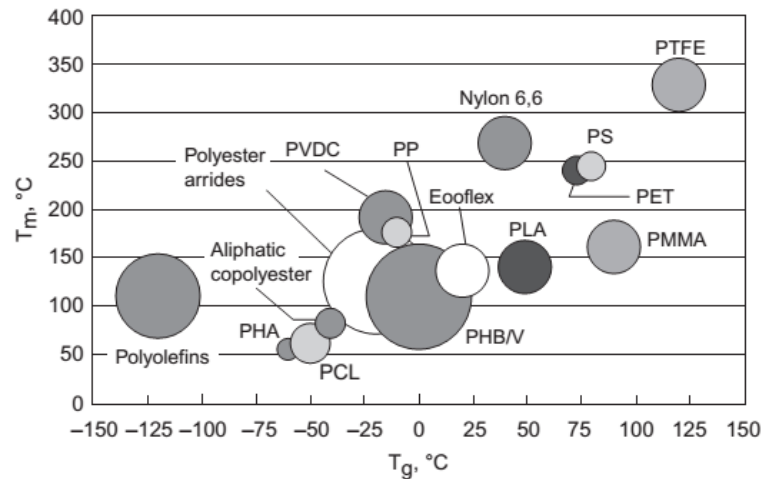
Figure 4.7.3 Comparison of Tg and Tm of polylactic acid (PLA) with other thermoplastics[195].

PLA has relatively high Tg and low Tm as compared to other thermoplastics[202]. PLA has properties similar to those of cellophane, PS, oriented polypropylene (OPP), and oriented polyethylene. The tensile strength and elastic modulus of PLA are comparable to those of PET.

Its manufacture results in 44% less carbon dioxide production and consumes 36% less energy compared to the production of a PET bottle[202]. PLA is a very brittle material, however, with less than 10% elongation at break. Its low deformation at break, high

modulus, and hydrophilic properties have limited its application primarily to rigid thermoformed packaging[203].

Also, the low melt strength of PLA creates limitations during melt processing. High melt strength is needed in the processing of PLA, such as film and sheet extrusion, blown film, and foam[195].

4.7.1.3   *Modification of PLA and its effect on physical properties*

To overcome the current issues with PLA, other ingredients have been incorporated into the PLA structure. Good distribution of additives or fillers in a PLA matrix is essential to produce PLA composite films.

Various materials such as plasticizers, polymers, nanoclays, carbon, and starch have been blended into the PLA matrix to modify its properties in order to improve mechanical and thermal properties [201–193]. PLA has been copolymerized also with other bio-polyesters and the copolymers showed excellent elongation and elastomeric properties[205,207,208,203]. PLA has also been blended with other bioplastics such as thermoplastic starch (TPS), PHA, Polycaprolactone or poly (butylene adipate-co-terephthalate) (PBAT) to exhibit improved ductility and toughness[206,208,209].

4.7.2   **Cyclodextrins (CyD)**

The first work on cyclodextrins was published in 1891 by a French scientist A. Villiers, who described the isolation of 3 g of crystalline substance from bacterial digest of 1000 g of starch. The substance appeared to be resistant towards acid hydrolysis and, like cellulose, did not show reducing properties. His experimental results indicated that the substance was a dextrin. He determined its composition as $(C_6H_{10}O_5)_2 \cdot 3H_2O$ and named it "cellulosine". It is now thought that Villiers detected both α - and β-cyclodextrin in the digest[160].

The early treatment of starch with amylase from *Bacillus macerans* gave a crude mixture of α -cyclodextrin (~60%), β-cyclodextrin (~20%) and γ-cyclodextrin (~20%) together with small amounts of cyclodextrins with more than eight glucose units.

The biotechnological advances that occurred in the 1970s lead to dramatic improvements in their production. Genetic engineering made different types of CGTases available, more active and more specific towards production of α-, β- or γ-cyclodextrin than the previously used enzymes. Their increased purity let them used also as pharmaceutical excipients[160].

Thanks to their peculiar chemical structure, CyDs can include various guest molecules, and nowadays they are widely employed in biomedical applications as drug carriers, in

food, cosmetics, textile, agricultural industries, in enantiomeric separations, and in other areas.

4.7.2.1   *Chemical Structure*

Cyclodextrins are macrocyclic oligosaccharides most commonly composed of 6, 7, or 8 glucosidic units bearing the names α-, β- or γ-cyclodextrins, in Figure 4.7.4, respectively. Other, usually smaller, molecules (called guests) can enter their cavity forming inclusion complexes with these hosts. After more than 50 years the structure of CyDs can be confirmed.
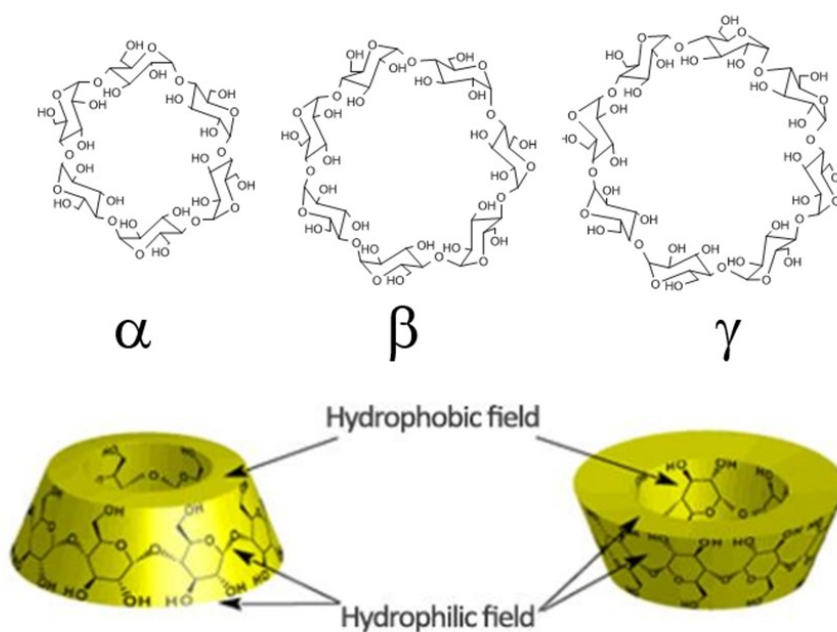
Figure 4.7.4 Chemical structure of CyDs structures.

They are environmentally friendly and deserve attention for their valuable properties: CyDs bind covalently or supramolecularly with other species to give a great number of products. The CyD molecule has a hydrophobic cavity and a hydrophilic outer part. The inclusion complexation of CyDs involves the supramolecular self-assembly having a crucial role in the creation of non-conventional, intelligent, often self-healing novel materials. The viscosity of aqueous solutions is not very different from that of pure water; the dependence of viscosity on temperature and concentration is the same as that shown by linear polysaccharides.

Various modifications of CyDs have been made to improve their properties expecially for the environmental field[155,210–213]. Indeed, they are potentially useful sorbents for

aromatic hydrocarbons. CyDs have a low-polarity cavity in which organic compounds of appropriate shape and size can form inclusion complexes [160,214–217]. This unique property provides CyDs with a capacity to significantly increase the apparent solubility of low polarity organic compounds. As a consequence, they can play a major role in environmental science in terms of solubilisation of organic contaminants, enrichment and removal of organic pollutants and heavy metals from soil, water and atmosphere[160,214–217].

In this study, β-cyclodextrins are added in different physical forms (in powder and solubilized) to PLA fibres in order to produce air filters for blocking VOCs and PMs.

4.7.2.2   *Synthesis of CyDs*

Cyclodextrins are usually prepared by enzymatic treatment of starch by a cyclising enzyme, cycloglycosyltransferase (CGTase). CGTase is produced by approximately 16 bacterial species, such as Klebsiella pneumonia, *Bacilllus macerans* or Bacillus circulans[218].

In general, two different types of CyD production processes can be distinguished: in "Solvent Processes", an organic complexing agent precipitates one type of CyD selectively and as such directs the enzyme reaction to produce mainly this type of CyD. In the "Non-Solvent Process" no complexing agent is added and therefore a mixture of different CyDs is formed. The ratio of CyDs produced depends only on the CGTase used and on the reaction conditions[74].

4.7.2.2.1   Solvent process

Figure 4.7.55a shows a typical flowsheet of a solvent process. On an industrial scale, most CyD is produced in solvent processes, where an organic solvent – mainly toluene, ethyl alcohol or acetone – acts as a complexing agent. The procedure starts with starch liquefaction (typical starch concentration 20–30%). The liquefaction is carried out using either heat-stable α-amylase, acids (e.g. HCl), mechanical disintegration or thermostable CGTases.

After liquefaction, the starch solution is cooled down to the enzyme reaction temperature, and CGTase and organic complexing agent are added. CyDs are enzymatically produced and the desired type of CyD forms a complex with the complexing agent and precipitates. After the conversion stops, the CyD-agent complex is separated from the reaction solution by centrifugation or filtration[74].

The remaining solution contains unused starch, linear dextrins, glucose, maltose, CGTase, unused organic complexing agent, some other by-products and water. The separated complex is washed, and the filtrate is distilled to recover excess complexing

agent. In the next step, the CyD-complex is suspended in water and cleaved by heating. The downstream process only separates the CyDs from the rest of the reaction solution, but does not separate different CyDs from each other[74].

4.7.2.2.2   Non-solvent process

Figure 4.7.5b shows a flowsheet of a typical non-solvent process. CyDs produced without an organic complexing agent can be applied in the food industry without restriction, in contrast to CyDs produced in solvent processes.

 β-CD production starts with starch liquefaction and enzymatic conversion identical to that used in solvent process, but with the exception that no complexing agent is used. At the end of the reaction, CGTase is inactivated, the pH is reduced and glucoamylase is added. The glucoamylase converts unused starch and other non-cyclic dextrins, which may disturb purification, to glucose and maltose[74]. The solution is then cleared using activated carbon, filtered and concentrated under reduced pressure to about 60% (w/v) dissolved solids. After crystallisation and recrystallisation, the precipitated β-CyD is isolated, washed, centrifuged and dried. The rest, consisting of glucose, maltose, α- and γ-CyD, is concentrated to a syrup and can be used as a food additive[74].
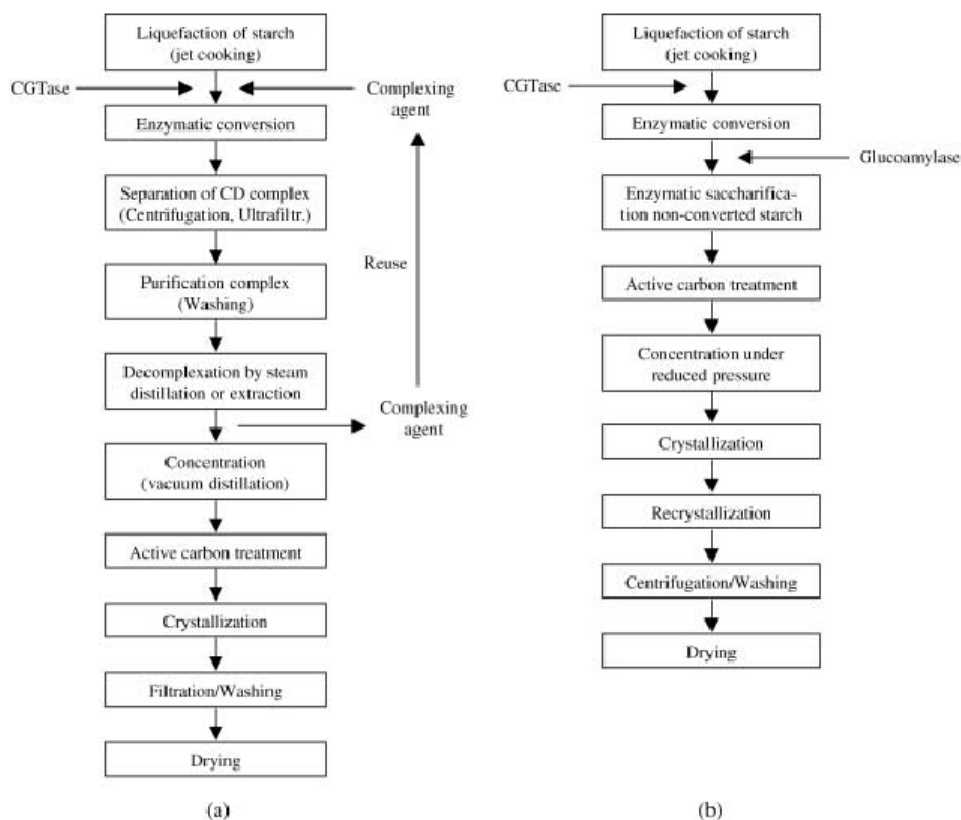
Figure 4.7.5 a) Solvent Process for CyDs synthesis; b) Non-Solvent Process for CyDs synthesis[74]

4.7.2.2.3   Purification

Using the typical solvent process purification procedures, purities of 98% can be achieved. Most impurities are non-cyclic dextrins, the content of the organic complexing agent is often less than 1 ppm [74]. However, solvent process purification only isolates the CyDs from the rest of the reaction mixture, but not the different CyD types from each other. Purification of the three types of cyclodextrins takes advantage of the different water solubility of the molecules: α-cyclodextrin 14.5 g / 100 mL; β-cyclodextrin 1.85 g / 100ml; γ-cyclodextrin 23.2 g / 100 mL.

Overall, the solubility of cyclodextrins is lower than that of acyclic oligosaccharides and the presence of organic substances reduces their solubility due to the formation of complexes. The solubility in ethanol and propanol solution is higher than in water.

4.7.2.2.4   Factors influencing the industrial production of cyclodextrins

  a. Starch Concentration

High starch concentrations reduce production costs but also lead to a low yield of cyclodextrin. The optimal concentration is 30%.

b. *Hydrolysis Time:*

CGTase produces three major cyclodextrins. The ratio depends on the time taken for the conversion; time that can be controlled with suitable reaction conditions.

c. *Origin CGTase*

Bacilllus macerans or *bacillus circulans* species mainly produce β-cyclodextrin, while that produced by Klebsiella pneumonia mainly produces α-cyclodextrin.

d. *Presence of organic substances in the reaction mixture*

The addition of medium and long chain alcohols, benzene, toluene, etc. alters the relative yield to the different types of cyclodextrins.

4.7.2.3   *Complex of Inclusion*

Cyclodextrins can form complexes of inclusion with numerous poorly soluble molecules, this is why they are commonly used in pharmaceutical chemistry as carriers. Hydrophobic molecules are maintained in the cavity of the cyclodextrin with the outer surface of the complex maintaining its hydrophilic characteristics[217,219]. Wen[173] incorporated cinnamon essential oil/beta-cyclodextrin into PLA nanofilm to give better antimicrobial activity compared to conventional nanofilm, to prolong the shelf life of food, as an active food packaging.

The formed structure, in which the host molecule spatially includes the guest molecule is defined as an adduct structure and the drug-cyclodextrin set is defined as an inclusion complex (Figure 4.7.6). When CyD is in aqueous solution (Figure 4.7.6), the water molecules occupy the cavity, giving rise to a thermodynamically un-favourable polar-apolar interaction[73,74,159,216,220,221].

If a drug, a VOCs or other lipophilic molecule is present in solution, it will displace the water molecules and take their place, creating an energetically more stable situation (apolar-apolar interaction)[211]. The driving force of the complexation is to obtain an energetically more stable system than that made up of the single components. No covalent bond is formed between the host molecule and the guest molecule but a simple association-dissociation equilibrium. The interaction between host molecule is optimal when the binding sites of the two molecules are stereoelectronically complementary[216].
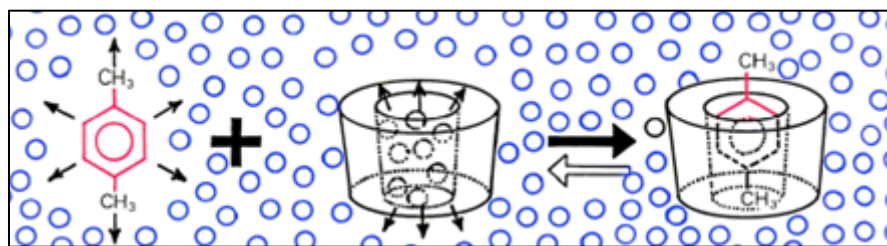
Figure 4.7.6 Representation of the Inclusion complex process

4.7.2.3.1   Prerequisites for the formation of complexes

a. Geometric compatibility

Cyclodextrins can form inclusion complexes with molecules that have a size compatible with their cavity. In some cases, even molecules larger than the cyclodextrin cavity can be complexed but, in this case, only a part of the host molecule penetrates inside the cyclodextrin cavity. Several cyclodextrins can complex a single molecule or a single Cyd can complex several molecules.

b. Polarity and charge

Molecules with high hydrophilicity or with ionic groups hardly form a complex. Only molecules with a polarity lower than that of water can be included. The stability of a complex is proportional to the hydrophobic character of any substituents.

c. Reaction environment

The complex could also form in the absence of solvent, but the times would be very long. Even in water the times are relatively long, in proportion to the solubility of the molecules to be included. The times for the complex formation are sufficiently short, when both the host molecule and the guest molecule are in solution. At the same time, however, the use of organic solvents which would prevent the formation or lead to the breakdown of the complex itself should be avoided.

4.8   **Methods**

The three phases of the filter development includes: the study of the formulation, which include the setting up of all the electrospinning parameters and the design of the support for the nanofibers; the characterization of the electrospun fibres and the filter before the tests; the PM generation and efficiency tests.

4.8.1   **Formulations**

Dichloromethane (DCM) and N,N-Dimethylformamide (DMF) of analytical grade are purchased from Sigma-Aldrich. PLA (Total Corbion Luminy LX930) has been used to prepare a polymeric solution of 8% w/V solubilized in DCM/DMF (80:20).

The electrospinning setup consists of a syringe pump, which needle is connected to the high potential (16kV). The flow rate is 0.5 ml/h and the needle/collector distance equal to 10 cm. Nanofibers are electrospun over a PLA-based 3D printed support, placed on a grounded aluminum foil, (1 mm thick) with large voids (60% fill). The dimensions of each side are 2.2 cm, with a length of 3.9 cm between the opposite sides and 4.9 cm between the two opposite angles. The design of the support is reported in Figure 4.8.1.

This hexagonal shape has been chosen because it makes the filter easy-modulable for panels of different sizes; furthermore, both support and nanofibers produced with electrospinning technique are made by the same polymer to improve the affinity, permitting a better adhesion between them [222,160,217].

Figure 4.8.1 PLA 3D-printed support and its dimensions.

In this study β-methyl-cyclodextrins (Carbosynth) have been also used either in association with fibers as such (in powder) or solubilized in the minimum necessary quantity of methanol (Sigma-Aldrich) and electrospun.

Three different formulations are proposed:

4.8.1.1   *PLA-series*

In this series, as reference, PLA samples (8% w/V) are solubilized in the solvent (DCM/DMF 80:20) and then electrospun at 0.5 mL/h, 16 kV, with a needle/collector distance equal to 10cm.

Figure 4.8.2 reports a sample of this series.

Figure 4.8.2 PLA filter

4.8.1.2   *PLA/CyD-series*

This formulation presents a three levels configuration where a layer of cyclodextrins in powder is placed in the middle of a bilayer of electrospun PLA (PLA/CyD).

Also in this case samples PLA (8% w/V) is solubilized in the solvent (DCM/DMF 80:20) and then electrospun at 0.5 ml/h, 16kV, with a needle/collector distance equal to 10cm.

In this series of samples, the electrospinning process is executed in two steps: the first one is directly on the support to realize the first layer of fibers; the second step is after the deposition of the CyDs powder (15%w/w).

In the second step attention should be payed in the homogenization of the process because the presence of powder makes the substrate thicker, causing a possible reduction in the conductivity between that part of the aluminum foil and the needle.

Figure 4.8.3 reports a picture of a sample of this series.

Figure 4.8.3 PLA/CyD filter

4.8.1.3   *PLA+CyD-series*

This series (PLA+CyD) of samples have CyDs (1.5% w/w) solubilized in few droplets of methanol (Sigma-Aldrich) and added in the same solution of PLA (8% w/V). The solution has been well mixed with an IKA Vortex 2 for 2 minutes and then electrospun at 0.5 mL/h, 16 kV, with needle/collector distance equal to 10cm.

Figure 4.8.4 reports a sample of this series.
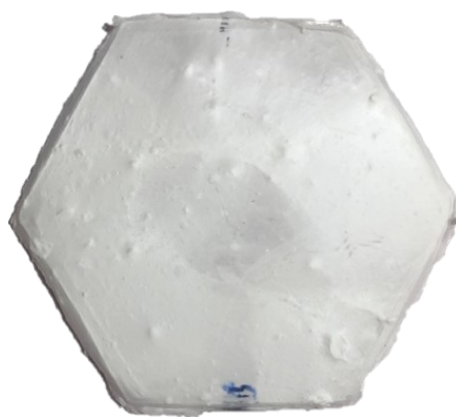
Figure 4.8.4 Picture of the PLA+CyD filter.

4.8.2   **Scanning Electron Microscope**

All the specimens have been analyzed with a ZEISS Scanning electron microscope for the characterization of the morphological aspect and to evaluate the interaction between PLA and CyDs.

4.8.3   **PM generation and efficiency tests**

In the filtration efficiency tests, PM particles are generated by burning incense in an 82 L box (Figure 4.8.5). The incense stick is a perfect source of PM and VOCs, because mainly composed by particles, metals (e.g. Al, As, Cd, Co, Cr) and various ions (as K^+, Ca^{2+}, F^-, Cl^-, NO_2^-, NO_3^-, SO_4^{2-} and PO_4^{3-})[223].

The smoke PM particles have a wide size distribution from <300 nm to 4 μm, with the majority of particles being <1 μm.

The so-generated particle stream is controlled by dilution with air. The PM particle number is measured with a GRIMM 1.108 particle counter. The removal efficiency is calculated by comparing the number before and after filtration, while the pressure drop in the filter medium is measured by a differential pressure meter (Honeywell 160 PC).

The wind velocity, measured in absence of the filter with a hot-wire anemometer, is equal to $1.4\,\mathrm{m\,s^{-1}}$.

VOCs removal tests are performed in the same box environments, with the injection of 100 µl Toluene, the test starts when its full vaporization occurred. VOCs concentration is measured with a ppb RAE 3000 with 1-min sample time, and the VOCs removal efficiency is calculated, likewise for PM, by comparing the number before and after filtration. All the tests are performed at T = 27±2°C and RH equal to 50±10%.
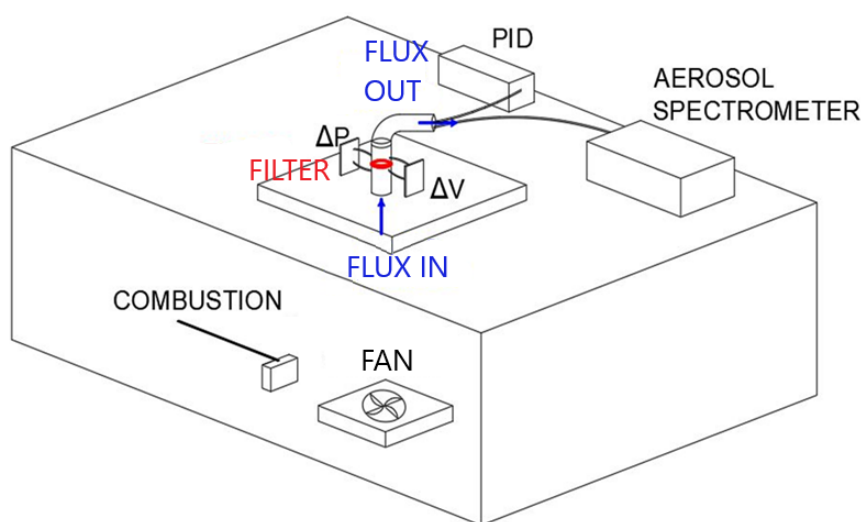
Figure 4.8.5 Model box for the efficiency tests.

4.8.4   Fourier-transform infrared spectroscopy (FTIR)

A Perkin-Elmer Spectrum GX1 spectrometer (PerkinElmer, Inc, Waltham, MA, USA) equipped with U-ATR accessory for the analysis of solid samples in reflectance mode has been used. On each sample, 5 spectra are acquired in the range between 4000 - 500 cm^{-1}, with a spectral resolution of 4 cm^{-1} and recording 64 scans. A background adsorption spectrum is recorded before each acquisition. Raw IR spectra are converted in absorbance, interpolated in the 1800-500 cm^{-1} spectral range and vector normalized in the same interval. An automatic baseline correction algorithm is used in all spectra to avoid errors due to baseline shifts. Atmospheric compensation is also performed. The average absorbance spectra of all samples are also calculated, and curve fitted in the 1800-800 cm^{-1} upon two-points baseline correction and vector normalization (Grams AI 9.1 software, Galactic Industries, Inc., Salem, NH). A Gaussian algorithm is adopted. For each underlying band, the positions in terms of wavenumbers, height and integrated area are calculated. Spectrum 5.3.1 (Perkin-Elmer) are used as the operating software.

4.9   Results and Discussion

4.9.1   Analysis of the morphology of the electrospun fibres

The morphological analysis at the SEM of the different samples shows very interesting results. As expected, the three series present a very different morphological aspect due to the different formulation. Two series, PLA and PLA/CyD, present very similar nanofibers in terms of shape, but their diameters are slightly different even if they have exactly the same polymer solution. In fact, PLA/CyD-series present a slightly thicker fibers, probably due to the presence of the powder in the bilayer, which can make a bit more difficult the migration of the polymer from the needle of the syringe to the collector causing a lower conductivity of the aluminum foil respect to the PLA-series. As previously reported, the size of the fiber is dependent by the conductivity level: higher conductivity permits to obtain fibers with a smaller diameter[183,185,189,190].

The SEM images of PLA filter are reported in Figure 4.9.1, Figure 4.9.2 and Figure 4.9.3.
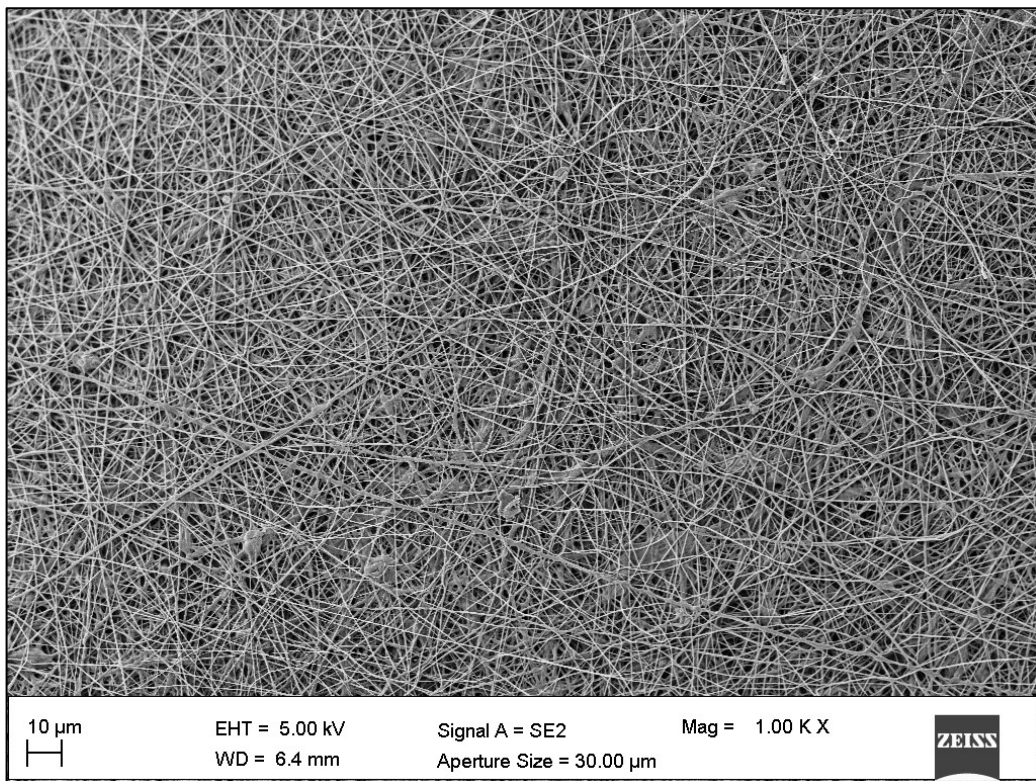
Figure 4.9.1 PLA overall view of the filter
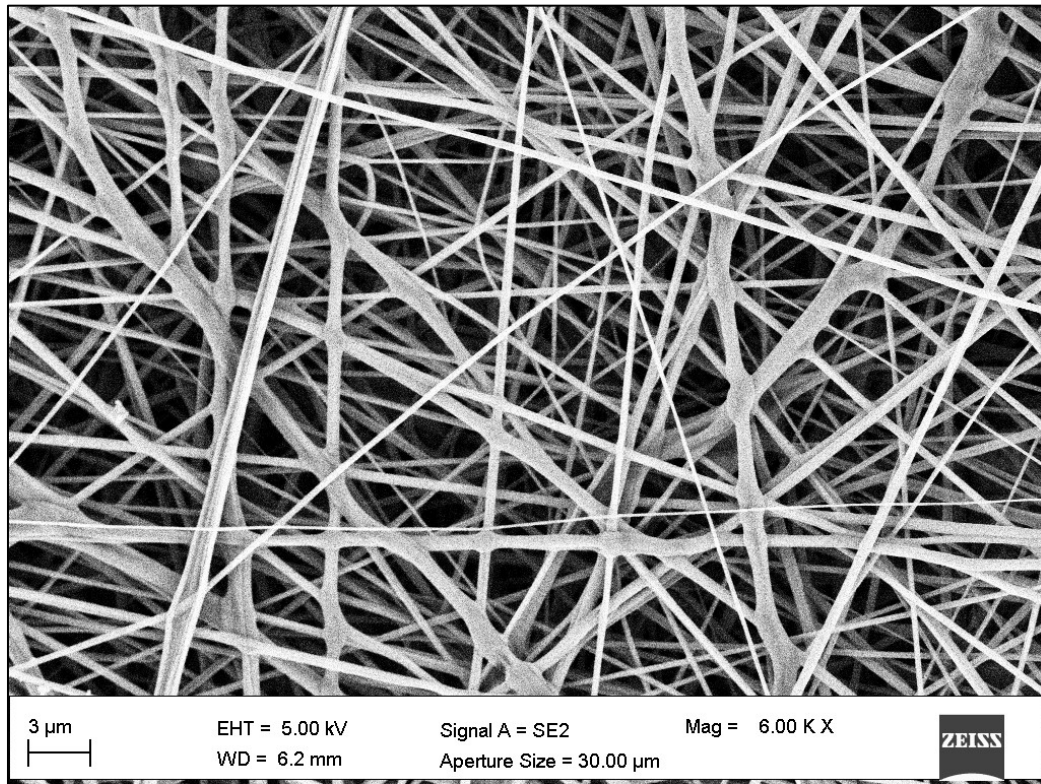
Figure 4.9.2 Enlargement of PLA fibres.
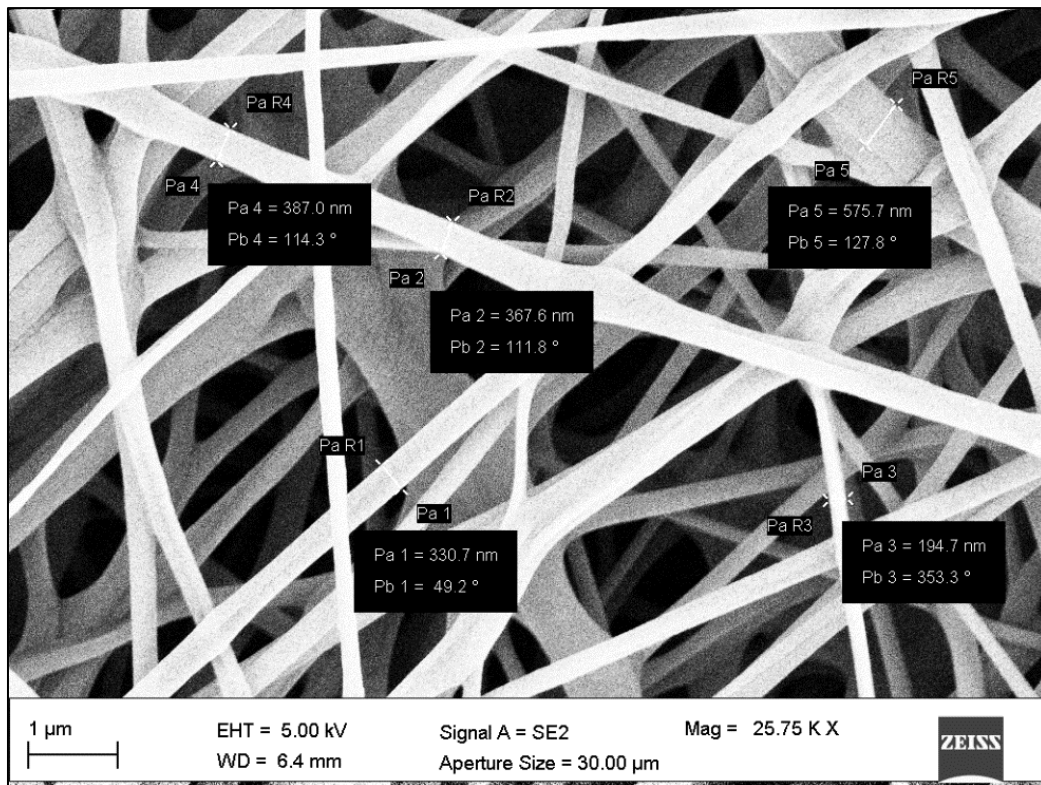
Figure 4.9.3 Measurement of the diameters of the fibre in PLA filter.

From Figure 4.9.1 the sample appears uniform, with thin fibers well overlapped. In Figure 4.9.2, the enlargement of the fibers shows very thin fibers and the homogeneity of the sample is confirmed. Figure 4.9.3 reports their size and the average diameter for PLA-series fibers is 350 nm.

Comparing this series with PLA/CyD-series previously mentioned, it is clear the difference in terms of size. In fact, with the same enlargement, the fibers appear thicker also in the overall view in Figure 4.9.4. Figure 4.9.5 show not only the shape of the fiber, but also how the powder interacts with the fiber in this particular bilayer configuration. Cyclodextrins are deposited on the fibers and well adhered thanks to the second layer of nanofibers. They tend to form agglomerates, which may or may not affect the filtration efficiency. At this stage, this aspect has not been studied yet, but it would be part of future studies. The average diameter for this series of samples is 530 nm (Figure 4.9.6) and also in this case the sample is uniform.
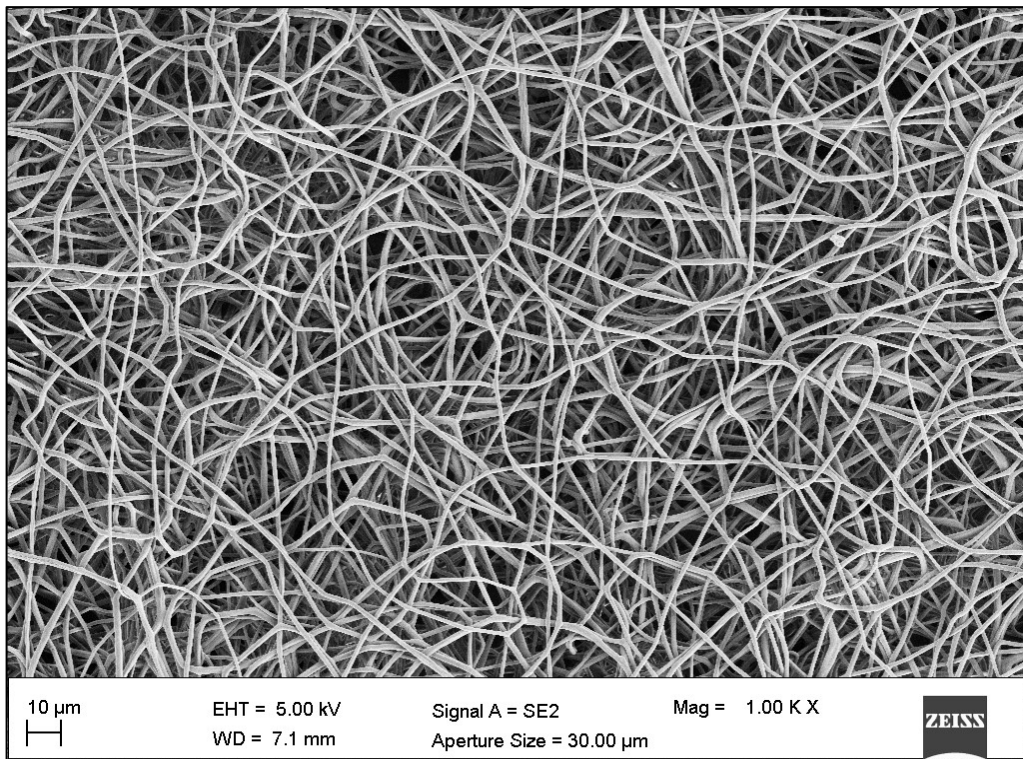
Figure 4.9.4 Overall view of the PLA/CyD filter.
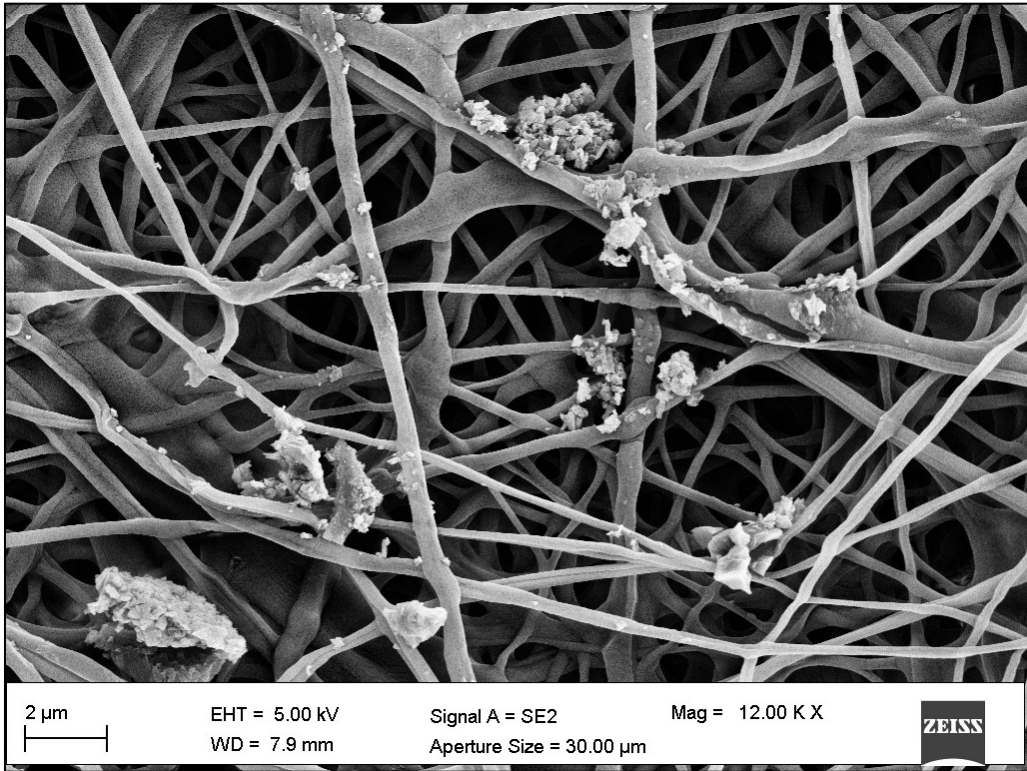
Figure 4.9.5 Enlargement of PLA/CyD filter
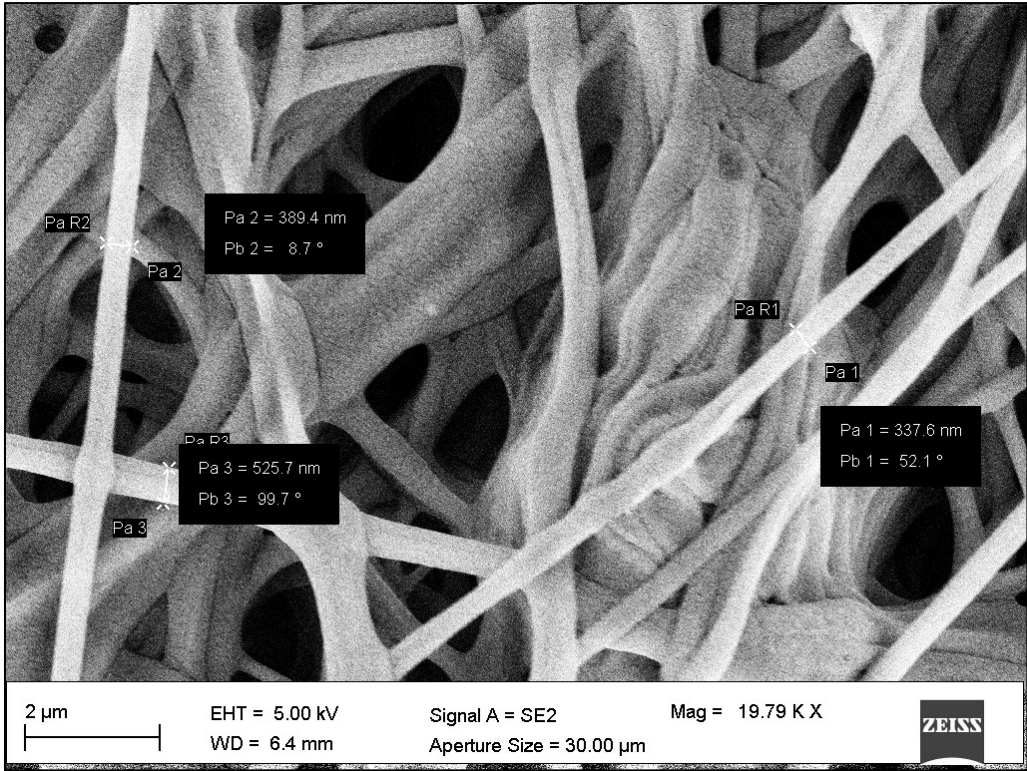
Figure 4.9.6 Measurement of the diameters of the fibre of PLA/CyD filter with the support in background.

The last series of filters present the most different shape and size due to the different formulation. In fact, adding the CyD directly in the solution, even if only by 1.5% w/w, increases the concentration of the polymeric solution, causing also the increase in size of the fibers (Figure 4.9.7).
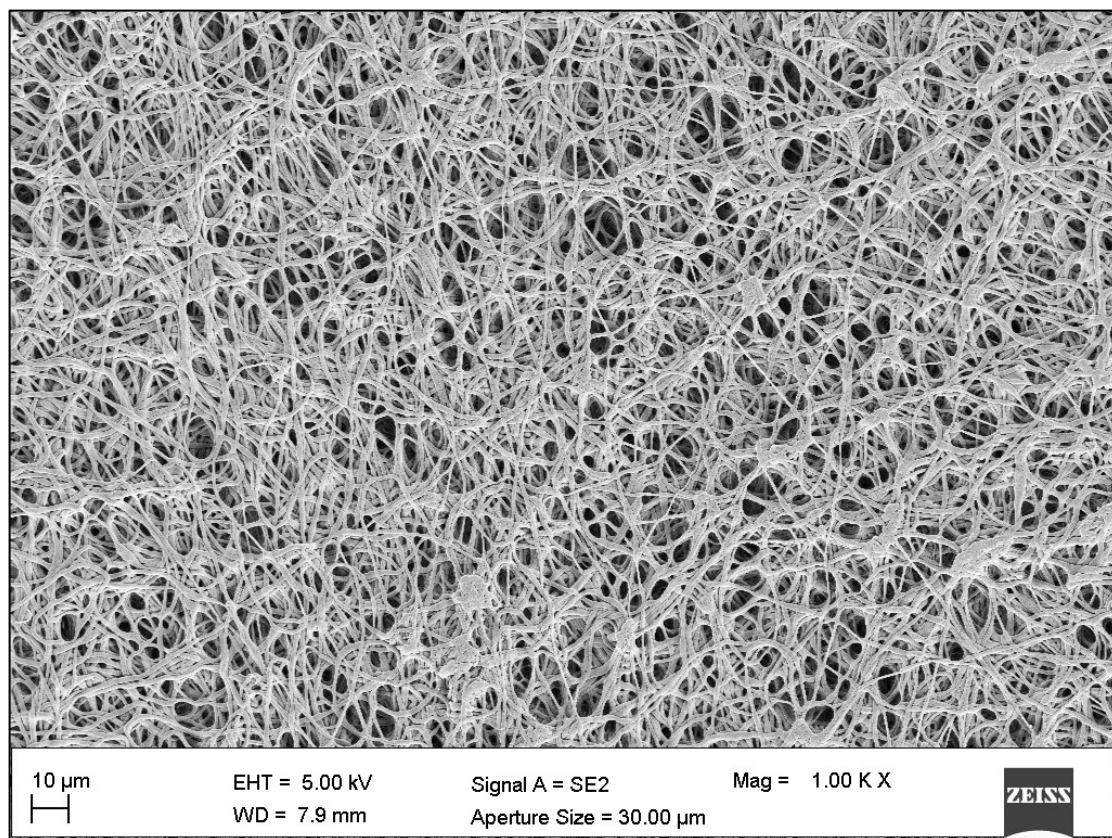
Figure 4.9.7 Overall view of PLA+CyD filter.

Extremely interesting is the shape of the fibers, which is clear in Figure 4.9.8: these fibers are still homogeneous, but the addition of CyD to the PLA totally changes their morphology, making them more attached to each other and with a surface that seems porous.

In this case the range of the diameters is larger, from 400 nm up to 1 μm, so the average diameter results to be 990 nm (Figure 4.9.9).
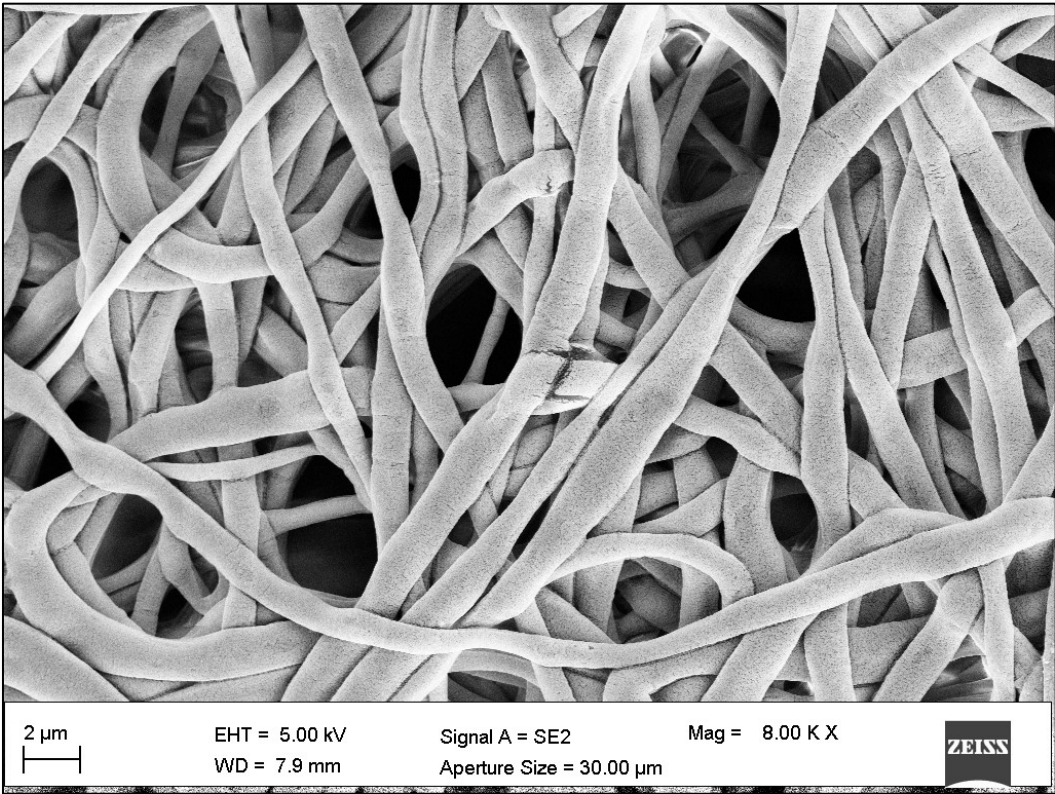
Figure 4.9.8 Enlargement of PLA+CyD filter.
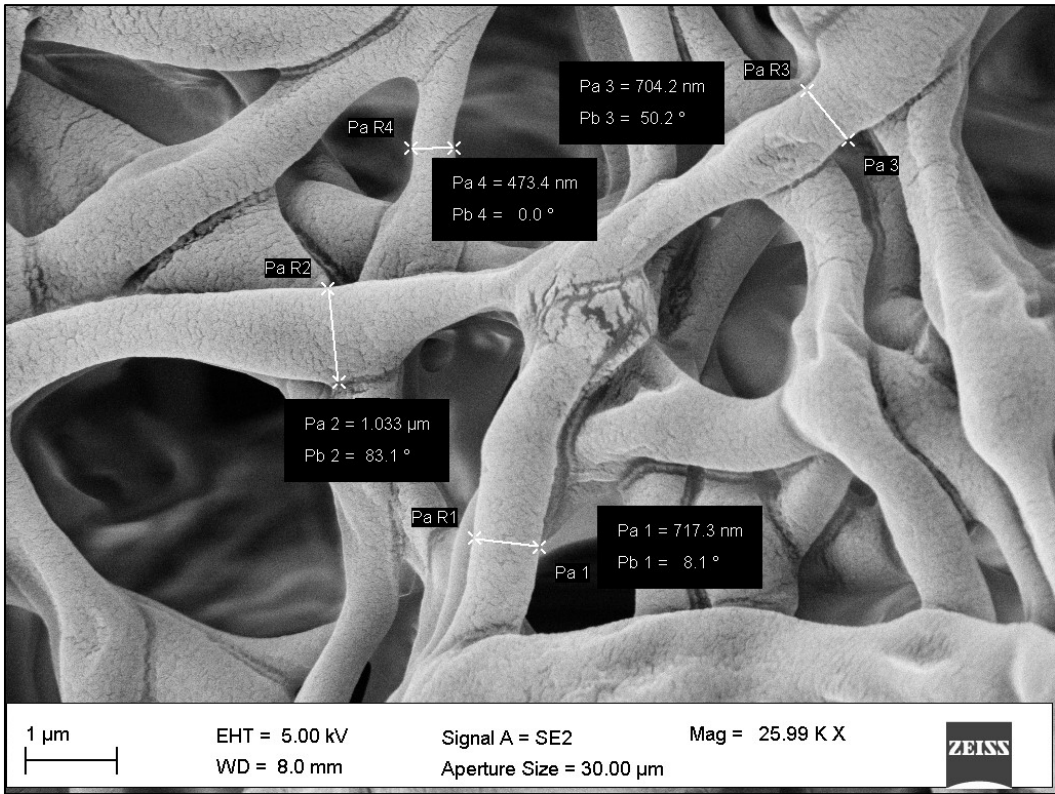
Figure 4.9.9 Measurement of the diameters of the fibre of PLA+CyD fibres

In Figure 4.9.10 the diameters distributions of the three series of samples are reported.
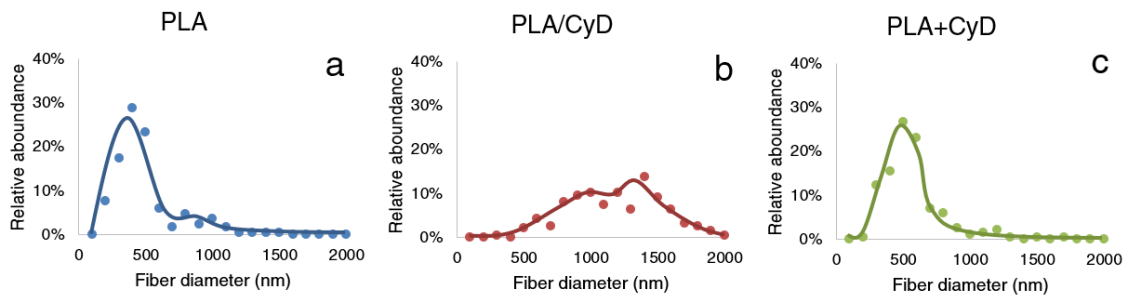
Figure 4.9.10 Fibre diameter distribution for (a) PLA, (b) PLA/CyD and (c) PLA+CyD electrospun nanofibers.

The morphological aspect is strictly related to the fibrous filter pressure drops, which have been measured at low face velocity. Pressure drop and outlet air velocity, as a function of the fiber type and fiber loading values, have been reported in Table 4.9-1.

Table 4.9-1 Composition and characterization of the electrospun filter media

Filter	solution		CyD	V outlet (m/s)	ΔP (Pa)	Filter loading (mg/cm^2)
	PLA	CyD				
PLA	100%	0	-	0.25	24.4	1.43
PLA/CyD	98.5%	1.5%	-	0.41	33.9	2.47
PLA+CyD	100%	-	1.5%	0.24	29.9	4.05

Crossing these data with the images analyses the correlations between dimensions and morphology of the fibers can be found.

Observing the three types of filters, the presence of cyclodextrins influences the result of electrospinning and the overall measured pressure drop (Table 4.9-1, ΔP 24.4, 33.9, and 29.9 respectively).

The pressure drop of air filters is an essential parameter to consider in the air filtration field because a high pressure drop means that the air handler has to work harder and consume more energy in order to maintain proper airflow.

Filters with the PLA/CyD formulation show apparently more bulky fibers (Table 4.9-1, filter loading (mg/cm^2), 1.43, 2.47, and 4.05) than the ones of PLA and PLA+CyD filters. This comparison justifies a higher drop pressure for this filter (33.9 Pa).

Furthermore, crossing fibers enhance thickness determining a probably augmented capacity of sieving phenomena, particularly for the PMs.

4.9.2   PM and VOC removal tests

The PM1, PM2.5 and PM10 removal by different fibrous filters is shown in Figure 4.9.11. From the PM efficiency removal comparison, it is possible to observe that the PLA+Cyd has the highest removal for smallest particles, while all the other samples exhibit an efficiency higher than 97% for particles having diameter greater than 2.5 μm. This contribution in the efficiency of filtration is due to the presence of CyDs.
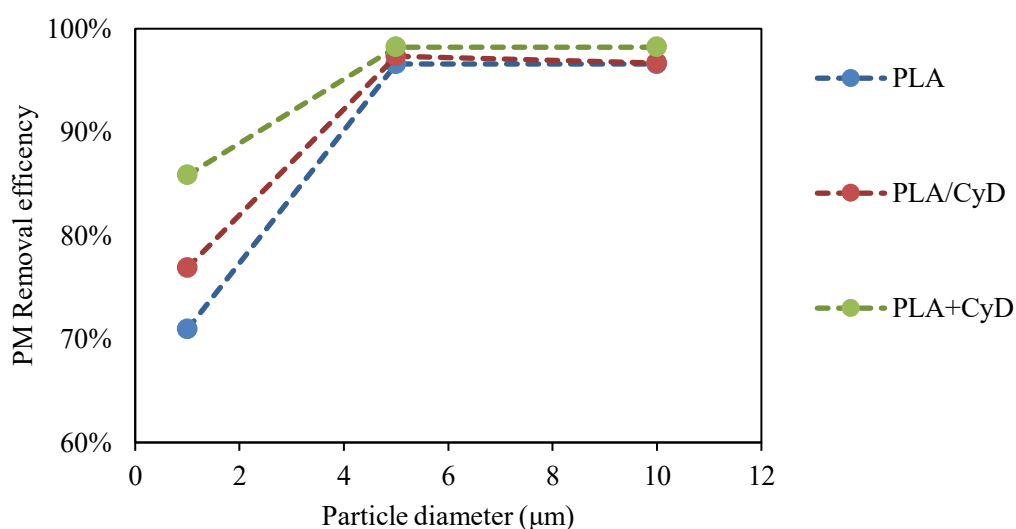
Figure 4.9.11 PM removal efficiency

The characteristic conical configuration of cyclodextrins[217], in fact, is suitable for the formation of complexes of inclusion through non-covalent interactions: for this reason, hydrophobic molecules are maintained in the cavity, blocking their passage through the filter.

This mechanism of filtration should be added, according to classical filtration theory, to the other five mechanism effects to catch particles (interception, inertial, diffusion, gravity, and static electricity effect)[170] to catch also other smaller molecules as VOCs.

In this way, CyD plays a role both in affecting the fiber morphology, resulting in thicker fibers and reduced cavities, and, actively, as surface centers for the capture of PM and VOCs, due to their dual hydrophilic/hydrophobic nature.

The presence of CyD molecules at the surface of the fibers has a large influence on the molecular filtration capability[224]. The presence of more CyDs on the surface of the fibers implies a higher availability of sites for the bond with the pollutants, so it is reasonable to assume that higher concentration of CyDs are beneficial for the overall filtration

efficiency. Nevertheless, the superficial availability of adsorption centers will affect also the blocking capacity of PMs and the resulting pressure drop.

For all these reasons, the amount of CyDs must be enough both to be bonded to the polymer and to have the possibility to create hydrogen bond with the pollutants.

During the electrospinning, CyD molecules could separate from PLA matrix and form heterogeneous dispersion during solvent evaporation in the electrospinning process: this is likely because CyD has a hydrophilic characteristic and PLA is a hydrophobic polymer[224]. A heterogenic solution may cause a not homogeneous presence of CyDs on the fiber surface, causing a not homogenous filter, not in terms of fibers but in terms of area with the presence of CyD.

VOCs removal curve is shown in Figure 4.9.12 where the three different tested filters are compared after two subsequent injections of certain quantities of toluene in the box in two different moments.
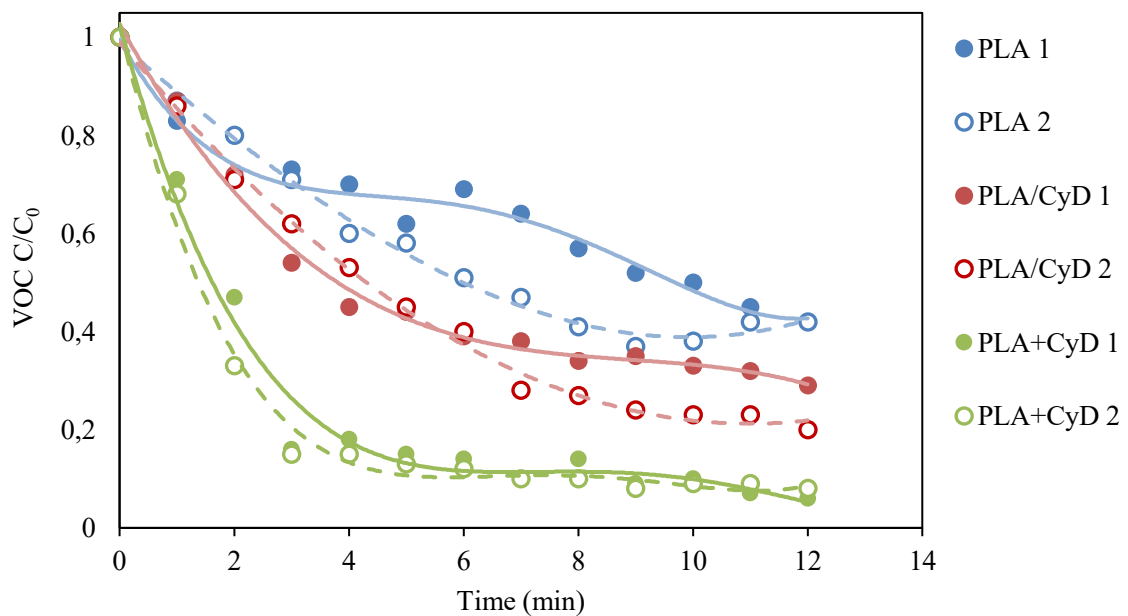
Figure 4.9.12 Normalized VOC concentration versus time in the presence of different fibrous filters

The curve 1 is the behavior with 100 µl of Toluene (in Figure 4.9.12 labelled with 1). After about 30 minutes and as curves reach a plateau or their background concentration, the second injection of Toluene has been carried out (20 µl). This second injection (in Figure 4.9.12 labelled with 2) is sufficient to obtain an initial concentration of Toluene comparable to the first one.

The purpose of this method consists in investigating repeatability of tests and in the first evaluation of the durability of filters. As expected, filters with cyclodextrins allow quicker removal of VOCs, referred to PLA only fibers.

Besides, it can be observed that the two normalized curves are almost overlapped, highlighting a factual constant behavior, for two subsequent tests at high concentration at least. The presence of cyclodextrins in filters points out an increased capacity in the removal of VOCs. This condition suggests that VOCs removal tests highlight the contribution of the CyD on adsorption.

A previous study[225] on the inclusion complex formation of benzene with β-cyclodextrin, demonstrates that, due to specific geometry, the aromatics and β-CyD in aqueous solution could form inclusion complexes with 1:1, 1:2, and 2:1 stoichiometry. The study of the values of stability constant (Ks) for 1:1 stoichiometry inclusion complex at different temperatures (in the range of 291–303 K) are rather small, and stability constant increases with diminishing of temperature. Therefore, it could be concluded, that interactions between β-CyD and benzene or its derivates are rather weak. Such interactions are typical for non-specific forces or inclusion complexes with VOCs.

Thermodynamic values in the study[225] of complex formation between b-cyclodextrin and benzene[231] demonstrates that the complex formation is the spontaneous and thermodynamically favored process. Formation of 1:1 ''β-cyclo- dextrin-benzene'' inclusion complex is an exothermal process, accompanied by the release of high-enthalpy water molecules and the decrease of entropy as a result of guest-molecule restriction in the cavity of β-CyD molecule.

In the case of this study, the bond between the two molecules is preferred because it respects the usual temperature present in indoor environments, so the stability constant could be compared to the one at 298K proposed in[225].

The exact nature of the driving force of complexation of cyclodextrins with guest molecules is not known. It is a combination of CyD-ring strain release upon complexation, geometrical compatibility, van der Waals forces, electrostatic, and hydrophobic interactions and, in some cases, hydrogen bonding between the cyclodextrin and the guest molecule[226].

Thus, the CyD can empower the removal of VOCs in two different ways. It is probable that in PLA/CyD filters VOCs are removed when CyD have their hole available. In PLA+CyD filters, VOCs are removed when they collide with CyD powder with an enhanced capacity of removal because of entire exposure to air, with a higher number of available sites.

A non-exhaustive comparison of the obtained results with the one reported in the literature is reported in Table 4.9-2.

Table 4.9-2 Comparison of the obtained filtration results with the ones reported in the literature

Electrospun Polymer	Efficiency	Comments	Ref
PLA	99.997% (165.3 Pa)	Small fiber diameter and the presence of additional mesopores on the beads were conducive to the capture and adsorption of particulates.	[227]
PLA/TiO2	99.996% (128.7 Pa)	Relative humidity of 45% and face velocity of 5.3 cm/s and a high antibacterial activity of 99.5%	[228]
PLA/CNPs	98.99% (147.60 Pa)	Air flow rate of 14 cm/s. PLA/chitosan fibers show a highly porous structure	[175]
PVA/CNCs	99.1% (91 Pa)	Tests with PM2.5 and airflow velocity of 0.2 m/s	[192]
Hierarchical structured nano-sized/porous PLA	99.999% (93.3 Pa)	PLA-N/PLA-P double-layer structured membrane with a mass ratio of 1/5. Face velocity equal to 5.3 cm/s	[171]
PAN	>99% (27 Pa)	Nanobeads are useful for reducing the packing density and the pressure drop through the filter. Ultrafine nanofibers guarantee the PM removal efficiency. Airflow rate e 4.2 cm/s	[174]
PLA/CyD	> 98% (30Pa)		This study

DMAC: dimethylacetamide; CNPs: Chitosan nanoparticles; CNCs: cellulose nanocrystals

4.9.3   **FTIR Spectroscopy**

FTIR spectroscopy has been used to determine the interaction between both PLA and CyD and the composite and pollutants[229]. Obviously, due to a large number of functional groups present due not only to the variability of the compounds in the polluting source used for the tests but also to the polymeric ones of the filter, the filtered molecules can not be identified with certainty.

It is instead possible to determine by difference the presence or absence of pollutants. In this regard, it has been necessary to outline a spectroscopic profile of the materials used to make the filter itself, to also study the interaction between the polymer and the CyDs.

Figure 4.9.13 reports a comparison between the untested (PLA_pre) and the tested (PLA_post) PLA filter (samples without CyDs). The spectra of the pristine filter show the main peaks attributable to the PLA: at 2997-2944cm^{-1} are related to the symmetrical and the asymmetrical stretching of CH_2 and CH_3; the characteristic peak of a carbonyl

group is at 1753 cm^{-1}; at 1453 cm^{-1} is the pick of methyl in α position respect to the carbonyl group and the region of 1380-1000cm^{-1} is related to the bending signals of CH$_2$ and CH$_3$.
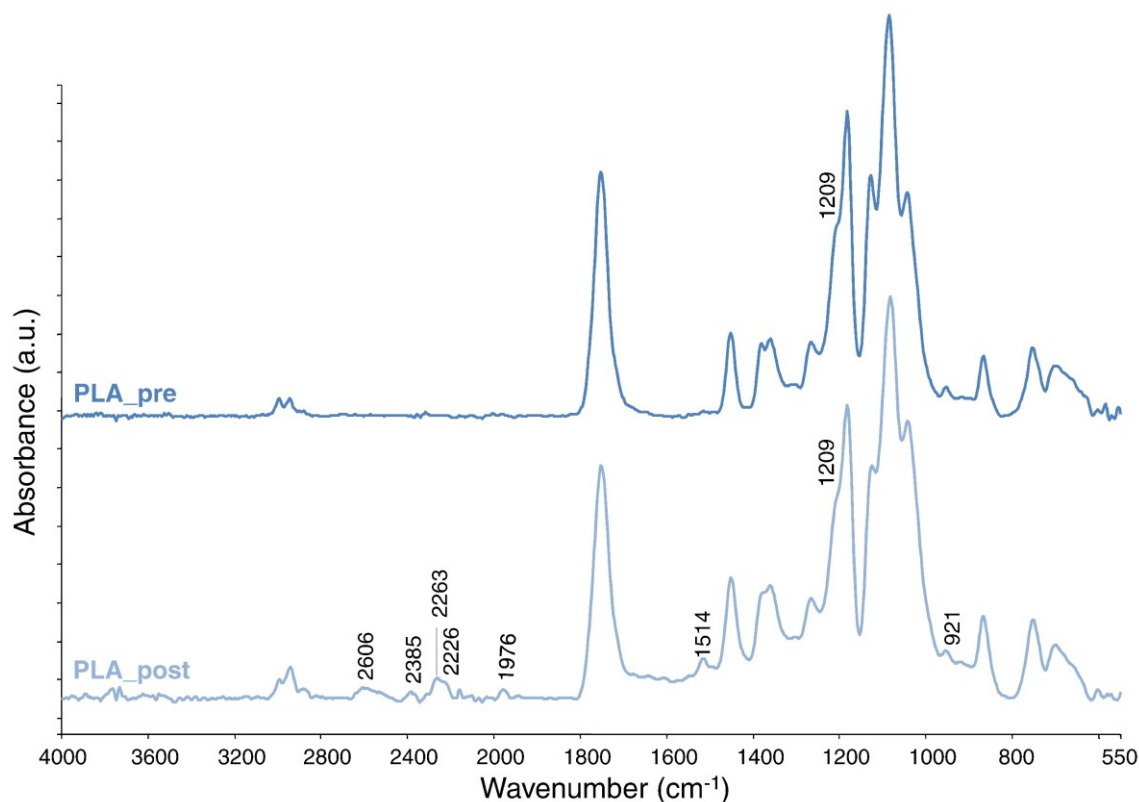
Figure 4.9.13 FTIR spectra of untested (PLA_pre) and tested (PLA_post) PLA filters.

In the other spectra, the different peaks caused by the interaction of the polymer with pollutants can be easily individuated: at 1644, 1541, 1514, 1301 cm^{-1} and 953 cm^{-1}. Confronting the peak of the carbonyl group at 1753 cm^{-1} of the no-tested and tested filter, the tested filter reports a shift caused by the interaction between the polymer and the pollutant. It is possible to suppose the presence of nitro groups, reported by the peaks in the range of 1541cm^{-1} and 1514 cm^{-1}; the presence of aldehydes because of the shift at 1754 cm^{-1} and the peak at 1644cm^{-1}; and a carbon-nitrogen bound, due to the presence of a peak at 1301cm^{-1}. The peak at 1514cm^{-1} is very sharp respect to the other spectra, it is reasonable to assume that this is due to the concentration of pollutant adsorbed. A peak at 1514cm^{-1} can be attributed or to a NO or a CN group. Moreover, it presents a series of peaks at 2601, 2385, 2263 and 1976cm^{-1}. Usually, in this range, signals from inorganic contaminants as, for example, thiocyanate fall.

Considering the CN at 1514cm^{-1}, at the level of bands' ratio, the signal of the triple bonds is present at 2200cm^{-1}; the -SH group is at 2600 cm^{-1} and the signal of SCN is at 2100 cm^{-1}.

The peak at 1209cm^{-1} is different in terms of height, therefore the concentration of the respective group increases after the filtration meaning that a pollutant containing this group is attached to the filter. Lastly, at 921 cm^{-1} a new peak appears, which was absent in the pristine filter, again probably relative to the deposited pollutant.

For what concerns the filters made with cyclodextrins (PLA/CyD and PLA+CyD), it is important to determinate the possible interaction between the polymer and the CyD molecules, because during the electrospinning process these two compounds could interact causing the presence of new peaks.

It is necessary to determine the shifts and the new peaks on a no-tested filter, not only to have a reference standard for the identification of the pollutant, but also to estimate the level of the bond between the two compounds.

Figure 4.9.14 reports the spectra of the untested filter, made by adding CyD not only in the between of two layers of the polymer (PLA/CyD), but also in the polymer solution (PLA+CyD).
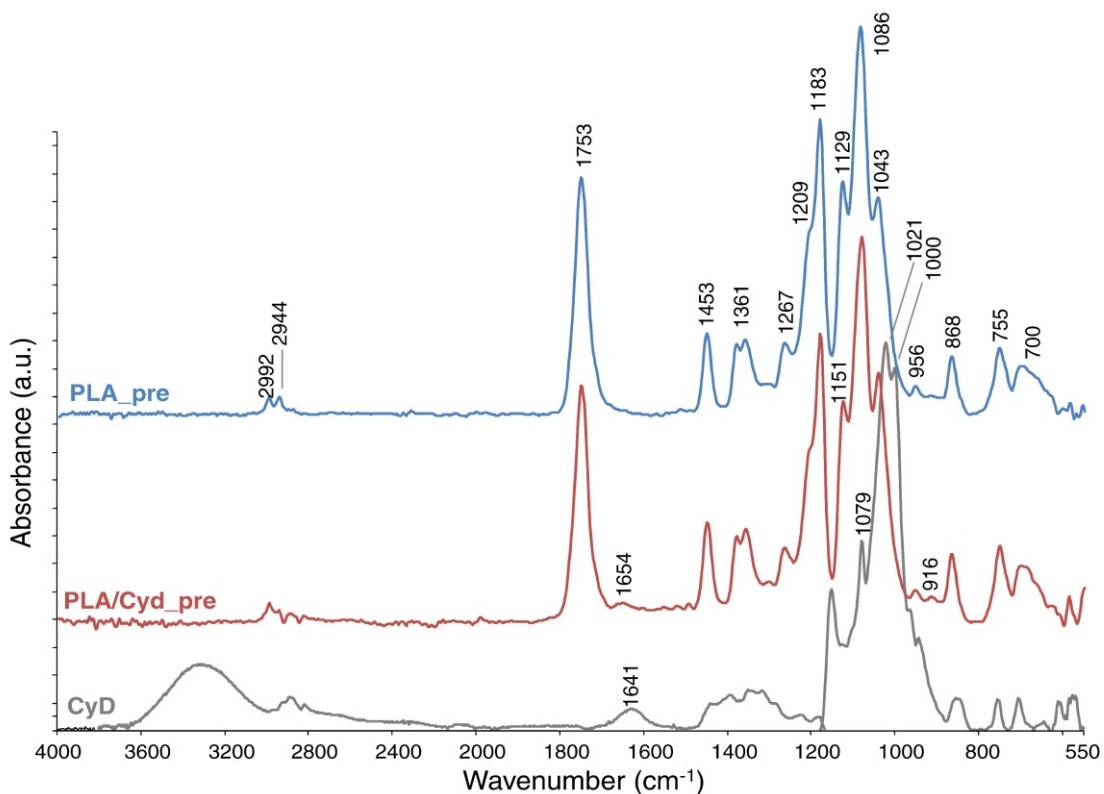
Figure 4.9.14 Comparison between the spectrum of pure CyD, the untested PLA filter and the spectra of untested filter containing PLA and CyDs (PLA/CyD).

Analyzing this spectrum, it is immediately notable the absence of the characteristic peak of the hydroxylic group at 3400cm^{-1}, because a large quantity of these groups is bonded

with PLA in hydrogen bonds; however the peak at 1654cm^{-1} indicates that there are still some free.

All the values at 1000, 1021, 1077 and 1151 cm^{-1} are shifted to 1040, 1082, 1124 and 1182 cm^{-1} because of the hydrogen bonds between the two compounds. Also, the peak at 850cm^{-1}, typical of C-C bond, is shifted to 916 cm^{-1}.

The shift of the signal can be caused not only by the formation of new bonds but also by the sum of two different signals in the same region.

After the reference spectra for the filters containing CyD, also the tested spectra were examined (Figure 4.9.15).
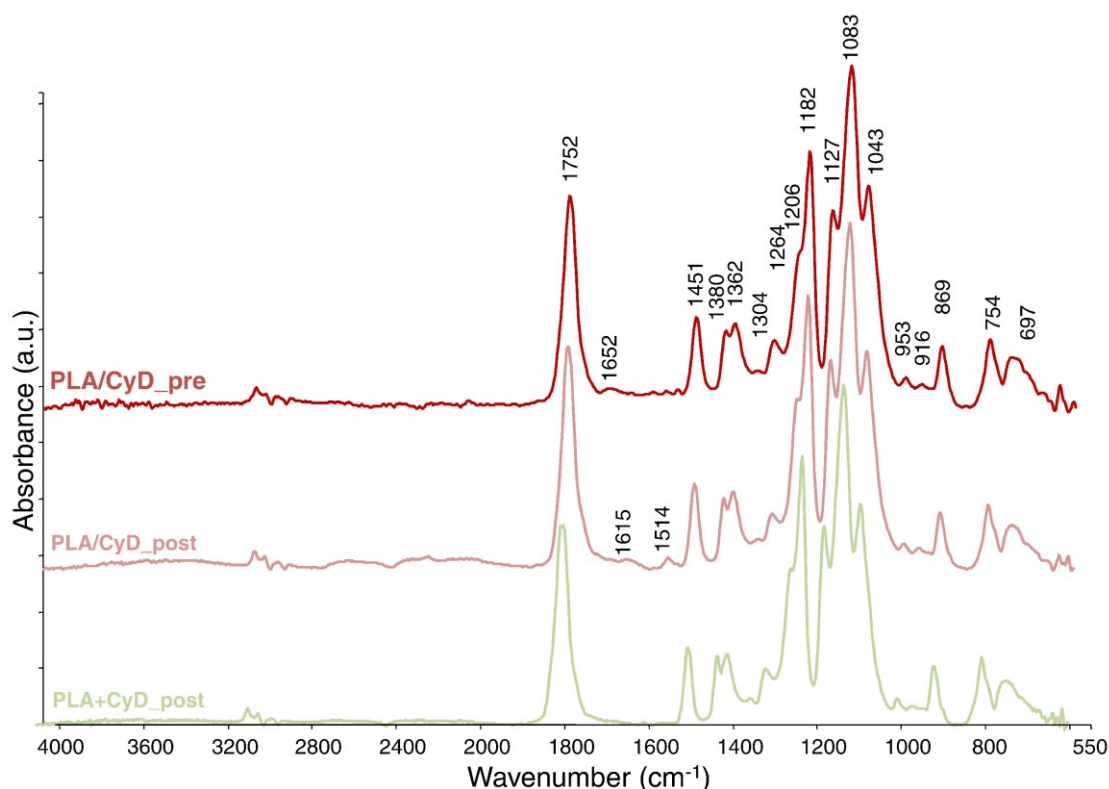
Figure 4.9.15 Comparison between the FT-IR spectra of all the filters containing cyclodextrins.

In these samples the presence of contaminates is represented by two main behaviors: the most important is the split of the carbonyl peak (Figure 4.9.16) and its slightly shift; the other is the shift of all the characteristic bands in the range from 1220 cm^{-1} to 1000cm^{-1} (Figure 4.9.17). The split of the carbonyl group can indicate the presence of another molecule with a similar configuration (for instance an aldehyde or a ketone). Moreover, these kinds of pollutants may cause also the shoulder at 1736cm^{-1}.

Other particular peaks (Figure 4.9.15) are present at 3377cm^{-1} for PLA/Cyd: the peak at 3377cm^{-1} can be attributed to a compound with NH group, there are also peaks at 1615 and 1514 cm^{-1}, which usually indicate the presence of NH$_2$ and of a carbon bonded to nitrogen.

The series of peaks in the range from 870 to 700cm^{-1} are typical of CH groups: in these cases, they are different from the reference because of their shape and their shift, indicating the presence of another compound different from Cyclodextrins or PLA.
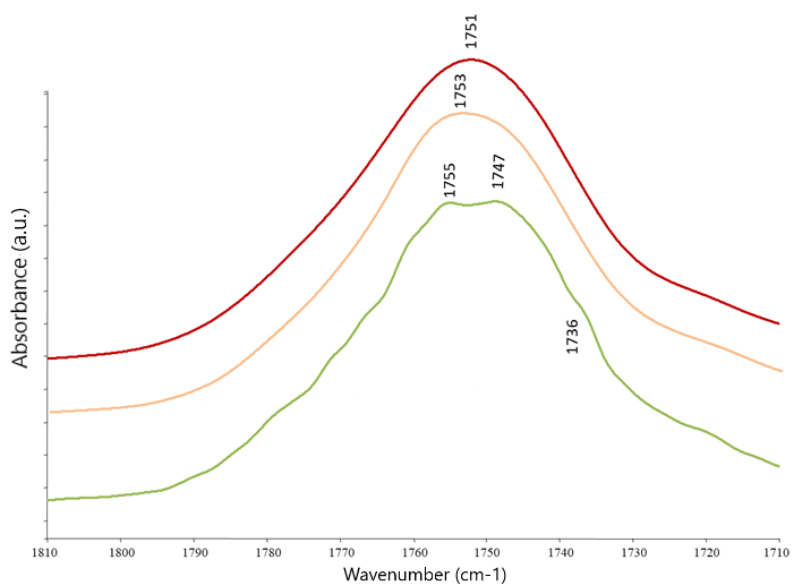
Figure 4.9.16 Enlargement on carbonyl group of the FTIR spectra in Figure 4.9.15
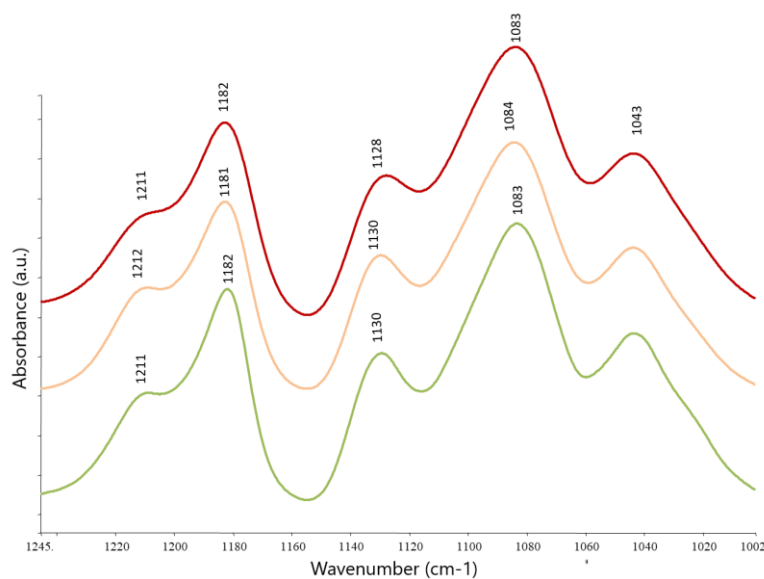
Figure 4.9.17 Enlargement of peaks in the range of 1200cm^{-1} -1000cm^{-1} of the FTIR spectra in Figure 4.9.15

4.10   **Conclusions**

The addition of CyD both in bulk and powder determines an increase of removal efficiency of VOCs and PM1 size fraction, due to two different effects: the CyD in bulk affects the PLA fibers morphology, while the superficially deposited CyD directly affects the removal of VOCs.

Efficiency tests highlight enhanced VOCs removal efficiency in PLA/CyD and PLA+CyD filters; the FTIR analysis confirms that in filters containing CyDs the traces of the interaction between the pollutants and the filter are more evident, showing shifted and larger bands, split and sharper peaks.

The use of this innovative air filtration system, combined with technology such as electrospinning, makes CyD-based filters a new resource for use in indoor air filtration applications.

This study, although preliminary, demonstrates that the reduction of pollutants such as VOCs is possible and proposes a solution to a problem already well known as harmful and dangerous to human health.

The next step of this preliminary study is focused on the perfecting of formulations, involving also the electrospray of a solution of cyclodextrins directly on PLA nanofibers, in order to increase the surface area of contact between the two components. Moreover, also the recovering of the solvents used for the formulation is going to be studied in order to make the procedure more green as possible.

After this step, further studies will involve the investigation of the VOCs type on the adsorption property, with the simultaneous addition of functional composites and the aim of synthesizing such composite from starch-food wastes.

The use of CyDs from food wastes, such as processing wastes and starch-rich wastewater, in air filtration systems will improve their positive environmental impact in a circular economy perspective and it will be the core of this project.

5. Chapter PHAs coming from WWTPs

Study on the effect of mechanical pre-treatments on the properties of polyhydroxyalkanoates extracted from a mixed culture biomass coming from wastewater treatment plants.

5.1   Introduction

One of the main problem nowadays is the production and the use of petroleum based plastics because of their non-biodegradable nature[230] that generates non-degradable wastes[31] during their processing and at the end of their service life.

For this reason, researchers are experimenting and studying substitutes for common plastics derived from petroleum, in order to develop more sustainable products.

The term "Bioplastic" comprises of a whole family of materials with different properties and applications. According to European Bioplastics[24], a plastic material is defined as a bioplastic if it is either biobased, biodegradable, or features both properties. There are two major advantages of biobased plastic products compared to their conventional versions: they save fossil resources by using biomass which regenerates (annually) and provides the unique potential of carbon neutrality. Furthermore, biodegradability is an add-on property of certain types of bioplastics. It offers additional means of recovery at the end of a product's life[24].

Bioplastics are largely classified on the basis of their biodegradability, type of monomer structure and source of raw materials used. It should be noted that biodegradability is an inherent property of a material and is not the same as being biobased. Biobased materials can be non-biodegradable while petroleum-based plastics can be biodegradable[231].

5.2   Polyhydroxyalkanoates: the new frontier for plastic

5.2.1   Polyhydroxyalkanoates

A green, eco-friendly and biodegradable alternative to petroleum based plastic are those based on Polyhydroxyalkanoates (PHAs)[41].

These are polyesters widely distributed in nature, accumulated intracellularly in microorganisms in the form of storage granules, with physical-chemical properties resembling petrochemical plastics.

PHA plays a pivotal role in priming microorganisms for stress survival and promotes the long-term survival of bacteria under nutrients-scarce conditions by acting as carbon and energy reserves for both non-sporulating and sporulating bacteria[79,232]. In particular, Poly(3-hydroxyalkanoates) (PHAs) are structurally simple macromolecules (biopolymers) synthesized by many gram-positive and gram- negative bacteria[233] in granular forms as lipid inclusions for energy storage within the cellular structure[234].

Once PHAs are extracted from the bacterial cell, these molecules show properties similar to polypropylene ones. The bacterial origin of the PHAs make these polyesters a natural

material: most of them are biodegradable and biocompatible, which makes them extremely interesting from the biotechnological point of view[79]. PHAs are recyclable like the petrochemical thermoplasts[231,235].

The number and size of the granules, the monomer composition, macro- molecular structure and physical-chemical properties vary, depending on the producer organism[236]. The presence of the polyester in the bacteria can be observed intracellularly as light-refracting granules or as electron-lucent bodies as previous studies reported[79] (Figure 5.2.1).
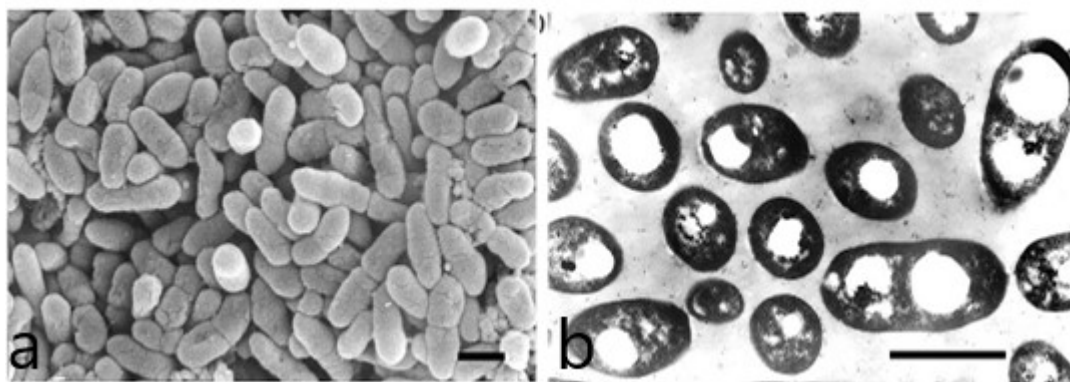
Figure 5.2.1 Scanning (a) and transmission (b) electron microphotographs of P. putida U cultured in a chemically defined solid medium containing 7-phenylheptanoic acid (5 mM) as a source of aromatic PHAs and 4-hydroxyphenylacetic acid (5 mM) as an energy source. Bar =1 μm[79]

5.2.2 PHA biosynthesis

The biosynthetic pathways of PHAs are intricately linked with the bacterium's central metabolic pathways including glycolysis, Krebs Cycle, β-oxidation, de novo fatty acids synthesis, amino acid catabolism, Calvin Cycle, and serine pathway[237,233].

Many common intermediates are also shared between PHA and these metabolic pathways, most notably being acetyl-CoA. In some PHA-producing microbes such as *Cupriavidus necator, Chromatium vinosum*, and *Pseudomonas aeruginosa*, the metabolic flux from acetyl-CoA to PHA is greatly-dependent on nutrient conditions[238]. Under nutrient-rich conditions, the production of high amounts of coenzyme A from Krebs Cycle blocks PHA synthesis by inhibiting 3-ketothiolase (PhaA) such that acetyl-CoA is channeled into the Krebs Cycle for energy production and cell growth[35].

Conversely, under unbalanced nutrient conditions (i.e. when an essential nutrient such as nitrogen and phosphorus is limiting in the presence of excess carbon), coenzyme A levels are non-inhibitory allowing acetyl-CoA to be directed towards PHA synthetic pathways for PHA accumulation[238,239]. This metabolic regulation strategy in turn enables the PHA-

accumulating microbes to maximize nutrient resources in their adaptation to environmental conditions[240].

In order to synthesize PHB, two molecules of acetyl-CoA condense to form acetoacetyl-CoA. This reaction is catalysed by β- ketoacyl-COA thiolase. Subsequently an enzyme named acetoacetyl-CoA reductase reduces acetoacetyl-CoA to (R)-3-hydroxybutyryl-CoA which is then used as a monomer to polymerize PHB by PHB synthase[240] (Figure 5.2.2).

A possible explanation to the accumulation of PHA under nutrient limiting conditions can be attributed to the inhibition of enzyme β-ketothiolase by CoA-SH. In conditions of oxygen limitation, the final electron acceptor is lacking, leading to an increased NADH/NADH+ ratio. As a result, many acetyl-CoA molecules cannot enter the TriCarboxylic Acid (TCA) cycle resulting in a decreased CoA-SH concentration. Moreover, nitrogen or phosphate limitation results in a reduced activity of anabolic pathways leading to ATP excess which causes acetyl CoA accumulation leading to PHA production in a manner similar to that for oxygen limitation. It has however been observed that complete depletion of a nutrient causes growth cessation resulting in a decreased PHA storage capacity[237,231]
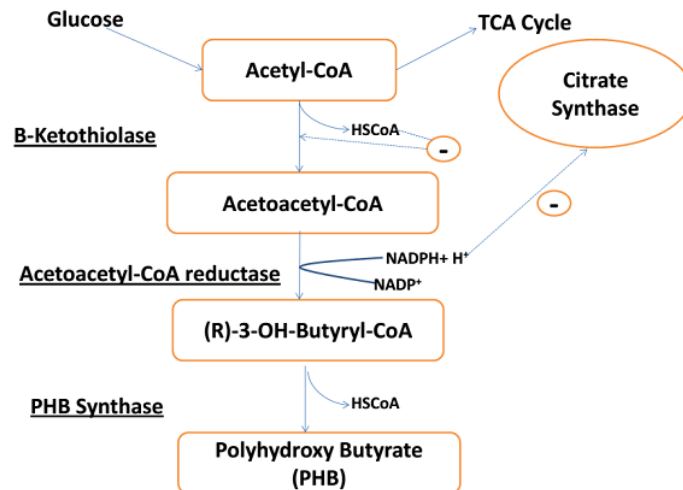
Figure 5.2.2 Biosynthesis of polyhydroxybutirrate [231]

Composition of the culture, specially the substrate, influences the polymer characteristics (e.g., side chains, range of polymers formed, molecular weight, crystallinity), which affects some of their chemical- physical properties (e.g., mechanical and tensile strength)[241].

5.2.3   **Chemical structure**

PHAs are classified into three classes based on their chain lengths: short (scl), medium (mcl) or long chain (lcl) (Figure 5.2.3). Different chain lengths give different properties to the polymer especially in terms of thermo-mechanical behaviour (as reported in Chapter 2). PHAs are insoluble in water, resistant to UV, biocompatible, biodegradable and have good resistance to hydrolytic attack[230].

In these polymers, the carboxyl group of one monomer forms an ester bond with the hydroxyl group of the neighbouring monomer (Figure 5.2.3).

In all PHAs that have been characterized so far, the hydroxyl-substituted carbon atom is of the R configuration, except in some special cases where there is no chirality. At the same C-3 or β position, an alkyl group which can vary from methyl to tridecyl is positioned.

Substituents in the side chains of PHAs can be modified chemically, for instance by cross-linking of unsaturated bonds[242]. This variation in the length and composition of the side chains and the ability to modify their reactive substituents is the basis for the diversity of the PHA polymer family[233].

P(3HB) is the most common type of PHA, and the ability of bacteria to accumulate P(3HB) is often used as a taxonomic characteristic[243–245]. Copolymers of P(3HB) can be formed by cofeeding of substrates and may result in the formation of polymers containing 3-hydroxyvalerate (3HV) or 4-hydroxybutyrate (4HB) monomers. Together, polymers containing such monomers form a class of PHAs typically referred to as short-side-chain PHAs (scl-PHAs)[233].

The vast majority of microbes synthesize either scl-PHAs containing primarily 3HB units or mcl-PHAs containing 3-hydroxyoctanoate (3HO) and 3-hydroxydecanoate (3HD) as the major monomers[239,233].

R group	Carbon no.	PHA polymer
methyl	C_4	Poly(3-hydroxybutyrate)
ethyl	C_5	Poly(3-hydroxyvalerate)
propyl	C_6	Poly(3-hydroxyhexanoate)
butyl	C_7	Poly(3-hydroxyheptanoate)
pentyl	C_8	Poly(3-hydroxyoctanoate)
hexyl	C_9	Poly(3-hydroxynonanoate)
heptyl	C_{10}	Poly(3-hydroxydecanoate)
octyl	C_{11}	Poly(3-hydroxyundecanoate)
nonyl	C_{12}	Poly(3-hydroxydodecanoate)
decyl	C_{13}	Poly(3-hydroxytridecanoate)
undecyl	C_{14}	Poly(3-hydroxytetradecanoate)
dodecyl	C_{15}	Poly(3-hydroxypentadecanoate)
tridecyl	C_{16}	Poly(3-hydroxyhexadecanoate)

Poly(3-hydroxyalkanoate)

Figure 5.2.3 Polyhydroxyalkanoates (PHA) chemical structure. The nomenclature and carbon number for PHA compounds is determined by the functional alkyl R *group. Asterisk denotes chiral centre of PHA-building block[239].*

5.2.4 Physical properties

The molecular mass of PHAs varies per PHA producer but is generally on the order of 50,000 to 1,000,000 Da. During the early research on aliphatic polyesters, their properties were not remarkable due to the use of relatively impure substrates at the time, which limited the molecular masses of these polymers to 20,000 to 30,000 Da[233].

Bacterially produced P(3HB) and other PHAs, however, have a sufficiently high molecular mass to have polymer characteristics similar to conventional plastics (such as polypropylene). Within the cell, P(3HB) exists in a fluid, amorphous state. After extraction from the cell with solvents, P(3HB) becomes highly crystalline[246] and in this state is a stiff but brittle material. Because of its brittleness, P(3HB) is not very stress resistant. Also, the relatively high melting temperature of P(3HB) (around 170°C) is close to the temperature where this polymer thermally decomposes and thus limits the ability to process the homopolymer. Initial biotechnological developments were therefore aimed at making PHAs easier to process[233]. The incorporation of 3HV into the P(3HB) resulted in a poly(3-hydroxybutyrate-co-3-hydroxyvalerate) [P(3HB-3HV)] copolymer that is less stiff and brittle than P(3HB). It can be used to prepare films with excellent water and gas barrier properties reminiscent of polypropylene, that can be processed at a lower temperature while retaining most of the other excellent mechanical properties of P(3HB). In contrast to P(3HB) and P(3HB-3HV), mcl- PHAs have a much lower level of crystallinity and are more elastic[245,247,248]. These mcl-PHAs potentially have a different range of applications from the scl-PHAs[233].

5.3   Overview of PHB production from Industrial residues

The growing concern about the harmful effects of plastics has given impetus to the search of biodegradable alternatives which can compete with the petrochemical based plastics being used worldwide currently. However to produce an economically viable biodegradable plastic, cost efficiency and yield properties should be focused: the substrate and recovery costs in PHB production by fermentation are very high, making their use unattractive[232]. Carbon source for PHB production accounts for up to 50% of the total production costs[249]. One of the ways to cut down the production cost for bioplastic is the use of cheap, readily available industrial and agricultural waste as carbon and nitrogen source[231].

All the extracted polymers coming from different resources can be applied again in different fields[34,250,251]. Urban wastewater treatment and agricultural waste plants permit to obtain different kind of biomass, which allow to recover diversified products (as cellulose[154], phosphorous or fatty acids[16]).

The following section discusses some industrial residues already used in the production of PHB's:

5.3.1   Molasses

It is a viscous by-product produced during refining of sugarcane, grapes, or sugar beets into sugar. It is extensively used as a carbon source in industrial scale fermentations due to its relatively low price and abundance[252]. The production of PHB using molasses is well known in literature, in fact different kind of molasses have been used (soy, sugar cane or sugar beet). The difference in sugar content and the growth conditions influence the percentage of accumulation in the bacteria[231]. For example, the production of mcl-PHA from soy molasses using Pseudomonas corrugate achieved a yield of 5-17% of PHA's such as 3-hydroxyl-dodecanoate, 3-hydroxyl-octanoate and 3-hydroxytetradecenoate[253].

5.3.2   Whey and whey hydrolysate

It is a by-product of diary and cheese industry, constituting the watery portion collected after the separation of fat and casein from whole milk. Cheese whey is normally produced in volumes almost equal to the milk processed in cheese manufactories. The disposal of whey therefore causes serious pollution problems in the surrounding environment due to its enormous biochemical oxygen demand[231].

5.3.3   Lignocellulosic material

Lignocellulosic biomass consists of 30-50% cellulose, 20-50% hemicellulose and 15-35% lignin. Cellulosic biomass is inedible therefore its usage is not in direct competition

with food or animal feed production. But one of the main drawbacks in the use of lignocellulosic raw materials for the production of PHAs are the pre-treatment/hydrolysis steps required to generate the sugar feed stocks that can be metabolized by microbes to produce the bioplastics[231].

5.3.4   Wastewater

Production of PHAs from wastewater provides an economically viable alternative. Various organic wastewaters, such as municipal wastewater[17,254], biodiesel wastewater[255], food processing waste effluent[6,56]and other wastewater[29,256] have been already tested for PHAs biosynthesis in previous studies. Most of the cases involve conversion of organic carbon into volatile fatty acids in aerobic activated sludge in the first step, followed by PHA production using mixing cell cultures in the second step. Although the final PHAs concentrations are still low at the current investigated conditions, PHAs could accumulate to around or even over 50% of the cell dry weight in some cases[231].

In a recent study[257], the selection of PHA storing bacteria was integrated with the side stream treatment of nitrogen removal via nitrite from sewage sludge reject water. A novel process was developed and applied where the alternation of aerobic-feast and anoxic-famine conditions accomplished the selection of PHA storing biomass and nitrogen removal via nitrite. The results showed that the selection of PHA storing biomass was successful either when the ammonium conversion to nitrite occurred in the same reactor in which the PHA selection process occurred, and when two separate reactors were used. On the contrary, the nitrogen removal efficiency was affected by the process configuration, in fact the efficiency was much higher (almost 90%) when two separate reactors were used[257].

Among the many advantages associated with the use of PHAs, one of the most interesting concerns the possibility to be produced from renewable resources as mixed culture and renewable organic waste[30,40,258]. In particular, activated sludge from wastewater treatment plants (WWTPs) is a well-known source of PHAs where organisms store these polymers as carbon and energy reserve for biomass growth[30,259].

Literature already reports the extraction of PHAs from different type of biomass[77,41] and from mixed culture[47,260], but the extraction from activated sludge from wastewater treatment plants is the more interesting for its environmental impact, since this impact concerns not only the production of bioplastic, but also the depuration of waste water[254,257,261,262].

5.4   Upstream Processing

A number of fermentation strategies have been reported for the production of PHAs[75,270–273] from municipal wastewater. Process selection depends upon the type of culture used,

substrates, physiological conditions, fermentation processes and methods employed for the recovery of the final products. This section highlights the various upstream and downstream processes used in PHA production[231].

5.4.1   PHA from pure culture

Pure cultures of PHA producing bacteria can be divided into two groups: Non-growth associated and Growth associated PHA producing bacteria.

The non-growth associated PHA producing bacteria, for example *C. necator* and *Pseudomonas* species require nutrient limitation to accumulate PHA. Biomass growth and PHA accumulation are typically performed in two separate stages: The first stage is associated with biomass growth due to the availability of nutrients. In the second stage, due to the limitation or depletion of one nutrient PHA production prevails[231].

In the second group, organisms such as *Alcaligenes latus* and recombinant *Escherichia coli* do not require nutrient limitation and PHA accumulation and growth occur simultaneously[231].

In fed-batch cultures of growth-associated PHA producing bacteria, a nutrient feeding strategy is essential for obtaining high PHA production yields. This is because both cell growth and PHA synthesis can be enhanced as both processes occur at the same time. The two processes need to be balanced in order to avoid low PHA levels[237].

5.4.2   PHA from mixed culture

Mixed Microbial Cultures (MMC) are defined as group of different micro-organisms growing together on the same substrate. At present, PHAs usually come from pure substrates, which require sterile conditions and therefore high costs[260]. This is the main reason why interest on the use of mixed culture and on the study of possible extraction and purification processes is high.

Three main processes are used to produce PHA from a mixed culture:

5.4.2.1   *Anaerobic-aerobic (AN/AE) process*

PHA production using the AN/AE system comprises of three steps. In the first Activated Sludge Treatment Plant (ASTP) is used for culture enrichment. This is followed by fermentations of industrial wastewater and agro-industrial residues through acidogenesis into substrate containing Volatile Fatty Acids (VFAs). These VFAs are then used for PHA production[231].

5.4.2.2 *Aerobic dynamic feeding (ADF) system (feast and famine)*

ADF is the strategy of transient carbon supply where long periods of substrate shortage (famine period) are alternated with short periods of substrate excess (feast period) in a fully aerobic reactor. The PHA production occurs due to an intracellular component limitation. In the long periods of carbon limitation (famine), the macromolecular composition of the cells changes. As a consequence, the micro-organisms need a physiological adaptation when they are exposed to high substrate concentrations (feast). Although product is only formed during the feast phase, the famine phase is also very important for the process feasibility. The famine periods should be short in order to obtain high volumetric productivities but on the other hand, they should be long enough to guarantee high and stable PHA storage capacities on the long term[231,235].

5.4.2.3 *Fed-batch process under nutrient growth limitation*

In this strategy, carbon substrate from industrial wastewater and organic wastes is fermented through acidogenesis into substrate containing VFAs which are used for PHA production in a fed-batch reactor. The sludge present in the PHA production reactor originates from ASTP in which AN/AE or ADF conditions are established. This strategy can only be applied if the cells are previously formed and PHA accumulation is the only goal[231].

In this work the attention has been focused on the recovery of PHAs coming from activated sludge of a wastewater treatment plants with a multistage process[49], as schematized in Figure 5.4.1. PHAs production integrated with the via-nitrite nitrogen removal from anaerobic reject water was investigated at pilot scale at long-term period.

The pilot plant is located inside of the Carbonera WWTP (Treviso, northern Italy). The main water line is composed by preliminary treatments, primary sedimentation, biological reactor (Schreiber process), secondary sedimentation, disinfection and final filtration. The sludge line is composed by a static pre-thickener followed by dynamic thickening (installed during the experimental period) of mixed primary and secondary sludge, equalization tank for thickened sludge, anaerobic digester and the Short-Cut Enhanced Nutrients Abatement (S.C.E.N.A.) system for the treatment of sludge reject water[49,267].

The pilot plant treated around 10% (1.5–3.0 m^3/day) of the daily produced anaerobic reject water, while the system comprised of six different units, as reported below: 1) rotating belt dynamic filter (RBDF) for the recovery of CPS; 2) sequencing batch fermentation reactor (SBFR) for the production of VFAs by acidogenic fermentation;3) ultrafiltration (UF) unit for S/L; 4) Nitration-SBR; 5) Selection-SBR; 6) Fed-batch accumulation reactor (A-SBR). The flowchart of the process is reported in Figure 5.4.1[49].
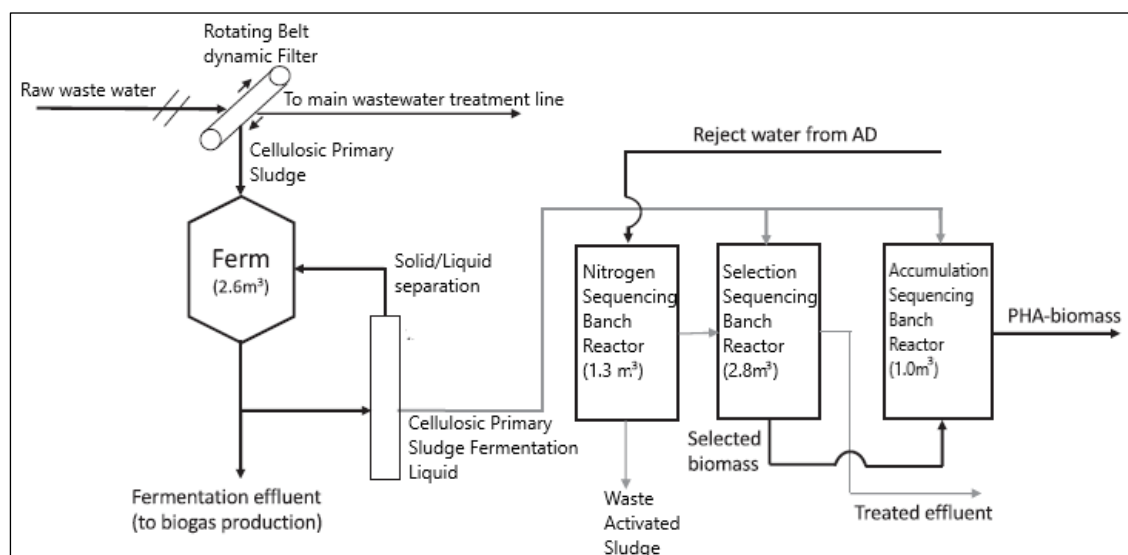
Figure 5.4.1 Schematic representation of the pilot plant in Carbonera (Treviso, Italy)[49]

The production of PHAs via-nitrogen is part of a project aimed to validate the long-term operation of an innovative pilot-scale plant integrating the via-nitrite nitrogen removal with PHAs production from the sidestream of Carbonera WWTP. A novel substrate derived from fermentation of CPS has been used as carbon source to evaluate the impacts on PHAs production. Each process unit has been investigated in Carbonera to assess the long-term stability of the process and to define the parameters required for the full-scale implementation.

5.5   Downstream Processing

Since PHA is an intracellular product, the method applicable for the effective separation of PHA from other biomass components can be complex and costly[268–270]. Various methods have been studied and reported in literature for the recovery and purification of PHAs from biomass. The steps of a proper downstream process are integrated with each other's and with the bioreaction stage to yield an optimal recovery scheme[268–270]. The principal approaches are based on the affinity with the polymer and the cell lysis.

5.5.1   Solvent Extraction

Solvent extraction is the most extensively adopted method to recover PHA from the cell biomass. Among various solvents, chloroform is the most preferred solvent to carry out PHA extraction without its degradation[271,269]. Other halogenated hydrocarbon solvents such as dichloromethane, dichloroethane and chloropropane can be also used to extract and purify PHA from the cell biomass though these solvents can be potentially hazardous to health and environment[271].

This method is also used routinely in the laboratory because of its simplicity and rapidity. Two main steps are involved, first is the modification of cell membrane permeability thus allowing release and solubilization of PHA. This is then followed by non-solvent precipitation[271]. Precipitation of PHA is commonly induced by non-solvent such as methanol and ethanol. Solvent extraction has undoubted advantages over the other extraction methods of PHA in terms of efficiency. This method is also able to remove bacterial endotoxin and causes negligible degradation to the polymers[272]. So, very pure PHA with high molecular weights can be obtained. Unfortunately, large-scale application of solvent extraction is generally viewed as not environmentally friendly[273]. In addition, several other factors discourage the use of solvents such as high capital and operational costs.

5.5.2   Digestion methods

While solvent extraction techniques involve the solubilization of the PHA granules, digestion methods involve the solubilization of the cellular materials surrounding the PHA granules. Digestion methods are well established approaches developed as an alternative to solvent extraction and can be classified into either chemical digestion or enzymatic digestion. Because of the ready availability of various chemicals with known properties many studies have been directed towards the development of chemical digestion methods compared to enzymatic digestion[29,43,274].

The approach of chemical digestion is based on the solubilization of non-PHA cellular mass and mainly utilizes sodium hypochlorite or surfactants. Nevertheless, the quality of the extracted PHA can be reduced, which is a very important disadvantage[272].

Recovery process of PHA using enzymatic digestion involves a rather complex procedure where solubilization of cell components other than PHA typically consists of heat treatment, enzymatic hydrolysis and surfactant washing. The enzyme technique is attractive because of its mild operation conditions, but because enzymes are very specific with respect to the reactions they catalyse, recovery of PHA with good quality could be expected. Nevertheless, the high cost of enzymes and complexity of the recovery process outweigh its advantages[55,274] .

5.5.3   Mechanical and physical disruption

Mechanical cell disruption is widely used to liberate intracellular products[275]. The concept has been tested in different studies to recover PHA from bacterial cells[34,77,269,270,276]. Among the various mechanical disruption methods, bead milling and high-pressure homogenization dominate the large scale cell disruption in pharmaceutical and biotechnology industries[270,277]. Unlike other recovery methods, mechanical disruption is favoured mainly due to economic advantageous and because it causes mild damage to the products[269,270]

Mechanical disruption of cells does not involve any chemicals, so it minimizes environmental pollution and contamination to the products. In general, the drawbacks of mechanical disruption method are, high capital investment cost, long processing time and difficulty in scaling up[272]. Physical pre-treatment is classified based on the nature of the forces causing cell wall disruption and could be sub- divided into thermal and mechanical (solid and liquid share forces, waves, and currents) methods. All these methods are pre-treatments applied directly on the biomass.

5.5.3.1   *Bead mill*

The principle of bead mills is based on the shearing action and energy transfer from beads to cells in the contact zones. The key parameters that affect the disruption process are the bead loading and bead diameter[270,278,279].

The extent of cell disruption also depends on numerous parameters such as residence time distribution, shear forces, type of microorganisms, cell concentration, feed rate of the suspension, agitator speed, geometry of the grinding chamber and design of the stirrer.

Bead mills disruption is recommended for PHA recovery as it requires less power supply, not susceptible to blockages and different diameter of beads did not significantly affect the disruption rate although micronization of P(3HB) is possible with smaller bead size[269,270,272].

5.5.3.2   *High pressure and high speed homogenization*

With high pressure homogenization, disruption of cell suspension occurs under high pressure through an adjustable, restricted orifice discharge valve[276–278].

Process parameters such as operating pressure, number of passes, suspension and homogenizer valve design must be care- fully scrutinized for efficient disruption[270,274]. The high-speed homogenizer combines hydrodynamic cavitation generated by stirring at high rpm and mechanical forces such as shear for cell wall disruption[280]. Process parameters are not the only factors that influence the cell disruption but microbial physiological parameters, namely type and growth phase of the microorganisms as well as cell concentration also affect the disruption efficiency. Generally, Gram-positive bacteria are more difficult to be disrupted compared to Gram-negative bacteria. Among the drawbacks associated with high pressure homogenization include the possibility of thermal degradation of desired products and formation of fine cellular debris that would interfere with the further downstream processing of PHA granules[270,274,280].

5.5.3.3   *Freeze-drying*

The freeze-fracture method involves a series of freezing-defrost cycles, and cell disruption is achieved due to ice crystal formation and cell expansion upon thawing. During freeze-drying (lyophilization) a pressure of about 1 kPa and temperatures of less

than -40°C are applied to slowly frozen samples. Cell walls become more porous due to formation of large ice crystals during slow freezing, and these crystals sublime in the lyophilization process[270,281,269].

5.5.3.4   *High temperature*

High-temperature methods are generally applied in biocrude oil and biogas production and are among the most per- formant cell wall disruption methods[269,270,274]. The use of steam improves heat transfer, and less energy is required to break the hydrogen bonds, provoking structural changes[269]. The pre-treatment is unspecific, promoting reactions on the different components of cell: under these conditions, lipids can release fatty acids, which are able to decompose into hydrocarbons[282]. The main operational parameters are the type of micro-organism, temperature, pressure, and time. Other advantages of thermal pre-treatments are cost-effectiveness, wide availability, and no use of chemicals[270].

5.5.3.5   *Microwaves*

Microwaves have been broadly applied as an alternative thermal pre-treatment of biomass feedstocks, including lignocellulosic, microalgae, and macroalgae biomass[283]. The frequency ranges from 0.3 to 300 GHz, of which 2450 MHz waves are typically used for microalgae cell wall disruption[280]. The mechanism is based on the interaction of electromagnetic waves with dielectric and polar molecules provoking local heating and an internal pressure increase. High concentrations of biomass benefit the specific energy consumption by increasing the energy directed to biomass. Apart from biomass concentration, pre- treatment time and power of microwaves are the main operation parameters[270].

5.5.3.6   *Ultrasonication*

Ultrasonication waves induce alternations of high- and low-pressure cycles in the liquid. Microbubbles created during low-pressure cycles ultimately implode in high-pressure cycles and produce local shock waves (cavitation) creating acoustic vibrations, extreme temperature peaks, and thermolysis of water around the bubbles forming highly reactive free radicals. Ultrasonic cavitation at low (18–40 kHz) frequency is much stronger than at high frequency (400–800 kHz). Nevertheless, its efficiency depends on the micro-organism (shape, size, intracellular structure), operational conditions (temperature, time, power, number of cycles), and biomass concentration[270,274,277,278] .

5.6   **Scope of the study**

Considering all these methods for the downstream process, 4 mechanical pre-treatments were chosen and applied to the biomass for the extraction of PHA in chloroform.

The first part of the work is focused on the extraction of the polymer and on the evaluation of the influence of various pre-treatments on the final extraction yield.

The second part deals with the realization of films with the polymer deriving from the various extractions, their characterization and comparison of relative properties.

To these aims, in particular, the procedure proposed in this work is:

(a) The selection and application of different pre-treatments to the biomass before extraction;
  - Fourier transform infrared (FTIR) spectroscopy, to quantify the extractive efficiency;

(b) The application of hot extraction (classical technique) and in continuous extraction (Soxhlet) to evaluate the corresponding extraction yields;

(c) The characterization of the different polymeric films by:

- Tensile test to study the mechanical behaviour and to calculate the relative parameters;
- Optical and electronic microscopy with the elemental distribution analysis (EDAX), to observe the morphology and to evidence the presence of elements different from C, H and O coming from possible impurities;
- ^{1}H-NMR analysis, to investigate the monomer's composition of the polymers;
- Thermogravimetrical analysis (TGA) and differential scanning calorimetry (DSC), to investigate the thermal behaviour of the polymeric films;

5.7   Materials

5.7.1   PHA extraction from biomass

5.7.1.1   *Biomass preparation*

The used biomass (Figure 5.7.1) comes directly from an urban wastewater treatment plant located in Carbonera (Province of Treviso, Italy). The supplied biomass is stabilized at a $pH = 2$, at concentration of 1% (w/V), with the total solids (TS) = 14.9% and total volatile solids (TVS)/TS = 86.9%.

The biomass used in this study has an initial hydroxybutyrate (HB) component in content is 60%, while the hydroxyvalerate (HV) is found to be between 40%, as reported by Smart-Plant project (https://cordis.europa.eu/project/id/690323/results/it).

25 kg of biomass is centrifuged (REMI XS R-10) at 6000 rpm for 4 minutes in 50 ml flasks to allow the separation of the two phases. The solid phase (wet biomass or biomass

at time zero) is collected and stored in the fridge at T = 5°C before to be used for extractions. The PHA quantity in the biomass represents the 100% of the yield.
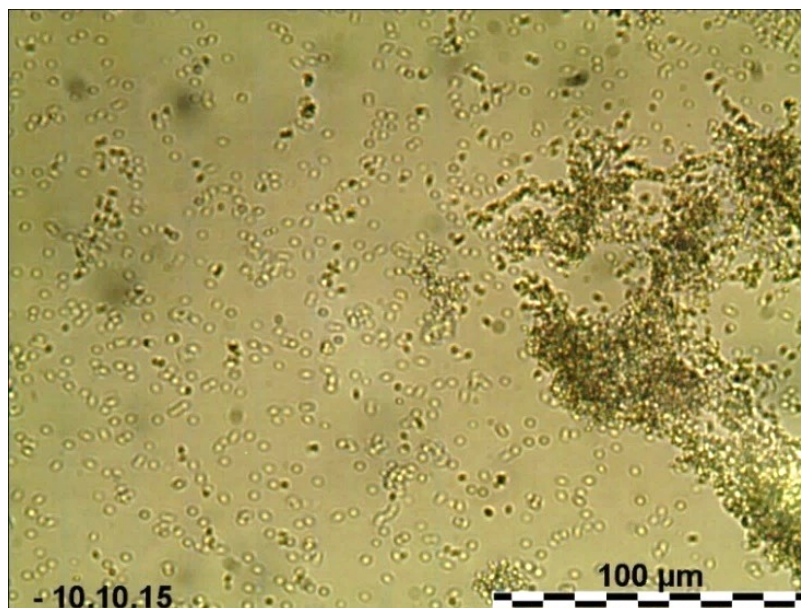
Figure 5.7.1 Biomass abserved at optical microscoscopy at time zero

5.7.1.2   *Biomass Pre-treatments*

The biomass is submitted to the following pre-treatments before the extraction procedures: (a) reference (without pre-treatment); (b) sonication; (c) homogenization with pressure (high-pressure homogenization); (d) homogenization with blades (high speed homogenization) and (e) glass spheres (bead mill); according to the procedures presented below.

These pre-treatments are chosen with the intention of destroying, or at least stressing, the bacterial cell wall so as to facilitate extraction[270,276–278]. The efficiency of different pre-treatments was evaluated according to the availability of the PHA present in the biomass at time zero.

5.7.1.3   *Sonication (Sonic)*

The disruption efficiency of sonication is strongly dependent on the ultrasonic strength (the power and frequency), the cell characteristics and the operation time[277]. In this case, the wet biomass is collected in a backer and put into a sonication bath for 15 minutes, 120 W and 40 KHz.

In this study, two samples following this pre-treatment are considered with the difference in the final drying method after classical extraction (Section 5.7.2.1): one sample is recovered by mechanical filtration (Sonic_mc) and subsequently dried at room conditions; the other is recovered and dried by rotavapor (Sonic_rt).

5.7.1.4   *Homogenization for pressure (Homo)*

High pressure homogenisation is one of the most widely known methods for large scale cell disruption. A positive displacement piston pump was used to draw the cell suspension through a check valve into the pump cylinder. On the return of the piston, the suspension was forced through the adjustable annular gap of a discharge valve and impinges on an impact ring. The discharge pressure, regulated by a spring-loaded valve rod, controlled the position of the valve in relation to the valve seat[274].

The wet biomass underwent this pre-treatment (American Instrument Company, AMINCO, Maryland) for 4 consecutive cycles at 1379 bar (20000 psi). Despite this, a complete break of the cell wall is not reached, as observed by optical microscopy (Figure 5.7.2) where the presence of intact cell walls is still visible. It is known that the performance of the homogenizer depends on the biomass concentration[274] that in this case is likely not sufficient.
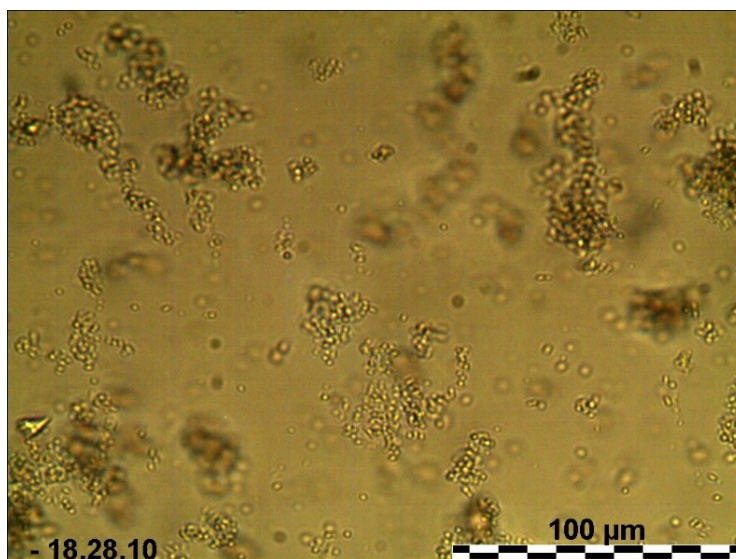
Figure 5.7.2 Biomass after 4 cycles at 1379 bar observed at optical microscope

5.7.1.5   *Homogenization with blades (Ultra)*

The high-speed homogenizer combines hydrodynamic cavitation generated by stirring at high rpm and mechanical forces such as the shear force for cell wall disruption[270]. In this study an ULTRA-TURRAX T25 basic IKA-WERKE is used on the wet biomass for 15

minutes at 9500 rpm, taking care that the blades passed over the whole sample uniformly. As for homogenization by pressure, also in this case a total disruption of the wall cell is not reached as observed by optical microscope (Figure 5.7.3).
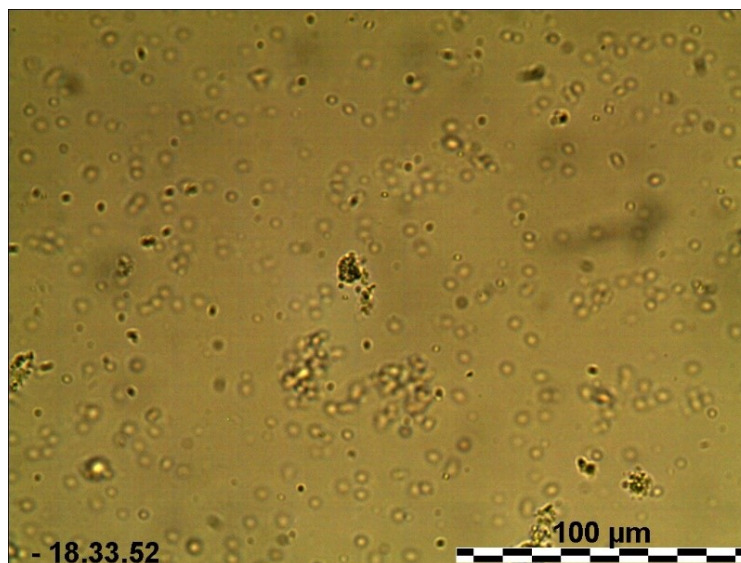
Figure 5.7.3 Biomass after 15 minutes of homogenization with blades at 9500 rpm observed at optical microscope

5.7.1.6 *Glass Spheres (Spheres)*

Studies of cell rupture using high speed bead mills have been carried out on yeast, Gram-positive and Gram-negative bacteria[279,284,285]. This complex process is influenced by a wide range of parameters such as relating to the number and energy of impacts, the energy transfer to the grinding elements, the liquid shear, the hydrodynamics, and the mixing as well as the bead diameter, density and loading, cell concentration in the feed, flow rate of the feed, agitator speed and configuration, geometry of the grinding chamber and temperature[276].

Glass spheres are mixed to the wet biomass (diluted 1:1 with water) with a vortex (IKA Vortex 2) for 5 minutes at room temperature.

5.7.2 **PHA Extraction**

The different extraction techniques that are applied to the non-pre-treated (used as a reference) and pre-treated biomass are compared in terms of yield and extract quality. All the extractions are also characterized in terms of the residual PHA's content by FTIR analysis to quantify the efficiency of extraction. The results are expressed in percentage (%) based on the maximum quantity of the PHA present (biomass at time zero).

The extraction methods studied in this work are two: (a) the conventional method or hot extraction; (b) Soxhlet or in continuous extraction.

5.7.2.1   *Conventional extraction*

Conventional extraction[241], based on the protocol already used in the Carbonera plant, is applied to all the samples. This method involves the use of 50 ml of chlorinated solvent (chloroform) (d= 1,49 g/cm³) for each gram of biomass. The solution is heated to the boiling point of the solvent for two hours. Then the solution is filtered to separate the liquid phase from the solid phase. FTIR spectroscopic analysis is performed on the residual biomass to evaluate the residual quantity of PHA present and then to calculate the extraction efficiency. Cold methanol (d=0.792 g/cm³) is added to the liquid phase to promote polymer precipitation[42,77,266,271,274,286] and to purify the polymer.

Following precipitation, the polymer is collected by filtration (except for the "Sonic_rt" sample, which is dried by rotavapor) and dried at room conditions.

5.7.2.2   *Soxhlet extraction*

In a Soxhlet extraction the sample is repeatedly brought into contact with fresh portions of solvent, in order to facilitates displacement of the transfer equilibrium. This permits the system to remain at high temperature thanks to the effect of the heat applied to the distillation flask[287–289]. In addition, the extracted is completely separated from the biomass, therefore no filtration is required. Typically this technique has a higher efficiency than conventional extraction because it permits a superior number of parallel extractions in 2 hours extraction (as for the conventional extraction described in Section 5.7.2.1). As aim is only to choose the extractive method to be adopted, the Soxhlet extraction is considered and compared to the conventional method only for the non-pre-treated sample (biomass t0).

5.7.2.3   *PHA Extraction Yield*

To evaluate the efficiency of each single extraction, the exact quantity of PHA present in the biomass batch should be known.

One of the biggest problems in working with by-products from wastewater treatment plants is the enormous variability among different biomass batches. Therefore, a method to easily calculate the percentage of PHA present in the biomass at time zero in order to define the various extractive efficiencies was necessary.

5.8   Methods

5.8.1   PHA films preparation

PHA-films are prepared by dispersing the polymer into chloroform. The total solid content is 4% (w/v). The polymer solutions are cast onto glass Petri dishes, and films are obtained after solvent evaporation at room temperature.

The PHA-films are kept at room temperature in dry conditions for 1 day before characterization.

5.8.2   Tensile Test

The tensile properties of the films are measured using a dynamometer INSTRON 5543 according to UNI EN 527: 1997. For each type of film, 5 samples are tested and the average results reported. The test specimen is extended along its major longitudinal axis at a constant speed until the specimen fractured or until the stress (load) or the strain (elongation) reached some predetermined value. Tests carried out on specimens of different dimensions, or prepared under different conditions, may produce results that are not comparable. Other factors, as the speed of testing and the specimens conditioning, can also influence the results. Consequently, samples 6×300 mm in dimensions are prepared and placed at controlled temperature (23 ± 2) °C and RH (50 ± 10) % before testing. During testing, the specimens are placed between the grip heads of the testing machine following the same procedure. The tensile strength (σ_M), Young's modulus (E), deformation at maximum load (e_M %), ductility, resilience and toughness, are calculated from the resulting stress-strain curves.

5.8.3   Micro-structural analysis

After the tensile test, the microstructure of the films is observed by using a Macroscopy (Wild Makroskop M420) at 10X and a Scanning Electron Microscope (SEM) (VEGA3 TESCAN) at 25.0 kV equipped with elemental distribution analysis (EDAX). In this way, the morphological analysis is carried out, but also, the presence of possible impurities is estimated, which might affect the film's mechanical properties.

5.8.4   ^{1}H-NMR Analysis

1H NMR spectra are recorded on a Bruker 400 MHz spectrometer with $CDCl_3$ as solvent. Chemical shifts (δ in p.p.m.) are referred to TMS and coupling constants (J) are given in Hz.

5.8.5   **Thermal analysis**

5.8.5.1   *TG Analysis*

As PHA undergoes rapidly decomposes with volatile products at T > 180 °C [290], thermal analysis is useful to investigate the thermal stability of different PHA films extracted from the biomass [291].In this case, TGA is conducted with a Mettler Toledo TGA/SDTA 851 under air atmosphere at the T = 25 - 500 °C with a heating rate of 20 °C/min.

5.8.5.2   *DSC Analysis*

Differential scanning calorimetry (DSC) measurements are conducted with a DSC Seiko Exstar 6000 to identify the phase transition temperatures of different PHA films extracted from biomass. A heating rate of 20 °C/min is used. Firstly, the polymer sample is equilibrated at 25 ∘C, heated at 20 ∘C/min to 200 ∘C. Then, the sample is cooled at 30 ∘C/min to −70 ∘C and heated again from -70°C to 200°C at 20°C/min. This method ensures the removal of the previous thermo-mechanical history of the sample. The third heating is used for the determination of the different phase transition temperatures according to UNI EN ISO 11357-1:2016. Also the associated crystallization (ΔHc) and melting enthalpies (ΔHm) are measured and the percentage of crystallinity is calculated[292,293].

5.8.6   **ATR-FTIR measurements**

Previous studies[294,295,296] have investigated the use of Fourier transform infrared (FTIR) spectroscopy as a method for a rapid quantification of the intracellular PHA in a mixed culture during the polymer accumulation phases in the bacterium. Attenuated Total Reflection Fourier Transform IR (ATR-FTIR) spectroscopy is the technique of choice for spectrum acquisition because of it ensures a short optical path for measurement without putting restraints on the geometry of the unit hosting the ATR element. In this study, ATR technique was performed at first to acquire the spectra of pure PHA and biomass at time zero, as reference spectra, then to investigate the biomass samples submitted to the above extraction procedures and to evaluate the percentage of the extracted polymer from each of them. A small amount of each sample was placed on the ATR crystal and measurements were carried out immediately without requiring any preparation.

The samples are analysed by using a *Perkin-Elmer Spectrum GX1* spectrometer (PerkinElmer, Inc, Waltham, MA, USA) equipped with U-ATR accessory for the analysis of solid samples in reflectance mode. On each sample, 5 spectra are acquired in the range between 4000 - 500 cm^{-1}, with a spectral resolution of 4 cm^{-1} and recording 64 scans. A background adsorption spectrum is recorded before each acquisition. Raw IR spectra are converted in absorbance, interpolated in the 1800-500 cm^{-1} spectral range and vector normalized in the same interval. An automatic baseline correction algorithm is used in all spectra to avoid errors due to baseline shifts. Atmospheric compensation is

also performed. The average absorbance spectra of all samples are also calculated, and curve fitted in the 1800-800 cm^{-1} upon two-points baseline correction and vector normalization (Grams AI 9.1 software, Galactic Industries, Inc., Salem, NH). A Gaussian algorithm is adopted. For each underlying band, the positions in terms of wavenumbers (cm^{-1}), height (H) and integrated area (A) are calculated. Spectrum 5.3.1 (Perkin-Elmer) are used as the operating software.

5.9   Results and Discussion

5.9.1   PHA extraction yields

The representative ATR-FTIR spectra of pure PHA (Goodfellow BV340) and the biomass samples are reported in Figure 5.9.1. The wavenumbers of the most significant IR peaks are identified by the curve fitting procedure and listed in Table 5.9-1 with the corresponding chemical assignments.

In the biomass spectrum, the bands related to the organic matter are detected at 1623, 1530 and 1382 cm^{-1} (respectively proteins and collagen). The bands of carbonate and phosphate groups are found in both of spectra (PHA and biomass) at 1458, 826 cm^{-1} and 1099, 1084 cm^{-1} respectively. The characteristic band of the carbonyl group is at 1732 cm^{-1} in the biomass spectrum and at 1721 cm^{-1} in the PHA spectrum, because it could shift according to the crystallinity degree of the polymer.
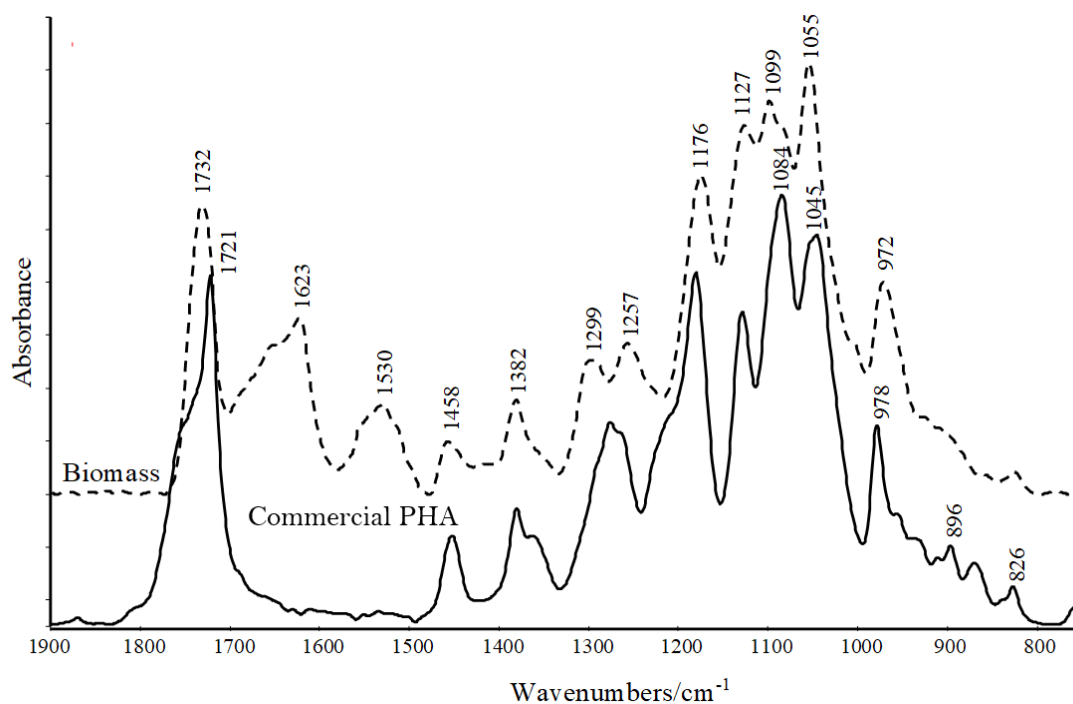
Figure 5.9.1 Comparison between the ATR-FTIR representative absorbance spectra of Commercial PHA polymer and biomass at zero time in the spectral range 1900-800 cm-1. From this analysis, 72% of PHA is present within the biomass at time zero

Table 5.9-1 Position (in terms of wavenumbers, cm⁻¹) and chemical assignment of the IR peaks identified by curve fitting analysis of pure polymer and biomass spectra

Wavenumber (cm⁻¹)	Chemical assignment
1721	Carbonyl group
1623, 1530	Amide I and Amide II of proteins
1458	Carbonate groups
1382	Collagen
1250-1300	Amide III of proteins
1176, 1127	Inorganic and Organic groups
1099, 1084	Phosphate groups

1045	Carbohydrate groups
978	PHA crystalline phase

All the residual biomass spectra obtained following the various extraction procedures are compared with the spectra of Commercial PHA and biomass at time zero (Figure 5.9.2).
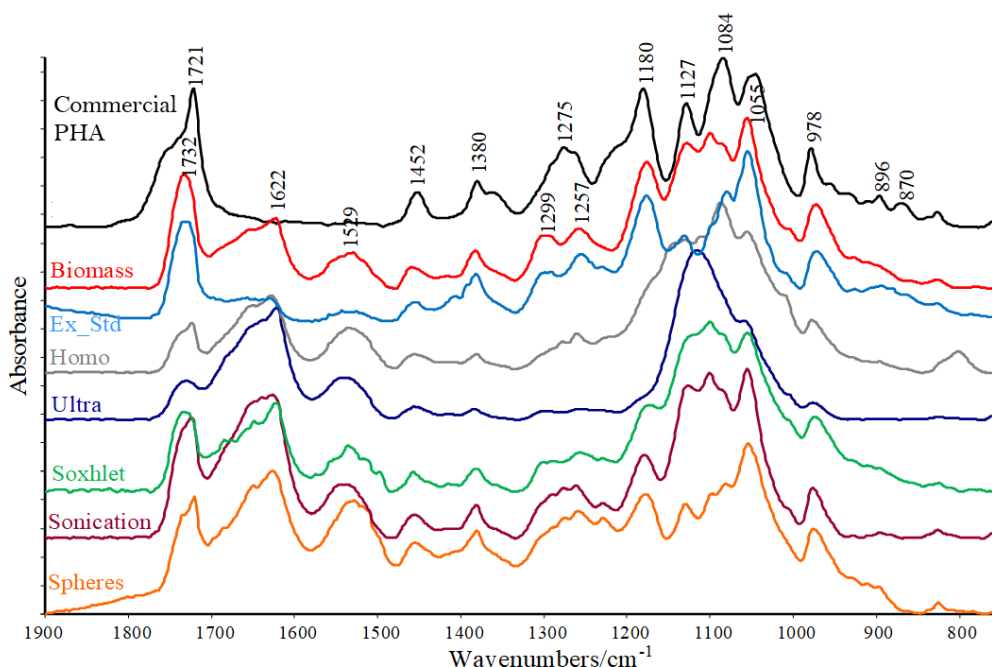
Figure 5.9.2 Comparison of ATR-FTIR representative absorbance spectra of PHA pure polymer and biomass together with the residual biomass spectra obtained following the various extraction procedures (spectral range 1900-800 cm^{-1})

Considering the bands at 1721 cm^{-1} and 1530 cm^{-1} as characteristic for the Commercial PHA and the biomass, respectively, the band area ratio A1721/A1530 is calculated for each representative spectra in order to investigate the residual percentage of PHA inside of the biomass and to evaluate the efficiency of the various extraction procedures adopted. All extraction yields are calculated considering the 72% of PHA available in the biomass as the maximum extractable quantity, so 100% of the possible yield (Table 5.9-2).

Table 5.9-2 Residual amount of PHA in the biomass and extracted amount of PHA (%) following the different extraction procedures.

	Residual PHA [%]	Extracted PHA [%]
Commercial PHA	100	-
Biomass (t0)	72*	-
Ex_Std	50	31
Soxhlet	47	35
Sonication	67	7
Spheres	55	24
Homo	35	51
Ultra	40	44

*Maximum amount of PHA that can be extracted from the biomass, therefore all the extracted PHA percentages are calculated assuming this value as the 100% of available PHA.

As shown, the homogenization pre-treatment gives the best extraction yields; in fact, the use of the French press (Homo) allows the extraction of 51% of the polymer contained in the biomass at time zero, whereas the blades (Ultra) extract the 44%. Instead, the pre-treatment by sonication is rather inefficient, allowing to obtain a yield of only 7%.

Regarding the influence of the extraction methods on yield, the two methods have almost the same efficiency since continuous extraction with Soxhlet (35%) is only 2% more efficient than conventional one (31%).

5.9.2 Characterization of the films

5.9.2.1 *Tensile Test*

The average stress strain curves of the different PHA films are compared in Figure 5.9.3. From the average stress strain curves, the maximum tensile strength (σ_M), the

elastic modulus (E), the ductility (%), the deformation at the maximum load (e%$_M$), the resilience (R) and the toughness (T) are measured and reported in Table 5.9-3 together with the thickness and cross-sectional area of the tested samples, since they affect the mechanical performances[297297,298].
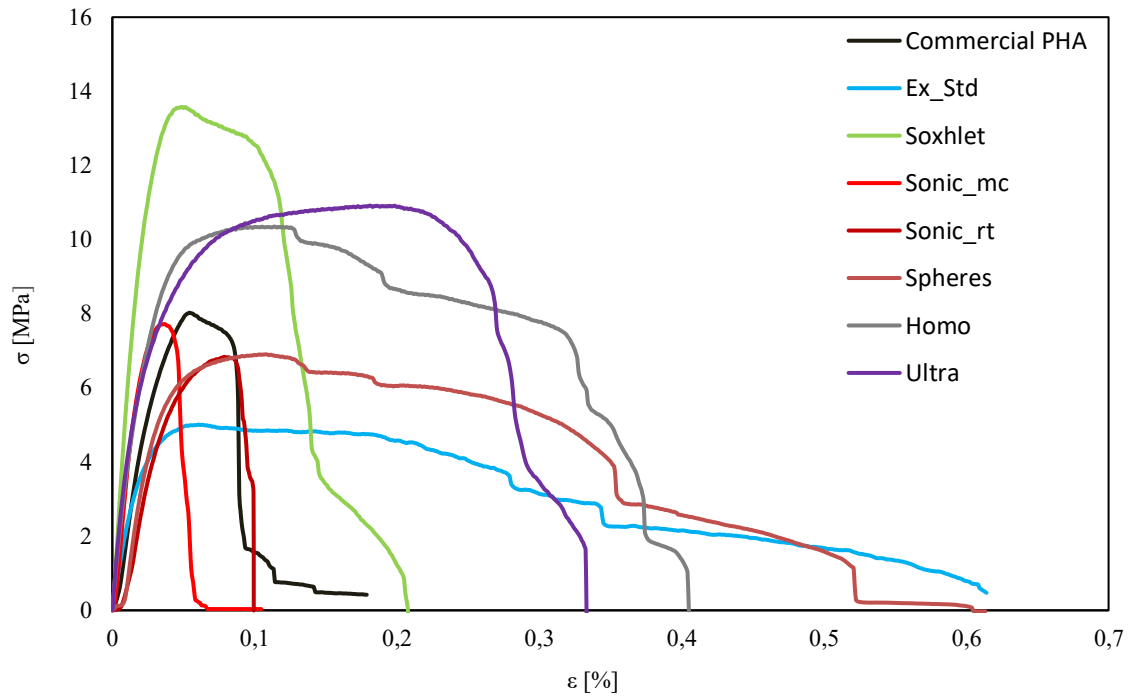
Figure 5.9.3 Average stress strain curves for different PHA films.

Table 5.9-3 Dimensions and mechanical properties of different PHA films characterized by tensile test.

Sample	Thickness [μm]	Cross-sectional area [mm²]	σ$_M$ [MPa]	ε$_M$ [%]	E [MPa]	R [MPa]	T [MPa]	Ductility [%]
Commercial PHA	55	0.03	8	7	137	0.2	0.2	10
Ex_Std	64	0.04	5	12	77	0.2	1.6	38
Soxhlet	66	0.04	14	3.4	252	0.4	1.0	14
Sonic_mc	75	0.04	8	3.6	147	0.1	0.1	4

Sonic_rt	62	0.04	7	9	158	0.2	0.1	10
Spheres	56	0.03	8	10	205	0.2	2.0	42
Homo	60	0.04	9	11	150	0.3	1.4	33
Ultra	61	0.04	11	20	230	0.5	1.8	29

Under a tensile stress, at first the elastic deformation occurs when the primary covalent chemical bonds inside the polymeric chains stretch but do not break. Once the limit of the elastic deformation (yield point) is reached, a polymer breaks or continues to deform depending on its fragility or ductility. In fragile materials, the inability of the atoms to flow causes the catastrophic breaking when the applied force exceeds the primary strong covalent bond strength. In ductile materials, including most thermoplastic polymers, such as PHA, the material undergoes a plastic permanent deformation since the molecular chains are stretched and flow over each other so as to align in the direction of the effort (the degree of crystallization of the polymer also influences these properties). The flow of atoms over each other's occurs thanks to the rupture of the weak secondary chemical bonds inside the same macromolecular chain or among different macromolecular chains. Only subsequently, when the applied force exceeds the primary strong covalent bond strength, does the rupture occurs[298,299].

Before breaking, a material absorbs energy: the energy absorbed during elastic deformation is R, which depends on the E and yield strength. The total energy absorbed before breaking, including that under the plastic behaviour, corresponds to T of the material which depends on ductility and σ_M.

The two extraction techniques and the different pre-treatments affect a lot the mechanical performances of the obtained PHA films.

In particular, regarding the two extraction techniques (Ex_std and Soxhlet), Soxhlet extraction gives PHA films with significantly higher mechanical performances in terms of σ_M (14 MPa), E (252 MPa) and R compared with conventional extraction. σ_M is proportional to the elastic modulus even if fragile materials are also sensitive also to the surface properties[298]. Ex_std sample shows a much higher ductility (and consequently T) than the Soxhlet sample. The Commercial PHA film used as reference, which has not undergone a hot extraction process but only a filming process at room temperature (solvent casting), shows an average σ_M of 8 MPa and an E of 137 MPa.

When conventional extraction has been used, the ductility is very variable, from 4% (Sonic_mc) to 42 % (Spheres), as well as R from 0.1MPa (Sonic_mc) to 0.5 MPa (Ultra) and T from 0.1 MPa (Sonic) to 1.9 MPa (Spheres). In particular, in comparing the effect of different pre-treatments on mechanical performances, sonication,

regardless of the filtration type, gives PHA films with the worst mechanical performances in terms of σ_M (~ 7 MPa), E, R, T and ductility, with values similar to those of reference PHA (Commercial PHA). On the other hand, the two homogenizations give films with the best mechanical performances in terms of the highest σ_M: 9 MPa (Homo) and 11 MPa (Ultra) and very high R, T and ductility. For what concerns E, homogenization using blades (Ultra) gives stiffer films (E = 230 MPa) than using pressure (Homo) (E = 147 MPa). E depends on the ability of atomic bonds to deform, the higher the bonding force, the greater the rigidity of the material. During homogenization with blades, the sample undergoes heating[276], which is not the case with pressure treatment. It is well known the effect of temperature on the mechanical properties of a polymer[298,300,301,302]; heating can lead to a change in the polymer structure by breaking some chemical bounds[46] and forming new ones during cooling. If the number of new formed bonds prevails over the number of broken bonds, the polymer becomes stiffer. The ductility and tenacity of PHA films obtained by homogenizations are overcame only by Ex_Std and Spheres even if with a lower σ_M.

The mechanical properties of the analysed PHAs are comparable with those found in literature [303] for similar polymers. In particular, the elongation of these films is comparable with that of PHBV analysed by Martin et all[303] (15-20%), but the Young's Modulus is much lower (252 MPa for Soxhlet and 900 MPa for PHBV). For what concerns E, the obtained PHAs are much more similar to polycaprolactone considered in the same study (260 MPa). The chemical composition of the polymer, in particular the ratio between the monomers of the copolymer, is determinant on its properties[83].

5.9.2.2   *Microstructural analysis*

The percentage of purity of the polymer largely affects its mechanical behaviour[38,296]. In particular, when defects act as stress concentrators, the process leading to the formation of voids at defects[304,305,306,307] begins first decreasing the mechanical performances. As the deformation proceeds, these micro-cavities tend to expand and merge with each other until an internal fissure is formed.

The purity is closely related to the pre-treatment type, extraction time and temperature. In this case, solvents and extraction time are fixed, therefore purity depends only on the type of pre-treatment.

5.9.2.2.1   Optical macroscopy

An optical macroscope has been used to observe the morphology of the sample and to evidence the presence of impurities. For all pictures the same enlargement was used (10X) (Figure 5.9.4).
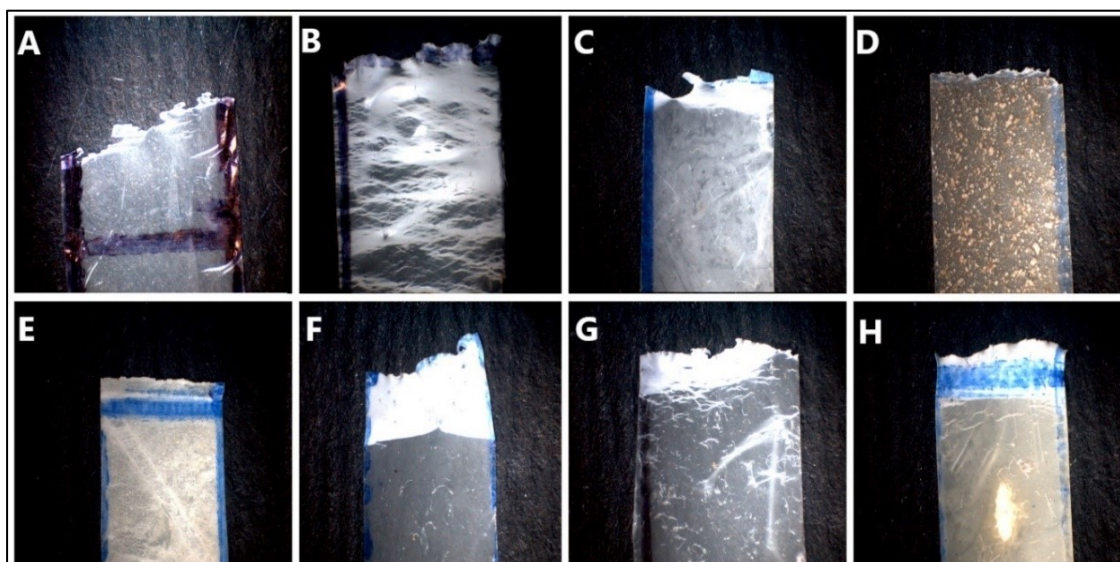
Figure 5.9.4 Morphological observations (10X) of films after the tensile test: a) Commercial PHA; b) Ex_std; c) Soxhlet; d) Sonic_mc; e) Sonic_rt, f) Spheres; g) Homo; h) Ultra.

Concerning the different pre-treatments, certain samples clearly have more macro-porosities than others. Sonic_mc and Sonic_rt samples appear yellowish in colour and spots of macroscopic impurities are well visible on the surface, giving them a wrinkled and porous aspect (especially Sonic_mc). It is probable that some impurities have gone into solution during the sonication process. The sonication process is considered very efficient to destroy the cell walls[45,276,308] therefore it can also remove more easily impurities[270] (based on carbonates groups and/or proteins) from the cell walls . The highest presence of impurities in Sonic_mc and Sonic_rt PHA films can explain their low mechanical performances as reported above (Figure 5.9.3 and Table 5.9-3). All other samples appear purer with a white transparent colour, except for the Ultra sample which is transparent but slightly yellowish.

Concerning different extraction procedures, during conventional extraction, high temperatures were constantly maintained, and the biomass was surrounded by the polymer and solvent solution. In Soxhlet extraction, the solvent is continuously re-condensed (therefore T is lower than the boiling point) and made to fall back into the sample holder, which is different from the solvent (and extracted polymer) holder. This permitted a minor risk of macro and micro-impurities caused by the extraction process (Figure 5.9.4) justifying the higher mechanical performances of the Soxhlet PHA film than Ex_Std film. Macroscopically, both samples appear with a good purity level, but some micro-impurities, possibly coming from cell walls and other biological components, unobservable by optical macroscope, could affect their properties.

By macroscopic observations, the part of the film stretched during the tensile test can be easily distinguished thanks to a completely different morphology from the bulk: it

appears white opaque in colour, sometimes with streaks, due to the orientation of the molecular chains in the direction of the stress before the rupture[307,88], which densifies the structure. As expected, higher is the ductility of the sample and longer is the stretched part of the film, following this decreasing order: Ex_std, Spheres, Ultra, Homo, Soxhlet, Commercial PHA and Sonic rt, and finally Sonic_mc.

5.9.2.2.2   Scanning Electron Microscopy

SEM analysis allows to investigate the microstructure at higher magnitude than optical microscopy. In Figure 5.9.5, Figure 5.9.6, Figure 5.9.7, Figure 5.9.8, Figure 5.9.9, Figure 5.9.10, Figure 5.9.11 and Figure 5.9.12 three images of every sample after the tensile test are reported and compared: the first reports the break zone, the second and the third give details of the stretched and not stretched area (where it has been possible to identify them) at greater enlargements.

(a)   (b)   (c)
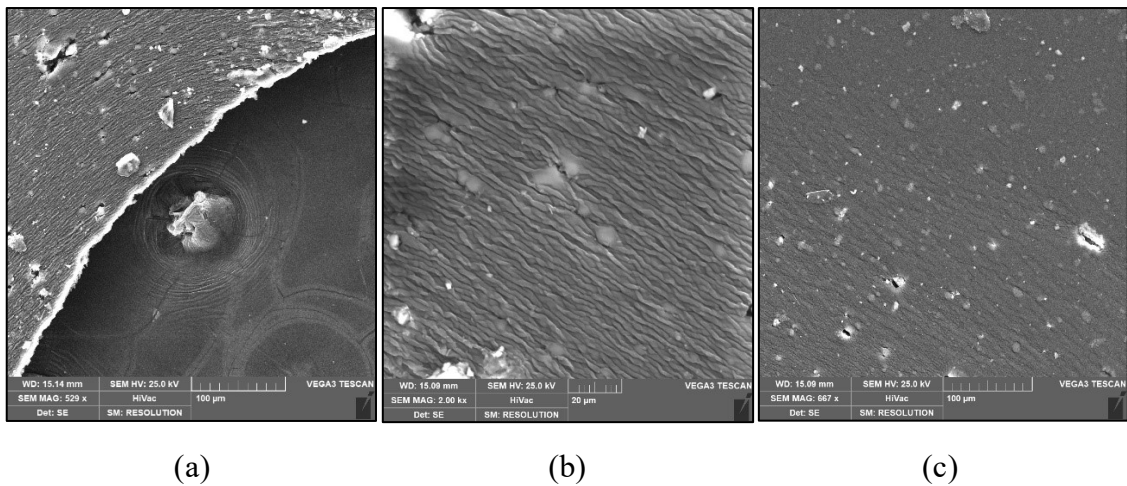
Figure 5.9.5 SEM analysis of Commercial PHA: a) cut section; b) stressed area; c) surface.

(a)   (b)   (c)
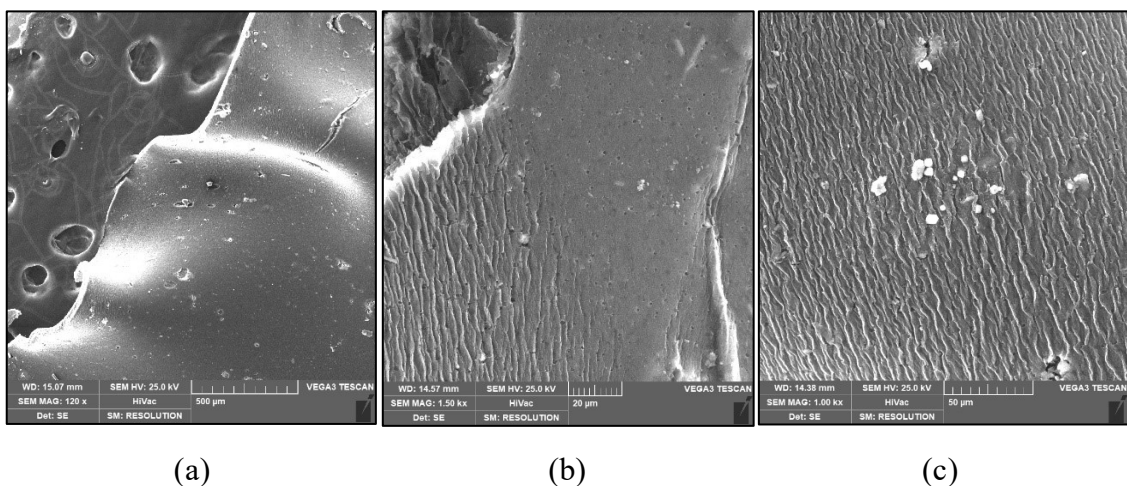
Figure 5.9.6 SEM analysis of Ex_Std: a) cut section; b) stressed area; c) surface

(a)   (b)   (c)
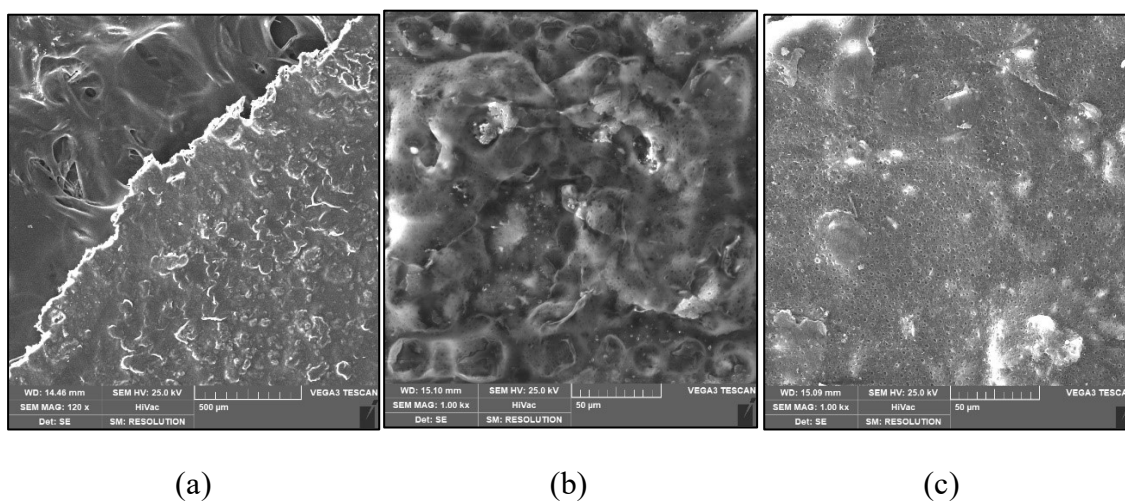
Figure 5.9.7 SEM analysis of Sonic_mc: a) cut section; b) stressed area; c) surface

(a)   (b)   (c)
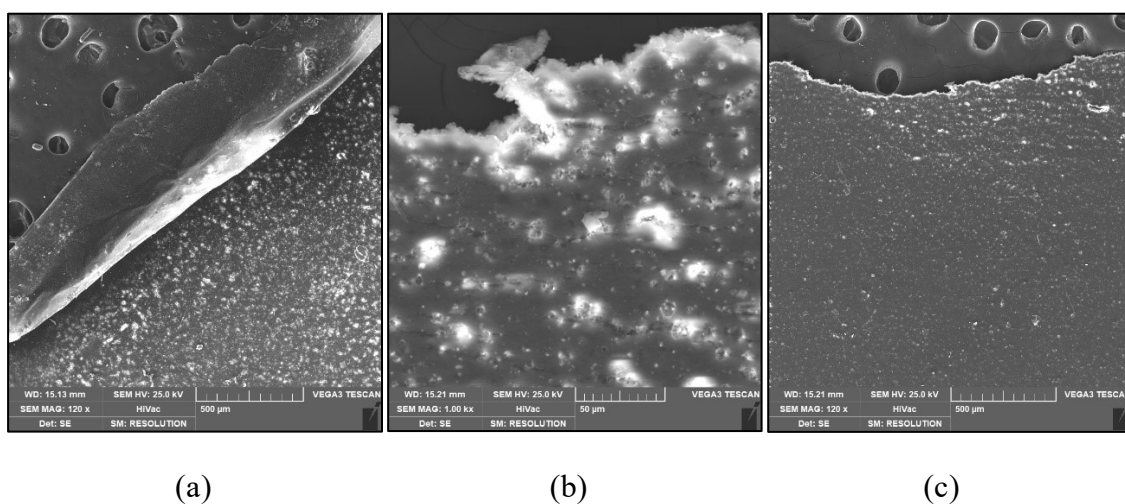
Figure 5.9.8 SEM analysis of Sonic_rt: a) cut section; b) stressed area; c) surface

(a)   (b)   (c)
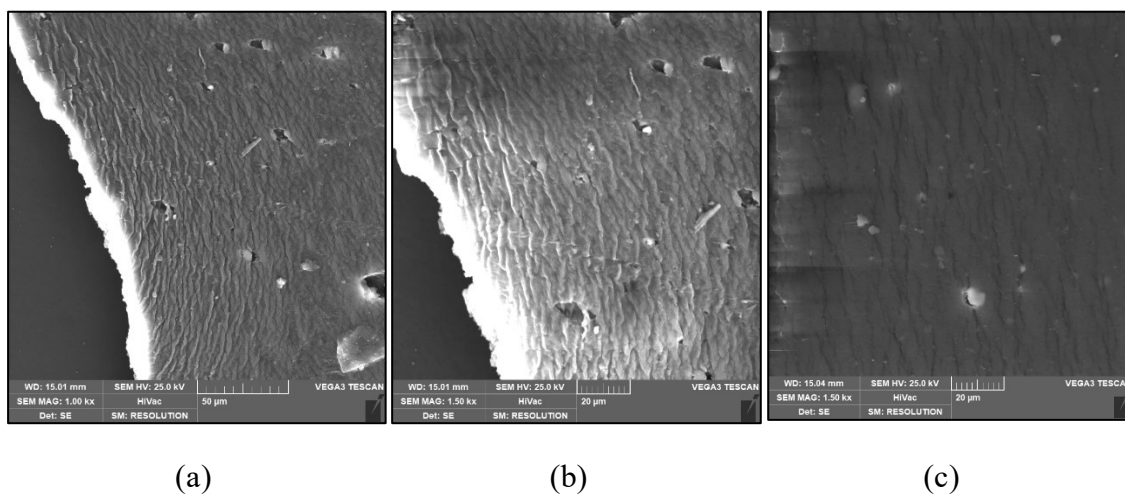
Figure 5.9.9 SEM analysis of Soxhlet: a) cut section; b) stressed area; c) surface
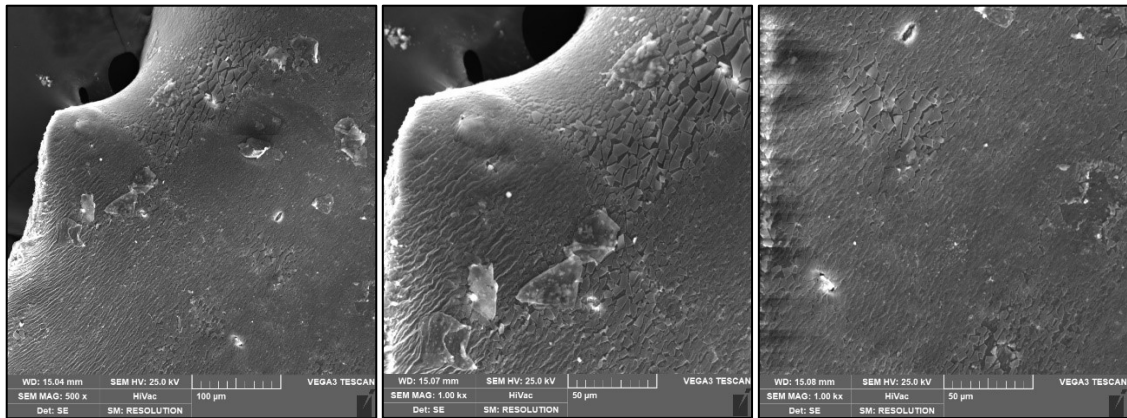
(a)   (b)   (c)

Figure 5.9.10 SEM analysis of Spheres: a) cut section; b) stressed area; c) surface
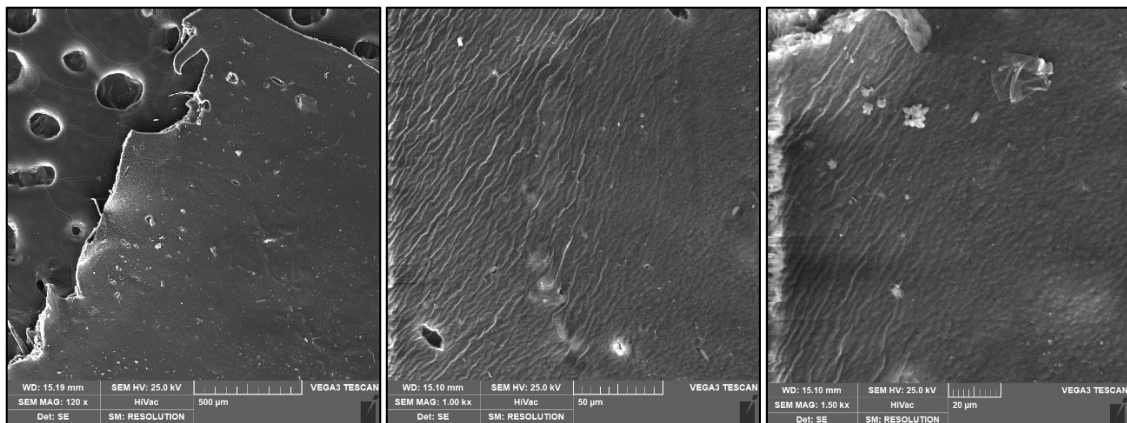
(a)   (b)   (c)

Figure 5.9.11 SEM analysis of Homo: a) cut section; b) stressed area; c) surface
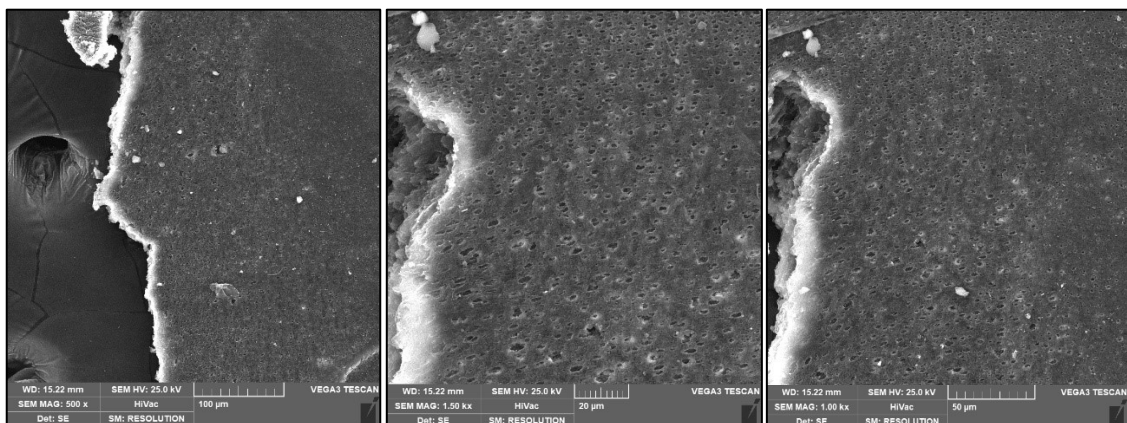
(a)   (b)   (c)

Figure 5.9.12 SEM analysis of Ultra: a) cut section; b) stressed area; c) surface

When a cast film is deformed, the randomly oriented molecules tend to orient towards the deformation direction. Especially when the sample is deformed quickly and at low temperatures, possible defects act as stress concentration and cracks are created giving the ultimate sample failure[309].

Comparing the morphology of the stretched and not stretched area, the formation of stripes due to the sample deformation during the tensile test is clearly visible. As expected, more ductile is the sample, as Ultra, Homo, Spheres, Ex_Std, and wider is the PHA film zone with stripes; more fragile is the sample, as Sonic_mc and Sonic_rt, and more restricted is the PHA film zone with stripes.

The high fragility of both Sonic samples is confirmed to be due to the high presence of impurities, already observed by optical macroscopy, that give high roughness to the surfaces observed by SEM.

Moreover, particularly Ultra, and both Sonic samples have a porous appearance: this morphology is found in literature [310,311] for co-polyester consisting of 3-hydroxybutyrate, 3-hydroxyhexanoate and PHB blended with salts. The presence of salts as impurities, especially in these polymeric films, is confirmed by the EDAX analysis (Table 4) which evidences the presence of elements, other than carbon (C) and oxygen (O) which are the main components of polymers. Table 5.9-4 reports the results of EDAX analysis of PHA films in terms of weight %.

Table 5.9-4 EDAX analysis of PHA films

	Commercial PHA	Ex_Std	Soxhlet	Sonic_mc	Sonic_rt	Spheres	Homo	Ultra
Element				Weight [%]				
C	70.23	57.92	62.5	58.35	58.03	61.62	58.55	59.22
O	26.55	39.85	34.85	38.84	32.32	35.85	38.26	34.88
Si	3.02	2.22	2.41	1.24	7.69	1.95	1.7	4.14
Ca	0.2	-	-	0.56	0.22	0.28	-	0.2
Cl	-	-	0.24	-	0.6	-	0.28	0.32
P	-	-	-	0.26	-	-	-	-
S	-	-	-	0.74	0.27	0.31	-	0.25

| Na | - | - | - | - | 0.73 | - | 1.21 | 1 |
| K | - | - | - | - | 0.13 | - | - | - |

After C e O, in every film Silicon (Si) is the third most present element with an amount ranging from 2 to 8% by weight; probably some particles were scratched from the Petri dish used to cast the polymer solution during the removal of the film from the support and they adhered to the film surface.

Some films (Soxhlet, Sonic_rt, Homo and Ultra) contain also small traces of chlorine (Cl), ranging from 0.24 to 0.6% by weight probably as residual of the solvent ($CHCl_3$) used for the extraction process and the filmation procedure.

Sulphur (S) ranging from 0.25% and 0.74% in Sonic_mc, Sonic_rt, Spheres and Ultra, and Phosphorus (P) 0.26% by weight in Sonic_mc are typical contaminants present in wastewater treatment plants[254,257].

Lastly, Calcium (Ca), Sodium (Na) and Potassium (K) are the most common cations of salts usually present in waste waters[29].

The formation of pores in the micro-structure can be caused also by the molecular composition of the PHA film and by the filmation process: when the polymer crystallizes after the casting, stresses are generated inside the polymer giving an irregular and porous film surface. A low crystallization degree produces less stress as well as a slow and mild crystallization process provides the polymer enough time to rearrange the molecules for releasing the stress produced by crystallization[310].

5.9.2.3   *^{1}H-NMR Analysis*

The ^{1}H-NMR analysis was carried out taking into account the typical signal of these kind of polymers as reported in the literature[312,313]. For comparison, a ^{1}H-NMR spectrum of the commercial sample has been recorded (Figure 5.9.13) and all the signal have been analized basing on the following points:

- the methyl doublets (J=7.12 Hz) at 1.28, accompanied by the multiplet at δ=2.47 ppm (corresponding coupled α proton) and by the multiplet at δ=5.19 ppm (the more deshielded proton close to oxygen), could be considered as "markers" of Me-PHB (methyl butyrate);

- the methyl doublet (J=7.12 Hz) at δ=1.58 accompanied by the multiplet at δ =2.60 ppm (two coupled α protons) the multiplets at δ = 5.27 ppm are typical of PHB.

- the -CH_3 1: 2: 1 triplet (J=7.32 Hz) at δ = 0.9, attributed to the methyl split by the -CH_2- in α position at δ= 1.62 ppm, are typical PHV resonances.

Upon these bases, the commercial sample (Figure 5.9.13) is mainly composed by Me-PHB (methyl butyrate), although contaminated by a very small amount of PHB.

Soxhlet (Figure 5.9.14) and Sonic_rt (Figure 5.9.15) appeared identical to that of the commercial PHA but contaminated by more impurities. However, the-CH$_3$ integration ratio for Soxhlet suggested an increase in the PHB content with respect to the commercial sample.
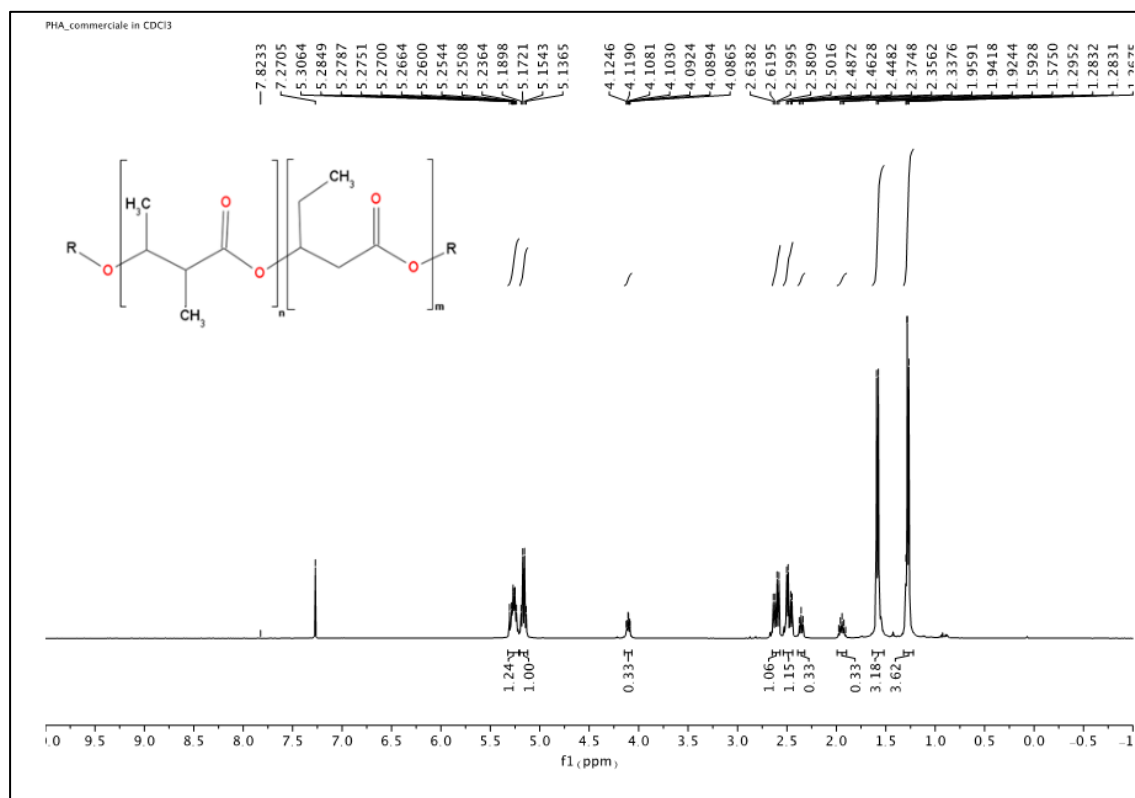
Figure 5.9.13 ^{1}H-NMR spectra of Commercial PHA
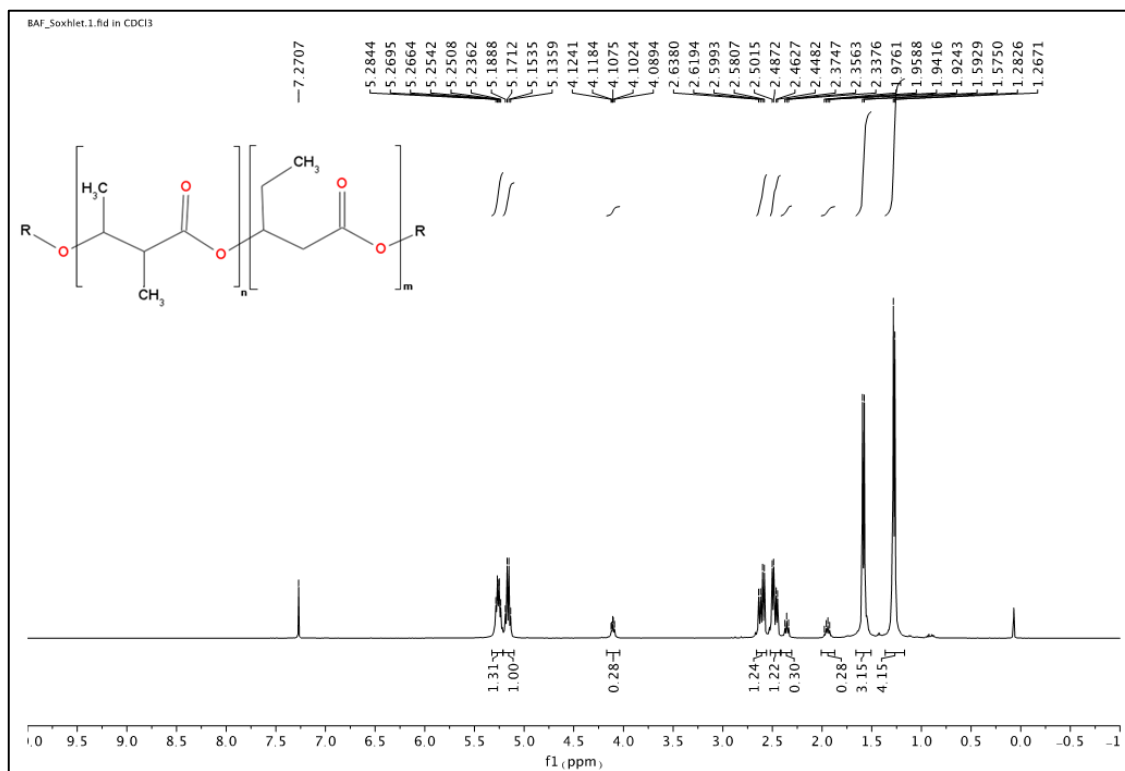
Figure 5.9.14 ^{1}H-NMR spectra of Soxhlet
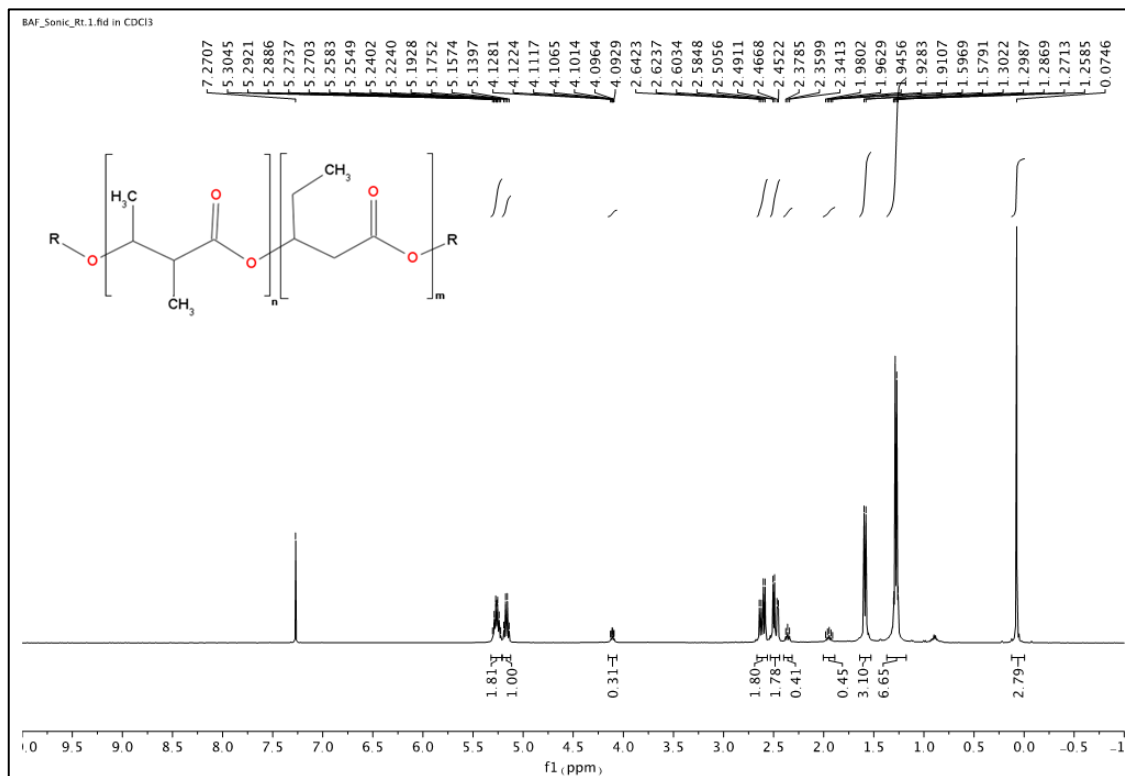
Figure 5.9.15 ^{1}H-NMR spectra of Sonic_rt

Sonic_mc (Figure 5.9.16) shows a different composition for the presence of PHV, recognizable by the typical -CH$_3$ 1: 2: 1 triplet (J=7.32 Hz) at δ = 0.9, splitted by the -CH$_2$- in α position at δ= 1.58 ppm, partially superimposed with the PHB -CH$_3$ doublet signal. As a consequence, the low field multiplet pattern at δ= 5.2 ppm slightly changes due to the PHV resonances. In this sample, the integration of the two methyl doublets at δ = 1.28 and 0.9 ppm allow the estimation of a PHB/PHV ratio of about 4.5 to 1.0 such a behaviour let hypothesize a composition dependence from the extraction method.

Spheres (Figure 5.9.18), Homo (Figure 5.9.19), Ultra (Figure 5.9.20) and Ex_Std (Figure 5.9.17) show a similar spectrum with respect to Sonic_mc, but with a different PHB/PHV ratio, which in the case of Ex_Std is about 1.0 to 2.9.
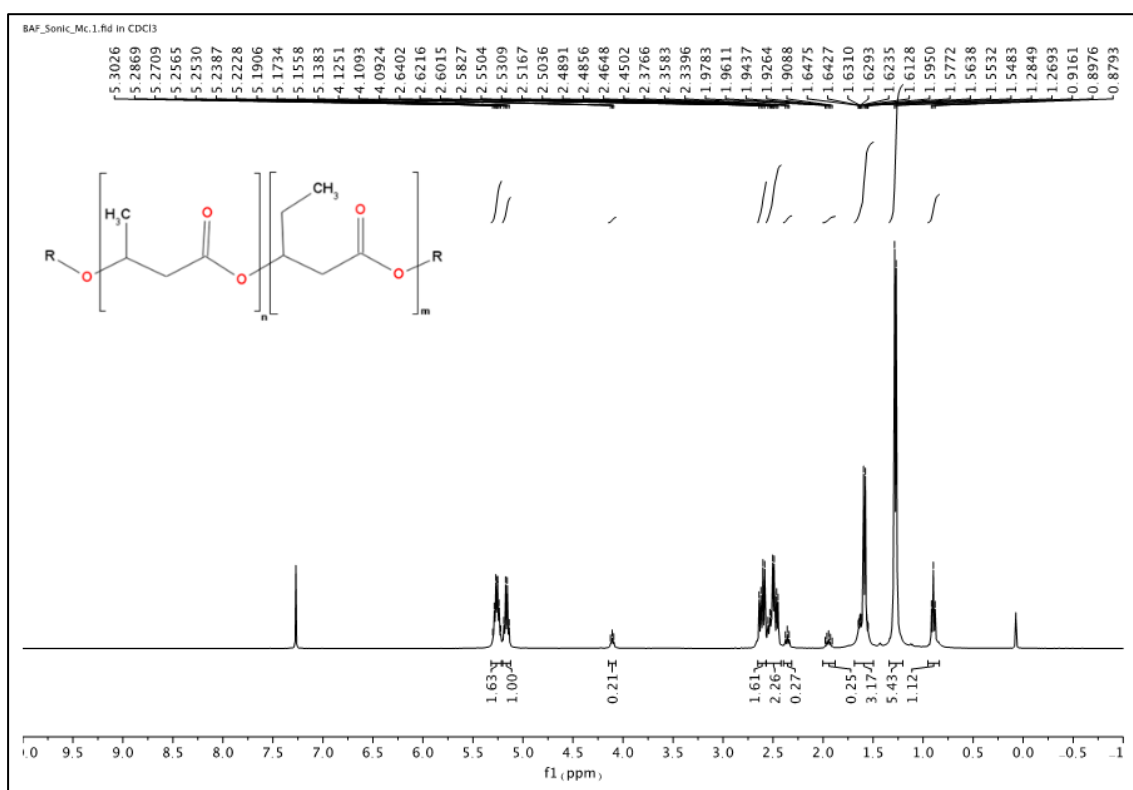
Figure 5.9.16 ^{1}H-NMR spectrum of Sonic_mc
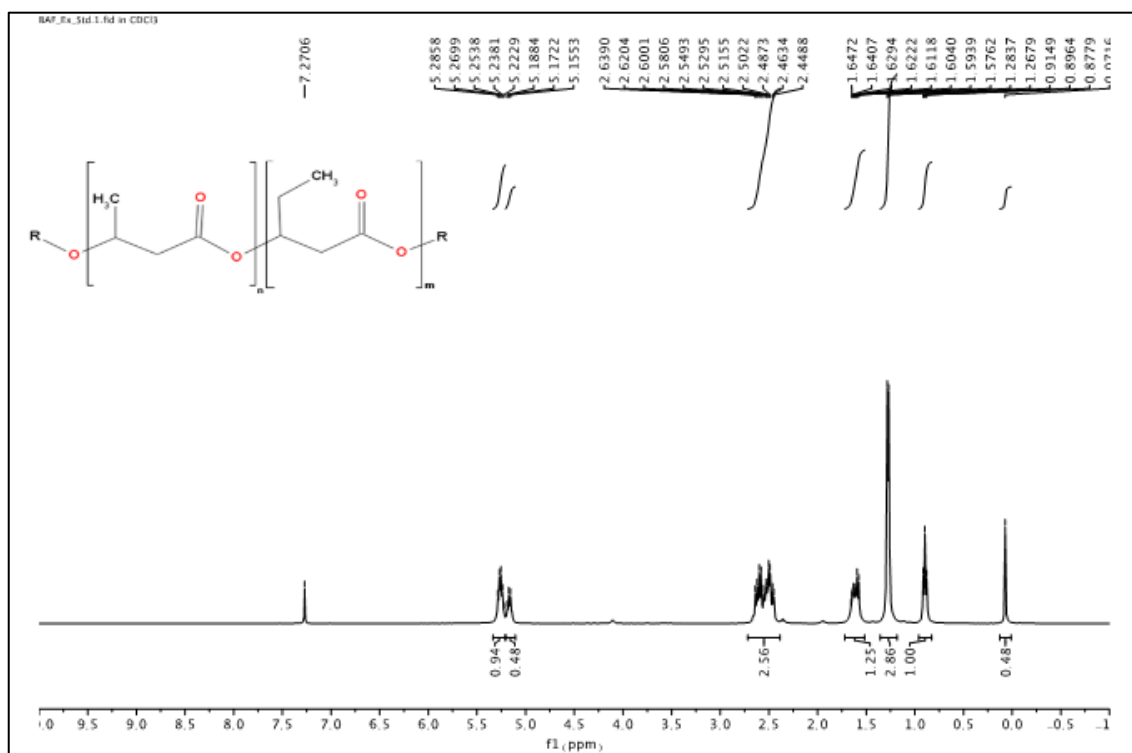
Figure 5.9.17 ^{1}HNMR spectrum of Ex_Std
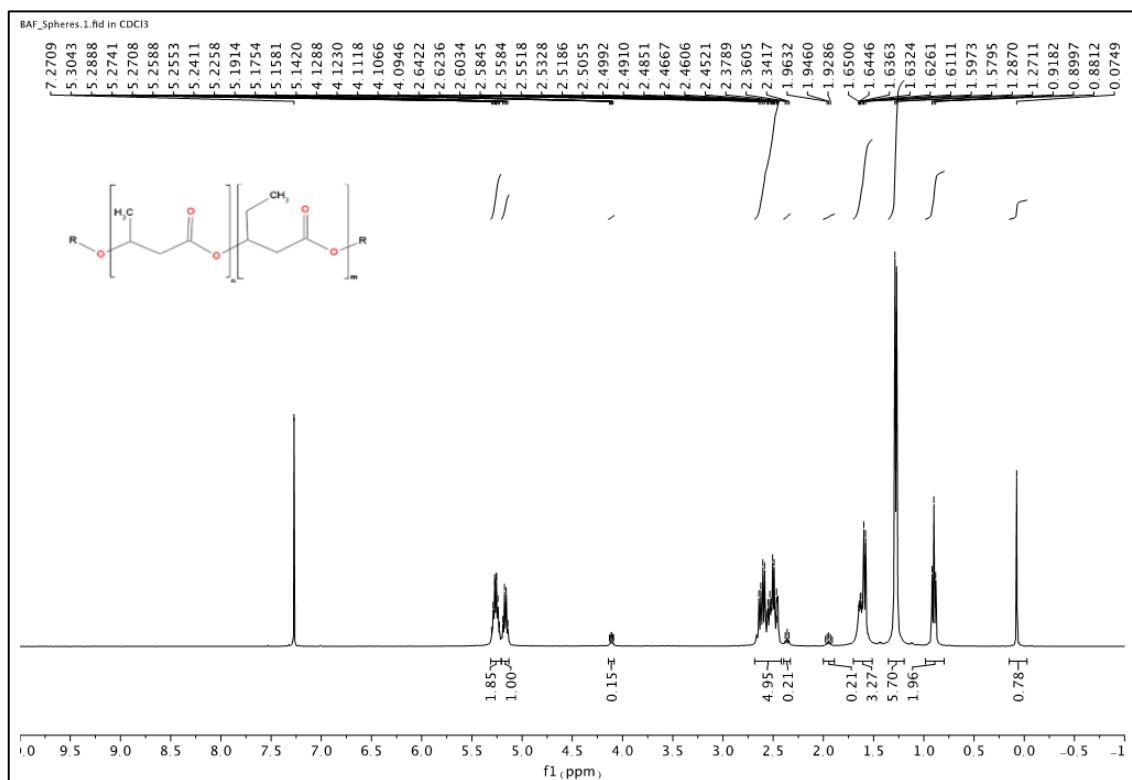
Figure 5.9.18 ^{1}H-NMR spectra of Spheres
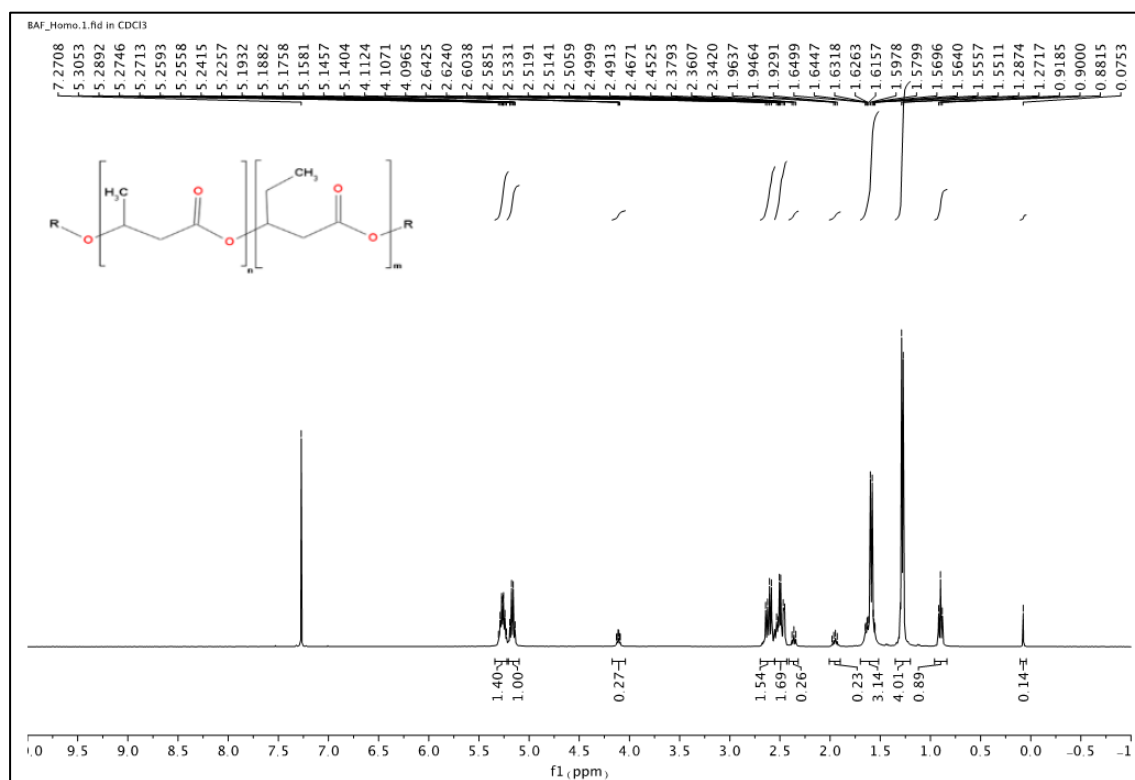
Figure 5.9.19 ^{1}H-NMR spectra of Homo
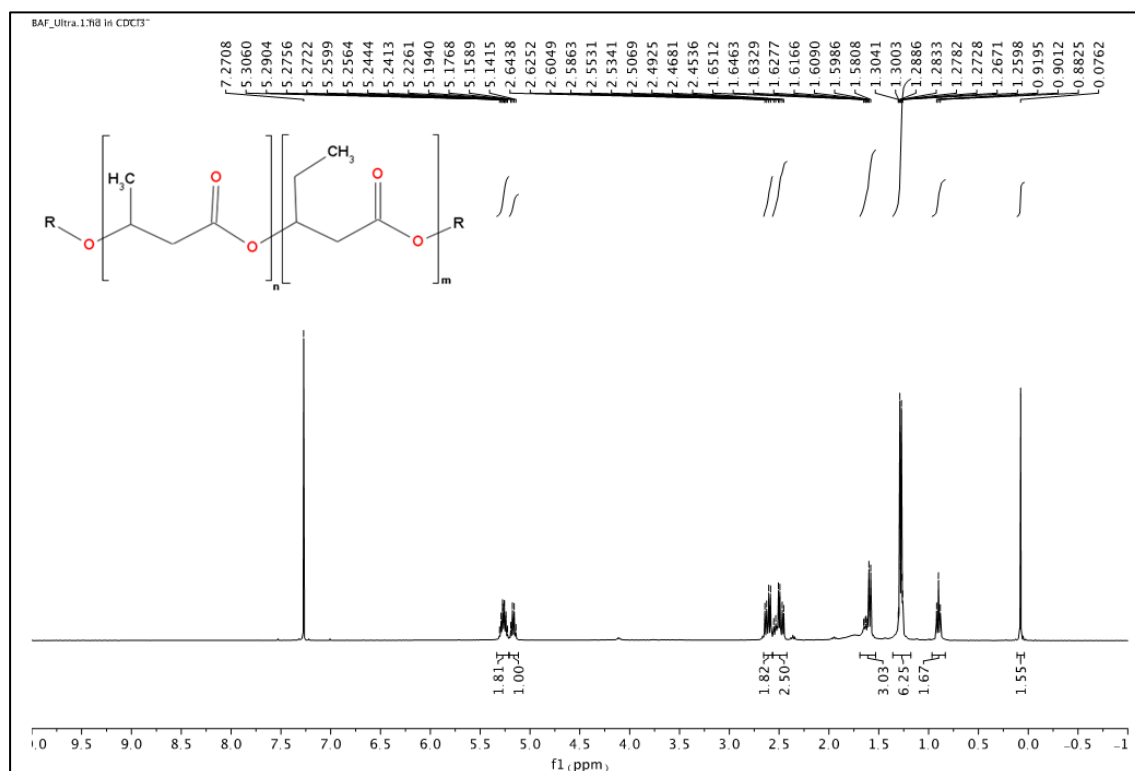
Figure 5.9.20 ^{1}H-NMR spectra of Ultra

5.9.2.4   *Thermal analysis*

5.9.2.4.1   TG Analysis

TG curves of the different PHA films, carried out to investigate the thermal stability of the polymer, are reported in Figure 5.9.21, Figure 5.9.22, Figure 5.9.23, Figure 5.9.24, Figure 5.9.25, Figure 5.9.26, Figure 5.9.27 and Figure 5.9.28.

Figure 5.9.21 TGA curves obtained by Commercial PHA
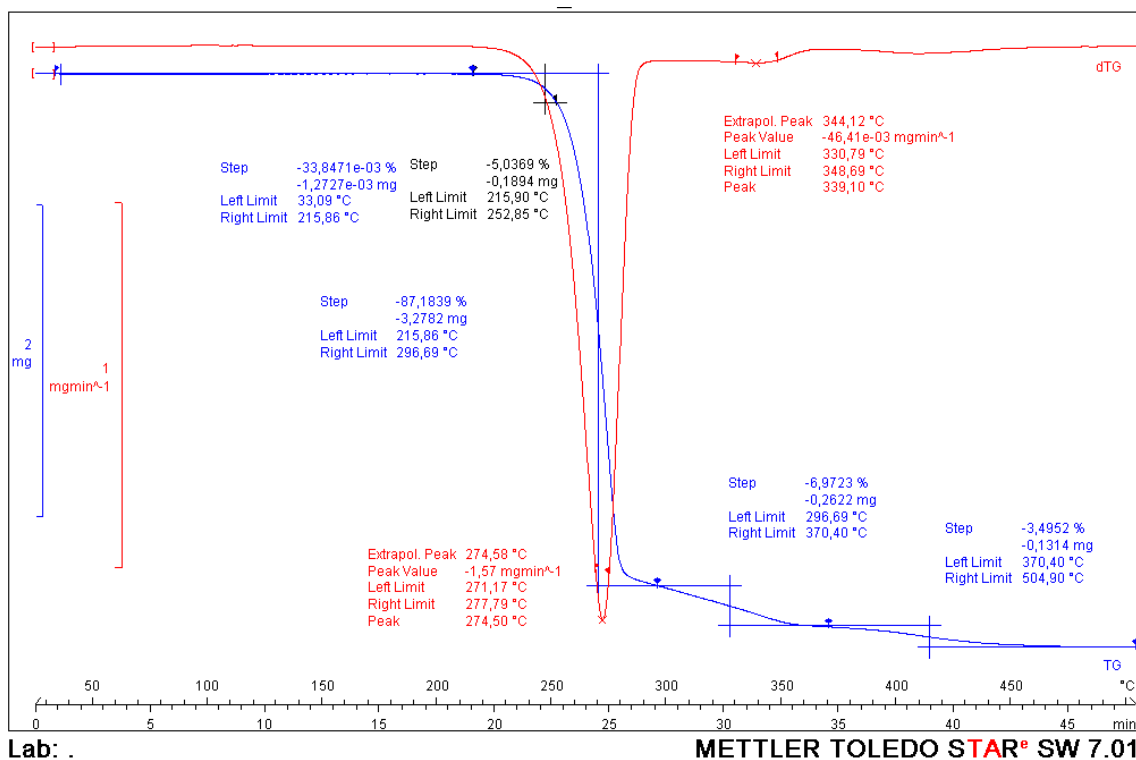
Figure 5.9.22 TGA curves obtained by Ex_Std
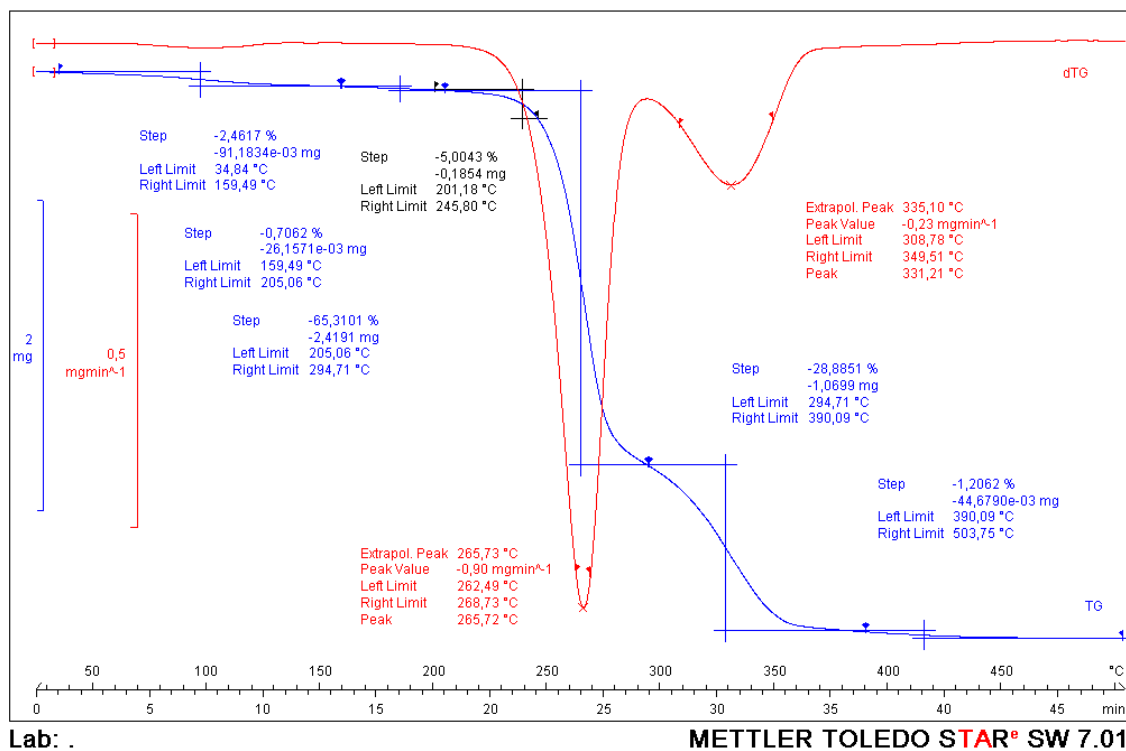
Figure 5.9.23 TGA curves obtained by Soxhlet
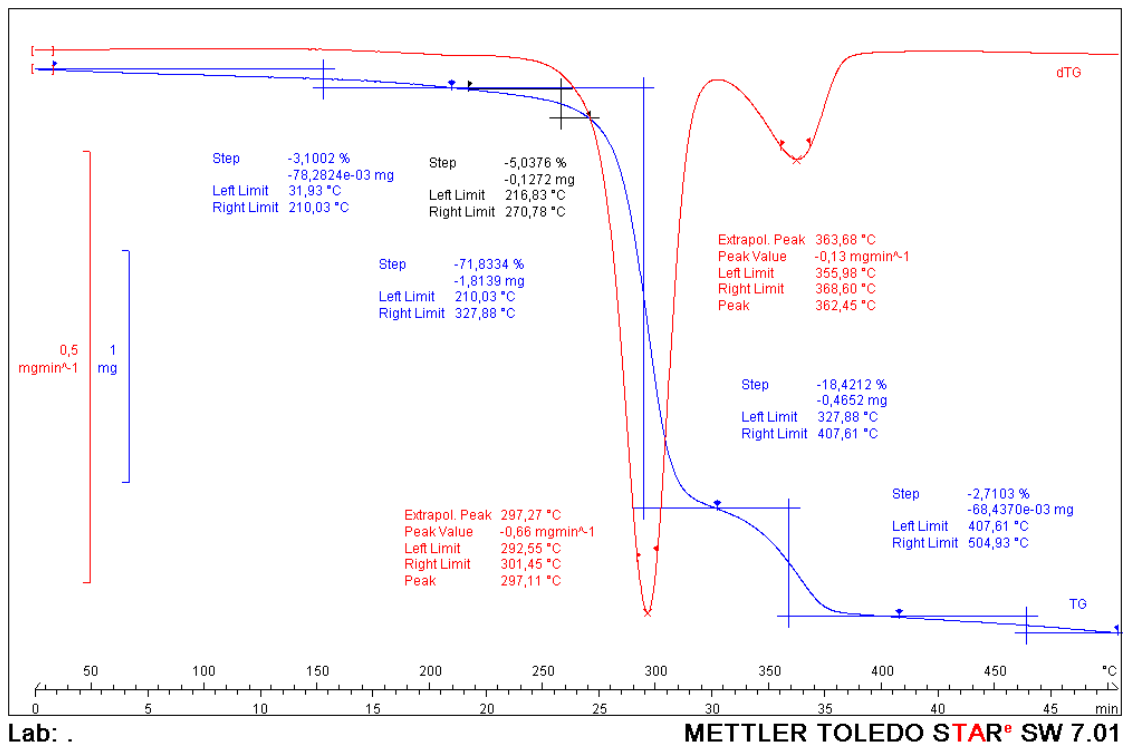
Figure 5.9.24 TGA curves obtained by Sonic_mc
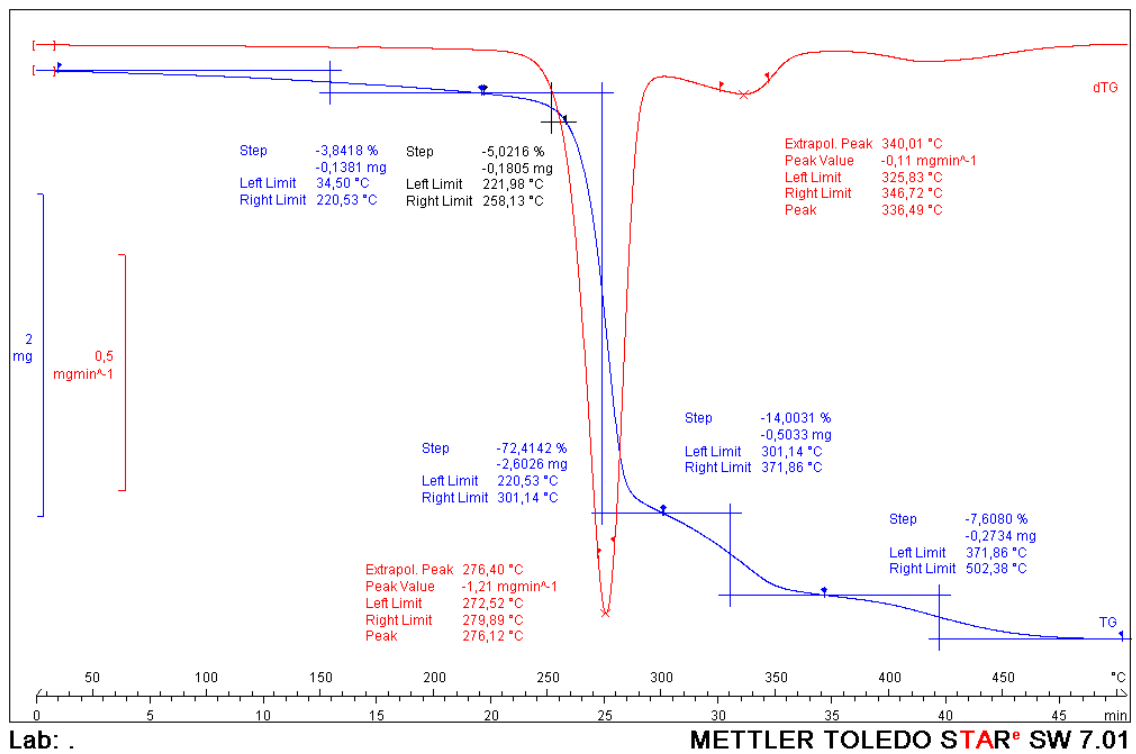
Figure 5.9.25 TGA curves obtained by Sonic_rt
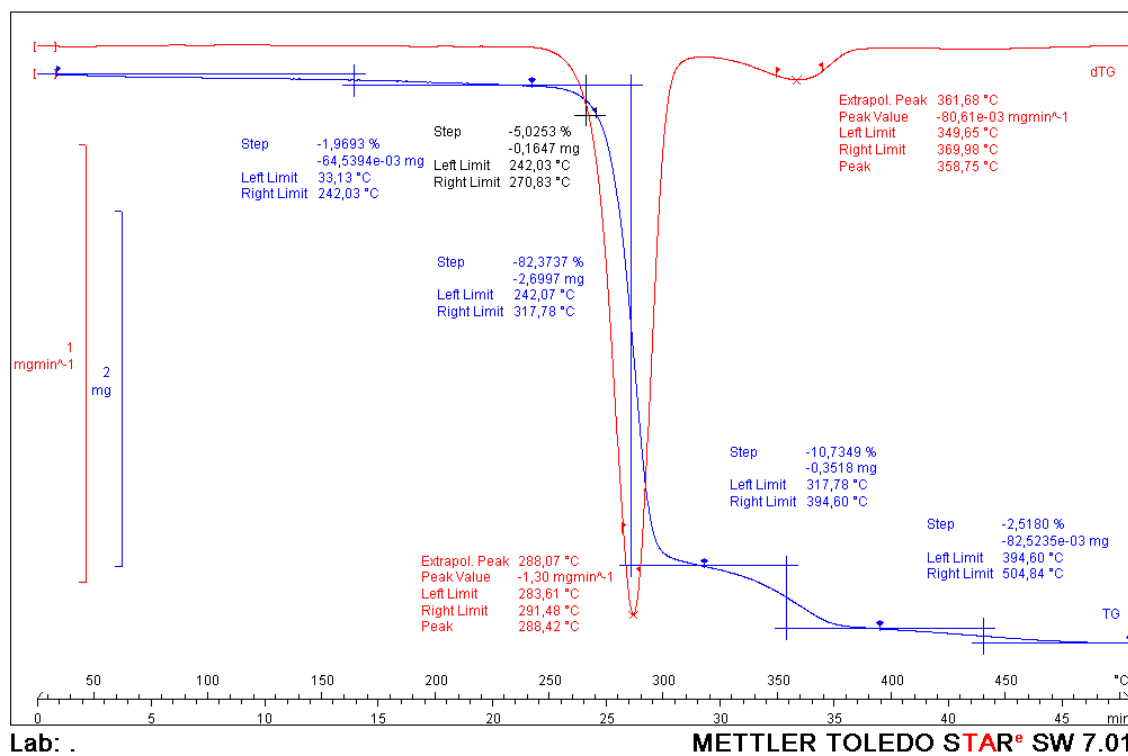
Figure 5.9.26 TGA curves obtained by Spheres
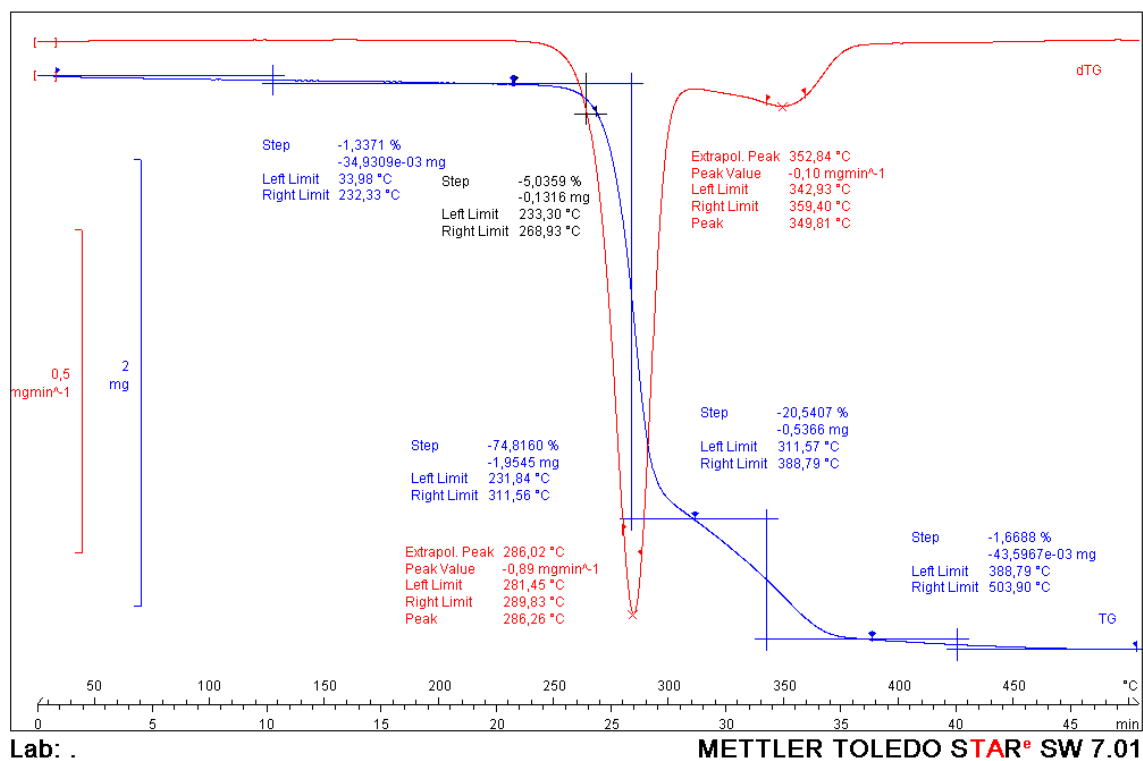
Figure 5.9.27 TGA curves obtained by Homo
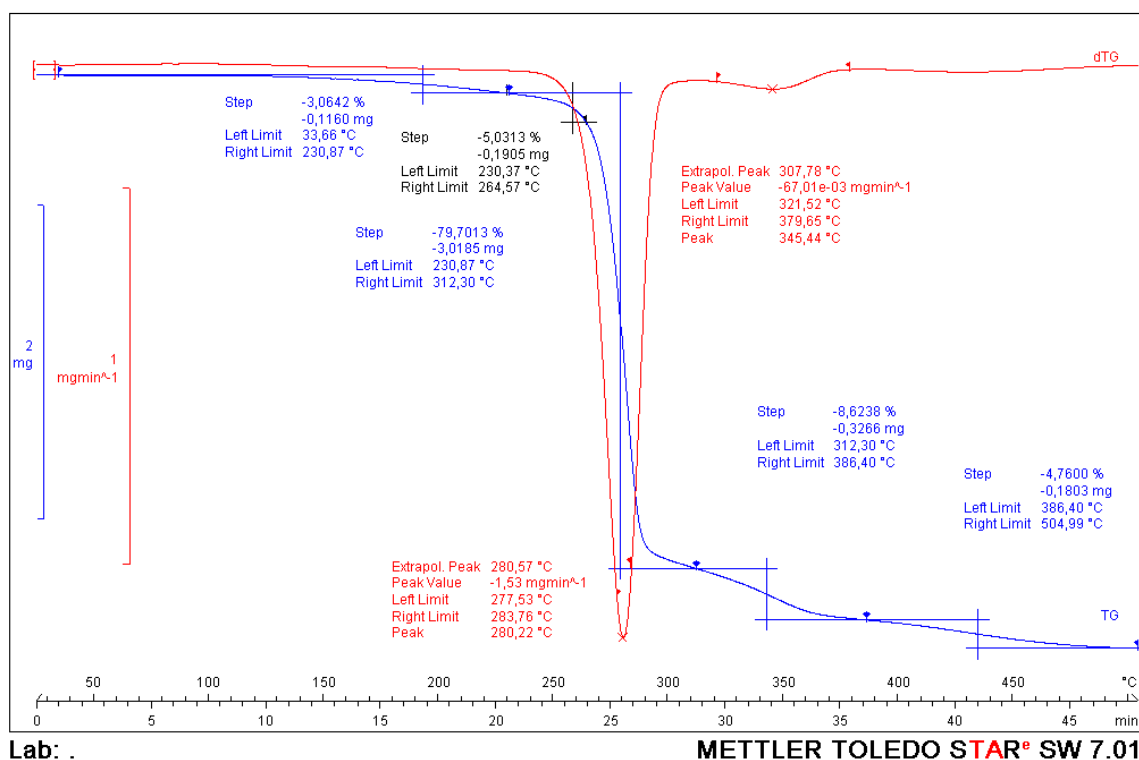
Figure 5.9.28 TGA curves obtained by Ultra

In air, the TG curves of polymers have a two-stage weight decrease. Firstly, thermal decomposition occurs with an endothermic pack; then oxidative decomposition occurs with an exothermic peak. However, during the first weight decrease, it is likely that endothermic and exothermic peaks overlap, and thermal and oxidative decomposition occur back to back. From TG curves, the decomposition temperature (Td), defined as the temperature at which the polymer loses the 5% of its weight, and the temperatures of maximum degradation (T1 and T2) were measured for each sample.

The rapid nature of PHA thermal decomposition generates well-defined peaks in dW/dT [290]. TGA measurements (Figure 5.9.21, Figure 5.9.22, Figure 5.9.23, Figure 5.9.24, Figure 5.9.25, Figure 5.9.26, Figure 5.9.27 and Figure 5.9.28) show that PHA films are generally thermally stable up to 250°C with a weight loss < 1.5 wt% at this temperature exception for Sphere (-2%), Soxhlet (-2.5%), Sonic_mc, Ultra (-3%) and Sonic_rt (-4%). Then PHA films degrade in two main steps37 at around T = 270 ± 10 ° C and around Y = 340 ± 10 °C, respectively. During the first step the decomposition of the sample begins and most of the mass loss occurs, on average 75%, whereas in the second step the mass loss is only about 20%. The weight loss during heating ranges from 95% for Homo to 88% for Sonic_rt; in particular the presence of remaining impurities from the process of PHA extraction[314] is higher in Ultra (22%), Sonic_rt (14%) and Sonic_mc (10%) than in other samples confirming the conclusions obtained by EDAX analysis (Table 5.9-4) where these PHA films appear those with the highest

percentages of elements different from C, and O. These impurities give a rough and porous surface to Ultra and both Sonic samples under SEM observations (Figure 5.9.5, Figure 5.9.6, Figure 5.9.7, Figure 5.9.8, Figure 5.9.9, Figure 5.9.10, Figure 5.9.11 and Figure 5.9.12), a yellowish wrinkled and porous aspect under optical macroscopy observations (Figure 5.9.4) and, in particular for Sonic_mc and Sonic_rt samples, very low mechanical properties (Figure 5.9.3).

Table 5.9-5 reports the thermal properties of PHA films measured by TGA in terms of mass loss, decomposition temperature (Td) and the temperatures of maximum degradation of different PHA films (T1 and T2).

Table 5.9-5 Thermal properties of PHA films measured by TGA

	Mass loss [%]	Total Mass Loss	Td [°C]	T1 [°C]	T2 [°C]
Commercial PHA	60		245	265	-
	34	94		-	334
Ex_Std	87		253	274	-
	7	94		-	339
Soxhlet	65	94	246	266	-
	29			-	331
Sonic_Mc	72	90	271	297	-
	18			-	362
Sonic_Rt	72	86	258	276	-
	14			-	336
Spheres	82	93	271	288	-
	11			-	359
Homo	74	95	269	286	-
	21			-	350

Ultra	79	88	265	280	-
	9			-	345

Td, related to a random degradation of the chain[80], varied from 245°C to 271°C for the different PHA films.

Concerning the different extraction processes, Td of Ex_std sample is 7°C higher than that of Soxhlet sample. After the beginning of thermal decomposition, T1 and T2 of Ex_std film remain 8°C higher than those of Soxhlet one.

Concerning the effect of the different pre-treatments on the thermal behaviour of the PHA films, Spheres, Sonic_mc, Homo, Ultra (Td = 271°C, 271°C, 269°C, 265°C, respectively), followed by Sonic_rt and Ex_std (Td = 258 and 253 °C, respectively) are the most resistant to thermal decomposition. Soxhlet and Commercial PHA films appear the less resistant to thermal decomposition with a Td = 266°C and 265°C, respectively. It is well known that the thermal stability of polyesters strongly depends on the length of the chains. An increase in thermal stability is related to an increase in molecular weight since if the molecular weight is higher, a higher number of bond breaking events are necessary to generate volatile oligomers which cause weight loss.

After the beginning of thermal decomposition, the differences in T1 and T2 for different PHA films are of about 30°C, again with higher values for Spheres, Sonic_mc, Homo, Ultra and lower values for Commercial PHA and Soxhlet samples.

It is worth to underline that all the 4 pre-treatments give PHA films with higher thermal stability (Td) than the not pre-treated polymer (Ex_std). A higher thermal stability means a wider fields of applications[33] since a higher decomposition temperature provides a broader separation between the required melting temperature for injection moulding and thermal degradation of the polymers[315].

Moreover, generally, the more thermally stable films are also those with the best mechanical properties in terms of high T coupled with high R, σ_M and E (Table 5.9-5, Figure 5.9.3). The only exception is the Sonic_mc film where the very high degree of impurities, as visually observed (Figure 5.9.4), probably affects its low mechanical performances.

5.9.2.4.2   DSC Analysis

Differential scanning calorimetry (DSC) measurements are carried out to identify the phase transition temperatures of different PHA films extracted from biomass. Figure 5.9.29 reports the DSC curves of the different samples.
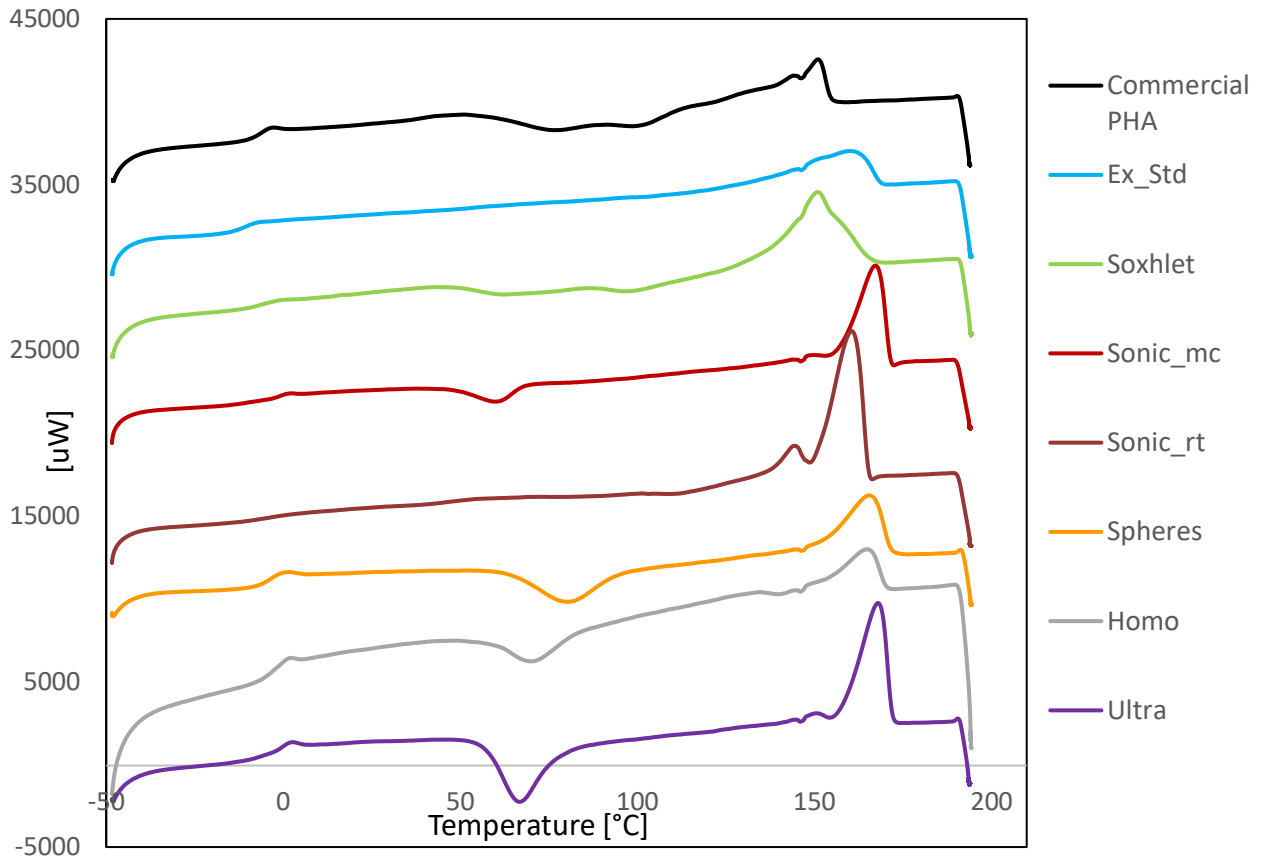
Figure 5.9.29 DSC curves of the obtained polymers

From these curves, the crystallization temperature (Tc) and melting temperature (Tm) are taken at the maximum peak of the exotherm (downward in the TGA figures) and endotherm (upward in the Figure 5.9.29) transition phase, respectively. The glass transition temperature (Tg) is taken at the mid-point of the specific heat increment. The crystallization and melting enthalpies (UNI EN ISO 11357-3), ΔHc and ΔHm respectively, are obtained by measuring the area of the corresponding peaks (Table 5.9-6). Also the corresponding crystallization degree is calculated by the equation:

$$X_c(\%) = \frac{\Delta Hm - \Delta Hc}{\Delta_{100\%}Hm}$$
(Equation 8)

where Xc (%) is the percentage crystallinity; ΔHm is the measured melting enthalpy (J/g); and the ΔH100%m is the melting enthalpy for fully crystalline PHB (146 J/g)[292].

Table 5.9-6 Thermal properties of PHA films measured by DSC.

	Tg	Cp	Tc	ΔHc	Tm1	Tm2	ΔHm	Xc
	[°C]	[mJ/°C·mg]	[°C]	[mJ\mg]	[°C]	[°C]	[mJ\mg]	[%]
Commercial PHA	-5	0.095	58	17	139	-	19	1
Ex_std	-11	0.171	-	-	138	-	25	17
Soxhlet	-4	0.060	59	4	140	151	40	25
Sonic_mc	0.4	0.050	55	12	148	157	22	7
Sonic_rt	-4	0.033	-	-	134	151	40	27
Spheres	-2	0.130	65	16	-	156	20	3
Homo	0.6	0.055	60	9	-	154	12	2
Ultra	0.6	0.130	48	31	143	156	36	3

From literature data, the thermal characteristics of PHA vary considerably with the molecular weight and the length of chains. In particular, Tg of P3HB varies between - 3 and 5 °C[316] according with the Tg values found in this work.

The different extraction methods and the different pre-treatments give polymers with Tg still comparable with that of reference Commercial PHA (- 6°C ± 5°C) even if, except for Ex_std, a little bit higher.

Tg depends on the mobility and flexibility of the polymeric chains[81]. If the mobility of the chains is restricted, then the glassy state is more stable because more energy is required to make the chains free reflecting in a higher Tg[81]. An increase in Tg is caused by a higher Mw[264] and the presence of more flexible chains[80]. In Table 5.9-6, Ex_std has the lower value of Tg; crossing this result with those obtained by 1H-NMR analysis, this is probably due to the ratio between PHB and PHV, which is almost 1:3 (while in Spheres, Homo, Ultra and Sonic_mc is 4.5:1). Also an increase in the amorphous phase might induce an increase of Tg[316]. On the other hand, side groups, increasing the free volume in the molecule, and short polymer chains acting as plasticizers, give a Tg decrease[316]. From ^{1}H-NMR analysis is evident that all samples have similar structures and, except for Ex_Std and Soxhlet, similar ratio between the two monomers, even if the exact Mw can not be obtained.

In Figure 5.9.29, a clear crystallization peak can be easily observed for Ultra, Spheres, Homo and Sonic_mc. This indicates that these compounds undergo a small amount of crystallization while heating. Tc varies from 55°C for Sonic_mc to 65°C for Spheres; higher Tc implies that the crystallisation ability of the polymer is better[316].

As Tg, also Tm is strictly related to the molecular weight[293], the polymerization degree, side chains and functional groups in PHAs structure[80]. PHAs with smaller crystals with larger imperfections, more side chain structures, less crystallinity and more amorphous structure melt at lower temperatures[316,317]. On the other hand, an increase in Tm suggests an increased symmetry in the polymer structure with higher number of average molecular weight. In this case, Tm varies from around 139°C for Commercial PHA to almost 160°C for Spheres, Sonic_mc, Homo and Ultra. Commercial PHA has the lowest Tm very probably because the introduction of inorganic nanoparticles to increase the nucleation density and decrease the spherulite size is a common practice in commercial PHAs[316] (also the presence of Ca in EDAX analysis induces this assumption) .

As expected, PHAs with higher Tm are those with the higher maximum thermal degradation temperature (T1 in Table 5.9-5) and the higher thermal stability temperature (Td in Table 5.9-5). PHAs with higher Tm and sharper melting peaks also show well defined crystallization peaks (Ultra, Spheres, Homo and Sonic_mc).

Two features characterize polymer during the melting process: polymer melts can move in their totality by Brownian motion; the diffusion of chains in a melt may also entail the cooperative movement of sub-chains. The behaviour of a polymer during the melting process is dependant by the main interactions presented on the structure. During flow, chains slip with respect to each other and when the chains are branched or when they carry bulky substituents, their relative motion is more difficult. The degree of freedom experienced by the polymer during melting depends closely on its molecular structure and in particular on its backbone[82,318] . In this case, all the chains are free to rotate and the structure is flexible and compact as result from 1H-NMR analysis.

As reported in Table 5.9-5, Figure 5.9.23, Figure 5.9.24, Figure 5.9.25 and Figure 5.9.28, some samples (Soxhlet, Sonic_mc, Sonic_rt and Ultra) show two melting peaks: this behaviour is typical of semi-crystalline polymers and it is related to the rotation of chains[80] (the ^{1}H-NMR analysis confirmed the presence of more methyl groups thanks to the higher ratio PHB/PHV). The phenomenon of multiple melting in semi-crystalline polymers is well explained by a new model, where a thermodynamically metastable polymer system may start to reorganize to achieve lower states of the free energy when it is perturbed by an increase of temperature. Such re-organization can happen through recrystallization of the metastable crystals initially formed at a low temperature to form thicker and more stable crystals[319].

The Tm of the analysed PHA ranging from 139°C up to 156°C agree with earlier data on polyesters (PHBV) with similar composition[303] (Tm = 144°C). The Tm parameter (Figure 5.9.21, Figure 5.9.22, Figure 5.9.23, Figure 5.9.24, F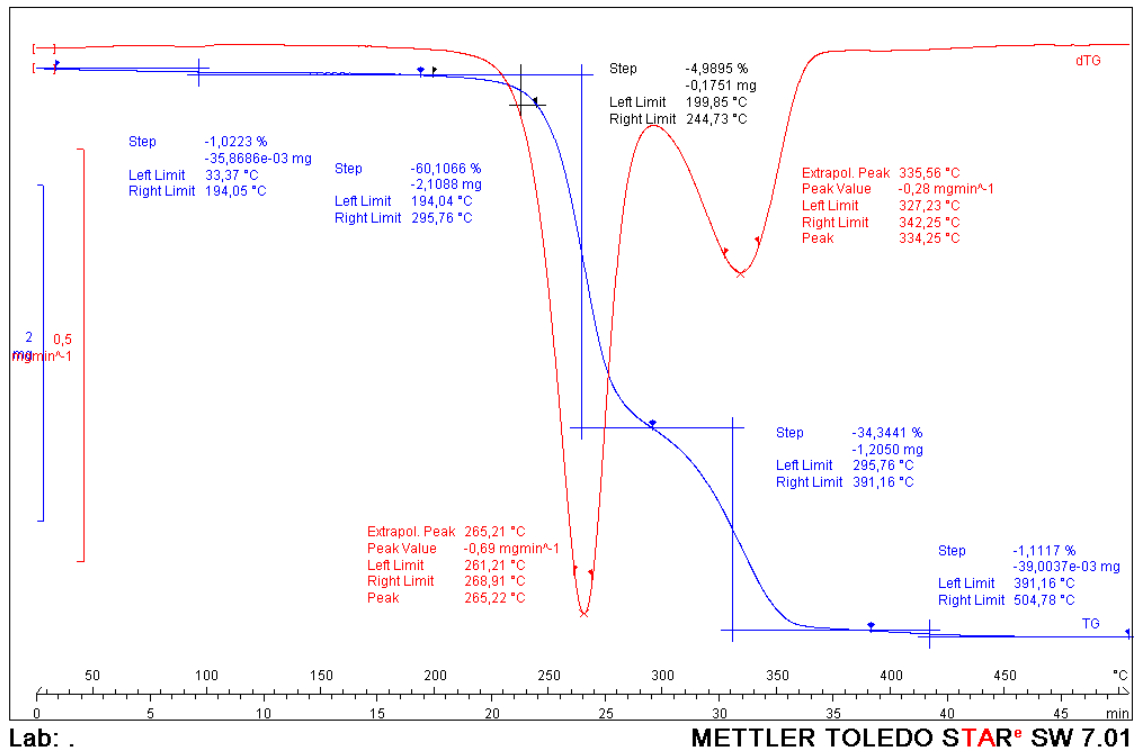igure 5.9.25, Figure 5.9.26, Figure 5.9.27 and Figure 5.9.28 and Table 5.9-6) significantly affects potential polymer applications because it affects their processings[88] and their recycling[314]. In particular, lower Tm makes the polymer processing easier and a decrease of 20°C in Tm is of great significance[320]. The higher Tm for Spheres, Sonic_mc, Homo, Ultra corresponds to the higher thermal stability measured by TGA (Table 5.9-5) and to the higher mechanical performances in terms of T together with σ_M and E measured by the stress-strain curves (Figure 5.9.3). The only exception is Sonic_mc sample for its high impurity. Probably, in Ultra, Spheres and Homo PHA films, the plastic deformation which contribute to rise the material T is due to the more linear and compact molecular structure, with less or short side chains, that facilitates chain movements and the sliding of the macromolecules one over the other. Also the presence of methyl groups (typical of PHB) may facilitate the rotation of chains.

The degree of crystallinity Xc is directly related to the processability and the industrial applications of PHAs[314]; crystallinity equal to or above 50% is considered high and detrimental for commercial and industrial purposes. Koller[321] suggests that a 3-hydroxyvalerate (3-HV) share of approximately 20% is required to reduce the crystallinity of the product (PHA) for most industrial applications. This is not necessary in this study once the majority of the PHAs exhibited crystallinity much lower than 50%[314].

Crossing all the results obtained by the thermal analysis, it is reasonable to assume that Soxhlet, Sonic_rt, Ultra, Spheres, Homo and Sonic_mc PHA films have higher molecular weight, more symmetrical and compact structure and side chains that rotates during heating than Commercial PHA film[80,316,322]. The side chains of these samples are mainly composed by methyl groups, which can rotate very easily and a higher presence of valerate with respect to commercial PHA gives slightly longer chains. In these polymers the PHB to PHV ratio is almost 5:1, causing a compact structure with a higher Tm value with respect to Commercial PHA (> 150°C).

On the other hand, the results obtained for Ex_Std PHA films suggest a lower Mw due to the higher presence of PHV with respect to PHB (almost 3:1) and flexible side chains which reduce the Tm at 138°C[80,316,322]. The similar Tm of Commercial PHA and Ex_std samples suggests a similar Mw, even if the presence of valerate in the structure is very different.

PHAs are generally thermally stable at temperatures below 160∘C, as found in this study (Table 5.9-5). Crossing the results obtained by TGA and DSC, it is clear that PHAs begin to melt long before their degradation temperature is reached (Td > 200°C). Plastic or viscous behaviours, which correspond to the partial or total irreversibility

of deformations in response to a mechanical stress, are imperative to apply[82] the usual techniques of polymer processing. Thus, these polymers are suitable for different processing as thermoforming, extrusion or compression[88], can be easily moulded by injection and are applicable to blown film processing confirming usefulness of produced PHA in many industrial applications.

5.10 **Conclusion**

This work has the purpose of comparing the effects of two different extraction methods (conventional extraction and Soxhlet extraction) and four different pre-treatments (homogenization with pressure and with blades, sonication and impact with glass spheres) on the extraction yields and properties of PHA extracted from biomass coming from a wastewater treatment plant.

The obtained results confirm a direct correlation between the adopted pre-treatment and extraction method with the extraction yields, impurities content and the mechanical and thermal properties of the obtained PHA films.

The extractive yield has proved to be highly influenced by pre-treatments: homogenization gave the best result leading approximately to 15% more extractive yield.

The two different extraction processes affect the crystallization degree of the polymer (17% for Ex_Std and 29% for Soxhlet) and the chemical composition (PHB/PHV for Ex_std and PHB/Me-PHB for Soxhlet).

Moreover, compared to standard extraction without pre-treatments, homogenization has proved to be the best pre-treatment in terms of purity, tensile strength (about 5 MPa higher) and Young's module (higher 153 MPa) of the obtained PHA films. There were not many differences in the PHA films obtained by homogenization with blades or at high pressures, except that the first gives films slightly more impure than the second.

Finally, as regards the thermal behaviour, conventional extraction gives PHA films with a Td 10°C higher than those obtained by Soxhlet extraction, whereas the four pre-treatments give PHA films with higher Td than that of not treated polymer. This means a higher thermal stability and therefore a wider field of applications thanks to their molecular structure mainly composed by PHB.

The best compromise among highest thermal degradation (T1 = 290°C), visual appearance (transparency and clearness) and mechanical performance (Toughness) are reached with pre-treatments based on homogenization and impact with glass spheres which give PHAs with the same PHB/PHV ratio equal to 4.5:1.

However, all the PHA film begin to melt long before their degradation temperature (over 200° C); this hopes for its possible use in the field of extrusion or compression moulding.

6 . Chapter

Preliminary study on PHAs Composites

Evaluation of the effect of natural reinforcing materials and manufacturing processes on PHA-composites properties.

6.1   **Introduction**

This part of the dissertation concerns the study of composites process carried out in collaboration with The University of Queensland, Brisbane, Australia.

The first phase of this research, reported in this Chapter, is focused on the properties induced by reinforcing filler/fibers and the type of polymer processing on composites based on polyhydroxyalkanoates.

The use of such polymers as the matrix in bio-based composites is one of the growing areas of interest because of the expanding Natural fibre-reinforced composites (NFRCs) and Wood Plastic Composites (WPCs) market[11] and the cost competitiveness achieved by taking advantage of cheap, abundant and biodegradable wood fibres or other bio-based materials as structural fillers[11].

Green agro-fibre thermoplastic bio-composites, also known as agro-plastics, where agro-fibres are bond with bioplastics, have been developed in different researches on lab-scales; rice straw – poly hydroxybutyrate-co-hydroxyvalerate (PHBV) bio-composites, rice straw-PLA and rice husk-PLA wheat straw – recycled petrol-based HDPE and rice husk bonded by recycled PVC are already available on the market[323].

Natural fibre-reinforced composites offer a unique solution where both the reinforcement and the matrix ingredients are entirely bio-sourced and also biodegradable [324]. The physical and mechanical properties of PHA biopolymers are particularly suitable for the manufacture of Natural fibre-reinforced composites; PHAs exhibit a low melt viscosity, which makes them suitable for polymer processing[323–327].

In this study, the attention is focused on the realization of composites through two of the more common techniques in polymer processing: compression moulding and extrusion.

The extrusion process comprises the forcing of a plastic or molten material through a shaped die by means of pressure. In modern process, different types of screws are used to progress the polymer in the molten or rubbery state along the barrel of the machine[88].

In the compression moulding method, the mould (containing the polymer) is closed with a top force or plug member, pressure is applied to force the material into contact with all mould areas, while heat and pressure are maintained until the moulding material has cured. The advantage of compression moulding is its ability to mould large, fairly intricate parts. Furthermore, it is one of the lowest cost moulding methods compared with other methods such as transfer moulding and injection moulding; moreover it wastes relatively little material, giving it an advantage when working with expensive compounds[88,89].

Formulations containing PHA of commercial source and a single reinforcing material are proposed so as to be able to evaluate the effects on the matrix. The considered materials (wood flour, macadamia shells and coffee grounds) have different origins and shapes, but they are all secondary by-products of Australians industries (*Radiata pine wood and macadamia shells, by MicroMilling Pty Ltd, Goulburn, NSW, Australia; Coffee grounds 100% arabica Merlo Coffee®, Brisbane, QLD, Australia*). Previous studies[323,325] in literature have already investigated on the use of different natural fibrous materials in association with polypropylene or other thermoplastics, but for author's knowledge this is the first study on the influence of the filler on the PHA-matrix analysed with two different processing techniques.

The final objective of the study is to evaluate how the composite manufacturing process and the filler addition can vary the performances (mechanical, thermal and structural) of the composite and how the interaction between the two phases changes. Four formulations were analysed in both techniques and compared each other's: a reference made with 100% of PHA with three other specimens containing the same amount of added filler.

6.2   Overview on Green reinforced composites

Over the past few decades, polymers have replaced many of the conventional metals/materials in various applications. This is possible because of the advantages that polymers offer over conventional materials as the ease of processing, productivity, and cost reduction[88,93]. These composites are finding applications in diverse fields from appliances to spacecrafts. In most of these applications, the properties of polymers are modified using fillers and fibers to suit the high strength/high modulus requirements. Natural fibre–reinforced composites (NFRCs) are increasingly being used in many engineering applications[339].

Polymer matrices can be divided into two types; one is synthetic petrochemical- based called synthetic matrix (polyester, polypropylene (PP), polyethylene (PE), epoxy, etc.) and the other is natural or bio-based called biodegradable matrix (PHA or PLA are some examples)[328].

Natural fibers are classified based on their origins, whether from plants, animals, or minerals[328–330]. Plant fibers include leaf fibers (pineapple, sisal, and abaca), core fibers (hemp, jute, and kenaf), grass and reed fibers (wheat, corn, and rice), seed fibers (cotton, kapok, and coir), bast fibers (flax, jute, hemp, ramie, and kenaf), and all other types (wood and roots) [328]. Jute, ramie, flax, and sisal are the most commonly used fibers for polymer composites. Green Reinforced Composites includes also all the composites reinforced with materials that are not in form of fibres, but they are always from natural source (as coffee grounds, seeds or starch).

A classification of natural fibres and fillers is reported in Figure 6.2.1.
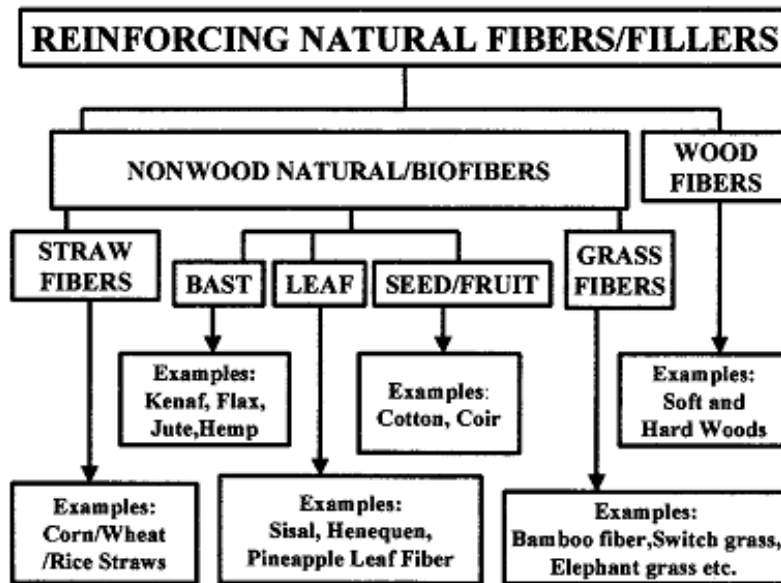
Figure 6.2.1 Classification of reinforcing natural fibres/fillers

Natural fibers in the form of wood flour have also been often used for preparation of natural fiber composites. The properties of these fibers have been investigated in previous studies[11,115,335–341,140,323,328,330–334] ; the specific modulus of natural fibers (modulus/specific gravity) show values comparable to or better than those of glass fibers. These higher specific properties are one of the major advantages of using natural fiber composites for applications wherein the desired properties also include weight reduction[329].

Natural fibers are low-cost, with low density and high specific properties, biodegradable and nonabrasive, unlike other reinforcing fibers. Also, they are readily available and their specific properties are comparable to those of other fibers used for reinforcements. However, certain drawbacks such as incompatibility with the hydrophobic polymer matrix, the tendency to form aggregates during processing, and poor resistance to moisture greatly reduce the potential of natural fibers to be used as reinforcement in polymers.

Natural fibre–based composites from renewable resources have low cost, lightweight, biodegradability[342], high thermal and acoustic insulation, and high specific strength and stiffness. Synthetic fibre– based composites, instead, have high cost, high energy consumption in machining and manufacturing processes, poor recycling and non-renewability properties, CO_2 emissions and health hazards when breathed in[328]. These

shortcomings have caused natural fibre composites to emerge as a promising alternative to synthetic fibre composites.

6.2.1   **Fiber Composition**

Natural fibers are cellulose fiber reinforced materials themselves as they consist of microfibrils in an amorphous matrix of lignin and hemicellulose with several minor components such as pectin, wax, protein, tannins, ash, and inorganic salts. These constituents vary depending on the source of the fibers, growing conditions, plant age, and digestion processes[330]. The hydrogen bonds and other linkages provide the necessary strength and stiffness to the fibers. A representation of the fiber structure is reported in Figure 6.2.2.
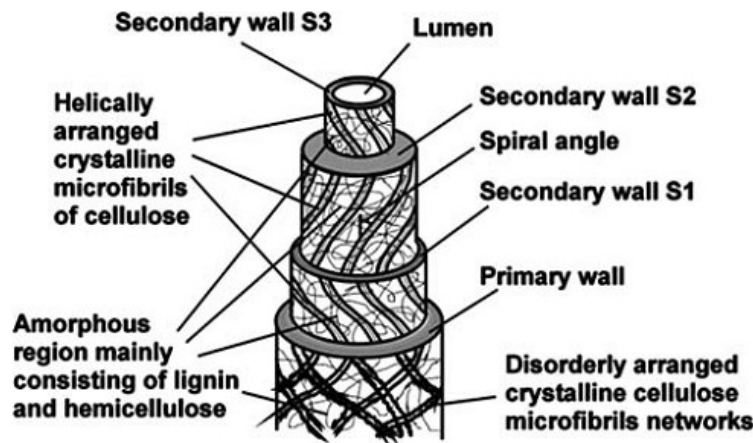
Figure 6.2.2 The structure of a single fibre cel [330].

Generally, the content of cellulose plays the largest role in governing the properties of the fibers and dictates the mechanical performance of the fibers when used as reinforcement within composites. Unlike the cellulose, increases in non-cellulosic components tend to reduce the strength and modulus of the fibers, leading to negative influences on natural fiber reinforced composites[330].

Hemicellulose is responsible for the biodegradation, moisture absorption, and thermal degradation of the fiber as it shows least resistance whereas lignin is thermally stable but it is responsible for the UV degradation. The percentage composition of each of these components varies for different fibers. Generally, the fibers contain 60–80% cellulose, 5–20% lignin, and up to 20% moisture[329].

All the main components are presented in the sections below.

6.2.1.1   *Cellulose*

Cellulose is the major building block of wood; as in most plants, it makes up between 40% and 50% of the dry mass of timber.

Glucose ($C_6H_{12}O_6$) is produced in plants and trees by the act of photosynthesis. The glucose units are then transported down to the cambial zone where they bond together linearly to form cellulose. Chemically, cellulose is the polymer of the hexose, ß-D-glucopyranose, with the polymer links being between the fourth and the first carbons on the molecules. This polymer has a crystalline structure (i.g. it is made up of repeating units), therefore it is easier to degrade[343]. The degree of polymerization (PDI) of wood cellulose is between 8000 and 10,000, making each cellulose chain approximately 4-5 μm and the molecular weight in the order of $1.5 \cdot 10^6$.

The length of a cellulose molecule is approximately 5 μm or 5000 nm. This length is higher than the length of the crystallinity area, which is approximately 60 nm[344]. This means that a molecule will pass through areas of high crystallinity as well as regions of low crystallinity, in which molecules are only loosely associated with each other[343].

6.2.1.2   *Hemicellulose*

Hemicellulose, second to cellulose in abundance, differs greatly from cellulose. The molecules are shorter with a PDI of between 150 and 200 and are built up of different heteroglycan sugar units, depending upon the species from which they are obtained, i.e., hardwood, softwood or angrifies. As well as glucose, hemicellulose can contain primarily the mannose and galactose, but they can also contain the pentoses xylose and arabinose.

In softwoods the majority of the hemicelluloses are known as Galacto-glucomannans; these are one to four polymers of glucose and mannose, in which the mannose predominates, while the galactose units are borne laterally on this main chain. Previous studies estimated that hemicellulose make up 25-40% of dry wood mass[119,122,140,344–346]. Typical components of hemicelluloses are a group of compounds called aldoses and may be linked together either in a linear or branched arrangement. Typical components present within hemicelluloses include D-xylose, D-mannose, D-glucose, D-galactose, L-arabinose, L-rhamnose, 4-O-methyl-D-glucuronic acid, D-glucuronic acid and D-galacturonic acid[343].

6.2.1.3   *Lignin*

Lignin is a highly complex non-crystalline molecule comprised of a large number of phenyl-propane units[344].

Lignin is a disordered, cross-linked polymer which gives rigidity to plants. It is an amorphous phenolic polymer with aromatic and aliphatic constituents formed by phenyl-

propane units. The molecular masses of isolated lignin are from 1,000 to 20,000 g/mol. The PDI of lignin is difficult to measure, since it easily becomes fragmented during extraction and consists of several types of substructures without a regular repeating pattern[343]. During biosynthesis of plant cell walls, lignin is developed between the polysaccharide fibers (cellulose and hemicellulose), binding them together. This lignification process causes a stiffening of cell walls. As a plant matures, lignin becomes more rigid. The structure of lignin depends on the original sources, but the basic composition is kept the same. Lignin is highly hydrophobic in nature and is not hydrolyzed by acids. It is soluble in hot alkali, readily oxidized, and easily condensable with phenol. The mechanical properties of lignin are lower than those of cellulose[343,344].

The large number of bond types in lignin means that the structure is hard to break down. About 25% of all the lignin in wood is found in the middle lamella an intercellular layer that made of lignin and pectin[343,330].

6.2.1.4   *Pectin*

Pectin is a collective name for heteropolysaccharides, which are a major matrix component of the cell wall in long non-wood fibers, particularly the important bast fibers. Pectin gives flexibility to plants. It is soluble in water only after a partial neutralization with alkali or ammonium hydroxide[343].

6.2.1.5   *Terpenes, waxes, acids and alcohols*

Due to the biosynthetic pathways of plants, each species is capable of producing its own individual range of chemical components. Many of the fragrances recognizable for wood and plant species are due to the combination of other compounds as VOCs.

Terpenoids are a range of compounds based on isoprene units derived naturally from mevalonic acid. The presence of terpenoids within a plant has been attributed to a protective system against biological attack or stress during growth, with the diverse needs of plant protection demonstrated by the more than 20,000 terpenoids known and classified. They are produced in cellular organelles, to be stored within a structure until needed[343].

In order to maintain an external protective layer, plants use cuticles. These are lipophilic structures deposited onto the outer side of epidermal cell walls. Two major components of plant cuticles are recognized through their levels of solubility: cuticular wax, comprising lipophilic components soluble in organic solvents, and cutin, which comprises non-extractable components. The waxes present on plants and tree materials represent a water-repellent barrier to aid in the bio-protection of the plant[343].

Cuticular wax contains a wide range of hydrocarbons from fatty acids, including medium to long chain alkanes such as undecane and eicosane. The cuticular waxes can also include hydroxy fatty acids, hydroxy fatty acid methyl esters and alkanols[343].

6.2.1.6   *Proteins*

Mature wood (both hard and soft types) contains only small amounts of proteins (up to max 0.5% of dry matter). These are of the elastin type and are important for cell wall growth. They have negligible effects on the mechanical properties of mature wood[343] 'Lignocellulosic' materials (fibers and fiber bundles/chips) sourced from annual crops contain more protein than wood but again the proteins have little influence on fiber/chip mechanical properties[343].

6.2.1.7   *Inorganic material*

The inorganic content of natural fibers is usually defined only as silica; these levels are often determined by thermal degradative processes. A range of metallic species may also be found in low concentrations, often linked to local growing conditions[343].

6.3   Coffee Grounds

Coffee has been consumed for many years, and the resulting coffee production is enormous worldwide. At present, significant coffee wastes are generated by its production and utilization with drinking water, and large amounts of coffee grounds (CG) are discharged worldwide. Brazil is the largest producer of coffee and produces about 80% of coffee. This corresponds to 28, 590 ,502 tonnes of coffee every year. About 50% of the total coffee is used as drinking water[347–349].

They are mainly composed of cellulose, hemicellulose, and lignin. Thus, they are very similar to natural fibers for their chemical composition, but their shape and size is totally different[348,350,351]. Nevertheless, they also contain proteins, lipids, fatty acids, tannins, polysaccharides, polyphenols and a non-negligible amount of minerals[350], which make their chemical composition more complex.

Numerous research studies have been carried out on coffee wastes, where researchers studied their composition trying to use it as resource[52,347–349,351–353] as "green materials" with many potentials uses in a variety of fields, such as bioenergy, biofuels, or polysaccharides productions. In some cases, they can be used as reinforcing agent in biopolymers to produce sustainable green composites with affordable cost.

However, their hydrophilicity constitutes a real barrier to their incorporation in polymer matrices due to the poor affinity between hydrophobic polymers and hydrophilic CG components, thereby leading to limited usage as bio-reinforcement. Currently, numerous

studies have been conducted on CG not only for improving their hydrophobicity for material applications, but also to reduce the risk related to disposal in landfill locations[348,350,351].

Among these studies, some focused on compatibilizers or coupling agents addition to the polymer matrix, other on chemical modification of CG by antimicrobial rosin, or by torrefaction, which is a mild thermal treatment (200−300 °C) under nitrogen, with the aim of obtaining a hydrophobic material[349].

The use of this lignocellulosic material combined with a polymer with low performances can enhance its applications as reinforcing agent, which shall be added to improve the polymer properties to meet desired applications, and decrease the final price of the product [349].

Nevertheless, the reinforcing effect depends upon microstructure configuration and interfacial adhesion between the polymer matrix and the filler. As previously exposed the percentage in cellulose, hemicellulose, lignin and other components are crucial on the reinforcement effect of a fill due to the influence on the interaction between the polymer matrix and the other phase. Moreover, in this case, the CG are a secondary products, which means that the percentages of the components can be much different from the usual amount [52,347–351,353].

6.4   Study of the reinforced composite

The matrix phase plays a crucial role in the performance of polymer composites. Both thermosets and thermoplastics are attractive as matrix materials for composites. In thermoset composites, formulation is complex because a large number of components are involved such as base resin, curing agents, catalysts, flowing agents, and hardeners. These composite materials are chemically cured to a highly cross-linked, thus highly solvent resistant, tough, and creep resistant. The fiber loading can be as high as 80% and because of the alignment of fibers, the enhancement in the properties is remarkable.

One of the advantages of thermoplastic matrix composites is their low processing costs. Another is design flexibility and ease of molding complex parts. Simple methods such as extrusion and injection molding are used for processing of these composites[88,93].

This is mainly because the processing temperature is restricted to temperatures below 200°C to avoid thermal degradation of the natural fibers[88,93].

For thermoplastic composites, the dispersion of the fibers in the composites is also an important parameter to achieve consistency in the product. Thermoplastic composites are flexible and tough and exhibit good mechanical properties. However, the amount of fibers is limited by the processability of the composite: a too high percentage of fibers may

induce the formation of voids, which will affect the mechanical properties[154,335,343,354]. In the composites the fiber orientation is random and accordingly the property modification is not as high as is observed in thermoset composites[88,93]. Properties of the fibers, the aspect ratio of the fibers, and the fiber–matrix interface decide the properties of the composites. The surface adhesion between the fiber and the polymer plays an important role in the transmission of stress from matrix to the fiber and, so the performance of the composite. Another important aspect is the thermal stability of these fibers [329,343,330].

Since most thermoplastics are processed at high temperatures, the thermal stability of the fibers at processing temperatures is important. Thus the key issues in development of natural reinforced composites are (i) thermal stability of the fibers, (ii) surface adhesion characteristics of the fibers, and (iii) dispersion of the fibers in the case of thermoplastic composites[329,343,330].

In this study, the polymer matrix is composed by polyhydroxyalkanoates (thermoplastic), with the addition of three types of filler in the same quantity, coming from industrial wastes: Wood Flour (WF), Macadamia nut shells (MS) and spent Coffee Grounds (CG).

The effect of two processing techniques and the three types of fillers on the mechanical, thermal and morphological properties of the composite are evaluated.

6.5   **Materials**

6.5.1   **Polyhydroxyalkanoates (PHA)**

Poly(3-hydroxybutyrate-co-3-hydroxyvalerate) (PHBV) biopolymer with 1 mol% HV 3-(hydroxyvalerate) content is purchased from TianAn Biopolymer, China in powder form under the trade name of ENMAT Y1000. ENMAT Y1000 has a density of 1.25 g/cm^3, and a reported melt flow index (MFI) of 5.2 g/10 min at 180 °C, using a weight of 2.16 kg, according to ISO 1133. The polymer has a Mn of 590 kDa and the melting temperature of 171 °C, as measured by Differential Scanning Calorimetry (DSC) in accordance with ASTM D3418-12. The particle size distribution, as provided by the supplier, ranges from granules having a diameter d =1 μm to d=80 μm, with the maximum pick at d =20 μm. The critical granular diameters, below which 50% (D_{50}) and 90% (D_{90}) of the total granules are included, are D_{50} = 17 μm, and D_{90} = 45 μm, respectively.

6.5.2   **Wood Flour (WF)**

Wood flour (WF) is hammer-milled and supplied as unbleached thermomechanical pulp from Radiata pine wood, *by MicroMilling Pty Ltd, Goulburn, NSW, Australia*. No chemicals are used to treat the fibres. The average length of the wood fibres is 300 μm with a density of 340g/L. The aspect of the fibre is fine homogenous, light-biscuit coloured powder (Figure 6.5.1).
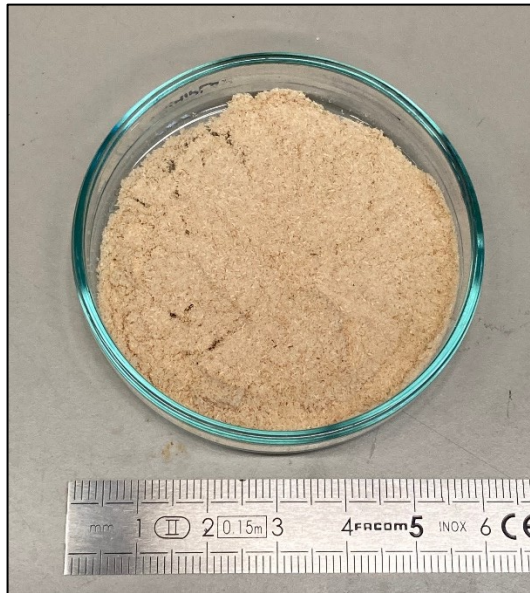
Figure 6.5.1 Wood flour

The specified particle size distribution of the as-received wood flour is summarised in Table 6.5-1.

Table 6.5-1 Specified particle size distribution of wood flour from manufacturer

Particle size (μm)	Smaller than 75	75-150	150-250	250-300	Larger than 300
Distribution	35%	30%	30%	5%	Max 1%

6.5.3   Macadamia nut shells

Macadamia nuts come from plants belonging to the family of *Proteaceae* and are native to Australia. The macadamia nut production is increasing annually as the associated waste shell generation which is 65% of total nut. Disposal of macadamia nut shells have created serious problems for the nut processing industries and hence sustainable recycling solution is critically required[339].

Macadamia nut shells (MS) flour are hammer-milled and supplied as unbleached thermomechanical pulp from macadamia shell nuts, *by MicroMilling Pty Ltd, Goulburn, NSW, Australia*. No chemicals are used to treat the fibres. The average length of the wood fibres is 212 μm with a density of 610 g/L. The aspect of the fibre is a fine homogenous, light-chocolate coloured powder (Figure 6.5.2).
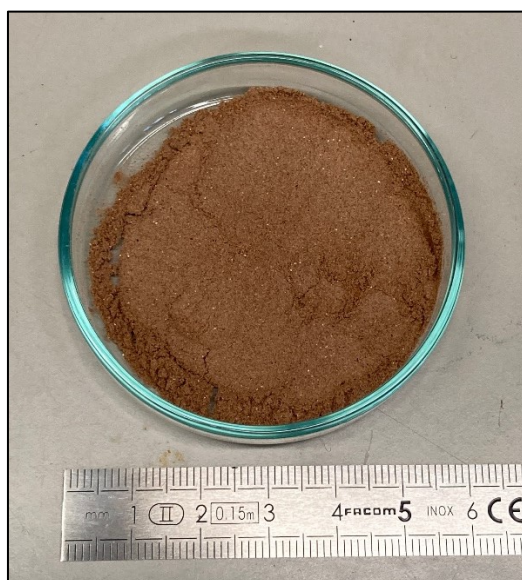
Figure 6.5.2 Macadamia nut shells

The specified particle size distribution of the as-received macadamia shells flour is summarised in Table 6.5-2

Table 6.5-2 Specified particle size distribution of Macadamia shells fibres from manufacturer

Particle size (μm)	Smaller than 85	85-110	110-150	150-180	Larger than 250
Distribution	55%	30%	10%	10%	Max 1%

6.5.4   Coffee grounds

Coffee grounds (CG) are supplied as spent secondary product by Merlo Coffee®, Brisbane, Queensland. The average size of coffee grounds is 100 μm and the density is equal to 1240 g/L. Figure 6.5.3 shows the spent coffee grounds used as filler.

Figure 6.5.3 Spent coffee grounds

All the materials are dried overnight at 35±5°C before the use to remove all the moisture.

6.6   **Methods**

6.6.1   **Compression moulding**

The first step of the study is the preparation of 4 formulations: a reference made with 100% of polymer (CP_Pm) and the specimens containing the reinforcing material (wood flour, macadamia shells and coffee grounds). For the other 3 samples, the same amount of WF, MS and CG is used: 70% w\w of polymer and 30 % w\w of filler. In Table 6.6-1 the four formulations are resumed.

Table 6.6-1 Formulations of compression moulded specimens

Name of the sample	Polymer (%)	Filler (%)
CP_Pm	100	-
CP_30WF_Pm	70	30 - wood flour (WF)
CP_30MS_Pm	70	30 - macadamia shells (MS)
CP_30CG_Pm	70	30 - coffee grounds (CG)

For all the compression moulded composites the polymer is solubilized in 50 mL of chloroform (Sigma-Aldrich) with the filler/fibres (when required). The solution is solvent casting in glass petri dishes (Figure 6.6.1) to promote the filmation process and, successively, the film is cut in pieces for the compression moulding process.

Figure 6.6.1 Filmation process of the three solution of PHA + filler: (from the right to the left) PHA +WF; PHA + MS; PHA +CG.

10 g of cut film was placed in the mould (Figure 6.6.2) and the Rondol Technology press (Figure 6.6.3) was closed applying 30kN at 200°C for 15 minutes.

Two metallic supports were necessary to increase the thickness of the mould because a space between the two heated platens of the hydraulic press was remained.

(a)   (b)

(c)   (d)

Figure 6.6.1 Preparation of the cut film in the mould for the compression moulding process: a)
100% PHA (CP_Pm); b) 70%PHA +30% WF (CP_30WF_Pm); c) 70%PHA +30% MS
(CP_30MS_Pm);d) 70%PHA +30% CG (CP_30CG_Pm).

(a)   (b)
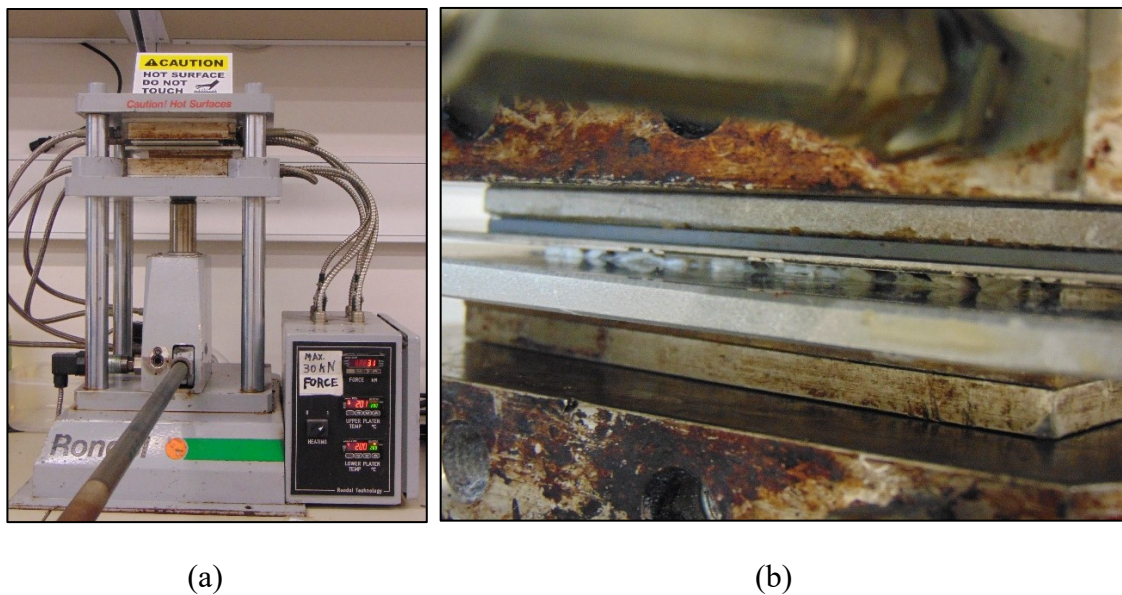
Figure 6.6.2 a) hydraulic press for compression moulding; b) Detail of the hydraulic press:
heated plates with the mould and the metallic supports. In the middle it is possible to see the cut
polymer film before the melting process.

Before to open the press, the specimen should be cooled down slowly, to avoid imperfection and cracks[88] and then removed from the mould (Figure 6.6.4).
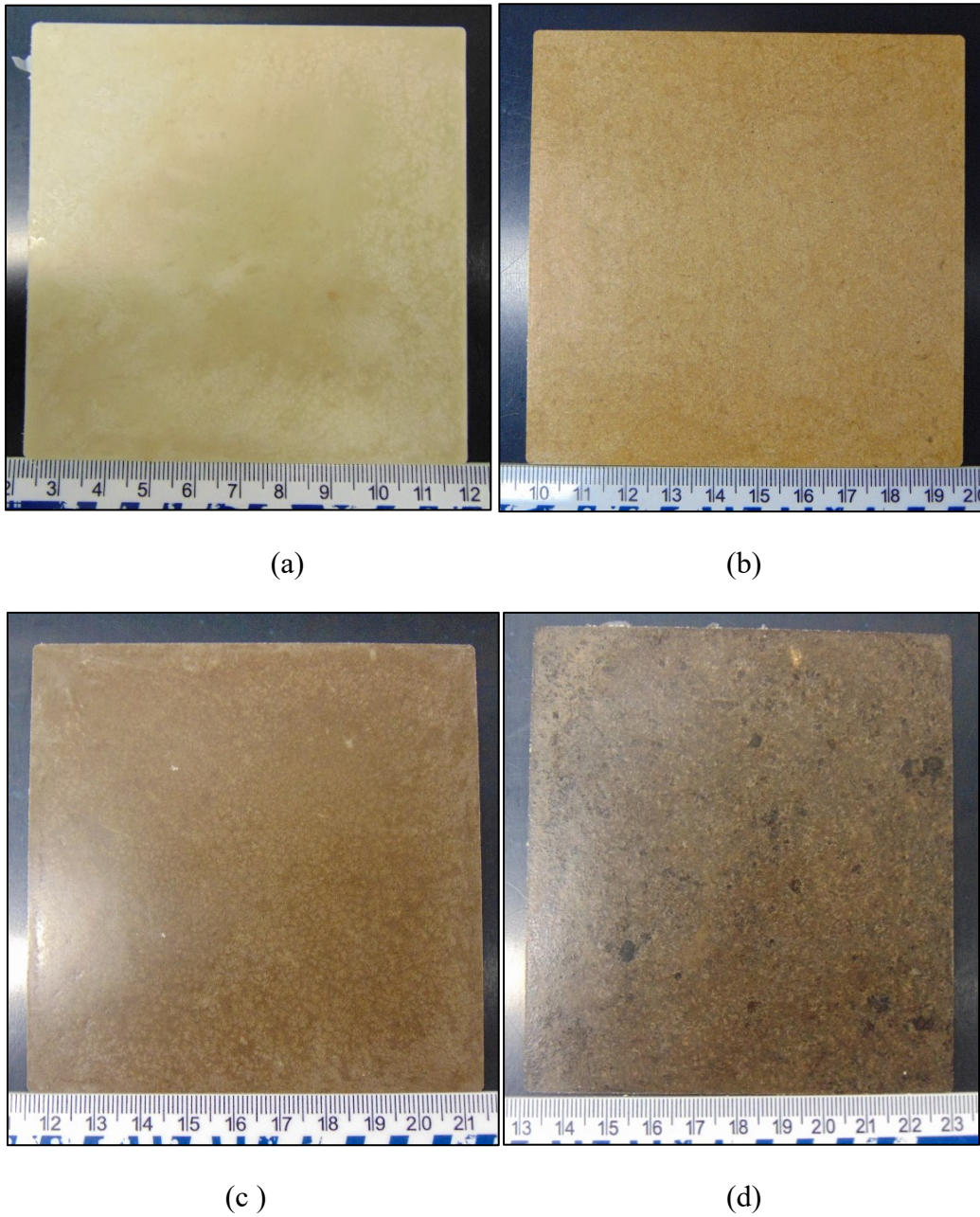
Figure 6.6.3 a)CP_Pm; b) CP_30WF_Pm; c) CP_30MS_Pm and d) CP_30CG_Pm specimens.

6.6.2   **Extrusion**

Processing of the extruded specimens is achieved by feeding the polymer powder directly into the extruder. For composite specimens, the filler and PHA powder are pre-mixed

(without the solvent) according to ratios listed in Table 6.6-2, which are in the same percentages of compression moulded specimens.

Table 6.6-2 Formulations of extruded specimens

Name of the sample	Polymer (%)	Filler (%)
CP_Ex	100	-
CP_30WF_Ex	70	30 - wood flour
CP_30MS_Ex	70	30 – macadamia shells
CP_30CG_Ex	70	30 – coffee grounds

A co-rotating twin screw extruder (EuroLab 16 XL, ThermoFisher Scientific Inc, Waltham, USA) with a diameter of 16mm and a length-to-diameter ratio of 40:1 is used (Figure 6.6.5). PHBV and Reinforced-PHBV blends are fed at flood feeding (full barrel). A volumetric feeding rate has been chosen for this work, to maintain a consistent occupied barrel volume across different fibre ratios. Between each extrusion run, the die element is removed and cleaned, the barrel is fully purged with PHBV polymer for 10 min, and the first 20 g of each run is discarded.

Figure 6.6.4 EuroLab16XL extruder

The feed screw elements in zones 2 to 6 ensured a clear feed throat and prevented jamming. The elevated temperatures in these zones caused higher melt flow (low viscosity).

Flood feeding and a decreasing temperature profile with a maximum barrel temperature of 180 °C and a die temperature of 160 °C are implemented. The screw profile consisted of forward conveying elements only with no mixing zones. The screw speed is maintained at 100 rpm which resulted in a residence time of around 1 min.

During extrusion, extrudates are cut and pressed through a roller to produce flat samples. All the extrusion details as temperatures (°C) and pression (bar) applied in the different zones are reported in Figure 6.6.6. Each extrusion run is exposed to an atmospheric vent in zone 5.
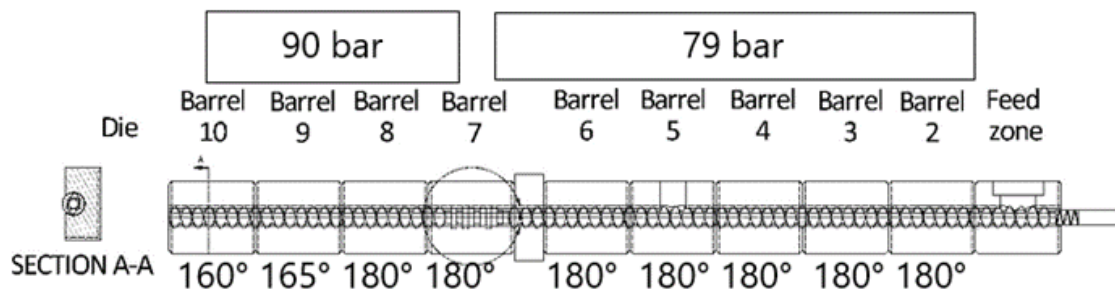
Figure 6.6.6 Extrusion profile of different zones with temperatures and pressure.

The last functional zone is where the shaping of the polymer takes place: the die forming zone is the most important functional zone because the actual shape of the final product develops in this zone. As exposed in Chapter 2, the geometry of the flow channel in the die, the flow properties of the polymer melt and the temperature distribution in the polymer melt are essential in this part of the process[92].

A slit die with cross sectional dimension of 13 by 2 mm is placed at the extruder exit to yield sections of rectangular specimens for mechanical testing (Figure 6.6.7).
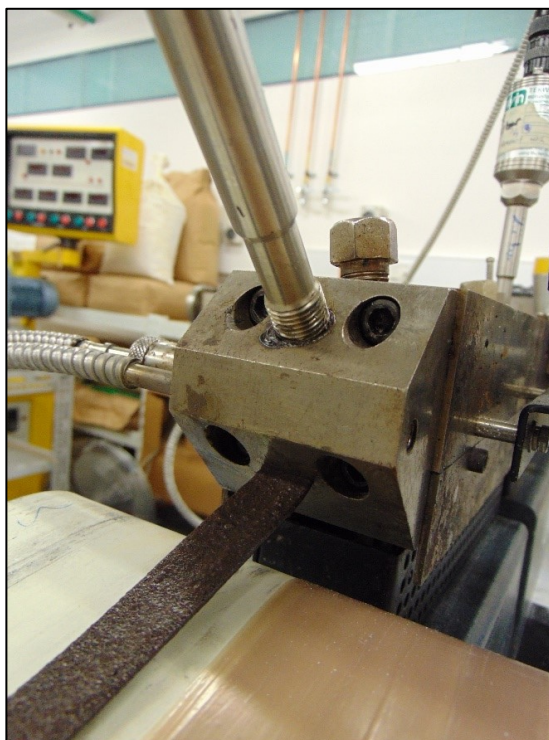
Figure 6.6.5 Slit die with cross sectional dimension of 13 by 2mm during the extrusion of CP_30CG_Ex

6.6.3 **Composite characterization**

6.6.3.1 *Gel permeation chromatography (GPC)*

Weight average molecular weight (Mw), number average molecular weight (Mn) and polydispersity index (PDI = Mw/Mn) are obtained using gel permeation chromatography (GPC)[355]. Specimens are dissolved in chloroform (HPLC grade) at room temperature for 30 minutes, with a concentration of 2.5 mg/mL. GPC analyses are performed using an Agilent 1260 Infinity Multi Detector Suite system (Cheshire, UK) equipped with a guard column followed by three columns in series. The columns are kept at 30°C. A refractometer, at 30°C, is equipped to detect the signals. A chloroform flow rate of 1 mL/min is used for the analysis. Narrowly distributed molecular weight polystyrene standards are used for calibration.

6.6.3.2 *Microstructural analysis*

After the tensile test, the microstructure of films is observed by using a Macroscopy (Wild Makroskop M420) at 10X and a Scanning Electron Microscope (SEM) (VEGA3 TESCAN) at 25.0 k.

6.6.3.3   *Tensile Test*

Prior to any characterisation, the samples are dried overnight at 35±5°C for 24 h to remove any absorbed moisture. Samples are cut in 5 dog-bone-shaped specimens (Figure 6.6.8) from each sample (compression moulded and extruded) and tested following ASTM D 638-5 for tensile test. All the tests are conducted using an electromechanical Instron model 5584 (Instron Pty Ltd, USA) with a 1 kN load cell. Specimens are clamped using pneumatic grips, and tested at constant cross-head displacement rate of 1 mm/min. A video-extensometer is used to obtain the strain value across the narrow region of the specimen. This contactless approach avoids any risk for introducing stress concentration and premature crack initiation and propagation. The reported values represent the mean of five replicate test specimens.
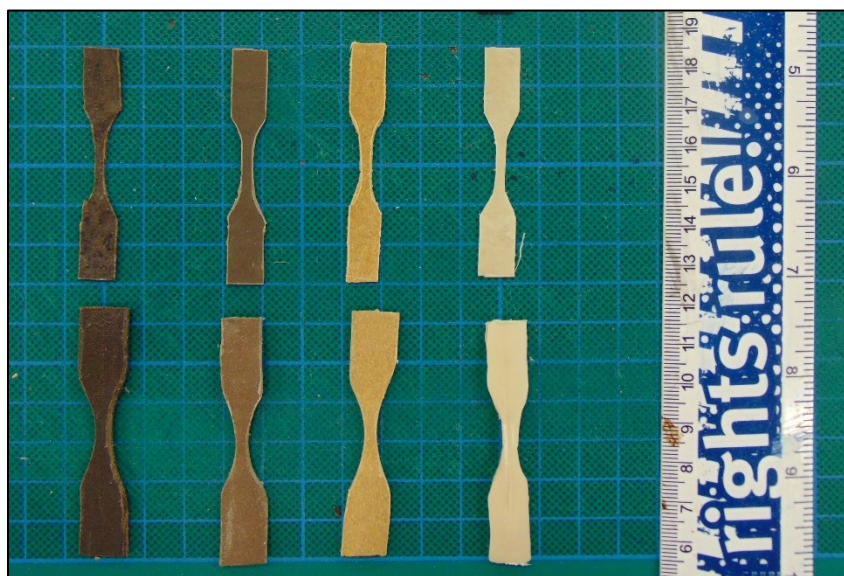
Figure 6.6.6 A specimen for each category is shown: in the top line (from the right to the left) CP_30CG_Pm; CP_30MS_Pm; CP_30WF_Pm; CP_Pm. In the bottom line (from the right to the left) CP_30CG_Ex; CP_30MS_Ex; CP_30WF_Ex; CP_Ex.

6.6.3.4   *Differential Scanning Calorimetry (DSC)*

DSC experiments are performed using a DSC instrument (DSC Q2000, TA Instruments) in order to determine the melting point (Tm) of the PHA-composites. About 2 mg of sample is heated to 185 °C at a heating rate of 20 °C min^{-1}, and subsequently cooled from 185 °C to –50 °C at a cooling rate of 10 °C min^{-1}, and then reheated to 185 °C at 10 °C min^{-1} heating rate under nitrogen gas.

6.6.3.5   *Thermogravimetric Analysis (TGA)*

TGA experiments are performed using a TGA instrument (Mettler Toledo TGA/SDTA 851) following the norm UNI EN ISO 1111358-1:2014 in order to determine the decomposition temperatures (Td) of the composites. About 5 mg of sample is heated from room temperature to 550 °C at a heating rate of 10 °C min^{-1} in air.

6.7   **Results and discussions**

Tensile strength, modulus and strain at break of extruded and compressed PHA-composites and PHA with 30% of filler content are measured (Figure 6.7.1, Figure 6.7.2 and Figure 6.7.3). Data are presented as box plots indicating the maximum, 3rd quartile, median, 1st quartile and minimum value among ten duplicates. The mean values are noted in text to the right of each box plot. From these data the influence of the fillers and the two techniques on the mechanical performances can be estimated.

All the extruded composites are more resistant to the tensile stress than the compression moulded series. Confronting the two references made with 100% of PHA (CP_Pm and CP_Ex) the main difference in the performance is in the stress at maximum load (4 MPa), whereas the tensile modulus (Figure 6.7.2) is comparable with average values equal to 3 GPa for CP_Ex and 2 GPa for CP_Pm. A totally opposite behaviour can be observed by the elongation at break, where elongation is almost 9% for the CP_Pm and only 2.1% for CP_Ex. Low values in tensile strain at break are expected for composites with PHBV and a low HV content (~1 mol%) as polymer matrix, since it is brittle under the processing conditions used without additional modifiers[356,357].
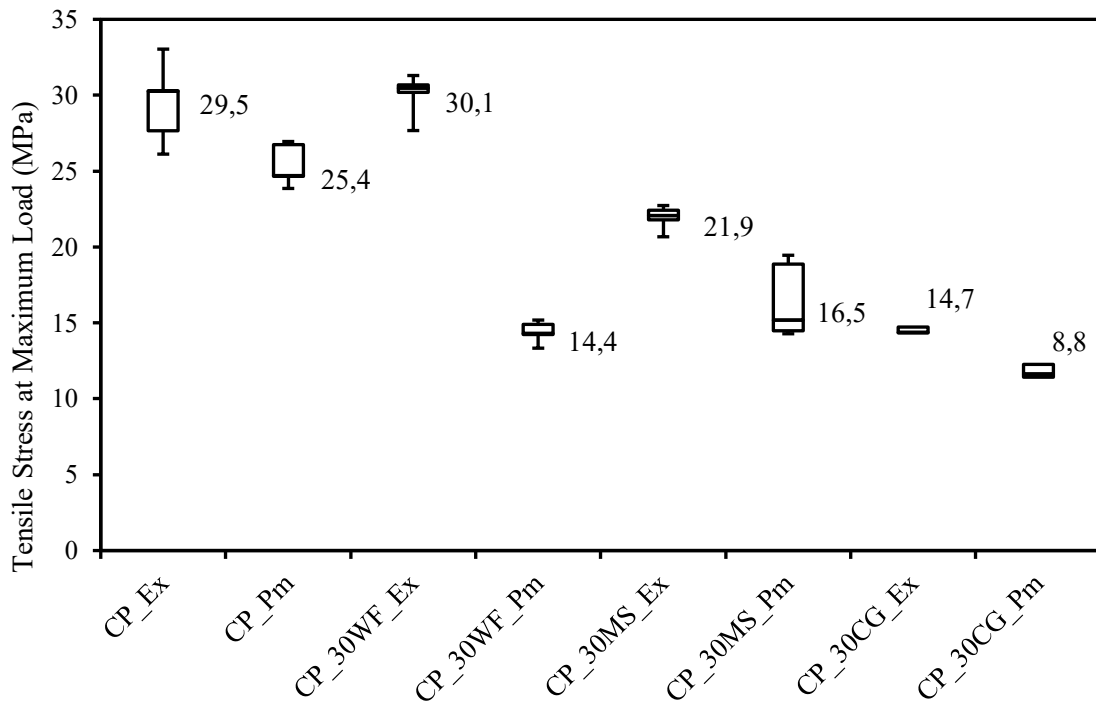
Figure 6.7.1 Tensile stress at maximum load
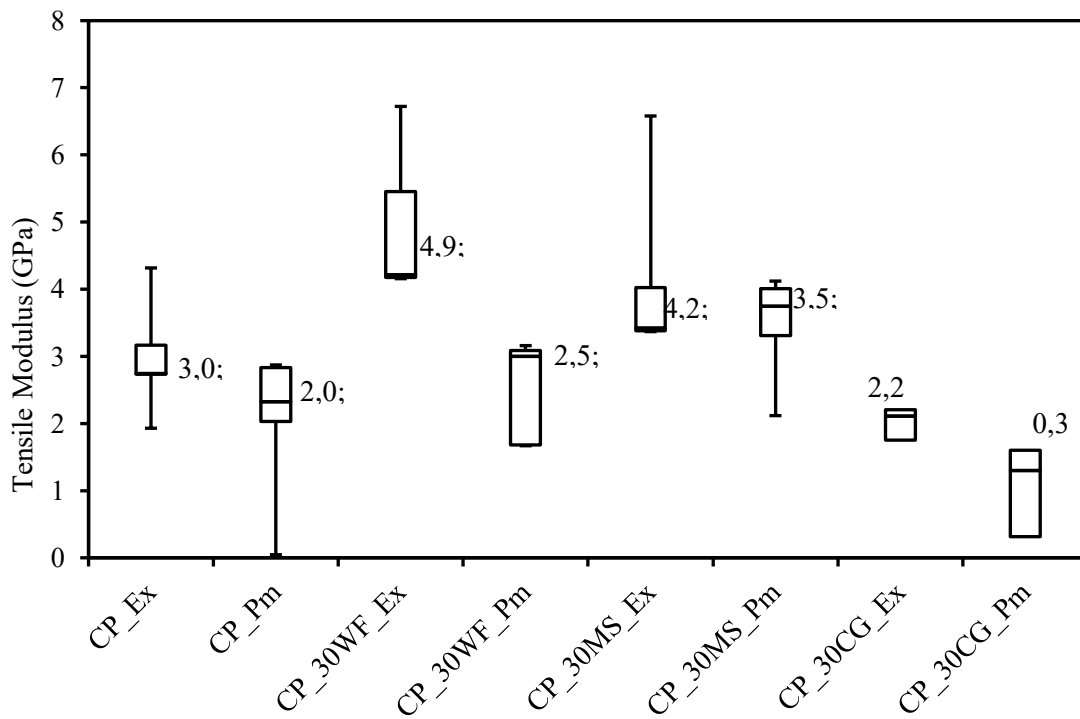
Figure 6.7.2 Tensile Modulus
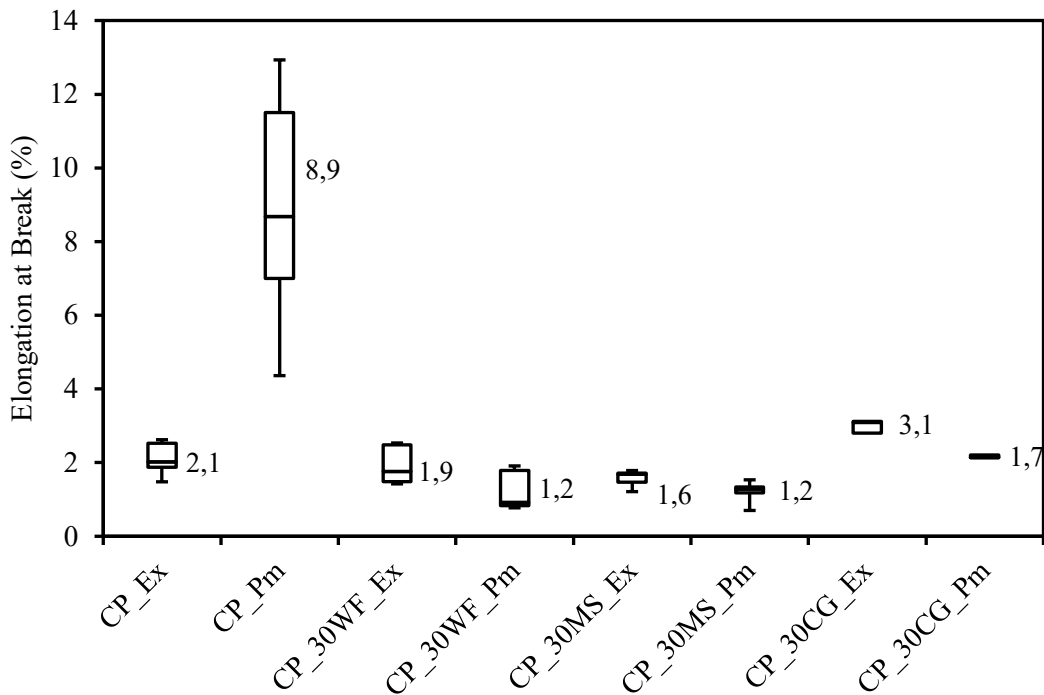
Figure 6.7.3 Elongation at break

The mean tensile strength decreased with increasing temperature profile: in fact, in the extruded samples, where the temperature is lower and more controlled, tensile strength (σ_M) is in a range between 30.1 MPa and 14.7 MPa. Possible reasons could include thermal degradation of the matrix (or the reinforcing materials) or a change in melt viscosity of the polymer which has influenced the mechanical properties. Further investigations into the molecular weight changes are summarised in Table 6.7-1.

Examining the obtained values from GPC analysis and the Mn on the datasheet of ENMAT Y1000, where the original value of Mn is 590 kDa, it is evident that the two process caused a degradation of the polymer, reducing the molecular weight. Moreover, comparing the two processes, all the compression moulded composites have a lower molecular weight (Mn and Mw) than the extruded series, which indicates a major degradation during the polymer processing, probably caused by the high temperature.

In fact, the temperature profile and the pressure conditions in the extrusion process are much more controlled than in the compression moulding, where the temperatures reach 200°C at 30 kN. These more extreme conditions, even if for a short time, are determinant for the reduction in the Mn, which causes losses in the mechanical performances[302,355,92,93].

PDI means polydispersity index and this refers to the ratio between the average molecular weight (Mw) and the average number (Mn) called as molecular weight distribution. PDI

is used to indicate distribution of polymer chain molecular weights in a given polymer[81]. As the PDI value increases the heterogeneity in cross-linking, network formation, chain length, branching, hyper branching will be with more random arrangement. In this case, the PDI value varies from 1.8 (CP_30MS_Pm) to 2.6 CP_30CG_Ex, showing a different heterogeneity between the specimens. More precisely, in all the extruded composites the values of PDI are higher. Both specimens including the WF in their formulation have similar values of PDI (2.0 for CP_30WF_Pm and 2.3 for CP_30WF_Ex), whereas in all the other samples the difference between the two series are more relevant. This particular factor implies that the level of polymer growth is not in a controlled manner and oligomers concentrations are more, but this happens in both of the specimens, giving similar results[81,83].

In the other specimens, as CP_30MS_Pm and CP_30MS_Ex, this behaviour is not comparable at all, because there are wide differences between the two series: thus the measured dispersity demonstrates a more inconsistent size, shape and mass distribution of the molecules in the series with higher values (extruded composites)[81].

Table 6.7-1 GPC analysis of PHA-composites.

Specimen	Mn (g/mol)	Mw (g/mol)	PDI
CP_Pm	77381	144155	1,9
CP_30WF_Pm	74942	150827	2,0
CP_30MS_Pm	62708	113013	1,8
CP_30CG_Pm	91179	176206	1,9
CP_Ex	155413	383718	2,5
CP_30WF_Ex	153031	344830	2,3
CP_30MS_Ex	141144	333268	2,4
CP_30CG_Ex	156625	405135	2,6

The mean tensile strength decreases increasing the fibres/filler content in almost all the samples, the only exception is CP_30WF_Ex. This reduction is in agreement with the trends reported in literature for reinforced composites[247,335,343,358,359,328–330,340,341,360–363], and can be explained by the concentration of stress around short fibres/fillers, which acts as defects and initiates crack propagation. For what concerns CP_30WF_Ex, the increase in σ_M from 29.5 MPa to 30.1 MPa is not very significant. Nevertheless, the behaviour of CP_30MS_Pm is particularly interesting: even if the 30% of macadamia nut shell fibres

addition causes the reduction of the tensile strength to 21.9 MPa, the difference between CP_30MS_Pm and CP_Pm is about 3 MPa.

The tensile modulus increased with increasing wood fibre ratio, as can be expected and is typically observed from the addition of a reinforcement material with higher stiffness than the matrix[87,94,333,337,339,364–367]. The main reason for the modulus variability of wood fibres is the difference between earlywood and latewood fibres, affecting cell wall thickness, fibril angle and secondary fibre wall[355]. So, the differences between the specimens with the same amount of fillers are so evident because of the differences in the fibre's composition, which is due to their origin. Composites with macadamia shells give comparable results in terms of tensile modulus for both of the series (4.2 GPa for extrusion and 3.5 GPa for the compression moulding), but the best result comes from CP_30WF_Ex (4.9 GPa).

In terms of elongation at break, almost all the results are comparable, only two of them stand out from the others: CP_Pm (8.9%) and CP_30CG_Ex (3.1%).

For CP_Pm the major elongation can be due to the thermal exposure: thermal exposure of PHBV during extrusion process, and consequently melt viscosity and crystallisation, are suggested to have a stronger influence on the intrinsic mechanisms which affect tensile strength, over the mechanisms affecting stiffness. A study in literature[368] reported that the tensile strength of PHBV is influenced by the morphology of the semi-crystalline structure. A higher temperature of the melt as well as lower molar mass of the polymer lead to a lower number of intrinsic nuclei for crystallisation and hence to a lower number of spherulites with greater diameter. As reported in literature[369], cracks are formed at the boundaries of the spherulites in PHBV when the diameter reaches a critical value. Moreover, also the presence of fibres can affect the performance due to their tendency to agglomerate in the mix, which cause inhomogeneous part in the matrix.

Previous studies in extruded composites found out that there are interactions between fibres content and the feeding rate, since the large variance generated by different wood content is minimised at higher feeding rates[355]. Short-fibre composites are heterogeneous materials, and tend to fail at the weakest cross-section, where the presence of microstructural heterogeneity or defects control the tensile strength. It was reported that for wood plastic composites, unwanted fibre agglomerates are likely to initiate tensile failure, as happened for all the composites including the fibres.

The fibre-matrix interface is a reaction or diffusion zone in which two phases or components are physically, mechanically and/or chemically combined. Interfacial adhesion between the fibre and matrix plays a fundamental role in terms of the factors governing the mechanical characteristics of the composite[324].

The higher elongation performance in CP_30CG_Ex can be explained by the type of filler: in fact, coffee grounds have a very different shape and size from the fibres, and this causes a different interaction with the polymer matrix respect to the composites with fibres.

Spent coffee grounds are highly hydrophilic and this leads to formation of aggregates as happens with the fibres; although individual particle size is fundamental to enhance the mechanical performances. The characteristics of the particles largely control the property of the alloy, and a spacing of 0.2–0.3 μm between particles usually helps optimize properties[348,349,351,353]. As particle size increases, less material is required to achieve the desired interparticle spacing[353]. Due to their particle shape and size, CGs do not permit to have a bridging effect as for the fibres reinforcing composites, in fact they act as a crack propagation and voids generation agent (Figure 6.7.4 and Figure 6.7.5). Nevertheless, it can have a positive effect on the elongation properties because the CG-clumps are smaller than fibres-clumps.
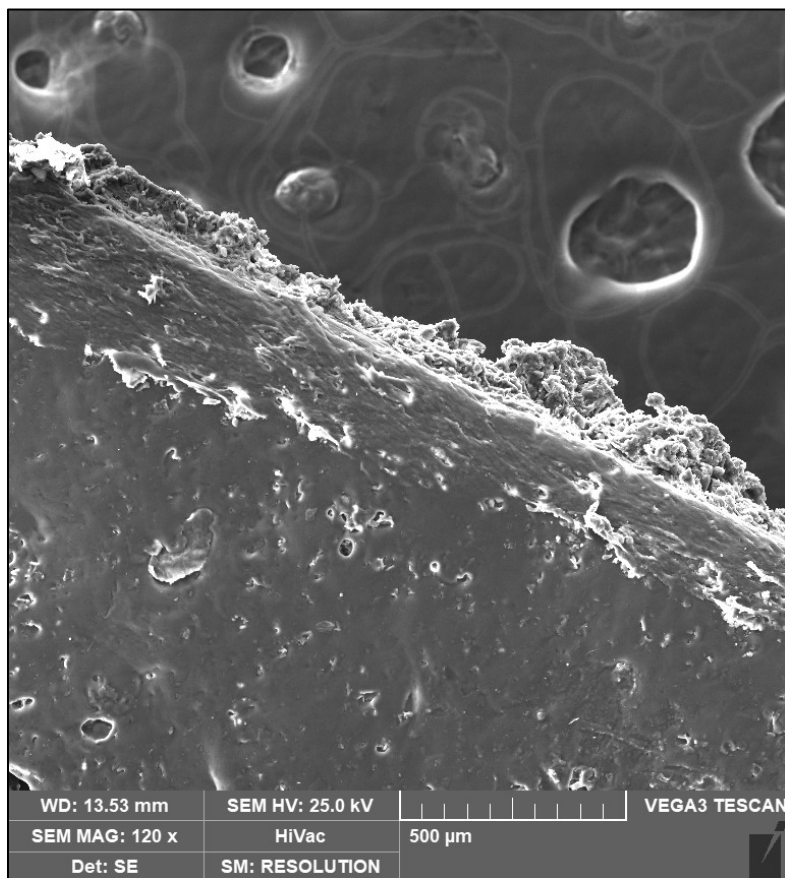
Figure 6.7.4 CP_30CG_Ex cut section: voids on the surface.
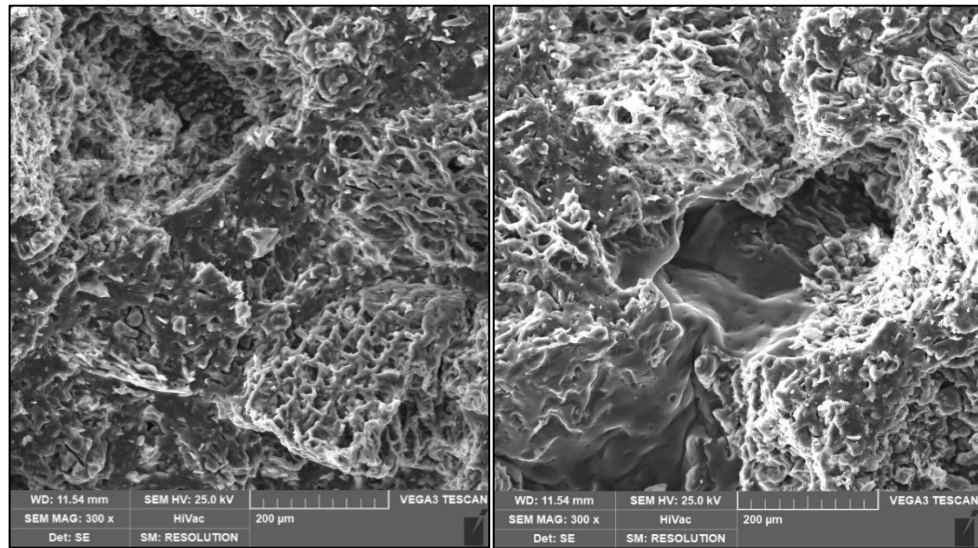
(a)   (b)

Figure 6.7.5 CP_30CG_Ex cross-sectional area and void structure.

As reported in the SEM images (Figure 6.7.6a) the interaction between the two phases is not homogeneous for the specimens of CP_30CG_Ex. Also in the other series (CP_30CG_Pm) the two phases have the same behaviour, but with the presence of more and larger voids (Figure 6.7.6b).
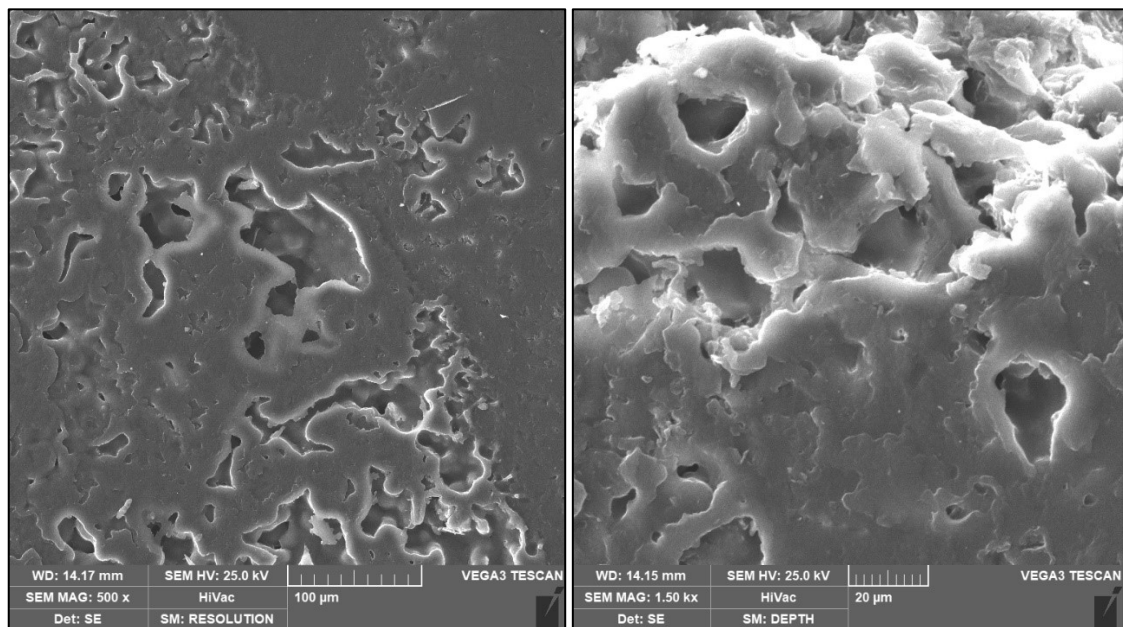
(a)   (b)

Figure 6.7.6 (a) Surface of CP_30CG_Pm and (b) voids structure

Analysing the morphology of the composites, the interfacial transition zone (ITZ) of the fibre reinforced composites in the cross sectional area (Figure 6.7.7, Figure 6.7.8, Figure 6.7.9) permits to evaluate the interaction between the two phases.
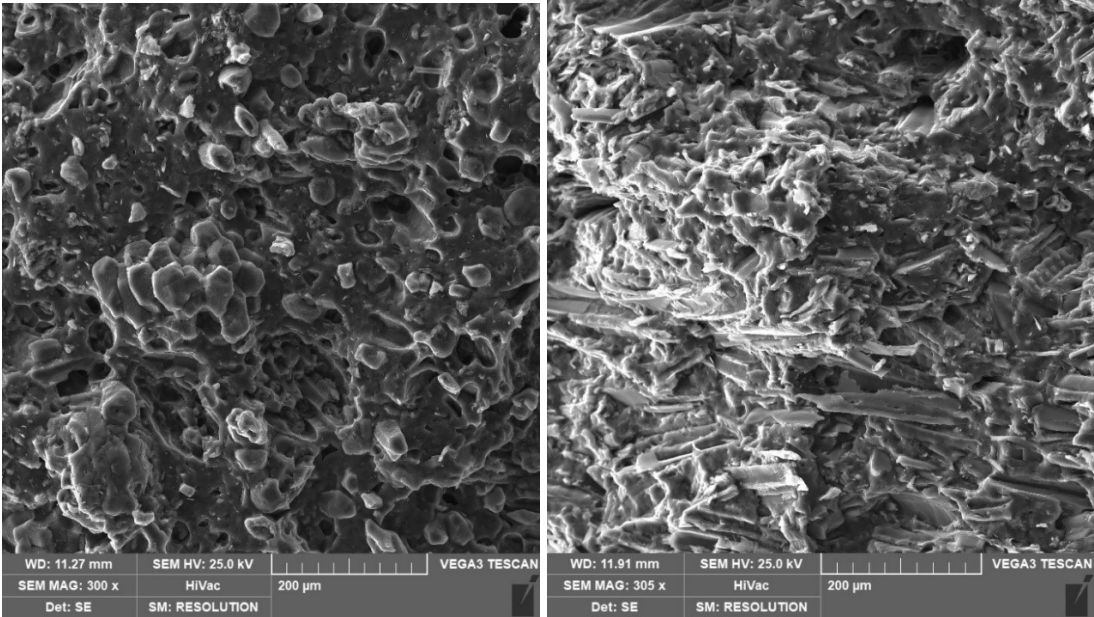
(a)   (b)

Figure 6.7.7 a) CP_30MS_Ex and b) CP_30WF_Ex
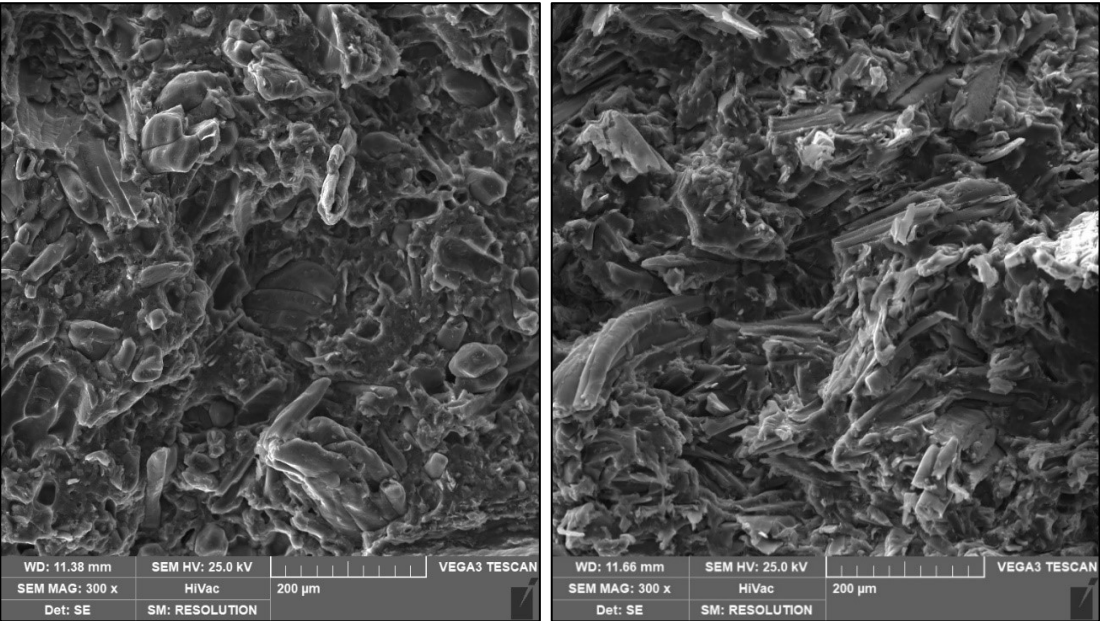
(a)   (b)

Figure 6.7.8 a) CP_30MS_Pm and b)CP_30WF_Pm

On the contrary, for the compression moulded composites, CP_30WF_Pm shows very long part of the fibres coming out from the matrix in the cross sectional area which means that the interaction between the two phases is better thanks to the adherence between the fibre and the polymer. This means that the bridging effect is predominant in this specimen and that the low performances are due to the presence of voids caused by fibre separation. Fibre separation or fibre segregation takes place when the fibre does not migrate with the polymer flow in the mould. As a consequence, the fibre content becomes non-uniform leading to a higher than nominal fibre content in the upstream and a lower than nominal fibre content in the downstream[93].

In Figure 6.7.9 ,Figure 6.7.10, Figure 6.7.11 and Figure 6.7.12 the surfaces of all the specimens are shown in order to compare the morphological differences of the two series.
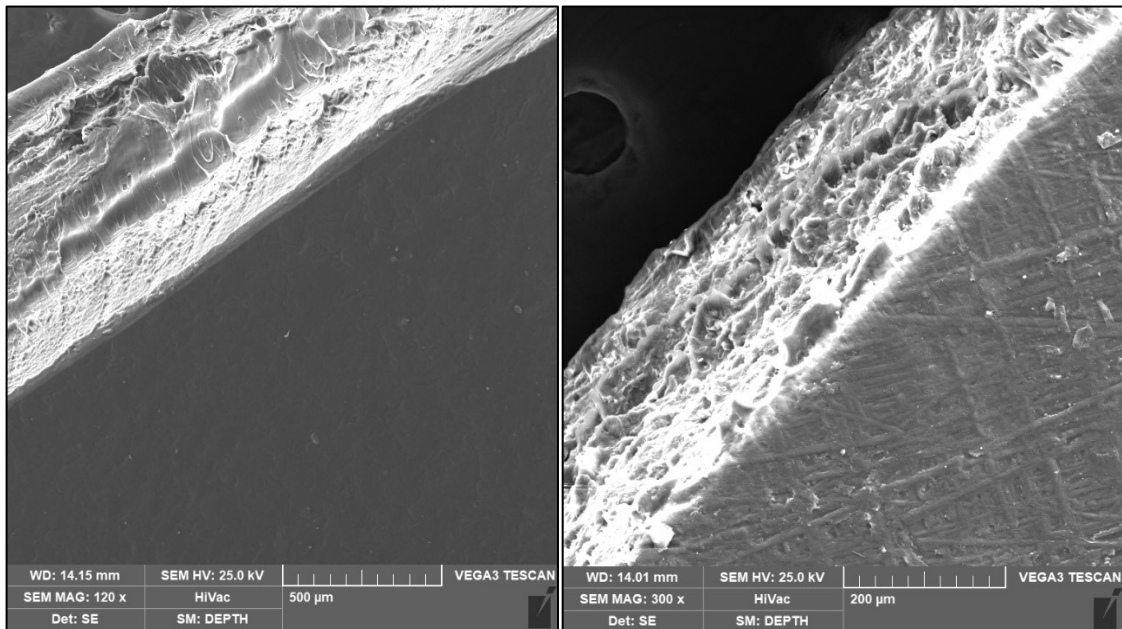
(a)   (b)

Figure 6.7.9 a) CP_Ex; b) CP_Pm
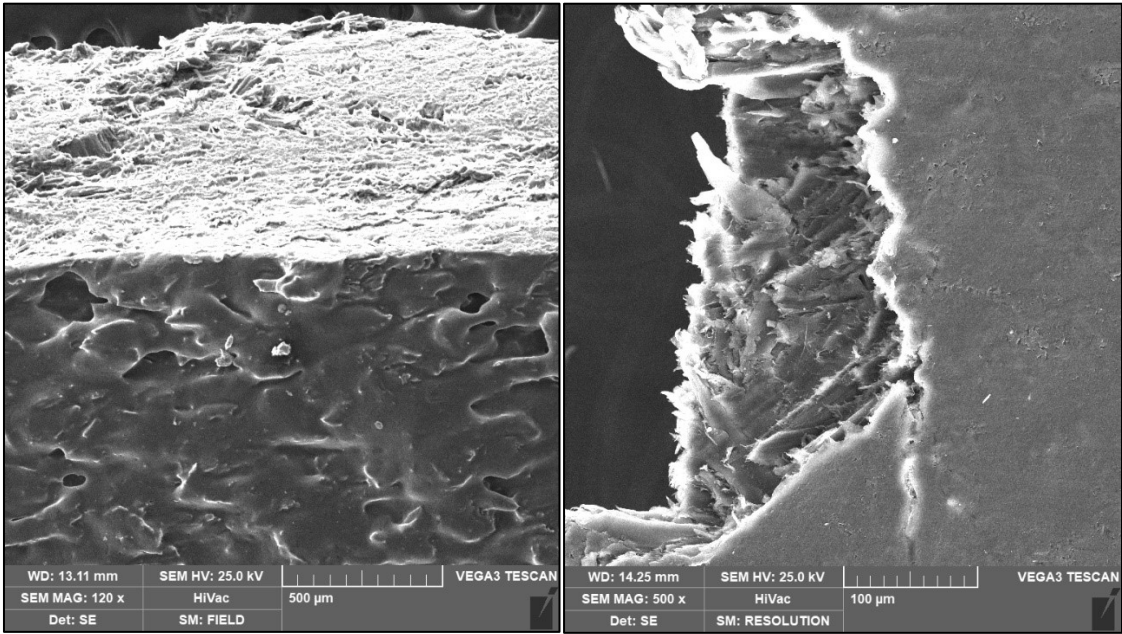
(a)   (b)

Figure 6.7.10 a) CP_30WF_Ex b) CP_30WF_Pm
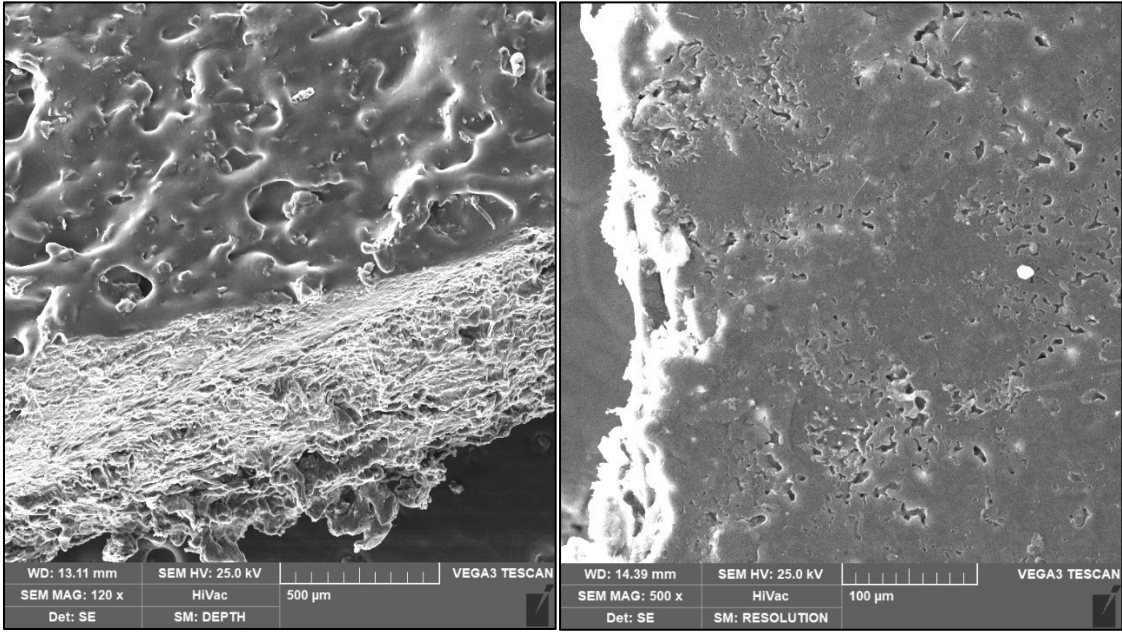
(a)   (b)

Figure 6.7.11 a) CP_30MS_Ex b) CP_30MS_Pm
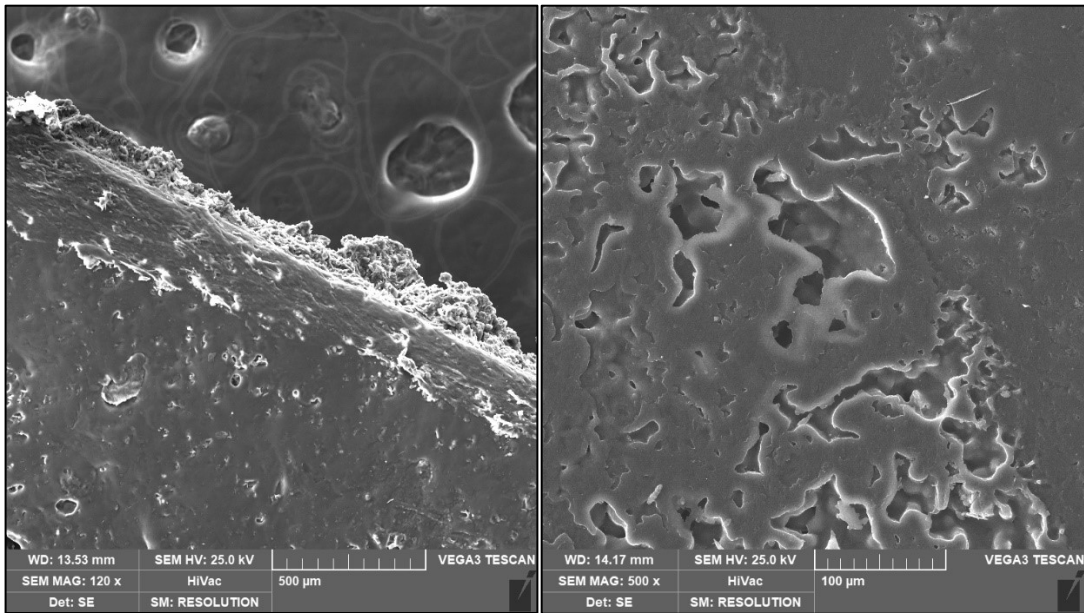
(a)   (b)

Figure 6.7.12 a) CP_30CG_Ex b) CP_30CG_Pm

Comparing the different samples all the defects coming from the processes are evident: in Figure 6.7.9, CP_Ex and CP_Pm have two different surfaces, but both of them are homogeneous.

CP_Ex present a very regular and smooth surface, whereas CP_Pm presents a wrinkly surface due to the polymer processing. The defects in CP_Pm are typical of a process with high temperature and high pressure and usually they can be avoided gently increasing the high pressure. For the production of the other samples this principle was considered, in fact the surface (Figure 6.7.10) does not appear wrinkled anymore, but it is smooth even with the presence of voids. The presence of voids is caused by more factors: the principal one is the possible segregation of the fibres (WF and MS) and the presence of the filler (CG), but also high temperature, high pressure and a not homogeneous disposition of the cut polymer on the mould can be the causes[88,93,298,370].

It is well known that the existence of interactions between the substrate (as the aluminium mould) and the polymer can strongly affect the physical properties of the polymer, such as the Tg and the molecular chain mobility, which in turn influence the crystallization kinetics of the polymer. The influence of a foreign surface on the crystallization kinetics of polymers is multifarious, depending on the sample thickness and the used polymer/substrate system, which determines the interaction between the substrate and the polymer melt[371]. Due to the enhanced nucleation ability caused by the presence of a

heterogeneous surface, the overall crystallization rate will be increased remarkably, especially for those with difficulty in homogeneous nucleation. The enhanced nucleation abilities of polymers on a foreign surface are best revealed by the formation of trans-crystalline layers in the fibre-reinforced polymer systems[87,88,93,371–374].

Considering that polymeric materials are directly in contact with some kinds of solid surfaces in a variety of applications, surface-induced crystallization of polymers has attracted considerable attention during the past decades. It has been shown that solid surfaces most generally accelerate the crystallization of the polymers, being the cause of possible defects as porosity, flowlines or blistering. If there are defects also on the surface of the mould they can be transmitted to the composite, having an impact on its performance[88,93,298,370].

In extrusion, certain die flow instabilities can occur that may seriously affect the entire extrusion process, damaging the product. All the extruded composites including the filler\fibres present a very rough surface known as shark skin effect.

Shark skin manifests itself as a regular ridged surface distortion, with the ridges running perpendicular to the extrusion direction. A less severe form of shark skin is the occurrence of matness of the surface, where the glossy surface cannot be maintained. This effect is generally formed in the die land or at the exit, and it is dependent primarily on the temperature and the linear extrusion speed. Factors such as shear rates, die dimensions, approach angle, surface roughness, L / D ratio, and material of construction seem to have little or no effect on shark skin. The mechanism of shark skin can be caused by the rapid acceleration of the surface layers of the extrudate when the polymer leaves the die: if the stretching rate is too high, the surface layer of the polymer can actually fail and form the characteristic ridges of the shark skin surface. High-viscosity polymers with narrow molecular weight distribution (MWD) seem to be most susceptible to shark skin instability. The shark skin problem can generally be reduced by reducing the extrusion velocity and increasing the die temperature, particularly at the land section or using an additive[92,375].

The set parameters used during the process for the composite production affect not only the morphological aspect of the composite, but also its thermal properties.

In Table 6.7-2 all the results from DSC and TGA analysis are reported.

Table 6.7-2 TGA and DSC results

PHA Sample	Tg [°C]	Tc [°C]	Tm [°C]	Xc [%]	Td [°C]	T1 [°C]	Endo-Peaks [°C]	Exo-Peaks [°C]
CP_Pm	3	123	175	7.6	275	298	177	291
								306
CP_30WF_Pm	4	120	172	1	272	287	181	277
						327		283
						421		296
								334
								456
CP_30MS_Pm	-0.5	120	170	2.7	273	292	175	285
						322		300
						450		323
								453
CP_30CG_Pm	-3	114	172	5.2	265	170	175	268
						275		271
						426		284
						495		322
								431
								499
CP_Ex	0	123	174	3.5	279	297	179	288
								295
								307
CP_30WF_Ex	-3	120	173	3.4	272	172	178	275
						288		281
						320		301
						427		326
								430
CP_30MS_Ex	-3	120	174	3.4	275	172	177	283
						291		286

						324		299
						461		328
								464
CP_30CG_Ex	-1	114	172	3.0	264	170	176	328
						272		431
						426		502
						499		

Form the DSC analysis the crystallization temperature (Tc) and melting temperature (Tm) are taken at the maximum peak of the exotherm (downward in the TGA figures) and endotherm (upward in the Figure 6.7.13, Figure 6.7.14, Figure 6.7.15, Figure 6.7.16, Figure 6.7.17, Figure 6.7.18, Figure 6.7.19 and Figure 6.7.20) transition phase, respectively. The Tg is taken at the mid-point of the specific heat increment. The crystallization and melting enthalpies (UNI EN ISO 11357-3), ΔHc and ΔHm respectively, are obtained by measuring the area of the corresponding peaks in order to calculate the corresponding crystallization degree is by the Equation 10 of the previous Chapter. As previously exposed, Xc(%) is the percentage crystallinity; ΔHm is the measured melting enthalpy (J/g); and the $\Delta H100\%m$ is the melting enthalpy for fully crystalline PHB (146 J/g)[292].

The Xc (%) has a value of $3 \pm 0.5\%$ in all the extruded composites, because the processing conditions are stable. Indeed, in the composite made through compression moulding, where pressure and temperature are more difficult to maintain at the same conditions for all the specimens, the Xc (%) varies from 1% up to almost 8%. This can be due to the nucleation process on the surface of the mould and for the cooling down process after the heating. In fact, the cooling process takes long time for each specimen (about 1 hour), this means that the heating can not be totally controlled, because the heated plates of the hydraulic press needs time before to reach the room temperature, thus they continue to give heat to the mould (and to the polymer).

Moreover, this aspect influences also the Tg: the controlled pressure during the extrusion permits to obtain similar values of Tg for all the extruded composites (from -1°C for CP_30CG_Ex up to -3°C for CP_30MS_Ex and CP_30WF_Ex); whereas all the compressed composites reach higher values (from -0.5°C for CP_30MS_Pm up to 4°C CP_30WF_Pm). The higher value of Tg can be caused by different factors: a lower crystallinity degree; the presence of pressure (in compression moulding the pressure is much higher than in the extruder); molecular rigidity and a major degree of cross-linking. In this case, compressed moulded composites are subjected to high pressure at high

temperature, thus the high temperature can facilitate the degradation of the polymer reducing the Mw, while the high pressure can increase the Tg value[80].

The extruded composites present similar Tg and Xc in all the samples, which implies a similar cross-linking of the polymer with similar molecular weight (as reported from the GPC). The compression moulding process caused a high degradation of the polymer due to the more extreme conditions respect to the extruded series (as reported from GPC the Mn and Mw are about 80 kDa lower than the extruded series).

For what concerns the melting temperature Tm the differences are not so significant, in fact they vary from 170°C for CP_30MS_Pm up to 175°C for CP_Pm. This means that both techniques are suitable for the manufacturing process due to the Tm. Usually in this field polymers with low Tm are preferable to the others for the conditions of polymer processing. The crystallization temperature (Tc) is in a larger range of values: from 114°C for the composites including CG up to 123°C for both of the references made with 100% PHA. In this case, it is clear that there is a correlation between the formulation of the composite and the Tc: in fact, the two references have the same Tc at 123°C; all the samples containing fibres have the Tc at 120°C and the CG-composites have it at 114°C. This means that even if the process influences the crystallization (and the morphology) of the composites, also the materials used for the reinforcing effect is determinant. The two reference for extrusion and compression moulding have no filler in their formulation, for this reason a higher value of temperature can be expected. In the reinforced composites, the chemical composition of the fibres\filler may interact with the polymer, creating new cross-links and bonds with the polymer matrix. Thus, the composition of the reinforced material can be another important factor for the nucleation and crystallization of the composites Macadamia shells fibres and wood flour have a similar chemical composition and structure in terms of quantity of lignin, hemicellulose and cellulose; whereas the components of coffee grounds are different. Also CGs contain substances as cellulose, hemicellulose and lignin, but they have also ashes, lipids, fatty acids and polysaccharides, which may be the cause for the lower Tc.

TGA analysis (Figure 6.7.13, Figure 6.7.14, Figure 6.7.15, Figure 6.7.16, Figure 6.7.17, Figure 6.7.18, Figure 6.7.19 and Figure 6.7.20) permits to evaluate the degradation and decomposition temperatures of the different components of the composite, thus also the influence of each addition in the final product.

Analysing the two references is possible to estimate the thermal behaviour of PHA in the TGA and how the two manufacturing processes can influence the composite. In CP_Pm the Td is at 275°C, whereas in CP_Ex is at 279°C: this result is in line with what was previously mentioned because the compression moulding process caused a major degradation of the polymer reducing the Mw, therefore a lower value of Td was predictable. Nevertheless, the maximum thermal degradation temperature (T1) is higher

than CP_Ex (298°C and 297°C). The DTG (green line in Figure 6.7.13 and Figure 6.7.14) shows an endothermic peak corresponding to the fusion of the polymer at 177°C for the CP_Pm and at 179°C for CP_Ex. The exothermic peaks of the same images permit to understand the decomposition of the polymer: in CP_Pm the decomposition occurs in two stages at 291°C and at 306°C, with a final residue less than 2% of the total PHA weight at 1000°C.

For CP_Ex, the exothermic peaks occur in three stages: the decomposition onset temperature at 288°C, and the maximum at 295°C and 307°C; which are the typical values for PHA[376,377].
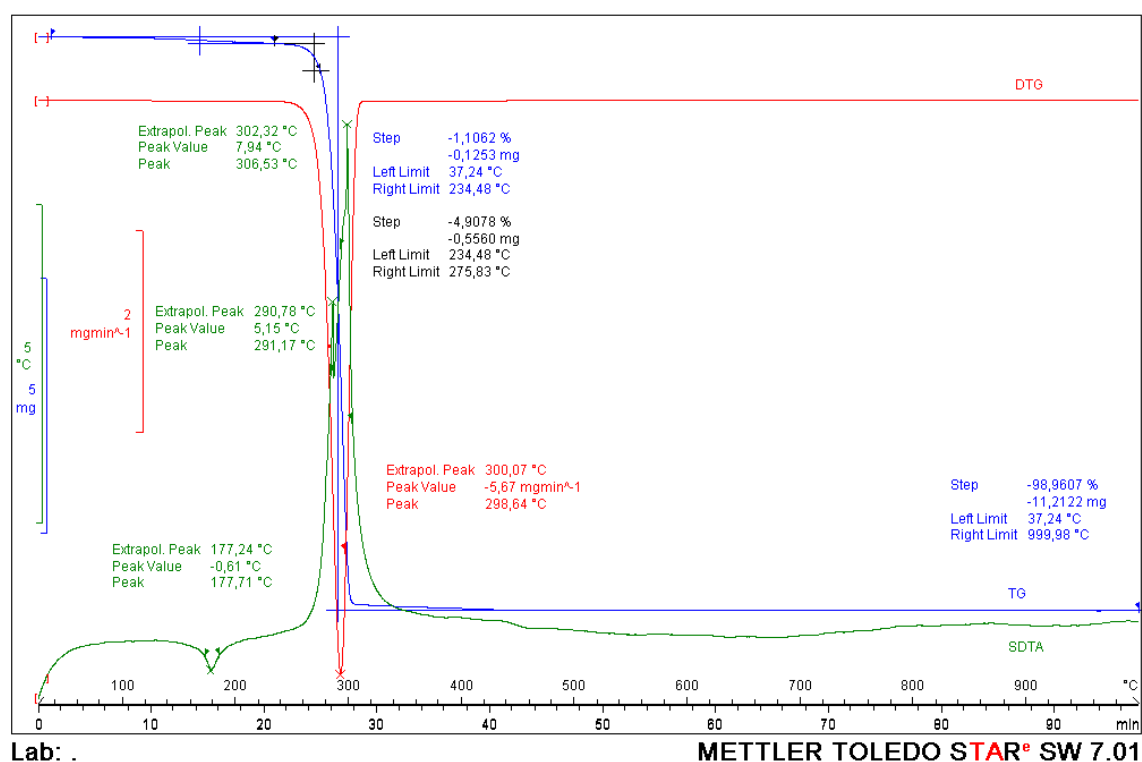
Figure 6.7.13 TGA of CP_Pm
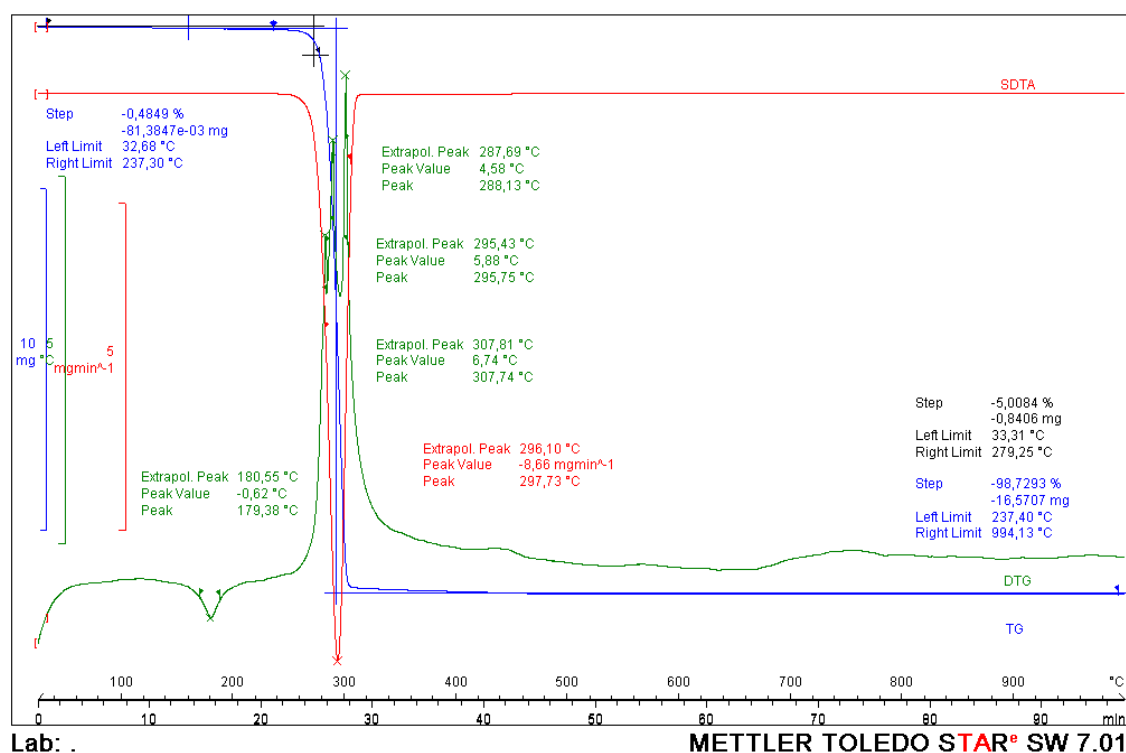
Figure 6.7.14 TGA of CP_Ex

The contribution due to the inclusion of fibers in the formulation can be seen in the TGA. In Figure 6.7.15, Figure 6.7.16, Figure 6.7.17 and Figure 6.7.18 the mass loss (%) occurs in more stages depending on the different components of the composite: during the first step of the process there is the loss of volatile compounds as moisture or residue of the solvent (1.7% for CP_30WF_Pm, 1.4% for CP_30WF_Pm, 2% for CP_30MS_Pm and 1.5% for CP_30MS_Ex). Successively the graph is characterized by two and three shoulders for WF and MS respectively) corresponding to the major mass loss: 74% and 13% for CP_30WF_Pm, 75% and 12% for CP_30WF_Ex, 78%, 10% and 10% for CP_30MS_Pm and, lastly, 81%, 8% and 6% for CP_30MS_Ex. The final stage of the analysis occurs at very extreme temperature (over 500°C up to 1000°C), which are generally inorganic residue or ashes with a mass loss $\leq$ 2% of the total weight of the PHA-composite.

The Td occurs at lower value compared to the 100% pure samples due to the presence of the fibres. In fact, the Td (Table 6.7-2) for CP_30WF_Pm, CP_30WF_Ex, CP_30MS_Pm and CP_30MS_Ex are at 272°C, 272°C 273°C and 275°C respectively.
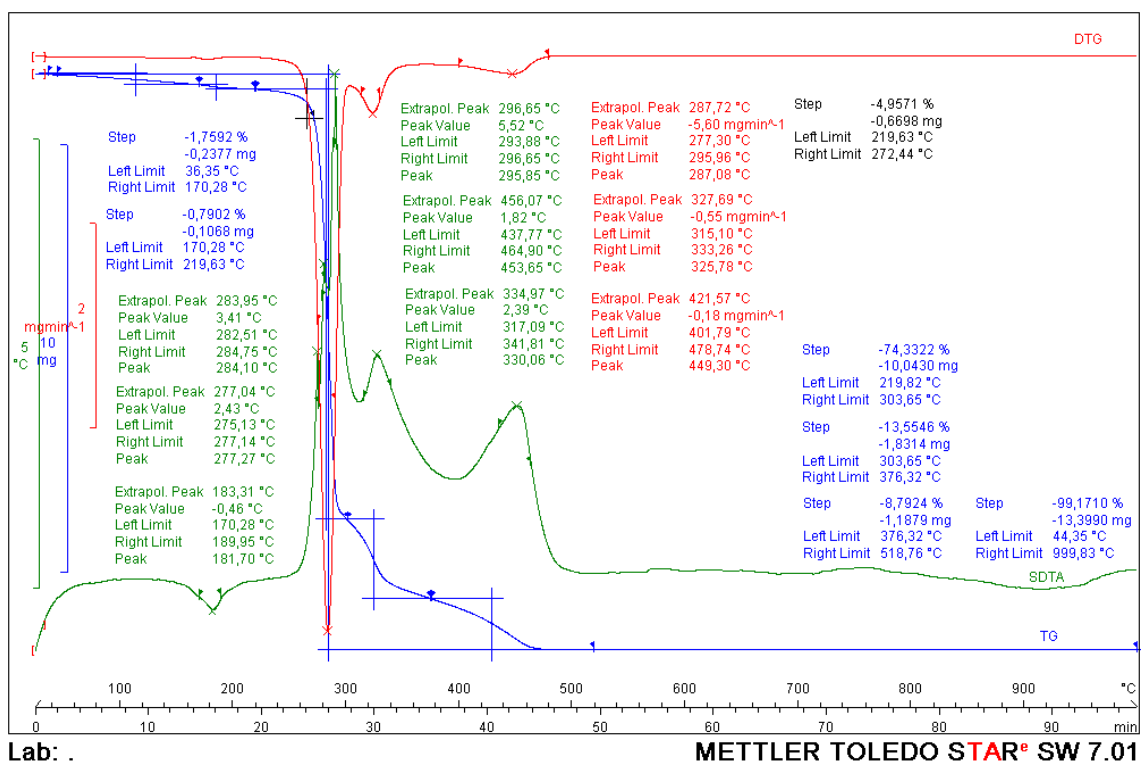
Figure 6.7.15 TGA of CP_30WF_Pm
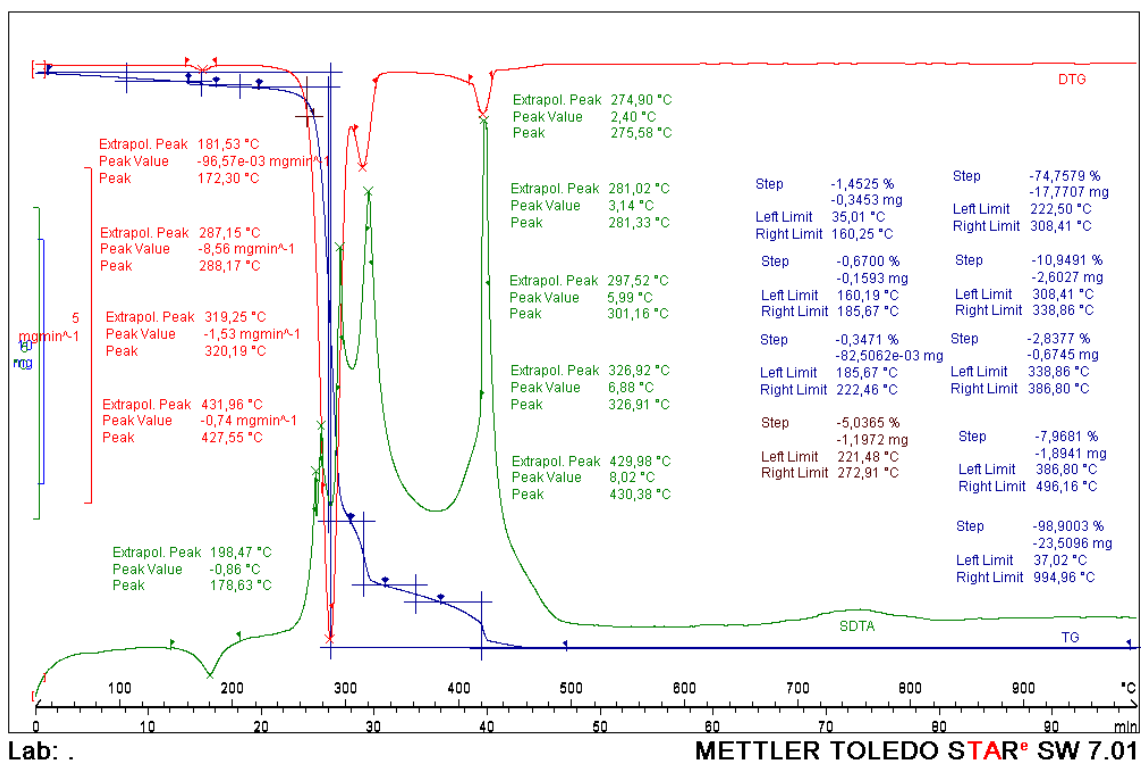
Figure 6.7.16 TGA of CP_30WF_Ex
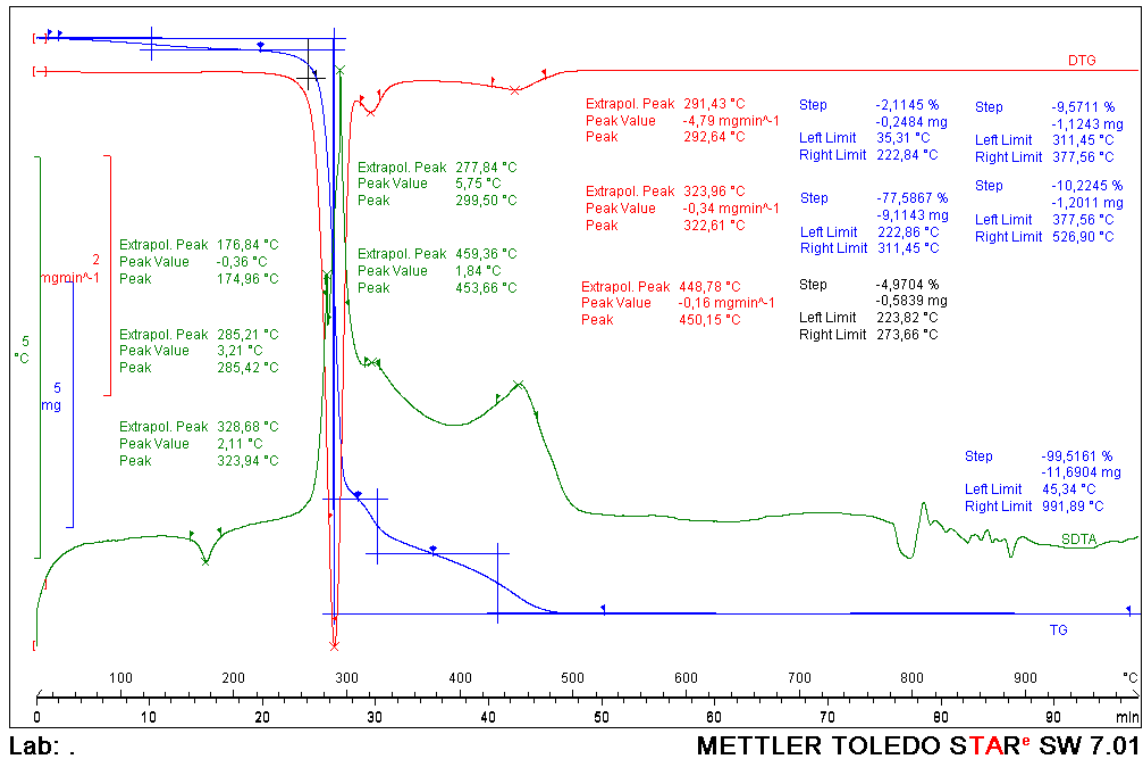
Figure 6.7.17 TGA of CP_30MS_Pm
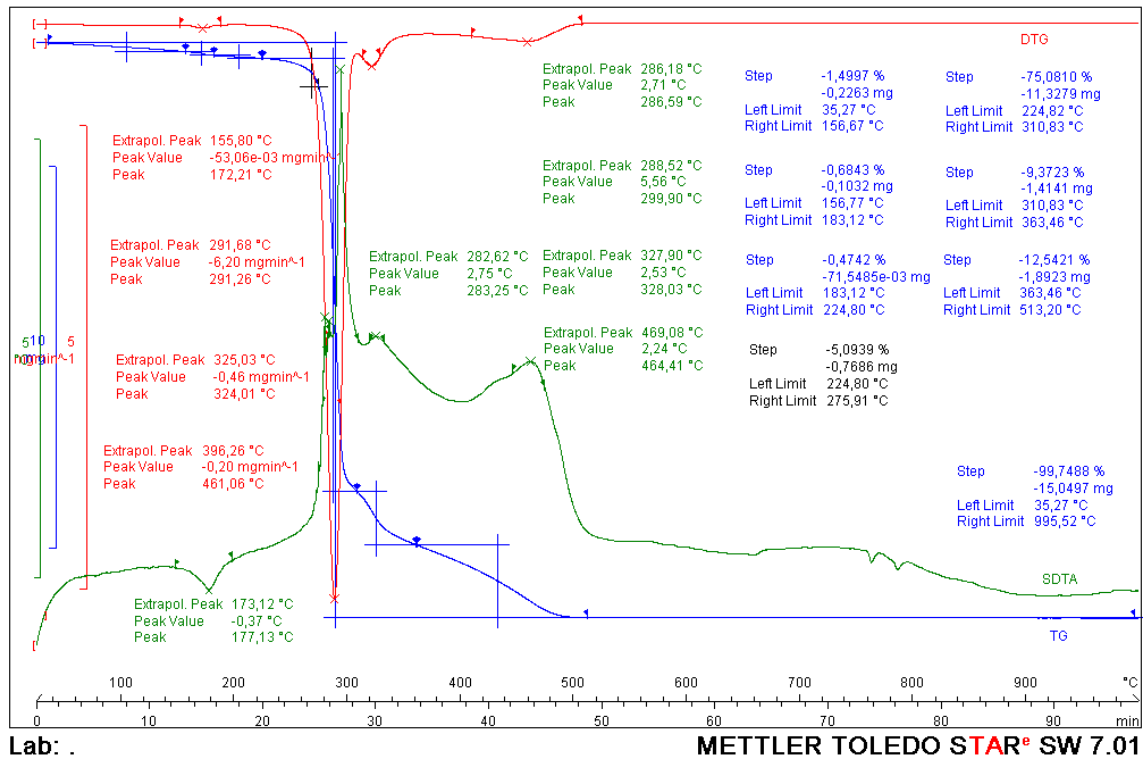
Figure 6.7.18 TGA of CP_30MS_Ex

In these cases, more peaks of the maximum thermal degradation (T1) are present in the graph (red line in Figure 6.7.19 and Figure 6.7.20) because of the different components present in the fibre.

Three recognizable peaks correspond to the thermal degradation of the PHA, lignin and cellulose and they are present in all the reinforced composites. The identifiable peak of PHA occurs at 287±1°C for CP_30WF_Ex and CP_30WF_Pm, at 292±1°C for CP_30MS_Ex and CP_30MS_Pm and at 273±2 °C for CP_30CG_Ex and CP_30CG_Pm. The difference in these values are due to the different chemical composition of the three additions, which influences the thermal properties of PHA.

For what concerns the degradation and decomposition temperatures of other components as lignin and cellulose, in literature different ranges of temperature are reported because basing on their amount in the fibre the onset temperature may be subjected to some changes. Generally, lignin onset temperature is reported to be in a range between 200°C and 400°C: during thermal decomposition of lignin, relatively weak bonds break at lower temperature whereas the cleavage of stronger bonds in the aromatic rings takes place at higher temperature. Thus, when the lignin content is lower, the degradation begins at a higher temperature, but the fibres do not have the oxidation resistance given by the aromatic rings in the lignin[378]. The range of cellulose is set at higher temperatures, usually from 350°C up to 520°C[325]. In this context, peaks at 327°C for CP_30WF_Pm, at 322°C for CP_30MS_Pm, at 320°C for CP_30WF_Ex and at 324°C for CP_30MS_Ex correspond to the lignin continent of the fibres. Different peaks at 421°C for CP_30WF_Pm, at 456°C for CP_30MS_Pm, at 427°C for CP_30WF_Ex and at 461°C for CP_30MS_Ex correspond to the degradation of cellulose.

In two samples another peak is present at temperature below 200°C (in this case at 172°C): from previous studies this is the degradation temperature of some tannins and flavonoids that are usually present in natural fibres (i.g. catechins or acetylated tannins)[379].

Studying the exothermic peaks of DTG (green line in the graphs), the decomposition temperature of each components of the reinforced composites can be recognized: as previously mentioned, the typical decomposition of PHA occurs at 290°C and 305°C; sulfuric acid lignin at 290°C-300°C[380]; hemicellulose at 250-350°C and some of its polysaccharides at 270°C; lastly lignin from 400°C up to 500°C.

The same components are present also in coffee grounds but being in different amounts some values are shifted. The peak at 170°C in Figure 6.7.19and Figure 6.7.20 indicates the thermal degradation of hemicellulose in spent CGs, as reported in previous studies[353]. The other main value corresponds to the exotherm peak at 502 °C of CP_30CG_Ex, that might indicate the presence of ashes, which are very common in spent coffee grounds[350].
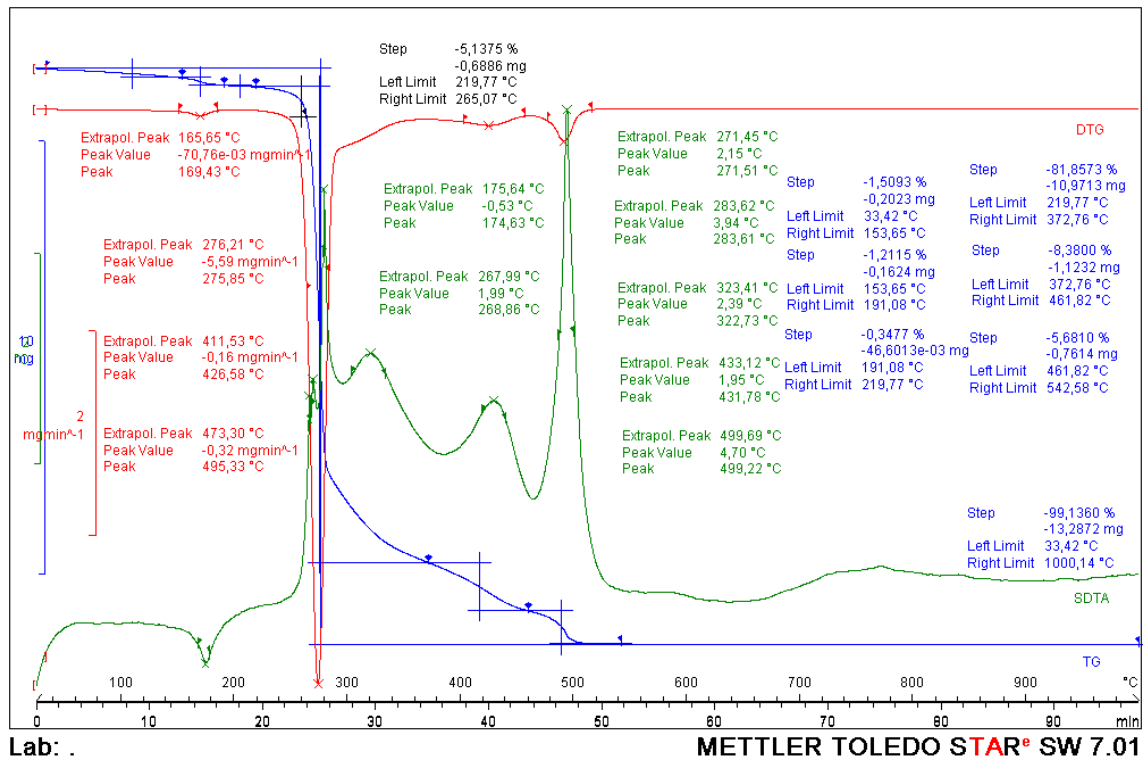
Figure 6.7.19 TGA of CP_30CG_Pm
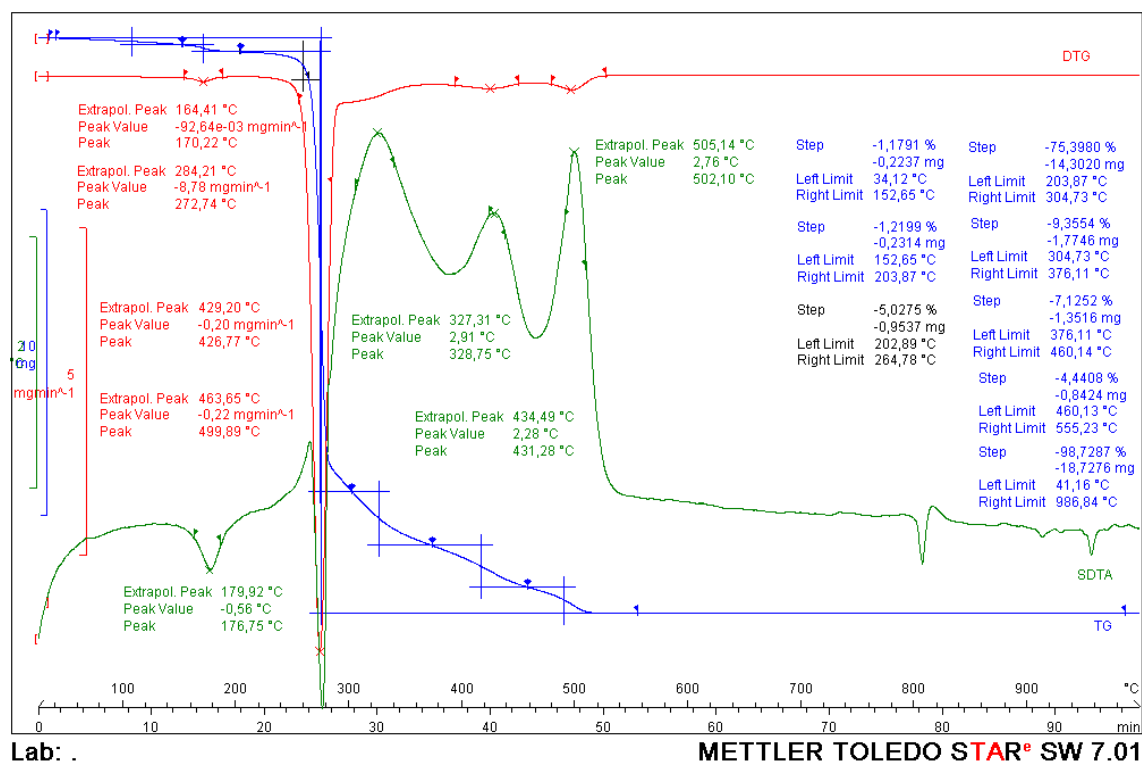
Figure 6.7.20 TGA of CP_30CG_Ex

6.8   **Conclusions**

In this chapter, the effect of the manufacturing techniques and reinforcing materials on the performance of the composite has been evaluated. This work is a preliminary study to estimate the best method for the realization of PHA-composites coming from a renewable resource that will be presented in the next chapter.

The obtained results suggest the following conclusions:

- The addition of the exhausted coffee grounds as a filler in the polymer matrix does not seem to valorize the composite in terms of mechanical performances or for the thermal properties. The resulting "filler effect" reduce the tensile strength to 14.7 MPa (from 29.5 MPa of the reference) in the extruded composite and to 8.8MPa (from 25.4MPa of CP_Pm) for the compression molded composite. Also the Tensile Modulus is reduced of 27% respect to the reference for CP_30CG_Ex and of 85% for CP_30CG_Pm. These results are due to the particles shape and size of coffee grounds, which induce defects in the morphology of the composites (shark skin and voids) and act as a crack propagator.

- The addition of the Wood Flour (WF) as a reinforcing agent in the polymer matrix valorize the composite in terms of Tensile Modulus for both of the series (4.9 GPa for the extruded composites and 2.5 GPa for the compression moulded). For what concerns the tensile strength, WF has a positive effect on the extruded series, in fact the value of σ_M is slightly increased; nevertheless, its effect on the compression molded series is negative, reducing the value up to 14.4 MPa. The elongation at break is slightly higher for CP_30WF_Ex (about 0.7%). Tensile modulus is increased in both of the series. Thanks to the fiber composition the morphology of the composites is homogeneous in both of the series, but in CP_30WF_Pm the interaction between the fiber and the matrix appears more homogeneous with a better adherence between the two phases. Also the surface of the compressed series appears very smooth and with smaller voids respect to all the other composites.

- The addition of the Macadamia nut shells (MS) as a reinforcing agent in the polymer matrix valorizes the composite in terms of Tensile Modulus for both of the series (4.2 GPa for the extruded composites and 3.5 GPa for the compression moulded). For what concerns the tensile strength, MS has a negative effect on both of the series, in fact the value of σ_M is reduced to 21.9 MPa for CP_30MS_Ex and to 3.5 MPa for CP_30MS_Pm. The elongation at break is less respect to WF for both of the series. Tensile modulus is increased in both of the series, but it is still comparable to the WF. Due to the fiber composition the morphology of the composites is not homogeneous: the presence of agglomerates induce the formation of large voids compared to WF. The interaction between the fiber and the matrix appears homogeneous, but the nature of the fibre induce a segregation effect in the compressed composites making the surface irregular. In the extrusion series the shark skin effect is still present. In terms of thermal properties both of the specimens are comparable to the WF series.

- For the evaluation of the two different manufacturing techniques is better to use the specimens made with 100% of PHA as references. In the extrusion processing, a major amount of PHA is necessary due to the cleaning process of the machine and for the setting of all the parameters, which will be an important disadvantage for the production of composite with PHA from renewable resource. Nevertheless, the extrusion process does not degrade the polymer as much as compression moulding. In fact, from GPC results, both of the processes degrade the polymer reducing its molecular weight from 590kD to 155kD (extrusion) and 77kD (compression moulding). Moreover, compression moulding can affect the Tg and Tc of the composites because of its processing conditions (higher pressure and temperature), but the differences in terms of mechanical properties are not so

significant. Indeed, the major difference is in terms of mechanical strength (29.5 MPa for CP_Ex and 25.4 MPa for CP_Pm), whereas for tensile modulus and elongation at break the differences are not so significant.

- For what concerns the reinforced composites, the two techniques in addition to the presence of the WF, MS and CG, caused defects in both of the samples as shark skin, wrinkly surface and voids, but these effects are limited in WF - composites made through compression moulding.

In view of the obtained results, it can be stated that for the aim of this preliminary study, which is the evaluation of the best reinforcing material and process for the production of PHA composite using PHA coming from biomass, the best results are achieved through compression moulding. The reason for this choice is based on the estimation of the advantages and disadvantages of this technique: even if the degradation of the polymer is higher, the mechanical and thermal performances are still comparable with the extrusion series. Moreover, the necessary amount of product (PHA) for the realization of the composite is much lower respect to the extrusion, which is determinant for the next study.

Wood Flour will be used as reinforcing fibers because it permits to achieve a better morphology, avoiding the segregation effect and the presence of bigger voids respect to Macadamia shells fibers and Coffee Grounds.

Therefore, the next phase of the research is mainly focused on the study of the extraction process of PHA from a selected biomass and on the production of PHA composites made with this PHA, comparing its performances with the one made with ENMAT Y1000.

7 . Chapter

Extraction of PHAs from PPB and their Composites

Explorative study on the extraction of Polyhydroxyalkanoates from Purple Phototrophic Bacteria biomass, production and characterization of composites and comparison with composites made with Commercial PHA.

7.1   **Introduction**

This chapter of the dissertation can be considered an exploratory study relating to the extraction of PHAs from a biomass composed of a well-selected culture. The activity has been carried out in collaboration with The University of Queensland (Brisbane, Australia), which represents one of the leaders in the sustainable research and development of PHAs from alternative sources to the usual cultures. In the various departments, new fermentation reactors for the production of PHA under different conditions and with selected cultures are developed, extraction methods are studied, the extracted polymers characterized and composite prototypes are manufactured, also in collaboration with local companies.

This multi sectorial study focuses on the extraction of the polymer from a biomass produced by the Advanced Water Management Center, evaluating different extraction conditions thanks to the School of Chemical Engineering. The Advanced Engineering Building (AEB) allowed the characterization of the polymer and its use for the production of composites. The realization of the composites was based on the preliminary study reported in the previous chapter.

A selected biomass rich of Purple Phototrophic Bacteria (PPB) is used as a substrate for the extraction of PHA. Purple phototrophic bacteria accumulate various storage materials, such as sulfur globules, glycogen or PHAs under appropriate conditions[381,21,393]. The interest in this particular culture is not only related to PHA production, but also to their structure and properties.

The research started with the study of the biomass, specifically from the bacteria structure, to understand how to extract the polymer disrupting the cell walls in the most efficient way, avoiding the damage of other substances as carotenoids.

The extraction process has been studied considering the effects of temperature, solvents, pre-treatments and purification processes on yields. The polymers deriving from the selected processes with the best yields, have been then characterized to estimate their quality in order to choose the best extraction process to be used for a scale up. The final selected process has been used for the large-scale extraction of PHA from PPB to produce composites for design products.

7.2   **Purple Phototrophic Bacteria (PPB)**

Purple Bacteria PPB are a diverse group of anoxygenic, phototrophic, facultative anaerobes. They are widely spread throughout the phylogenetic tree of bacteria, with many subdivisions, particularly within the *Proteobacteria*. Many genera of purple

bacteria are known and the organisms share many basic properties with their non-phototrophic relatives.

Anoxygenic phototrophic purple bacteria are a major group of phototrophic microorganisms that inhabit aquatic and terrestrial environments. Purple bacteria that inhabit oxic habitats and which carry out photosynthesis only aerobically are called 'aerobic anoxygenic phototrophs[45].

Anoxygenic phototrophic bacteria have always attracted scientists for numerous reasons: PPB are gram-negative prokaryotes that convert light energy into chemical energy by the process of anoxygenic photosynthesis. Purple bacteria contain photosynthetic pigments as bacteriochlorophylls and carotenoids, which make them extremely valuable as sub products. Moreover, they can grow autotrophically with CO_2 as sole carbon source [45,383,384].

The application of purple phototrophic bacteria (PPB) for resource recovery from waste streams is gaining increasing attention, specifically in mixed culture photoheterotrophic growth mode[385].

PPB consist of purple sulfur bacteria (PSB) and purple non-sulfur bacteria (PNSB), which often coexist in the same environment[386,382]

7.2.1   Purple sulfur bacteria (PSB)

PSB are predominantly photoautotrophic, using reduced sulfur compounds as electron donor to reduce inorganic carbon. PSB have limited photoheterotrophic and dark metabolic capabilities and most of them require sulfur for their growth. Many species of purple sulfur bacteria are 'extremophilic' species, including in particular, species that grow best at high salt and/or pH[386,382].

The physiology of purple sulfur bacteria is intimately linked to sulphide, and large populations of purple sulfur bacteria are observed in nature only in illuminated environments where sulphide is present[387]. This implies that the growth of purple sulfur bacteria in nature is primarily phototrophic. If growth is photoautotrophic, sulphide, thiosulfate or H_2 are used as photosynthetic electron donors.

In addition to autotrophic growth, a few organic carbon sources are photo-assimilated by purple sulfur bacteria. Organic acids and fatty acids are the preferred substrates, but short-chain alcohols and even carbohydrates are used by certain species[386].

7.2.2   Purple non-sulfur bacteria (PNSB)

In contrast to the previous section, PNSB have photoautotrophic capabilities in addition to diverse capacities for (aerobic/ anaerobic) dark chemotrophy. All purple non-sulfur

bacteria are proteobacteria, and phylogenetic trees show the various species to be closely related to non-phototrophic species[386].

Purple non-sulfur bacteria are a physiologically versatile group of purple bacteria that can grow well both phototrophically and in darkness. Growth of some purple non-sulfur bacteria is possible under phototrophic conditions with either CO_2 or organic carbon, or in darkness by respiration, fermentation, or chemolithotrophy[386].

The diverse range of potential PPB applications arises from the exploitation of their metabolic versatility: PPB grow under anaerobic conditions, by (1) photo-autotrophy, using light for anabolism and CO_2 as carbon source, with a range of inorganic electron donors; (2) photoheterotrophy, using light as energy source and organic carbon as carbon source, and (3) fermentation, without light and using organics molecules as energy and carbon source.

Photoautotrophic growth is typical of purple and green sulfur bacteria, while photoheterotrophic growth is typical of purple non-sulfur bacteria.

Chemoheterotrophic growth in the presence of oxygen is common among purple non-sulfur bacteria, but is also found in some purple sulfur bacteria. While some species are very sensitive to oxygen, others grow equally well under aerobic conditions in the dark at the full oxygen tension of air. Under anaerobic dark conditions, growth of some species is also supported by respiratory electron transport in the presence of nitrate, nitrite, nitrous oxide, dimethyl sulfoxide (DMSO), or trimethylamine-N-oxide (TMAO) as electron acceptors.

In the absence of external electron acceptors, a number of substrates allow for energy generation and slow growth by a fermentative metabolism. In addition to these diverse methods for energy generation, there is considerable variation in the utilization of carbon, nitrogen and sulfur compounds for assimilatory and dissimilatory purposes, as well as in the enzymatic reactions and pathways involved in these processes.

Organic carbon sources have principally different functions under phototrophic, respiratory and fermentative conditions. Under phototrophic growth conditions they serve primarily as a source of cellular carbon, but in addition may function as an electron source for photosynthetic electron transport.

The purple bacteria have a Gram-negative cell wall organization; which means that the percentage of peptidoglycan is lower compare to Gram positive and their structure is mainly maintained by the external membrane. The cell wall composition (Figure 7.2.1) can be determinant to study the conditions of extraction for the recovery more products.
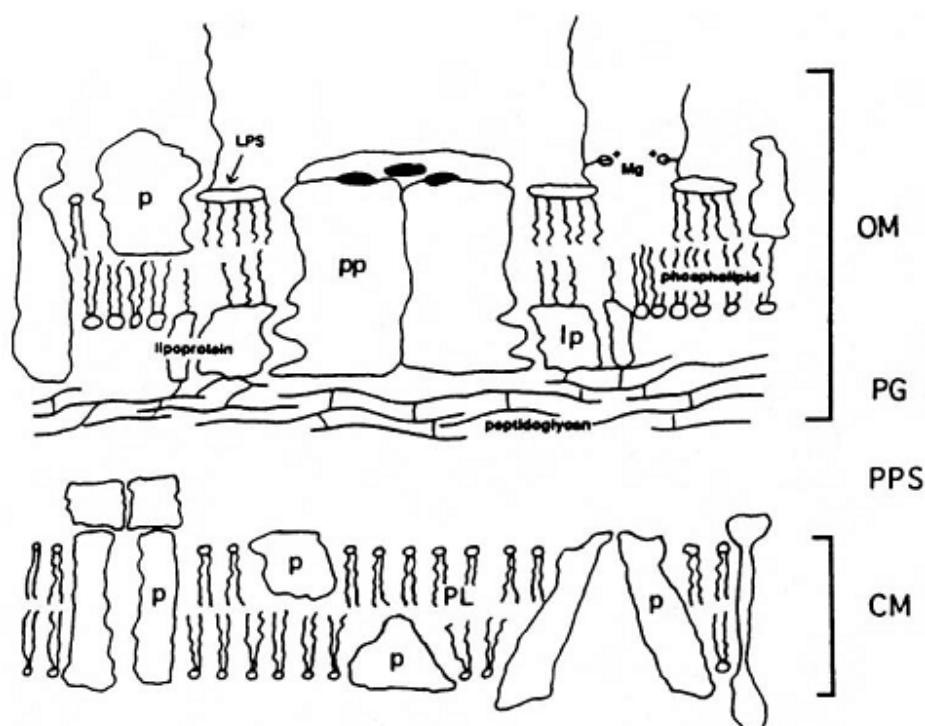
Figure 7.2.1 Cell envelope of Gram (-) bacteria: Cytoplasmatic membrane(CM), lipopolysaccharide(LPS); lipoprotein (LP); outer membrane (OM); proteins(p); peptidoglycan (PG); Phospholypidus (PL); porins proteins (pp); periplasmatic space (PPS)[384].

In order to recover the PHA granules stored inside of the cell wall, it is necessary to rupture the bacterial cell and remove the protein layer that coats the PHA granules. Alternatively, the PHA must be selectively dissolved in a suitable solvent. In fact, modifying the cell wall's permeability and then the PHA dissolution in the solvent are the mechanisms for PHA extraction. Thus, the conformation of the structure permits to estimate the best protocol for the recovery of the polymer and other substances as carotenoids in order to reach the highest yield[270,276–278,284,308,388–390]. It is possible to extract the polymer after the creation of pores on the barrier with solvents or using pre-treatments. The use of a pre-treatment on the biomass is the easiest way to modify the cell wall's permeability to simplify the access of the solvent to the granule of polymer.

7.2.3   Carotenoids

Regular human cellular metabolism continuously generates free radicals; almost 95% of them are used for body metabolism and 5% of oxygen is converted as reactive oxygen species (ROS). The damaged macromolecules cause dysfunction or alteration of various stress-response genes, which initiates further formation of ROS, e.g., hydroxyls radicals or reactive non-radical compounds like singlet oxygen and hydrogen peroxide. The

antioxidant effects from the ingested carotenoid significantly neutralize the ROS, which further demolishes the oxidative stress in the body[391]. For this reason, the recovery of carotenoids from PPB can be an extremely added value.

The photosynthetic pigment protein complexes that carry out light harvesting and the initial photochemical reactions contain coloured carotenoids as usual constituents. Besides contributing to light absorption, these pigments provide protection against harmful photosensitized oxidations by quenching the metastable excited states of chlorophylls and oxygen that are unavoidably formed as by-products of the primary photo-processes. The protective function of carotenoids appears to be essential for the survival of phototrophic organisms in aerobic environments[392]. In these micro-organisms the other major pigments present are bacteriochlorophyll a or b (BChl a and BChl b) and the corresponding pheophytin (Figure 7.2.2). Carotenoids necessarily exist in reaction center (RC), RC-light-harvesting 1 (LH1) and LH2 antenna complexes, and have functions of light-harvesting and/or photoprotection, as well as playing possible structural roles. Most aerobic photosynthetic bacteria have the purple bacteria-like photosynthetic apparatus including BChl a, and many species have spirilloxanthin, as well as additional polar 'non-photosynthetic' carotenoids[386,392].
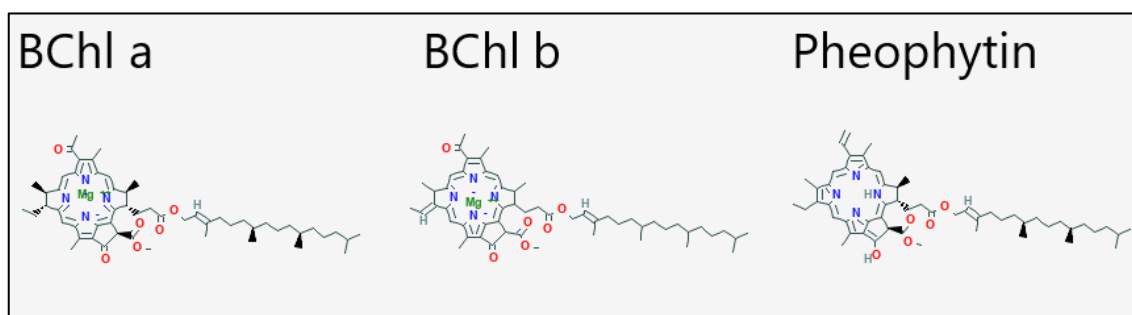
Figure 7.2.2 Structure of bacteriochlorophyll a or b (BChl a and BChl b) and the corresponding pheophytin.

7.3   Pre-Treatments

In literature, different processes are reported to weaken the integrity of the cell wall and membrane layers; biological, chemical (as alcohols or chlorinated solvents), and/or physical processes (as pressure or sonication), to release the polyester molecules or the PHA granules and increase extraction yield[77,268,270,278,393].

Some of them have been described in previous Section 5.5.3.

In this study, three chemical pre-treatments in combination with ultrasonication have been analysed in order to compare their effects on the yield with that of a conventional extraction process reported in literature[271]. The three considered pre-treatments are:

sodium hypochlorite, ethanol and a mixture of acetone and methanol. These pre-treatments have been chosen for their efficiency as cell wall disruption agents basing on previous work found in literature[270,274,276–278,308,394,395] and for their low environmental impact.

7.3.1   Sodium Hypochlorite (NaClO)

Most methods to recover intracellular PHA involve the use of digestion methods (described in Section 5.5.2). Such a method can reduce the use of large quantities of solvent making the procedure economically and environmentally unattractive. Recently, another recovery method becomes an alternative to the usual digestion: the use of sodium hypochlorite for differential digestion of the biomass or non-PHA cellular materials. This method, in previous studies, obtained high purity levels of PHA (more than 86%)[43].

7.3.2   Ethanol (EtOH)

Ethanol has been shown to inhibit the assembly of cross-linked peptidoglycan and to induce cell lysis in *Escherichia coli*. These effects of ethanol appear to result from the weakening of hydrophobic interactions by ethanol rather than from the intercalation of ethanol into membranes. The addition of ethanol to aqueous solutions weakens hydrophobic associations and has been used to solubilize hydrophobic compounds, to increase membrane permeability, and to destabilize nucleic acids and proteins[393,34]. The use of ethanol as pre-treatment can facilitate the extraction of carotenoids, which have high affinity with alcohols and chlorinated solvents[391].

7.3.3   Acetone/Methanol (Ac/MeOH)

Acetone (Ac) is another of the more common and largely used green solvent. Ac is the most commonly used solvent in mcl-PHA extraction while methanol is usually employed as the mcl-PHA non-solvent both for biomass pre-treatment and PHA precipitation from solution in acetone[396]. In this study, acetone and methanol are used as a mixture in order to purify the product and as a pre-treatment on the biomass. This choice is based on the properties of the two solvents: methanol, as ethanol, can be effective on peptidoglycan. Also acetone, can have a high influence on the cell wall lysis thanks to its ability to dissolve the lipid components of the membrane. Moreover, MeOH and Ac are very good solvent for the extraction of carotenoids from plants[391].

To explore the extraction process, the effects of the common parameters, including solutes/solvent ratio, size of the raw material, extraction duration, solvent (Chloroform and 2-Buthanol) and temperature, on the PHA extraction yield have been investigated. After the extraction, considering the obtained yields, a first skimming process is carried on in order to decide the best extraction for the scale up.

The obtained polymer from the selected extraction processes is characterized through Gel permeation chromatography (GPC), Nuclear Magnetic Resonance (NMR), Differential Scanning Calorimetry (DSC) and Thermogravimetric Analysis (TGA).

7.4   **Compression Moulded Composites**

The final aim of this work is to produce composites with the extracted PHA from PPB, through compression moulding process, and compare them to a series made with commercial PHA. As discussed in Chapter 6, the main advantage of this technique is the low need of polymer for the procedure. In fact, due to the limited time, the bigger amount of materials for the extrusion process can not be collected .

The compressed composite combines the polymer with one of the commonest Australian waste from industry: Wood Flour (WF). The Wood Flour already described in the previous chapter have been used. This waste has been chosen for the good interaction with the polymer matrix, essential for a good adhesion between the two phases of a reinforced composite. The addition of wood fibres not only positively influences the mechanical properties of the composite, as found in literature[87,307,354,397,398] and in the preliminary study of Chapter 6, but it is an added value for the circular economy perspective[154–47]. From previous studies[247,356], the use of industrial wastes as wood flour in association with biopolymers in composite materials could result in a reduced product entry cost equal to 21% of neat PHA cost[11].

7.5   **Materials and Methods**

Some of the materials used such as commercial PHA (ENMAT Y1000) and Wood flour (WF) have already been introduced and described in Chapter 6 (Section 6.5.1 and Section 6.5.2).

7.5.1   **Biomass Pre-Treatment**

The biomass (Figure 7.5.1) was taken from a selected mixed PPB PHA-accumulating culture. The biomass has been selected and enriched in a 60 L flat plate anaerobic lab-scale photobioreactor, fed with acetic acid (500 mg COD/l) as a sole artificial carbon source and under 24 h artificial illumination. The imposed feeding regime, based on feast and famine condition with limitation of nitrogen source (35 mg NH_4Cl/l), lead the PPB towards the accumulation of PHA. These conditions permitted to obtain a biomass with a PHA continent of 35%. This value is considered the maximum quantity of extractable PHA (100%) to calculate the yields.

Figure 7.5.1 Freeze-dried biomass used for all the extractions

After the freeze-drying process, the biomass is treated with the selected pre-treatments: sodium hypochlorite (7% by volume), ethanol (100%) or acetone/methanol (7:2) (Sigma Aldrich analytic grade) using sonication for 15 minutes followed by 30 minutes of stirring to homogenize the solution. All the conditions of the different pre-treating process are resumed in Table 7.5-1.

At the end of each pre-treatment procedure, the solution is filtered by using a vacuum filtration apparatus with a paper filter (45µm pore size), then the solute has been dried overnight at 30±5 °C.

Table 7.5-1 List of pre-treatments and their conditions

Pre-treatment	Temperature	Concentration of the solution	Quantity for each gram of biomass
Sodium Hypochlorite	Room temperature	7% by volume	80ml
Ethanol	Boiling Point	100%	80ml
Acetone/Methanol	Boiling Point	7:2	80ml

Ethanol and the mixture Ac/MeOH are used at the boiling point to extract more carotenoids, giving a clearer polymer at the end of the procedure.

In Figure 7.5.2 two solutions of 1 mL of biomass and ethanol after the pre-treatment at two different temperature are shown: the orange one is at room temperature, the green one is at the boiling temperature. The two solutions have the same solute/solvent ratio.
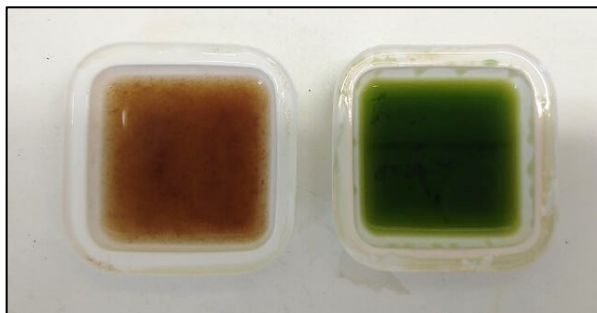
Figure 7.5.2 1 mL solution of biomass and ethanol after the pre-treatment at two different temperatures: room temperature (right) and boiling point (left)

7.5.2   **Extractions**

One of the oldest method of PHA extraction uses organic solvents to extract the polymer from the cells[271,265]. Methods to recover PHA would typically involve cell wall/cell membrane lysis, solubilization and purification of PHA component, and precipitation of PHA polymer[239]. The extraction procedures explore the use of two possible solvents: chloroform and 2-buthanol. Chloroform is the most known solvent for the extraction of PHA and with a high yield efficiency[403]. Nevertheless, it can be dangerous for human health and environment. 2-Buthanol is a greener option, but previous studies have given an inferior extraction efficiency[243]. In Table 7.5-2 the different extraction conditions are resumed.

7.5.2.1   *Extraction in chloroform:*

1gr of freeze-dried and pre-treated biomass is stirred with 50mL of solvent in a Parr Reactor (Figure 7.5.3) at the same temperature for 2 hours. The Parr reactor is able to control maintain all the variables that may affect the extraction process as the stirring speed, temperature and pression.

Then, the solution is cooled down and filtered by a vacuum filtration system to separate the liquid phase from the biomass, avoiding the presence of macro impurities. Successively, the liquid phase is left to evaporate overnight to facilitate the film formation process.

The film is then purified by the addition of Ac/MeOH co-solvent (7:2) followed by sonication for 30 minutes to dissolve all the residual carotenoids. Only one sample is left not purified as reference to evaluate the influence of this step on the polymer

characteristics. The last filtration of the solution by paper filter separates PHA from the solution of carotenoids as a film.

7.5.2.2   *Extraction in 2-Buthanol:*

1 gr of freeze-dried and pre-treated biomass is stirred with 50 ml of solvent in a Parr Reactor at constant temperature (140°C) for 2 hours.

Then, it is necessary to cool down the solution and filter it by a vacuum filtration system to separate the liquid phase from the biomass. Successively, 50 ml of chloroform is added to the solid phase and stirred at room temperature for 45 minutes. Another filtration occurs to avoid the presence of macro impurities. Successively, the liquid phase is left to evaporate overnight to facilitate the film formation process.

Figure 7.5.3 Parr Reactor (100 mL capacity)

The film is then purified by the addition of a Ac/MeOH co-solvent (7:2) followed by sonication for 30 minutes to dissolve all the residual carotenoids. The last filtration by paper filter allows to separate the PHA film from the carotenoid's solution. Each extraction process is repeated three times and the yield reported as the average value calculated considering the maximum quantity of PHA in the biomass (35%) as 100% yield.

Table 7.5-2 List of all the extractions and their conditions.

	Pre-treatment	Solvent	Temperature	Purification post extraction
1	-	$CHCl_3$	Boiling Point	Ac/MeOH (7:2)
2	-	$CHCl_3$	140°C	Ac/MeOH (7:2)
3	Ac/MeOH	$CHCl_3$	140°C	-
4	EtOH	$CHCl_3$	140°C	Ac/MeOH (7:2)
5	NaClO	$CHCl_3$	140°C	Ac/MeOH (7:2)
6	Ac/MeOH	$CHCl_3$	140°C	Ac/MeOH (7:2)
7	-	2-Buthanol	140°C	Ac/MeOH (7:2)
8	EtOH	2-Buthanol	140°C	Ac/MeOH (7:2)
9	NaClO	2-Buthanol	140°C	Ac/MeOH (7:2)
10	Ac/MeOH	2-Buthanol	140°C	Ac/MeOH (7:2)

7.5.3   **Extracted polymer characterization**

Only 4 of the 10 obtained polymers are selected and characterized to measure their properties and purity level. The polymers are characterized by the following procedures.

7.5.3.1   *Differential Scanning Calorimetry (DSC)*

DSC experiments are performed using a DSC Q2000, TA Instruments to determine the melting point (Tm). About 2 mg of sample is heated at 185 °C with a heating rate of 20 °C min^{-1}, subsequently cooled to –50 °C with a cooling rate of 10 °C min^{-1}, and then reheated to 185 ∘C at 10 ∘C min^{-1} heating rate under nitrogen gas.

7.5.3.2   *Thermogravimetric Analysis (TGA)*

TGA experiments are performed following the norm UNI EN ISO 1111358-1:2014 by using a Netzsch Jupiter STA449 F3 TGA instrument to determine the decomposition temperatures (Td) of the purified PHA polymers and the PPB biomass. About 5 mg of sample is heated from room temperature to 550 °C with a heating rate of 10 °C min^{-1} under nitrogen gas.

7.5.3.3   *Nuclear Magnetic Resonance (NMR)*

Proton NMR (^{1}H-NMR) spectroscopy is used to characterize the chemical structure of the purified PHA polymers. PHA samples are dissolved in deuterochloroform (CDCl$_3$) (10 mg/mL). ^{1}H 1D NMR spectra acquisition at 25°C is preceded using a Bruker Avance 500 MHz high-resolution NMR spectrometer by 64 scans with a spectral width of 11 ppm (5500 Hz). 4 dummy scans are used prior. TopSpin 3.5 software is used to obtain the quantitative parameters including the relative peak intensities and chemical shifts. Chemical shifts are referenced against the proton peak of CDCl$_3$ at 7.26 ppm.

7.5.3.4   *Gel permeation chromatography (GPC)*

Weight average molecular weight (Mw), number average molecular weight (Mn) and polydispersity index (PDI = Mw/Mn) are obtained using gel permeation chromatography (GPC)[355]. Specimens are dissolved in chloroform (HPLC grade) at room temperature for 30 minutes, at a concentration of 2.5 mg/mL. GPC analyses are performed using an Agilent 1260 Infinity Multi Detector Suite system (Cheshire, UK) equipped with a guard column followed by three columns in series. The columns are kept at 30°C. A refractometer, at 30°C, is equipped to detect the signals. A chloroform flow rate of 1 mL/min is used for the analysis. Narrowly distributed molecular weight polystyrene standards were used for calibration.

7.5.4   **Preparation of the composites**

Four composites are made with the two different polymers: one is the result of the selected extraction processes from PPB (named as recovered PHA or RP); the other is a commercial PHA (ENMAT Y1000) produced by TianAn Biopolymer (described in Section 6.5.1) (named as Commercial PHA or CP). The same amount of polymer (70% w/w) is mixed with wood flour (for the characterization see Section 6.5.2), which is used as a reinforcing material. Table 7.5-3 shows the formulations used for each sample.

Table 7.5-3 Formulations of the composites made with compression moulding

Sample	Commercial PHA (Enmat Y1000)	PHA from PPB	Wood Flour
CP_Pm	100%	-	-
RP_Pm	-	100%	-
CP_30WF_Pm	70%		30%
RP_30WF_Pm	-	70%	30%

All the composites are made with the same procedure of Chapter 6, Section 6.6.1.

7.5.5   Composite characterization

7.5.5.1   *Microstructural analysis*

After the tensile test, the microstructure of composites is observed by using a Macroscopy (Wild Makroskop M420) at 10X and a Scanning Electron Microscope (SEM) (VEGA3 TESCAN) at 25.0 kV equipped with EDAX for the analysis of elements.

7.5.5.2   *Tensile Test*

Samples are cut in 5 dog-bone-shaped specimens from each compression moulded square samples and tested following ASTM D 638-5 for tensile test. All the tests are conducted using an electromechanical Instron model 5584 (Instron Pty Ltd, USA) with a 1 kN load cell. Specimens are clamped using pneumatic grips, and tested at constant cross-head displacement rate of 1 mm/min. A video-extensometer is used to obtain the strain value across the narrow region of the specimen. This contactless approach avoids any risk for introducing stress concentration and premature crack initiation and propagation. The reported values represent the mean of five replicate test specimens.

7.5.5.3   *Differential Scanning Calorimetry (DSC)*

DSC measurement on the composites have been carried out in the same conditions of the extracted polymers (Section 7.5.3.1).

7.5.5.4   *Thermogravimetric Analysis (TGA)*

TGA experiments are performed using a TGA instrument (Mettler Toledo TGA/SDTA 851) following the norm UNI EN ISO 1111358-1:2014 in order to determine the decomposition temperatures (Td) of the composites made with PHA from PPB and

TianAn PHA polymers. About 5 mg of sample is heated from room temperature to 550°C with a heating rate of 10 °C min^{-1} under nitrogen gas.

7.6   Results and Discussion

7.6.1   Extraction

The various factors influencing the extraction yields and the characteristics of the obtained polymer were decisive for the skimming process and for the selection of the most effective method. From the extraction procedures the obtained results are very different. All the results reported in Table 7.6-1 are calculated considering a content of 35% of PHA in the biomass, considered as 100% of the yield.

Table 7.6-1 Extraction yields for all the considered extraction processes

	Pretreatment	Solvent	Temperature	Purification	Yield (%)
1	-	CHCl$_3$	Boiling Point	Ac/MeOH (7:2)	21%
2	-	CHCl$_3$	140°C	Ac/MeOH (7:2)	40%
3	Ac/MeOH	CHCl$_3$	140°C	-	40%
4	EtOH	CHCl$_3$	140°C	Ac/MeOH (7:2)	70%
5	NaClO	CHCl$_3$	140°C	Ac/MeOH (7:2)	40%
6	Ac/MeOH	CHCl$_3$	140°C	Ac/MeOH (7:2)	44%
7	-	2-Buthanol	140°C	Ac/MeOH (7:2)	37%
8	EtOH	2-Buthanol	140°C	Ac/MeOH (7:2)	16%
9	NaClO	2-Buthanol	140°C	Ac/MeOH (7:2)	14%
10	Ac/MeOH	2-Buthanol	140°C	Ac/MeOH (7:2)	24%

Considering the yields reported in Table 7.6-1, temperature is determinant for this type of extraction, since the yield difference between chloroform extraction at the boiling point and at 140°C is 19%. It is well known that increasing the temperature the solvent efficiency increases, permitting to solubilize more solute[404,405]. Nevertheless, it is essential to avoid high temperatures because the decomposition temperature of the polymer can occur.

The use of 2-Butanol at 140°C and without pre-treatments gives similar results of the extraction in chloroform at the same conditions, but the extraction procedure, articulated in more steps, can cause more losses in the yield. The differences between the pre-treated samples extracted in chloroform and in 2-buthanol is explicative. Considering that all the samples are extracted from the same substrate and underwent the same pre-treatment, those extracted in chloroform give much higher yield percentages (70% for ethanol, 40% for sodium hypochlorite and 44% for Acetone/Methanol) than those in 2-buthanol (16%, 14% and 24% respectively).

Concerning the single pre-treatment, the use of boiling ethanol as cells wall disruption agent is effective in both cases, but the results on the extraction in chloroform are impressive. Indeed, it permitted to reach a yield of 70%, which is the highest of this study. The ethanol pre-treatment in the 2-buthanol extraction does not give the same results, probably due to the procedure. The use of the mixture of Acetone/Methanol permits to reach 44% in chloroform and 24% in 2-buthanol. The worse cell disrupting agent is sodium hypochlorite, which gives 10% in chloroform and 14% in 2-Buthanol. Moreover, its use with biomass, even if in low concentration, produces a small amount of bubbles which require washes to be removed.

At the end of this phase of the study, the authors decided to carry on the analysis of only four of the ten polymers extracted: the choice has been made basing on the difficulty of the extraction procedure, on the pre-treatment effect and on the best yield. For these reasons, only the polymers coming from the extraction in chloroform at 140°C and pre-treated with Acetone/Methanol (6) and Ethanol (4) have been analysed. In addition to these samples, also the extraction in chloroform at 140°C without pre-treatments (2) and the one pre-treated with Acetone\Methanol but without the purification process in Acetone/Methanol (3) have been compared to the others to understand not only the differences caused by these processes on the polymer structure, but also if it purification can be avoided in order to reduce the use of solvents.

7.6.2   **Polymer characterization**

7.6.2.1   *Thermogravimetric Analysis (TGA) of extracted polymers*

TGA monitors weight loss trends in real-time, in addition to initial and final values, during the sample thermal decomposition treatment. From TG curves, the decomposition temperature (Td), defined as the temperature at which the polymer loses the 5% of its weight, and the temperatures of maximum degradation (T1, T2) has been measured for each sample, considering as references the temperatures for the evaporation of solvents (120°C) and decomposition of organic matters (400°C).

All the results are reported in Table 7.6-2 and the graphs are shown in Figure 7.6.1.

Table 7.6-2 TGA results of PPB biomass and the extracted polymers

Sample	Extraction Conditions	Reference Temperature [°C]	Mass Loss [%]	Td [°C]	T1 [°C]	T2 [°C]
PPB biomass	-	-	5	95	-	-
		120	10	-	-	-
		-	33	-	280	-
		-	44	-	-	309
		400	66	-	-	-
Standard_extractio n_Ac\MeOH purification	No pre-treatment	120	< 1	-	-	-
	CHCl$_3$	-	5	272	-	-
	140°C	-	40	-	288	-
	Acetone\Methanol purification (7:2)	400	97	-	-	-
Ac\MeOH pretreatment_No purification	CHCl$_3$	120	< 1	-	-	-
	140°C	-	5	250	-	-
	No purification	-	52	-	289	-
		400	92	-	-	-
EtOH Pretreatment_ Ac\MeOH purification	Ethanol pre-treatment	120	< 1	-	-	-
	CHCl$_3$	-	5	272	-	-
	140°C	-	60	-	292	-
	Acetone\Methanol purification (7:2)	400	98	-	-	-
Ac\MeOH Pretreatment_ Ac\MeOH purification	Acetone\Methanol pre-treatment (7:2)	120	< 1	-	-	-
	CHCl$_3$	-	5	272	-	-
	140°C	-	46	-	288	-
	Acetone\Methanol purification (7:2)	400	97	-	-	-

The TGA curve for the PPB biomass shows weight loss in **more stages**. The **first** mass loss occurrs in the temperature range from room temperature to **120°C**. In this sample Td occurs at 95°C, where the loss weight is 5%. At 120°C the loss is equal to 10% due to volatile components and moisture evaporation. In this case, also other unknown substances (as carotenoids[406]) are lost. Previous studies in literature describes the thermal behaviour of PHA[264,37,34] and the range of maximum decomposition occurs between 250°C and 290°C. The presence of the polymer, in fact, is evident at **280°C,** where the

first peak of decomposition occurs. Another peak is at **309°C,** but this is not caused by the polymer but rather by the other components of the biomass[34,407]. The last decomposition step is at **400°C**, for the decomposition of organic compounds. After 400°C remain the 44% of other substances probably inorganic and high-temperature resistant. It is very difficult to estimate the influence of carotenoids and other compounds in the thermal behaviour of the biomass, because of the wide variability of the substrate and the biomass.

Analysing the extracted polymer, the differences respect the PHA stored in the biomass are evident, especially for Td. Td is much higher in all the purified polymers (272°C instead of 250°C). The purification process removes all the residual carotenoids and other substances from the polymer and avoid the reduction in the thermal stability.

For all the extracted PHA up to 120°C the mass loss is approximately around 1% due to the evaporation of physically adsorbed solvents (water or chloroform) on the polymer. Further, the second or the major step of degradation of the polymer begins after 250°C, after the melting point of PHA, which is usually in the range of 150-170°C[264,37,34]. This decomposition temperature, considerably greater than the melting temperature (Tm), permits an extensive thermal space of workability. The degradation process involves reduction in molecular weight, which includes chain scission and hydrolysis. The thermal degradation of PHA that occurs in this stage is due to the random chain scission process which involves the cleavage of C=O and C—O bonds in ester moieties by β-scission[408] destruction of crystalline regions, and scissions of the chain in different monomers. The second step of weight loss occurs with a further rise in temperature, causing the chain scission with subsequent formation of crotonic acid, as described in literature [244]. Figure 7.6.1 shows that for PHA T1 is at 290±2°C for all the samples (except PPB biomass), where the mass loss is from 40% for the extraction without pre-treatment to 60% for the PHA pre-treated with ethanol. The trend of the curve in this stage of the process is evident in Figure 7.6.1. Similarly, the residual mass is less than 2% after 400°C for almost all the samples: the only exception is the PHA without the purification process after the extraction, which lose only the 92% of its total weight. This behaviour highlights that the purification is strictly necessary to avoid a reduction of 20°C in the Td. The presence of these other unknown substances that influence the Td and the maximum decomposition temperatures may cause difference also in the glass transition temperature (Tg), crystallization temperature (Tc) and in the melting temperature (Tm), which are determinant for the workability of the polymer in composites.

Comparing the curves in Figure 7.6.1 the different behaviours of the extracted polymers are clear: at 400°C the polymers subjected to the purification process in acetone / methanol have approximately the same residual mass (around 2-3%). On the other hand, at the same temperature, the sample that has not undergone this process shows a higher

residual mass (about 8%), exactly as biomass as it is. This implies that during the purification process not only the residual carotenoids are extracted, but also other not identified substances which affect the thermal stability and the final purity of the polymer limiting the range of workability and applications.
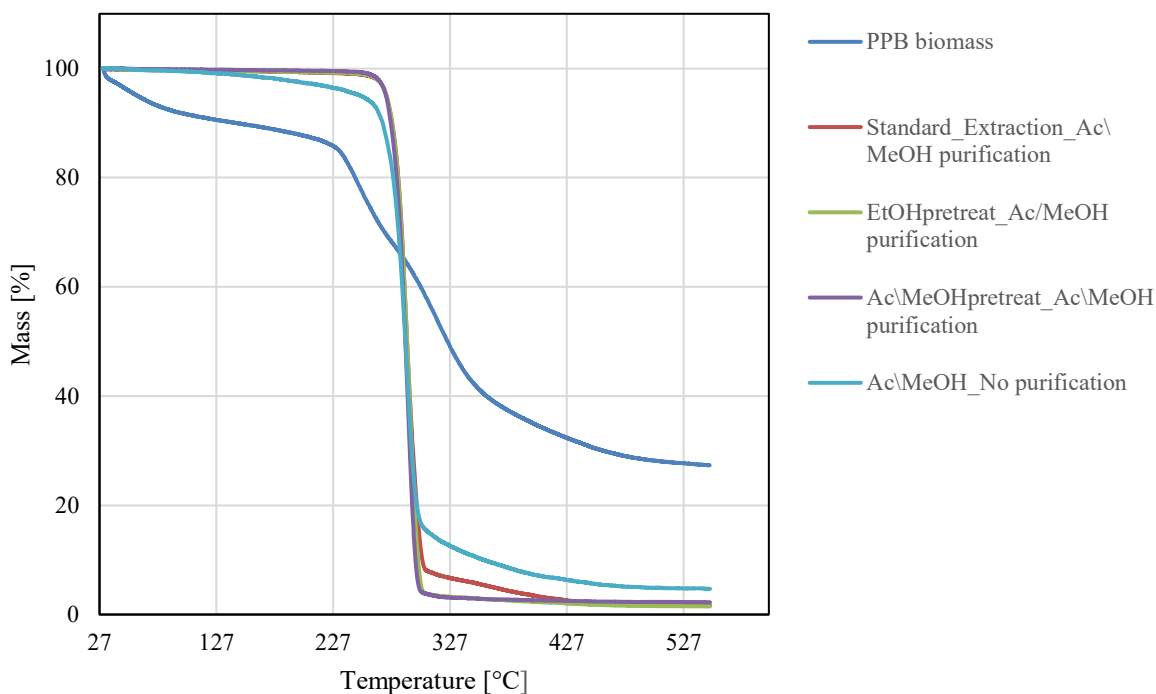
Figure 7.6.1 TGA of PPB biomass and extracted polymers.

7.6.2.2   *Differential Scanning Calorimetry (DSC)*

Differential scanning calorimetry (DSC) measurements are carried out to identify the phase transition temperatures of different PHA extracted from PPB biomass. From these curves, the crystallization temperature (Tc) and melting temperature (Tm) are taken at the maximum peak of the transition phase, respectively. The glass transition temperature (Tg) is taken at the mid-point of the specific heat increment. The crystallization and melting enthalpies (UNI EN ISO 11357-3), ΔHc and ΔHm respectively, are obtained by measuring the area of the corresponding peaks (Table 7.6-3). Also the corresponding crystallization degree is calculated by the Equation 8 in Chapter 5, where Xc(%) is the percentage crystallinity; ΔHm is the measured melting enthalpy (J/g); and the $\Delta H_{100\%}m$ is the melting enthalpy for fully crystalline PHB (146 J/g)[265].

From the results found in the literature, the thermal characteristics of PHA vary considerably with the molecular weight and the length of chains. In particular, the Tg of

P3HB has been reported to vary between -3 and 5 °C[313,403]and our Tg values are aligned to these values.

In this case, the different extraction methods and the different pre-treatments give polymers with Tg still comparable with a reference of commercial PHA (TianAn Biopolymer ENMAT Y1000) with Tg values in the range 3°C ± 4°C. All the results of this analysis are reported in Table 7.6-3.

Tg depends on the mobility and flexibility of the polymeric chains[313]. If the mobility of the chains is restricted, then the glassy state is more stable, and restrictions are more difficult to break. This causes the immobility of the polymer chains at higher temperature, because more energy is required to make the chains free, and this reflects in a higher Tg[313,403]. An increase in Tg is also commonly caused by a higher polymer Mw [308] and the presence of more flexible chains[313].

In Table 7.6-3, **EtOH Pretreatment_ Ac\MeOH purification** specimens have the lower value of Tg: an increase in the amorphous phase might induce an increase of Tg[313]. On the other hand, side groups, increasing the free volume in the molecule and short polymer chains, act as plasticizers, both resulting in a Tg decreasing[314] .

A clear crystallization peak can be easily observed for all the samples, which indicates that these compounds undergo some small amount of crystallization while heating. **Tc** varies from 88°C for **Ac\MeOH Pretreatment_No purification** to 113±4°C for **Commercial PHA, Standard_extraction_Ac\MeOH purification, EtOH Pretreatment_ Ac\MeOH purification and Ac\MeOH Pretreatment_ Ac\MeOH purification**; high Tc implies that the polymer crystallisation ability of the material is better[313].

As Tg, also **Tm** is strictly related to the molecular weight and the polymerization degree of the polymer. Presence of side chains and functional groups in PHAs structure impact Tm[80]. PHAs with smaller crystals with larger imperfections, more side chain structures, less crystallinity and more amorphous in the structure melt at lower temperatures[316,317] . On the other hand, an increase in Tm suggests an increased symmetry in the polymer structure with higher number of average molecular. The small differences in Tm values may be due to the variation in molecular weight of the PHA polymers[29]. In this case, Tm varies from around 173°C for **Commercial PHA** to 166°C for **EtOH Pretreatment_ Ac\MeOH purification and Ac\MeOH Pretreatment_ Ac\MeOH purification. Ac\MeOH Pretreatment _No purification** has the lowest Tm very probably because of the presence of inorganic particles and other substances (as carotenoids or inorganic salts) that reduce the Tm value.

As expected, the high temperature obtained for the maximum thermal degradation temperature (T1 in Table 7.6-2) predicts also high values for Tm in the extracted polymers meaning a higher thermal stability temperature (Td in Table 7.6-2).

The behaviour of a polymer during the melting process is dependant by the main interactions presented in the structure. During flow, chains slip with respect to each other and when the chains are branched or when they carry bulky substituents, their relative motion is made more difficult. The phenomenon of multiple melting in semi-crystalline polymers is well explained by a new model, where a thermodynamically metastable polymer system may start to reorganize to achieve lower states of free energy when it is perturbed by an increase of temperature. Such re-organization can happen through recrystallization of the metastable crystals initially formed at a low temperature to form thicker and more stable crystals[293].

The thermal behaviour of the analysed PHA agrees with earlier data on polyesters with similar composition as reported in literature[293]. PHBV in literature[293] has a Tm = 144°C and in this study the reported Tm are in the range from 160°C to 173°C (the results of DSC analysis are shown in Table 7.6-3).

The **Tm** parameter significantly affects potential polymer applications because it affects their processings[409] and it is essential for understanding the chemical recycling of polymeric materials[314]. A decrease in Tm is of great significance [316] since in particular, lower **Tm** makes the polymer better for a varied number of applications and.

The degree of crystallinity Xc is directly related to the processability and the industrial applications of PHAs[314]; crystallinity equal to or above 50% is considered high and detrimental for commercial and industrial purposes. Koller[42]suggests that 20% of a 3-hydroxyvalerate (3-HV) is required to reduce the crystallinity of the product (PHA) for most industrial applications. This is not necessary in this study once the majority of the PHAs exhibited much lower crystallinity than 50%[314].

PHAs are generally considered thermally stable at temperatures below 160°C, which corresponds with the values obtained in this study. Analysing and crossing the results obtained by TGA and DSC (Table 7.6-2 and Table 7.6-3), it is clear that PHAs begin to melt long before their degradation temperature (over 200° C). Thus, these polymers are suitable for different processing as extrusion or compression[306], can be easily moulded by injection and are applicable to blown film processing confirming usefulness of produced PHA in many industrial applications.

Table 7.6-3 DSC results of Commercial PHA and PHAs coming from PPB

PHA Sample	Tg [°C]	Tc [°C]	Tm [°C]	ΔHc [J/g]	ΔHm [J/g]	Xc [%]
Commercial PHA	5	117	173	52	56	3

Standard_extraction_Ac\MeOH purification	3	114	168	56	59	2
Ac\MeOH Pretreatment_No purification	3	88	160	46	57	8
EtOH Pretreatment_ Ac\MeOH purification	-1	115	167	80	85	3
Ac\MeOH Pretreatment_ Ac\MeOH purification	2	109	166	63	74	7

7.6.2.3   *Gel Permeation Chromatography (GPC)*

Polymer molecular weight determines various physical properties such as melt viscosity, tensile strength, toughness, thermal behaviour, chemical resistance, and weatherability. Universally, higher molecular weights are associated with higher physical properties whereas, lower molecular weights are associated with lower properties. During polymerization after a certain molecular weight is reached, the increase in properties plateaus off, since additional increase in molecular weight does not improve mechanical performance of the polymer. Larger molecular weight polymers demonstrate higher viscosity, reducing the melt flow characteristics making the melt-processing difficult[264,410].

The molecular weight average number (Mn) measuring system requires counting the total number of molecules in a polymeric unit mass irrespective of their shape or size. This means all molecules are treated equally. This kind of measuring system is required in cases where certain properties are dependent only upon the number of molecules or repeating units and not upon their weight or sizes. Average molecular weight (Mw) measuring system includes the mass of individual chains, which contributes to the overall molecular weight of the polymer. It is based on the fact that bigger molecules contain more mass than smaller molecules[366,410,411].

The polydispersity index (PDI) is a measure of the broadness of a molecular weight distribution of a polymer, and is defined by[410]:

$$PDI = \frac{Mw}{Mn}$$

The larger the polydispersity index, the broader the molecular weight. A monodisperse polymer where all the chain lengths are equal (such as a protein) has an Mw/Mn = 1[410].

The gel permeation chromatography permits to calculate the molecular weight of the extracted polymer. In Table 7.6-4 Mn, Mw and the PDI of the pre-treated and not pre-treated extractions are reported. These results are compared to those of commercial PHA (TianAn ENMAT Y1000), with a Mn of 590 kDa as reported in the data sheets.

Table 7.6-4 GPC results of PHAs coming from PPB.

	Mn [KDa]	Mw [KDa]	PDI
EtOH Pretreatment_ Ac\MeOH purification	512	369	7.2
Ac\MeOH Pretreatment_ Ac\MeOH purification	328	952	2.9
Ac\MeOH Pretreatment_No purification	159	641	4.0

From the GPC results appear evident that all the molecular weights of the samples are very high. For this reason, their thermal properties are not very different from those of commercial PHA, with the exception of **Ac\MeOH Pretreatment _No purification.** Crossing the GPC results and the thermal behaviour, the lower Mn of the **Ac\MeOH Pretreatment _No purification** sample causes a lower value in Tc and Tm respect to all the other samples. For all the other polymers, the small differences in Mn do not cause very valuable differences in the thermal properties, in fact Tg and Tm are still comparable with the Commercial PHA. The most interesting result is the values of PDI: all the samples show values higher than 2, which imply that as the PDI value increases the heterogeneity in cross-linking, network formation, chain length, branching, hyper branching are with a more random arrangement[412,94,207].

7.6.2.4   *Nuclear Magnetic Resonance (NMR)*

To discern the PHA microstructure of the polymers obtained from PPB biomass, ^{1}H NMR (Figure 7.6.2, Figure 7.6.3, Figure 7.6.4) is used to determine the nearest chemical structure and the level of purity. From the spectra also the type of polymer chain can be determinate as well as the ratio between hydroxyvalerate (HV) and hydroxybutyrate (HB).

All the spectra present a peak at the same ppm and with similar. It is reasonable to assume this peak as an impurity of the solvent because this peak is present also in the sample of commercial PHA, which has been used as a reference for its purity.

The peak integration uses the peak of the solvent (CDCl3) at 7.29 ppm as calibration reference. ^{1}H-NMR spectrum of Commercial PHA indicates three characteristic signals for PHB homopolymer: a peak at 1.25 ppm for a methyl group coupled to a proton; doublet of quadruplet at 2.58 ppm for a methylene group neigh- boring an asymmetrical carbon atom with a proton; and multiplet at 5.27 ppm characteristic of the methylene group (Figure 7.6.2). These results confirms that commercial PHA is composed by PHB as found in literature[265] .

The spectra of extracted polymers are different: they present two single peaks with different heights in the range between 0.9 and 1.4 ppm, which indicates two different types of methyl group in different ratio. The triplet at 0.9 ppm is the -CH3 of HV and the other corresponds to HB. Moreover, there is also another peak at 1.6ppm, which is the CH_2 of the HV chain. Also the signals from CH_2 in α position are different because they come from two different monomers. At the same ppm small amount of water in all the extracted samples appears. In the region of 5.0 ppm, two different signals from CH appear, CH of HV at 5.2ppm and HB at 5.3 ppm.

The ratio between the height of all these signals permits to calculate the quantity of PHV and PHB in each polymer coming from PPB. Through this analysis also the presence of impurities can be estimated, confronting the smaller peaks with those of commercial PHA.

The only sample with a very different level of purity is **Ac\MeOH pretreatment_No purification** (Figure 7.6.3) one, which presents more peaks in the range between 1 and 2.8 ppm that can not be attributed to the PHA molecule.
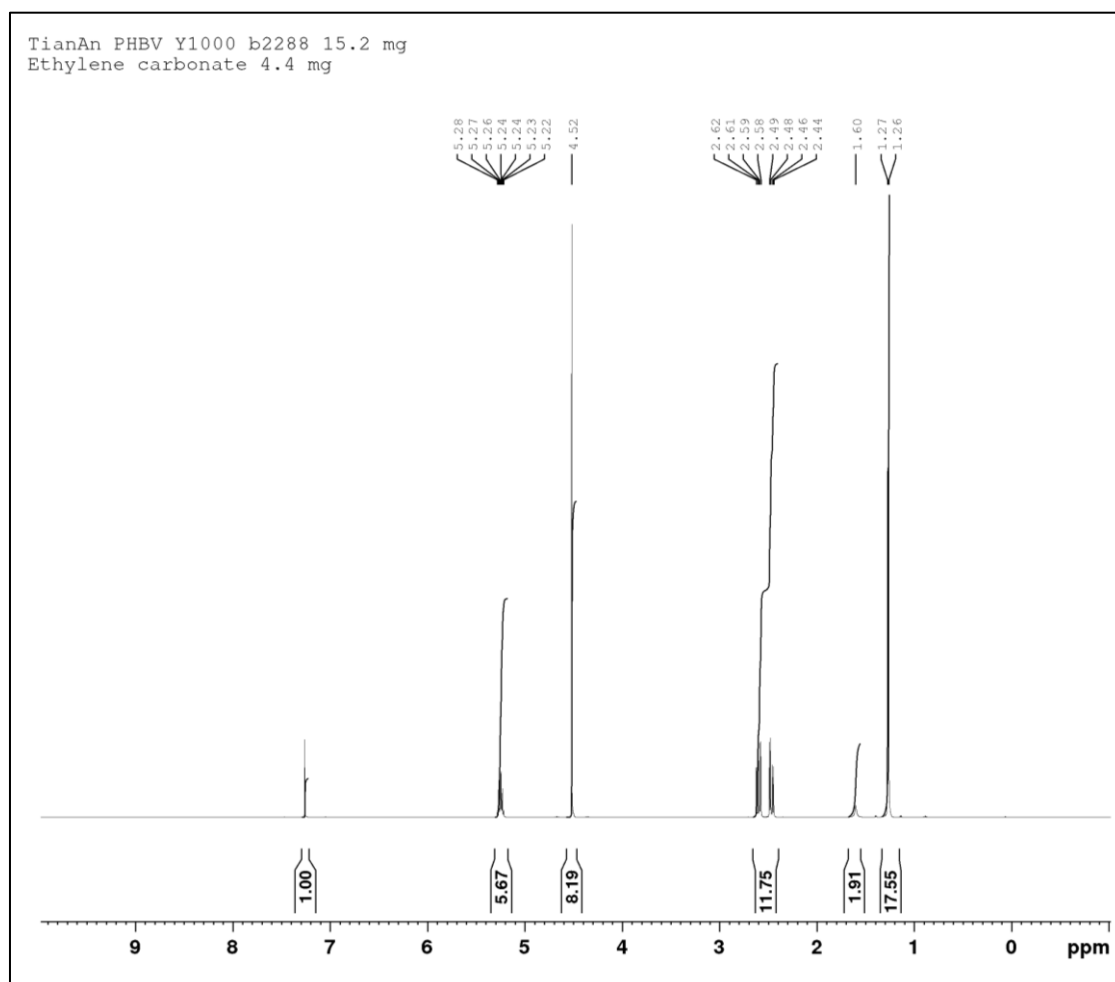
Figure 7.6.2 1H-NMR of Commercial PHA used as reference.

The analysis of the peaks integration permits to estimate the percentage of PHB and PHV in the polymers extracted from PPB biomass: the **Standard extraction_Ac\MeOH purification** and **Ac\MeOH pre-treatment_Ac\MeOHpurification** samples are composed by the 7% of PHV; **EtOH pre-treatment_Ac\MeOH purification** (Figure 7.6.4) sample has a lower amount equal to 5% and **Ac\MeOH pre-treatment_No purification** sample has 9% of PHV.

Crossing ^{1}H-NMR results with the previous analysis of GPC and DSC evidences that **Ac\MeOH pre-treatment_No purification sample** (Figure 7.6.3) presents the lowest thermal properties due to the low molecular weight and the presence of impurities, which affect also the mechanical properties of the polymers. All these reasons made **Ac\MeOH pre-treatment_No purification sample** not suitable for the realization of composites because thermal characteristics are crucial in polymer processing[68-81].

In fact, **Ac\MeOH pre-treatment_No purification** sample has the highest percentage of PHV (9%) respect to the other samples. This highest percentages, joined to the value of Mn, justify the low thermal properties of the polymer: the presence of more side chains of PHV causes higher value of Tg, even if the Mn is the lowest, making the molecular structure more compact and flexible (rotations are permitted) respect to the other samples. Indeed, also the value of Tm is the lowest (160°C) due to the molecular flexibility and the length of the chains.

Also in the other samples the presence of PHV affects the thermal characteristics of the polymer: **Standard extraction_Ac\MeOH purification** and **Ac\MeOH pre-treatment_Ac\MeOHpurification** samples are composed by the 7% of PHV and presents very similar thermal behaviour in terms of Tg (3°C and 2°C respectively) and Tm (168°C and 166°C, respectively). **EtOH pre-treatment_Ac\MeOH purification sample** with only the 5% of PHV and the highest Mn, has the highest thermal performances and PDI. All these characteristics give better mechanical performances according to literature[68, 208–84]
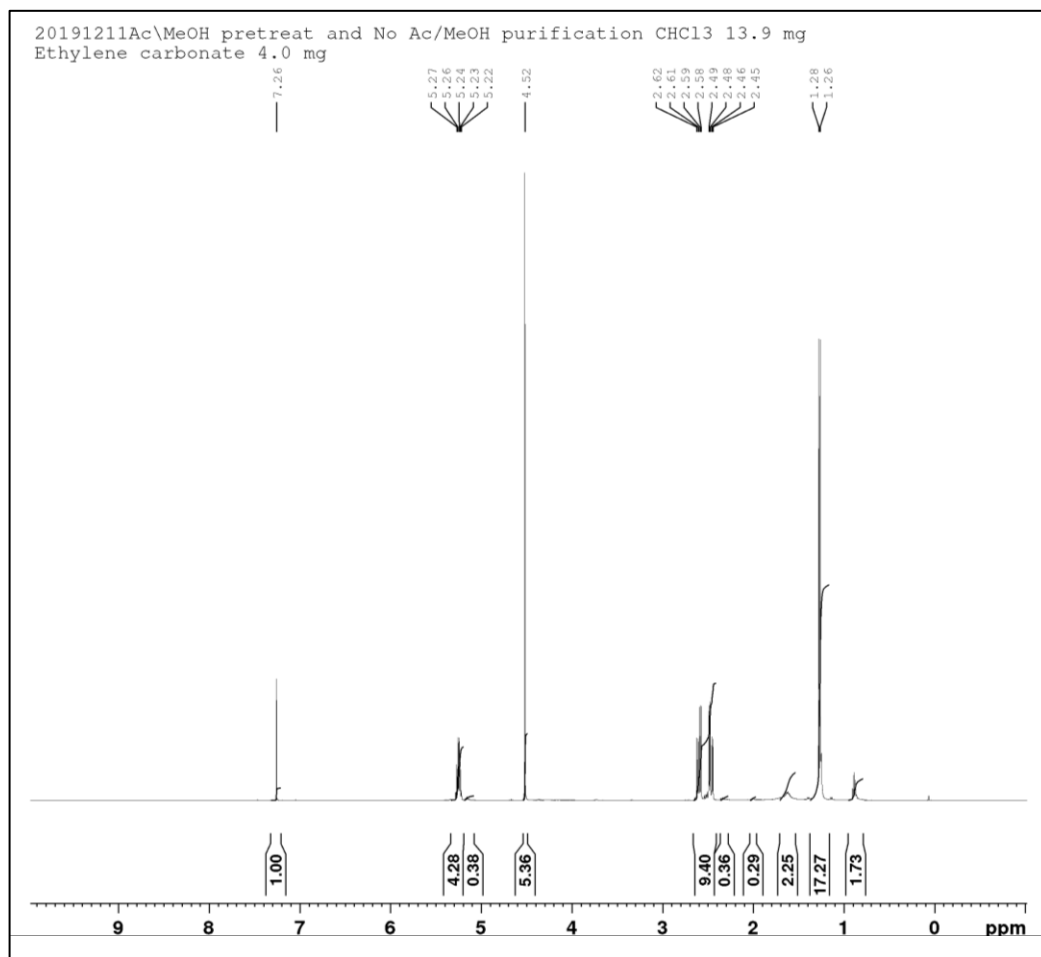
Figure 7.6.3 ¹H-NMR of Ac/MeOH pretreatment_No purification

Crossing all the results obtained from polymers extracted from PPB, the extraction using boiling Ethanol appears to give the best results in terms of degradation temperature (Td=272°C), maximum decomposition temperature (about 10°C higher than the other polymers), Tg (-1°C), Mn and PDI, which make the polymer suitable for the production of composites. Moreover, these conditions permit to achieve the 70 % of the yield, which is 30% higher respect to the others.
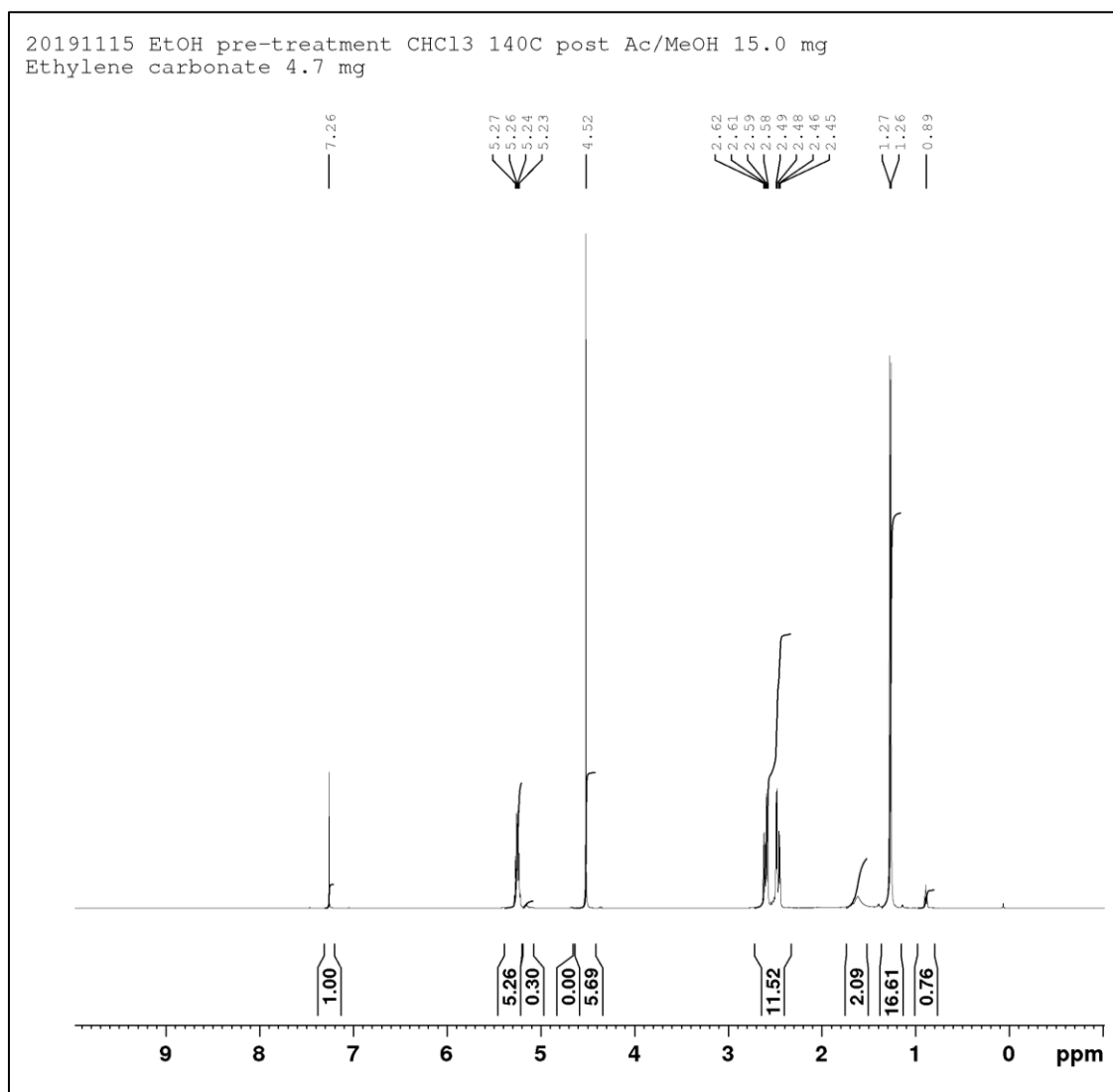
Figure 7.6.4 ^{1}H-NMR of EtOH pre-treatment_Ac/MeOH purification

At this point of the study, several extractions have been carried out following the same protocol used for **EtOH pre-treatment_Ac\MeOH purification** with a Paar Reactor of 1.5 L in order to obtain enough polymer to realize composites made with PHA from PPB.

7.6.3   Composite characterization

In Table 7.5-3 all the formulations of the different composites are reported and in Figure 7.6.5 the composites are shown. For the author's knowledge it is the first time that PHA from PPB has been used to realized composites in association with wood flour.

(a)   (b)

(c)   (d)
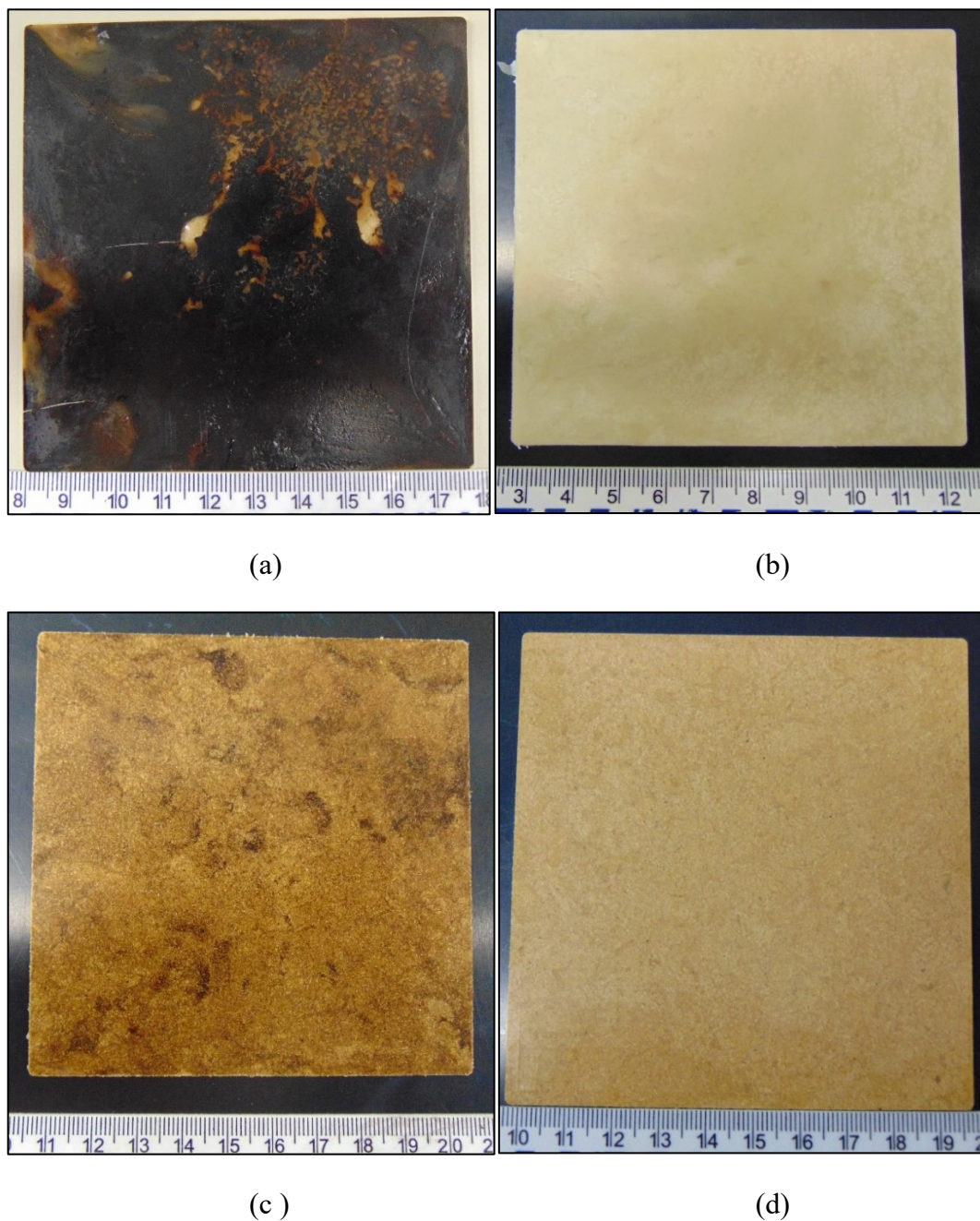
Figure 7.6.5 Compression moulded composites: a)100%PHA from PPB (RP_Pm); b) 100% commercial PHA (CP_Pm); c)70% PHA from PPB and 30% of WF (RP_30WF_Pm); d) 70% commercial PHA and 30% of WF (CP_30WF_Pm)

The four composites have a different appearance (as shown in Figure 7.6.5), especially RP_Pm. The dark colour of the composite is due to the presence of impurities as carotenoids. The presence of wood in the matrix permits to have a more homogeneous colouration in the composites, nevertheless, it is always darker respect to the commercial series (CP_30WF_Pm). For the characterization of the composites, small samples have been cut in the homogeneous parts, making sure to avoid the inhomogeneous or defected parts of the sample (as the small hole in RP_Pm). For the determination of the homogeneous parts, the thickness of each specimen has been measured with a calliper and the samples for tensile test have been cut where the thickness was constant.

Figure 7.6.6, Figure 7.6.7 and Figure 7.6.8 reports the tensile strength, Young's modulus and strain at break of all composites. The bars in the tensile strength, Young's modulus and strain at break indicate the minimum and the maximum value. Data are presented as box plots indicating the maximum, 3rd quartile, median, 1st quartile and minimum value among five duplicates. The mean values are noted in text on the top of each box.
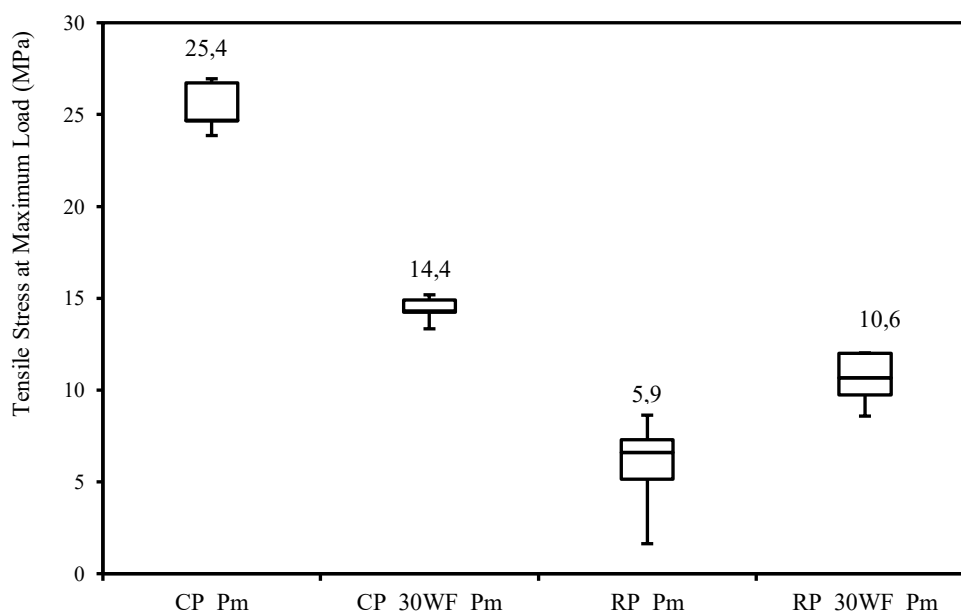
Figure 7.6.6 Tensile stress at maximum load of PHA composites
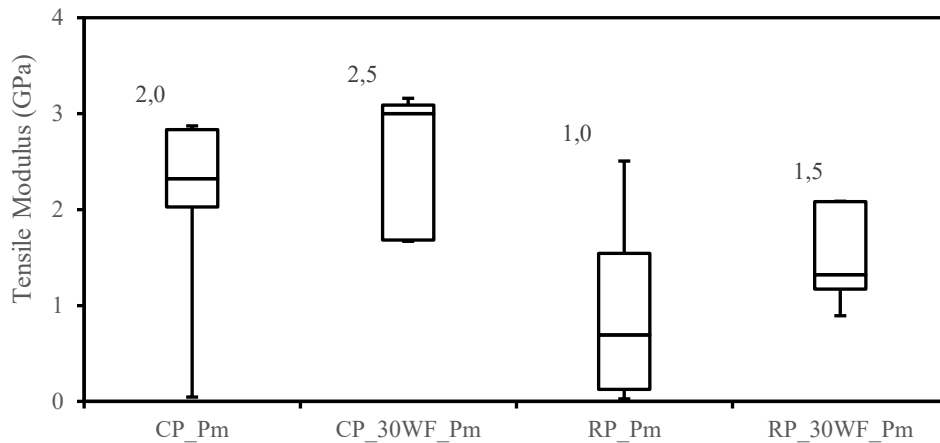
Figure 7.6.7 Tensile modulus of PHA composites
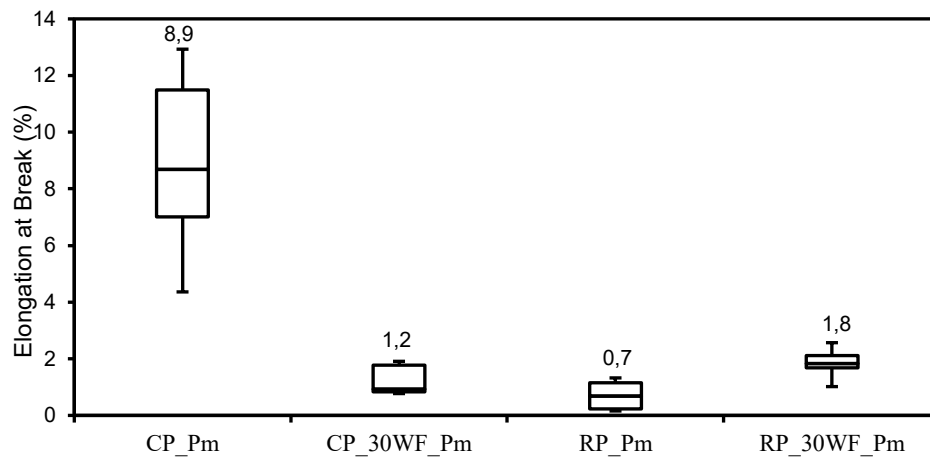
Figure 7.6.8 Elongation at break of PHA composites

The origin of the polymer and the filler largely influence the mechanical performances of composites[343,247,356]. Studies demonstrate that shape, size or chemical composition of the fibres affect the interaction between the waste and the matrix[88,343]. WF is in form of fibres (300μm) and in compression moulding where fibrous fillers are well distributed, not disturbed or oriented during processing[88] this shape enhances the mechanical properties in the composites[415]. Considering the chemical structure of the reinforcing material, the percentage of cellulose, hemicellulose and lignin can affect the stiffness and strength of the material[416,144,115].

Comparing the effect of WF on the composite made with commercial PHA, a reduction of the mechanical properties in terms of tensile stress, Young's modulus and elongation at break respect to the reference for this series (CP_Pm) as shown in Table 7.6-5:

Table 7.6-5 Resume of Tensile test results

	Tensile stress (MPa)	Tensile Modulus (GPa)	Elongation at break (%)
CP_Pm	25.4	2	8.9
CP_30WF_Pm	14.4	2.5	1.2
RP_Pm	5.9	1	0.7
RP_30WF_Pm	10.6	1.5	1.8

According to literature, fibrous fillers added to PHA gives better performances in composites, thanks to the "bridging effect" of the fibres[338,417]. Fibres with higher stiffness than the matrix increase the modulus of the composites, but generally fillers cause a dramatic decrease in the elongation at break. If the adhesion between the reinforcing material and the matrix is good, a decrease of the elongation at break, even with small amounts of addition, can be expected. On the other hand, if the adhesion is poor, the elongation at break may decrease more gradually[418]. In this study the elongation at break is almost the same for the reinforced composites.

In Figure 7.6.9, Figure 7.6.10 and Figure 7.6.9 the cut section of the 4 composites are shown. The specimen with 100% commercial PHA (CP_Pm) presents a different morphology compared with the one made with 100% of PHA coming from PPB (RP_Pm). CP_Pm (Figure 7.6.9) appears more compact and with a rigid and homogenous structure; nevertheless, the surface (Figure 7.6.11) is wrinkly due to the polymer processing. The defects are typical of a high temperature and high pressure process and usually they can be avoided gently increasing the pressure. For the production of the other samples this principle was considered, in fact the surface of the composite with the inclusion of WF does not appear wrinkled anymore, but smooth even with the presence of voids. The presence of voids is caused by more factors: the principal one is the possible segregation of the fibres[88,93].

RP_Pm (Figure 7.6.10) appears homogeneous but the structure of the composite in the cut line seems to be very fragile and easily crumbling. This differences in the morphological structure are due to the purity level of the composites, in fact RP_Pm presents various impurities caused by carotenoids and inorganic compounds. In this case, the surface is very smooth (Figure 7.6.12), but some defects are still present (as small particles that can act as crack propagator). The presence of impurities or imperfections very common in semi-crystalline polymers, influences the deformation behaviour of polymers[84,85].

The GPC results of the composites (Table 7.6-6) show a large decrease in the molecular weights compared to the extracted polymer (Table 7.6-4) caused by the polymer processing. A reduction in molecular weight, which is about 313 kDa for RP_Pm and 290 kDa for RP_30WF_Pm affects the mechanical performances of the composite: in fact low values of ductility and fracture energy is seen for low-molecular-weight polymers[371]. Also the PDI is reduced from 7.2 for the **EtOH Pretreatment_ Ac\MeOH purification** sample to approximately 2 for all the composites.

Table 7.6-6 Results of GPC analysis on the composites.

	Mn (g/mol)	Mw (g/mol)	Mz (g/mol)	PDI
CP_Pm	77381	144155	237460	1.86
CP_30WF_Pm	74942	150827	260499	2.01
RP_Pm	29039	55859	98898	1.93
RP_30WF_Pm	41357	76133	119577	1.84

This behaviour can due also to the differences in the purity level of the polymers and how WF and other residual substances in the biomass (as carotenoids or inorganic molecules for example) interact with the polymer matrix. The presence of impurities reduces also the thermal stability of the extracted PHA, in fact the GPC results of the composites shows a massive degradation after the melting process (< 60 kDa, when PHA loses mechanical integrity) compared to 150 kDa for commercial PHA. The presence of imperfection or impurities on the surface can affect the structure providing regions with relatively easy paths for crack propagation[419,310,418,345].

Confronting the two references made with 100% of polymer, it is undeniable that the commercial PHA outperformed the one extracted from PPB accumulation. In fact, the tensile stress at maximum load between the two samples has a difference of almost 20 MPa and the Young's modulus of CP is twice the one of RP. Also the elongation behaviour at the break point is totally different between the two samples: RP has an elongation of 0.7% and CP of 8.9%.
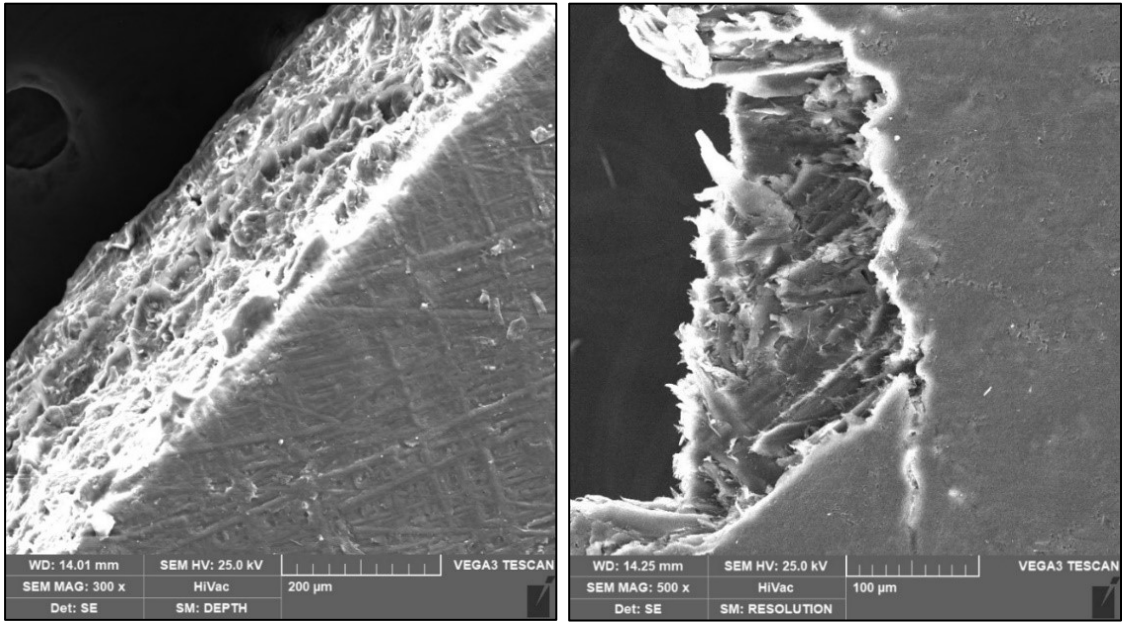
(a)   (b)

Figure 7.6.9 Cut-section of a)Composite made with 100% of commercial PHA (CP_Pm); b) Composite made with 70% of commercial PHA and 30% wood flour (CP_30WF_Pm);
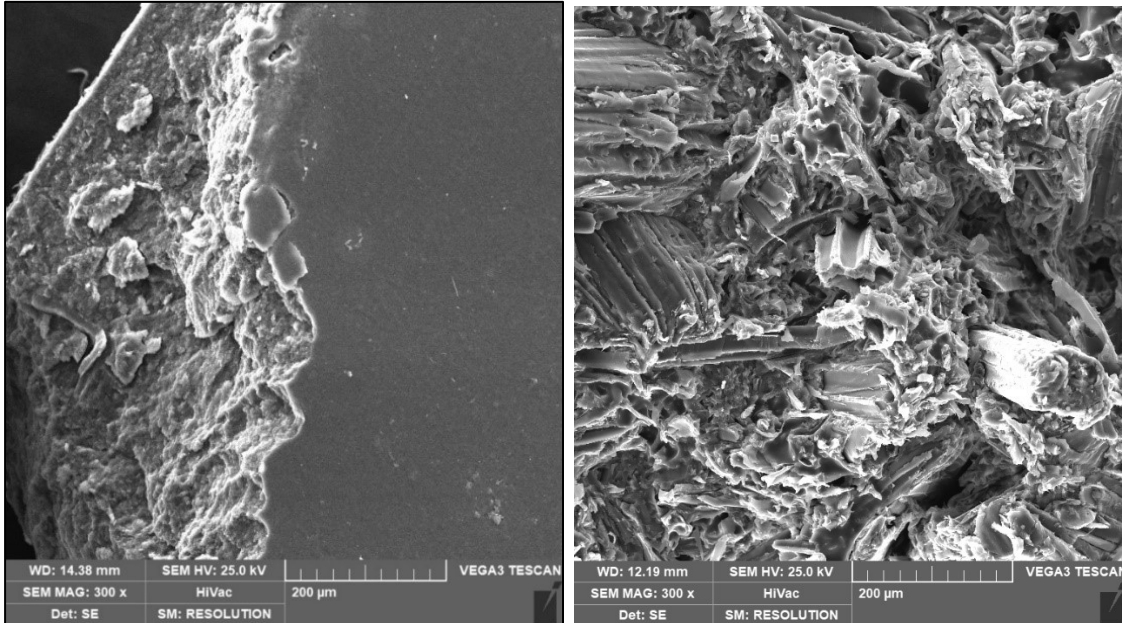
(a)   (b)

Figure 7.6.10 Cut-section of a) Composite made with 100% of PHA from PPB (RP_Pm); b) Composite made with 70% of PHA from PPB and 30% wood flour (RP_30WF_Pm);

(a)   (b)
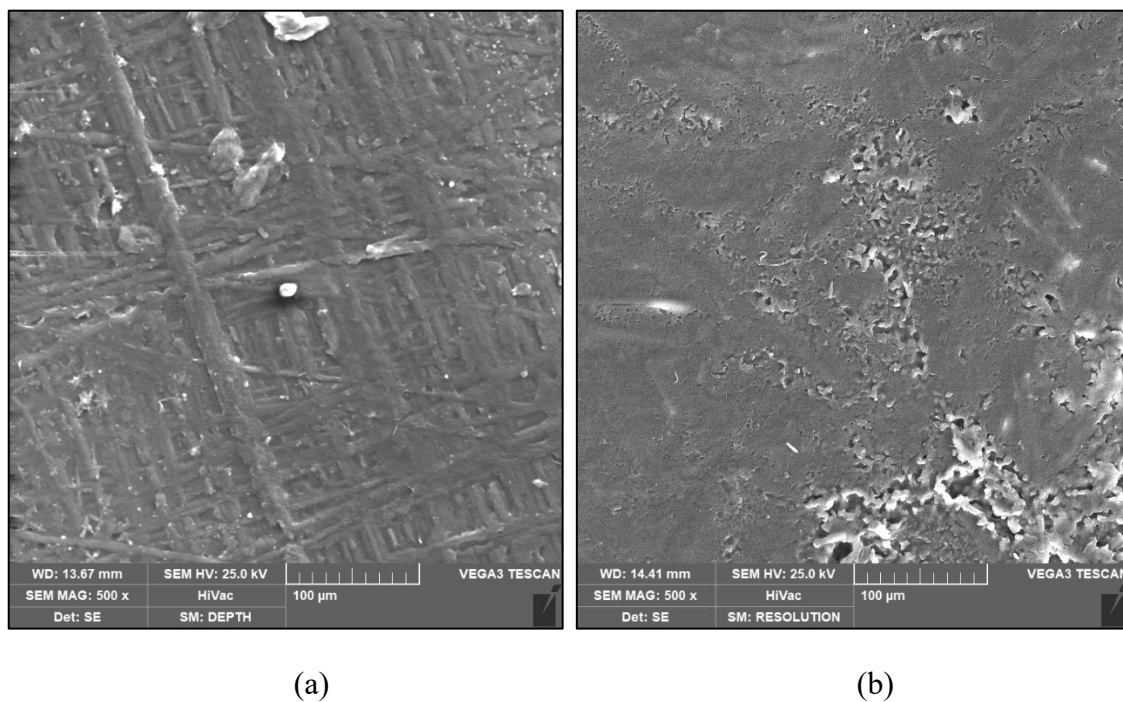
Figure 7.6.11 Surface of a)Composite made with 100% of commercial PHA (CP_Pm); b) Composite made with 70% of commercial PHA and 30% wood flour (CP_30WF_Pm);

(a)   (b)
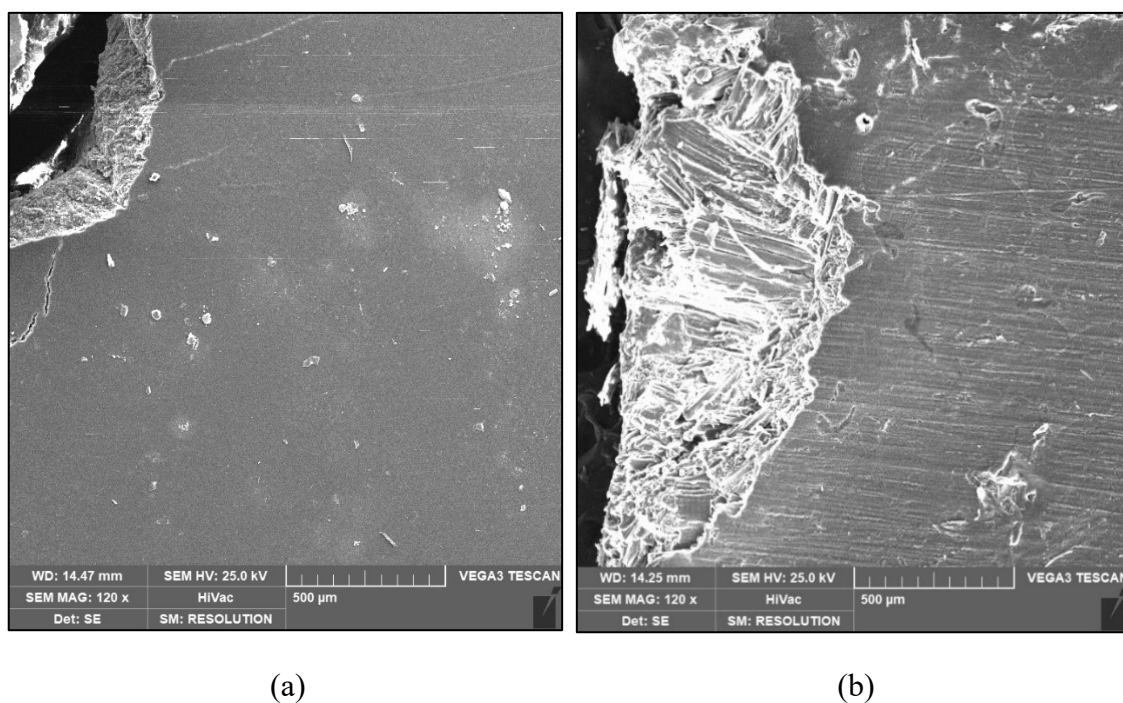
Figure 7.6.12 Surface of a) Composite made with 100% of PHA from PPB (RP_Pm); b) Composite made with 70% of PHA from PPB and 30% wood flour (RP_30WF_Pm);

For what concerns the addition of WF (Figure 7.6.12 and Figure 7.6.12) to the polymer, it is evident that the fibre has a reinforcing effect on the recovered specimen and an anti-reinforcing effect on the commercial PHA. There is good adhesion between the PHA matrix and the wood fibre surfaces in both composites; fracture paths have passed through the wood fibre in both cases[418].

The addition of fibres in CP_30WF_Pm caused a reduction in all the tensile properties compared with CP_Pm: tensile stress at the maximum load is equal to 14.4 MPa; the tensile modulus is 2.5 GPa and the elongation at break is equal to 1.2%. Nevertheless, in RP_30WF_Pm, all the mechanical performances increased thank to the bridging effect of the fibres[143,338,358] . This difference in the fibre effect can be caused by the interaction between fibre and matrix. In both of the samples fibres are well mixed, but in CP_30WF_Pm (Figure 7.6.10), their presence caused small voids (present also on the surface), which reduced the tensile strength of the composite. An increase in tensile strength, as happens to RP_WF_Pm, means that the stress has been transferred from the PHA matrix to the WF[418], so there is a better interaction between fibre and polymer .

The presence of impurities is confirmed by the EDAX analysis (Table 7.6-7).

Table 7.6-7 EDAX analysis on the composites

Element (%weight)	CP_Pm	RP_Pm	CP_30WF_Pm	RP_30WF_Pm
C	59.65	61.94	60.12	58.58
O	38.03	37.37	39.88	37.98
Cl	0.64	-	-	-
Na	1.68	0.2	-	1.41
K	-	-	-	0.22
P	-	-	-	0.5
S	-	0.49	-	0.53
Ca	-	-	-	0.37

The presence of carbon (C) and oxigen (O) is typical for organic compounds as natural fibres and biopolymer. Sodium (Na) in CP_Pm can be a residue of the polymer production, the purity level reported on the datasheet is (>98%). Chloride (Cl), in very small amount, can be a residue of the filmation process.

In PHA from PPB series, the presence of other elements as phosphorous (P) and sulphur (S) is remarkable probably due to impurities coming from the biomass. This confirms the reason for the low performances.

The processing conditions have a great effect on the mechanical properties of PHA composites and on the molecular weight. After special treatments, highly orientated crystals can be formed to enhance the mechanical properties of scl-PHA[420]. In this study, the two polymers had notable differences: the ethanol pre-treatment and the presence of residual substances[421] influence the chemical and physical properties of the extracted polymer as the feeding during accumulation, as reported in literature[264,422]. All these factors, influencing the cross-linking bonds between the polymer chains and the chemical structure of the waste (mainly cellulose and lignin), determine a different behaviour of the composite, also conditioned by the physical form of the wasted material[345].

TGA curves (Figure 7.6.13, Figure 7.6.14, Figure 7.6.15, Figure 7.6.16 and Table 7.6-8) show that the thermal degradation of the composite combines the thermal degradation of WF and PHA. The processing conditions affect also the thermal behaviour of the composites with shifted peaks respect those of PHA from PPB and the commercial reference. Tg and Tm increase for all composites, probably due to the presence of the reinforcing material (Table 7.6-2 and Table 7.6-3). The shift of Tc towards lower temperature indicates that crystallisation is occurring with a higher under-cooling energy (driving force). A short difference between the starting and the ending temperatures of crystallization peaks mean that a shorter time is needed for the completion of crystallisation, which can be caused by the mould. Also the Tg value depends on the degree of crystallinity and typically increases with crystallinity due to less mobile polymer chains: in this case, the observed higher Tg may be due to the addition of WF and to the process conditions, which influences the PDI of the composites and molecular weight[356].

In CP_Pm and RP_Pm Td is 275°C and 276°C respectively, whereas in the composites including the fibres is 272°C and 271°C.

The exothermic peaks (green lines in Figure 7.6.13, Figure 7.6.14, Figure 7.6.15 and Figure 7.6.16) are related to the decomposition of the polymer: in CP_Pm the decomposition occurs in two stages at 291°C and at 306°C, with a final residue weight less than 2% at 1000°C. Three recognizable peaks are present in all the reinforced composites, corresponding to the thermal degradation of PHA, lignin and cellulose typical of wood-PHA composites. Generally, lignin onset temperature is reported in the range 200°C - 400°C. During thermal decomposition of lignin, relatively weak bonds break at lower temperature whereas the cleavage of stronger bonds in the aromatic rings takes place at higher temperature. Thus, when the lignin content is lower, the degradation begins at a higher temperature, but the fibres do not have the oxidation resistance given

by the aromatic rings in the lignin[378]. The range of cellulose decomposition is set at higher temperatures, usually from 350°C to 520°C[325].

In Table 7.6-8, CP_30WF_Pm and RP_30WF_Pm samples, in addition to the typical PHA peak of maximum degradation around 280°C, have two further peaks: at 325±5°C and over 400°C, which respectively correspond to the lignin and cellulose contained in the fibres as reported in literature[325,423].

Table 7.6-8 Results of TGA on the composites

PHA Sample	Tg [°C]	Tc [°C]	Tm [°C]	Td [°C]	T1 [°C]	T2 [°C]	T3 [°C]	Endo-Peaks [°C]	Exo-Peaks [°C]
CP_Pm	3	123	175	275	298	-	-	177	291
									306
RP_Pm	3	82	154	276	293	-	-	166	292
			168					180	300
									304
									351
									471
CP_30WF_Pm	4	120	172	272	287	327	421	181	277
									283
									296
									334
									456
RP_30WF_Pm	4	87	160	271	279	320	441	162	274
			172					172	281
									294
									322
									450

Studying the exothermic peaks of DTG (green lines in the graphs), the decomposition temperature of each components of composites can be recognized: the typical decomposition of PHA occurs at 290°C and 305°C; hemicellulose at 250-350°C[380] and some of its polysaccharides at 270°C; lastly lignin from 400°C to 500°C.

The same components are present also in coffee grounds but being in different amounts some values are shifted. In Figure 6.7.19 and Figure 6.7.20, the peak at 170°C indicates the thermal degradation of tannins and other carotenoids[353,391,406,424].

The endothermic peak around 177°C for CP_Pm indicates the melting temperature. In samples containing PHA from PPB a peak at lower temperatures, around 165°C, appears due to some impurities left by the extraction process.

Exothermic reactions generally indicate decomposition processes and, in this case, five peaks generally appear: the exothermic peaks of PHA in samples without WF are at 290°C and 300°C. In samples containing WF, the two peaks are approximately at 275°C and 280°C. Previous studies[423,380,426] on wood components report exothermic peaks caused by hemicellulose and lignin, respectively at T ~ 295°C, T = 300°C -350°C and 450°C. Lastly, the sample RP_Pm presents three peaks at 304°C, 351°C and 471°C, which can be attributed to some components used as feedstock of the biomass during the accumulation process, as butyric acid, propionic acid, acetic acid and cellulosic residual components[427–429].
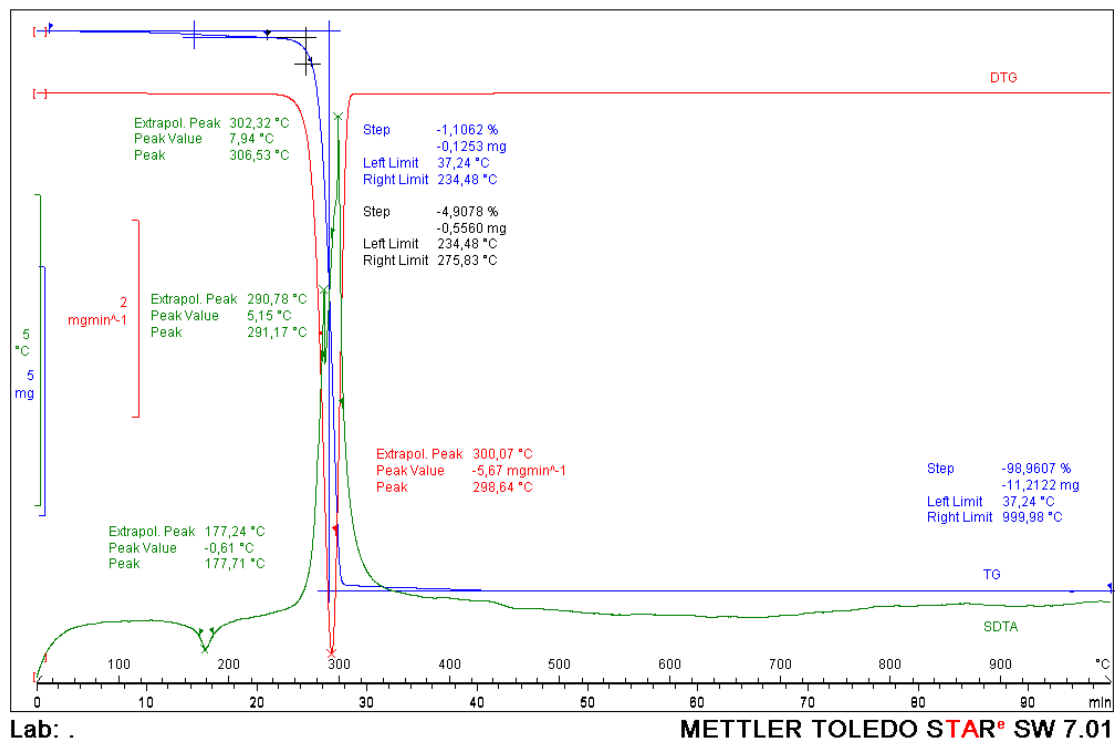
Figure 7.6.13 TGA of CP_Pm
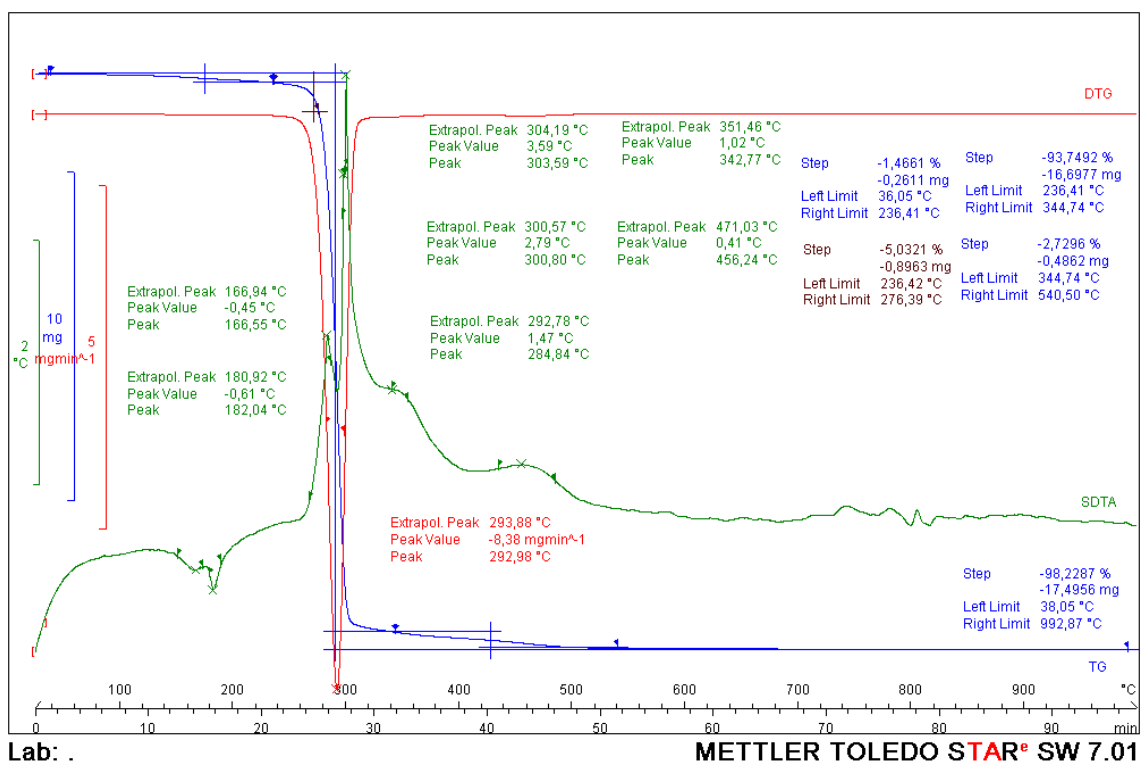
Figure 7.6.14 TGA of RP_Pm
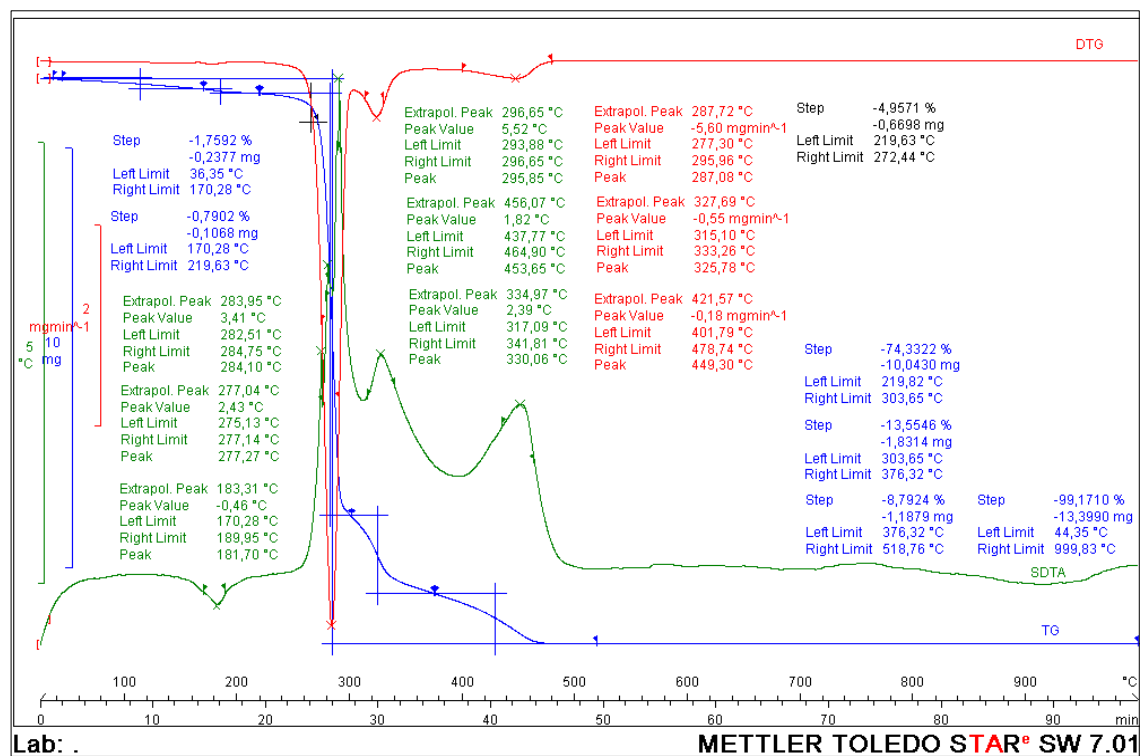
Figure 7.6.15 TGA of CP_30WF_Pm
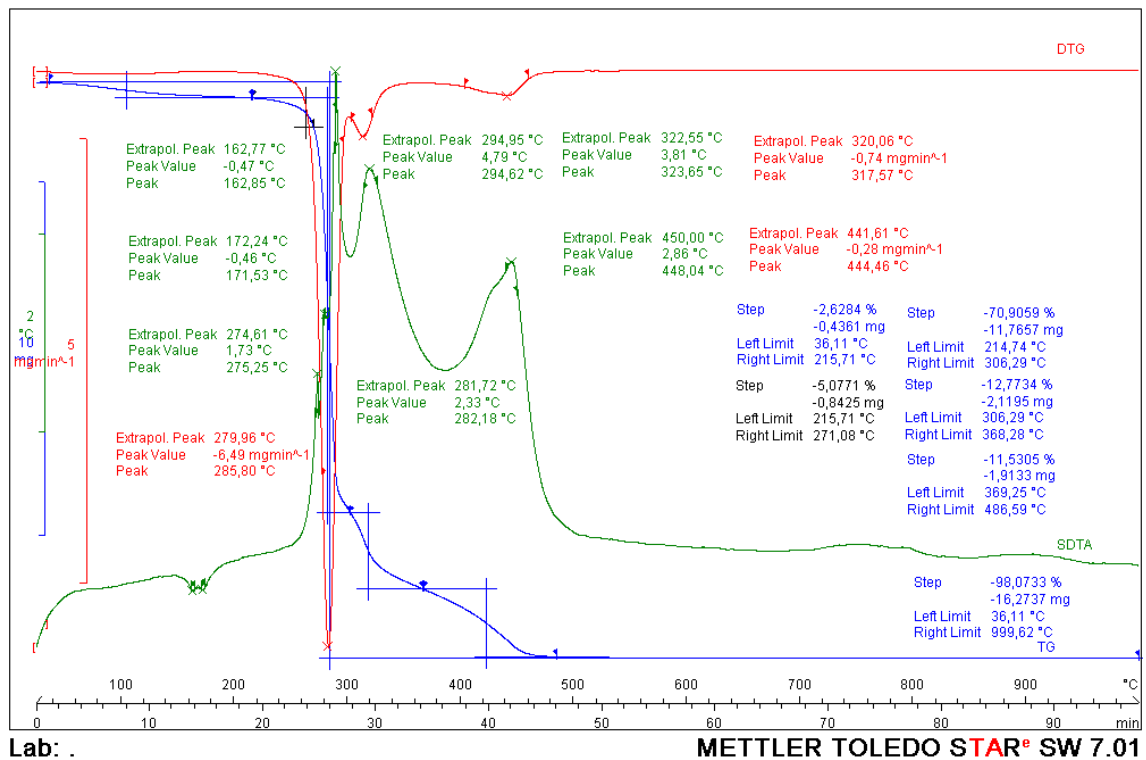
Figure 7.6.16 TGA of RP_30WF_Pm

7.7   **Conclusion**

In this work the possibility to use polyhydroxyalkanoates extracted from a biomass containing purple phototrophic bacteria for the realization of wood composites is explored.

In the first part of the study, different types of extractions have been considered in order to choose the best process in terms of yields, purity and quality of the polymer. Various solvents and pre-treatments have been considered and compered in order to recover not only the polymer, but also other important compounds contained in the biomass, as carotenoids. The extracted PHAs have been characterized to determine their chemical and physical properties and to decide the best extraction parameters to apply in a larger scale (from 100ml up to 1.5 L) in order to collect enough polymer for the composite production through compression moulding.

A pre-treatment based on boiling ethanol has been selected for its low cost, green properties and sustainability characteristics. The extracted polymer from the selected process has a Mn of 512kDa, PDI equal to 7.2 and composed by 5% of PHV as revealed by the[1]H-NMR analysis. From TA, its Tg is at -1 °C and Tm at 166 °C, with a Td at

272°C and the maximum decomposition at 292°C, which make the polymer suitable for compressing moulding application.

The second stage of the study consisted in the realization of composites with one of the more common Australian industrial waste (wood flour), chosen in a circular economy perspective. In order to evaluate the influence of the polymer origin and the reinforcing effect on the performances of the product, two series of composites have been made with commercial PHA and PHA from PPB. As expected, these two parameters are essential for the tensile characteristics. Indeed, the type of filler, the chemical composition and the interaction with the polymer matrix have an important impact on the performances of the composite. The four composites have been characterized in terms of mechanical properties, thermal behaviour and morphology. Our results show an increase in the mechanical properties of the composites containing wood flour and PHA from PPB, with performances comparable to commercial composites with the same formulation.

The added fibers have a reinforcing effect for the sample coming from PPB (RP_30WF_Pm), but a negative effect for the sample containing commercial PHA (CP_30WF_Pm). The addition of fibers permits a "bridging effect" in the first sample, bringing the tensile stress from 6 MPa of the respective reference to almost 11 MPa. In the other sample, the fibers caused the formation of voids, which reduced their mechanical properties from 25 MPa to 14MPa. The mechanical properties have also been influenced by the manufacturing thermal process of the various composites where the polymer can be subjected to thermal degradation, that causes a decrease in molecular weight (as confirmed by the GPC analysis). The thermal properties of the composites depend on their composition, however the samples deriving from PPB had comparable thermal stability as the others (Td at 275°C for the 100% PHA composites and at 272°C for the wood-composites).

Further research might explore the optimization of the process during the extraction and the polymer manufacturing. This would allow a full investigation of the extraction and processability properties of PHA from PPB: the use of substrates coming from non-pure cultures would permit to recover more components (i.e. carotenoids) and reduce the cost for the maintenance and feedstock of the culture. It is also attractive to further explore other greener solvents in order to reduce the environmental impact of the extraction procedure. Lastly, also improving the composite toughness using fillers from other origins could be investigated.

8 . Chapter LCA of the extraction protocol of PHAs from WWTPs

Life Cycle Assessment of the protocol used for the extraction of PHAs from biomass coming from wastewater treatment plants.

8.1   Introduction

This chapter examines the extraction procedure presented in Chapter 5, where different mechanical pre-treatments are applied on a biomass coming from wastewater treatment sludge composed by mixed microbial culture (MMC).

It is focused on the evaluation of the efficiency of the process in terms of greenhouse gases (GHG) emissions, expressed as equivalent mass of CO_2 (CO_2 eq.), under a life cycle assessment (LCA) approach.

This study analyses how the application of different pre-treatments on the substrate could reduce the environmental impact, particularly global warming potential, of PHA's extraction with chloroform. Therefore, a short presentation of advantages and disadvantages of all the considered cases is described with a *reduction-in-CO_2 eq.-emission* perspective of the process.

In this Chapter the extraction in continuous (named as Soxhlet in Section 5.7.2.2) has not been considered due to the difficulties on the applicability of this technique in industrial processes. The environmental issues in the production of bioplastics and all the variables to consider are presented. Also a modelling of the extraction process with the description of the mass-energy balance is proposed. In the methodology section, the two main cases with the various scenarios of pre-treatments are described in detail with the power demands of each single step. Lastly, the results are discussed reporting the GHG emissions of each scenario in kilogram of CO_2 equivalent per gram of PHA and the reduction of emissions compared to the standard extraction. The same labelled of Chapter 5 is used in this Chapter.

8.2   Environmental issues and bioplastics production

Climate change, global warming and greenhouse gases have become common terms in everyday life due to their impact on the planet and on human health. Despite rising prices and apparent depletion of resources, fossil fuel consumption has increased and led to higher GHG emissions, thus contributing to global warming[430].

It is well known that conventional plastics derived from the fossil fuels pose a threat to the global environment due to their non-degradable nature and their large applicability sectors. Application of plastics in regular life is inevitable[431], so problems associated with global warming and solid waste management has generated interest in the development of novel plastics. For these reasons, biopolymers have become the new frontier of polymer science.

In fact, biopolymers are renewable, largely biodegradable and can have very similar properties to conventional polyolefin polymers. Conventional plastics are produced from fossil fuels and resource depletion may become a determining factor in future production. Since biopolymers represent a possible solution to the problem of conventional plastics, it is also essential to understand their environmental impact before the total replacement. Indeed, sometimes the environmental benefits that could occur in replacing conventional polymers with biopolymers may however come at an economic loss[432] and, sometimes, also the production of biopolymers might have a considerable environmental impact.

Cost of bioplastics serves as a hindrance to the development of bioplastics for food and drink packaging as happens for the conventional plastic. This is due to large consumptions and also to the fact that biopolymers are produced by harvesting natural resources. Therefore, the final application of the bioplastic should be also evaluated: for biopolymer as hygienic packaging, hygienic standards must be respected, which normally require high costs. For all other types of packaging, the use of biopolymers deriving from agricultural waste or other sources is generally allowed, and this usually reduces the overall cost of the product. As in the case of the production of petroleum-based plastics, for the production of biopolymers large sums of energy are needed, as electricity and heating, that consume non-renewable sources.

Thanks to their degradation properties, the use of bioplastics reduces the waste accumulation on the areas surrounding us. Moreover, their degradation does not produce any toxicity to the environment and no harmful gas is emitted thus no greenhouse gas and no global warming. They can be considered as a real environment friendly product[433]. For this reason, researchers are focusing on new production methods that involve the use of secondary products such as biomass to be used as substrates instead of pure culture[41,46,263,434,435]. One of the most interesting sources for the production of biopolymers are bacteria in wastewater plants[13,18,28,29,75,262]. As largely introduced, during the last years wastewater treatment plants (WWTPs) have moved from the concept of 'waste treatment', aimed at discharging treated wastewaters. The recovery of by-products from WWTPs can generate value-added products such as renewable energy, biofertilizers and water for different purposes, which are new resources. The recycling of resources through innovative recovery processes is only a recent objective in wastewater treatment systems and makes the processes of the plants more efficient: it reduces the amount of waste and it provides environmental and economic benefits[13]. In this context, resource recovery from wastewater treatment processes can have a role also in the plastic's circular economy[28].

Among the various biodegradable plastic available, PHAs are considered strong candidates as they have very similar properties to synthetic polymers[11,241,436,437], but they degrade completely to water and carbon dioxide under aerobic conditions[267].

Commercialisation of PHAs is still in its early stages, and although its global production capacity is one of the fastest growing amongst biopolymers, small capacities and volumes are associated with relatively higher costs, which makes it challenging to compete up-front on just price with petroleum-based plastics that are produced on a very large scale[438] As a relatively new family of polymers, PHAs need to gain further end-user acceptance and grow their own market, including for target/niche applications. Potential applications for PHAs include, consumer goods, agriculture, packaging, furniture, and personal care products[11].

The use of mixed microbial cultures (MMC) present in waste waters is promising because it will help to reduce the production costs of PHAs, since MMCs do not require sterile conditions and have a wider metabolic potential than single strains. This allow them to utilize a large number of cheaper substrates such as wastes , that avoids the use of expensive carbon sources[28]. This is one of the key points to enhance the production of biopolymers as PHAs.

Besides, downstream PHA recovery technologies significantly affects the overall process economics and its environmental sustainability since traditional extraction methods mostly employ halogenated solvents (as chloroform)[271]. The challenge in the recovery process is to achieve, in a cheap and environmentally friendly manner, a high recovery efficiency and a high degree of purity of the extracted polymer but, maintaining at the same time its molecular weight and thermal and mechanical properties[272]. Nevertheless, the use of green solvents does not permit to achieve the same extraction yields of chlorinated solvents (as discussed in Chapter 7), so the use of disrupting agents (chemical and physical) is very common in order to modify the cell wall permeability[23–27].

This study analyses, from a life cycle assessment (LCA) approach, how the application of different pre-treatments (sonication, bead milling, homogenization through pressure and blades) on the substrate could reduce the environmental impact of PHA extraction with chloroform in terms of global warming potential. This research is based on previous studies in laboratory scale presented in Chapter 5 and this preliminary analysis of potential environmental impacts can provide useful information to better orient the development and scale-up phases.

The LCA of the process is extremely important to correlate and estimate the possible environmental impact of the procedure, because the improvement of the efficiency can involve an increase in variables (such as electricity) that may cause an increment on the environmental impact increasing the level of GHG.

A large part of global climate change and the greenhouse effect is due to carbon dioxide (CO_2) emissions and other greenhouse gases[439]. The CO_2 emissions are considered as the

source of 90% of all emitted greenhouse gases (GHGs). Therefore, CO_2 emissions have received considerable attention regarding reduction of polluting gases[440].

Energy consumption is an important factor in economic growth process, but it also has a negative impact on the environment. In fact, the higher the kg oil equivalent per capita energy consumed, the higher the economic growth, and hence increases in CO_2 emissions. On the other hand, economic growth stimulates increase in kg equivalent per capita of energy consumed. The more the increase in kg oil equivalent per capita of energy consumed, the higher the CO_2 emissions level[440].

This concept can be applied to this study because each single variable in the procedure implies a different consumption of energy, which might have a negative environmental impact. The energy consumption can change the intentional positive effect of the whole study, determining if it is an effective growth in the recovery of resources and the substitution of conventional plastics. Each of the stages of the process are represented in Figure 8.2.1, indicating the main energy (yellow arrow) and resources (in purple) interchanges.
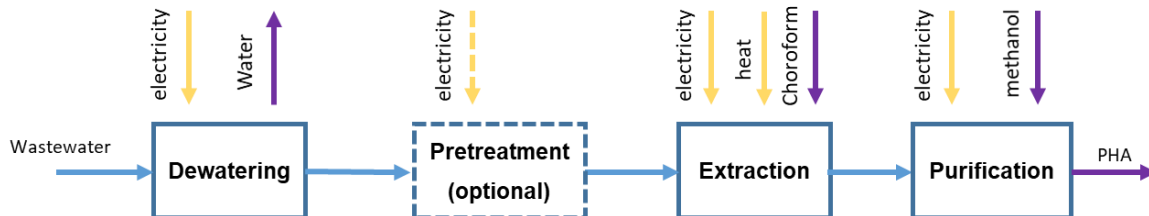
Figure 8.2.1 Simplified main stages of the PHA extraction process with the energy demand and resources recovery.

Clearly, also the type of energy (renewable or not) can affect the emissions: for this reason, energy and environmental policies are controlled by European Union (EU).

Following the trend in industrial economies, CO_2 emissions in Italy had risen in the late of 1940's reaching 76% until 1974 when it sharply falls to 46%, mainly due to replacing oil with natural gas. Italy joined the Kyoto Protocol with the other 28-EU countries and was able to reduce the gap between GHG emissions and Kyoto target from 37.09 in 2008 to −0.87 in 2012. Regarding the Europe 2020 Strategy, Italy launched National Reform Programme (NRP) in 2013 to achieve three set out targets; the reduction of GHG emissions; the increase of renewable energy generation; and the increase in energy efficiency[440]. A study[440] demonstrated that even with the increase in kg oil equivalent per capita of energy consumed, CO_2 emissions level of Italy has been declining overtime. By

implication, Italy energy and environmental policies are in line with their macroeconomic objectives. Thus, the economy appears to have achieved their environmental sustainability targets, a move towards cleaner environment for both the immediate and future generation.

Another target for the EU is to increase the energy consumption from renewable energy sources to 20% of the total energy demand. One of the justifications to increase renewable energy is to mitigate CO_2 emissions, as they offer clean alternatives to fossil fuels by releasing almost no emissions to the atmosphere (Directive 2009/28/EC). Unlike the GHG target, there is not an EU-wide policy instrument to reach the renewable energy target. Indeed, the renewable energy target was divided among the EU member states and each country has developed national policies to meet its share of the target. Italy put in place a variety of support schemes to develop renewable energy. They go from green certificates to feed-in tariffs and premium tariffs. The Italian renewable energy incentives (REI) created a huge surge in installed capacity, especially in wind and solar photovoltaic (PV) in recent years.

Italy experienced an impressive growth in wind and PV capacity and energy production in the years 2000–2011. The results indicate that the annual carbon surcharge for wind energy was 165 €/tCO_2 on average, while the implicit carbon price was 179 €/tCO_2. For solar energy, the carbon surcharge, as well as the implicit carbon price, were much higher, respectively 990 €/tCO_2 and 1003 €/tCO_2. The difference between wind and solar was due to the different level of remunerations: the incentive scheme for solar allowed higher remunerations per megawatt-hour (MWh) of generated electricity than those for wind[441].

8.3   Modelling of the extraction process

Industrial scale extraction of PHAs with chloroform using pre-treatments is not yet established, resulting in lack of direct input/output data for the Life Cycle Inventory (LCI). Therefore, the extraction processes have been simulated by a preliminary design based on the obtained laboratory-scale results (Chapter 5). One of the most limiting steps in laboratory experimentation is the recovery of solvents due to the available equipment.

This phase is already well known at the industrial level, so in the model the chemical make-up will be significantly reduced including a recirculation stream for the recycling of the two chemicals: chloroform and methanol (as reported in Figure 8.3.1).

Apart from the standard extraction case (Ex_std), when pre-treatment is included, there are four scenarios based on the type of pre-treatments (Sonic, Spheres, Homo and Ultra). All the pre-treatments are applied at the same stage on the wet biomass before the extraction procedure. While it is recognized that the actual scale-up would require extensive research efforts, this simplified approach is considered adequate for the purpose

of explorative LCA studies[442]. The material balance for the envisaged process flow diagram have been quantified with the support of Engineering Equation Solver (EES) software. Results are shown in Table 8.3-1, Table 8.3-2, Table 8.3-3, Table 8.3-4, and Table 8.3-5. Calculation is based on 1kg of wastewater used.
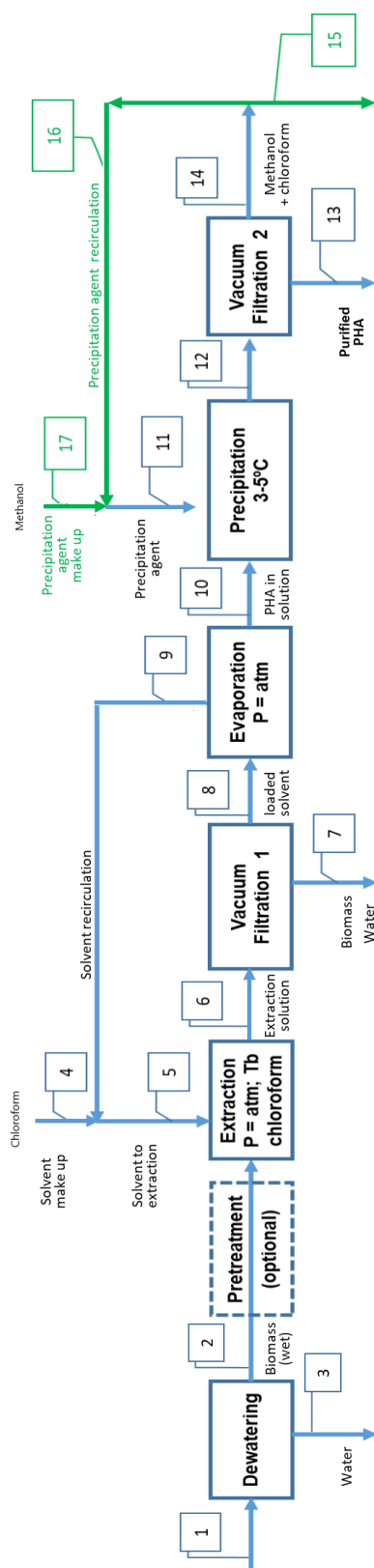
Figure 8.3.1 Representation of the whole process used for the mass and energy balance. The recovery of solvents is also included

Table 8.3-1 Mass balance of standard extraction (Ex_Std)

Stream	Water (g)	Total solids(g)	Biomass (dry) (no PHA) (g)	PHA (g) (dry)	CHCl3 (ml) 1.49 g/ml	MeOH (ml) 0.792 g/ml
1	998.6	1.40	0.350	1.050	-	-
2	8.6	1.40	0.350	1.050	-	-
3	990.0	-	-	-	-	-
4	-	-	-	-	15	-
5	-	-	-	-	70	-
6	8.6	1.400	0.350	1.050	70	-
7	8.6	1.085	0.350	0.735	-	-
8	-	0.315	-	0.315	70	-
9	-	-	-	-	55	-
10	-	0.315	-	0.315	15	-
11	-	0.158	-	0.158	15	75
12	-		-	0.315	15	75
13	-		-	0.158	-	-
14	-	0.315	-	0.315	30	75
15	-	0.158	-	0.158	15	37.5
16	-	0.158	-	0.158	15	37.5
17	-	-	-	-	-	37.5

Table 8.3-1 Mass balance of Sonication pre-treatment (Sonic)

Stream	Water (g)	Total solids (g)	Biomass (dry) (no PHA) (g)	PHA (g) (dry)	CHCl3 (ml) 1.49 g/ml	MeOH (ml) 0.792 g/ml
1	998.6	1.4	0.35	1.05	-	-
2	8.6	1.4	0.35	1.05	-	-
3	990	-	-	-	-	-
4	-	-	-	-	15	-
5	8.6	1.4	0.35	1.1	70	-
6	8.6	1.4	0.35	1.05	-	-
7	-	-	-	-	70	-
8	-	-	-	0.017	15	75
9	-	-	-	0	55	-
10	-	-	-	0.017	15	-
11	-	0.017	-	-	15	75
12	-	0.074	-	0.074	15	75
13	-	0.057	-	0.057	-	-
14	-	0.114	-	0.114	15	75
15	-	0.057	-	0.057	15	37.5
16	-	0.057	-	0.057	15	37.5
17	-	-	-	-	-	37.5

Table 8.3-2 Mass balance of bead milling pre-treatment (Spheres)

Stream	Water (g)	Total solids(g)	Biomass (dry) (no PHA) (g)	PHA (g) (dry)	CHCl3 (ml) 1.49 g/ml	MeOH (ml) 0.792 g/ml
1	998.6	1.4	0.35	1.05	-	-
2	8.6	1.4	0.35	1.05	-	-
3	990	0	0	0	-	-
4	0	0	0	0	15	-
5	8.6	1.4	0.35	1.05	70	-
6	8.6	1.148	0.35	0.798	0	-
7	0	-	0	0.252	70	-
8	-	-	-	0.252	15	75
9	0	-	0	0	55	-
10	0	-	0	0.252	15	-
11	-	0.139	-	0.139	15	75
12	-	0.113	-	0.113	15	75
13	-	0.139	-	0.278	0	0
14	-	0.278	-	0.113	15	75
15	-	0.139	-	0.139	15	37,5
16	-	0.139	-	0.139	15	37,5
17	-	-	-	-	-	37,5

Table 8.3-3 Mass balance of homogenization with pressure pre-treatment (Homo)

Stream	Water (g)	Total solids(g)	Biomass (dry) (no PHA) (g)	PHA (g) (dry)	CHCl3 (ml) 1.49 g/ml	MeOH (ml) 0.792 g/ml
1	998.6	1.4	0.35	1.05	-	-
2	8.6	1.4	0.35	1.05	-	-
3	990	-	-	-	-	-
4	-	-	-	-	15	-
5	8.6	1.4	0.35	1.05	70	-
6	8.6	0.865	0.35	0.515	0	-
7	-	-	-	0.536	70	-
8	-	-	-	0.536	15	75
9	-	-	-	-	55	-
10	-	-	-	0.536	15	-
11	-	0.285	-	0.285	15	75
12	-	0.251	-	0.251	15	75
13	-	0.285	-	0.285	-	-
14	-	0.570	-	0.570	15	75
15	-	0.285	-	0.285	15	37,5
16	-	0.285	-	0.285	15	37,5
17	-	-	-	-	-	37,5

Table 8.3-4 Mass balance of homogenization with blades pre-treatment (Ultra)

Stream	Water (g)	Total solids(g)	Biomass (dry) (no PHA) (g)	PHA (g) (dry)	CHCl3 (ml) 1.49 g/ml	MeOH (ml) 0.792 g/ml
1	998.6	1.4	0.35	1.05	-	-
2	8.6	1.4	0.35	1.05	-	-
3	990	-	-	-	-	-
4	-	-	-	-	15	-
5	8.6	1.4	0.35	1.05	70	-
6	8.6	0.938	0.35	0.588	0	-
7	-	-	-	0.462	70	-
8	-	-	-	0.462	15	75
9	-	-	-	-	55	-
10	-	-	-	0.462	15	-
11	-	0.207	-	0.207	15	75
12	-	0.255	-	0.255	15	75
13	-	0.207	-	0.207	0	0
14	-	0.414	-	0.414	15	75
15	-	0.207	-	0.207	15	37.5
16	-	0.207	-	0.207	15	37.5
17	-	-	-	-	-	37.5

8.4 LCA Methodology

The main goal of the study is to estimate and compare life cycle global warming potential of the extraction methods of PHA from biomass coming from urban wastewaters. Systems under study are: Case 1, that represents the standard extraction (Ex_Std); Case 2, that analysed well-known physical methods usually employed as cell wall disruption techniques to recover intracellular products in various industries[270,276], described in details in Sections 5.7.1.3, 5.7.1.4, 5.7.1.5 and 5.7.1.6. Case 2 is divided in four scenarios

where a different pre-treatment is applied on the biomass: sonication (Sonic), bead milling (Spheres), homogenization through pression (Homo) and through blades (Ultra). Sonication is only considered as a pre-treatment, so the division reported in Chapter 5 in Sonic_mc and Sonic_rt is not considered because it is referred to the last step of the process, which could not be applied in this modelling for industrial scale due to the recovery of the solvents. In order to compare each scenario to Case 1, to estimate the possible differences induced by each single pre-treatment, in these scenarios yield, efficiency, consumption and emissions have been considered and studied as Case 1. As the function of the systems is the extraction of PHA, the functional unit chosen for comparison is 1 g of extracted PHA. Main chemical and energy consumptions are included within the boundary limits of the study. Any possible environmental credits obtained from by-products selling are not considered due to the lack of information about the needed treatment. Life Cycle Inventory for chemicals are obtained directly from mass balance results reported in Table 8.3-1, Table 8.3-3, Table 8.3-4 and Table 8.3-5.

The LCI is the methodology step that involves creating an inventory of input and output flows for a product system. Such flows include inputs of water, energy, and raw materials. The energy consumption in terms of heat and electricity has been estimated basing on mass balance results from previous section and the conditions of the process by using next literature data and considerations:

- Dewatering: 3.1 kWh/m^3 ([443]). Relative density of wastewater is assumed to be equal to 1.
- Extraction reactor (2 h at chloroform's boiling point): 300 kJ/m^3·day for stirring electricity consumption[444]. Relative density of chloroform = 1.49 [445], heat capacity of the stream obtained by mass ponderation of specific heat capacity of each of the component: 116 J/mol chloroform[445], 4.18 kJ/(kg·ºC) water; 4.18 kJ/(kg·ºC) biomass (assumed). 10 % heat losses considered. Chloroform boiling point (atmospheric pressure) = 334.3 K; atmospheric temperature = 298 K.
- Vacuum filtration 1: 5 kWh/m^2 with 25cm^2 filtration area[445].
- Chloroform recovery (evaporation): 32 kJ/mol at atmospheric pressure[445]
- Vacuum filtration 2: same assumption than Vacuum filtration 1.
- Precipitation (4 ºC): electricity efficiency of refrigeration 60 %. Relative density of methanol = 0.792 and heat capacity of methanol = 79 J/mol[445].

Table 8.4-1 summarise Life Cycle Inventory data.

Table 8.4-1 Inventory data. Consumptions of Chemicals, Electricity and Heat per g/PHA and related kgCO2eq of all the scenarios

	Consumptions per g/PHA	Ex_Std	Sonic	Spheres	Homo	Ultra
Chemicals (g)	CHCl₃ for extraction	**201,4**	**210,3**	**167,9**	**65,4**	**108**
	MeOH for precipitation	**267,6**	**279,4**	**223,1**	**87**	**143,5**
Electricity (kWh)	Dewatering	2,80E-02	2,90E-02	2,30E-02	9,10E-03	1,50E-02
	Extraction	1,20E-02	1,30E-02	1,00E-02	3,90E-03	6,40E-03
	Filtration 1	1,50E-03	1,60E-03	1,30E-03	4,90E-04	8,10E-04
	Precipitation	8,20E-04	8,60E-04	6,80E-04	2,70E-04	4,40E-04
	Filtration 2	1,50E-03	1,60E-03	1,30E-03	4,90E-04	8,10E-04
	Pretreatment	0,00E+00	1,30E-05	1,30E-05	1,30E-05	1,30E-05
	Total	**4,40E-02**	**4,60E-02**	**3,70E-02**	**1,40E-02**	**2,30E-02**
Heat	Extraction	54,2	56,6	45,2	17,6	29
	Evaporation	210,8	220,1	175,8	68,5	113
	Total	**265**	**276,7**	**221**	**86,1**	**142,1**

Global Warming Potential (GPW) as equivalent CO_2 emissions is calculated using the literature GWP impact factors showed in Table 8.4-2.

Table 8.4-2 GWP impact factors

		GWP impact factor	Units	Reference
Chemicals (g)	CHCl₃	1.77	kgCO₂eq / kg	[446]
	MeOH for precipitation	0.649	kgCO₂eq / kg	[447]
Energy (kWh)	Electricity	0.265	kgCO₂eq / kWh	[447]
	Heat	7.45E-05	kgCO₂eq / kJ	[447]

8.5   **Results and Discussion**

Environmental performances of extraction processes of PHA from wastewater biomass considering two alternative (with and without pre-treatments of the biomass) and four different pre-treating procedures for polymer recovery are presented in Figure 8.3.1. The four scenarios of Case 2 (Sonic, Spheres, Ultra and Homo) are compared to the reference scenario of Case 1 (Ex_Std), which represents the standard extraction (Ex_Std). The relative contributions to environmental performance by life cycle stage for each scenario are also shown in detail in Table 8.4-1, Table 8.4-2 and Table 8.5-1.

Almost all the extraction processes through pre-treatment of the biomass show environmental performances better than the scenario of Ex_Std for what concerns the total CO_2 emission. The only exception is the scenario where sonication is applied (Sonic). GHG emissions due to extract process through chloroform in the standard extraction are 0,56 kgCO_2eq/gPHA; in the other scenarios, there is a reduction from 30% (Spheres) to 64% (Homo). Nevertheless, the extraction procedure using sonication of the biomass produce almost 5% of CO_2 emission **more** than the standard extraction. These data have been calculated considering the energy need of each step in the extraction process. Moreover, also the obtained yield and its process efficiency is fundamental to the estimation of environmental impact. A low yield reduces the efficiency of the process, causing too high consumptions respect to the other scenarios, that could be avoided choosing other processes.

The results in Table 8.5-1 show that the higher influence on the CO_2 emissions is the use of solvents, in fact in Ex_Std 63.48% of the emission are caused by chloroform, 30.93% by Methanol and only the 5.59% by electricity and heating processes. The influence of solvents in CO_2 emission largely increase with the reduction of the yield, in fact Sonic presents the final CO_2 emission equal to 0.58 kgCO_2eq/gPHA, with 0.02 kgCO2eq/gPHA more than Ex_Std caused only by chloroform. The influence of pre-treatments stage on the emissions of the entire process is highlighted in energy demands as electricity and heating.

Confronting the total electricity demands for all the scenarios, CO_2 emissions are in a range from 0.0038 kgCO_2eq/gPHA (Homo) up to 0.0121 kgCO_2eq/gPHA (Sonic). The use of pre-treatments reduces the electricity impact for almost all the scenarios respect to the Ex_Std (0.0116 kgCO_2eq/gPHA), in fact the total electricity emission is 0.0038 kgCO_2eq/gPHA for Homo, 0.0062 kgCO_2eq/gPHA for Ultra and 0.0097 kgCO_2eq/gPHA for Spheres.

Table 8.5-1 CO2 emissions for kgCO2eq/g PHA for chemicals, electricity and heat and their related percentages

	consumptions per g/PHA	Ex_Std CO2 emissions kgCO2eq/g PHA	%	Sonic CO2 emissions kgCO2eq/g PHA	%	Spheres CO2 emissions kgCO2eq/gPHA	%	Homo CO2 emissions kgCO2eq/gPHA	%	Ultra CO2 emissions kgCO2eq/g PHA	%
Chemicals (g)	CHCl3 for extraction	0.3564	63.48%	0.3720	123.63%	2.97E-01	98.72%	1.16E-01	38.47%	0.1911087	63.48%
	MeOH for precipitation	0.1737	30.93%	0.1813	60.24%	0.1448	48.10%	0.0564	18.75%	0.0931	30.93%
Electricity (kWh)	Dewatering	0.0074	1.32%	0.0077	2.57%	0.0062	2.05%	0.0024	0.80%	0.0040	1.32%
	Extraction	0.0032	0.57%	0.0033	1.10%	0.0027	0.88%	0.0010	0.34%	0.0017	0.57%
	Filtration 1	0.0004	0.07%	0.0004	0.14%	0.0003	0.11%	0.0001	0.04%	0.0002	0.07%
	Precipitation	0.0002	0.04%	0.0002	0.08%	0.0002	0.06%	0.0001	0.02%	0.0001	0.04%
	Filtration 2	0.0004	0.07%	0.0004	0.14%	0.0003	0.11%	0.0001	0.04%	0.0002	0.07%
	Pretreatment	0.0000	0.00%	0.0000	0.00%	0.0000	0.00%	0.0000	0.00%	0.0000	0.00%
Total for electricity		0.0116	2.07%	0.0121	4.02%	0.0097	3.21%	0.0038	1.25%	0.0062	2.07%
Heat (kJ)	Extraction	0.0040	0.72%	0.0042	1.40%	0.0034	1.12%	0.0013	0.44%	0.0022	0.72%
	Evaporation	0.0157	2.80%	0.0164	5.45%	0.0131	4.35%	0.0051	1.70%	0.0084	2.80%
Total for heat		0.0197	3.52%	0.0206	6.85%	0.0165	5.47%	0.0064	2.13%	0.0106	3.52%
TOTAL		0.5614	kgCO2eq/gPHA	0.5862	kgCO2eq/gPHA	0.4681	kgCO2eq/gPHA	0.1824	kgCO2eq/gPHA	0.3010	kgCO2eq/gPHA

Wasted solvents produce a significant carbon footprint and associated expenditure independently of being incinerated on-site or disposed of through outsourced services: it is extremely important to highlight that the main quantity of emissions in this cases is due to the used solvents and their amounts (about 63% of the total emissions in the standard extraction). For this reason, in the ideal plant the recovery of the solvents to reduce the chemical wastes and the environmental impact should be considered. From a sustainability point of view, recovered solvent can be used again in situ where it was used in the first place[448]. Preferably solvents need to be recycled on-site using distillation, adsorption or membrane processing.

Due to the importance of rapid time-to-market speed in chemical businesses, solvent recovery and recycling is not considered in the early stages of process development. On the other hand, once a process is well established, solvent recovery is often one of the key upgrades considered to improve profit margins[448]. The most common technologies for solvent recovery and reuse include distillation processes such as pressure swing,

azeotropic or extractive distillation; adsorption and membrane processes such as organophilic pervaporation and solvent-resistant nanofiltration. According to literature[448], in our case pervaporation represent the best option in terms of carbon footprint and efficiency because pervaporation is a membrane process employed for the separation of liquid mixtures: also in dehydration applications, water is removed from solvent-water mixtures by selective permeation through a dense hydrophilic pervaporation membrane. Table 8.5-2 summarize the advantages and disadvantages of the three techniques; Figure 8.5.1 reports a literature study[449] comparing energy and Carbon Footprint for the recovery of chloroform and methanol by distillation and nanofiltration.

Table 8.5-2 Advantages and disadvantages of different techniques for solvent recovery

Technique	Advantages	Disadvantages
Distillation	Well-established technology High recovery High savings	Consumes large amount of energy
Adsorption processes	High efficiency Low cost Low energy consumption Less carbon footprint than others	Difficult to remove water in organic solvents (which can cause side reactions)
Membrane processes	Simplicity Energy efficiency Less carbon footprint than others Stable in harsh conditions	-

Solvent	Waste Solvent Generated in 2006 (10^6 kg/year)	Q_{dist} (kWh)	Q_{OSN} (kWh)	Q_{dist}/Q_{OSN}	CO_2 Footprint (10^6 kg/year)
Methanol	44.8	150	0.023	6,453	18
Chloroform	3.71	131	0.012	10,543	0.4

Q_{dist}, and Q_{OSN} represent energy required for solvent recovery by distillation and OSN processes. The carbon footprint of the waste solvent is estimated based on their disposal using incineration. *OSN*, organic solvent nanofiltration.

Figure 8.5.1 Comparison of Energy. and Carbon Footprint Required for Solvent Recovery by Distillation and Nanofiltration[449,448]

To the best of our knowledge, this is the second report to give a set of LCA results for PHB production. The first one was by Harding[432]. Both works report GHG emissions expressed as CO_2-equivalent and the values per functional units are well comparable

(about 1 kg versus 2 kg. respectively) considering that the study[432] included also the cultivation phase, the other impact categories are not comparable since the characterization methods used are different.

Comparing the four scenarios related to the novel protocol, the extraction applied to pre-treated biomass is preferable to the standard one (except for Sonic process). Such a result is dependent on two main factors: yield and efficiency of the process. Considering these two factors, two of the analysed pre-treatments (Homo and Ultra) give better yields (51% and 44% respectively) compared to the standard extraction (30%). Also, for efficiencies, the obtained values are very different: 27% for Homo, 20% for Ultra and only 15% for Ex_Std. The Spheres sample can be defined as comparable to the standard extraction, as the yield and efficiency of the process are not much lower. On the contrary, the limit case is the sonication process: not only it gives the worse yield (7%), but also the process efficiency is very low (only 5%). All the results are shown in Table 8.5-3.

Table 8.5-3 Resume of yield, process efficiency and the percentage of reduction in CO_2 emission for all the scenarios.

	Case 1	Case 2			
	Ex_Std	Sonic	Homo	Ultra	Spheres
Yield (%)	30	7	51	44	24
Process Efficiency (%)	15	5	27	20	13
CO_2 Emission Reduction (%) respect to Case 1	-	+4.42	-64.64	-46.38	-30.98

Due to the evaporating procedure and the precipitation in methanol the GHGs are high, but from previous studies [442] the precipitation phase appears more suitable from the ecotoxicological point of view than evaporation.

The process analysis permits to evaluate where the process is lacking. In fact, the main losses are during the filtration process. In the lab scale experiments the losses were due to the impossibility of work on larger amount of substrate because of the equipment availability. In a larger scale with the use of industrial equipment and in a in continuous line the losses during the filtration processes should be reduced. In fact, the second filtration is the step with more losses. To reduce losses process means to increase the process efficiency, recovering a higher amount of PHA.

The LCA study of Case 1 and Case 2 demonstrate that standard extraction causes emissions of 0.56 kgCO2eq/gPHA, whereas three of the four scenarios examined in Case 2 permit to reduce the emissions in a range between 30.98% up to 64.64%. These results are very promising, because thanks to the integration of a pre-treatment in the plant line, the high cost of PHA production can be balanced with the environmental impact.

8.6   Conclusions

This study analyses the environmental impact of the extraction procedure described in Chapter 5 highlighting the weak points of the entire procedure applied in a modelling plant. The environmental impact assessment has shown that, even with the use of solvents such as methanol and chloroform, the environmental impact can be reduced by carrying out mechanical pre-treatments on biomass, so as to increase not only the yield but also the efficiency of the entire extraction process.

The study of Case 1 and Case 2 demonstrates that standard extraction causes emissions of 0.56 kgCO$_2$eq/gPHA, whereas the scenarios examined in Case 2 (Ultra, Spheres and Homo) reduces emissions in a range between 31% up to 65%. Considering all the variables examined in the study, the most promising procedure is the homogenization through pression (Homo) which has 51% of yield, 27% of process efficiency and almost 65% of reduction in CO$_2$ eq emission.

These results are very promising: thanks to the inclusion of a pre-treatment the recovery of PHA can be increased and at the same time, the environmental impact reduced, in terms of global warming potential. Moreover, including the recirculation line for solvents, an already well-known technique, the use of new solvent can be reduced, further decreasing the impact on the environment.

9. *Chapter*

Final

Remarks

Conclusions; critical analysis of results and future developments

In this thesis work, various by-products from industrial waste and / or wastewater have been studied and analysed. These include some of the most common waste materials: cellulose from toilet paper, starch derivatives and polymers produced by microorganisms commonly found in wastewater treatment plants.

Normally, these materials are directly disposed of, triggering a cascade process not only for the loss in terms of product, but also in terms of energy consumption for their disposal and for the exploitation of new raw materials.

The work aimed to enhance these materials based on their composition, so as to propose a new application and prolong their life.

9.1   Research progresses and results

9.1.1   Cellulose from toilet paper

The recovery of cellulose in toilet paper from municipal wastewater is one of the most innovative actions in the circular economy context. In fact, fibres could address possible new uses in the building sector as reinforcing components in binder-based materials.

The addition of recovered cellulose fibres in mortars bring benefits in terms of lightness, microstructure and moisture buffering value (0.17 g/m %UR). Concerning mechanical properties, flexural strength is improved with the addition of 20% of recovered cellulose fibres. In addition, a simplified economic assessment is reported for two possible pre-mixed blends with 5% and 20% of recovered fibres content.

9.1.2   Cyclodextrins: a starch derivate

Starch is one of the more common natural polymer thanks to the diversity and sheer number of end-use applications in both food and non-food industries. Although there is a large consume of conventional sources of starch, such as corn and potato. The application of non-conventional raw materials as complementary sources may provide cost reduction of raw material in industries, besides offering new products with differentiated characteristics. A large quantity of starch can be collected by waste waters of agro-food industries and can be converted in other products. Cyclodextrins (CyDs) are glucose-based molecules and produced from the enzymatic degradation of starch by bacteria. The most characteristic feature of CyDs is the ability to form inclusion compounds with various organic molecules through host–guest interactions: the interior cavity of the molecule provides a relatively hydrophobic environment into which a pollutant can be trapped. In this preliminary study, electrospun PLA-based nanofibers are functionalized with cyclodextrins in order to provide adsorptive properties to the composite. The aim of this work is to investigate a hybrid composite from renewable sources for the combined filtration of particulate matter (PM) and adsorption of volatile organic compounds

(VOCs). The addition of CyD, both in bulk and powder, determines an increase of removal efficiency of VOCs and PM1 size fraction due to two different effects: the CyD in bulk affect the PLA fibers morphology, while the superficially deposited CyD directly affects the removal of VOC. Efficiency tests highlight enhanced VOC removal efficiency in PLA/CyD and PLA + CyD filters; the FTIR analysis confirms that in filters containing CyDs the traces of the interaction between the pollutants and the filter are more evident, showing shifted and larger bands, and split and sharper peaks.

9.1.3   **PHA**

As far as these biopolymers are concerned, the work has been approached from different points of view: PHAs from mixed cultures deriving from urban wastewater and from selection culture (PPB) have been extracted and analysed. Various extraction methods have been also evaluated, taking into account the fundamental variables such as pre-treatments (mechanical and chemical), extraction temperatures and purification methods. Furthermore, these extracted polymers have been also compared in terms of mechanical, thermal and morphological performances to commercial PHA. Composites have been also produced by solvent casting, extrusion and compression moulding in order to evaluate not only the manufacturing processes, but also the different characteristics.

9.1.3.1   *PHA from WWTPs*

The effects of 2 different extraction methods (conventional extraction and Soxhlet extraction) and 4 different pre-treatments (homogenization with pressure and with blades. sonication with mechanical filtration and with rotavapor and impact with glass spheres) on the extraction yields and properties of PHA extracted from biomass coming from a wastewater treatment plant were investigated. The obtained results show that the two different extraction processes affect the crystallization degree of the polymer (17% for conventional and 29% for Soxhlet extraction) and the chemical composition (PHB/PHV for conventional and PHB/Me-PHB for Soxhlet extraction). On the other hand. the extractive yield is highly influenced by pre-treatments: homogenization gives 15% more extractive yield than the others. Homogenization, especially at high pressure, has proved to be the best pre-treatment also in terms of purity, visual appearance (transparency and clearness), thermal stability and mechanical performances of the obtained PHA films. However, all the PHA films begin to melt long before their degradation temperature (Td > 200° C) allowing their use in the field of extrusion or compression moulding.

An LCA study has evaluated the GHG emission referring to the CO_2 levels. The use of pre-treatments permits to reduce the GHG emission from 31% up to almost 65% respect to the standard extraction. The only exception is the pre-treatment through sonication, which causes an increase of almost 5% in the total emissions. Thanks to the well-known techniques and procedures, this protocol permits a reduction of emissions with a good

efficiency of the process as express in the modelling, thus it could be applied in a possible plant.

9.1.3.2   *PHA composites*

Three different common Australian waste have been studied and analysed in order to be used as reinforcing material in association with PHA to make composites for design products. The effects of the reinforcing materials (coffee grounds, macadamia shell nuts fibres and wood flour) have been evaluated in order to investigate the best formulation in terms of mechanical performances, thermal properties and morphological aspect of the composite. The analysed techniques are extrusion and compression moulding. Advantages and disadvantages of the techniques and the fillers have been considered to be applied successively in composite made with PHA extracted from a biomass composed by purple phototrophic bacteria for the same application.

The addition of the exhausted coffee grounds as a filler in the polymer matrix does not seem to valorize the composite in terms of mechanical performances or for the thermal properties.

The addition of the Wood Flour (WF) as a reinforcing agent in the polymer matrix valorize the composite in terms of tensile modulus for both of the series. For what concerns the tensile strength, WF has a positive effect on the extruded series and a negative effect on the compression molded series. Thanks to the fiber composition, the morphology of the composites is homogeneous in both of the series, but in the compression moulded composite the interaction between the fiber and the matrix appears more homogeneous with a better adherence between the two phases. Also the surface of the compressed series appears very smooth and with smaller voids respect to all the other composites.

The addition of the Macadamia nut shells valorizes the composite in terms of mechanical properties. The interaction between the fiber and the matrix appears homogeneous but the nature of the fiber induces a segregation effect in the compressed composites making the surface irregular. In the extrusion series the shark skin effect is still present. In terms of thermal properties both of the specimens are comparable to the WF series.

In the extrusion processing, a major amount of PHA is necessary due to the cleaning process of the machine and for the setting of all the parameters, which will be an important disadvantage for the production of composite with PHA from renewable resource. Nevertheless, the extrusion process does not degrade the polymer as much as compression moulding.

Compression moulding can affect the Tg and Tc of the composites because of its processing conditions, but the differences in terms of mechanical properties a not so significant.

9.1.3.3   *PHA from PPB*

In this study a selected biomass rich of Purple Phototrophic Bacteria (PPB) is used as a substrate for the extraction of PHA. Purple phototrophic bacteria accumulate various storage materials under appropriate conditions. The interest in this particular culture is not only related to PHA production but also because of their structure and properties: PPB are capable of producing their own food via photosynthesis. They are pigmented with bacteriochlorophyll a or b together with various carotenoids.

The extraction process has been studied following different approaches: temperature (at 140°C and at the boiling point), solvents (chloroform and 2-buthanol), pre-treatments (sodium hypochlorite, ethanol and a mixture of acetone/methanol) and purification processes (with and without acetone/methanol) have been examined to consider their effects on yields. After collecting these data, the authors decided to make a selection of the best processes based on the extracted yields obtained. The polymers deriving from the selected processes have been characterized to estimate their quality with the aim of deciding the best extraction process to be used for a scale up. The final selected process has been used for the large-scale extraction of PHA from PPB, which was used for the first time to produce composites in association with wood flour, one of the more common industrial waste in Australia.

In the composites, the added fibers have a reinforcing effect for the sample coming from PPB, but a negative effect for the sample containing commercial PHA. The addition of fibers permits a "bridging effect" in the first sample, increasing the tensile stress. In the other sample, the fibers caused the formation of voids, which reduced their mechanical properties. The mechanical properties have also been influenced by the manufacturing process of the various composites. In fact, being a thermal process, the polymer can be subjected to thermal degradation, that causes a decrease in molecular weight (as confirmed by the GPC analysis). As far as the thermal properties of the composites are concerned, they strictly depend on their composition. However, the samples deriving from PPB had the same thermal stability as the others (Td at 275°C for the 100% PHA composites and at 272°C for the wood-composites).

9.2   **Scientific contribution and future developments**

The present dissertation opens a new line of study on the improvement of wasted materials with new functionalities and adds knowledge to the field of materials sciences and technologies through the development of novel composites.

The search for new techniques and formulations for the enhancement of mechanical properties and life cycle of recovered materials has been followed by the development of other functionalities, in particular by increasing the mechanical properties of the composites (PHAs-composites and cellulose-based mortars), their pollutants removal (Cyclodextrins) and the extraction techniques for biopolymers.

Heretofore, research on the biopolymers were disconnected, being focused only either on the extraction either on the composite's properties. On the contrary, this research focused on the connection line between the two topics, on the production of low-cost composites, easily producible and usable on a large scale, thanks to the introduction of recycled fillers.

The results obtained propose new methods for the recycling of industrial waste within the building sector. The used recovered cellulose proved to be very effective in increasing the mechanical strength and IAQ of the mortars.

The use of Cyclodextrins has proven effective in increasing the removal of VOCs and PM, thanks to the inclusion of cyclodextrins in the filter formulation. This permitted to achieve comparable results respect to the actual air filtration systems, being a good preliminary study on the recovery and transformation of starch in an even more valuable resource.

However, some analyzed parameters showed scientific gaps which require a theoretical investigation and further steps of experimentation. In particular, for what concerns the preliminary studies on PHAs-composites and on the PLA-cyclodextrins air filtration systems, it is essential to investigate more the extraction parameters and the processing in order to avoid the degradation process and the loss of Mw of PHA. In the air filtration system is essential to study the mechanism of filtration and to extend the filtration efficiency tests to the biological sector (bacteria and viruses).

This dissertation represents a small step towards an industry closer to the needs of the society and environment since it is based on the use of technologies able to improve the quality of life of human beings.

References

1. Stahel WR. Circular economy. *Nature*. 2016:6-9.

2. World Resources Institution. World Resources Institution. 2018;2018:2018.

3. Lieder M, Rashid A. Towards circular economy implementation : a comprehensive review in context of manufacturing industry. *J Clean Prod*. 2016;115:36-51. doi:10.1016/j.jclepro.2015.12.042

4. Gustavsson J, Cederberg C, Sonesson U, The Swedish Institute for Food and Biotechnology. Global Food Losses and Food Waste-Congress, Save Food. In: *Global Food Losses and Food Waste-Congress, Save Food*. ; 2011.

5. Ingrao C, Faccilongo N, Di L, Messineo A. Food waste recovery into energy in a circular economy perspective : A comprehensive review of aspects related to plant operation and environmental assessment. *J Clean Prod*. 2018;184:869-892. doi:10.1016/j.jclepro.2018.02.267

6. Principato L, Ruini L, Guidi M, Secondi L. Adopting the circular economy approach on food loss and waste : The case of Italian pasta production. *Resour Conserv Recycl*. 2019;144(January):82-89. doi:10.1016/j.resconrec.2019.01.025

7. Food and Agriculture Organization of the United Nations. Technical Platform on the Measurement and Reduction of Food Loss and Waste. 2019:2019. https://ec.europa.eu/info/index.

8. European Commission. *Global Food Losses and Food Waste: Extent, Causes and Prevention, 2019*.; 2019. https://ec.europa.eu/info/index.

9. Morseletto P. Targets for a circular economy. *Resour Conserv Recycl*. 2020;153(October 2019):104553. doi:10.1016/j.resconrec.2019.104553

10. Bressanelli G, Perona M, Saccani N. Challenges in supply chain redesign for the Circular Economy : a literature review and a multiple case study. *Int J Prod Res*. 2019;7543. doi:10.1080/00207543.2018.1542176

11. Vandi LJ, Chan CM, Werker A, Richardson D, Laycock B, Pratt S. Wood-PHA composites: Mapping opportunities. *Polymers (Basel)*. 2018;10(7):1-15. doi:10.3390/polym10070751

12. Zion Research Analysis. Global Wood-Plastic Composites Market Set for Rapid Growth, to Reach around Usd 6.0 Billion by 2020. 2015. http://www.marketresearchstore.com/news/global- wood-plastic-composites-market-set-for-rapid-101. Published 2020.

13. Cardoso M, Scholz M, Antunes M. A framework for resource recovery from wastewater treatment plants in megacities of developing countries. *Environ Res*. 2020;188(March):109745. doi:10.1016/j.envres.2020.109745

14. Akyol Ç, Foglia A, Ozbayram EG, Frison N, Eusebi AL, Fatone F. Technology Validated innovative approaches for energy- efficient resource recovery and re-use from municipal wastewater : From anaerobic treatment systems to a biorefinery concept. *Crit Rev Environ Sci Technol*. 2019;0(0):1-34. doi:10.1080/10643389.2019.1634456

15. Ruiken CJ, Breuer G, Klaversma E, Santiago T, van Loosdrecht MCM. Sieving

wastewater - Cellulose recovery, economic and energy evaluation. *Water Res*. 2013;47(1):43-48. doi:10.1016/j.watres.2012.08.023

16. Crutchik D, Frison N, Eusebi AL, Fatone F. Biorefinery of cellulosic primary sludge towards targeted Short Chain Fatty Acids, phosphorus and methane recovery. *Water Res*. 2018;136:112-119. doi:10.1016/j.watres.2018.02.047

17. Kumar M, Ghosh P, Khosla K, Shekhar I. Recovery of polyhydroxyalkanoates from municipal secondary wastewater sludge. *Bioresour Technol*. 2018;255(December 2017):111-115. doi:10.1016/j.biortech.2018.01.031

18. Fernández-Dacosta C, Posada JA, Kleerebezem R, Cuellar MC, Ramirez A. Microbial community-based polyhydroxyalkanoates (PHAs) production from wastewater: Techno-economic analysis and ex-ante environmental assessment. *Bioresour Technol*. 2015;185:368-377. doi:10.1016/j.biortech.2015.03.025

19. Southeast Green – Business depends on the environment and the environment depends on business. How Much Toilet Paper Is Used Per Year? http://www.southeastgreen.com/index.php/seg- features/tips-a-faqs/tips-to- green-your738life/10551-how-much-toilet-paper-is-used-per-year. Published 2018. Accessed December 1, 2018.

20. Toilet Paper History. www.toiletpaperhistory.net. Published 2018. Accessed November 21, 2018.

21. Matters of Scale – Into the Toilet | Worldwatch Institute. www.worldwatch.org. Published 2018.

22. Industrial Shredders. www.industrialshredders.com. Published 2018. Accessed November 21, 2018.

23. Raheem A, Sikarwar VS, He J, et al. Opportunities and Challenges in Sustainable Treatment and Resource Reuse of Sewage Sludge : A Review. *Chem Eng J*. 2017. doi:10.1016/j.cej.2017.12.149

24. European Bioplastics Association. European Bioplastics. 2013.

25. PlasticsEurope- Assosiation of Plastics Manufactures,. https://www.plasticseurope.org/. Published 2020. Accessed July 10, 2020.

26. Brockhaus S, Petersen M, Kersten W. A crossroads for bioplastics : exploring product developers ' challenges to move beyond petroleum-based plastics. *J Clean Prod*. 2016;127:84-95. doi:10.1016/j.jclepro.2016.04.003

27. Akaraonye E, Keshavarz T, Roy I, et al. Production of polyhydroxyalkanoates: The future green materials of choice. *J Chem Technol Biotechnol*. 2010;85(6):732-743. doi:10.1002/jctb.2392

28. Mannina G, Presti D, Montiel-jarillo G, Suárez-ojeda ME. Bioplastic recovery from wastewater : A new protocol for polyhydroxyalkanoates (PHA) extraction from mixed microbial cultures. *Bioresour Technol*. 2019;282(March):361-369. doi:10.1016/j.biortech.2019.03.037

29. Puyol D, Batstone DJ, Hülsen T, Astals S, Peces M, Krömer JO. Resource recovery from wastewater by biological technologies: Opportunities, challenges, and prospects. *Front Microbiol*. 2017;7(JAN). doi:10.3389/fmicb.2016.02106

30. Frison N, Katsou E, Malamis S, Oehmen A, Fatone F. Development of a Novel Process

Integrating the Treatment of Sludge Reject Water and the Production of Polyhydroxyalkanoates (PHAs). *Environ Sci Technol*. 2015;49(18):10877-10885. doi:10.1021/acs.est.5b01776

31. Akaraonye E, Keshavarz T, Roy I. Production of polyhydroxyalkanoates: The future green materials of choice. *J Chem Technol Biotechnol*. 2010;85(6):732-743. doi:10.1002/jctb.2392

32. Chen G. Industrial Production of PHA. 2010;14. doi:10.1007/978-3-642-03287

33. Sathiyanarayanan G, Bhatia SK, Song HS, et al. Production and characterization of medium-chain-length polyhydroxyalkanoate copolymer from Arctic psychrotrophic bacterium Pseudomonas sp. PAMC 28620. *Int J Biol Macromol*. 2017;97:710-720. doi:10.1016/j.ijbiomac.2017.01.053

34. Akdoğan M, Çelik E. Purification and characterization of polyhydroxyalkanoate (PHA) from a Bacillus megaterium strain using various dehydration techniques. *J Chem Technol Biotechnol*. 2018;93(8):2292-2298. doi:10.1002/jctb.5572

35. Madison LL, Huisman GW. Metabolic engineering of poly(3-hydroxyalkanoates): from DNA to plastic. *Microbiol Mol Biol Rev*. 1999;63(1):21-53. doi:<p></p>

36. Wang Y, Yin J, Chen GQ. Polyhydroxyalkanoates, challenges and opportunities. *Curr Opin Biotechnol*. 2014;30:59-65. doi:10.1016/j.copbio.2014.06.001

37. Villano M, Valentino F, Barbetta A, Martino L, Scandola M, Majone M. Polyhydroxyalkanoates production with mixed microbial cultures: From culture selection to polymer recovery in a high-rate continuous process. *N Biotechnol*. 2014;31(4):289-296. doi:10.1016/j.nbt.2013.08.001

38. Arcos-Hernandez M V, Gurieff N, Pratt S, et al. Rapid quantification of intracellular PHA using infrared spectroscopy: an application in mixed cultures. *J Biotechnol*. 2010;150(3):372-379. doi:10.1016/j.jbiotec.2010.09.939

39. Peoples OP. PHA Production in Plants : Enabling a Sustainable Plastics Biorefinery . :2139.

40. Dionisi D, Carucci G, Petrangeli Papini M, Riccardi C, Majone M, Carrasco F. Olive oil mill effluents as a feedstock for production of biodegradable polymers. *Water Res*. 2005;39(10):2076-2084. doi:10.1016/j.watres.2005.03.011

41. Davis R, Kataria R, Cerrone F, et al. Conversion of grass biomass into fermentable sugars and its utilization for medium chain length polyhydroxyalkanoate (mcl-PHA) production by Pseudomonas strains. *Bioresour Technol*. 2013;150:202-209. doi:10.1016/j.biortech.2013.10.001

42. Koller M, Niebelschütz H, Braunegg G. Strategies for recovery and purification of poly[(R)-3-hydroxyalkanoates] (PHA) biopolyesters from surrounding biomass. *Eng Life Sci*. 2013;13(6):549-562. doi:10.1002/elsc.201300021

43. Salmiati ZU, Salim MR, Olsson G. Recovery of Polyhydroxyalkanoates (PHAs) from Mixed Microbial Cultures by Simple Digestion and Saponification. *Proc 3rd Int Water Assoc (IWA)-ASPIRE Conf Exhib*. 2009;(December 2013):8-15. doi:10.1080/03043790320000101863

44. Mesquita DP, Amaral AL, Leal C, Oehmen A, Reis MAM, Ferreira EC. Polyhydroxyalkanoate granules quantification in mixed microbial cultures using image analysis: Sudan Black B versus Nile Blue A staining. *Anal Chim Acta*. 2015;865(1):8-15.

doi:10.1016/j.aca.2015.01.018

45. Blankenship RE, Madigan MT, Bauer CE. *Anoxygenic Photosynthetic Bacteria*. (Blankenship RE, Madigan MT, Bauer CE, eds.). New York, Boston, Dordrecht, London, Moscow: Kluwer Academic Publishers; 1995.

46. Oh YH, Eom IY, Joo JC, et al. Recent advances in development of biomass pretreatment technologies used in biorefinery for the production of bio-based fuels , chemicals and polymers. 2015;32(10):1945-1959. doi:10.1007/s11814-015-0191-y

47. Albuquerque MGE, Martino V, Pollet E, Avérous L, Reis MAM. Mixed culture polyhydroxyalkanoate (PHA) production from volatile fatty acid (VFA)-rich streams: Effect of substrate composition and feeding regime on PHA productivity, composition and properties. *J Biotechnol*. 2011;151(1):66-76. doi:10.1016/j.jbiotec.2010.10.070

48. Gahlawat G, Soni SK. Study on Sustainable Recovery and Extraction of Polyhydroxyalkanoates (PHAs) Produced by Cupriavidus necator Using Waste Glycerol for Medical Applications. *Chem Biochem Eng Q*. 2019;33(1):99-110. doi:10.15255/CABEQ.2018.1471

49. Conca V, Valentino F, Laura A, Frison N, Fatone F. Long-term validation of polyhydroxyalkanoates production potential from the sidestream of municipal wastewater treatment plant at pilot scale. *Chem Eng J*. 2020;390(March):124627. doi:10.1016/j.cej.2020.124627

50. United Nations Environment Programme (UNEP). https://www.unenvironment.org/.

51. Evans D, Campbell H, Murcott A. A brief pre-history of food waste and the social sciences. 2013;26:5-26. doi:10.1111/1467-954X.12035

52. Zabaniotou A, Kamaterou P. Food waste valorization advocating Circular Bioeconomy - A critical review of potentialities and perspectives of spent coffee grounds biore fi nery. *J Clean Prod*. 2019;211:1553-1566. doi:10.1016/j.jclepro.2018.11.230

53. La G, Micale R, Paolo P, et al. Reducing waste and ecological impacts through a sustainable and efficient management of perishable food based on the Monte Carlo simulation. *Ecol Indic*. 2019;97(June 2018):363-371. doi:10.1016/j.ecolind.2018.10.041

54. Santana L, Zabot GL, Osorio-tob JF, et al. Starch recovery from turmeric wastes using supercritical technology. *J Food Eng J*. 2017;214:266-276. doi:10.1016/j.jfoodeng.2017.07.010

55. Baiano A. Recovery of Biomolecules from Food Wastes — A Review. *Molecules*. 2014:14821-14842. doi:10.3390/molecules190914821

56. Vasanthan T, Bergthaller W, Driedger D, Yeung J, Sporns P. Starch from Alberta potatoes : wet-isolation and some physicochemical properties. *Food Res Int*. 1999;32.

57. Hanna MA. Starch-Based Plastic Foams From Various Starch Sources. *Eng Process*. 1996;73(5):601-604.

58. Catarino J, Mendonc E, Picado A, Anselmo A, Partida P. Getting value from wastewater : by-products recovery in a potato chips industry. 2007;15:927-931. doi:10.1016/j.jclepro.2005.12.003

59. Delval F, Crini G, Vebrel J, Knorr M, Sauvin G, Conte E. Starch-Modified filters for the removal of dyes from waste water. *Macromol Symp*. 2003:165-171. doi:10.1002/masy.200351315

60. Jin B, Leeuwen HJ Van, Patel B, Doelle HW, Yu Q. Production of fungal protein and glucoamylase by Rhizopus oligosporus from starch processing wastewater. *Process Biochem*. 1999;34:59-65.

61. Commission E. Internal Market, Industry, Entrepreneurship and SMEs Directorate General. *Eur Constr Sect A Glob Partn*. 2016:2016.

62. S.Vaclav. Making the Modern World: Materials and Dematerialization. *Lulu Press*. 2016.

63. Han B, Yu X, Ou J. *Self-Sensing Concrete in Smart Structures*.; 2014. doi:10.1016/C2013-0-14456-X

64. Roy D, Brown P, Shi D, Scheetz B, May W. Concrete Microstructure Porosity and Permeability. *Strateg Highw Res Program, Natl Res Counc ,washingt DC*. 1993.

65. Brownjohn JMW. Structural health monitoring of civil infrastructure. *Philos Trans R Soc A Math Phys Eng Sci*. 2007;365(1851):589-622. doi:10.1098/rsta.2006.1925

66. Dittenber DB, Gangarao HVS. Critical review of recent publications on use of natural composites in infrastructure. *Compos Part A Appl Sci Manuf*. 2012;43(8):1419-1429. doi:10.1016/j.compositesa.2011.11.019

67. Wei S, Jiang Z, Liu H, Zhou D, Sanchez-Silva M. Microbiologically induced deterioration of concrete - A review. *Brazilian J Microbiol*. 2013;44(4):1001-1007. doi:10.1590/S1517-83822014005000006

68. Giosuè C, Pierpaoli M, Mobili A, Ruello ML, Tittarelli F. Influence of binders and lightweight aggregates on the properties of cementitious mortars: From traditional requirements to indoor air quality improvement. *Materials (Basel)*. 2017;10(8). doi:10.3390/ma10080978

69. Andrés FN, Beltramini LB, Guilarducci AG, Romano MS, Ulibarrie NO. Lightweight Concrete: An Alternative for Recycling Cellulose Pulp. *Procedia Mater Sci*. 2015;8:831-838. doi:10.1016/j.mspro.2015.04.142

70. Liu C, Hsu PC, Lee HW, et al. Transparent air filter for high-efficiency PM 2.5 capture. *Nat Commun*. 2015;6:1-9. doi:10.1038/ncomms7205

71. World Health Organization. *Burden of Disease from the Joint Effects of Household and Ambient Air Pollution for 2016*.; 2016. doi:https://www.who.int/airpollution/data/cities/en/

72. Signoretta PE, Buffel V, Bracke P. Health & Place Mental wellbeing , air pollution and the ecological state. *Health Place*. 2019;57(March):82-91. doi:10.1016/j.healthplace.2019.03.003

73. Buckholz, Richard; Gleeson M. Production of cyclodextrins, a novel carbohydrate, in the tubers of transgenic potato plants. *Nat Biotechnol*. 1991;9:1067-1072. doi:10.1038/nm0798-822

74. Biwer A, Antranikian G, Heinzle E. Enzymatic production of cyclodextrins. *Appl Microbiol Biotechnol*. 2002:609-617. doi:10.1007/s00253-002-1057-x

75. Blanco KC, Lima CJB De, Monti R, Jr JM. Bacillus lehensis — an alkali-tolerant bacterium isolated from cassava starch wastewater : optimization of parameters for cyclodextrin glycosyltransferase production. *Ann Microbiol*. 2012:329-337. doi:10.1007/s13213-011-0266-x

76. Anto H, Trivedi UB, Patel KC. Glucoamylase production by solid-state fermentation using

rice flake manufacturing waste products as substrate. *Bioresour Technol*. 2006;97:1161-1166. doi:10.1016/j.biortech.2005.05.007

77. Steinbuchel A, Madkour MH, Heinrich D, Alghamdi AM, Shabbaj II. PHA Recovery from Biomass. *Biomacromolecules*. 2013.

78. Ibarra VG, Sendón R, Quirós AR De. *Antimicrobial Food Packaging Based on Biodegradable Materials*. Elsevier Inc.; 2016. doi:10.1016/B978-0-12-800723-5.00029-2

79. Luengo JM, García B, Sandoval A, Naharro G, Olivera ER. Bioplastics from microorganisms. *Curr Opin Microbiol*. 2003;6(3):251-260. doi:10.1016/S1369-5274(03)00040-7

80. Van Krevelen DW. *PROPERTIES OF POLYMERS:THEIR CORRELATION WITH CHEMICAL STRUCTURE; THEIR NUMERICAL ESTIMATION AND PREDICTION FROM ADDITIVE GROUP CONTRIBUTIONS*. Elsevier; 2009.

81. Balani K, Verma V, Agarwal A, Narayan R. Physical, thermal, and mechanical properties of polymers. In: *Biosurfaces: A Materials Science and Engineering Perspective,*. ; 2015:329-344.

82. Gnanou Y, Fontanille M. *Organic and Physical Chemistry of Polymers*. (Wiley-Interscience, ed.).; 2008.

83. Nicholson JW. *The Chemistry of Polymers*. (Publishing R, ed.).; 2006.

84. Alfonso GC. *Polymer Crystallization II From Chain Microstructure to Processing*.

85. Alfonso GC. *Polymer Crystallization I From Chain Microstructure to Processing*.

86. Balani K, Verma V, Narayan A, Agarwal R. *Biosurfaces*. John Wiley & Sons, Inc.; 2015.

87. Mitchell BS. *MATERIALS ENGINEERING AND SCIENCE: AN INTRODUCTION TO MATERIALS ENGINEERING AND SCIENCE FOR CHEMICAL AND MATERIALS ENGINEERS*. JOHN WILEY & SONS, INC; 2004.

88. Morton-Jones DH. *Polymer Processing*. (Chapman and Hall, ed.). London: Chapman and Hall; 1989.

89. TADMOR Z, GOGOS CG. *Principles of Polymer Processing*. 2nd ed. (John Wiley & Sons I, ed.). Wiley; 2006.

90. Han CD. *Rheology and Processing of Polymeric Materials*. (Oxford University Press, ed.). Oxford University Press, Inc.,; 2007.

91. Mark J, Ngai K, Graessley W, et al. *Physical Properties of Polymers*. the press syndicate of the university of cambridge; 2003.

92. Rauwendaal C. *Polymer Extrusion*. Hanser Publications; 2013.

93. Morton-Jones DH, Ellis JW. *Polymer Products*. (Chapman and Hall, ed.). Chapman and Hall; 1986.

94. Rosato D V, Rosato D V, Rosato M V. *Plastic Product Material and Process Selection Handbook*.; 2004.

95. Advani SG, Hsiao K-T. *Manufacturing Techniques for Polymer Matrix Composites (PMCs)*. (Woodhead Publishing Limited, ed.). Woodhead Publishing Limited; 2012.

96. Oksanen T, Pere J, Paavilainen L, et al. What happens to cellulosic fibers during papermaking and recycling? A review. *Cem Concr Compos*. 1997;47(8):43-48.

doi:10.3390/ma10080978

97. Jacobsen T. Sennacherib's Aqueduct at Jerwan. *Orient Inst Publ*. 1935;24.

98. Sparavigna AC, Fisica D, Torino P. Ancient concrete works. *Anc Concr Work*. 2011.

99. The History of Concrete. *Dept Mater Sci Eng Univ Illinois, Urbana-Champaign*. 2012.

100. Gromicko N. The History of Concrete. *Int Assoc Certif Home Insp*. 2013;(January).

101. Herring B. The Secrets of Roman Concrete. *Romanconcrete.com*. 2012.

102. Courland R. Concrete planet : the strange and fascinating story of the world's most common man-made material. *Amherst, NY Prometh Books*. 2015.

103. Schieweck A, Uhde E, Salthammer T, et al. Smart homes and the control of indoor air quality. *Renew Sustain Energy Rev*. 2018;94(May):705-718. doi:10.1016/j.rser.2018.05.057

104. The European Commission's science and knowledge service, Improving safety in construction, avaible from: https://ec.europa.eu/jrc/en/research-topic/improving-safety-construction.

105. B. Han, L. Zhang and JO. Smart and Multifunctional Concrete Towards Sustainable Infrastructures. *Springer Singapore*. 2017:2017.

106. Mounir S, Abdelhamid K, Maaloufa Y. Thermal Inertia for Composite Materials White Cement-cork, Cement Mortar-cork, and Plaster-cork. *Energy Procedia*. 2015;74:991-999. doi:10.1016/j.egypro.2015.07.830

107. Zeng Q, Mao T, Li H, Peng Y. Thermally insulating lightweight cement-based composites incorporating glass beads and nano-silica aerogels for sustainably energy-saving buildings. *Energy Build*. 2018;174:97-110. doi:10.1016/j.enbuild.2018.06.031

108. Tittarelli F, Giosuè C, Mobili A, Ruello ML. Influence of binders and aggregates on VOCs adsorption and moisture buffering activity of mortars for indoor applications. *Cem Concr Compos*. 2015;57:75-83. doi:10.1016/j.cemconcomp.2014.11.013

109. Loh K, Gaylarde CC, Shirakawa MA. Photocatalytic activity of ZnO and TiO2'nanoparticles' for use in cement mixes. *Constr Build Mater*. 2018;167:853-859. doi:10.1016/j.conbuildmat.2018.02.103

110. Hospodarova V, Stevulova N, Briancin J, Kostelanska K. Investigation of Waste Paper Cellulosic Fibers Utilization into Cement Based Building Materials. *Buildings*. 2018;8(3):43. doi:10.3390/buildings8030043

111. Mohamed MAS, Ghorbel E, Wardeh G. Valorization of micro-cellulose fibers in self-compacting concrete. *Constr Build Mater*. 2010;24(12):2473-2480. doi:10.1016/j.conbuildmat.2010.06.009

112. Mohammed BS, Fang OC. Assessing the properties of freshly mixed concrete containing paper-mill residuals and class F fly ash. 2011;2(February):17-26.

113. Ogi K, Shinoda T, Mizui M. Strength in concrete reinforced with recycled CFRP pieces. *Compos Part A Appl Sci Manuf*. 2005;36(7):893-902. doi:10.1016/j.compositesa.2004.12.009

114. Faruk O, Bledzki AK, Fink H, Sain M. Biocomposites reinforced with natural fibers : 2000 – 2010. *Prog Polym Sci*. 2012;37(11):1552-1596. doi:10.1016/j.progpolymsci.2012.04.003

115. Ardanuy M, Claramunt J, Toledo Filho RD. Cellulosic fiber reinforced cement-based composites: A review of recent research. *Constr Build Mater*. 2015;79:115-128. doi:10.1016/j.conbuildmat.2015.01.035

116. Couvreux M. Selecting a Natural Hydraulic Lime - What to Look For. 2014;(62):8-10.

117. Kim HK, Nam IW, Lee HK. Enhanced effect of carbon nanotube on mechanical and electrical properties of cement composites by incorporation of silica fume. *Compos Struct*. 2014;107:60-69. doi:10.1016/j.compstruct.2013.07.042

118. Du H, Pang SD. Enhancement of barrier properties of cement mortar with graphene nanoplatelet. *Cem Concr Res*. 2015;76:10-19. doi:10.1016/j.cemconres.2015.05.007

119. Wistara N, Young RA. Properties and treatments of pulps from recycled paper. Part I. Physical and chemical properties of pulps. *Cellulose*. 1999;6(4):291-324. doi:10.1023/A:1009221125962

120. Howard RC, Bichard W. The basic effects of recycling on pulp properties. *J pulp Pap Sci*. 1992;18(4):151-159. doi:10.1557/PROC-266-195

121. Hubbe MA, Venditti RA, Rojas OJ. What happens to cellulosic fibers during papermaking and recycling? A review. *BioResources*. 2007;2(4):739-788. doi:10.15376/biores.2.4.739-788

122. Wan J, Wang Y, Xiao Q. Effects of hemicellulose removal on cellulose fiber structure and recycling characteristics of eucalyptus pulp. *Bioresour Technol*. 2010;101(12):4577-4583. doi:10.1016/j.biortech.2010.01.026

123. Oksanen T, Buchert J, Viikari L. The role of hemiocelluloses in the hornification of bleached kraft pulps. *Holzforschung*. 1997;51(4):355-360.

124. Hospodarova V, Stevulova N. Investigation of Waste Paper Cellulosic Fibers Utilization into Cement Based Building Materials. 2018:10-12. doi:10.3390/buildings8030043

125. Jongvisuttisun P, Negrello C, Kurtis KE. Effect of processing variables on efficiency of eucalyptus pulps for internal curing. *Cem Concr Compos*. 2013;37(1):126-135. doi:10.1016/j.cemconcomp.2012.11.006

126. Collet F, Pretot S. Experimental investigation of moisture buffering capacity of sprayed hemp concrete. *Constr Build Mater*. 2012;36:58-65. doi:10.1016/j.conbuildmat.2012.04.139

127. Collet F, Bart M, Serres L, Miriel J. Porous structure and water vapour sorption of hemp-based materials. *Constr Build Mater*. 2008;22(6):1271-1280. doi:10.1016/j.conbuildmat.2007.01.018

128. Maslinda AB, Abdul Majid MS, Ridzuan MJM, Afendi M, Gibson AG. Effect of water absorption on the mechanical properties of hybrid interwoven cellulosic-cellulosic fibre reinforced epoxy composites. *Compos Struct*. 2017;167:227-237. doi:10.1016/j.compstruct.2017.02.023

129. Khedari J, Suttisonk B, Pratinthong N, Hirunlabh J. New lightweight composite construction materials with low thermal conductivity. *Cem Concr Compos*. 2001;23:65-71.

130. Osanyintola OF, Simonson CJ. Moisture buffering capacity of hygroscopic building materials: Experimental facilities and energy impact. *Energy Build*. 2006;38(10):1270-1282. doi:10.1016/j.enbuild.2006.03.026

131. Tran Le AD, Maalouf C, Mai TH, Wurtz E, Collet F. Transient hygrothermal behaviour of a hemp concrete building envelope. *Energy Build*. 2010;42(10):1797-1806. doi:10.1016/j.enbuild.2010.05.016

132. Mazhoud B, Collet F, Pretot S, Chamoin J. Hygric and thermal properties of hemp-lime plasters. *Build Environ*. 2016;96:206-216. doi:10.1016/j.buildenv.2015.11.013

133. Gonçalves H, Gonçalves B, Silva L, Raupp-Pereira F, Senff L, Labrincha JA. Development of porogene-containing mortars for levelling the indoor ambient moisture. *Ceram Int*. 2014;40(10):15489-15495. doi:10.1016/j.ceramint.2014.07.010

134. Wang Y, Wu HC, Victor L. Concrete reinforcement with recycled fibers. *J Mater Civ Eng*. 2000;(November):314-319.

135. Slanina P, Šilarová Š. Moisture transport through perforated vapour retarders. *Build Environ*. 2009;44(8):1617-1626. doi:10.1016/j.buildenv.2008.10.006

136. Abadie MO, Mendonça KC. Moisture performance of building materials: From material characterization to building simulation using the Moisture Buffer Value concept. *Build Environ*. 2009;44(2):388-401. doi:10.1016/j.buildenv.2008.03.015

137. Kawashima S, Shah SP. Early-age autogenous and drying shrinkage behavior of cellulose fiber-reinforced cementitious materials. *Cem Concr Compos*. 2011;33(2):201-208. doi:10.1016/j.cemconcomp.2010.10.018

138. Anju TR, Ramamurthy K, Dhamodharan R. Surface modified microcrystalline cellulose from cotton as a potential mineral admixture in cement mortar composite. *Cem Concr Compos*. 2016;74:147-153. doi:10.1016/j.cemconcomp.2016.09.003

139. Mwaikambo LY, Ansell MP. Chemical modification of hemp, sisal, jute, and kapok fibers by alkalization. *J Appl Polym Sci*. 2002;84(12):2222-2234. doi:10.1002/app.10460

140. Sgriccia N, Hawley MC, Misra M. Characterization of natural fiber surfaces and natural fiber composites. *Compos Part A Appl Sci Manuf*. 2008;39(10):1632-1637. doi:10.1016/j.compositesa.2008.07.007

141. Plagué T, Desmettre C, Charron JP. Influence of fiber type and fiber orientation on cracking and permeability of reinforced concrete under tensile loading. *Cem Concr Res*. 2017;94:59-70. doi:10.1016/j.cemconres.2017.01.004

142. Bentur A, Mindess S. Fibre reinforced cementitious composites. *Taylor Fr*. 2007. doi:ISBN10: 0–415–25048–X (hbk)

143. Fan M, Fu F. *Advanced High Strength Natural Fibre Composites in Construction*.

144. Savastano H, Agopyan V. Transition zone studies of vegetable fibre-cement paste composites. *Cem Concr Compos*. 1999;21(1):49-57. doi:10.1016/S0958-9465(98)00038-9

145. Bentchikou M, Guidoum A, Scrivener K, Silhadi K, Hanini S. Effect of recycled cellulose fibres on the properties of lightweight cement composite matrix. *Constr Build Mater*. 2012;34:451-456. doi:10.1016/j.conbuildmat.2012.02.097

146. Collins F, Aly T, Sanjayan JG. Effect of polypropylene fibers on shrinkage and cracking of concretes. *Mater Struct Constr*. 2008:1741-1753. doi:10.1617/s11527-008-9361-2

147. Mobili A, Belli A, Giosuè C, Bellezze T, Tittarelli F. Metakaolin and fly ash alkali-activated mortars compared with cementitious mortars at the same strength class. *Cem Concr Res*. 2016;88:198-210. doi:10.1016/j.cemconres.2016.07.004

148. Latif E, Lawrence M, Shea A, Walker P. Moisture buffer potential of experimental wall assemblies incorporating formulated hemp-lime. *Build Environ*. 2015;93(P2):199-209. doi:10.1016/j.buildenv.2015.07.011

149. Giosuè C, Mobili A, Toscano G, Ruello ML, Tittarelli F. Effect of Biomass Waste Materials as Unconventional Aggregates in Multifunctional Mortars for Indoor Application. *Procedia Eng*. 2016;161:655-659. doi:10.1016/j.proeng.2016.08.724

150. Giosuè C, Yu QL, Ruello ML, Tittarelli F, Brouwers HJH. Effect of pore structure on the performance of photocatalytic lightweight lime-based finishing mortar. 2018;171:232-242. doi:10.1016/j.conbuildmat.2018.03.106

151. Honda S, Miyata N, Iwahori K. Recovery of biomass cellulose from waste sewage sludge. *J Mater Cycles Waste Manag*. 2002;4(1):46-50. doi:10.1007/s10163-001-0054-y

152. Claramunt J, Ardanuy M, García-Hortal JA. Effect of drying and rewetting cycles on the structure and physicochemical characteristics of softwood fibres for reinforcement of cementitious composites. *Carbohydr Polym*. 2010;79(1):200-205. doi:10.1016/j.carbpol.2009.07.057

153. Alhuthali A, Low IM, Dong C. Characterisation of the water absorption, mechanical and thermal properties of recycled cellulose fibre reinforced vinyl-ester eco-nanocomposites. *Compos Part B Eng*. 2012;43(7):2772-2781. doi:10.1016/j.compositesb.2012.04.038

154. Palmieri S, Cipolletta G, Pastore C, et al. Pilot scale cellulose recovery from sewage sludge and reuse in building and construction material. *Waste Manag*. 2019;100:208-218. doi:10.1016/j.wasman.2019.09.015

155. Ozmen EY, Sezgin M, Yilmaz A, Yilmaz M. Synthesis of -cyclodextrin and starch based polymers for sorption of azo dyes from aqueous solutions. 2008;99:526-531. doi:10.1016/j.biortech.2007.01.023

156. Ayadi-Zouari D, Kammoun R, Jemli S, Chouayekh H, Bejar S. Secretion of cyclodextrin glucanotransferase in E. coli using Bacillus subtilis lipase signal peptide and optimization of culture medium. *Indian J Exp Biol*. 2012;50(1):72-79.

157. Vorgias CE. Glycosyl Hydrolases from Extremophiles. 1996:141-145.

158. Kaulpiboon J, Hansakul P. Comparative studies on the synthesis of cyclodextrin from two bacterial CGTases in the presence of organic solvents.

159. Mikuš P, Šebesta R, Kaniansky D, Sališová M. *Cyclodextrins and Their Complexes - Structure and Interactions*. Vol 96.; 2002.

160. Loftsson T, Duchêne D. Cyclodextrins and their pharmaceutical applications. *Int J Pharm*. 2007;329(1-2):1-11. doi:10.1016/j.ijpharm.2006.10.044

161. Alsbaiee A, Smith BJ, Xiao L, Ling Y, Helbling DE, Dichtel WR. Rapid removal of organic micropollutants from water by a porous β-cyclodextrin polymer. *Nature*. 2016;529(7585):190-194. doi:10.1038/nature16185

162. Arkas M, Allabashi R, Tsiourvas D, Mattausch EM, Perfler R. Organic/inorganic hybrid filters based on dendritic and cyclodextrin "nanosponges" for the removal of organic pollutants from water. *Environ Sci Technol*. 2006;40(8):2771-2777. doi:10.1021/es052290v

163. European Environmental Agency. Health impact of PM mass concentrations (μg/m3). Loss in statistical life expectancy (months) that can be attributed to anthropogenic

contributions to PM2.5 for the year 2000 (left) and for 2020 (right) for the CAFE baseline scenario. 2012. https://www.eea.europa.eu/data-and-maps/figures/health-impact-of-pm-mass-concentrations-g-m3-loss-   in-statistical-life-expectancy-months-that-can-be-attributed-to-anthropogenic-contributions-to-pm2-5-for-   the-year-2000-left-and-for-2020-right-for-the-cafe-baseline-scenario. Published 2009.

164.   Lee TG, De Biasio D, Santini A. HEALTH AND THE BUILT ENVIRONMENT : INDOOR AIR QUALITY. In: *Vital Signs*. ; 1996.

165.   Kampa M, Castanas E. Human health effects of air pollution. 2008;151:362-367. doi:10.1016/j.envpol.2007.06.012

166.   European Environmental Agency. Key industrial air pollutant and GHG emissions for EEA-33 in 2007 to 2016 by industry sector. 12 Dec 2019. https://www.eea.europa.eu/data-and-maps/figures/key-industrial-air-pollutant-and. Published 2019. Accessed September 17, 2020.

167.   World Health Organization. *Guideline for Indoor Air Quality: Selected Pollutants*.; 2010. https://www.who.int/.

168.   Liu G, Xiao M, Zhang X, Gal C, Chen X, Liu L. A review of air filtration technologies for sustainable and healthy building ventilation. *Sustain Cities Soc*. 2017;32(December 2016):375-396. doi:10.1016/j.scs.2017.04.011

169.   Doshi J, Reneker DH. Electrospinning process and applications of electrospun fibers. *Conf Rec 1993 IEEE Ind Appl Conf Twenty-Eighth IAS Annu Meet*. 1993;35:151-160. doi:10.1109/IAS.1993.299067

170.   Qin X, Wang S. Filtration Properties of Electrospinning Nanofibers. *J Appl Polym Sci*. 2006;(March). doi:10.1002/app.24361

171.   Wang Z, Pan Z. Preparation of hierarchical structured nano-sized/porous poly(lactic acid) composite fibrous membranes for air filtration. *Appl Surf Sci*. 2015;356:1168-1179. doi:10.1016/j.apsusc.2015.08.211

172.   Zander NE, Gillan M, Sweetser D. Recycled PET nanofibers for water filtration applications. *Materials (Basel)*. 2016;9(4):1-10. doi:10.3390/ma9040247

173.   Wen P, Zhu DH, Feng K, et al. Fabrication of electrospun polylactic acid nanofilm incorporating cinnamon essential oil/β-cyclodextrin inclusion complex for antimicrobial packaging. *Food Chem*. 2016;196:996-1004. doi:10.1016/j.foodchem.2015.10.043

174.   Huang JJ, Tian Y, Wang R, Tian M, Liao Y. Fabrication of bead-on-string polyacrylonitrile nanofibrous air filters with superior filtration efficiency and ultralow pressure drop. *Sep Purif Technol*. 2020;237:116377. doi:10.1016/j.seppur.2019.116377

175.   Li H, Wang Z, Zhang H, Pan Z. Nanoporous PLA/(Chitosan Nanoparticle) Composite Fibrous Membranes with Excellent Air Filtration and Antibacterial Performance. *Polymers (Basel)*. 2018;10(10):1085. doi:10.3390/polym10101085

176.   Lala NL, Ramaseshan R, Bojun L, Sundarrajan S. Fabrication of Nanofibers With Antimicrobial Functionality Used as Filters : Protection Against Bacterial Contaminants. 2007;97(6):1357-1365. doi:10.1002/bit

177.   Kim M, Lim G, Kim Y, Han B, Gyu C, Kim H. A novel electrostatic precipitator-type small air puri fi er with a carbon fi ber ionizer and an activated carbon fi ber fi lter. 2018;117(December 2017):63-73. doi:10.1016/j.jaerosci.2017.12.014

178. Brincat J, Sardella D, Muscat A, et al. A review of the state-of-the-art in air fi ltration technologies as may be applied to cold storage warehouses. *Trends Food Sci Technol*. 2016;50:175-185. doi:10.1016/j.tifs.2016.01.015

179. Di Natale F, Carotenuto C, D'Addio L, et al. Capture of fine and ultra fine particles in a wet electrostatic scrubber. *J Environ Chem Eng*. 2015;3(1):349-356. doi:10.1016/j.jece.2014.11.007

180. Bian Y, Wang S, Zhang L, Chen C. Influence of fiber diameter , filter thickness , and packing density on PM 2 . 5 removal efficiency of electrospun nanofiber air filters for indoor applications. *Build Environ*. 2020;170(December 2019):106628. doi:10.1016/j.buildenv.2019.106628

181. Xia T, Bian Y, Zhang L, Chen C. Relationship between Pressure Drop and Face Velocity for Electrospun Nanofiber Filters. *Energy Build*. 2017. doi:10.1016/j.enbuild.2017.10.073

182. Schnelle KB, Ternes ME, Dunn R. Fundamentals of Particulate Control. In: *Air Pollution Control Technology Handbook*. ; 2002:305-314.

183. Greiner A, Wendorff JH. Electrospinning: A fascinating method for the preparation of ultrathin fibers. *Angew Chemie - Int Ed*. 2007;46(30):5670-5703. doi:10.1002/anie.200604646

184. Yang F, Murugan R, Wang S, Ramakrishna S. Electrospinning of nano/micro scale poly(l-lactic acid) aligned fibers and their potential in neural tissue engineering. *Biomaterials*. 2005;26(15):2603-2610. doi:10.1016/j.biomaterials.2004.06.051

185. Mohammadian M, Haghi AK. Systematic parameter study for nano-fiber fabrication via electrospinning process. *Bulg Chem Commun*. 2014;46(3):545-555. doi:10.1016/j.polymer.2005.05.068

186. Chakraborty S, Liao IC, Adler A, Leong KW. Electrohydrodynamics: A facile technique to fabricate drug delivery systems. *Adv Drug Deliv Rev*. 2009;61(12):1043-1054. doi:10.1016/j.addr.2009.07.013

187. Cavaliere S. *ELECTROSPINNING for ADVANCED ENERGY and ENVIRONMENTAL APPLICATIONS*. (Group T& F, ed.). CRC Press; 2016.

188. Reneker DH, Yarin AL, Zussman E, Xu H. ELECTROSPINNING OF NANOFIBERS FROM POLYMER SOLUTIONS. *Polymer (Guildf)*. 2007. doi:10.1016/S0065-2156(06)41002-4

189. Beachley V, Wen X. Effect of electrospinning parameters on the nano fi ber diameter and length. *Mater Sci Eng C*. 2009;29(3):663-668. doi:10.1016/j.msec.2008.10.037

190. Li D, Xia Y. Electrospinning of nanofibers: Reinventing the wheel? *Adv Mater*. 2004;16(14):1151-1170. doi:10.1002/adma.200400719

191. Ding B, Kimura E, Sato T, Fujita S, Shiratori S. Fabrication of blend biodegradable nanofibrous nonwoven mats via multi-jet electrospinning. *Polymer (Guildf)*. 2004;45(6):1895-1902. doi:10.1016/j.polymer.2004.01.026

192. Zhang Q, Li Q, Young TM, Harper DP, Wang S. A Novel Method for Fabricating an Electrospun Poly(Vinyl Alcohol)/Cellulose Nanocrystals Composite Nanofibrous Filter with Low Air Resistance for High-Efficiency Filtration of Particulate Matter. *ACS Sustain Chem Eng*. 2019;7(9):8706-8714. doi:10.1021/acssuschemeng.9b00605

193. Clark JH, Kraus GA. *A Handbook of Applied Biopolymer Technology: Synthesis,*

Degradation and Applications. (Clark JH, Kraus GA, eds.). RSC Green Chemistry Series; 2011.

194. Hagen R, Gmbh UI. Polylactic Acid. In: *Polymer Science:A Comprehensive Reference*. Vol 10. Elsevier B.V.; 2012:231-236. doi:10.1016/B978-0-444-53349-4.00269-7

195. Byun Y, Kim YT. Bioplastics for Food Packaging: Chemistry and Physics. In: *Innovations in Food Packaging*. Elsevier Ltd; 2014:349-366. doi:10.1016/B978-0-12-394601-0.00014-X

196. Park J, Lee I. Controlled release of ketoprofen from electrospun porous polylactic acid (PLA) nanofibers. 2011:1287-1291. doi:10.1007/s10965-010-9531-0

197. Lemos PC, Viana C, Salgueiro EN, et al. Electrospun poly lactic acid (PLA) fibres: Effect of different solvent systems on fibre morphology and diameter. *Polym (United Kingdom)*. 2014;55(18):4728-4737. doi:10.1016/j.polymer.2014.06.032

198. Li Y, Teck C, Kotaki M. Study on structural and mechanical properties of porous PLA nano fi bers electrospun by channel-based electrospinning system. 2015;56:572-580. doi:10.1016/j.polymer.2014.10.073

199. Id JS, Shen J, Chen S, Cooper MA, Wu D, Yang Z. Nanofiller Reinforced Biodegradable PLA / PHA Composites : Current Status and Future Trends. :1-22. doi:10.3390/polym10050505

200. Jain JP, Kumar N. Self Assembly of Amphiphilic (PEG) ₃ -PLA Copolymer as Polymersomes: Preparation, Characterization, and Their Evaluation As Drug Carrier. *Biomacromolecules*. 2010;11(4):1027-1035. doi:10.1021/bm1000026

201. Ogata N, Jimenez G, Kawai H, Ogihara T. Structural and thermal mechanical properties of PLA CLAY nanocomposites.pdf. *J Polym Sci Part B Polym Phys*. 1997:389-396.

202. Auras R, Harte B, Selke S. An Overview of Polylactides as Packaging Materials. *Macromol Biosci*. 2004:835-864. doi:10.1002/mabi.200400043

203. Okamoto K, Ichikawa T, Yokohara T, Yamaguchi M. Miscibility , mechanical and thermal properties of poly (lactic acid)/ polyester-diol blends. *Eur Polym J*. 2009;45(8):2304-2312. doi:10.1016/j.eurpolymj.2009.05.011

204. Wu C, Liao H. Study on the preparation and characterization of biodegradable polylactide / multi-walled carbon nanotubes nanocomposites. *Polymer (Guildf)*. 2007;48(15):4449-4458. doi:10.1016/j.polymer.2007.06.004

205. Rasal RM, Janorkar A V, Hirt DE. Poly (lactic acid) modifications. *Prog Polym Sci*. 2010;35(3):338-356. doi:10.1016/j.progpolymsci.2009.12.003

206. Liao H, Wu C. Preparation and characterization of ternary blends composed of polylactide , poly (e -caprolactone) and starch. *Mater Sci Eng A*. 2009;515:207-214. doi:10.1016/j.msea.2009.03.003

207. Jiang L, Zhang J. Biodegradable and Biobased Polymers. In: *Applied Plastics Engineering Handbook*. Elsevier; 2011:145-158. doi:10.1016/B978-1-4377-3514-7.10009-1

208. Stolt M. Properties of lactic acid based polymers and their correlation with composition. *Prog Polym Sci*. 2002;27. doi:DOI: 10.1016/s0079-6700(02)00012-6

209. Yokesahachart C, Yoksan R. Effect of amphiphilic molecules on characteristics and tensile properties of thermoplastic starch and its blends with poly (lactic acid). *Carbohydr Polym*. 2011;83(1):22-31. doi:10.1016/j.carbpol.2010.07.020

210. Palmieri S, Pierpaoli M, Riderelli L, Qi S, Ruello ML. Preparation and Characterization of an Electrospun PLA-Cyclodextrins Composite for Simultaneous High-E ffi ciency PM and VOC Removal. *Compos Sci*. 2020:1-11.

211. Favier IM, Baudelet D, Fourmentin S. VOC trapping by new crosslinked cyclodextrin polymers. *J Incl Phenom Macrocycl Chem*. 2011;69(3-4):433-437. doi:10.1007/s10847-010-9776-6

212. Arkas M, Allabashi R, Tsiourvas D, Mattausch EM, Perfler R. Organic/inorganic hybrid filters based on dendritic and cyclodextrin "nanosponges" for the removal of organic pollutants from water. *Environ Sci Technol*. 2006;40(8):2771-2777. doi:10.1021/es052290v

213. Han R, Li J, Shin H, et al. Recent advances in discovery , heterologous expression , and molecular engineering of cyclodextrin glycosyltransferase for versatile applications. *Biotechnol Adv*. 2014;32(2):415-428. doi:10.1016/j.biotechadv.2013.12.004

214. Valle EMM Del. Cyclodextrins and their uses : a review. *Process Biochem*. 2004;39:1033-1046. doi:10.1016/S0032-9592(03)00258-9

215. Crini* G. Review : A History of Cyclodextrins. *Chem Rev*. 2014. doi:10.1021/cr500081p

216. Sliwa W, Girek T. *Cyclodextrins. Properties and Application*. (Wiley-VCH, ed.).; 2017.

217. Aulton ME, Taylor KMG. *Tecnologie Farmaceutiche-Progettazione e Allestimento Dei Medicinali*. (Edra, ed.). London; 2015.

218. Suan H, Wei C, Noriznan M, et al. Extractive bioconversion of cyclodextrins by Bacillus cereus cyclodextrin glycosyltransferase in aqueous two-phase system. *Bioresour Technol*. 2013;142:723-726. doi:10.1016/j.biortech.2013.05.087

219. Favier IM, Baudelet D, Fourmentin S. VOC trapping by new crosslinked cyclodextrin polymers. In: *Journal of Inclusion Phenomena and Macrocyclic Chemistry*. Vol 69. Springer; 2011:433-437. doi:10.1007/s10847-010-9776-6

220. Sliwa W, Girek T. *Cyclodextrins: Properties and Applications*. (Sliwa W, Girek T, eds.). Weinheim, Germany: wiley; 2017. doi:10.1002/9783527695294

221. Blanco KC, Moraes FFDE, Bernardi NS. Cyclodextrin Production by Bacillus lehensis Isolated from Cassava Starch : Characterisation of a Novel Enzyme. *Czech J Food Sci*. 2014;32(1):48-53.

222. Pierpaoli M, Riderelli L, Palmieri S, Fava G, Ruello ML. Transparent electrospun PLA-nanofibers on 3D-printed honeycomb for a high-efficient air filtration . In: ; 2017:2-3.

223. See SW, Balasubramanian R. Characterization of fi ne particle emissions from incense burning. *Build Environ*. 2011;46(5):1074-1080. doi:10.1016/j.buildenv.2010.11.006

224. Uyar T, Havelund R, Hacaloglu J, Besenbacher ḰF, Kingshott P. Cyclodextrins : Comparison of Molecular Filter Performance. *ACS Nano*. 2010;4(9):5121-5130.

225. Trofymchuk IM, Belyakova LA, Grebenyuk AG. Study of complex formation between b -cyclodextrin and benzene. *J Incl Phenom Macrocycl Chem*. 2011:371-375. doi:10.1007/s10847-010-9757-9

226. Chalumot G, Yao C, Pino V, Anderson JL. Determining the stoichiometry and binding constants of inclusion complexes formed between aromatic compounds and □ -cyclodextrin by solid-phase microextraction coupled to high-performance liquid chromatography. *J Chromatogr A J*. 2009;1216:5242-5248.

doi:10.1016/j.chroma.2009.05.017

227. Wang Z, Zhao C, Pan Z. Porous bead-on-string poly(lactic acid) fibrous membranes for air filtration. *J Colloid Interface Sci*. 2015;441:121-129. doi:10.1016/j.jcis.2014.11.041

228. A Novel Hierarchical Structured Poly(lactic acid)/Titania Fibrous Membrane with Excellent Antibacterial Activity and Air Filtration Performance. doi:10.1155/2016/6272983

229. Medhurst LJ. FTIR Determination of Pollutants in Automobile Exhaust : An Environmental Chemistry Experiment Comparing Cold-Start and Warm-Engine Conditions. *J Chem Educ*. 2005;82(2).

230. Raza ZA, Abid S, Banat IM. Polyhydroxyalkanoates: Characteristics, production, recent developments and applications. *Int Biodeterior Biodegrad*. 2018;126(September 2017):45-56. doi:10.1016/j.ibiod.2017.10.001

231. Khajuria R, Kaur L, Parihar L, Singh GD. Polyhydroxyalkanoates : Biosynthesis to commercial production- A review. *J Microbiol Biotechnol food Sci*. 2017;(February). doi:10.15414/jmbfs.2017.6.4.1098-1106

232. Lee SY. Plastic bacteria ? Progress and prospects for polyhydroxyalkanoate production in bacteria. *Trends Biotechnol*. 1996;14(November):431-438.

233. Madison LL, Huisman GW. Metabolic Engineering of Poly (3-Hydroxyalkanoates): From DNA to Plastic. *Microbiol Mol Biol Rev*. 1999;63(1):21-53.

234. Poli A, Di Donato P, Abbamondi GR, Nicolaus B. Synthesis, production, and biotechnological applications of exopolysaccharides and polyhydroxyalkanoates by Archaea. *Archaea*. 2011;2011. doi:10.1155/2011/693253

235. Kourmentza C, Ntaikou I, Kornaros M, Lyberatos G. Production of PHAs from mixed and pure cultures of Pseudomonas sp . using short-chain fatty acids as carbon source under nitrogen limitation. *DESALINATION*. 2009;248(1-3):723-732. doi:10.1016/j.desal.2009.01.010

236. Anderson AJ, Dawes EA. Occurrence , Metabolism , Metabolic Role , and Industrial Uses of Bacterial Polyhydroxyalkanoates. *Microbiol Rev*. 1990;54(4):450-472.

237. Khanna S, Srivastava AK. Recent advances in microbial polyhydroxyalkanoates. *Process Biochem*. 2005.

238. Steinbüchel A, Hein S. Biochemical and Molecular Basis of Microbial Synthesis of Polyhydroxyalkanoates in Microorganisms. In: *Advances in Biochemical Engineering/ Biotechnology*. Vol 71. ; 2001.

239. Tan GYA, Chen CL, Li L, et al. Start a research on biopolymer polyhydroxyalkanoate (PHA): A review. *Polymers (Basel)*. 2014;6(3):706-754. doi:10.3390/polym6030706

240. Rehm BHA. Polyester synthases : natural catalysts for plastics. *Biochem J*. 2003;33:15-33.

241. Rass-Hansen J, Falsig H, Jørgensen B, Christensen CH. Chemical characterization of medium-chain-length polyhydroxyalkanoates (PHAs) recovered by enzymatic treatment and ultrafiltration. *J ofChemical Technol Biotechnol*. 2007;82(May):329–333. doi:10.1002/jctb

242. Gagnon KD, Lenzt RW, Farris RJ, Science P, Fuller RC. Chemical modification of bacterial elastomers: 1. Peroxide crosslinking. *Polymer (Guildf)*. 1994;35(20):4358-4367.

243. Fei T, Cazeneuve S, Wen Z, Wu L, Wang T. Effective recovery of poly- β - hydroxybutyrate (PHB) biopolymer from Cupriavidus necator using a novel and environmentally friendly solvent system Effective Recovery of Poly- b -Hydroxybutyrate (PHB) Biopolymer from Cupriavidus necator Using a Novel a. *Am Inst Chem Eng*. 2016;(February). doi:10.1002/btpr.2247

244. Pradhan S, Dikshit PK, Moholkar VS. Production, ultrasonic extraction, and characterization of poly (3-hydroxybutyrate) (PHB) using Bacillus megaterium and Cupriavidus necator. *Polym Adv Technol*. 2018;29(8):2392-2400. doi:10.1002/pat.4351

245. Arcos-hernández M V, Laycock B, Donose BC, et al. Physicochemical and mechanical properties of mixed culture polyhydroxyalkanoate (PHBV). *Eur Polym J*. 2013;49(4):904-913. doi:10.1016/j.eurpolymj.2012.10.025

246. Doi Y. MICROBIAL SYNTHESIS, PHYSICAL PROPERTIES, AND BIODEGRADABILITY OF POLYHYDROXYALKANOATES. *Macromol Symp*. 1995.

247. Vandi L, Chan CM, Werker A, Richardson D. Extrusion of wood fibre reinforced poly(hydroxybutyrate-co-hydroxyvalerate) (PHBV) biocomposites: Statistical analysis of the effect of processing conditions on mechanical performance. *Polym Degrad Stab*. 2018. doi:10.1016/j.polymdegradstab.2018.10.015

248. Ten E, Jiang L, Zhang J, Wolcott MP. *Mechanical Performance of Polyhydroxyalkanoate (PHA)-Based Biocomposites*. Fourteenth. Elsevier Ltd.; 2015. doi:10.1016/B978-1-78242-373-7.00008-1

249. Shivakumar S. Polyhydroxybutyrate (PHB) production using agro-industrial residue as substrate by Bacillus. *Int J ChemTech Res*. 2018;(June).

250. Bhardwaj U, Dhar P, Kumar A, Katiyar V. Polyhydroxyalkanoates (PHA)-cellulose based nanobiocomposites for food packaging applications. *ACS Symp Ser*. 2014;1162:275-314. doi:10.1021/bk-2014-1162.ch019

251. Stevulova N, Schwarzova I, Hospodarova V, Junak J. Implementation of waste cellulosic fibres into building materials. *Chem Eng Trans*. 2016;50(January):367-372. doi:10.3303/CET1650062

252. Zhang Y, Sun W, Wang H, Geng A. Bioresource Technology Polyhydroxybutyrate production from oil palm empty fruit bunch using Bacillus megaterium R11. *Bioresour Technol*. 2013;147:307-314. doi:10.1016/j.biortech.2013.08.029

253. Foglia TA, Marmer WN. Conversion of agricultural feedstock and coproducts into poly (hydroxyalkanoates). *Appl Microbiol Biotechnol*. 2006:783-789. doi:10.1007/s00253-006-0451-1

254. Basset N, Katsou E, Frison N, Malamis S, Dosta J, Fatone F. Integrating the selection of PHA storing biomass and nitrogen removal via nitrite in the main wastewater treatment line. *Bioresour Technol*. 2016;200:820-829. doi:10.1016/j.biortech.2015.10.063

255. Dobroth ZT, Hu S, Coats ER, Mcdonald AG. Bioresource Technology Polyhydroxybutyrate synthesis on biodiesel wastewater using mixed microbial consortia. *Bioresour Technol*. 2011;102(3):3352-3359. doi:10.1016/j.biortech.2010.11.053

256. Bhatnagar A, Sillanpää M. Utilization of agro-industrial and municipal waste materials as potential adsorbents for water treatment-A review. *Chem Eng J*. 2010;157(2-3):277-296. doi:10.1016/j.cej.2010.01.007

257. Frison N, Katsou E, Malamis S, Oehmen A, Fatone F. Development of a Novel Process

Integrating the Treatment of Sludge Reject Water and the Production of Polyhydroxyalkanoates (PHAs). *Environ Sci Technol*. 2015;49(18):10877-10885. doi:10.1021/acs.est.5b01776

258. Bengtsson S, Pisco AR, Johansson P, Lemos PC, Reis MAM. Molecular weight and thermal properties of polyhydroxyalkanoates produced from fermented sugar molasses by open mixed cultures. *J Biotechnol*. 2010;147(3-4):172-179. doi:10.1016/j.jbiotec.2010.03.022

259. Adsul M, Tuli DK, Annamalai PK, Depan D, Shankar S. Polymers from Biomass : Characterization , Modification , Degradation , and Applications. 2016;2016:2-4.

260. Martínez-Sanz M, Villano M, Oliveira C, et al. Characterization of polyhydroxyalkanoates synthesized from microbial mixed cultures and of their nanobiocomposites with bacterial cellulose nanowhiskers. *N Biotechnol*. 2014;31(4):364-376. doi:10.1016/j.nbt.2013.06.003

261. De-Bashan LE, Bashan Y. Recent advances in removing phosphorus from wastewater and its future use as fertilizer (1997-2003). *Water Res*. 2004;38(19):4222-4246. doi:10.1016/j.watres.2004.07.014

262. Van Der Hoek JP, De Fooij H, Struker A. Wastewater as a resource: Strategies to recover resources from Amsterdam's wastewater. *Resour Conserv Recycl*. 2016;113:53-64. doi:10.1016/j.resconrec.2016.05.012

263. Ghosh S, Gnaim R, Greiserman S, Fadeev L, Gozin M, Golberg A. Macroalgal biomass subcritical hydrolysates for the production of polyhydroxyalkanoate (PHA) by Haloferax mediterranei. *Bioresour Technol*. 2019;271(July 2018):166-173. doi:10.1016/j.biortech.2018.09.108

264. Matthew C, Johansson P, Magnusson P, et al. Mixed culture polyhydroxyalkanoate-rich biomass assessment and quality control using thermogravimetric measurement methods. *Polym Degrad Stab*. 2017;144:110-120. doi:10.1016/j.polymdegradstab.2017.07.029

265. Jiang G, Johnston B, Townrow DE, et al. Biomass extraction using non-chlorinated solvents for biocompatibility improvement of polyhydroxyalkanoates. *Polymers (Basel)*. 2018;10(7). doi:10.3390/polym10070731

266. Furrer P, Zinn M, Panke S. Efficient recovery of medium-chain-length poly([R]-3-hydroxyalkanoate) from bacterial biomass. *EMPA Act*. 2006;69(2006):43. doi:10.1016/j.mimet.2007.01.002

267. Longo S, Frison N, Renzi D, Fatone F. Is SCENA a good approach for side-stream integrated treatment from an environmental and economic point of view ? *Water Res*. 2017;125:478-489. doi:10.1016/j.watres.2017.09.006

268. Heinrich D, Madkour MH, Al-Ghamdi MA, Shabbaj II, Steinbüchel A. Large scale extraction of poly(3-hydroxybutyrate) from Ralstonia eutropha H16 using sodium hypochlorite. *AMB Express*. 2012;2(1):1-6. doi:10.1186/2191-0855-2-59

269. Koller M, Niebelschütz H, Braunegg G. Strategies for recovery and purification of poly[(R)-3-hydroxyalkanoates] (PHA) biopolyesters from surrounding biomass. *Eng Life Sci*. 2013;13(6):549-562. doi:10.1002/elsc.201300021

270. D'Hondt E, Martín-Juárez J, Bolado S, et al. Cell disruption technologies. *Microalgae-Based Biofuels Bioprod From Feed Cultiv to End-Products*. 2017:133-154. doi:10.1016/B978-0-08-101023-5.00006-6

271. Ramsay' JA, Berger E, Voyer R, Chavarie C, B.A. Ramsay. EXTRACTION OF POLY-3-HYDROXYBUTYRATE USING CHLORINATED SOLVENTS. *Biotechnol Tech*. 1994;8(8):589-594.

272. Kunasundari B, Sudesh K. Isolation and recovery of microbial polyhydroxyalkanoates. *eXPRESS Polym Lett Vol5,*. 2011;5(7):620-634. doi:10.3144/expresspolymlett.2011.60

273. Hu X. Separation Science and Technology Recovery of Chloroform from Effluent with Solvent Extraction – Distillation Process. *Sep Sci Technol*. 1997;(January 2015). doi:10.1080/01496399708000753

274. Jacquel N, Lo CW, Wei YH, Wu HS, Wang SS. Isolation and purification of bacterial poly(3-hydroxyalkanoates). *Biochem Eng J.* 2008;39(1):15-27. doi:10.1016/j.bej.2007.11.029

275. Christi Y. Strategies in Downstream processing. In: *Bioseparation and Bioprocessing: A Handbook*. ; 1998.

276. Harrison STL. Bacterial cell disruption: A key unit operation in the recovery of intracellular products. *Biotechnol Adv*. 1991;9(2):217-240. doi:10.1016/0734-9750(91)90005-G

277. Hwang KJ, You SF, Don TM. Disruption kinetics of bacterial cells during purification of polyhydroxyalkanoate using ultrasonication. *J Chinese Inst Chem Eng*. 2006;37(3):209-216.

278. Geciova J, Bury D, Jelen P. Methods for disruption of microbial cells for potential use in the dairy industry - A review. *Int Dairy J*. 2002;12(6):541-553. doi:10.1016/S0958-6946(02)00038-9

279. Limon-Lason J, Hoare M, Orsborn CB, Doyle DJ, Dunnill P. Reactor properties of a high-speed bead mill for microbial cell rupture. *Biotechnol Bioeng*. 1979;21(5):745-774. doi:10.1002/bit.260210503

280. Ghatnekar MS, Pai JS, Ganesh M. Production and recovery of poly-3-hydroxy- butyrate from Methylobacterium sp V49. *J ofChemical Technol Biotechnol*. 2002;448(July 2001):444-448. doi:10.1002/jctb.570

281. Sudesh K, Abe H, Doi Y. Synthesis , structure and properties of polyhydroxyalkanoates : biological polyesters. 2000;25:1503-1555.

282. Patel B, Guo M, Izadpanah A, Shah N, Hellgardt K. A Review on Hydrothermal Pre-treatment Technologies and Environmental Profiles of Algal Biomass Processing. *Bioresour Technol*. 2015. doi:10.1016/j.biortech.2015.09.064

283. Ju E, Taek H, Mun K, et al. Pretreatment and saccharification of red macroalgae to produce fermentable sugars. *Bioresour Technol*. 2016;199:311-318. doi:10.1016/j.biortech.2015.08.001

284. Hedenskog G, Mogren Hår, Enebo L. A method for obtaining protein concentrates from microorganisms. *Biotechnol Bioeng*. 1970;12(6):947-959. doi:10.1002/bit.260120607

285. Mao HH, Moo-young M. DISRUPTION OF BAKER'S YEAST BY A NBN BEAU MILL. *Biotechnol tec*. 1990;4(5):335-340.

286. Raza ZA, Riaz S, Banat IM. Polyhydroxyalkanoates: Properties and chemical modification approaches for their functionalization. *Biotechnol Prog*. 2018;34(1):29-41. doi:10.1002/btpr.2565

287. Luque de Castro MD, Priego-Capote F. Soxhlet extraction: Past and present panacea. *J Chromatogr A*. 2010;1217(16):2383-2389. doi:10.1016/j.chroma.2009.11.027

288. Mezzomo N, Maestri B, Lazzaris R, Maraschin M, Ferreira SRS. Pink shrimp (P . brasiliensis and P . paulensis) residue : Influence of extraction method on carotenoid concentration. *Talanta*. 2011;85:1383-1391. doi:10.1016/j.talanta.2011.06.018

289. Timbart L, Renard E, Tessier M, Langlois V. Monohydroxylated poly(3-hydroxyoctanoate) oligomers and its functionalized derivatives used as macroinitiators in the synthesis of degradable diblock copolyesters. *Biomacromolecules*. 2007;8(4):1255-1265. doi:10.1021/bm060981t

290. Arcos-hernandez MVM, Gurieff N, Pratt S, et al. Mixed culture polyhydroxyalkanoate-rich biomass assessment and quality control using thermogravimetric measurement methods. *Polym Degrad Stab*. 2018;150(3):372-379. doi:10.1016/j.jbiotec.2010.09.939

291. W.J. Sichina. Characterization of Polymers Using TGA. *Therm Anal Appl note*. 2011:1-4.

292. Radecka I, Irorere V, Jiang G, et al. Oxidized Polyethylene Wax as a Potential Carbon Source for PHA Production. 2016:1-16. doi:10.3390/ma9050367

293. Stanley A, Vijayendra PSKMSVN. Characterization of Polyhydroxyalkanoate Produced by Halomonas venusta KT832796. *J Polym Environ*. 2020;28(3):973-983. doi:10.1007/s10924-020-01662-6

294. Kansiz K, Billman-Jacobe H, McNaughton D. Quantitative determination of the biodegradable polymer poly(β-hydroxybutyrate) in a recombinant Escherichia coli strain by use of mid-infrared spectroscopy and multivariative statistics. *Appl Environ Microbiol*. 2000;66(8):3415-3420. doi:10.1128/AEM.66.8.3415-3420.2000

295. Arcos-hernandez M V, Gurieff N, Pratt S, et al. Rapid quantification of intracellular PHA using infrared spectroscopy : An application in mixed cultures. *J Biotechnol J*. 2010;150:372-379. doi:10.1016/j.jbiotec.2010.09.939

296. Hong K, Sun S, Tian W, Chen GQ, Huang W. A rapid method for detecting bacterial polyhydroxyalkanoates in intact cells by Fourier transform infrared spectroscopy. *Appl Microbiol Biotechnol*. 1999;51(4):523-526. doi:10.1007/s002530051427

297. Goracci C, Sadek FT, Monticelli F, Cardoso PEC, Ferrari M. Influence of substrate, shape, and thickness on microtensile specimens' structural integrity and their measured bond strengths. *Dent Mater*. 2004;20(7):643-654. doi:10.1016/j.dental.2003.08.009

298. Brown R. *Handbook of Polymer Testing*.; 1999. doi:10.1201/9781482270020

299. Richeton J, Ahzi S, Vecchio KS, Jiang FC, Adharapurapu RR. Influence of temperature and strain rate on the mechanical behavior of three amorphous polymers: Characterization and modeling of the compressive yield stress. *Int J Solids Struct*. 2006;43(7-8):2318-2335. doi:10.1016/j.ijsolstr.2005.06.040

300. Reddy N, Chen L, Yang Y. Thermoplastic films from peanut proteins extracted from peanut meal. *Ind Crops Prod*. 2013;43(1):159-164. doi:10.1016/j.indcrop.2012.06.051

301. Modesti M, Besco S, Lorenzetti A. Effect of Processing Conditions on the Morphology and Properties of Polymer Nanocomposites. *Optim Polym Nanocomposite Prop*. 2010:369-405. doi:10.1002/9783527629275.ch17

302. Vandi LJ, Chan CM, Werker A, Richardson D, Laycock B, Pratt S. Experimental data for extrusion processing and tensile properties of poly(hydroxybutyrate-co-hydroxyvalerate)

(PHBV) polymer and wood fibre reinforced PHBV biocomposites. *Data Br*. 2019;22:687-692. doi:10.1016/j.dib.2018.12.084

303. Martin O, Schwach E, Avérous L, Couturier Y. Properties of biodegradable multilayer films based on plasticized wheat starch. *Starch/Staerke*. 2001;53(8):372-380. doi:10.1002/1521-379X(200108)53:8<372::AID-STAR372>3.0.CO;2-F

304. Misra SK, Valappil SP, Roy I, Boccaccini AR. Polyhydroxyalkanoate (PHA)/inorganic phase composites for tissue engineering applications. *Biomacromolecules*. 2006;7(8):2249-2258. doi:10.1021/bm060317c

305. Weng L, Fan T, Wen M, Shen Y. Three-dimensional multi-particle FE model and effects of interface damage , particle size and morphology on tensile behavior of particle reinforced composites. *Compos Struct*. 2019;209(October 2018):590-605. doi:10.1016/j.compstruct.2018.11.008

306. Meng Q, Wang T. An improved crack-bridging model for rigid particle-polymer composites. *Eng Fract Mech*. 2019;211(February):291-302. doi:10.1016/j.engfracmech.2019.02.028

307. Nielsen LE, Landel RF. *Mechanical Properties of Polymers and Composites*. (Inc MD, ed.).; 1994.

308. Byreddy AR, Gupta A, Barrow CJ, Puri M. Comparison of Cell Disruption Methods for Improving Lipid Extraction from Thraustochytrid Strains. *Mar Drugs*. 2015:5111-5127. doi:10.3390/md13085111

309. Lenz RW, Stein RS. *POLYMER SCIENCE AND TECHNOLOGY: STRUCTURE AND PROPERTIES OF POLYMER FILMS*. Vol 1.; 1972.

310. Kai Z, Ying D, Guo-qiang C. Effects of surface morphology on the biocompatibility of polyhydroxyalkanoates. *Biochem Eng J*. 2003;16:115-123. doi:10.1016/S1369-703X(03)00029-9

311. Sasaguri K, Hoshino S, Stein RS. Relationship between Morphology and Deformation Mechanisms of Polyolefins. *J Appl Phys*. 2008;47(1964):46-54. doi:10.1063/1.1713097

312. Dai Y, Lambert L, Yuan Z, Keller J. Characterisation of polyhydroxyalkanoate copolymers with controllable four-monomer composition. 2008;134:137-145. doi:10.1016/j.jbiotec.2008.01.013

313. Arslan H, Yeşilyurt N, Hazcr B. Brush type copolymers of poly(3-hydroxybutyrate) and poly(3- hydroxyoctanoate) with same vinyl monomers via "grafting fromæ technique by using atom transfer radical polymerization method. *Macromol Symp*. 2008;269(1):23-33. doi:10.1002/masy.200850905

314. Leonardo P, Ribeiro L, Cezar A, et al. Impact of different by-products from the biodiesel industry and bacterial strains on the production , composition , and properties of novel polyhydroxyalkanoates containing achiral building blocks. *Ind Crop Prod*. 2015;69:212-223. doi:10.1016/j.indcrop.2015.02.035

315. Inomata M, Vilas T, Figueiredo B, Santos L, Izabel J. The influence of crude glycerin and nitrogen concentrations on the production of PHA by Cupriavidus necator using a response surface methodology and its characterizations. *Ind Crop Prod*. 2014;52:338-346. doi:10.1016/j.indcrop.2013.11.008

316. Castell P, Garcia-Quiles L, Cuello A. Sustainable Materials with Enhanced Mechanical Properties Based on Industrial Polyhydroxyalkanoates Reinforced with Organomodified

Sepiolite. *Polymers (Basel)*. 2019.

317. Cha S, Son J, Jamal Y, Zafar M, Park H. Characterization of polyhydroxyalkanoates extracted from wastewater sludge under different environmental conditions. *Biochem Eng J*. 2016;112:1-12. doi:10.1016/j.bej.2015.12.021

318. Wunderlich B. *Macromolecular Physics - Crystal Melting Volume 3(, Academic Press) - Libgen.Lc.Pdf*. (Press A, ed.).; 1980.

319. Melnikov AP, Rosenthal M, Rodygin AI, Doblas D, Anokhin D V, Burghammer M. Re-exploring the double-melting behavior of semirigid-chain polymers with an in-situ combination of synchrotron nano- focus X-ray scattering and nanocalorimetry. *Eur Polym J*. 2016;81:598-606. doi:10.1016/j.eurpolymj.2015.12.031

320. El-abd MAE, El-sheikh HH, Desouky S, Shehab A. Identification , Biodegradation and bio-evaluation of biopolymer produced from Bacillus thuringenesis. 2017;(March 2018). doi:10.7324/JAPS.2017.70414

321. Koller M, Bona R, Braunegg G, et al. Production of Polyhydroxyalkanoates from Agricultural Waste and Surplus Materials. *Biomacromolecules*. 2005;(year 2002):561-565.

322. Ghaffari Mosanenzadeh S, Naguib HE, Park CB, Atalla N. Effect of biopolymer blends on physical and Acoustical properties of biocomposite foams. *J Polym Sci Part B Polym Phys*. 2014;52(15):1002-1013. doi:10.1002/polb.23522

323. Dahy H. Biocomposite materials based on annual natural fibres and biopolymers – Design, fabrication and customized applications in architecture. *Constr Build Mater*. 2017;147:212-220. doi:10.1016/j.conbuildmat.2017.04.079

324. Zhou Y, Fan M, Chen L. *Interface and Bonding Mechanisms of Plant Fibre Composites: An Overview*. Vol 101. Elsevier Ltd; 2016. doi:10.1016/j.compositesb.2016.06.055

325. Cruz-ramos CA. Natural Fiber Reinforced Thermoplastics. In: *Mechanical Properties of Reinforced Thermoplastics*. ; 1986:65-81.

326. Kim JK, Pal K. *Recent Advances in the Processing of Wood–Plastic Composites*. (Springer Heidelberg, ed.). Springer Heidelberg

327. Bhardwaj R, Mohanty AK, Drzal LT, Pourboghrat F, Misra M. Renewable resource-based green composites from recycled cellulose fiber and poly(3-hydroxybutyrate-co-3-hydroxyvalerate) bioplastic. *Biomacromolecules*. 2006;7(6):2044-2051. doi:10.1021/bm050897y

328. Lotfi A, Li H, Dao DV, Prusty G. Natural fiber – reinforced composites : A review on material , manufacturing , and machinability. *J Thermoplast Compos Mater*. 2019. doi:10.1177/0892705719844546

329. Saheb DN, Jog JP. Natural Fiber Polymer Composites : A Review. *Adv Polym Technol*. 1999;18(4):351-363.

330. Fuqua MA, Huo S, Ulven CA. Natural Fiber Reinforced Composites. *Polym Rev*. 2016;3724(October). doi:10.1080/15583724.2012.705409

331. Ramakrishna G, Sundararajan T. Studies on the durability of natural fibres and the effect of corroded fibres on the strength of mortar. *Cem Concr Compos*. 2005;27(5):575-582. doi:10.1016/j.cemconcomp.2004.09.008

332. Cinelli P, Mallegni N, Gigante V, et al. Biocomposites Based on Polyhydroxyalkanoates

and Natural Fibres from Renewable Byproducts. *Appl food biotechology*. 2019;6(1):35-43.

333. Devasahayam S, Yarlagadda P. Mechanics of Polyropylene-Seed-Coat-Fibres Composites AndPolyropylene – Wood Fibres Composites-A Comparative Study. *Procedia Eng*. 2014;97:1915-1928. doi:10.1016/j.proeng.2014.12.345

334. Sedan D, Pagnoux C, Smith A, Chotard T. Mechanical properties of hemp fibre reinforced cement: Influence of the fibre/matrix interaction. *J Eur Ceram Soc*. 2008;28(1):183-192. doi:10.1016/j.jeurceramsoc.2007.05.019

335. A.K. Bledzki JG. Composites reinforced with cellulose based fibre. *Prog Polym Sci*. 1999;24:221-274.

336. Poletto M, Ornaghi Júnior HL, Zattera AJ. Native cellulose: Structure, characterization and thermal properties. *Materials (Basel)*. 2014;7(9):6105-6119. doi:10.3390/ma7096105

337. Chan CM, Vandi L, Pratt S, et al. Composites of Wood and Biodegradable Thermoplastics : A Review. *Polym Rev*. 2018;58(3):444-494. doi:10.1080/15583724.2017.1380039

338. Gamstedt EK. Fatigue Propagation of Fibre-Bridged Cracks in Unidirectional Polymer-Matrix Composites. *Appl Compos Mater*. 2001:385-410.

339. Sahajwalla V. Composite panels obtained from automotive waste plastics and agricultural macadamia shell waste. *J Clean Prod*. 2017. doi:10.1016/j.jclepro.2017.03.074

340. BUIXANSKY B, FLECK NA. COMPRESSIVE FAILURE OF FIBRE. *J Mech Phys Solids*. 1993;41(I).

341. Friedrich K, Zhang Z, Schlarb AK. Effects of various fillers on the sliding wear of polymer composites. *Compos Sci Technol*. 2005;65:2329-2343. doi:10.1016/j.compscitech.2005.05.028

342. Mohanty AK, Misra M, Drzal LT. Sustainable Bio-Composites from Renewable Resources in Green Materials world. *J ofPolymers Environ*. 2002;10(April):19-26.

343. Fan M, Fu F. *Advance High Strength Natural Fibre Composites in Costruction*.

344. Desch HE, Dinwoodie JM. *Timber: Structure, Properties, Conversion and Use*. (MACMILLAN PRESS L TO Houndmills, Basingstoke H, ed.). MACMILLAN PRESS L TO Houndmills, Basingstoke, Ham; 1996.

345. Wistara N, Zhang X, Young RA. Properties and treatments of pulps from recycled paper. Part II. Surface properties and crystallinity of fibers and fines. *Cellulose*. 1999;6(4):325-348. doi:10.1023/A:1009255808215

346. Singh K, Risse M, Das KC, Worley J. Determination of Composition of Cellulose and Lignin Mixtures Using Thermogravimetric Analysis. *J Energy Resour Technol*. 2009;131(2):022201. doi:10.1115/1.3120349

347. Wu C. Renewable resource-based green composites of surface-treated spent coffee grounds and polylactide : Characterisation and biodegradability. *Polym Degrad Stab*. 2015;121:51-59. doi:10.1016/j.polymdegradstab.2015.08.011

348. Yoo J, Chang SJ, Wi S, Kim S. Spent coffee grounds as supporting materials to produce bio- composite PCM with natural waxes. *Chemosphere*. 2019;235:626-635. doi:10.1016/j.chemosphere.2019.06.195

349. Dufresne A. Utilization of Torrefied Coffee Grounds as Reinforcing Agent To Produce High-Quality Biodegradable PBAT Composites for Food Packaging Applications. *Sustain Chem Eng*. 2017. doi:10.1021/acssuschemeng.6b02633

350. Pujol D, Liu C, Gominho J, et al. The chemical composition of exhausted coffee waste. *Ind Crop Prod*. 2013;50:423-429. doi:10.1016/j.indcrop.2013.07.056

351. Lessa EF, Nunes ML, Fajardo AR. Chitosan/waste coffee-grounds composite: An efficient and eco-friendly adsorbent for removal of pharmaceutical contaminants from water Authors: *Carbohydr Polym*. 2018. doi:10.1016/j.carbpol.2018.02.018

352. Sung SH, Chang Y, Han J. Development of polylactic acid nanocomposite films reinforced with cellulose nanocrystals derived from coffee silverskin. *Carbohydr Polym*. 2017;169:495-503. doi:10.1016/j.carbpol.2017.04.037

353. García-García D, Carbonell A, Samper MD, García-Sanoguera D, Balart R. Green composites based on polypropylene matrix and hydrophobized spend coffee ground (SCG) powder. *Compos Part B Eng*. 2015;78:256-265. doi:10.1016/j.compositesb.2015.03.080

354. Cinelli P, Mallegni N, Gigante V, et al. Biocomposites Based on Polyhydroxyalkanoates and Natural Fibres from Renewable Byproducts. 2019;6(1):35-43.

355. Vandi LJ, Chan CM, Werker A, Richardson D, Laycock B, Pratt S. Extrusion of wood fibre reinforced poly(hydroxybutyrate-co-hydroxyvalerate) (PHBV) biocomposites: Statistical analysis of the effect of processing conditions on mechanical performance. *Polym Degrad Stab*. 2019;159(2019):1-14. doi:10.1016/j.polymdegradstab.2018.10.015

356. Matthew C, Vandi L, Pratt S, Halley P, Richardson D. Mechanical performance and long-term indoor stability of polyhydroxyalkanoate (PHA) -based wood plastic composites (WPCs) modified by non-reactive additives. *Eur Polym J*. 2018;98(September 2017):337-346. doi:10.1016/j.eurpolymj.2017.11.041

357. Luzier WD. Materials derived from biomass / biodegradable materials NNCH \ O ./ H-. *Proc Nati Acad Sci*. 1992;89(February):839-842.

358. Węcławski BT, Fan M, Hui D. Compressive behaviour of natural fibre composite. *Compos Part B Eng*. 2014;67:183-191. doi:10.1016/j.compositesb.2014.07.014

359. Kalia S, Dufresne A, Cherian BM, Kaith BS, Njuguna J, Nassiopoulos E. Cellulose based biocomposites and nanocomposites – a review. 2011;2011:1-103.

360. Taylor P, Netravali AN, Huang X, Mizuta K. Advanced ' green ' composites. *Adv Compos Mater*. 2007;(January 2014):37-41. doi:10.1163/156855107782325230

361. Luo S, Netravali AN. Interfacial and mechanical properties of environment-friendly " green " composites made from pineapple fibers and poly (hydroxybutyrate-co-valerate) resin. *J Mater Sci*. 1999;4:3709-3719.

362. Ozaki SK, Monteiro MBB, Yano H, Imamura Y, Souza MF. Biodegradable composites from waste wood and poly (vinyl alcohol). *Polym Degrad Stab*. 2005;87:293-299. doi:10.1016/j.polymdegradstab.2004.08.011

363. Youngquist JA, Myers GE, Muehl JH, Krzysik AM, Clemens CM, Brown L. *COMPOSITES FROM RECYCLED WOOD AND PLASTICS*.; 1994.

364. James F, Shackelford EJF, Alexander W. *MATERIALS SCIENCE ENGINEERING*.; 2001.

365. Mohamed MAS, Ghorbel E, Wardeh G. Valorization of micro-cellulose fibers in self-

compacting concrete. *Constr Build Mater*. 2010;24(12):2473-2480. doi:10.1016/j.conbuildmat.2010.06.009

366. Chanda Ma, Roy SK. *Plastics Fundamentals, Properties, and Testing*. (Donald E. Hudgin Professor, ed.). CRC Press; 2009.

367. Thakur VK, Thakur MK, Kessler MR. *Handbook of Composites from Renewable Materials*. Scrivener Publishing; Wiley; 2017.

368. Hoffmann A, Kreuzberger S, Hinrichsen G, Physics P. Influence of thermal degradation on tensile strength and Young's modulus of poly(hydroxybutyrate). *Polym Bullettin*. 1994;359:355-359.

369. Holmes PA. BIOLOGICALLY PRODUCED (R)-3-HYDROXY- ALKANOATE POLYMERS AND COPOLYMERS. In: *Development of Crystalline Polymers -2*. ; 1988:1-65.

370. Beecher JF, Marker L, Bradford RD. Morphology and Mechanical Behavior of Block Polymers. 1969;134(26):117-134.

371. Quipeng G. *Polymer Morphology*. (Wiley, ed.).; 2016.

372. Park CH, Lee WI. *Compression Molding in Polymer Matrix Composites*. Woodhead Publishing Limited; 2012. doi:10.1533/9780857096258.1.47

373. Chuayjuljit S. Properties and morphology of injection- and compression-molded thermoplastic polyurethane/polypropylene-graft-maleic anhydride/wollastonite composites. *J Thermoplast Compos Mater*. 2015;(November). doi:10.1177/0892705711431104

374. Landry B, Hubert P. Experimental study of defect formation during processing of randomly-oriented strand carbon / PEEK composites. *Compos Part A*. 2015;77:301-309. doi:10.1016/j.compositesa.2015.05.020

375. Molenaar J, Koopmans RJ, Doelder CFJ Den. Onset of the sharkskin phenomenon in polymer extrusion. *Phys Rev E*. 1998;58(4):4683-4691.

376. Seggiani M, Cinelli P, Mallegni N, et al. New Bio-Composites Based on Polyhydroxyalkanoates and Posidonia oceanica Fibres for Applications in a Marine Environment. *Materials (Basel)*. doi:10.3390/ma10040326

377. Guo W, Duan J, Geng W, et al. A Statistical approach to optimize the production of Polyhydroxyalkanoates from Wickerhamomyces anomalus VIT-NN01 using Response Surface Methodology. *Int J Biol Macromol*. 2013;168(4):231-237. doi:10.1016/j.micres.2012.11.003

378. Manfredi LB, Rodrı ES. Thermal degradation and fire resistance of unsaturated polyester , modified acrylic resins and their composites with natural fibres. *Polym Degrad Stab*. 2006;91:255-261. doi:10.1016/j.polymdegradstab.2005.05.003

379. Gaugler M, Grigsby WJ. Thermal Degradation of Condensed Tannins from Radiata Pine Bark. *J Wood Chem Technol*. 2009;(August 2013):37-41. doi:10.1080/02773810903165671

380. Beal BFC. Differential Calometric Analysis of Wood and Wood Components *. *Wood Sci Technol*. 1971;5:159-175.

381. Fulop A, Beres R, Tengolics R, Rakhely G, Kovacs KL. Relationship between PHA and hydrogen metabolism in the purple sulfur phototrophic bacterium Thiocapsa

roseopersicina BBS. *SciVerse Sci*. 2011;7:1-10. doi:10.1016/j.ijhydene.2011.12.019

382. Capson-tojo G, Batstone DJ, Grassino M, et al. Purple phototrophic bacteria for resource recovery : Challenges and opportunities. *Biotechnol Adv*. 2020;43(May):107567. doi:10.1016/j.biotechadv.2020.107567

383. Nagatsuma S, Gotou K, Yamashita T, et al. Phospholipid distributions in purple phototrophic bacteria and LH1-RC core complexes. *BBA - Bioenerg*. 2019;1860(April):461-468. doi:10.1016/j.bbabio.2019.04.001

384. Fujita Y, Yamakawa H. *Biochemistry of Chlorophyll Biosynthesis in Photosynthetic Prokaryotes*. doi:10.1007/978-3-319-51365-2

385. Cao K, Zhi R, Zhang G. Photosynthetic bacteria wastewater treatment with the production of value- added products : A review. *Bioresour Technol*. 2019;(December):122648. doi:10.1016/j.biortech.2019.122648

386. Hunter NC, Daldal F, Thurnauer MC, Beatty TJ. *The Purple Phototrophic Bacteria*. (Hunter NC, Daldal F, Thurnauer MC, Beatty TJ, eds.). Springer Netherlands; 2009.

387. Pfennig N. PHOTOTROPHIC GREEN AND PURPLE BACTERIA : a comparative survey. *Ann Rev Microbiol*. 1977:275-290.

388. Tan GA, Chen C, Li L, et al. Start a Research on Biopolymer Polyhydroxyalkanoate (PHA): A Review. 2014;(March). doi:10.3390/polym6030706

389. Van Loosdrecht MCM, Nielsen PH, Lopez-Vazquez CM, Brdjanovic D. *Experimental Methods in Wastewater Treatment*. 1st edithi. (Van Loosdrecht MCM, Nielsen PH, Lopez-Vazquez CM, Brdjanovic D, eds.). IWA Publishing; 2016.

390. Saini RK, Keum YS. Carotenoid extraction methods: A review of recent developments. *Food Chem*. 2018;240(June 2017):90-103. doi:10.1016/j.foodchem.2017.07.099

391. Nagarajan J, Ramanan RN, Raghunandan ME, Galanakis CM, Krishnamurthy NP. *Carotenoids*. Elsevier Inc.; 2017. doi:10.1016/B978-0-12-805257-0.00008-9

392. Zurdo J, Lozano RM, Fernandez-cabrera C, Ramirez JM, C CDIBCSI. Dimeric carotenoid interaction in the light-harvesting antenna of purple phototrophic bacteria. *Biochem J*. 1991;274:881-884.

393. Ingram L. Mechanism of Lysis of Escherichia coli by Ethanol and Other Chaotropic Agentst. *J BACTOLOGY,*. 1981;146(1):331-336.

394. Corredor C, Hou WC, Klein SA, et al. Disruption of model cell membranes by carbon nanotubes. *Carbon N Y*. 2013;60:67-75. doi:10.1016/j.carbon.2013.03.057

395. Samorì C, Abbondanzi F, Galletti P, et al. Extraction of polyhydroxyalkanoates from mixed microbial cultures : Impact on polymer quality and recovery. 2015;189:195-202. doi:10.1016/j.biortech.2015.03.062

396. Jiang X, Ramsay JA, Ramsay BA. Acetone extraction of mcl-PHA from Pseudomonas putida KT2440. *J Microbiol Methods*. 2006;67:212-219. doi:10.1016/j.mimet.2006.03.015

397. Kyszewski M, Galeski A, Martuscelli E. *POLYMER BLENDS*. SPRINGER SCIENCE+BUSINESS MEDIA, LLC; 1984.

398. Wu C, Liao H. Fabrication , characterization , and application of polyester / wood flour composites. 2017:1-10. doi:10.1515/polyeng-2016-0284

399. Moosberg-Bustnes H, Lagerblad B, Forssberg E. The function of fillers in concrete. *Mater Struct*. 2004;37:74-81. doi:10.1617/13694

400. Avérous L, Pollet E. Biorenewable nanocomposites. *MRS Bull*. 2011;36(9):703-710. doi:10.1557/mrs.2011.206

401. Bordes P, Pollet E, Avérous L. Nano-biocomposites: Biodegradable polyester/nanoclay systems. *Prog Polym Sci*. 2009;34(2):125-155. doi:10.1016/j.progpolymsci.2008.10.002

402. Achukwu E. Development of waste glass particle-reinforced Unsaturated polyester composites. 2017;(May):15-20.

403. Arslan H, Hazer B, Yoon SC. Grafting of poly(3-hydroxyalkanoate) and linoleic acid onto chitosan. *J Appl Polym Sci*. 2007;103(1):81-89. doi:10.1002/app.24276

404. Silvestroni P. *Fondamenti Di Chimica*. CEA; 1988.

405. Ege S, Kleinman RW, Ziteck P. *Organic Chemistry*. (Solutions macmillan learning curriculum, ed.). macmillan learning curriculum solutions; 2018.

406. Prates P, Jesus V, Frias M, Cristina E. Thermal degradation kinetics of carotenoids : Acrocomia aculeata oil in the context of nutraceutical food and bioprocess technology. *J Therm Anal Calorim*. 2020;(0123456789). doi:10.1007/s10973-020-09303-9

407. Burhenne L, Messmer J, Aicher T, Laborie M. The effect of the biomass components lignin , cellulose and hemicellulose on TGA and fixed bed pyrolysis. *J Anal Appl Pyrolysis*. 2013;101:177-184. doi:10.1016/j.jaap.2013.01.012

408. Hablot E, Bordes P, Pollet E, Ave L. Thermal and thermo-mechanical degradation of poly (3-hydroxybutyrate) -based multiphase systems. 2008;93:413-421. doi:10.1016/j.polymdegradstab.2007.11.018

409. Meng DC, Shi ZY, Wu LP, et al. Production and characterization of poly(3-hydroxypropionate-co-4-hydroxybutyrate) with fully controllable structures by recombinant Escherichia coli containing an engineered pathway. *Metab Eng*. 2012;14(4):317-324. doi:10.1016/j.ymben.2012.04.003

410. Stokes VK. Polymerization. In: *Introduction to Plastics Engineering*. ; 2018. doi:10.1016/B978-0-323-39500-7.00002-2

411. Ruiden A. Mechanical Properties of Polymer Solids and Liquids. In: *Mechanical Properties of Polymer Solids and Liquids*. ; 1999.

412. Srikanth Pilla. *Handbook of Bioplastic and Biocomposites Engineering Applications*. Vol 6. (Scrivener Publishing LLC, ed.). Salem, Massachusetts: John Wiley & Sons; 2011.

413. Hamad WY, Hu TQ. Structure–process–yield interrelations in nanocrystalline cellulose extraction. *Can J Chem Eng*. 2010;(August). doi:10.1002/cjce.20298

414. Lide D. Handbook of Chemistry and Physics. *82nd Ed Boca Raton, Florida, USA CRC Press*. 2001.

415. Thakur VK, Thakur MK. Processing and characterization of natural cellulose fibers/thermoset polymer composites. *Carbohydr Polym*. 2014;109:102-117. doi:10.1016/j.carbpol.2014.03.039

416. Pacheco-Torgal F, Jalali S. Cementitious building materials reinforced with vegetable fibres: A review. *Constr Build Mater*. 2011;25(2):575-581. doi:10.1016/j.conbuildmat.2010.07.024

417. Yao L, Alderliesten R, Zhao M, Benedictus R. Bridging effect on mode I fatigue delamination behavior in composite laminates. *Compos PART A*. 2014;63:103-109. doi:10.1016/j.compositesa.2014.04.007

418. Oksman K, Clemons C. Mechanical Properties and Morphology of Impact Modified Polypropylene – Wood Flour Composites. *J Appl Polym Sci*. 1997:1503-1513.

419. Surfaces P, Series ACSS, Society AC. *Microstructure and Microtribology of Polymer Surfaces About the Cover*.; 1999.

420. Wang S, Chen W, Xiang H, Yang J, Zhou Z, Zhu M. Modification and Potential Application of Short-Chain-Length Polyhydroxyalkanoate (SCL-PHA) Shichao. *Polymers (Basel)*. 2016. doi:10.3390/polym8080273

421. Matthew C, Vandi L, Pratt S, et al. Understanding the effect of copolymer content on the processability and mechanical properties of polyhydroxyalkanoate (PHA)/ wood composites. *Compos Part A*. 2019;124(May):105437. doi:10.1016/j.compositesa.2019.05.005

422. Lemos PC, Viana C, Salgueiro EN, Ramos AM, Crespo JPSG, Reis MAM. Effect of carbon source on the formation of polyhydroxyalkanoates (PHA) by a phosphate-accumulating mixed culture. *Enzyme Microb Technol*. 1998;0229(97):662-671.

423. Awal A, Ghosh SB, Sain M. Thermal properties and spectral characterization of wood pulp reinforced bio- composite fibers. *J Therm Anal Calorim* ·. 2010;(February). doi:10.1007/s10973-009-0100-x

424. Abdul-hammed M, Bolarinwa IF, Adebayo L. Kinetics of the Degradation of Carotenoid Antioxidants in Tomato Paste Kinetics of the Degradation of Carotenoid Antioxidants in Tomato Paste. 2016;(August). doi:10.19026/ajfst.11.2772

425. Naya S, Sebio-pun T, Lo J, Ethanol-extractives FÁPÁ. Thermogravimetric analysis of wood , holocellulose , and lignin from five wood species. *J Therm Anal Calorim*. 2012:1163-1167. doi:10.1007/s10973-011-2133-1

426. Arseneau DF. The differential thermal analysis o f wood. *Can J Chem*. 1961;39.

427. Ahmed I, Bilal M, Niazi K, Hussain A, Jahan Z. Influence of Amphiphilic Plasticizer on Properties of Thermoplastic Starch Influence of Amphiphilic Plasticizer on Properties of Thermoplastic Starch Films. *Polym Plast Technol Eng*. 2017;0(0):1-11. doi:10.1080/03602559.2017.1298803

428. Blake PG, Jackson GE. The Thermal Decomposition of Acetic Acid. *J Chem SOC*. 1966;(3):1966-1968.

429. González M, Dupont C, Thiéry S, Meyer X, Gourdon C. Biomass and Bioenergy Impact of biomass diversity on torrefaction : Study of solid conversion and volatile species formation through an innovative TGA-GC / MS apparatus. *Biomass and Bioenergy*. 2018;119(August):43-53. doi:10.1016/j.biombioe.2018.09.002

430. Ortiz FJG, Alonso-Fariñas B, Campanario FJ, Kruse A. Life cycle assessment of the Fischer-Tropsch biofuels production by supercritical water reforming of the bio-oil aqueous phase. *Energy*. 2020:118648. doi:10.1016/j.energy.2020.118648

431. Jayakrishna SVK, Joy D. Environmental impact assessment of an automotive component using eco-indicator and CML methodologies. *Clean Techn Env Policy*. 2012:333-344. doi:10.1007/s10098-011-0405-x

432. Harding KG, Dennis JS, Blottnitz H Von, Harrison STL. Environmental analysis of plastic production processes : Comparing petroleum-based polypropylene and polyethylene with biologically-based poly- □ -hydroxybutyric acid using life cycle analysis. *J Biotechnol 1*. 2007;130:57-66. doi:10.1016/j.jbiotec.2007.02.012

433. Tiwari A, Ramirez AM, Jain R, Saxena A. Green Chemistry for the Production of Biodegradable Polymers as Solid Substrate and the Formation of Sustainable Biofilm. *Nov Non-Conventional Mater Technol Sustain*. 2012;517:755-762. doi:10.4028/www.scientific.net/KEM.517.755

434. De Paula F, De Paula CB., Contiero J. Prospective Biodegradable Plastics from Biomass Conversion Processes. *Biofuels - state Dev*.

435. Lei P, Schmidt M, Wei W. Conversion of Biomass into Bioplastics and Their Potential Environmental Impacts. *Biotechnol Biopolym*.

436. M;Visakh P IR. *Polyhydroxyalkanoate (PHA) Based Blends , Composites and Nanocomposites*. (Roy I, P.M. V, eds.). The Royal Society of Chemistry; 2015. doi:10.1039/9781782622314

437. Yang S, Madbouly SA, Schrader JA, Grewell D, Kessler MR, Graves WR. Processing and characterization of bio-based poly (hydroxyalkanoate)/ poly (amide) blends : Improved flexibility and impact resistance of PHA-based plastics. 2015;42209:1-10. doi:10.1002/app.42209

438. Rodriguez-Perez S, Serrano A, Pantion AA, Alonso-Farinas B. Challenges of scaling-up PHA production from waste streams . A review. *J Environ Manage*. 2018;205. doi:10.1016/j.jenvman.2017.09.083

439. Kyung D, Kim M, Chang J, Lee W. Estimation of greenhouse gas emissions from a hybrid wastewater treatment plant. *J Clean Prod*. 2015;95:117-123. doi:10.1016/j.jclepro.2015.02.032

440. Akadiri S Saint, Alkaw MM, Sevin U, Akadiri AC. Towards achieving environmental sustainability target in Italy . The role of energy , real income and globalization ☆. *Sci Total Environ J*. 2019;671:1293-1301. doi:10.1016/j.scitotenv.2019.03.448

441. Marcantonini C, Valero V. Renewable energy and CO 2 abatement in Italy. *Energy Policy*. 2017;(April 2016):1-14. doi:10.1016/j.enpol.2016.12.029

442. Righi S, Baioli F, Samorì C, Galletti P, Stramigioli C. A life-cycle assessment of poly-hydroxybutyrate extraction from microbial biomass using dimethylcarbonate. In: *10th Italian LCA Conference*. ; 2016.

443. Niewersch C, Stemann J. Sustainable sewage sludge management fostering phosphorus recovery and energy efficiency Deliverable D 5 . 1. In: *P-REX*. ; 2014:1-67.

444. Ferrer I, Serrano E, Font X. Enhancement of Thermophilic Anaerobic Sludge Digestion by 70ºC Pre-Treatment : Energy Considerations. *J Residuals Sci Technol*. 2009;6(1):11-18.

445. National Institute of Standard Technologies. NIST Chemistry WebBook. 2018. doi:https://doi.org/10.18434/T4D303

446. Tozzi P V, Wisniewski CM, Zalewski NJ, Savelski MJ, Slater CS, Richetti FA. Life cycle assessment of solvent extraction as a low-energy alternative to distillation for recovery of N-methyl-2-pyrrolidone from process waste. *Green Process Synth*. 2018:277-286.

447. Wernet G, Bauer C, Steubing B, Reinhard J, Moreno-ruiz E, Weidema B. The ecoinvent database version 3 (part I): overview and methodology. *Int J Life Cycle Assess*. 2016;3(part I). doi:10.1007/s11367-016-1087-8

448. Cseri L, Razali M, Pogany P, Szekely G. Organic Solvents in Sustainable Synthesis and Engineering. In: *Green Chemistry*. Elsevier Inc.; 2018:513-553. doi:10.1016/B978-0-12-809270-5.00020-0

449. Livingston AG, Szekely G, Jimenez-solomon MF, Marchetti P, Kim JF, Livingston AG. Sustainability assessment of organic solvent nanofiltration: from fabrication to application. *Green Chem*. 2014;16(10):4440-4473. doi:10.1039/c4gc00701h